

INFORMATION TO USERS

This manuscript has been reproduced from the microfilm master. UMI films the text directly from the original or copy submitted. Thus, some thesis and dissertation copies are in typewriter face, while others may be from any type of computer printer.

The quality of this reproduction is dependent upon the quality of the copy submitted. Broken or indistinct print, colored or poor quality illustrations and photographs, print bleedthrough, substandard margins, and improper alignment can adversely affect reproduction.

In the unlikely event that the author did not send UMI a complete manuscript and there are missing pages, these will be noted. Also, if unauthorized copyright material had to be removed, a note will indicate the deletion.

Oversize materials (e.g., maps, drawings, charts) are reproduced by sectioning the original, beginning at the upper left-hand corner and continuing from left to right in equal sections with small overlaps.

Photographs included in the original manuscript have been reproduced xerographically in this copy. Higher quality 6" x 9" black and white photographic prints are available for any photographs or illustrations appearing in this copy for an additional charge. Contact UMI directly to order.

**ProQuest Information and Learning
300 North Zeeb Road, Ann Arbor, MI 48106-1346 USA
800-521-0600**

UMI[®]

University of Alberta

Radical Alkylation of Substituted η^3 -Allyltitanocene Complexes. Amino- and Alkyl-Substituted Bis(indenyl) Templates for Titanacyclobutane Synthesis and Conversion to Cyclobutanone Derivatives

by

Grace Greidanus



A thesis submitted to the Faculty of Graduate Studies and Research in partial fulfillment of the requirements for the degree of Doctor of Philosophy

Department of Chemistry

Edmonton, Alberta

F a l l 2001



**National Library
of Canada**

**Acquisitions and
Bibliographic Services**

395 Wellington Street
Ottawa ON K1A 0N4
Canada

**Bibliothèque nationale
du Canada**

**Acquisitions et
services bibliographiques**

395, rue Wellington
Ottawa ON K1A 0N4
Canada

Your file *Votre référence*

Our file *Notre référence*

The author has granted a non-exclusive licence allowing the National Library of Canada to reproduce, loan, distribute or sell copies of this thesis in microform, paper or electronic formats.

The author retains ownership of the copyright in this thesis. Neither the thesis nor substantial extracts from it may be printed or otherwise reproduced without the author's permission.

L'auteur a accordé une licence non exclusive permettant à la Bibliothèque nationale du Canada de reproduire, prêter, distribuer ou vendre des copies de cette thèse sous la forme de microfiche/film, de reproduction sur papier ou sur format électronique.

L'auteur conserve la propriété du droit d'auteur qui protège cette thèse. Ni la thèse ni des extraits substantiels de celle-ci ne doivent être imprimés ou autrement reproduits sans son autorisation.

0-612-68938-7

Canada

University of Alberta

Library Release Form

Name of Author: Grace Greidanus

Title of Thesis: Radical Alkylation of Substituted η^3 -Allyltitanocene Complexes.
Amino- and Alkyl-Substituted Bis(indenyl) Templates for Titanacyclobutane Synthesis
and Conversion to Cyclobutanone Derivatives

Degree: Doctor of Philosophy

Year this Degree Granted: 2001

Permission is hereby granted to the University of Alberta Library to reproduce single copies of this thesis and to lend or sell such copies for private, scholarly or scientific research purposes only.

The author reserves all other publication and other rights in association with the copyright in the thesis, and except as herein before provided, neither the thesis nor any substantial portion thereof may be printed or otherwise reproduced in any material form whatever without the author's prior written permission.



10705 84th Ave.

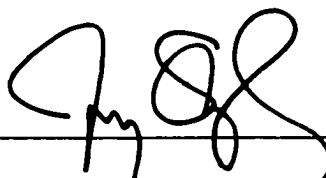
Edmonton, Alberta, T6E 2H8

April 18, 2001

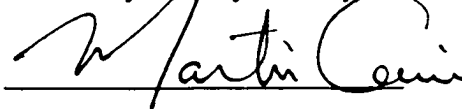
University of Alberta

Faculty of Graduate Studies and Research

The undersigned certify that they have read, and recommended to the Faculty of Graduate Studies and Research for acceptance, a thesis entitled **Radical Alkylation of Substituted η^3 -Allyltitanocene Complexes. Amino- and Alkyl-Substituted Bis(indenyl) Templates for Titanacyclobutane Synthesis and Conversion to Cyclobutanone Derivatives** submitted by **Grace Greidanus** in partial fulfillment of the requirements for the degree of Doctor of Philosophy.



Dr. Jeffrey M. Stryker (Supervisor)



Dr. Martin Cowie



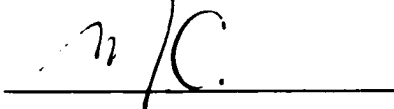
Dr. Steve H. Borgens



Dr. Rik R. Tykwinski



Dr. Michael C. Williams



Dr. Douglas W. Stephan

June 20, 2001

To my parents

Abstract

Electron rich bis(2-methoxyindenyl)- and bis(2-*N,N*-dimethylaminoindenyl)-titanium(III) templates were developed for the regioselective addition of both stabilized and unstabilized radicals to the central carbon of 1-substituted allyl complexes. One pot procedures were developed allowing these titanium(III) chloride complexes to be converted to titanacyclobutane complexes without the isolation of sensitive allyl titanocene intermediates. For the synthesis of 2,3-disubstituted titanacyclobutane complexes it is the two step methodology employing the use of allylmetal reagents, as compared to the samarium(II) mediated methodology, that affords higher overall yields.

A crystallographic investigation of bis(aminoindenyl)Ti(III) and Ti(IV) complexes was undertaken to rationalize the differences in reactivity observed between the 2-piperidinoindenyl and 2-*N,N*-dimethylaminoindenyl templates. What became apparent was that these ancillary ligands are capable of providing greater electron density than is required by the metal. Our investigation then turned to the development of simpler, less electron-rich indenyl templates. Surprising was the relatively minimal level of electron density necessary to promote clean conversion of substituted allyl complexes; however, a reasonable level of electron density provided to the metal center by the indenyl ancillary ligands is necessary to observe central carbon alkylation in good yields.

This investigation also revealed a new decomposition pathway for titanacyclobutane complexes. Various Ti(III) η^3 -allyl complexes undergo *reversible* regioselective central carbon alkylation when treated with allyl or benzyl radical. No trend was detected to rationalize the relative stability of these titanacyclobutane complexes and it is likely that stability is dictated by a combination of steric and electronic factors imparted by the ancillary ligand system onto the titanacyclobutane core.

This research also demonstrates that functionalization of titanacyclobutanes with carbon monoxide and isonitriles affords organic cyclobutanones and cyclobutanamines, respectively, in high yield under mild reaction conditions. Unexpectedly, carbonylation of bis(2-*N,N*-dimethylaminoindenyl)titanacyclobutane complexes generates an as yet uncharacterized paramagnetic Ti(III) intermediate that compromises approximately 50% of the material balance; the other 50% is isolated as bis(dimethylaminoindenyl)titanium dicarbonyl. This paramagnetic Ti(III) complex, on oxidative or hydrolytic workup, releases the cyclobutanone in very high yields, indicating that this complex contains all the organic material. The synthetic practicality of this reaction process was demonstrated by carrying out the cyclobutanone synthesis in one pot starting with bis(2-*N,N*-dimethylaminoindenyl)titanium chloride, again avoiding the isolation of sensitive intermediates.

Acknowledgements

I would like to thank my research advisor, Professor Jeffrey M. Stryker for all his great stories, guidance and encouragement in my pursuit of a scientific career. Your help has been truly appreciated.

I would also like to thank my doctoral committee, Professors Cowie, Bergens, Tykwinski, Williams and Stephan. In particular, I would like to thank Professor Cowie for his helpful discussions and his dedication to the inorganic division and inorganic graduate students. I have also enjoyed the seminars and lecture series put on by both the inorganic and organic division and have found these to be stimulating and highly informative.

I would also like to acknowledge and thank the current and former members of the Stryker group I have known: Trevor Dzwiniel, Christina Older, Jian-Xin Chen, Paul Tiege, Andy Skauge, Udo Verkerk, Megumi Fugita, Xin Qui, Jason Norman, Ross Witherell, Molla Endeshaw, Anne Hearn, James Sochan, Makoto Yasuda, Sensuke Ogoshi. Thank you for providing a stimulating atmosphere for doing research. Particular gratitude is to group members who made me laugh uncontrollably – you may or may not know who you are; some days it's not about what you do, but who you work with that makes life bearable.

I would also like to thank my good friends, Jennifer VanWijngaarden, Lesley Liu, Jennifer Doubt and Peggy Daley. Your interdisciplinary contributions to my scientific career gave me balance and perspective, but more importantly provided great suppers, coffee breaks, hockey and soccer games and one great ski trip.

The University of Alberta has provided me with great technical staff to help with characterization of many air sensitive compounds. Particularly, thanks goes to Darlene Mahlow, who suffered with me in trying to obtain all those difficult elemental analyses, and Dr. R. McDonald, for many crystallographic X-ray structure determinations. Gratefully acknowledged are NSERC of Canada and the Department of Chemistry, University of Alberta for financial support for this project.

Most importantly, my family, especially my parents, have given me support and never ending encouragement during these last four years, and throughout my life, which has enabled me to make these accomplishments. Mom and Dad, I don't know how to begin to say thank you. To Graham, my fiancé, your love and support is greatly appreciated, and, specifically to you Graham, the thesis doesn't end here: please, read further to catch a glimpse of what organometallic chemistry is about and what inspires me.

Table of Contents

	page
Chapter 1. Introduction	1
A. Metal-Templated Free Radical Reactions	1
B. Central Carbon Alkylation of η^3 -Allyl Complexes: Introduction and Historical Perspectives	6
1. Nucleophilic Additions to η^3 -Allyl Complexes	6
2. Radical Additions to η^3 -Allyl Complexes	14
C. Spectroscopic Characterization of Titanacyclobutane Complexes	26
D. Functionalization of Titanacyclobutane Complexes	27
E. Project Goals	32
F. References	34
Chapter 2. Bis(2-methoxyindenyl)titanacyclobutane Complexes via Organic Free Radical addition to Ti(III) allyl complexes	44
A. Synthesis of 2-Methoxyindenyl Titanocene η^3 -Allyl Complexes	44
B. Radical Addition to Allyl, Crotyl and Cinnamyl Complexes	47
C. Functionalization of Cinnamyl Derived Titanacyclobutanes	58
D. Conclusions	59
E. Experimental Procedures, Spectroscopic and Analytical Data	59
F. References	80
Chapter 3. Central Carbon Radical Alkylation of Bis(2-<i>N,N</i>-dimethylaminoindenyl)titanium(III) η^3-Allyl Complexes	84
A. Synthesis of Bis(2- <i>N,N</i> -dimethylaminoindenyl)titanium(III) η^3 -Allyl Complexes	84
B. Radical Addition to Crotyl and Cinnamyl Complexes	89

C. Crystallographic Investigation of Substituted Allyltitanium(III) and Titanacyclobutane Complexes	100
1. Introduction	100
2. Crystallographic Analysis of Titanium(III) Complexes 96 •LiCl(THF) ₂ , 98 , and 99	100
3. Crystallographic Analysis of Titanium (IV) Complexes 55a and 101a	117
D. β -Carbon Cleavage: A New Decomposition Pathway for Titanacyclobutane Complexes	124
E. One Pot all-Samarium Mediated Synthesis of Titanacyclobutane Complexes	138
F. Experimental	145
G. References	185
Chapter 4. Development of Less Electron Rich Indenyl Templates for Central Carbon Alkylation of Titanium(III) Allyl Complexes	194
A. Introduction	194
B. Bis(indenyl)titanium(III) as a Template for Central Carbon Alkylation	194
1. Preparation of Bis(indenyl)titanium(III) η^3 -Allyl Complexes	194
2. Radical Additions to Substituted and Unsubstituted Allyl Complexes of Bis(indenyl)titanium(III)	196
C. Bis(2-methylindenyl)titanium(III) as a Template for Central Carbon Alkylation	204
1. Preparation of Bis(2-methylindenyl)titanium(III) η^3 -Allyl Complexes	204
2. Radical Additions to Cinnamyl and Crotyl	206

Bis(2-methylindenyl)titanium(III) Complexes	
D. Bis(2-isopropylindenyl)titanium(III) as a Template for Central Carbon Alkylation	212
1. Preparation of Bis(2-isopropylindenyl)titanium(III) η^3 -Allyl Complexes	212
2. Radical Additions to Cinnamyl and Crotyl	217
Bis(2-isopropylindenyl)titanium(III) Complexes	
E. Conclusions	221
F. Experimental	222
G. References	267
Chapter 5. Chapter 5 Functionalization of Titanacyclobutane Complexes: Synthesis of Cyclobutane Derivatives	269
A. Introduction	269
B. Single Insertions of Carbon Monoxide. Synthesis of Cyclobutanones	270
C. Single Insertions of Isonitrile. Synthesis of Cyclobutanamines	279
D. Experimental	284
E. References	302
Chapter 6. Conclusions	307
Appendix I	309
Part A. Crystallographic details for complex 96•LiCl(THF)₂	310
Part B. Crystallographic details for complex 98	316
Part C. Crystallographic details for complex 99 and 99'	323
Part D. Crystallographic details for complex 101a	335
Part E. Crystallographic details for complex 55a	342

Part F. Crystallographic details for complex 139c	350
Part G. Crystallographic details for complex 145	358

List of Tables

	Page
Table 2.1 Selected Room Temperature ^1H NMR Resonances of Titanacyclobutane Complexes 55a and 89a-c	50
Table 2.2. Selected Room Temperature ^1H NMR Resonances of Titanacyclobutane Complexes 90a-d	53
Table 3.1 Room Temperature ^1H NMR Resonances of Titanacyclobutane Complexes 101a-d	92
Table 3.2 Yields of One Pot Procedure for Titanacyclobutane Complexes 101a-d	95
Table 3.3 Room Temperature ^1H NMR Resonances of Titanacyclobutane Complexes 102a-e	97
Table 3.4 Selected Bond Lengths and Angles for 96 • $\text{LiCl}_2(\text{THF})_2$	104
Table 3.5 Selected Bond Lengths and Angles for 98	105
Table 3.6 Selected Bond Lengths and Angles for 99 and 99'	106
Table 3.7 Comparison of Bond Lengths (Å) and Angles (°) for (allyl)Ti(III) Complexes	107
Table 3.8 Structural Data For Indenyl Coordination	111
Table 3.9 Indenyl Carbon-Carbon Bond Lengths (Å)	112
Table 3.10 Structural Data for Amino Group	113
Table 3.11 Selected Bond Lengths (Å) and Angles (°) for Complex 101a	120
Table 3.12 Selected Bond Lengths (Å) and Angles (°) for Complex 55a	121
Table 3.13 Titanacyclobutane Formation using Samarium Mediated Methodology	142
Table 4.1 Room Temperature ^1H NMR Resonances of Titanacyclobutane Complexes 139a-d	207
Table 4.2 Yields of One Pot Procedure for Titanacyclobutane	208

Complexes 139a-d	
Table 4.3 Selected Bond Lengths (Å) and Angles (°) for Complex 139c	210
Table 4.4 Structural Data For Indenyl Coordination	211
Table 4.5 Selected Bond Lengths (Å) and Angles (°) for Complex 145	216
Table 4.6 Bond Lengths (Å) and Angles (°) for Crotyl Ti(III)	217
Complex 145	
Table 4.7 Structural Data for Indenyl Coordination	217
Table 4.8 Room Temperature ¹H NMR Resonances of	219
Titanacyclobutane Complexes 146a-d	
Table 4.9 Yields of One Pot Procedure for Titanacyclobutane	220
Complexes 146a-d	
Table 5.1 Titanacyclobutane Formation and Carbonylation to Yield	274
Cyclobutanones	
Table 5.2 Isonitrile Insertion to Yield Cyclobutanamines	281

List of Figures

		page
Figure 1.1	Charge control argument for regioselectivity of nucleophilic addition.	7
Figure 1.2	EHMO energy level diagram for d ⁰ group IV metallocene π -allyl complexes.	12
Figure 1.3	EHMO energy level diagram for d ¹ group IV metallocene π -allyl complexes.	15
Figure 1.4a	$\eta^3 \leftrightarrow \eta^1$ Equilibrium for substituted allyl titanocene complexes.	22
Figure 1.4b	Unfavourable steric interactions between substituted allyl and ancillary ligand.	22
Figure 2.1	Numbering scheme for NMR spectroscopy of indenyl Ligand system.	49
Figure 3.1	The molecular structure of 96 •LiCl(THF) ₂ .	86
Figure 3.2	Proposed structures for non-interconverting structures of 101c at -60 °C.	94
Figure 3.3	The molecular structure of 98 .	101
Figure 3.4a	The molecular structure of 99 .	102
Figure 3.4b	The molecular structure of 99' .	103
Figure 3.5	The molecular structure of 53 .	108
Figure 3.6	Schematic diagram illustrating the folding axes of the indenyl ligand.	109
Figure 3.7	The molecular structure of 101a .	118
Figure 3.8	The molecular structure of 55a .	119
Figure 4.1	The molecular structure of 139a .	209
Figure 4.2	The molecular structure of 145 .	215

List of Abbreviations

Å	angstrom
AIBN	2,2'-azobisisobutyronitrile
Atm	atmosphere
Bu	butyl
calcd.	calculated
Cp	cyclopentadienyl
Cp*	pentamethylcyclopentadienyl
Cy	cyclohexyl
COSY	correlated spectroscopy
d	doublet
EMHO	extended Hückel Molecular Calculations
Et	ethyl
equiv	equivalent
FMO	frontier molecular orbital
g	grams
GC	gas chromatography
h	hour(s)
HMQC	heteronuclear multiple quantum correlation
Hz	Hertz
HOMO	highest occupied molecular orbital
<i>i</i>	iso
IR	infrared
L	liter
LUMO	lowest occupied molecular orbital
m	medium
M	metal

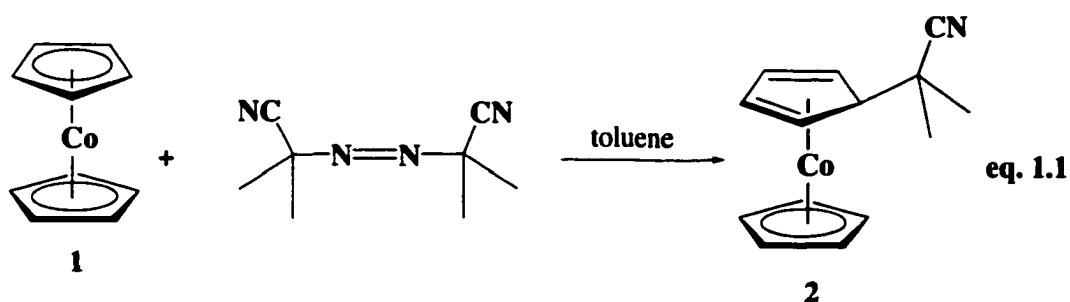
Me	methyl
mL	milliliter
MS	mass spectrometry
NMR	nuclear magnetic resonance
OTf	trifluoromethanesulfonate
Ph	phenyl
Pr	propyl
psig	pounds per square inch gauge pressure
q	quartet
R	alkyl group
s	singlet
s	strong
SOMO	singly occupied molecular orbital
t	tert
t	triplet
THF	tetrahydrofuran
TMEDA	<i>N,N,N',N'</i>-tetramethylethylenediamine
TMS	trimethylsilyl
w	weak
X	halide
η	hapticity
μL	microliter
↔	correlation

Chapter 1. Introduction

A. Metal-Templated Free Radical Reactions

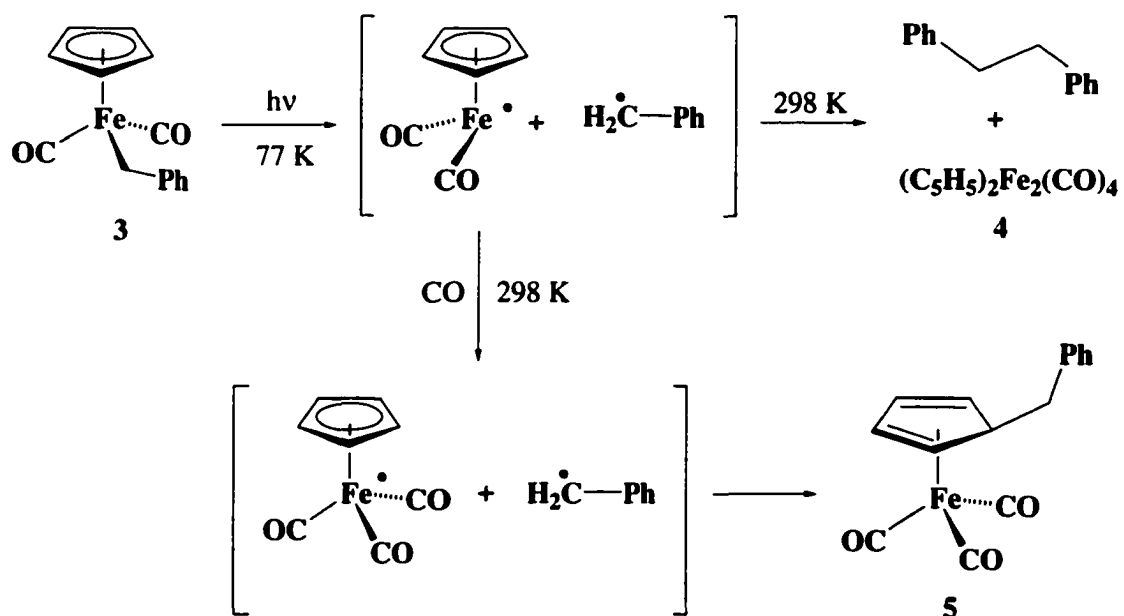
One of the fastest growing areas of organic chemistry is the application of organometallic and coordination compounds to synthetic problems, taking advantage of the control elements inherent in metal-templated reactions. Nucleophilic and electrophilic additions to unsaturated hydrocarbon ligands coordinated to transition metals have received considerable attention and resulted in many synthetically relevant metal-mediated methodologies.¹ Metal-templated free radical additions, however, remain a largely undeveloped field despite numerous reports of methods using transition metal complexes to initiate organic free radical reactions.² Organic radical reactions, once thought to be 'messy', are now generally recognized as being highly rate dependent and control of reaction conditions can result in high chemo- and regioselectivity.³ Further development of this field to include reactions of metal-templated hydrocarbyl ligands offers the synthetic chemist potentially valuable additions to the arsenal of selective carbon-carbon bond forming reactions.

The first direct investigation of radical addition to a transition metal coordinated hydrocarbyl ligand was reported in 1970 by Herberich and Schwartzer.⁴ Thermal decomposition of azoisobutyronitrile (AIBN) in the presence of cobaltocene produces the corresponding cyclopentadienyl-[5-*exo*-(1-cyano-1-methylethyl)cyclopentadiene]cobalt complex **2** in high yield (eq. **1.1**). This observation gives support to a proposed radical mechanism for the addition of organic halides to 19- and 20-electron metallocene and bis(η^6 -arene) complexes,⁵ as well as the migration of a benzyl ligand observed upon photolysis of iron complex **3** (Scheme **1.1**) to yield complex **5**.⁶ The most common radical reactions in organometallic complexes involve ligand to ligand dimerization reactions; these have been observed for a wide range of odd-electron metal complexes.⁷



Radical addition pathways have also been established for reactions of radicals with the free olefin moiety of α,β -unsaturated carbene,⁸ carbyne,⁹ vinyl,¹⁰ η^2 -alkenyne,¹¹ η^1 -allyl,¹² and η^1 -cyclopentadienyl ligands.¹² One electron oxidation of transition metal-alkynyl and alkylidene complexes followed by radical dimerization has led to a convenient pathway to conjugated carbon linkers between two metals.^{10,13}

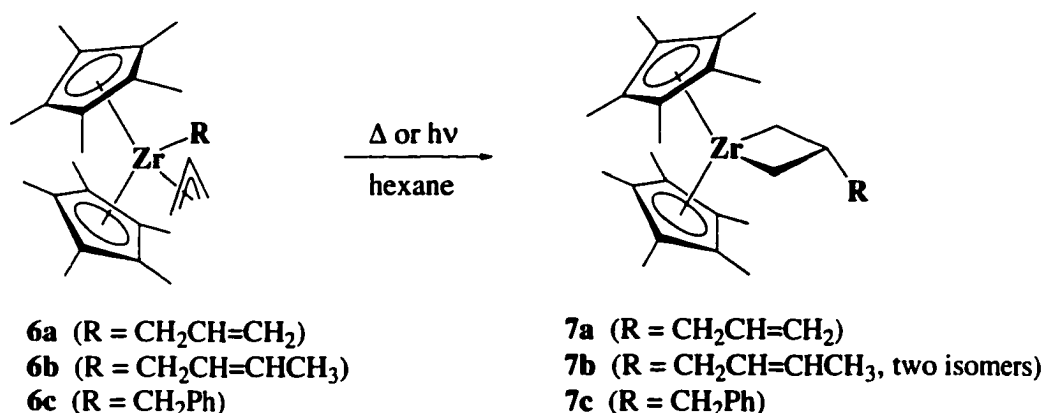
Scheme 1.1

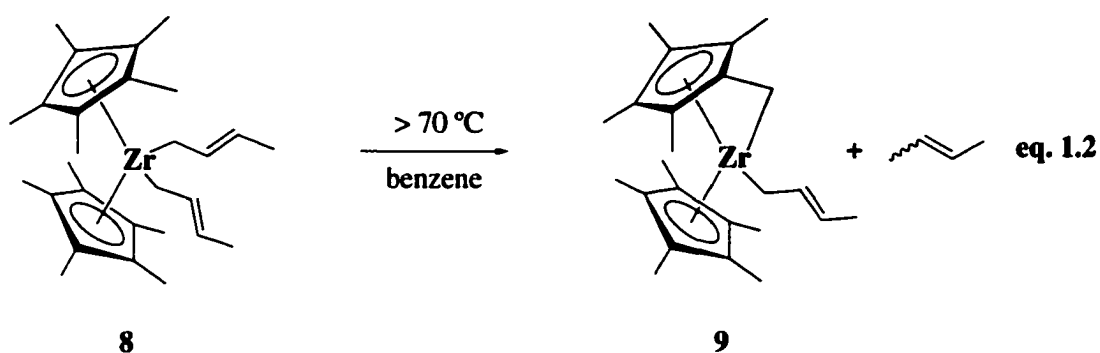


More recently, the Stryker group reported an unprecedented entry into the formation of group 4 metallacyclobutanes via thermal and photolytic rearrangement of

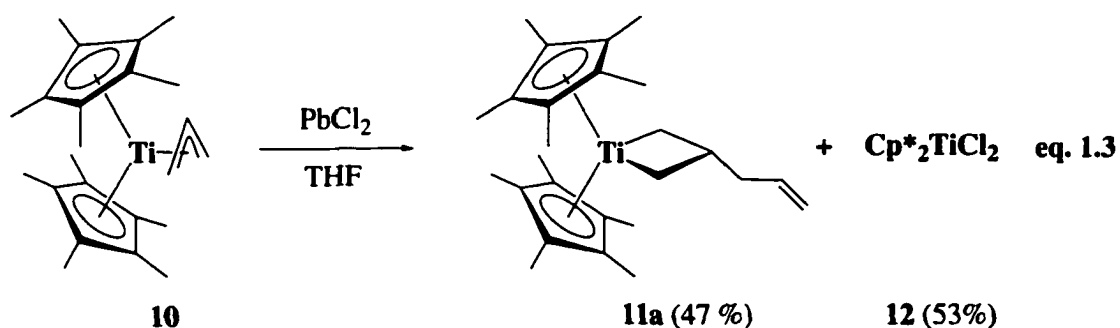
zirconocene bis(allyl) **6a** and related complexes (Scheme 1.2).^{14,15} Mechanistic investigations (kinetics and solvent effects) suggest that a free radical pathway is operative; the ligand rearrangement involves homolytic cleavage of the hydrocarbyl ligand followed by migration to the β -carbon of an Zr(III) η^3 -allyl moiety. This result prompted the investigation into hydrocarbyl radical additions to titanium(III) allyl complexes, which will be described in detail (*vide infra*). This zirconium rearrangement reaction, however, is specific to activated hydrocarbyl ligands migrating to unsubstituted allyl ligands. In zirconocene bis(crotyl) complex **8**, for example, no reaction is observed at temperatures less than 70 °C, at which point the complex undergoes slow σ -bond metathesis, giving ‘tuck-in’ crotyl complex **9** and 2-butene (eq. 1.2). This was attributed to a preference of the crotyl ligands to be η^1 -coordinated, underscoring the effect substituents have on hapticity in allyl ligand coordination in d^0 -metal complexes. This study was complemented by the observation that the oxidative chlorination of titanocene allyl complex **10** with PbCl_2 ,¹⁶ gives β -allyltitanacyclobutane **11a** and titanocene dichloride **12**, instead of the expected $\text{Cp}^*_2\text{Ti}(\text{allyl})\text{Cl}$ (eq. 1.3).

Scheme 1.2





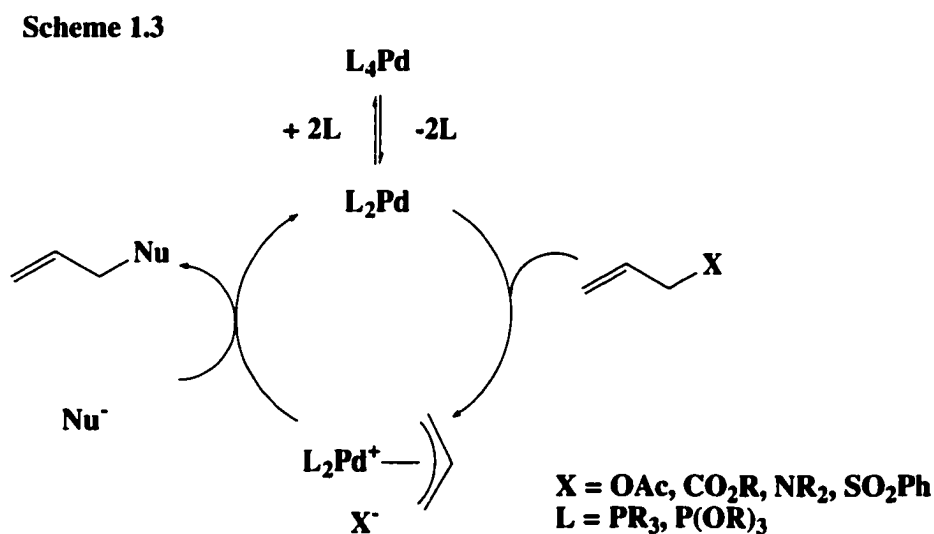
Central carbon radical alkylation of titanium(III) allyl complexes is only the latest of several useful methods to make titanacyclobutane complexes. Grubbs and coworkers successfully isolated titanacyclobutane complexes **13** by the treatment of Tebbe's reagent **14** with alkenes in the presence of a Lewis base such as *N,N*-dimethylaminopyridine (eq. 1.4).¹⁷ The addition of Grignard reagent **15** to titanocene dichloride also results in the formation of titanacyclobutane **16** (eq. 1.5).¹⁸ More recently, Bergman has reported that thermolysis of terminal alkenes in the presence of η^2 -*N*₂-dialkane titanocene complex **17** yields *trans*- α,β -disubstituted titanacyclobutane complexes **18** in a regio- and stereoselective manner (eq. 1.6).¹⁹ These methods are not entirely satisfactory, as titanacyclobutane complexes **13** are thermally unstable and complexes **18** are produced by multistep synthesis with low overall yield.



B. Central Carbon Alkylation Reactions of η^3 -Allyl Complexes: Introduction and Historical Perspectives

1. Nucleophilic Additions to η^3 -Allyl Complexes

Electrophilic transition metal η^3 -allyl complexes are known to undergo nucleophilic additions to either the terminal or the central carbon of the allyl ligand. Historically, interest has been focused on regioselective attack at the terminal carbon by a nucleophile as a means of obtaining allylically substituted organic compounds after decomplexation from the metal.²⁰ Significant contributions in this area emerged from the groups of Tsuji and Trost,²¹ where proallylic substrates reacted with stabilized nucleophiles in the presence of a catalytic amount of Pd(0), in a manner analogous to the displacement of an allylic leaving group by an S_N2 or S_N2' mechanism (Scheme 1.3). Nucleophilic additions to the terminal allylic carbon in several other transition metal η^3 -allyl systems have been reported in the literature, emphasizing the generality of this reactivity.²²



Central carbon alkylation of an allyl ligand was first reported by M. L. H. Green, et al.²³ This investigation revealed that cationic molybdocene and tungstenocene allyl complexes **19** and **20**, when treated with nucleophiles, experienced exclusive attack at the central carbon of the allyl ligand giving metallacyclobutane complexes **21** and **22**, respectively (Scheme 1.4). This surprising result was rationalized using a “charge control” argument (Figure 1.1).²⁴ Based on a perturbational approach, the Davies-Green-Mingos (DGM) rules predict that nucleophilic addition will be directed to the most electrophilic carbon of the allyl ligand. The effect of complexing an allyl ligand to an electron rich metal fragment, such as the d^2 Cp_2M systems ($M = Mo, W$) used in the

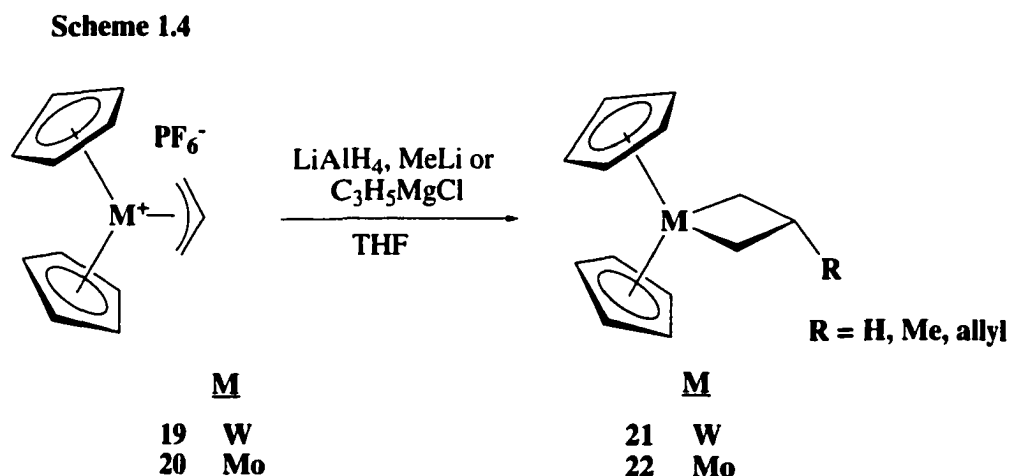
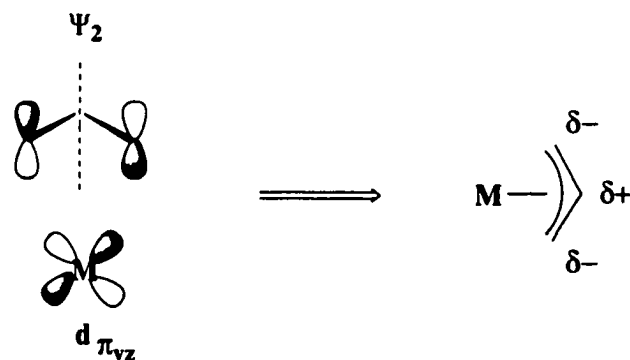


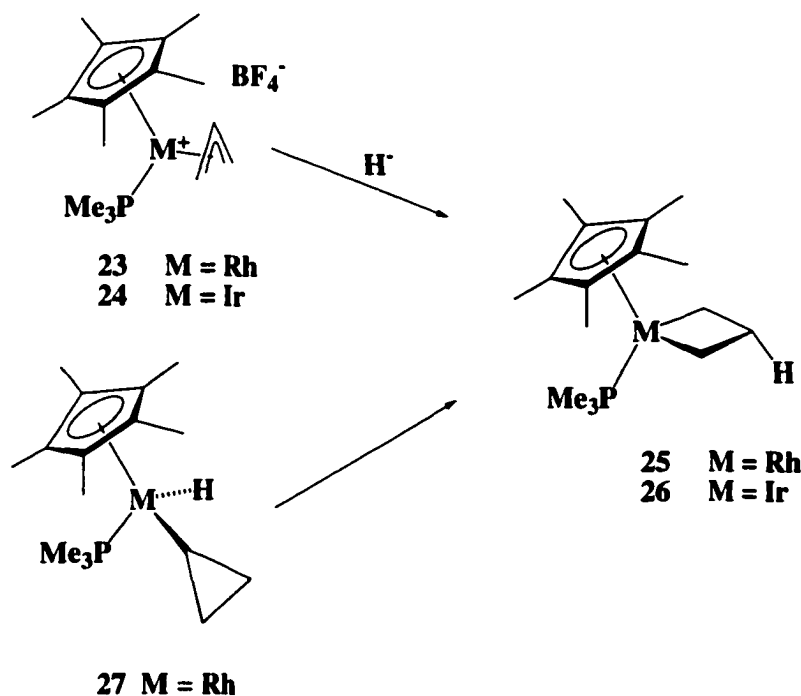
Figure 1.1 Charge control argument for regioselectivity of nucleophilic addition.



investigation, is partly negatively charged terminal carbons relative to the central carbon, as the metal fragment donates electron into the HOMO Ψ_2 of the allyl ligand.

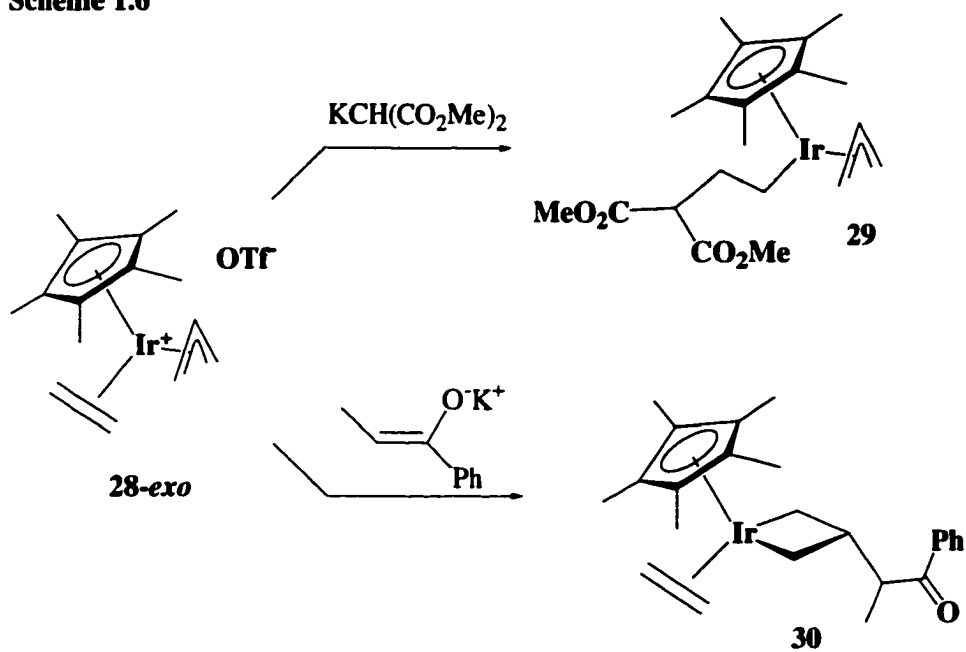
This rationale adequately explained the reactivity observed for many subsequently investigated transition metal π -allyl complexes.²⁵ However, a detailed investigation into half-sandwich group IX metallocene π -allyl complexes $[\text{Cp}^*(\text{L})\text{M}(\eta^3\text{-allyl})]^+\text{X}^-$ ($\text{M} = \text{Rh}, \text{Ir}$; $\text{X} = \text{BF}_4, \text{PF}_6, \text{OTf}$; $\text{L} = \text{PMe}_3$, $\text{Cp}^* = \text{C}_5\text{Me}_5$) yielded interesting findings, some in direct contradiction to the DGM rules. The addition of hydride reagents to $[\text{Cp}^*(\text{PMe}_3)\text{M}(\eta^3\text{-allyl})]^+\text{BF}_4^-$ ($\text{M} = \text{Rh}, \text{Ir}$) **23** and **24** to give metallacyclobutane complexes **25** and **26**, respectively, was first reported by Bergman (Scheme 1.5).²⁶ Rhodacyclobutane complex **25** can also be formed from an intramolecular thermal rearrangement of the hydrido cyclopropyl complex **27** at low temperature. Deuterium labeling studies in these complexes show that the nucleophilic addition reaction proceeds by direct hydride addition to the central carbon of the π -allyl metal complex, and not by initial metal addition followed by rearrangement.^{6a-c}

Scheme 1.5

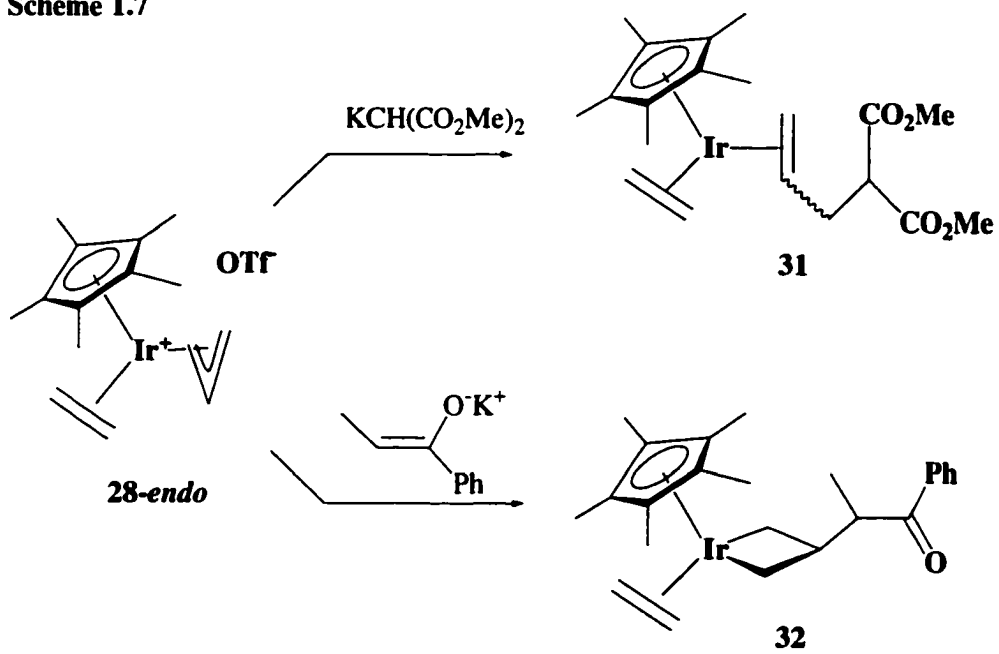


The Stryker group furthered the investigation by examining nucleophilic addition to the ethylene ($L = C_2H_4$) analogue of $[Cp^*(L)M(\eta^3\text{-allyl})]^+X^-$ ($X = OTf$, $Cp^* = C_5Me_5$) **28** ($M = Ir$).²⁷ Findings indicated that regioselectivity was not only dependent on the nature of the nucleophile, but also on the configuration of the allyl ligand. When *exo*-iridium allyl ethylene complex **28-*exo*** is treated with the potassium enolate of dimethylmalonate, the nucleophile attacks the ethylene carbon exclusively giving allyl iridium complex **29** (Scheme 1.6). In this case, the DGM rule, predicting kinetic nucleophilic attack preferentially occurring at an even, open polyene over addition to an odd, open polyene, is adhered to. Treating complex **28-*exo*** with the potassium enolate of propiophenone violates this DGM rule and results in exclusive formation of iridacyclobutane complex **30**, the result of central carbon addition to the η^3 -allyl. For the *endo*-iridium allyl ethylene complex **28-*endo***, nucleophilic addition is directed to the allyl ligand; not at the ethylene group as the DGM rule predicts. Using the potassium enolate of dimethylmalonate nucleophilic addition is directed at the *terminal* carbon of the allyl ligand, resulting in a mixture of bis(olefin) stereoisomers of complex **31**; the potassium enolate of propiophenone gives exclusively the central carbon alkylation product complex **32** (Scheme 1.7). Similarly, both terminal and central carbon alkylation are observed treating $[Cp^*(PMe_3)Rh(\eta^3\text{-allyl})]^+PF_6^-$ **33** with the potassium enolate of propiophenone. Altogether, this strongly indicates that coordination geometry and the strength of the nucleophile, in addition to electron-richness, are important factors in determining the regiochemistry of nucleophilic addition to transition metal π -allyl complexes.

Scheme 1.6



Scheme 1.7



Various molecular orbital calculations^{28,29} have been employed to explain the regioselectivity of nucleophilic addition to π -allyl complexes, such as those described above. Computations have shown, without exception, that the central carbon is positively charged with respect to the terminal carbons in all η^3 -allyl complexes;²⁸ kinetic regioselectivity is thus likely frontier orbital controlled. The position undergoing nucleophilic attack must be included in a vacant low energy LUMO to accept electrons from the incoming nucleophile. In the case of most late metal π -allyl complexes, the metal d orbitals overlap with both the π -allyl nonbonding orbital (n) and the antibonding orbital (π^*) of the π -allyl moiety. Of the resultant molecular orbitals, the combination which acts as the LUMO determines the regiochemical outcome of the reaction. Nucleophilic addition to a terminal allyl carbon occurs if the LUMO is a combination between a metal d orbital and the allyl nonbonding orbital, as this combination possesses coefficients only on the terminal carbons. Central carbon alkylation, on the other hand, occurs when the LUMO is a combination between a metal d orbital and the allyl π^* orbital, as the coefficient on the central carbon is larger than those on the terminal carbon atoms.²⁸

Curtis and Eisenstein tentatively predicted that cationic group 4 metallocene complexes, $[\text{Cp}_2\text{M}(\eta^3\text{-allyl})]^+$ might also experience nucleophilic attack at the central carbon to give metallacyclobutanes.²⁸ Inspection of the MO energy level diagram for d^0 group 4 metallocene π -allyl complexes (Figure 1.2) indicates that the LUMO is the bonding combination between the metal $d(3a_1)$ -orbital and allyl π^* -orbital.^{28,30} In corroboration of this theory, the Stryker group reported^{15,31} the addition of sterically imposing nucleophiles to zirconocene π -allyl complex **34**, giving exclusively β -substituted zirconacyclobutanes **35** (Scheme 1.8); smaller nucleophiles, however, attack the metal center, giving alkyl allyl zirconocene **36**. A nucleophile with an intermediate steric profile, benzylpotassium, shows a kinetic partitioning between the metal and

Central carbon positions giving rise to allyl benzyl zirconium complex **37** and zirconacyclobutane complex **38**. Allyl addition is favoured at lower temperatures and, at room temperature, zirconium complex **37** slowly rearranges to zirconacyclobutane complex **38** indicating that the later is the thermodynamically more stable of the two products.

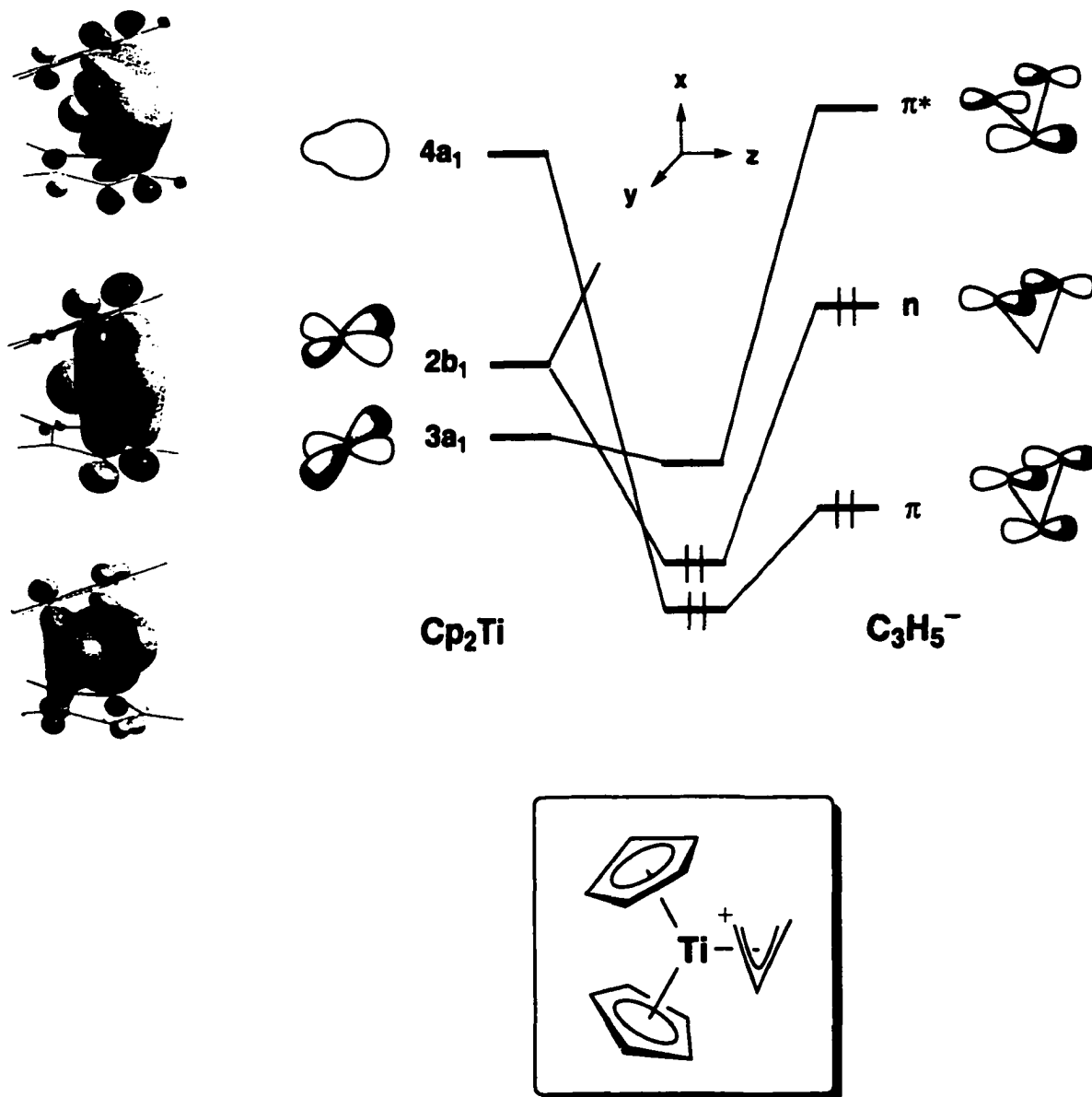
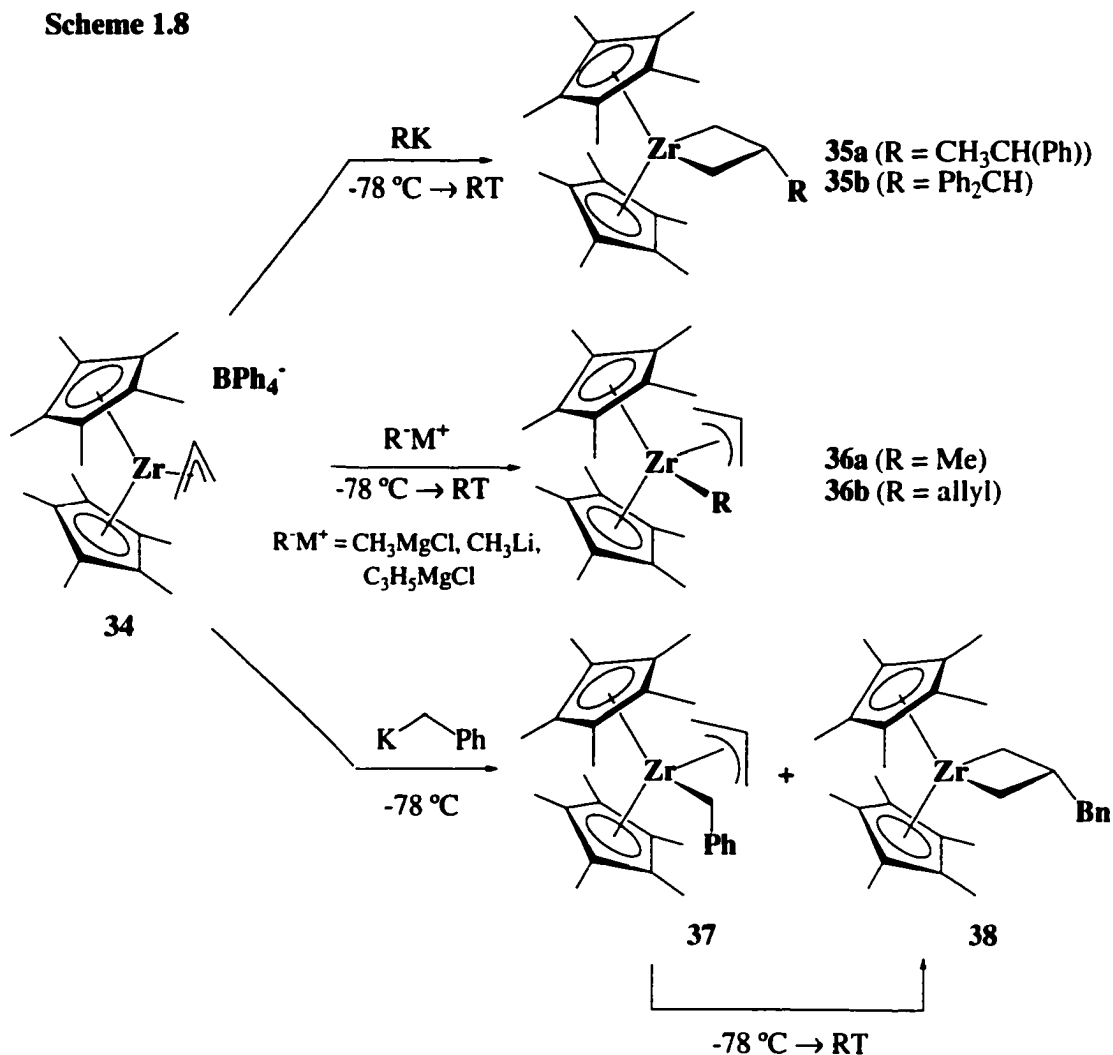


Figure 1.2 EMHO energy level diagram for d^0 group IV metallocene π -allyl complexes.

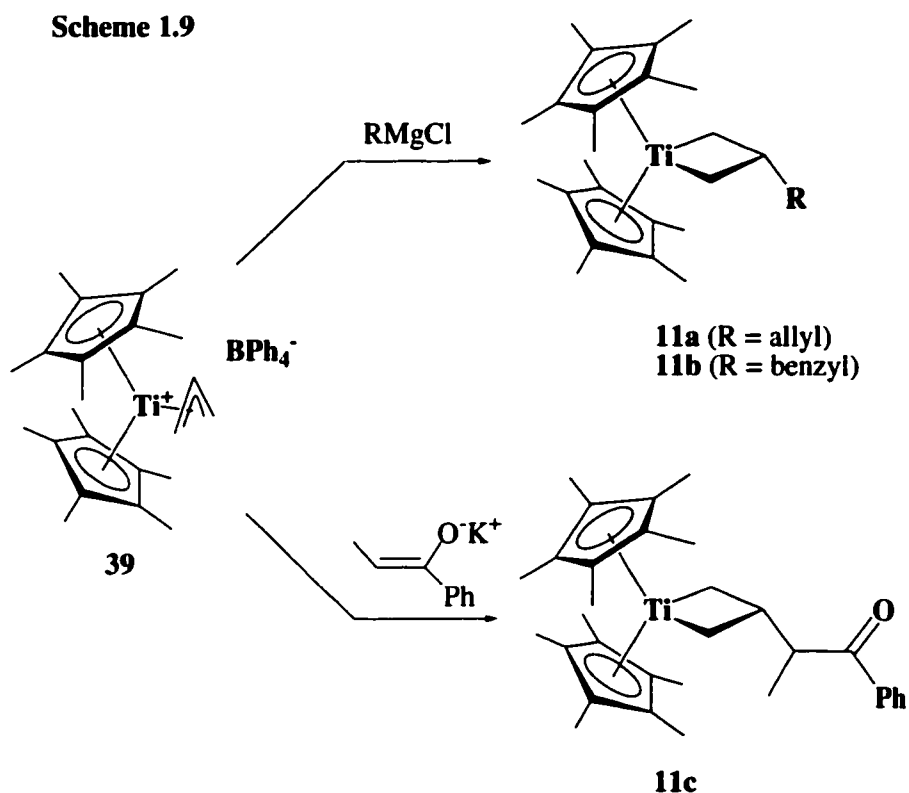
Scheme 1.8



Treating $[\text{Cp}^*_2\text{Ti}(\eta^3\text{-allyl})]^+\text{BF}_4^-$, **39**, with nucleophiles of various steric profiles and nucleophilicities gives central carbon alkylation products exclusively,^{31,32,33} in direct support of the Curtis and Eisenstein postulate (Scheme 1.9). One explanation for the observed reactivity compared to zirconium is that the smaller ionic radius of titanium restricts access to the metal center by the approaching nucleophile.

Attempts to extend the scope of this reactivity were met with some disappointment. Neither small (MeLi , LiAlH_4)³⁴ nor highly hindered ($\text{KCH}(\text{Ph})_2$) nucleophiles add to the allylic central carbon in complex **39** to give the desired

titanacyclobutane. The use of substituted η^3 -allyl complexes also generally failed to give 2,3-disubstituted titanacyclobutane complexes.³³ Nucleophiles added to cationic 1-phenylallyl complex $[\text{Cp}^*_2\text{Ti}(\eta^3\text{-C}_3\text{H}_4\text{Ph})]\text{BPh}_4$ **40**, appear to attack the metal center which then ejects the 1-phenylallyl ligand as a radical fragment (*vide infra*).



2. Radical Additions to η^3 -Allyl Complexes

Extending the FMO prediction^{28,30} to include free radical additions to neutral d^1 titanium (III) allyl complexes requires that the $3a_1$ orbital of the organometallic template 'house' one electron. The electron from the incoming free radical is expected to add to the singly occupied molecular orbital (SOMO) bonding combination between $3a_1$ and the π^* orbital of the allyl ligand (Figure 1.3). As this is the same combination that directs central carbon nucleophilic attack, free radical addition is also expected to be directed to the central carbon of the π -allyl Ti(III) complex.

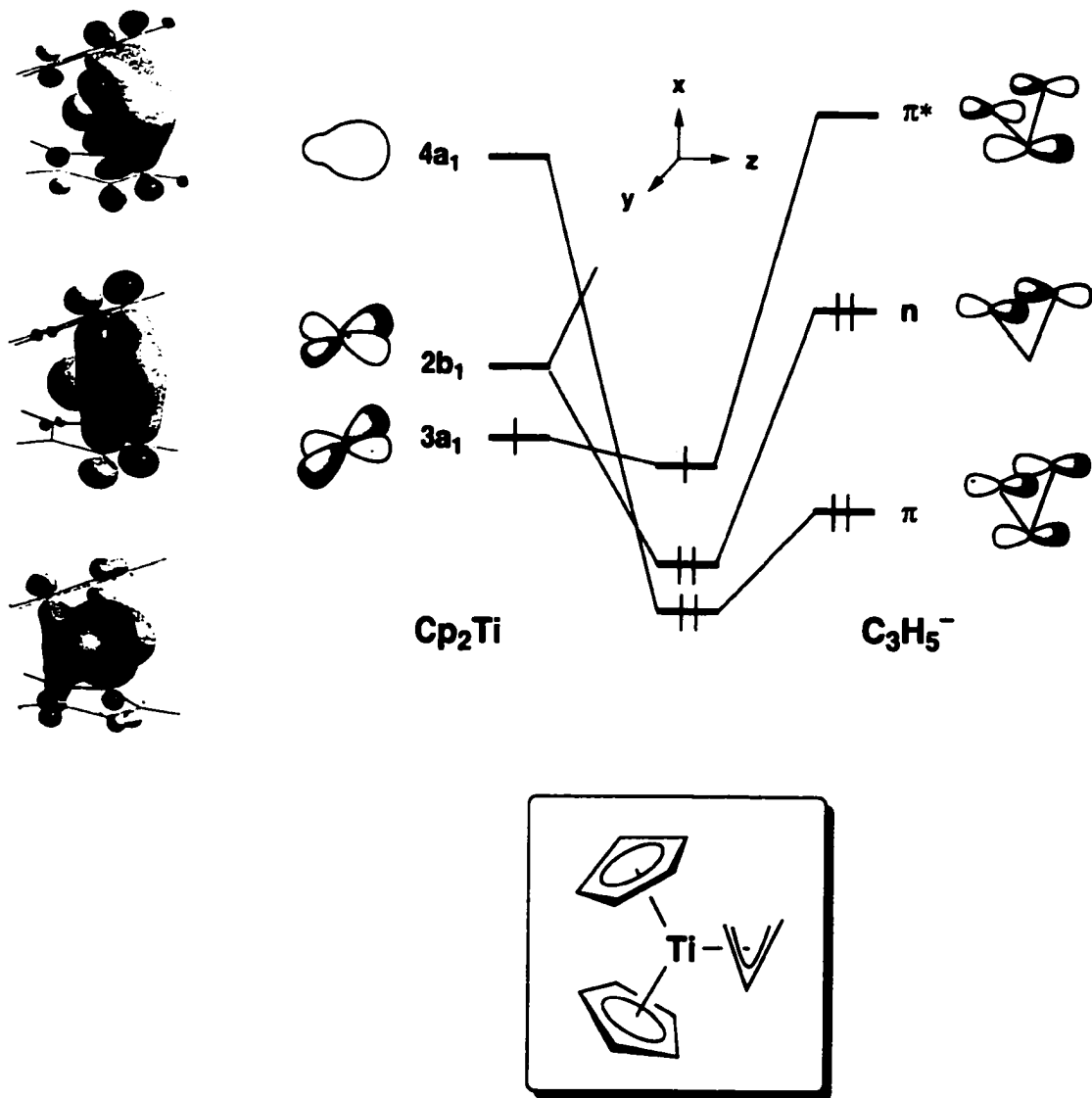


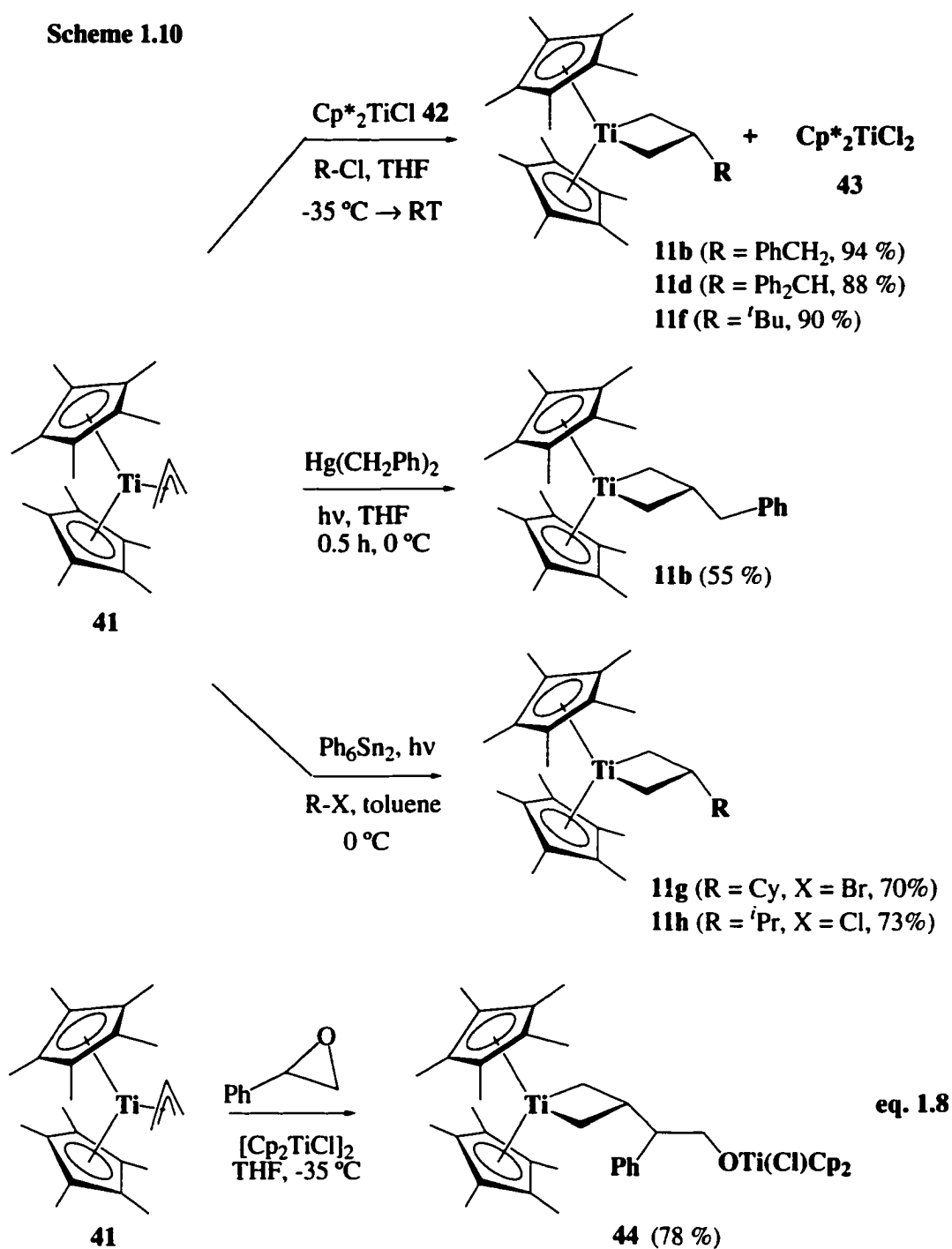
Figure 1.3 EMHO energy level diagram for d^1 group IV metallocene π -allyl complexes.

Recently Casty and Stryker reported the first highly regioselective free radical addition to a Ti(III) η^3 -allyl complex (eq. 1.7) under a variety of radical generating reaction conditions.^{32,35} When $\text{Cp}^*_2\text{Ti}(\eta^3\text{-allyl})$ **41** was treated with an equivalent both of Cp^*_2TiCl **42** and an alkyl halide, the reaction yielded the central carbon alkylation product, β -substituted titanacyclobutanes **11b,d** and **f** and titanocene dichloride **43** (Scheme 1.10). The procedure is limited to activated organic halides; the addition of secondary or primary alkyl halides to a solution of complexes **41** and **42** does not result in titanacyclobutane formation. Titanocene complex **42**, believed to be responsible for reacting with the alkyl halide to generate an alkyl radical, does not easily generate non-activated radicals under ambient conditions. The use of benzyl mercuric salts to generate radicals³⁶ resulted in the isolation of β -benzyltitanacyclobutane **11b**, albeit in lower yield. Photolytic initiation by hexaphenylditin³⁷ in the presence of secondary alkyl halides resulted in the formation of titanacyclobutane complexes **11g** and **11h**, but failed when more activated tertiary and benzylic halides were employed (Scheme 1.10). β -Oxyalkyl radicals, generated by titanium (III)-mediated opening of epoxides,³⁸ also successfully added to allyl complex **41** to give oxygen-containing titanacyclobutane **44** in good yield (eq. 1.8). Taken together, these experiments provide strong evidence for a radical process, however, they lack the generality required for synthetic applications.



Samarium diiodide,³⁹ a halophilic one electron reductant, proved to be the most general and synthetically practical reagent for the preparation of titanacyclobutane complexes. Samarium diiodide successfully mediates the formation of stabilized and unstabilized radicals for central carbon alkylation of allyl complex **41** using alkyl halides

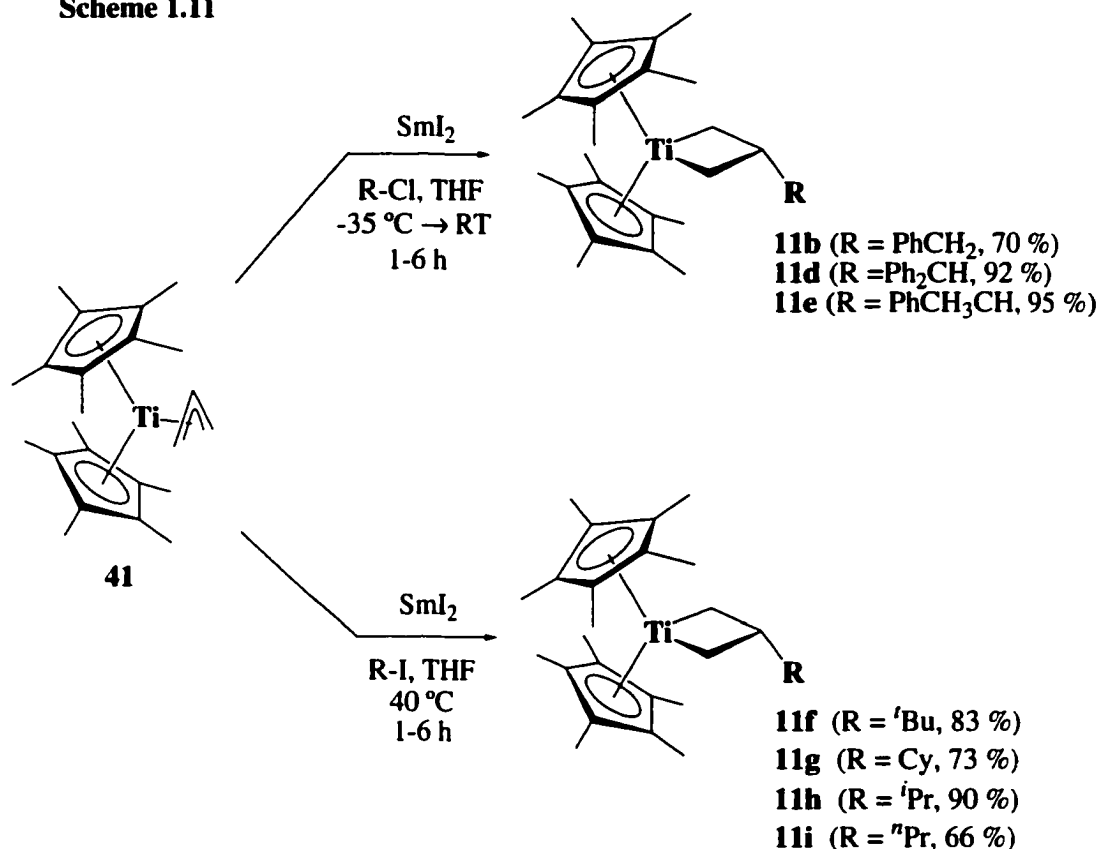
Scheme 1.10



as radical precursors. For the benzylic cases, the use of low temperature and the less reactive chloride is necessary to inhibit both SmI₂-induced radical dimerization and competitive reaction of the organic halide with the titanocene allyl complex (Scheme 1.11). For alkyl halides, the use of the iodide and higher temperatures are needed to

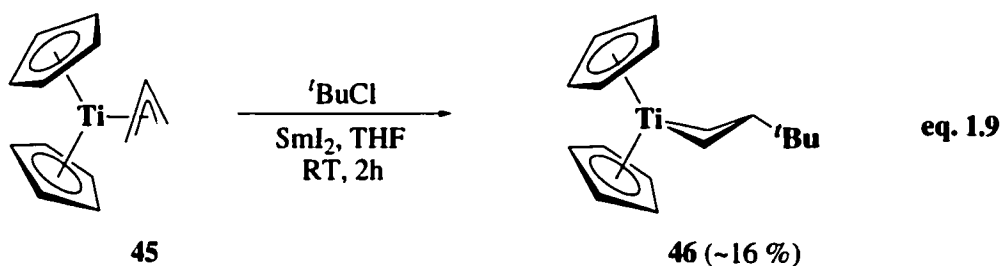
generate titanacyclobutanes **11f-i** in good to excellent yields; however, these reaction conditions also generate allyl titanacyclobutane complex **11a** as a byproduct, which is difficult to separate from the desired titanacyclobutane complex. In all cases, the Sm(III) byproducts can easily be separated from the titanacyclobutane complexes by trituration of the crude reaction mixture with pentane.

Scheme 1.11



Under identical reaction conditions, the less electron rich and sterically more open complex $\text{Cp}_2\text{Ti}(\eta^3\text{-allyl})$ **45** generally fails to undergo central carbon alkylation when treated with an alkyl halide and SmI_2 .^{32,40} The only 'successful' case is the addition of *tert*-butyl radical to give titanacyclobutane complex **46** in low yield (eq. 1.9). We propose that it is the steric bulk of *tert*-butyl chloride which hinders interaction with titanium; interaction with samarium iodide generates the *tert*-butyl radical which then

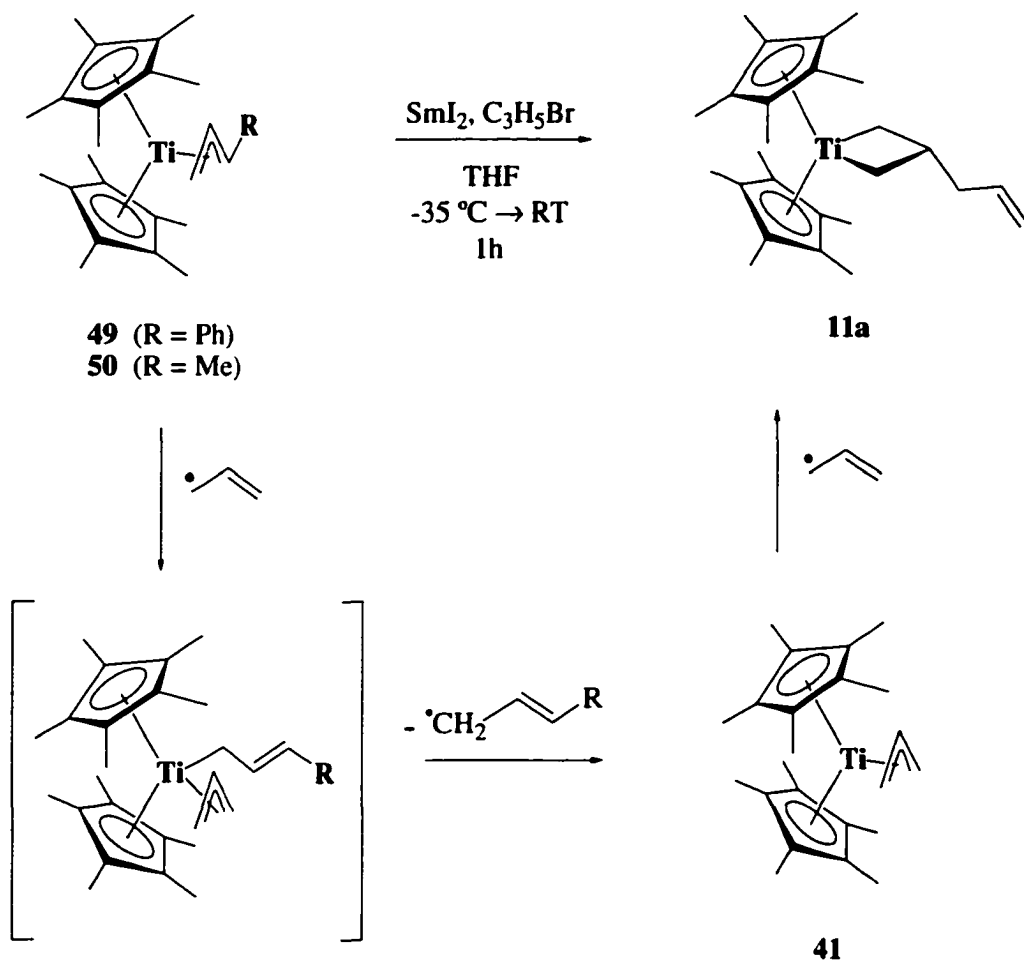
adds to allyl complex **46**. The failure of all other alkyl halides strongly suggests that there is a minimum electron density requirement for central carbon alkylation; high electron density may destabilize the metal-based SOMO in d^1 -systems creating more effective $d \rightarrow \pi^*$ backbonding into the π^* -orbital of the allyl ligand.²⁸ Consequently, the increased preference for η^3 -coordination and delocalization of the odd-electron density onto the central carbon may facilitate alkylation. Increasing the electron density at the metal center by using more electron rich ancillary ligands does activate the system toward central carbon radical alkylation: allyl complexes of both 1,1'-bis(*tert*-butylcyclopentadienyl)titanium(III) **47** and (cyclopentadienyl)(pentamethylcyclopentadienyl)titanium(III) **48** react with a range of organic radicals to produce titanacyclobutane complexes.^{32,41}



None of these titanocene systems tolerates substitution on the allyl ligand; instead, radical addition appears to occur at the metal center rather than at the central carbon of the allyl ligand.^{32,33,41} The permethylated metallocene template, very successful at mediating central carbon radical alkylation of the η^3 -allyl ligand, failed in all attempts to extend this reaction to substituted η^3 -allyls. Treating 1-phenylallyl (cinnamyl) and 1-methylallyl (crotyl) titanocene complexes **49** and **50**, in the presence of SmI_2 , with allyl bromide resulted only in producing a low yield of the β -allyl titanacyclobutane complex **11a** (Scheme 1.12). It is suspected that the allyl radical attacks the metal to afford a neutral Ti(IV) bis(allyl) intermediate, which then ejects the more stable substituted allyl

ligand as a radical. The resultant allyl complex **41** further reacts in a typical manner to give titanacyclobutane **11a**.

Scheme 1.12

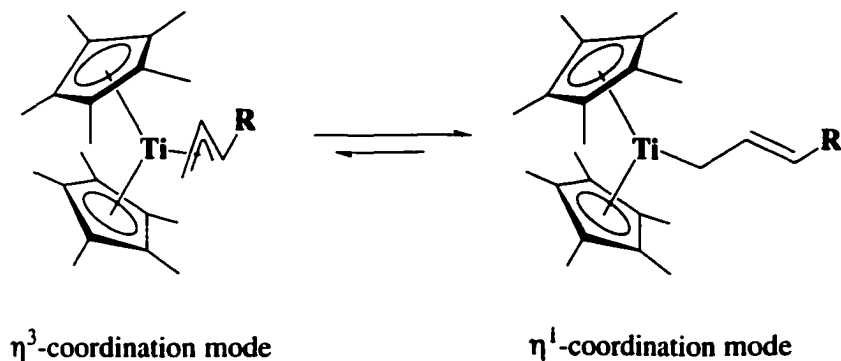


The reason for this change in reactivity is not well understood; little information is available regarding the solution structure and dynamics of d^1 -metallocene allyl complexes.⁴² However, a hapticity change in allyl ligand coordination from η^3 - to η^1 - or to η^1, η^2 -(σ, π)-bonding upon addition of alkyl substituents is frequently observed for d^0 -metallocene complexes of zirconium and titanium.⁴³ Regardless of the thermodynamic coordination mode, the allylic ligands in such d^0 -complexes are kinetically labile,

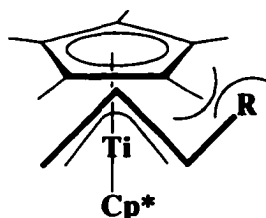
undergoing rapid $\eta^3 \leftrightarrow \eta^1$ equilibration. It is, therefore, reasonable to propose that substituents on the allyl ligand also significantly influence the equilibrium between η^3 - and η^1 -coordination modes in d^1 -metallocenes, particularly in donor solvents such as tetrahydrofuran. A d^1 -metallocene allyl complex, with one electron available for backbonding, should stabilize η^3 -coordination of the allyl group, relative to d^0 -complexes, as the η^1 -coordination mode disrupts the weak one-electron $d(3a_1) \rightarrow \pi^*$ allyl backbond^{28,30,35} thought to be responsible for controlling the regioselectivity of η^3 -allyl radical alkylation (Figure 1.4a). The bias toward η^1 -allyl coordination in substituted permethyltitanocene(III) allyl complexes then arises from the confluence of unfavourable steric interactions between the allyl and ancillary ligands and the inherently weaker metal-carbon bonding anticipated at the substituted position (Figure 1.4b). However, even the less sterically demanding (cyclopentadienyl)-(pentamethylcyclopentadienyl)titanium **47**,⁴¹ 1,1'-bis(*tert*-butylcyclopentadienyl)titanium **48**³² and 1,1'-bis(trimethylsilylcyclopentadienyl)titanium **51**³³ systems fail to undergo central carbon radical alkylation at substituted allyl ligands.

Given this analysis, research in this group was directed toward the use of strongly electron-donating templates to enhance the $d(3a_1) \rightarrow \pi^*$ one-electron backbond, as well as the use of templates that provide a more sterically relaxed environment to promote regioselective central carbon alkylation at substituted allyl ligands. This hypothesis proved to be correct: regioselective central carbon alkylation of substituted allyl complexes was recently reported by using the bis(2-piperidinoindenyl)titanium(III) template **52**, providing a stereoselective synthesis of 2,3-disubstituted titanacyclobutane complexes.⁴⁴ Cinnamyl and crotyl complexes **53** and **54** were obtained on upon treatment of chloride complex **52** with cinnamyllithium and crotylmagnesium chloride respectively

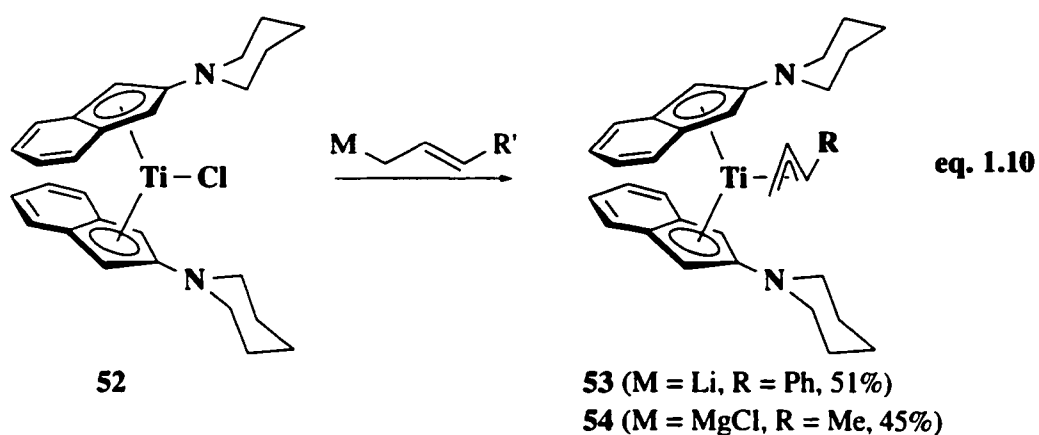
Figure 1.4 (a) $\eta^3 \leftrightarrow \eta^1$ Equilibrium for Substituted Allyl Titanocene Complexes



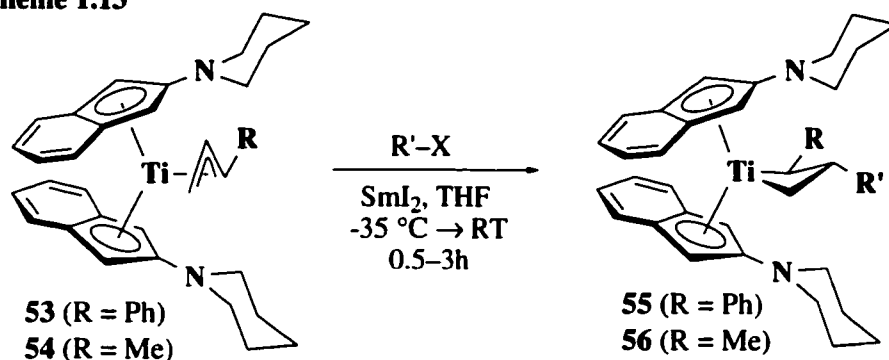
(b) Unfavourable Steric Interactions Between Substituted Allyl and Ancillary Ligand



(eq. 1.10). Addition of 2-iodopropane, iodocyclohexane or *tert*-butyl chloride to a solution of cinnamyl complex **53** and SmI_2 in THF leads to the formation of 3-alkyl-2-phenyltitanacyclobutane complexes **55a-c** in high yield (Scheme 1.13). Similar results are obtained upon treatment of crotyl complex **54** with unstabilized radicals, albeit in somewhat lower yields (Scheme 1.13). Titanacyclobutane complexes **56a-c**, however, are thermally sensitive, degrading via β -hydride elimination from the α -methyl substituent. Unfavourable steric interactions generated by the relatively large piperidino substituent on the indenyl rings were suggested to be at least partly responsible for the relative facility of this β -hydride elimination. Disappointingly, the use of the piperidinoindenyl template appears to be limited to alkylations using unstabilized alkyl radicals.³³



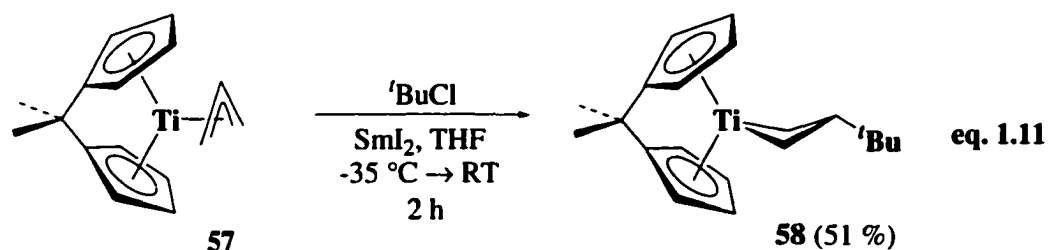
Scheme 1.13



Starting complex	R'X	Product	Yield
53	ⁱ PrI	55a	72%
53	CyI	55b	80%
53	^t BuCl	55c	88%
54	ⁱ PrI	56a	69%
54	CyI	56b	70%
54	^t BuCl	56c	36%

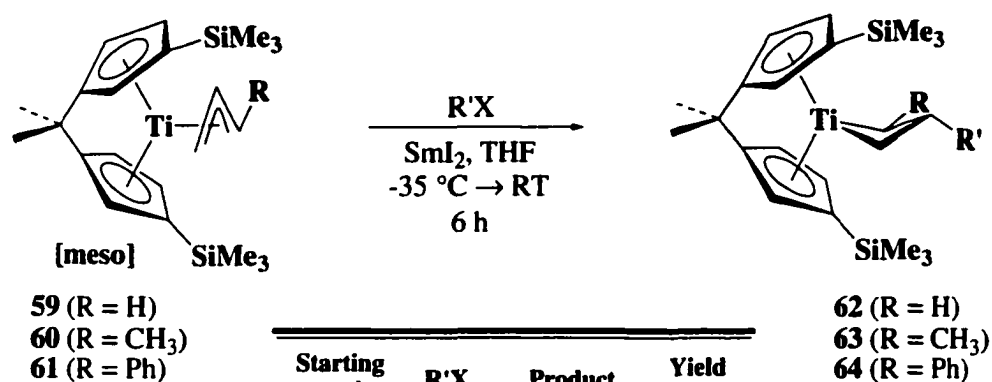
The use of sterically open *ansa*-bridged titanocene templates⁴⁵ for radical alkylation illustrates the influence of the electronic nature of the ancillary ligands, providing some unique reactivity.³³ The only successful free radical alkylation of unsubstituted *ansa*-

bridged allyltitanocene complex **57** resulted from of addition of *tert*-butyl radical, giving the 3-*tert*-butyl titanacyclobutane complex **58** (eq. 1.11). This limited reactivity is similar to that observed for bis(cyclopentadienyl)titanium allyl complex **45**.³²



Appending electron releasing groups to the cyclopentadienyl rings was investigated to provide greater delocalization of the odd-electron density of the metal onto the allyl moiety and promote central carbon radical alkylation. Consequently, the *meso ansa*-[1]-bis(3,3'-trimethylsilylcyclopentadienyl)titanium π -allyl complexes **59-61** were prepared and subjected to radical alkylation (Scheme 1.14). Alkylation of allyl complex **59** affords the 3-*iso*-propyl- and 3-*tert*-butyl titanacyclobutane complexes **62a** and **62b**. The crotyl complex **60** also undergoes successful central carbon alkylation, furnishing 2,3-disubstituted titanacyclobutanes **63a-c** in very high yields. Crotyl-derived titanacyclobutanes **63a-c**, however, are not stable in solution at room temperature, decomposing *via* β -hydride elimination as observed for crotyl-derived bis(piperidinoindenyl)titanacyclobutane RT complexes **56a-c**. Thermally stable 3-alkyl-2-phenyltitanacyclobutane complexes **64a-c** are obtained in high yield upon treatment of cinnamyl complex **61** with 2-iodopropane, iodocyclohexane and *tert*-butyl chloride, respectively, and SmI_2 in THF. The improved efficiency of these reactions illustrates the benefit of electron-rich ancillary ligands to ensure successful titanacyclobutane formation.

Scheme 1.14

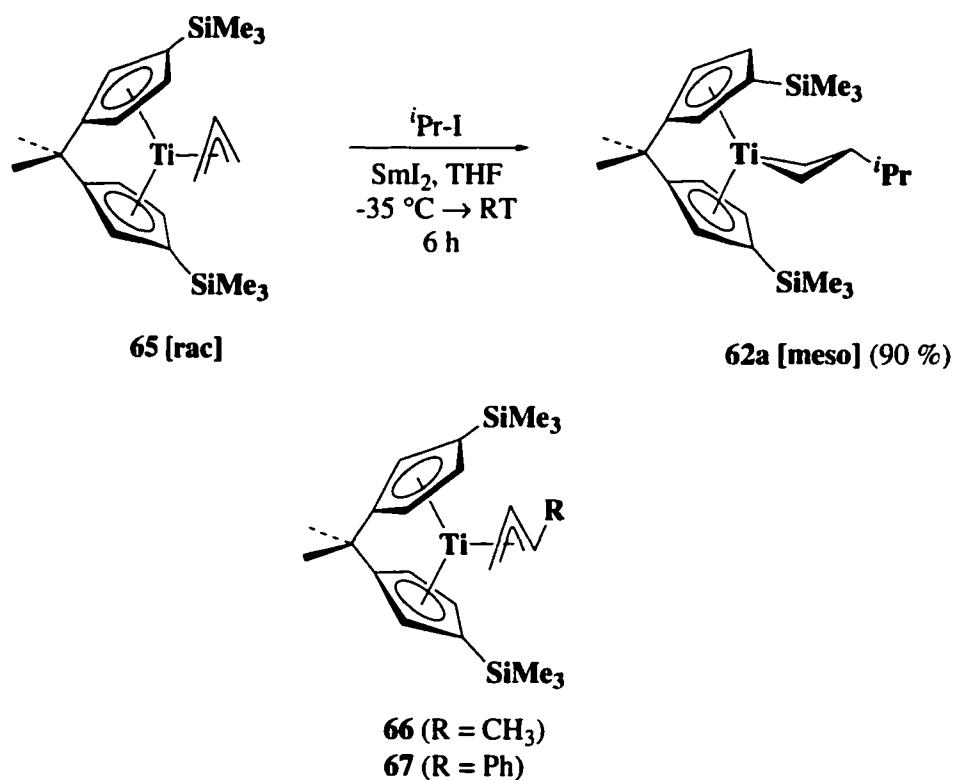


Starting complex	R'X	Product	Yield (%)
59	ⁱ PrI	62a	80
59	^t BuCl	62b	40
60	ⁱ PrI	63a	95
60	CyI	63b	97
60	^t BuCl	63c	81
61	ⁱ PrI	64a	73
61	CyI	64b	87
61	^t BuCl	64c	95

The isomeric *rac ansa*-bridged diastereomers of complexes **59-61** were investigated to determine whether the spatial orientation of the substituents on the Cp-rings influences radical reactivity. The diastereomer of complex **59**, *rac ansa* [1] bis(3,3'-trimethylsilylcyclopentadienyl)titanium π -allyl complex **65**, showed unprecedented reactivity toward isopropyl radical (Scheme 1.15). Complex **65** undergoes central carbon alkylation with concomitant isomerization to give the *meso*-titanacycle **62a** in high yield.⁴⁶ This reaction seems specific to isopropyl radical: all attempts to generate titanacycles by alkylation with other radicals fail. Radical alkylation of the substituted *rac* complexes **66** and **67** give primarily decomposition products, regardless of the alkyl radical used. ¹H NMR spectroscopic studies of the product mixtures from the alkylation of complex **67** shows trace amounts of titanacyclobutane formation, but optimization of reaction conditions proved unsuccessful.

A significant limitation of the ansa-bridged systems is that central carbon alkylation could not be achieved for stabilized radicals such as allyl and benzyl. All attempts to increase the scope of this reaction to include stabilized radicals gave primarily the titanocene dihalide and organic products resulting from dimerization of the free radical. The use of the alternative radical-generating protocol involving Ti(III)-mediated epoxide-opening³⁸ also failed to give titanacyclobutane complexes.

Scheme 1.15



C. Spectroscopic Characterization of Titanacyclobutane Complexes

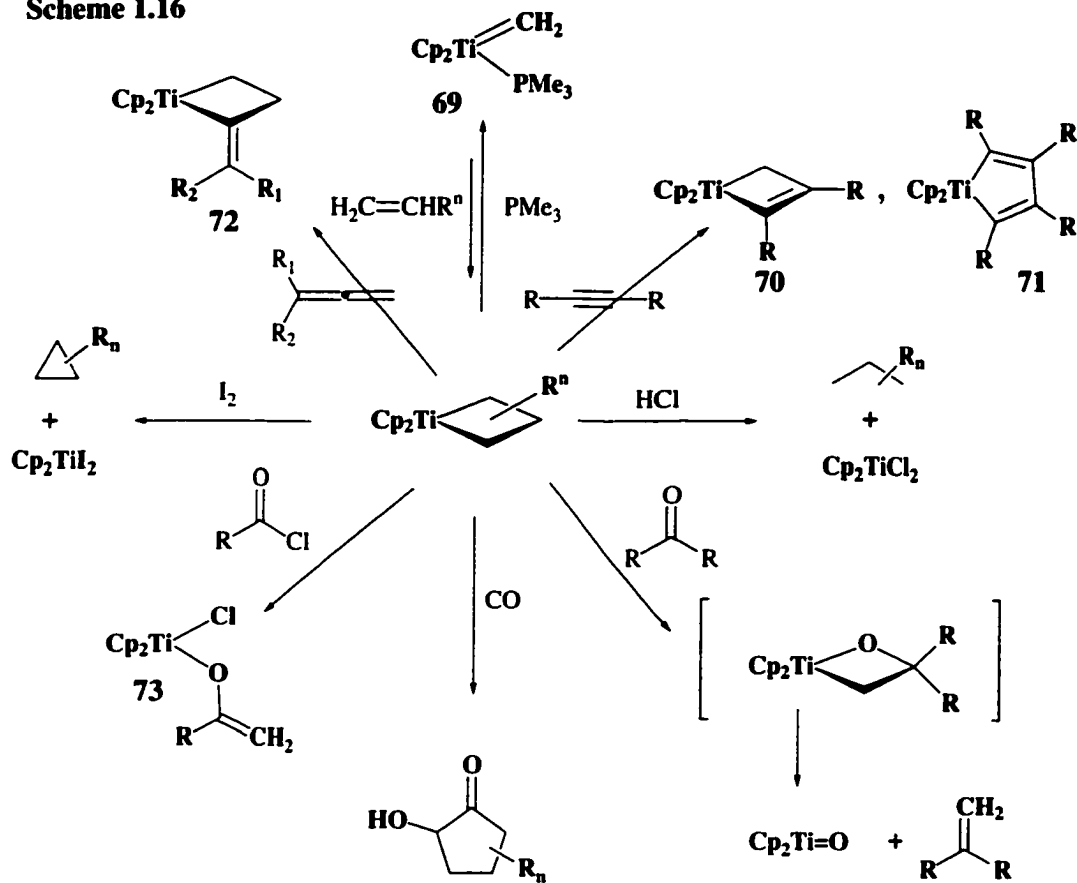
Several spectroscopic features of group 4 metallacyclobutane complexes are structurally diagnostic. The ^1H NMR spectra of β -substituted titanacyclobutanes display modestly shielded α -protons resonances (between 1.0 to 2.0 ppm), typically separated by no more than 0.4 ppm for the inequivalent *cis* and *trans* protons, and a highly shielded β -proton resonance (upfield of 0.5 ppm).^{15,17,33,47} This effect has been attributed to the

proximity of the β -carbon to the Cp_2Ti fragment and the inherent diamagnetic anisotropy of cyclopentadienyl rings in a magnetic field.^{17,18} In ^{13}C NMR spectra, the more deshielded α -carbons resonate between 60 and 70 ppm, whereas the relatively shielded β -carbon resonates between 20 and 30 ppm.^{15,17,19,32,33,47} The ^1H NMR spectra of α,β -disubstituted titanacyclobutanes differ somewhat; the α -proton resonance attached to the substituted α -carbon is often more deshielded (> 2.0 ppm). The inequivalent α -methylene protons have been observed to resonate at significantly different chemical shifts; the *cis* proton (relative to the α -methine proton) appears downfield (> 2.0 ppm) and the *trans* proton is often observed to be more shielded than the β -methine proton (< 1.0 ppm) as determined by 2-dimensional NMR techniques.^{19,33,47}

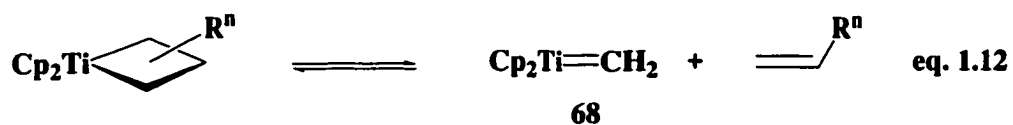
D. Functionalization of Titanacyclobutane Complexes

Titanacyclobutane complexes are known to undergo many interesting transformations to produce important organic and organometallic compounds (Scheme 1.16).⁴⁸ Bis(cyclopentadienyl)titanacyclobutane complexes are thermally sensitive, undergoing facile [2+2] cycloreversion to release an olefin (eq. 1.12). The organometallic product, the highly reactive titanium methyldene complex **68**, can be trapped by coordination of trimethylphosphine to yield complex **69**.⁴⁹ Methyldene complex **68** can also be trapped with alkynes; the addition of one equivalent results in formation of metallacyclobutenes **70** and the addition of two equivalents, following reductive cyclization, gives metallacyclopentadienes **71**.⁵⁰ Trapping complex **68** with allenes gives methylene-substituted titanacyclobutanes **72**.⁵¹ The organic fragment can also be cleaved from the titanacycle; oxidizing agents induce reductive elimination to give cyclopropanes, while electrophiles such as acids or acid chlorides simply cleave titanium-carbon bonds (e.g., **73**).⁵² Methylenation of carbonyl groups in esters, lactones, imides and acid anhydrides proceeds smoothly from the methyldene intermediate.⁵³ Grubbs has reported that titanacyclobutane complexes give α -hydroxycyclopentanones in modest yield when

Scheme 1.16



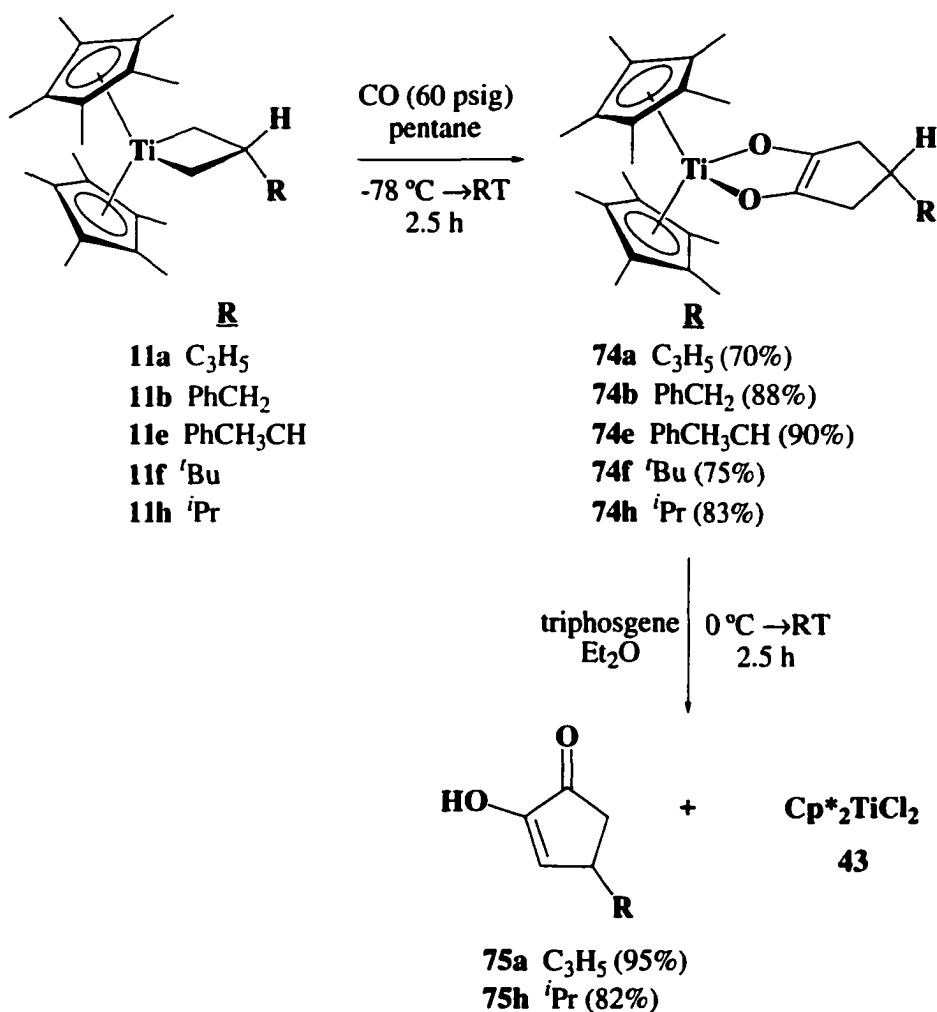
treated with two equivalents of carbon monoxide to give an intermediate enediolate complex, followed by protonolysis.⁵⁴ The mechanism for this reaction is believed to be two successive insertions of CO followed by rearrangement to give the isolable enediolate complex.⁵⁵



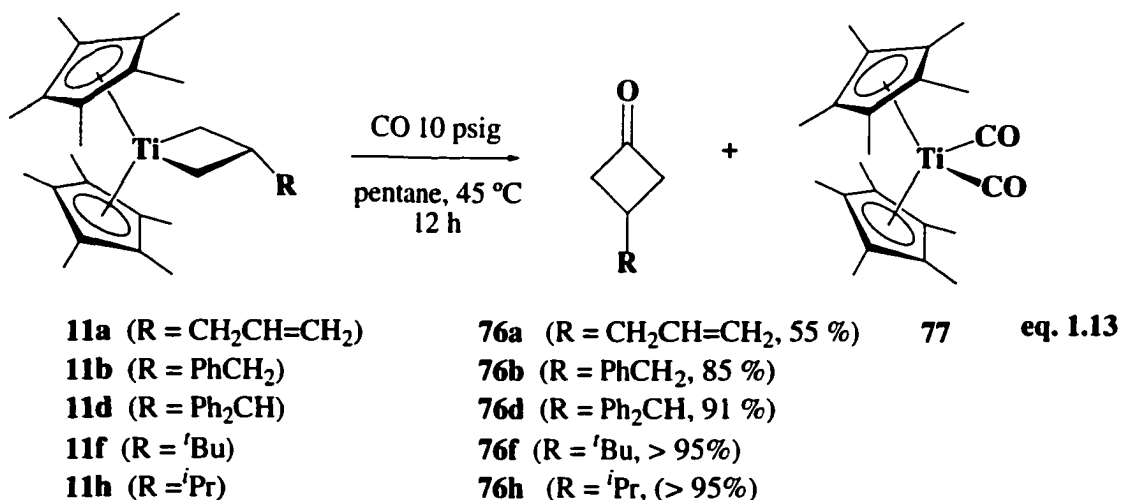
Recently, methodology has been developed in this group to convert titanacyclobutane complexes into four- and five-membered carbocyclic ring compounds via ring-expansion using polar unsaturated small molecules.^{32,33,56} Under conditions of high CO pressure and low temperature various β -alkyl substituted

bis(pentamethylcyclopentadienyl)titanacyclobutanes expectedly insert 2 equivalents of CO to yield isolable endiolate complexes **74** in excellent isolated yields (Scheme 1.17). The highest yielding demetallation of the 5-membered carbocycle involves treatment of the endiolate complexes **74a** and **74h** with one equivalent of triphosgene to yield, surprisingly, 2-hydroxy-2-cyclopentanones **75a** and **75h**, respectively. Demetallation of acyclic bis(cyclopentadienyl)titanium(pentenediolates) under these conditions had previously been reported to yield cyclic carbonates.⁵⁷

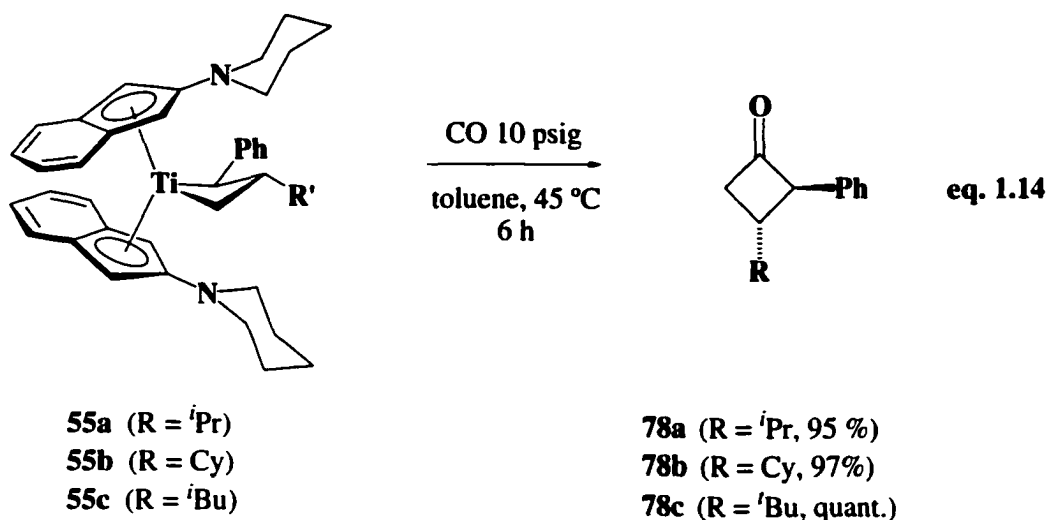
Scheme 1.17



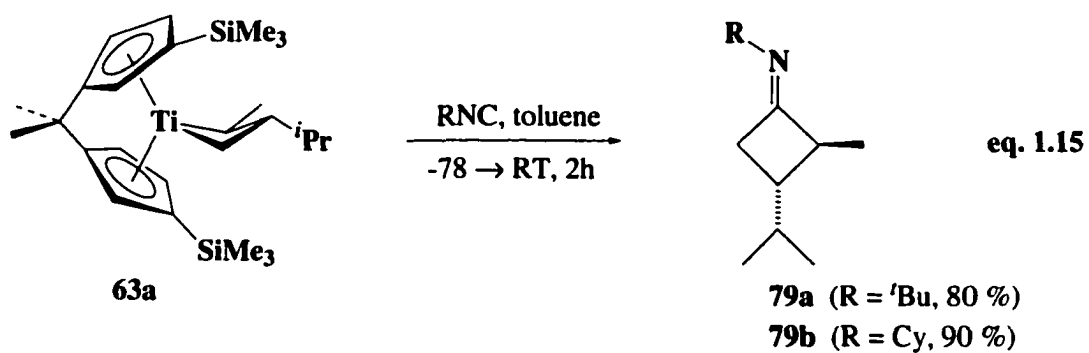
Controlled *single* insertion of carbon monoxide or isonitrile into titanium-carbon bonds, unprecedented in titanacyclobutane chemistry, yields cyclobutanones and cyclobutanamines, respectively, following spontaneous reductive elimination of the presumed acyltitanium intermediates. Thus, treatment of various 3-alkyltitanacyclobutane complexes **11**, pre-heated to 45 °C, with 10 psig of CO provides the corresponding 3-alkylcyclobutanones **76**, generally in high yield (eq. 1.13).³³ The organometallic product of the reaction is Cp*₂Ti(CO)₂,⁵⁸ **77**, recovered in high yield by precipitation from the reaction medium. Similarly, more highly substituted cyclobutanones **78a-c** can be obtained by carbonylation of bis(2-piperidinoindenyl)titanacyclobutane complexes **55a-c** (eq. 1.14). Unfortunately under the reaction conditions for single insertion no tractable organometallic product was isolated from the piperidinoindenyl system.³³



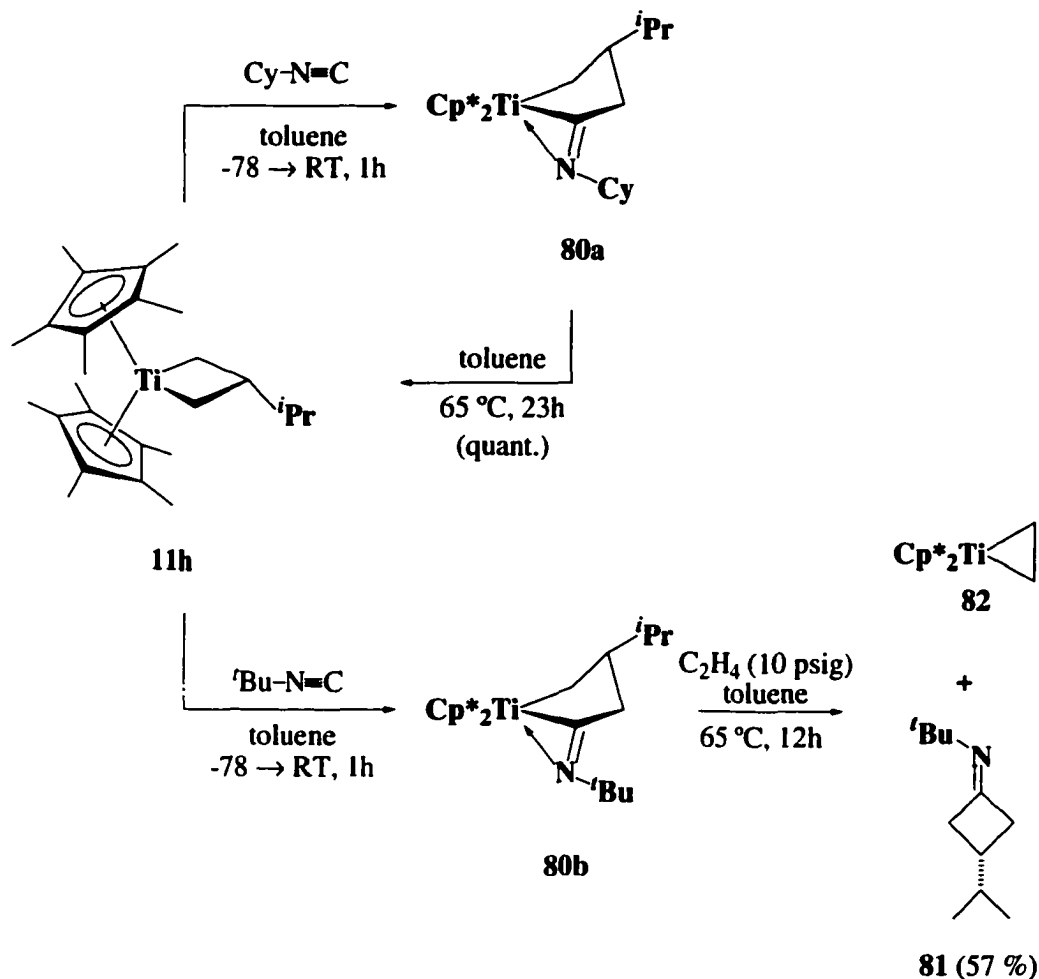
Isonitrile insertion also provides four-membered ring products: one equivalent of cyclohexyl or *tert*-butyl isonitrile at low temperature inserts cleanly into crotyl-derived titanacyclobutane complex **63a**, which then undergoes reductive elimination to afford cyclobutanamines **79a** and **79b**.³³ No tractable organometallic fragment is recovered, even in the presence of a trapping agent (eq. 1.15). In contrast,



permethyltitanacyclobutane complex **11h**, when treated with *tert*-butyl or cyclohexyl isonitrile, yields the isolable iminoacyl complexes **80a** and **80b** in high yield. Although, thermolysis of **80b** in the presence of ethylene gives the expected cyclobutanimine **81** and ethylene adduct **82**, under similar reaction conditions, **80a** surprisingly deinserts isonitrile to reform titanacyclobutane **11h** (Scheme 1.18).³³



Scheme 1.18



E. Project Goals

The potential for application of central carbon alkylation as a synthetically useful carbon-carbon bond formation strategy prompted efforts into extending the formation of titanacyclobutane complexes from substituted allyl complexes. Determination of the electron density and steric requirements at the metal center necessary to efficiently obtain central carbon alkylation of substituted allyl complexes was the primary focus of this study.

The regioselective central carbon alkylation of substituted allyl complexes recently obtained from the bis(2-piperidinoindenyl)titanium(III) template **52**, providing a stereoselective synthesis of 2,3-disubstituted titanacyclobutane complexes,⁴⁴ supports the postulate that central carbon radical alkylation should be particularly facile in d^1 -systems with significant $d \rightarrow \pi^*$ backbonding.²⁸ The use of the piperidinoindenyl template is, however, not suitable for practical application due to the limited stability of crotyl-derived titanacyclobutanes and the apparent unreactivity of stabilized radicals for central carbon alkylation. We thought that the use of strongly electron-donating, sterically unencumbered, alkoxy- or dialkylamino-substituted titanocene templates would provide an environment to facilitate regioselective central carbon alkylation at substituted allyl ligands as well as inhibit β -hydride elimination from α -methyl substituents on the resultant titanacyclobutane complexes. For these reasons, an investigation into sterically undemanding electron-rich templates was initiated.

The recently reported crystal structure of bis(piperidinoindenyl)titanium(III) cinnamyl complex, **53**, revealed some interesting features.⁴⁴ Notable are the *syn*-orientation of the ancillary ligands, the long $C_{\text{Ind}}\text{-N}$ bond lengths, and the varied hybridization of the nitrogen atoms on the ancillary ligands, all diagnostic of poor donation of the lone pair on the nitrogen atom into the indenyl ring. In fact, of the structurally characterized amino substituted group(IV) metallocenes, only the *ansa*-bridged bis(dialkylaminoindenyl)zirconium(IV) systems exhibit nitrogen pyramidalizations and $C_{\text{Ind}}\text{-N}$ bond lengths that approach the values present in complex **53**, although these features were attributed to specific steric interactions with the ligand bridges.⁵⁹ Following the development of a template of synthetic utility, a structural study was envisioned to provide insight into the minimum electron density requirement for the central carbon alkylation reaction. As well, a better understanding of the steric and

electronic environment favouring η^3 -coordination of the substituted allyl ligand was sought.

Continued investigation of the conversion of titanacyclobutane complexes into cyclic organic compounds was another goal in this study. The primary focus was ring expansions using carbon monoxide and isonitriles to convert the titanacyclobutane complexes into cyclobutanones and cyclobutanimes, respectively, as this reactivity is very rare for early transition metal metallacyclobutane complexes.⁶⁰

F. References

1. (a) Collman, J. P.; Hegedus, L. S.; Norton, J.; Finke, R. G. *Principles and Applications of Organotransition Metal Chemistry*; University Science Books: Mill Valley, CA, 1987. (b) Davies, S. G. *Organotransition Metal Chemistry: Applications to Organic Synthesis*; Pergamon: Oxford, England, 1982. (c) Harrington, R. J. *Transition Metals in Total Synthesis*; John Wiley & Sons: New York, NY, 1990. (e) Crabtree, R. H. *The Organometallic Chemistry of the Transition Metals*; John Wiley & Sons: New York, NY, 1994.
2. Iqbal, J.; Bhatia, B.; Nayyar, N. K. *Chem. Rev.* **1994**, *94*, 519.
3. Curran, D. P.; Porter, N. A.; Giese, B. *Stereochemistry of Radical Reactions*; VCH Publishers, Inc.: New York, NY, 1996.
4. Herberich, G. E.; Schwartzer, J. *Angew. Chem. Int. Ed. Engl.* **1970**, *9*, 897.
5. (a) Herberich, G. E.; Bauer, E. Schwartzer, J. *J. Organomet. Chem.* **1969**, *17*, 445. (b) Madonik, A. M.; Astruc, D. *J. Am. Chem. Soc.* **1984**, *106*, 2437. (c) Koelle, U.; Khouzami, F. *Angew. Chem. Int. Ed. Engl.* **1980**, *19*, 641. (d) Herberich, G. E.; Carstensen, T.; Klein, W.; Schmidt, M. U. *Organometallics*, **1993**, *12*, 1439. (e) Green, M. L. H.; Pratt, L.; Wilkinson, G. *J. Chem. Soc.* **1959**, 3753.
6. Blaha, J. P.; Wrighton, M. S. *J. Am. Chem. Soc.* **1985**, *107*, 2694.

7. Reviews: (a) Torraca, K. E.; McElwee-White, L. *Coord. Chem. Rev.* **2000**, in press. (b) Astruc, D. *Electron-Transfer and Radical Processes in Transition Metal Chemistry*; VCH Publishers, Inc.: New York, NY, 1995. (c) Trogler, W. C., ed.; *Organometallic Radical Processes*, Journal of Organometallic Chemistry Library, Vol. 22, Elsevier: Amsterdam, 1990. (d) Astruc, D. *Chem. Rev.* **1988**, *88*, 1189. (e) Drago, R. S. *Coord. Chem. Rev.* **1980**, *32*, 97.
8. (a) Merlic, C. A.; Xu, D. *J. Am. Chem. Soc.* **1991**, *113*, 9855. (b) Merlic, C. A.; Xu, d.; Nguyen, M. C.; Truong, V. *Tetrahedron Lett.* **1993**, *34*, 227.
9. (a) McElwee-White, L. *Synlett.* **1996**, 806. (b) Schoch, T. K.; Orth, S. D.; Zerner, M. C.; Jorgensen, K. A.; McElwee-White, L. *J. Am. Chem. Soc.* **1995**, *117*, 6475. (c) Main, A. D.; McElwee-White, L. *J. Am. Chem. Soc.* **1997**, *119*, 4551. (d) Torraca, K. E.; Storhoff, D. A.; McElwee-White, L. *J. Organomet. Chem.* **1998**, *554*, 13. (e) Mortimer, M. D.; Carter, J. D.; McElwee-White, L. *Organometallics* **1993**, *12*, 4493. (f) Torraca, K. E.; Abboud, K. A.; McElwee-White, L. *Organometallics* **1998**, *17*, 4413.
10. (a) Mahais, V. Cron, S.; Toupet, L.; Lapinte, C. *Organometallics* **1996**, *15*, 5399. (b) Paul, F.; Lapinte, C. *Coord. Chem. Rev.* **1998**, *180*, 431. (c) Cron, S.; Morvan, V.; Lapinte, C. *J. Chem. Soc., Chem. Commun.* **1993**, 1611.
11. Melikyan, G. G.; Vostrowsky, O.; Bauer, W.; Bestmann, H. J.; Khan, M.; Nicholas, K. M. *J. Org. Chem.* **1994**, *59*, 222.
12. (a) Gupta, B. D.; Funabiki, T.; Johnson, M. D. *J. Am. Chem. Soc.* **1976**, *98*, 6697. (b) Fabian, B. D.; Labinger, J. A. *J. Am. Chem. Soc.* **1979**, *101*, 2239. (c) Fabian, B. D.; Labinger, J. A. *Organometallics* **1983**, *2*, 659. (d) Rosenblum, M.; Waterman, P. S. *J. Organomet. Chem.* **1980**, *187*, 267. (e) Waterman, P. S. Giering, W. P. *J. Organomet. Chem.* **1978**, *155*, C47.
13. (a) Astruc, D. *Acc. Chem. Rev.* **1997**, 383. (b) Tolbert, L. M. *Acc. Chem. Rev.* **1992**, 561. (c) Le Narvor, N.; Lapinte, C. *J. Chem. Soc., Chem. Commun.* **1993**, 357. (d) Le

- Narvor, N.; Toupet, L.; Lapinte, C. *J. Am. Chem. Soc.* **1995**, *117*, 7129. (e) Beddoes, R. L.; Bitcon, C.; Grime, R. W.; Ricalton, A.; Whiteley, M. W. *J. Chem. Soc., Dalton Trans.* **1995**, 2873. (f) Densiovich, L. I.; Filatova, T. V.; Peterleitner, M. G.; Ustynyuk, A.; Vinogradova, V. N.; Leont'eva, L. I. *Russ. Chem. Bull.* **1998**, *47*, 1901. (g) Iyer, R. S.; Selegue, J. P. *J. Am. Chem. Soc.* **1987**, *109*, 910. (h) Bruce, M. I. *Chem. Rev.* **1991**, *91*, 197. (i) Rabier, A.; Lugan, N.; Mathieu, R.; Geoffroy, G. L. *Organometallics* **1994**, *13*, 4676. (j) Woodworth, B. E.; White, P. S.; Templeton, J. L. *J. Am. Chem. Soc.* **1997**, *119*, 828. (k) Beevor, R. G.; Freeman, M. J.; Green, M.; Morton, C. E.; Orpen, A. G. *J. Chem. Soc., Chem. Commun.* **1985**, 68.
14. Tjaden, E. B.; Stryker, J. M. *J. Am. Chem. Soc.* **1993**, *115*, 2083.
15. Tjaden, E. B. Ph. D. Thesis, Indiana University, 1993.
16. Luinstra, G. A.; Teuben, J. H. *Organometallics* **1992**, *11*, 1793.
17. (a) Howard, T. R.; Lee, J. B.; Grubbs, R. H. *J. Am. Chem. Soc.* **1980**, *102*, 6876. (b) Lee, J. B.; Ott, K. C. Grubbs, R. H. *J. Am. Chem. Soc.* **1982**, *104*, 7491. (c) Ikariya, T.; Ho, S. C. H.; Grubbs, R. H. *Organometallics* **1985**, *4*, 199.
18. (a) Seetz, J. W. F. L.; Schat, G.; Akkerman, O. S.; Bickelhaupt, F. *Angew. Chem. Int. Ed. Engl.* **1983**, *22*, 248. (b) Seetz, J. W. F. L.; Van de Heisteeg, B. J.; Schat, G.; Akkerman, O. S.; Bickelhaupt, F. *J. Mol. Catal.* **1985**, *28*, 71.
19. Polse, J. L.; Kaplan, A. W.; Anderson, R. A.; Bergman, R. G. *J. Am. Chem. Soc.* **1998**, *120*, 6316. (b) Polse, J. L.; Anderson, R. A.; Bergman, R. G. *J. Am. Chem. Soc.* **1996**, *118*, 8737.
20. (a) Feldman, J.; Schrock, R. R. *Prog. Inorg. Chem.* **1991**, *39*, 1. (b) Grubbs, R. H.; Tumas, W. *Science* **1989**, *243*, 907. (c) Lindner, E. *Adv. Heterocyclic Chem.* **1986**, *39*, 237. (d) Dragutan, V.; Balaban, A.T.; Dimonie, M. *Olefin Metathesis and Ring Opening Polymerization of Cycloolefins*; Wiley: New York, 1986. (e) Krauss, H.L.; Hagen, K.; Hums, K. *J. Mol. Catal.* **1985**, *28*, 233. (f) Ivin, K. J. *Olefin Metathesis*; Academic: London, 1983. (g) Chappell, S. D.; Dole-Hamilton, D. J. *Polyhedron*

- 1982, 1, 739. (h) Grubbs, R. H.; In *Comprehensive Organometallic Chemistry*; Wilkinson, G.; Stone, F. G. A., Abel, E. W.; Eds.; Pergamon: Oxford, U. K., 1982, Vol. I, Ch 54. (i) Puddephatt, R. J. *Coord. Chem. Rev.* **1980**, *33*, 149. (j) Grubbs, R. H. *Prog. Inorg. Chem.* **1978**, *24*, 1. (k) Katz, T. J. *Adv. Organomet. Chem.* **1977**, *16*, 283. (l) Graziani, M.; Lenarda, M.; Ros, R.; Belluco, U. *Coord. Chem. Rev.* **1975**, *16*, 35. (m) Hérisson, J. –L.; Chauvin, Y. *Macromol. Chem.* **1970**, *141*, 161.
21. Tsuji, J. In *The Chemistry of the Carbon-Carbon Bond, Vol 3. Carbon-Carbon Bond Formation Using Organometallic Compounds*, Hartley, F. R.; Patai, S., Eds.; Wiley: New York, 1985; Ch 3, Part 2. (b) Trost, B. M. *Acc. Chem. Res.* **1980**, *13*, 385. (c) Trost, B. M.; Verhoeven, T. R. *J. Am. Chem. Soc.* **1980**, *102*, 4730. (d) Heck, R. F. *Acc. Chem. Res.* **1979**, *12*, 146. (e) Tsuji, J. *Acc. Chem. Res.* **1969**, *2*, 144.
22. For Mo: (a) Faller, J. W.; Chao, K. H. *J. Am. Chem. Soc.* **1984**, *106*, 887. (b) Faller, J. W.; Chao, K. H.; Murray, H. H. *Organometallics*, **1984**, *3*, 1231. (c) Schilling, B. E. R.; Hoffman, R.; Faller, J. W. *J. Am. Chem. Soc.* **1979**, *101*, 592. (d) Adams, R. D.; Chadosh, D. F.; Faller, J. W. *J. Am. Chem. Soc.* **1979**, *101*, 2570. For Co: (e) Heck, R.F. In *Organic Synthesis via Metal Carbonyls*; Wender, I.; Pino, P.; Eds.; Wiley: New York, 1968; Vol. 1, pp. 379-384. (f) Heck, R. F.; Breslow, D. S. *J. Am. Chem. Soc.* **1963**, *85*, 2779. (g) Hegedus, L. S.; Inoue, Y. *J. Am. Chem. Soc.* **1982**, *104*, 4917. (h) Hegedus, L. S.; Perry, J. P. *J. Org. Chem.* **1984**, *49*, 2570. For Fe: (i) Whitesides, T. H.; Arhart, R. W.; Slaven, R. W. *J. Am. Chem. Soc.* **1973**, *95*, 5792. (j) Pearson, A. J. *Aust. J. Chem.* **1976**, *29*, 1841. For Rh: (k) Tsuji, J.; Minami, I.; Shimizu, I. *Chem. Lett.* **1984**, 1721. (l) Semmelhack, M. F. *Org. React.* **1972**, *19*, 115. Baker, R. *Chem Rev.* **1973**, *73*, 487. (m) Hegedus, L. S.; *J. Organomet. Chem. Lib.* **1976**, *1*, 329. (n) Billington, D. C. *Chem. Soc. Rev.* **1985**, *14*, 93. (o) Ikeda, S.; Maruyama, Y.; Ozawa, F. *Organometallics* **1998**, *17*, 3770. For Ni (l-n) and: (p) Benfield, F. H.; Francis, B. R.; Green, M. L. H.; Luong-Thi, N. –T.; Moser, G.; Poland, J. S.; Roe, D. M. *J. Less Common Metals* **1974**, *36*, 187.

23. (a) Ephritikhine, M.; Francis, B. R.; Green, M. L. H.; MacKenzie, R. E.; Smith, M. J. *J. Chem. Soc., Dalton Trans.* **1977**, 1131. (b) Ephritikhine, M.; Green, M. L. H.; MacKenzie, R. E. *J. Chem. Soc., Chem. Commun.* **1976**, 619.
24. Davies, S. G.; Green, M. L. H.; Mingos, D. M. P. *Tetrahedron* **1978**, *34*, 3047.
25. (a) Hegedus, L. S.; Darlington, W. H.; Russell, C. E. *J. Org. Chem.* **1980**, *45*, 5193. (b) Carfagna, C.; Mariani, L.; Musco, A.; Sallese, G.; Santi, R. *J. Org. Chem.* **1991**, *56*, 3924. (c) Hoffman, H. M. R.; Otte, A. R.; Wilde, A. *Angew. Chem. Int. Ed. Engl.* **1992**, *31*, 234. (d) Benyunes, S. A.; Brandt, L.; Green, M.; Parkins, A. W. *Organometallics* **1991**, *10*, 57. (e) Carfagna, C.; Galarini, R.; Musco, A.; Santi, R. *Organometallics* **1991**, *10*, 3956. (f) Aranyos, A.; Szabo, K. J.; Castano, A. M.; Backvall, J. E. *Organometallics* **1997**, *16*, 1058. (g) Suzuki, T.; Fujimoto, H. *Inorg. Chem.* **1999**, *38*, 370. (g) Kadota, J.; Korori, S.; Fukumoto, Y.; Murai, S. *J. Org. Chem.* **1999**, *64*, 7523.
26. (a) McGhee, W. D.; Bergman, R. G. *J. Am. Chem. Soc.* **1988**, *110*, 4246. (b) Periana, R. A.; Bergman, R. G. *J. Am. Chem. Soc.* **1986**, *108*, 7346. (c) McGhee, W. D.; Bergman, R. G. *J. Am. Chem. Soc.* **1985**, *107*, 3388. (d) Periana, R. A.; Bergman, R. G. *J. Am. Chem. Soc.* **1984**, *106*, 7272.
27. (a) Schwiebert, K. E.; Stryker, J. M. *Organometallics* **1993**, *12*, 600. (b) Tjaden, E. B.; Casty, G. L.; Stryker, J. M. *J. Am. Chem. Soc.* **1993**, *115*, 9814. (c) Tjaden, E. B.; Stryker, J. M. *Organometallics* **1992**, *11*, 16. (d) Tjaden, E. B.; Schwiebert, K. E.; Stryker, J. M. *J. Am. Chem. Soc.* **1992**, *114*, 1100. (e) Wakefield, J. B.; Stryker, J. M. *J. Am. Chem. Soc.* **1991**, *113*, 7057. (f) Wakefield, J. B.; Stryker, J. M. *Organometallics* **1990**, *9*, 2428. (g) Tjaden, E. B.; Stryker, J. M. *J. Am. Chem. Soc.* **1990**, *112*, 6420.
28. Curtis, M. D.; Eisenstein, O. *Organometallics* **1984**, *3*, 887.
29. (a) Aranyos, A.; Szabó, K. J.; Castaño, A. M.; Bäckvall, J. –E. *Organometallics* **1997**, *16*, 1058. (b) Carfagna, C.; Galarini, R.; Linn, K.; López, J. A.; Melli, C.; Musco, A.

- Organometallics* **1993**, *12*, 3019. (c) Hoffman, H. M. R.; Otte, A. R.; Wilde, A.; Menzer, S.; Williams, D. J. *Angew. Chem. Int. Ed. Engl.* **1995**, *34*, 100. (d) Hoffman, H. M. R.; Otte, A. R.; Wilde, A. *Angew. Chem. Int. Ed. Engl.* **1992**, *31*, 234. (e) Wilde, A.; Otte, A. R.; Hoffmann, H. M. R. *J. Chem. Soc. Chem. Commun.* **1993**, 615. (f) Otte, A. R.; Wilde, A.; Hoffman, H. M. R. *Angew. Chem. Int. Ed. Engl.* **1994**, *33*, 1280.
30. Lauher, J. W.; Hoffman, R. *J. Am. Chem. Soc.* **1976**, *98*, 1729. (b) Green, J. *Chem. Rev.* **1998**, *27*, 263.
31. Tjaden, E. B.; Casty, G. L.; Stryker, J. M. *J. Am. Chem. Soc.* **1993**, *115*, 9814.
32. Casty, G. L. Ph. D Thesis, Indiana University, 1994.
33. Carter, C. A. G. Ph. D Thesis, University of Alberta, 1994.
34. Only Super-Hydride (LiEt₃BH) under an atmosphere of ethylene was seen to give the desired titanacyclobutane complex.
35. Casty, G. L.; Stryker, J. M. *J. Am. Chem. Soc.* **1995**, *117*, 7814.
36. Wardell, J. L. In *Comprehensive Organometallic Chemistry Vol. 2*. Wilkinson, G. ed. Pergamon Press, New York, 1982, p. 910 and references therein.
37. Giese, B. *Radicals in Organic Synthesis: formation of Carbon-Carbon Bonds*. Pergamon, Oxford, 1986.
38. RajanBabu, T. V.; Nugent, W. A. *J. Am. Chem. Soc.* **1994**, *116*, 986 and references therein. (b) RajanBabu, T. V. Nugent, W. A.; Beattie, M. S. *J. Am. Chem. Soc.* **1992**, *114*, 6408. (c) Nugent, W. A.; RajanBabu, T. V. *J. Am. Chem. Soc.* **1989**, *111*, 8561. (d) RajanBabu, T. V.; Nugent, W. A. *J. Am. Chem. Soc.* **1989**, *111*, 4525.
39. (a) Girard, P.; Namy, J. L.; Kagan, H. B. *J. Am. Chem. Soc.* **1980**, *102*, 2693. (b) Review: Imamoto, T. *Lanthanides in Organic Synthesis*; Academic Press: SanDiego, 1994.

40. In addition it has been reported the addition of allyl halides to Ti(III) allyl complexes provide Ti(IV)-allyl compounds $\text{Cp}_2\text{Ti}(\text{allyl})\text{X}$. Sato, F.; Iida, K.; Moriya, H.; Sato, M. *J. Chem. Soc., Chem. Commun.* **1981**, 1140.
41. Costa, E. M.; Stryker, J. M. Unpublished results.
42. Infrared spectroscopy has been used to suggest that the allylic ligands are η^3 -coordinate in $(\text{C}_5\text{Me}_5)_2\text{Ti}(\text{C}_3\text{H}_4\text{R})$ (R = H, Me): Luinstra, G. A.; ten Cate, L. C.; Heeres, H. J.; Pattiasina, J. W. Meetsma, A.; Teuben, J. H. *Organometallics* **1991**, *10*, 3227.
43. (a) Martin, H. A.; Lemaire, P. J.; Jellinek, F. J. *Organomet. Chem.* **1968**, *14*, 149. (b) Yasuda, H.; Kajihara, Y.; Mashima, K.; Nagasuna, K.; Nakamura, A. *Chem. Lett.* **1981**, 671. Mashima, K.; Yasuda, H.; Asami, K.; Nakamura, A. *Chem. Lett.* **1983**, 219. (c) Blenkins, J.; de Liefde Meijer, H. J.; Teuben, J. H. *J. Organomet. Chem.* **1981**, *218*, 383. (d) McDade, C.; Bercaw, J. E. *J. Organomet. Chem.* **1985**, *279*, 281. (e) Highcock, W. J.; Mills, R. M.; Spencer, J. L.; Woodward, P. *J. Chem. Soc., Dalton Trans.* **1986**, 829, and references therein. (f) Larson, E. J.; van Dort, P. C.; Lakanen, J. R.; O'Neill, D. W.; Pederson, L. M.; McCandless, J. J.; Silver, M. E.; Russo, S. O.; Huffman, J. D. *Organometallics* **1988**, *7*, 1183. Vance, P. J.; Prins, T. J.; Hauger, B. E.; Silver, M. E.; Wemple, M. E.; Pederson, L. M.; Kort, D. A.; Kannisto, M. R.; Geerligs, S. J.; Kelly, R. S.; McCandless, J. J.; Huffman, J. D.; Peters, D. G. *Organometallics* **1991**, *10*, 917. (g) Tjaden, E. B.; Stryker, J. M. *J. Am. Chem. Soc.* **1993**, *115*, 2083.
44. Carter, C. A. G.; McDonald, R.; Stryker, J. M. *Organometallics* **1999**, *18*, 820
45. (a) Smith, J. A.; J., V. S.; Huttner, G.; Brintzinger, H. H. *J. Organomet. Chem.* **1979**, *173*, 175. (b) Nifant'ev, I. E.; Butakov, K. A.; Aliev, Z. G.; Urazovskii, I. F. *Organometallic Chemistry in the USSR* **1991**, *4*, 622.
46. Recently the *meso* to *rac* diastereomeric rearrangement was reported in which a diastereomeric mixture of ethylene bis(indenyl)Zr(NR₂)₂ was converted thermally to

- a mixture enriched in the *rac* diastereomer. (a) Diamond, G. M.; Rodewald, S.; Jordan, R. F. *Organometallics* **1995**, *14*, 5. (b) Diamond, G. M.; Jordan, R. F.; Petersen, J. L. *Organometallics* **1996**, *15*, 4045. (c) Diamond, G. M.; Jordan, R. F.; Petersen, J. L. *Organometallics* **1996**, *15*, 4030. (d) Christopher, J. N.; Diamond, G. M.; Jordan, R. F.; Petersen, J. L. *Organometallics* **1996**, *15*, 4038. (e) Yoder, J. C.; Day, M. W.; Bercaw, J. E. *Organometallics* **1998**, *17*, 4946.
47. (a) Lee, J. B.; Gajda, G. J.; Schaefer, W. P.; Howard, T. R.; Ikariya, T.; Straus, D. A.; Grubbs, R. H. *J. Am. Chem. Soc.* **1981**, *103*, 7358. (b) Gilliom, L. R.; Grubbs, R. H. *Organometallics* **1986**, *5*, 721. (c) Straus, D. A.; Grubbs, R. H. *J. Mol. Catal.* **1985**, *28*, 9. (d) Stille, J. R.; Santarsiero, B. D.; Grubbs, R. H. *J. Org. Chem.* **1990**, *55*, 843.
48. Brown-Wensley, K. A.; Buchwald, S. L.; Cannizzo, L.; Clawson, L.; Ho, S.; Meinhardt, D.; Stille, J. R.; Straus, D.; Grubbs, R. H. *Pure & Appl. Chem.* **1983**, *55*, 1733 and references therein.
49. Meinhardt, J. D.; Anslyn, E. V.; Grubbs, R. H. *Organometallics* **1989**, *8*, 583.
50. (a) McKinney, R. J.; Tulip, T. H.; Thorn, D. L.; Coolbaugh, T. S.; Tebbe, F. N. *J. Am. Chem. Soc.* **1981**, *103*, 5584. (b) Lappert, M.F. In *Comprehensive Organometallic Chemistry*; Wilkinson, G.; Stone, F. G. A.; Abel, E. W. Eds.: Pergamon, 1995; vol 4.
51. Recent and leading references: (a) Bohme, U.; Beckhaus, R. *J. Organomet. Chem.* **1999**, *585*, 179. (b) Beckhaus, R.; Oster, J. *J. Organomet. Chem.* **1998**, *553*, 427. (c) Beckhaus, R.; Oster, J.; Wang, R. M.; Bohme, U. *Organometallics* **1998**, *17*, 2215. (d) Beckhaus, R. *J. Chem. Soc., Dalton Trans.* **1997**, 1991. (e) Beckhaus, R.; Oster, J.; Sang, J.; Strauss, I.; Wagner, M. *Synlett* **1997**, 241. (f) Beckhaus, R. *Angew. Chem. Int. Ed. Engl.* **1997**, *36*, 687.
52. (a) Ho, S. C. H.; Straus, D. A.; Grubbs, R. H. *J. Am. Chem. Soc.* **1984**, *106*, 1533. (b) Tumas, W.; Wheeler, D. R.; Grubbs, R. H. *J. Am. Chem. Soc.* **1987**, *109*, 6182. (c) Burk, M. J.; Staley, D. L.; Tumas, W. *J. Chem. Soc., Chem. Commun.* **1990**, 809. (d) Burk, M. J.; Tumas, W.; Wheeler, D. R. *J. Am. Chem. Soc.* **1990**, *112*, 6133.

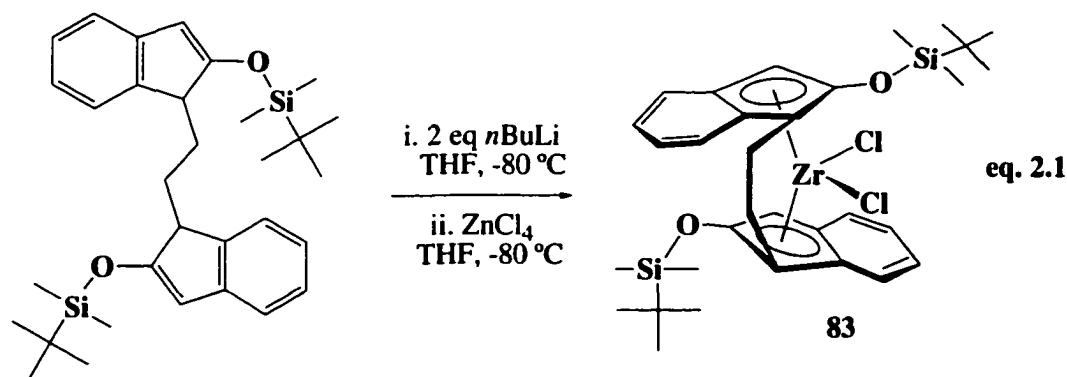
53. (a) Pine, S. H.; Zahler, R.; Evans, D. A.; Grubbs, R. H. *J. Am. Chem. Soc.* **1980**, *102*, 3270. (b) Clawson, L.; Buchwald, S. L.; Grubbs, R. H. *Tetrahedron Lett.* **1984**, *25*, 5733. (c) Pine, S. H.; Pettit, R. J.; Geib, G. D.; Cruz, S. G.; Gallego, C. H.; Tijerina, T.; Pine, R. D. *J. Org. Chem.* **1985**, *50*, 1212. (d) Cannizzo, L. F.; Grubbs, R. H. *J. Org. Chem.* **1985**, *50*, 2316.
54. Brown-Wensley, K.A.; Buchwald, S. L.; Cannizzo, L.; Clwson, L.; Ho, S.; Meinhardt, D.; Stille, J. R.; Straus, D.; Grubbs, R. H. *Pure Appl. Chem.* **1983**, *55*, 1733. (b) Dennehy, R. D.; Whitby, R. J. *J. Chem. Soc., Chem. Commun.* **1990**, 1060. (c) Petersen, J. L.; Egan, J. W., Jr. *Organometallics* **1987**, *6*, 2007. (d) Beckhaus, R.; Wilbrandt, D.; Flatau, S.; Bohmer, W. -H. *J. Organomet. Chem.* **1992**, *423*, 211.
55. Manriques, J. M.; McAllister, D. R.; Sanner, R. D.; Bercaw, J. E. *J. Am. Chem. Soc.* **1978**, *100*, 2716. (b) Roddick, D. M.; Bercaw, J. E. *Chem. Ber.* **1989**, *122*, 1579. (c) Hofmann, P.; Stauffert, P.; Frede, M.; Tatsumi, K. *Chem. Ber.* **1989**, *122*, 1559. (d) Petersen, J. L.; Egan, J. W.; *Organometallics* **1987**, *6*, 2007. (e) Berg, F. J.; Petersen, J. L. *Organometallics* **1991**, *10*, 1599. (f) Valero, C.; Grehl, M.; Wingbermuehle, D.; Koppenburg, L.; Carpenetti, D.; Erker, G.; Peterson, J. L. *Organometallics* **1994**, *13*, 415.
56. Carter, C. A. G.; Greidanus, G.; Chen, J.-X.; Stryker, J. M., submitted.
57. Durr, S.; Hohlein, U.; Schobert, R. *J. Organomet. Chem.* **1993**, *458*, 89.
58. Bercaw, J. E.; Marvich, R. H.; Bell, L. G.; Brintzinger, H. H. *J. Am. Chem. Soc.* **1972**, *94*, 1219.
59. (a) Barsties, E.; Schaible, S.; Prosenc, M. -H.; Rief, U.; Röhl W.; Weyand, O.; Dorer, B.; Brintzinger, H. -H. *J. Organomet. Chem.* **1996**, *520*, 63. (b) Luttikhedde, H. J. G.; Leino, R.; Ahlgrén, M. J.; Pakkanen, T. A.; Näsman, J. H. *J. Organomet. Chem.* **1998**, *557*, 227.
60. (a) Erker, G.; Czisch, P.; Schlund, R.; Angermund, K.; Kruger, C. *Angew. Chem. Int. Ed. Engl.* **1986**, *25*, 364. (b) Rietveld, M. H. P.; Hagen, H.; van de Water, L.; Grove,

D. M.; Kooijman, H.; Veldman, N.; Spek, A. L.; van Koten, G. *Organometallics*
1997, *16*, 168.

Chapter 2. Bis(2-methoxyindenyl)titanacyclobutane Complexes via Organic Free Radical Addition to Ti(III) Allyl Complexes

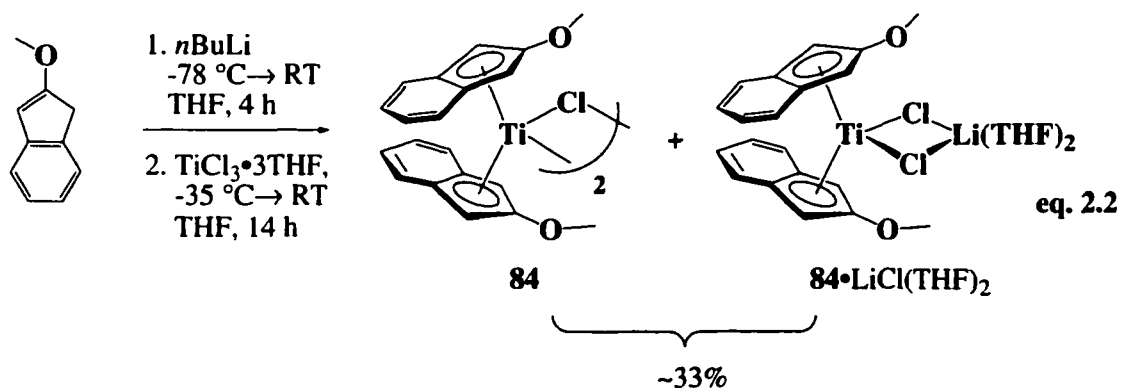
A. Synthesis of Bis(2-methoxyindenyl)titanium(III) η^3 -Allyl Complexes

Methoxycyclopentadiene¹ was considered an ideal ancillary ligand for this study, particularly because of the small steric profile of the methoxy group. However, due to difficulties associated with the preparation and storage of methoxycyclopentadiene, this study was aborted and the use of 2-methoxyindene² as an ancillary ligand was investigated. Although Rausch reported that an attempt to make (1-methoxyindenyl)trichlorotitanium failed,^{3a} Näsman reported zirconocene complex **83** sporting tethered siloxy-substituted indenyl ligands (eq. 2.1).^{3b}



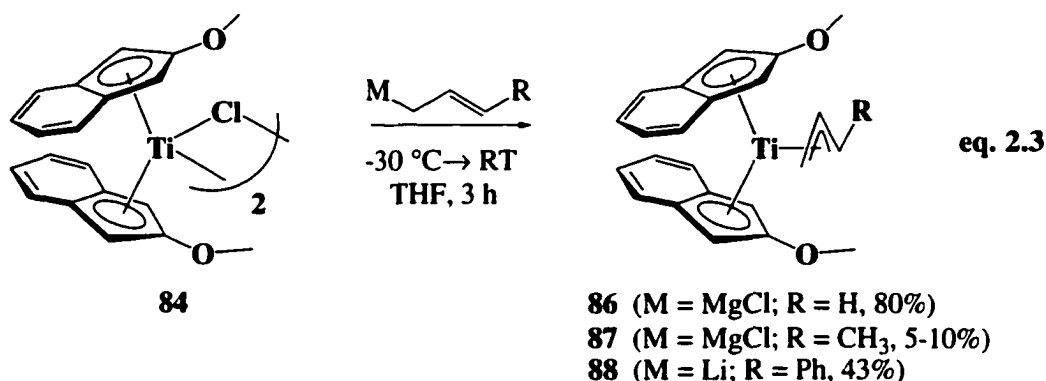
The preparation of the 2-methoxyindenyl template for radical central carbon alkylation of substituted allyl complexes was readily accomplished by mixing the lithium salt of 2-methoxyindene, prepared by metallation using *n*-butyllithium, and TiCl₃·3THF⁴ as solids, cooling to -35 °C and adding THF. Crystallization from THF layered with hexane results in a mixture of bis(2-methoxyindenyl)titanium chloride **84** and a tentatively assigned lithium chloride adduct **84**·LiCl(THF)₂ (*vide infra*) in a relatively low yield (eq. 2.2).⁵ It remains unknown whether the solid state structure of chloride complex **84** exists as a chloride-bridged dimer or is monomeric as the complex could not

be obtained as single crystals. Titanocene(III) chloride complexes typically adopt monomeric structures in the case of sterically significant ancillary ligands such as pentamethylcyclopentadienyl^{6a} or 1,3-di-*tert*-butylcyclopentadienyl.^{6c} Chloride-bridged dimers are observed for complexes with smaller ligands such as cyclopentadienyl^{6f} or isopropylcyclopentadienyl.^{6c} Tentatively, we assign the structure as a chloride-bridged dimer, a consequence of the intermediate steric demand of the 2-methoxyindenyl ligand. While HRMS analysis only indicated the presence of monomeric titanocene **84**, elemental analysis indicated that crystallization afforded a mixture of two complexes, **84** and presumably **84**•LiCl(THF)₂. Further characterization of paramagnetic complexes **84** and **84**•LiCl(THF)₂ was accomplished by PbCl₂ oxidation to the corresponding dichloride complex **85**, which was characterized spectroscopically.



Allyl, crotyl (η^3 -1-methylallyl) and cinnamyl (η^3 -1-phenylallyl) complexes **86**, **87** and **88** were obtained by treating the chloride complex **84** with allylmagnesium chloride, crotylmagnesium chloride and cinnamyl lithium respectively, in THF at $-35\text{ }^\circ\text{C}$ (eq. 2.3). The cinnamyl complex **88** was isolated as a green crystalline material in 43% yield. The green colour of complex **88** is attributed to the extended conjugation afforded by the phenyl substituent on the allyl ligand; by comparison, the unsubstituted allyl complex **86** is light brown. Consistent with this hypothesis, bis(2-piperidinoindenyl)titanium(η^3 -1-phenylallyl) **53** is also green.⁷ Characterization of **88** was accomplished by infrared

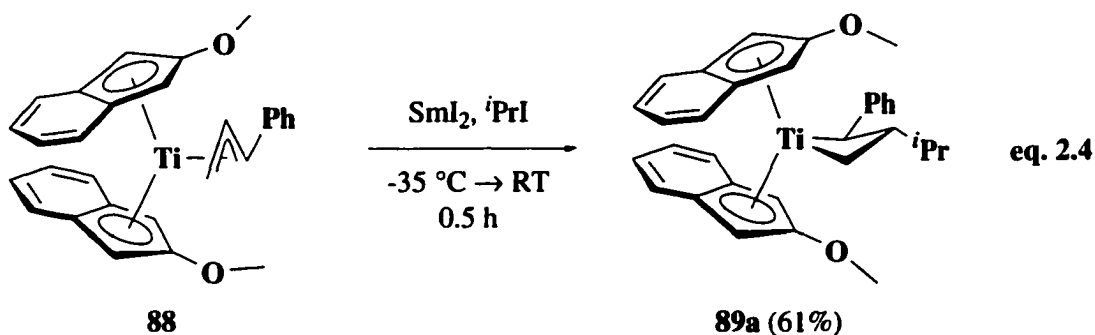
spectroscopy, elemental analysis and high resolution mass spectroscopy. The crotyl complex **87** was isolated as a dark brown oil in very low yield (10%). Elemental analysis of this paramagnetic complex was not within tolerable allowances and high resolution mass spectrometry failed to provide a parent ion peak.



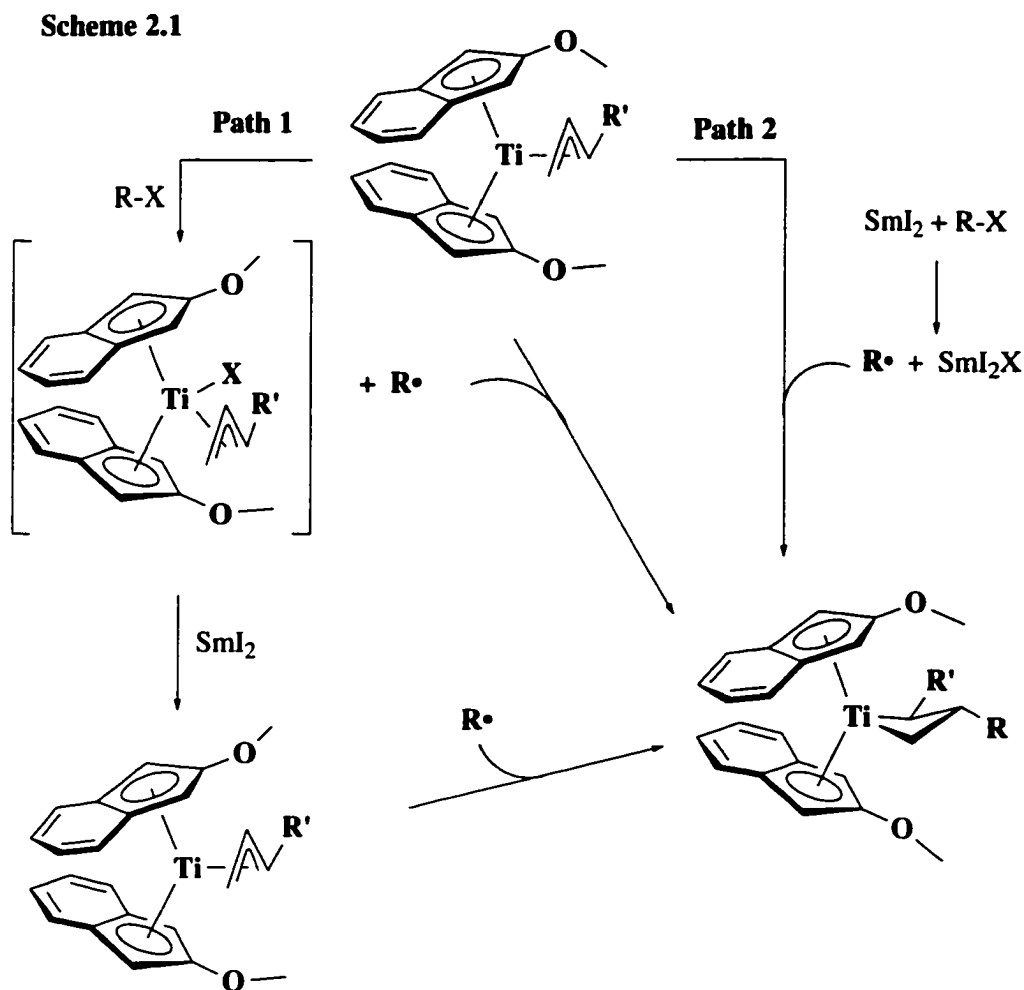
Alkali and transition metal complexes possessing a π -bonded allylic fragment are known to display an infrared absorption band between 1480 and 1540 cm^{-1} of moderate to strong intensity for the asymmetric allylic C=C stretch.^{8,9} To illustrate, the absorption bands for $\text{Cp}_2\text{Ti}(\eta^3\text{-C}_3\text{H}_5\text{-R}_n)$ are as follows: (allyl) = 1509 cm^{-1} ; (1-methylallyl) = 1533 cm^{-1} ; (2-methylallyl) = 1480 cm^{-1} ; (1,3-dimethylallyl) = 1546 cm^{-1} . The frequency of the $\text{C}=\text{C}_{\text{asym}}$ stretch of the allylic anions increases according to the sequence: 2-methylallyl < *anti*-1-methylallyl < allyl < *syn*-1-methylallyl.⁹ In the crude crotyl complex **87**, three absorption bands (1536, 1517, 1495 cm^{-1}) are seen in the region for the $\text{C}=\text{C}_{\text{asym}}$. This suggests either the presence of an impurity or that the complex may exist in more than one coordination mode (both η^3 - and η^1 -coordination) or may adopt either a distorted η^3 -coordination or η^1, η^2 -(σ, π)-coordination.¹⁰ Allyl complex **86**, obtained in good yield, was also characterized by IR spectroscopy. In contrast to crotyl complex **87**, only one $\text{C}=\text{C}_{\text{asym}}$ stretch was observed at 1496 cm^{-1} .

B. Radical Addition to Allyl, Crotyl and Cinnamyl Complexes

As was observed for the 2-piperidinoindenyl template **53**,⁷ cinnamyl and crotyl complexes **88** and **87** proved to be good traps for organic radicals, affording 2,3-disubstituted titanacyclobutane complexes in the process. The best results were obtained by treating a cold (-35 °C) THF solution containing one equivalent each of the cinnamyl complex **88** and SmI₂ with one equivalent of 2-iodopropane. Upon warming this reaction mixture to room temperature, the central carbon alkylation product **89a** can be isolated as brown crystals in moderate yield (eq. 2.4). The short reaction time and low temperature required for the central carbon alkylation step contrast the elevated temperatures required for the reaction of secondary alkyl iodides with samarium iodide¹¹ and for the samarium-mediated alkylation of (C₅Me₅)₂Ti(η³-allyl) **41** with isopropyl iodide (*vide supra*).¹² We suspect that under these reaction conditions, SmI₂ itself is not responsible for the initial radical generation. Instead, we believe that the electron-rich Ti(III) complex **88**, or an adventitious Ti(III) catalyst, reacts directly with the haloalkane, leading to the formation of an allyltitanium(IV) halide intermediate and the isopropyl radical, the latter of which alkylates the remaining Ti(III) allyl complex (path 1, Scheme 2.1). The allyltitanium(IV) halide intermediate is then reduced by SmI₂ to regenerate the allyltitanium(III) complex, as proposed for related alkylations of propargyl titanium(III) complexes.¹³

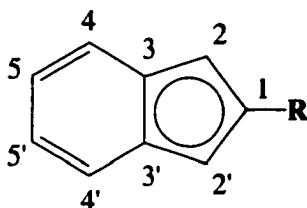


Characterization of titanacyclobutane **89a** rests on analysis of spectroscopic data. The numbering scheme used to simplify spectroscopic assignments for the indenyl ligand



is illustrated in Figure 2.1. 1H NMR spectroscopy of complex **89a** shows resonances characteristic of a four-membered titanacyclobutane ring: the expected doublet of doublets for each of the diastereotopic α -methylene protons appear as triplets at δ 2.56 ($J = 8.5$ Hz) and 0.79 ($J = 9.3$ Hz), and the α -methine proton resonates at δ 2.24 (d, $J = 10.5$ Hz). That $^3J_{cis}$ is similar to $^3J_{trans}$, resolving each methylene proton into a triplet, has been observed in all titanacyclobutane complexes.^{14,15,16,17,18} The expected doublet of doublet of triplets for the β -methine proton appears upfield of the α -protons as a quintet at δ 0.63 ($J = 8.7$ Hz). The 1.8 ppm difference between the two α -methylene hydrogen atoms, relatively rare in 2,3-disubstituted metallacycles,¹⁷ indicates that the α -methylene hydrogen with the high field signal is located in a highly shielded environment, possibly

Figure 2.1 Numbering scheme for NMR spectroscopy of the indenyl ligand system.



under one of the indenyl ligands where it would experience significant anisotropic shielding.^{15,19} Also noteworthy is the downfield shift from typically highly shielded resonances for the β -methine hydrogen. This β -hydrogen atom experiences a similarly shielded environment to one of the α -methylene protons, an occurrence uncharacteristic of group 4 metallacyclobutane complexes.^{14-18,20} The presence of the isopropyl substituent is confirmed by the diastereotopic methyl doublets at δ 1.09 ($J = 6.5$ Hz) and 0.91 ($J = 6.6$ Hz) and the complex methine multiplet at δ 1.23. The *trans* orientation assigned to the phenyl and isopropyl substituents on the titanacyclobutane ring is based on spectroscopic similarity to the rigorously established *trans* geometry in isostructural 2-piperidinoindenyl titanacyclobutane complex **55a** (*vide supra*).¹⁷ The top to bottom, as well as side to side, dissymmetry expected in 2,3-disubstituted titanacyclobutane complex **89a** is indicated by the observation of four methine resonances representing the five-membered ring protons (H2 and H2'), appearing at δ 5.58, 5.41, 5.06 and 4.62, and the inequivalency of the methoxy substituents on the indenyl rings, observed at δ 3.09 and 2.86. These data have been tabulated in Table 2.1. The remaining signals represent resonances for the α -phenyl substituent and indenyl ancillary ligands. Two-dimensional ^1H - ^1H correlated NMR spectroscopy (GCOSY) fully supports these assignments. Characteristic ^{13}C NMR resonances for the titanacyclobutane ring, determined by heterocorrelated ^{13}C - ^1H NMR (HMQC) experiments, occur at δ 96.8 and 89.3 for the α -methine and α -methylene carbons, respectively, with a high field signal at δ 25.1 for the β -carbon. Analytically pure complex **89a** is obtained from a concentrated THF solution layered with pentane (1 : 5) and cooled to -35 °C.

Table 2.1. Selected Room Temperature ^1H NMR Resonances of Titanacyclobutane Complexes **55a** and **89a-c**

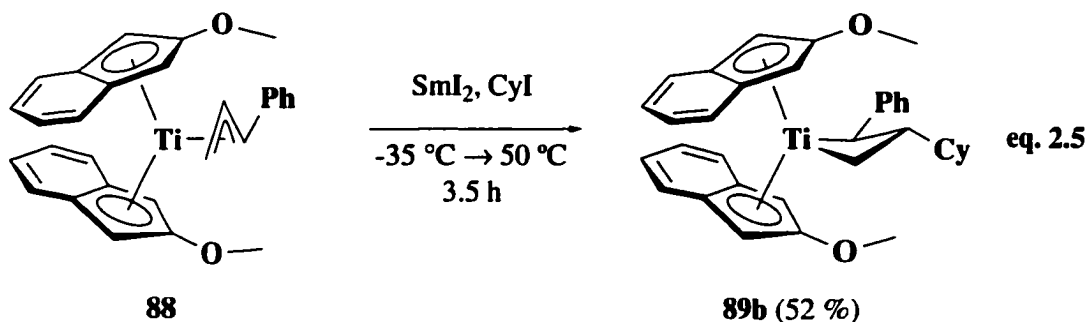
	R = 'Pr, 55a [‡] δ (m, J, I)*	R = 'Pr, 89a δ (m, J, I)*	R = Cy, 89b δ (m, J, I)*	R = Bn, 89c δ (m, J, I)*
Ti-CH(Ph)	2.48 (d, 11.6, 1H)	2.24 (d, 10.5, 1H)	2.26 (br d, 9.6 1H)	1.66 (d, 12.5, 1H)
Ti-CH ₂	2.61 (t, 10.0, 1H) 0.04 (t, 10.0, 1H)	2.56 (t, 8.5, 1H) 0.79 (t, 9.3, 1H)	2.62 (t, 8.6, 1H.) 0.82 (m, 1H)	2.34 (t, 10.9, 1H) 0.47 (t, 12.1, 1H.)
β -CH	0.84 (m, 1H)	0.63 (pentet, 8.7, 1H)	0.66 (m, 1H)	0.88 (m, 1H)
R	1.54 (m, 1H) 1.04 (d, 6.6, 3H) 0.95 (d, 6.6, 3H)	1.23 (m, 1H) 1.09 (d, 6.5, 3H) 0.91 (d, 6.6, 3H)	2.07 (d, 12.5, 1H) 1.89 (br d, 11.4, 1H) 1.61 (m, 3H) 1.20 (m, 2H) 1.05 (m, 1H) 0.94 (m, 3H)	2.83 (obscured signal, 1H, CH ₂ Ph) 2.00 (dd, 15.9, 10.9 1H, CH ₂ Ph),

[‡] 2-phenyl-3-benzyl-bis(piperidinoindenyl)titanacyclobutane

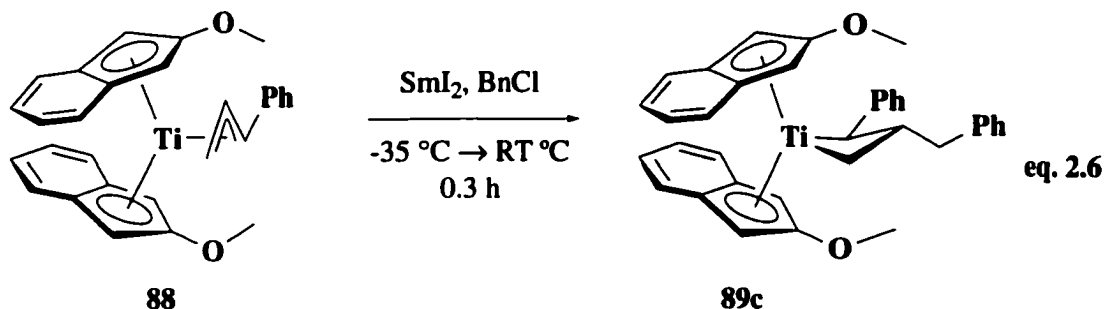
* δ = chemical shift, m = multiplicity, J = J_{HH} in Hz, I = integral.

Cinnamyl complex **88** also traps cyclohexyl radicals to give the expected 3-cyclohexyl-2-phenyl titanacyclobutane **89b** (eq. 2.5), albeit at slightly warmer temperature. These reaction conditions suggest that a different reaction mechanism may be operative. It is likely that, in this reaction, samarium diiodide generates the cyclohexyl radical by halide abstraction from iodocyclohexane, which then attacks cinnamyl complex **88** to generate titanacyclobutane complex **89b** (path 2, Scheme 2.1). Characterization of this complex was accomplished in a manner similar to complex **89a**. Pertinent ^1H NMR spectroscopic data for complex **89b** are given in Table 2.1, confirming the structural similarity to the isopropyl complex **89a**. Again, 2-dimensional NMR spectroscopy confirms that the α -methylene and α -methine resonances in the ^1H NMR spectrum occur at δ 2.62, 0.82 and 2.26, respectively. All of these signals are coupled to the β -methine signal, again observed upfield at δ 0.66. HMQC correlations identify the α -methylene and α -methine carbon signals in the ^{13}C NMR spectrum at δ 96.3 and 89.2,

respectively. The upfield signal for the β -carbon occurs at δ 23.6. Cyclohexyl-substituted titanacyclobutane complex **89b** powders out of a cold, concentrated pentane solution containing a nonstoichiometric amount of THF, but cannot be crystallized per se.

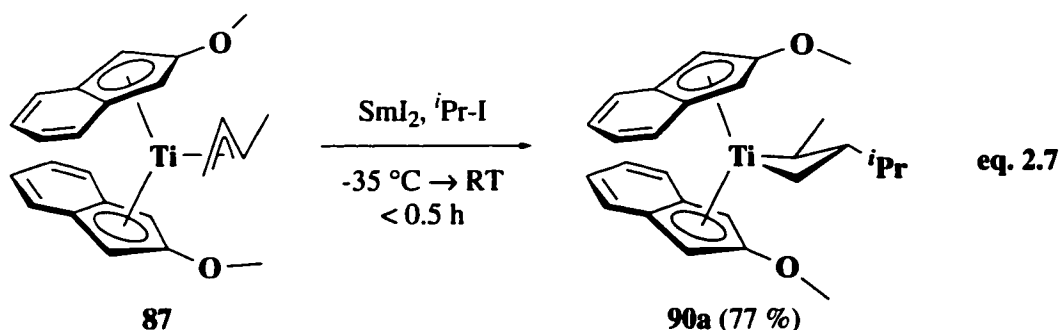


Cinnamyl complex **88** was also observed to trap benzyl radicals to give 3-benzyl-2-phenyl titanacyclobutane complex **89c** (eq. 2.6). However, all attempts to isolate the complex by cooling concentrated solutions of pentane resulted in intractable oils. Characterization of this complex is based only on ^1H NMR spectroscopy of the crude product and the similarity in signals to ^1H NMR spectra observed for titanacyclobutane complexes **89a** and **89b**. The α -methylene protons, well separated in chemical shift, were observed as triplets at δ 2.34 ($J = 10.9$ Hz) and 0.47 ($J = 12.1$ Hz); the α -methine proton resonates at δ 1.66 (d, $J = 12.5$ Hz). The addition of benzyl radical was confirmed by the diastereotopic benzyl protons at δ 2.83 (obscured signal) and δ 2.00 (dd, $J = 15.9, 10.9$ Hz). Paralleling titanacyclobutanes **89a** and **89b**, the β -proton exists in a shielded environment and resonates at δ 0.88.



Surprisingly, the addition of the less sterically encumbering allyl radical to cinnamyl complex **88** failed to generate the expected titanacyclobutane complex.

The corresponding crotyl complex **87**, when mixed with equal amounts of SmI_2 and 2-iodopropane, affords 3-isopropyl-2-methyl titanacyclobutane **90a** as purple agglomerated needles in good yield (eq. 2.7). The ^1H NMR spectrum of complex **90a** shows the characteristic signals for a 2,3-disubstituted titanacyclobutane core. The inequivalent α -methylene protons resonate at δ 2.68 (t, $J = 8.8$ Hz) and 1.14, in addition to the multiplet at δ 1.88 for the α -methine proton and the coincidental doublet of quartets (expected ddt) at δ -0.33 ($J = 6.7, 9.0$ Hz) for the β -methine proton. The remaining spectroscopic details are given in Table 2.2. Thermal instability of the product precluded further characterization, presumably due to β -hydride elimination from the α -methyl group.



Because isolation of crotyl titanium(III) complex **87** was so difficult, a one pot alkylation procedure was used to obtain crotyl derived titanacyclobutane complexes without the isolation of this intermediate. Thus, chloride complex **84** was alkylated *in situ* with crotyl Grignard, followed by addition of an equivalent of both isopropyl iodide and samarium diiodide, providing titanacyclobutane complex **90a** in an overall 98% yield

(Scheme 2.2). Extending this methodology to cinnamyl derived titanacyclobutane **89a** also resulted in an improvement of overall yield (Scheme 2.2).

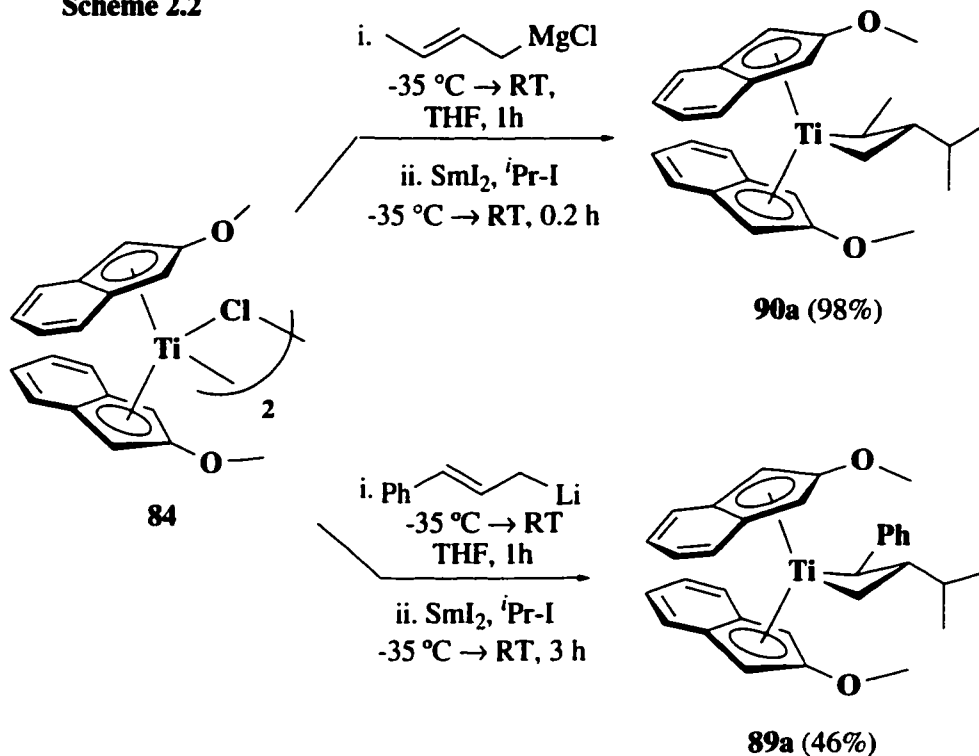
Table 2.2. Selected Room Temperature ^1H NMR Resonances of Titanacyclobutane Complexes **90a-d**

	R = <i>i</i> Pr, 90a δ (m, <i>J</i> , I)*	R = Cy, 90b δ (m, <i>J</i> , I)*	R = Bn, 90c δ (m, <i>J</i> , I)*	R = <i>t</i> Bu, 90d δ (m, <i>J</i> , I)*
Ti-CH(CH ₃)	1.88 (m, 1H)	1.84 (m, 1H)	1.72 (m, 1H)	1.82 (m, 1H)
Ti-CH(CH ₃)	1.80 (d, 6.5, 3H)	1.80 (d, 6.6, 3H)	1.69 (d, 6.8, 3H)	1.78 (d, 8.0, 3H)
Ti-CH ₂	2.68 (t, 8.8, 1H) 1.14 (obscured, 1H)	2.71 (t, 8.8, 1H) 1.30 (m, 4H)	2.59 (t, 8.4, 1H) 1.05 (t, 8.3, 1H)	2.60 (t, 8.7, 1H) 1.11 (t, 8.6, 1H)
β -CH	-0.33 (dq, 6.7, 9.0, 1H)	-0.33 (m, 1H)	0.75 (m, 1H)	0.021 (q, 8.6, 1H)
R	1.53 (octet, 6.7, 1H) 1.16 (d, 6.5, 3H) 1.09 (d, 6.6, 3H)	2.03 (d, 12.1, 1H) 1.96 (m, 1H) 1.72 (m, 2H) 1.64 (m, 2H) 1.52 (m, 2H) 1.30 (m, 4H)	2.24 (dd, 10.5, 8.0, 1H)	0.83 (s, 9H)

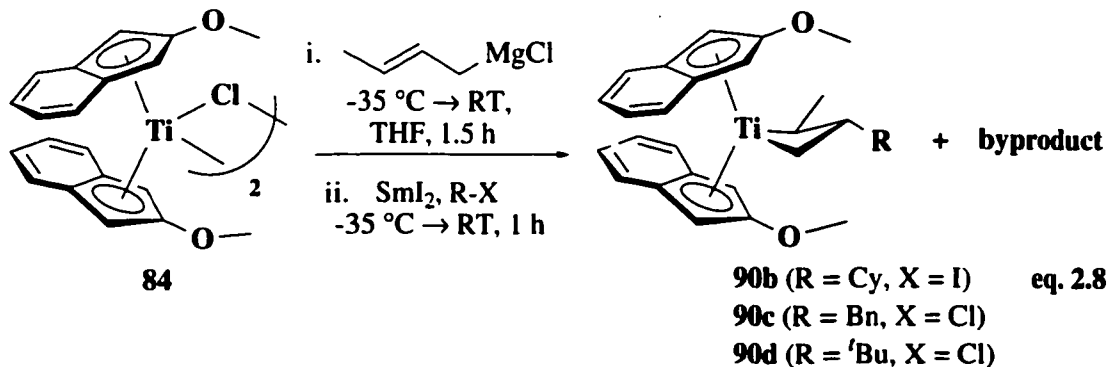
* δ = chemical shift, m = multiplicity, $J = J_{\text{HH}}$ in Hz, I = integral.

Utilizing this one pot methodology, 3-cyclohexyl-2-methyl titanacyclobutane **90b** is obtained by alkylating chloride complex **84** with crotyl Grignard, followed by addition of an equivalent of both iodocyclohexane and samarium diiodide (eq. 2.8). The ^1H NMR spectrum of the crude product revealed the formation of the desired titanacyclobutane: a characteristic triplet at δ 2.71 ($J = 8.8$ Hz) and a signal at δ 1.30 (obscured) are assigned to the inequivalent α -methylene hydrogen atoms, and multiplets at δ 1.84 and -0.33 are assigned to the α -methine and β -methine hydrogen atoms respectively. Also present in the ^1H NMR spectrum are signals attributable to a small amount of an uncharacterized byproduct. Further purification and characterization of this thermally unstable titanacyclobutane complex was not attempted.

Scheme 2.2



Benzyl and *tert*-butyl radicals also trap the crotyl complex **87** (generated *in situ*) (eq. 2.8); the spectroscopic details for the resultant complexes **90c** and **90d** are listed in Table 2.2. However, ^1H NMR spectra taken of the crude reaction mixtures also indicates that an increasing amount of the same byproduct is formed under the reaction conditions. In fact, the alkylation of chloride complex **84** with crotyl Grignard, followed by addition of crotyl bromide and samarium diiodide does not generate any of the expected

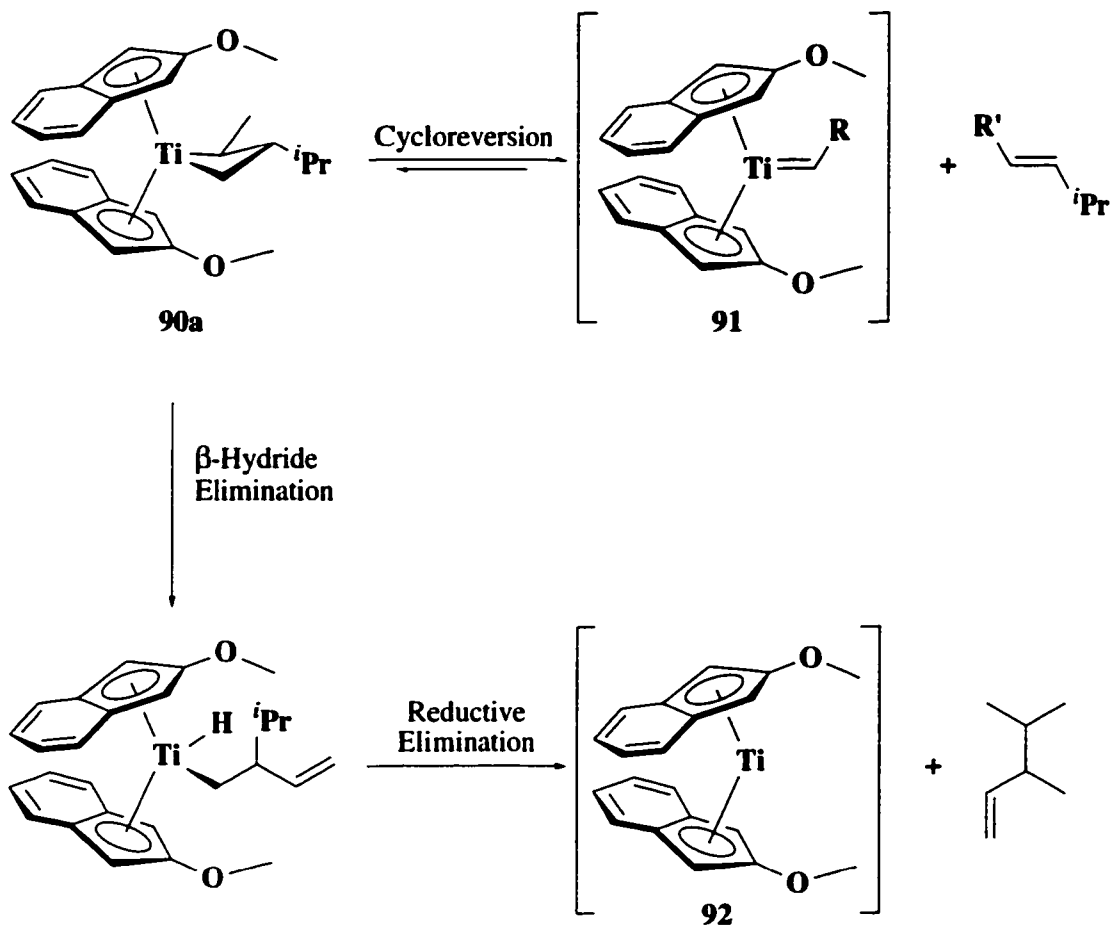


titanacyclobutane, returning only the unidentified 'byproduct'. The same result is obtained on addition of allyl bromide. This 'byproduct' is also generated by oxidizing crotyl complex **87** with one equivalent of PbCl_2 . This result confirms that some alkyl halides can act as halide-transfer one-electron oxidants, leading to byproduct formation, in addition to acting as radical sources for central carbon alkylation.

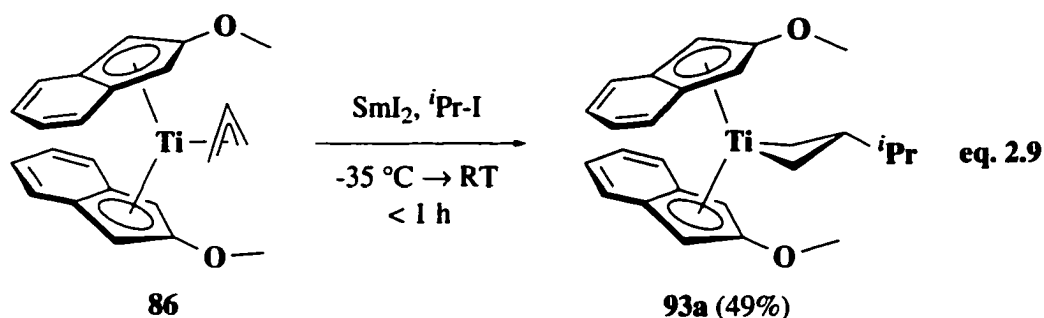
None of the 2,3-disubstituted titanacyclobutane complexes derived from the crotyl ligand are indefinitely stable in solution at room temperature. However, 3-isopropyl-2-methyl titanacyclobutane **90a** persists for longer periods of time when stored at low temperature (especially so in the solid state), but it too eventually decomposes. The two logical pathways by which decomposition can occur are cycloreversion and β -hydride elimination (Scheme 2.3). If cycloreversion of the titanacyclobutane is the operative decomposition pathway, the formation of one of two possible titanium alkylidenes **91**, in addition to an olefin product will result. If, on the other hand, β -hydride elimination from the α -methyl group followed by reductive elimination occurs, 3,4-dimethylpentene and an unstable Ti(II) species **92** would be generated. After allowing titanacyclobutane complex **90a** to decompose in solution at room temperature, ^1H NMR spectroscopy identified 3,4-dimethylpentene as the organic fragment arising from the titanacyclobutane core. This result was verified by GC-IR analysis, establishing β -hydride elimination as the principal decomposition pathway.

The inability of stabilized radicals to form stable titanacyclobutane complexes upon addition to cinnamyl complex **88** and the formation of the unidentified byproduct observed in the crotyl derived series of titanacyclobutane complexes prompted a brief examination of the reactivity of unsubstituted allyl complex **86**. The treatment of allyl complex **86** with equimolar amounts of samarium diiodide and 2-iodopropane at low temperature resulted in the formation of the expected 3-isopropyl substituted titanacycle

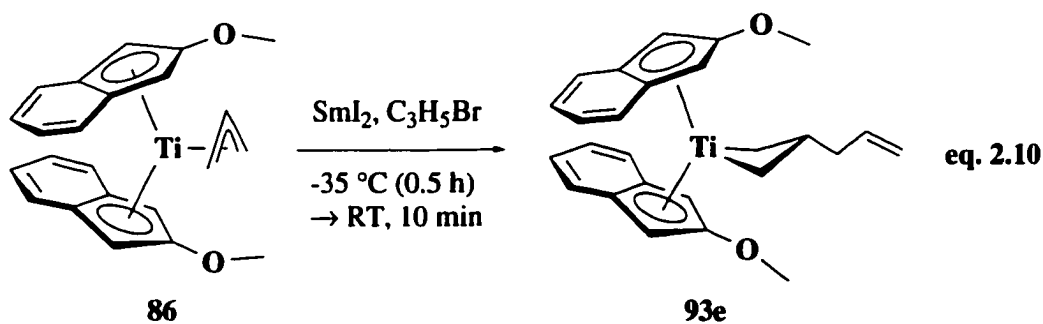
Scheme 2.3



93a in moderate yield after crystallization from cold pentane (eq. 2.9). The ^1H NMR spectrum of this stable complex clearly indicates a β -substituted titanacyclobutane: characteristic signals at δ 2.22 (dd, $J = 10.4, 8.7$ Hz) and 1.91 (t, $J = 8.5$ Hz) are observed for the α -methylene protons and the expected doublet of triplet of triplets for the β -methine signal appears at δ 0.02 ($J = 8.6$ Hz) as a coincidental sextet. The methyl groups on the isopropyl substituent are not diastereotopic (*cf.*, **89a** and **90a**). These assignments are in complete agreement with ^1H - ^1H NMR correlated spectroscopy of the complex. HMQC correlations identify the α -methylene and β -methine carbon signals in the ^{13}C NMR at δ 87.5 and 21.3, respectively.



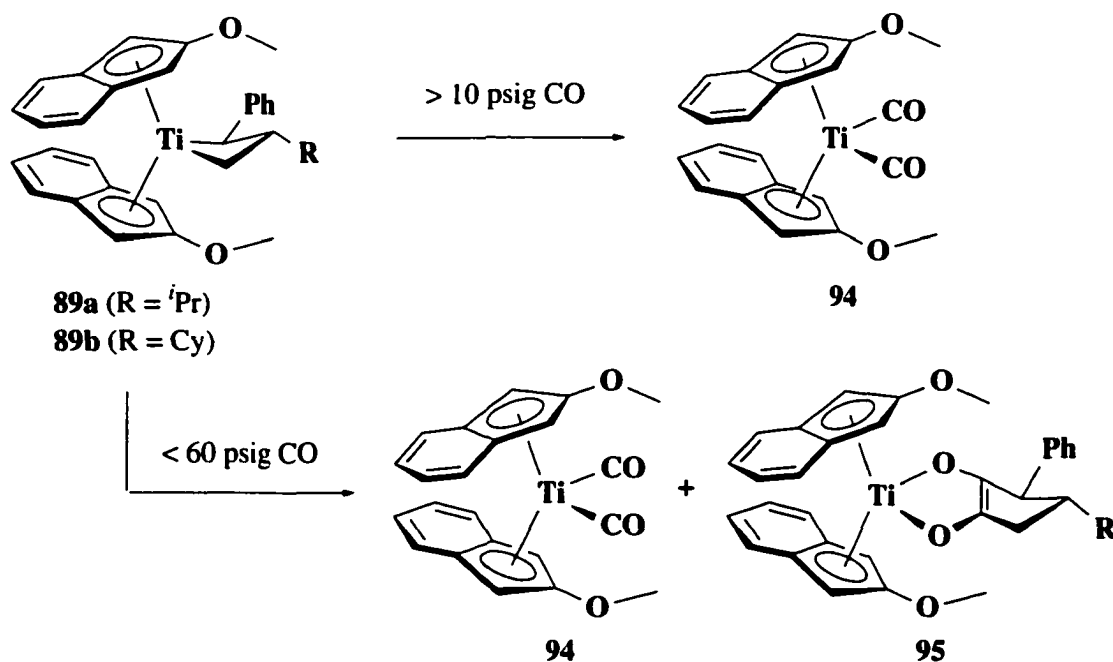
Treatment of allyl complex **86** with allyl bromide in the place of 2-iodopropane under similar reaction conditions, results in the formation of an unstable titanacyclobutane complex **93e** (eq. 2.10). The identity of complex **93e** rests only on assignment by ^1H NMR spectroscopy of the crude product, but the signals observed irrefutably point to its formation. The titanacyclobutane core is consistent with a β -allyl titanacyclobutane complex:¹⁶ a doublet of doublets is observed for one set of α -methylene protons at δ 2.41 ($J = 10.9, 8.7$ Hz) with the other set appearing at δ 1.91 as a triplet ($J = 8.0$ Hz), with the β -methine proton observed as a multiplet at δ 0.45. Resonances consistent with an allyl substituent are also observed; the doublet of doublet of triplets at δ 6.14 ($J = 16.2, 9.4, 6.0$ Hz) observed for the internal vinyl proton is coupled to the two overlapping signals for the terminal methylene group observed at δ 5.15. The internal methylene signal appears as a multiplet at δ 2.22. Further characterization was not possible, for within 10 minutes, the bright red complex decomposes to give paramagnetic material.



C. Functionalization of Cinnamyl Derived Titanacyclobutanes

Cinnamyl derived titanacyclobutanes **89a** and **89b** were treated with carbon monoxide under reaction conditions known to result in cyclobutanone formation for permethyltitanacyclobutane complexes **11** and 2-piperidinoindenyl complexes **55**.¹⁷ However, no cyclobutanone was isolated under these conditions, nor under various modifications of these reaction conditions. Under lower pressures of CO, the major product identified in the ¹H NMR spectrum was assigned to bis(2-methoxyindenyl)titanium dicarbonyl **94**.²¹ Under higher pressures of CO, in addition to the formation of presumed dicarbonyl complex **94**, signals possibly correlating to enediolate complex **95** were also detected in solution (Scheme 2.4). Additional interpretation of these results was made possible by the more extensive investigation of aminoindenyl systems (*vide infra*).

Scheme 2.4



D. Conclusions

This investigation provides further substantiation that electron richness at the metal enables central carbon radical alkylation of substituted allyl complexes. The fleeting existence of titanacycles resulting from the addition of stabilized radicals indicates that such titanacyclobutanes can be formed. Importantly, the one pot procedure allows for the titanium chloride complex **84** to be converted to titanacyclobutanes without the isolation of sensitive allyl titanocene intermediates.

The limitations of this system, however, caused us to abandon further work on this template. In addition to the low yields obtained in the synthesis of the bis(2-methoxyindenyl)titanium chloride complex **84**, the crotyl-derived titanacyclobutane series is plagued with the formation of an uncharacterizable byproduct. Allyl, crotyl and cinnamyl complexes **86-88** either do not give the expected titanacyclobutane complex on the addition of stabilized radicals or quickly decompose to paramagnetic material even when the desired titanacyclobutane complex is formed. Furthermore, functionalization of the stable 2,3-disubstituted titanacyclobutane complexes obtained using this template was not successful.

E. Experimental Procedures, Spectroscopic and Analytical Data

General: All manipulations on air sensitive compounds were performed under a nitrogen atmosphere using standard Schlenk techniques, or in nitrogen filled drybox equipped with a freezer maintained at -35°C . Unless stated otherwise, all reactions were carried out under a nitrogen atmosphere. The high vacuum line (10^{-5} mm Hg) was used to add solvent and volatile reagents to reaction mixtures at -198°C via vacuum transfer and to remove volatile compounds from reaction mixtures. Photolysis was carried out using a Hanovia 450 Watt high pressure mercury lamp filtered through Pyrex. Reactions requiring greater than

atmospheric pressure were carried out in reactors consisting of a thick-walled bottle, commercially available from Fisher-Porter, fitted with a safety pressure release, a sample withdrawal port, and a quick-connect hookup.²² IR spectra were recorded on a Nicolet Magna IR 750 or a Nicolet 20SX spectrophotometer and are reported in reciprocal wave numbers (cm^{-1}) calibrated to the 1601 cm^{-1} absorption of polystyrene. All infrared determinations were done on compounds applied as a thin film on KBr or KCl plates and are referred to as 'casts'. The infrared absorption band (between 1480 and 1530 cm^{-1}) for the asymmetric C=C stretch of all allyl and crotyl complexes were assigned tentatively, based on comparison with literature values.^{8,9} Celite filtration in the drybox was performed using a plug of Hyflo Super Cel™ (Fisher) over glass wool in a disposable pipette or through a sintered glass funnel under reduced pressure. Cylindrical medium-walled Pyrex vessels equipped with Kontes K-826510 Teflon vacuum stopcocks are referred to as glass bombs.

Nuclear magnetic resonance spectra (^1H NMR and ^{13}C NMR) were recorded on Bruker AM-400 (^1H , 400 MHz; ^{13}C , 100 MHz), Bruker AM-360 (^1H , 360 MHz), Bruker AM-300 (^1H , 300 MHz; ^{13}C , 75 MHz), Varian Unity-Inova 300 (^1H , 300 MHz) and Unity Inova 500 (^1H , 500 MHz; ^{13}C , 125 MHz) spectrometers. Chemical shifts are reported relative to residual protiated solvent ($\text{CD}_2\text{HC}_6\text{D}_6 = \delta 2.09$, $\text{C}_4\text{HD}_7\text{O} = \delta 1.73$, $\text{C}_6\text{D}_5\text{H} = \delta 7.15$, $\text{CHCl}_3 = \delta 7.26$, $\text{CDHCl}_2 = \delta 5.33$). In ^1H NMR spectral data, values of the coupling constants are either obtained directly from the spectrum, or extracted using standard homonuclear decoupling techniques. Although generally measured to ± 0.1 Hz, J values are self-consistent only to ± 0.5 Hz. Multiplicities are reported as observed, *e.g.* the α -methylene hydrogens of the titanacyclobutane complexes are observed as triplets (doublet of doublets with nearly identical coupling constants) and reported as such even though they arise from coupling between chemically different hydrogens. GCOSY denotes the standard COSY experiment, acquired using field gradients. Data for the ^1H - ^1H COSY or GCOSY is presented such that correlations are listed only once. HMQC

experiments are recorded at the ^1H frequency. Abbreviations used in the assignment of metallacyclobutane resonances are “ α ” (positions adjacent to the metal) and “ β ” (positions distal to the metal). In the assignment of ^1H NMR and ^{13}C NMR spectra, the numbering scheme used for the indenyl ligand is illustrated in Figure 2.1. Primes are used to designate symmetry imposed inequivalency of aryl positions. In complexes where additional aromatic resonances overlap with the indenyl resonances a ubiquitous designation of “aryl” is used.

High resolution mass spectra (HRMS) were obtained on a Kratos MS-50 spectrometer (electron impact ionization (EI)) and elemental analyses were performed by the University of Alberta Microanalysis Laboratories. All air sensitive compounds (2-3 mg) were wrapped in thick-walled pre-weighed tin boats and then further wrapped in pre-weighed tin foil and kept in nitrogen-filled one-dram vials prior to analysis.

X-ray crystallography intensity data were collected on either a Bruker P4/RA/SMART 1000 CCD or a Bruker PLATFORM/SMART 1000 CCD at -80°C with $\text{MoK}\alpha$ radiation. In each case a semiempirical absorption correction was applied to the data. All crystal structures were solved using direct methods (SHELXS-86 or DIRDIF-96)²³ and refined against F^2 using SHELXL-93.²⁴ All non-hydrogen atoms were refined anisotropically.

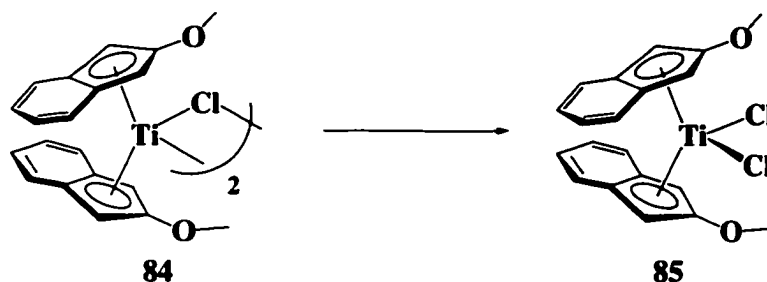
Materials: Unless indicated otherwise, solvents and reagents were purchased from commercial vendors, distilled or passed down a plug of neutral or basic alumina and degassed prior to use by repeated freeze-pump-thaw cycles on a vacuum line. Toluene, benzene, tetrahydrofuran, diethyl ether, hexane and pentane were distilled from sodium/benzophenone ketyl or potassium/benzophenone ketyl. Methylene chloride and chloroform were distilled from calcium hydride and degassed prior to use.

Preparation of cinnamylolithium: In a Schlenk flask, a THF solution (25 mL) of freshly distilled 3-phenylpropene (5.0 mL, 37.7 mmol) was cooled to -78 °C. *n*-Butyllithium (18.1 mL, 2.5 M in hexanes) was transferred via cannula into the flask and the reaction mixture was left to stir for one hour at -78 °C. The reaction mixture was allowed to warm to room temperature and stirred for an additional hour. Removal of the solvent *in vacuo* yielded a yellow solid residue which was washed repeatedly with hexane (4 x 25 mL) to give a brilliant yellow powder (3.98 g, 85%). This material was used without further characterization.

Preparation of crotylmagnesium chloride with activated magnesium:²⁵ In a Schlenk flask, 50 mL of dry THF was added to magnesium turnings (5.0 g) that had previously been vigorously stirred for 6 hours under a nitrogen atmosphere. Crotylchloride (5.0 mL in 15 mL THF) was added dropwise to the turnings over the course of 4 hours. The solution was left to stir for over 14 hours and then allowed to settle. The supernatant was removed via cannula and the concentration determined by titration of 100 µL aliquots of the Grignard with 0.18 M menthol in Et₂O using 1,10-diphenylanthracene as an indicator.

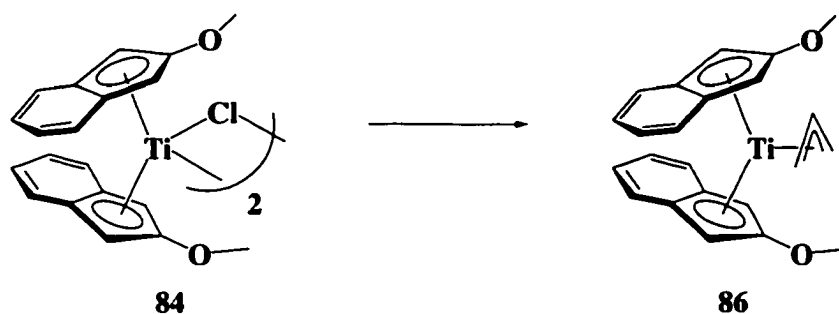
The following compounds were prepared according to published procedures: Cp*₂Ti(C₃H₅) **41**,¹² 2-methylindene,²⁶ 2-methoxyindene,²⁷ TiCl₃•3THF.²⁸

Bis(2-methoxyindenyl)titanium Dichloride 85 from Bis(2-methoxyindenyl)titanium Chloride 84:



Bis(2-methoxyindenyl)titanium dichloride 85. A small sample of chloride complex **84** was oxidized using 0.5 equivalent PbCl_2 in THF at room temperature. After 1 h the residual lead was removed via filtration yielding the corresponding diamagnetic dichloride complex **85**. The material obtained was spectroscopically homogeneous and was not further purified. ^1H NMR (300.1 MHz, C_6D_6): δ 7.43 (2nd order m, 4H, H4/H5), 6.84 (2nd order m, 4H, H4/H5), 4.92 (s, 4H, H2), 3.27 (s, 6H, OCH_3).

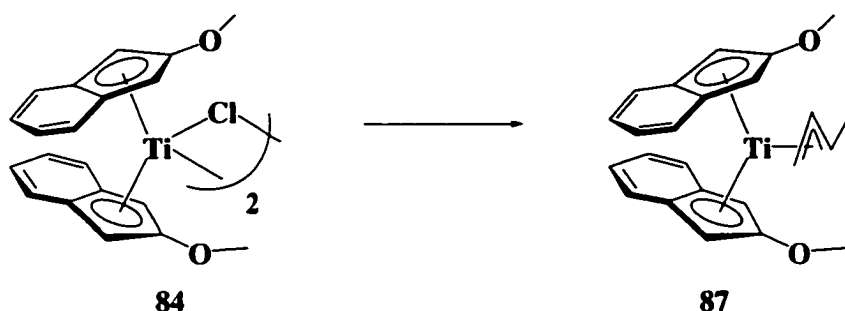
Bis(2-methoxyindenyl)titanium(allyl) 86 from Bis(2-methoxyindenyl)titanium Chloride 84:



Bis(2-methoxyindenyl)titanium(allyl) 86. In the drybox, a vial containing a THF solution (5 mL) of bis(2-methoxyindenyl)titanium chloride **84** (0.114 g, 0.305 mmol) was cooled to $-35\text{ }^\circ\text{C}$. Cold allylmagnesium chloride (0.320 mL, 1.0 M in THF at $-35\text{ }^\circ\text{C}$) was added to chloride complex **84** and the reaction was left overnight at $-35\text{ }^\circ\text{C}$. The

following day, the reaction was evaporated to dryness and the army green residue was triturated with hexane and filtered through a sintered-glass funnel layered with Celite. The solution was concentrated and cooled to $-35\text{ }^{\circ}\text{C}$ affording light brown agglomerates (116 mg) in 80 % yield. IR (cm^{-1} , THF cast): 2956 (m), 2917 (s), 2849 (m), 1606 (m), 1579 (w), 1538 (w), 1496 (m), 1464 (m), 1435 (w), 1422 (w), 1351 (w), 1323 (m), 1260 (w), 1229 (w), 1195 (w), 1141(m), 1018 (m), 799 (s), 746 (s), 694 (m), 649 (w).

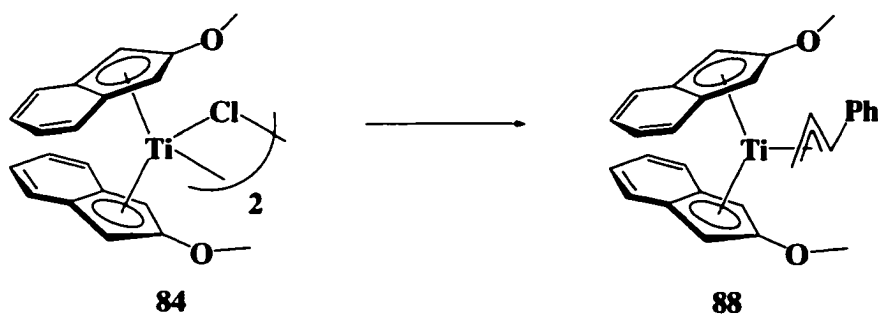
Bis(2-methoxyindenyl)titanium(crotyl) 87 from Bis(2-methoxyindenyl)titanium Chloride 84:



Bis(2-methoxyindenyl)titanium(crotyl) 87. In the drybox, a vial containing a THF solution (7 mL) of bis(2-methoxyindenyl)titanium chloride **84** (0.199 g, 0.524 mmol) was cooled to $-35\text{ }^{\circ}\text{C}$. Crotylmagnesium chloride (0.418 mL, 1.5 M in THF) was added via syringe to the cold solution. The reaction mixture was allowed to warm to room temperature and stir an additional 1.5 h. The solvent was removed under reduced pressure and the dark residue was extracted using benzene. Evaporation of the benzene and further purification from diethyl ether layered with hexane cooled to $-35\text{ }^{\circ}\text{C}$ yielded a dark brown oil (20.6 mg, 10%). IR (cm^{-1} , THF cast): 2936 (m), 1651 (m), 1606 (m), 1536 (m), 1517 (s), 1495 (vs), 1463 (s), 1446 (s), 1422 (vs), 1384 (m), 1350 (s), 1322 (s), 1290 (m), 1240 (m), 1194 (s), 1141 (s), 1125 (s), 1066 (s), 1016 (vs), 803 (s), 748 (vs), 716 (s), 667 (s), 646 (s) 594 (s), 575 (s), 550 (s). HRMS calcd. for $\text{C}_{24}\text{H}_{25}\text{O}_2\text{Ti}$ m/z

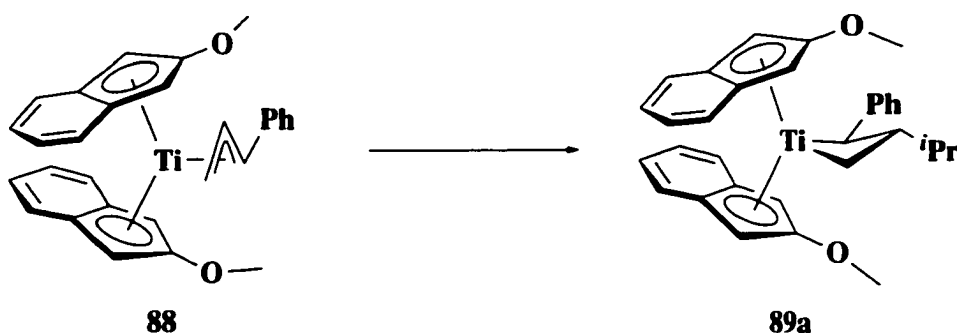
393.341; not found. Calculated for $C_{20}H_{18}O_2Ti$ (titanocene template): m/z 338.0786; found, 338.0797 (100%).

Bis(2-methoxyindenyl)titanium(cinnamyl) 88 from Bis(2-methoxyindenyl)titanium Chloride 84:



Bis(2-methoxyindenyl)titanium(cinnamyl) 88. In the drybox, to a 25 mL round bottomed flask containing a THF solution (10 mL) of bis(2-methoxyindenyl)titanium chloride **84** (0.568 g, 1.518 mmol) cooled to $-35\text{ }^{\circ}\text{C}$, was added a cold THF solution (5 mL) of cinnamyllithium (0.207 g, 1.668 mmol). The reaction mixture was left to warm to room temperature and stir an additional 3 h. The red colour of the chloride complex **84** disappeared quickly and within 1 h the solution turned deep green colour. The THF was removed under reduced pressure and the green residue was extracted into benzene and filtered through a sintered-glass funnel layered with Celite. Evaporation of the benzene and recrystallization from THF carefully layered with hexane cooled to $-35\text{ }^{\circ}\text{C}$ affords dark green hexagons (0.294 g, 43%). IR (cm^{-1} , THF cast): 3009 (m), 2962 (m), 1652 (m), 1593 (s), 1532 (s), 1496 (vs), 1449 (s), 1424 (vs), 1385 (m), 1352 (vs), 1253 (s), 1195 (s), 1141 (vs), 1070 (s), 1025 (vs), 953 (s), 842 (m), 802 (vs), 742 (vs), 698 (s), 667 (s), 649 (s), 550 (m). HRMS calcd. for $C_{29}H_{27}O_2Ti$ m/z 455.1490, found 455.1490. Anal. calcd. C, 76.48; H, 5.98; found C, 75.99; H, 6.16.

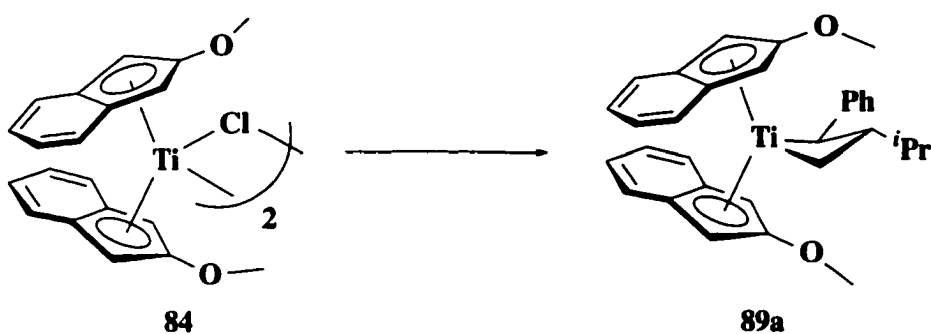
Titanacyclobutane **89a** from Cinnamyl Complex **88**:



3-Isopropyl-2-phenyl-bis(2-methoxyindenyl)titanacyclobutane **89a.** In the drybox, a vial containing a THF solution (2 mL) of bis(2-methoxyindenyl)titanium cinnamyl **88** (154.4 mg, 0.339 mmol) and SmI₂ (3.7 mL, 0.1 M in THF) was cooled to -35 °C and treated with 2-iodopropane (33.8 μL, 0.339 mmol). After 20 minutes at -35 °C, the reaction was left to stir at room temperature for 0.5 h, during which time the colour of the reaction turned from blue/green to dark brown. The solvent was removed *in vacuo*, the residue extracted into benzene and filtered. Evaporation of the benzene followed by crystallization from THF layered with pentane (1 : 5) cooled to -35 °C yielded brown agglomerates of complex **89a** (103.1 mg, 61%). ¹H NMR (360.1 MHz, C₆D₆): δ 7.35 (d, *J* = 8.4 Hz, 1H, C₆H₅), 7.21 (m, 4H, H4/H5), 6.94 (m, 6H, C₆H₅, H4/H5), 6.77 (t, *J* = 7.3 Hz, 1H, C₆H₅), 6.23 (d, *J* = 8.3 Hz, 1H, C₆H₅), 5.58 (d, *J* = 2.1 Hz, 1H, H2), 5.41 (s, 1H, H2'), 5.06 (s, 1H, H2''), 4.62 (s, 1H, H2'''), 3.09 (s, 3H, OCH₃), 2.86 (s, 3H, OCH₃), 2.56 (t, *J* = 8.5 Hz, 1H, α-CH₂), 2.24 (d, *J* = 10.5 Hz, 1H, α-CH), 1.23 (m, 1H, CH(CH₃)₂), 1.09 (d, *J* = 6.5 Hz, 3H, CH(CH₃)₂), 0.91 (d, *J* = 6.6 Hz, 3H, CH(CH₃)₂), 0.79 (t, *J* = 9.3 Hz, 1H, α-CH₂), 0.63 (apparent quintet, *J* = 8.7 Hz, 1H, β-CH). GCOSY (300 MHz, C₆D₆) select data only: δ 2.56 (α-CH₂) ↔ δ 0.79 (α-CH₂) ↔ δ 0.63 (β-CH), δ 2.24 (α-CH) ↔ 0.63 (β-CH), δ 0.63 (β-CH) ↔ δ 1.23 (CH(CH₃)₂) ↔ δ 1.09 (CH(CH₃)₂), δ 0.91 (CH(CH₃)₂). ¹³C NMR (125.7 MHz, C₆D₆): δ 157.5 (C1), 155.0 (C1'), 128.3 (C_{aryl}),

128.1 (C_{aryl}), 127.9 (C_{aryl}), 125.7 (C_{aryl}), 125.5 (C_{aryl}), 125.3 (C_{aryl}), 125.1 (C_{aryl}), 124.2 (C_{aryl}), 124.2 (C_{aryl}), 123.9 (C_{aryl}), 123.8 (C_{aryl}), 121.5 (C_{aryl}), 120.1 (C_{aryl}), 118.9 (C_{aryl}), 117.0 (C_{aryl}), 96.8 ($\alpha\text{-CH}$), 92.2 (C2), 91.3 (C2'), 89.4 (C2''), 89.3 ($\alpha\text{-CH}_2$), 86.4 (C2'''), 56.9 (OCH_3), 56.4 (OCH_3), 35.2 ($\underline{\text{C}}\text{H}(\text{CH}_3)_2$), 25.1 ($\beta\text{-CH}$), 23.9 ($\text{CH}(\underline{\text{C}}\text{H}_3)_2$), 23.0 ($\text{CH}(\underline{\text{C}}\text{H}_3)_2$), three aryl signals not observed are likely obscured by solvent signal. HMQC (300 MHz, C_6D_6) select data only: δ 96.8 ($\alpha\text{-CH}$) \leftrightarrow δ 2.24 ($\alpha\text{-CH}$); δ 92.2 (C2) \leftrightarrow δ 5.58 (H2); δ 91.3 (C2') \leftrightarrow δ 4.62 (H2'); δ 89.4 (C2'') \leftrightarrow δ 5.58 (H2''); δ 89.3 ($\alpha\text{-CH}_2$) \leftrightarrow δ 2.56 ($\alpha\text{-CH}_2$), δ 0.79 ($\alpha\text{-CH}_2$); δ 56.9 (OCH_3) \leftrightarrow δ 3.09 (OCH_3); δ 56.4 (OCH_3) \leftrightarrow δ 2.86 (OCH_3); δ 35.2 ($\underline{\text{C}}\text{H}(\text{CH}_3)_2$) \leftrightarrow δ 1.23 ($\underline{\text{C}}\text{H}(\text{CH}_3)_2$); δ 25.1 ($\beta\text{-CH}$) \leftrightarrow δ 0.63 ($\beta\text{-CH}$); δ 23.9 ($\text{CH}(\underline{\text{C}}\text{H}_3)_2$) \leftrightarrow δ 1.09 ($\text{CH}(\underline{\text{C}}\text{H}_3)_2$); δ 23.0 ($\text{CH}(\underline{\text{C}}\text{H}_3)_2$) \leftrightarrow δ 0.91 ($\text{CH}(\underline{\text{C}}\text{H}_3)_2$). HRMS calcd. for $C_{32}H_{34}O_2Ti$, not found; $C_{20}H_{18}O_2Ti$ (titanocene template) m/z 338.07861, found 338.07883 (100 %). ^1H NMR spectroscopy indicated that the isolated crystals contained a nonstoichiometric amount of entrained THF; anal. calcd. for a THF adduct of complex ($C_{32}H_{34}O_2Ti \cdot C_4H_8O$): C, 75.73; H, 7.41; anal. calcd. for $C_{32}H_{34}O_2Ti$ C, 77.08; H, 6.87; found C, 75.99; H, 7.16.

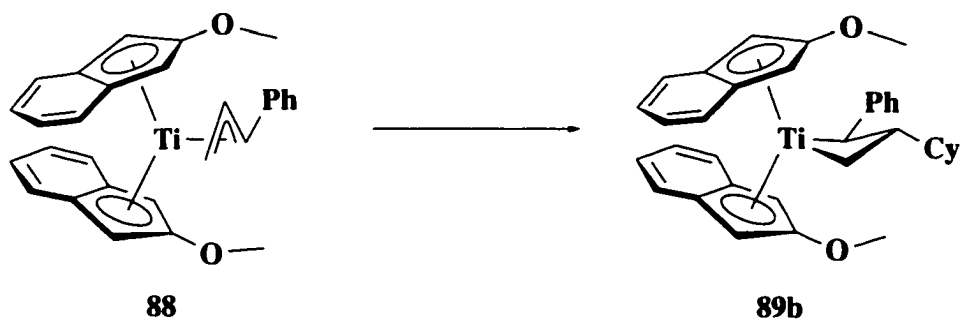
Titanacyclobutane 89a from Bis(2-methoxyindenyl)titanium Chloride 84:



3-Isopropyl-2-phenyl-bis(2-methoxyindenyl)titanacyclobutane 89a. In the drybox, to a vial containing a THF solution (5 mL) of bis(2-methoxyindenyl)titanium chloride **84** (102.9 mg, 0.275 mmol), cooled to $-35\text{ }^\circ\text{C}$, was added an equally cold THF solution (2

mL) of cinnamyl lithium (35 mg, 0.281 mmol). The reaction mixture was left to warm to room temperature and stir an additional 2 h, and was then re-cooled to $-35\text{ }^{\circ}\text{C}$. Following treatment with one equivalent of SmI_2 (2.8 mL, 0.1 M in THF) and, 1 h later, one equivalent of 2-iodopropane (28.0 μL), the reaction mixture was allowed to warm to room temperature and stir an additional 2 h. Upon warming the colour of the reaction turned from blue/green to dark brown. The solvent was removed *in vacuo* and the residue extracted into benzene and filtered. Evaporation of the benzene and crystallization from THF layered with pentane (1 : 5) at $-35\text{ }^{\circ}\text{C}$ yielded brown agglomerates (63.0 mg, 46 %). The recovered material was spectroscopically homogeneous and identical to the material prepared above.

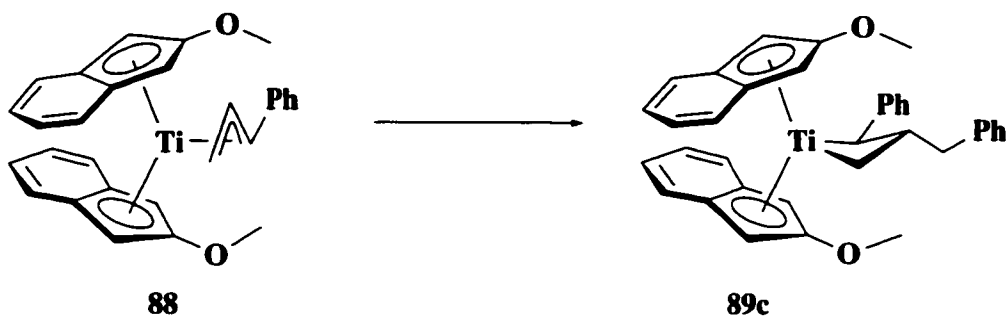
Titanacyclobutane 89b from Cinnamyl Complex 88:



3-Cyclohexyl-2-phenyl-bis(2-methoxyindenyl)titanacyclobutane 89b. In the drybox, a vial containing a THF solution (2 mL) of bis(2-methoxyindenyl)titanium cinnamyl **88** (21.3 mg, 0.0468 mmol) and SmI_2 (0.51 mL, 0.1 M in THF) was cooled to $-35\text{ }^{\circ}\text{C}$. Iodocyclohexane (33.8 μL , 0.339 mmol) was added via syringe to this solution and the resultant reaction mixture was allowed to warm to room temperature and stir for 1 h. The reaction mixture was transferred to a reaction bomb, removed from the drybox, and heated at $40\text{ }^{\circ}\text{C}$ for 1 h and $50\text{ }^{\circ}\text{C}$ for 1.5 h. The solvent was removed *in vacuo* and the reaction bomb was returned to the drybox where the dark brown residue was extracted with pentane. The pentane extracts were filtered, concentrated to approximately 2 mL

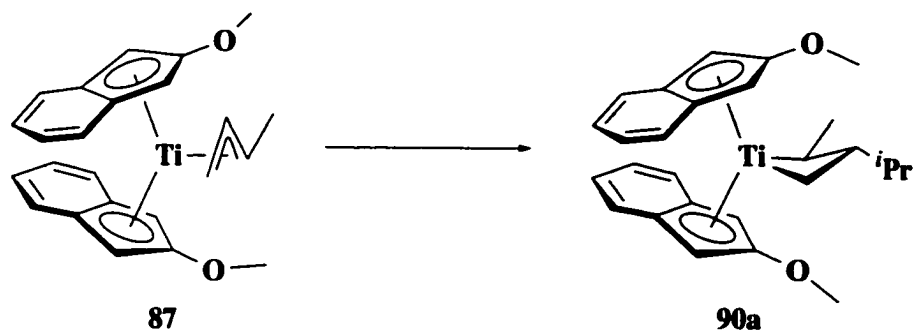
and cooled to $-35\text{ }^{\circ}\text{C}$ to yield titanacyclobutane **89b** as a dark brown powder (13.1 mg, 52%). $^1\text{H NMR}$ (360.1 MHz, C_6D_6): δ 7.34 (d, $J = 7.9$ Hz, 1H, C_6H_5), 7.19 (m, 4H, H4/H5), 6.93 (m, 6H, C_6H_5 , H4/H5), 6.75 (t, $J = 7.4$ Hz, 1H, C_6H_5), 6.22 (d, $J = 8.1$ Hz, 1H, C_6H_5), 5.57 (d, $J = 2.1$ Hz, 1H, H2), 5.20 (s, 1H, H2'), 5.06 (s, 1H, H2''), 4.62 (s, 1H, H2'''), 3.09 (s, 3H, OCH_3), 2.88 (s, 3H, OCH_3), 2.62 (t, $J = 8.6$ Hz, 1H, $\alpha\text{-CH}_2$), 2.26 (br d, $J = 9.6$ Hz, 1H, $\alpha\text{-CH}$), 2.07 (d, $J = 12.5$ Hz, 1H, H_{cy}), 1.89 (br d, $J = 11.4$ Hz, 1H, H_{cy}), 1.61 (m, 3H, H_{cy}), 1.20 (m, 2H, H_{cy}), 1.05 (m, 1H, H_{cy}), 0.94 (m, 3H, H_{cy}), 0.82 (m, 1H, $\alpha\text{-CH}_2$), 0.66 (m, 1H, $\beta\text{-CH}$). GCOSY (300 MHz, C_6D_6) select data only: δ 2.62 ($\alpha\text{-CH}_2$) \leftrightarrow δ 0.82 ($\alpha\text{-CH}_2$) \leftrightarrow δ 0.66 ($\beta\text{-CH}$); δ 2.26 ($\alpha\text{-CH}$) \leftrightarrow 0.66 ($\beta\text{-CH}$). $^{13}\text{C NMR}$ (75.5 MHz, C_6D_6): δ 157.4 (C1), 155.2 (C1'), 125.5 (C_{aryl}), 125.2 (C_{aryl}), 125.1 (C_{aryl}), 124.8 (C_{aryl}), 123.9 (C_{aryl}), 123.7 (C_{aryl}), 123.5 (C_{aryl}), 121.3 (C_{aryl}), 119.8 (C_{aryl}), 118.9 (C_{aryl}), 118.6 (C_{aryl}), 116.7 (C_{aryl}), 96.3 ($\alpha\text{-CH}$), 91.9 (C2), 91.1 (C2'), 89.7 (C2''), 89.2 ($\alpha\text{-CH}_2$), 86.1 (C2'''), 56.6 (OCH_3), 56.1 (OCH_3), 45.1 (C_{cy}), 34.4 (C_{cy}), 33.7 (C_{cy}), 29.9 (C_{cy}), 27.4 (C_{cy}), 27.2 (C_{cy}), 23.6 ($\beta\text{-CH}$), 4 missing aryl signals are likely obscured by solvent signal or coincidental isochrony. HMQC (300 MHz, C_6D_6) select data only: δ 96.3 ($\alpha\text{-CH}$) \leftrightarrow δ 2.26 ($\alpha\text{-CH}$); δ 91.9 (C2) \leftrightarrow δ 5.57 (H2); δ 91.9 (C2') \leftrightarrow δ 4.62 (H2'''); δ 89.7 ($\alpha\text{-CH}_2$) \leftrightarrow δ 2.62 ($\alpha\text{-CH}_2$) \leftrightarrow δ 0.82 ($\alpha\text{-CH}_2$); δ 89.2 (C2'') \leftrightarrow δ 5.20 (H2'); δ 86.1 (C2''') \leftrightarrow δ 5.06 (H2''); δ 56.6 (OCH_3) \leftrightarrow δ 3.09 (OCH_3); δ 56.1 (OCH_3) \leftrightarrow δ 2.88 (OCH_3); δ 45.1 (C_{cy}) \leftrightarrow δ 0.94 (H_{cy}); δ 34.4 (C_{cy}) \leftrightarrow δ 1.61 (H_{cy}), 0.94 (H_{cy}); δ 33.7 (C_{cy}) \leftrightarrow δ 2.07 (H_{cy}), 0.94 (H_{cy}); δ 29.9 (C_{cy}) \leftrightarrow δ 1.20 (H_{cy}); δ 27.4 (C_{cy}) \leftrightarrow δ 1.89 (H_{cy}), 1.05 (H_{cy}); δ 27.2 (C_{cy}) \leftrightarrow δ 1.61 (H_{cy}); δ 23.6 ($\beta\text{-CH}$) \leftrightarrow δ 0.66 ($\beta\text{-CH}$). $^1\text{H NMR}$ spectroscopy indicated that the isolated crystals contained a stoichiometric amount of entrained THF; anal. calcd. for a THF adduct of complex ($\text{C}_{30}\text{H}_{36}\text{O}_2\text{Ti} \cdot \text{C}_4\text{H}_8\text{O}$): C, 74.44; H, 7.08; anal. calcd. for $\text{C}_{30}\text{H}_{36}\text{O}_2\text{Ti}$ C, 75.62; H, 7.61; found C, 74.49; H, 7.58.

Titanacyclobutane 89c from Cinnamyl Complex 88:



3-Benzyl-2-phenyl-bis(2-methoxyindenyl)titanacyclobutane 89c. In the drybox, a vial containing a THF solution (2 mL) of bis(2-methoxyindenyl)titanium cinnamyl **88** (30.7 mg, 0.0674 mmol) and SmI_2 (0.75 mL, 0.1 M in THF) cooled to $-35\text{ }^\circ\text{C}$, was treated with benzyl chloride (7.7 μL , 0.0674 mmol). The resultant reaction mixture was left to warm to room temperature and, after 20 minutes at this temperature, the blue/green solution turned red brown. The solvent was removed under reduced pressure, the product extracted into pentane, filtered and evaporated to dryness. A ^1H NMR spectrum taken of the crude product suggests the formation of titanacyclobutane complex **89c**. Attempted crystallization from concentrated solutions of pentane gave an intractable brown oil. ^1H NMR (360.1 MHz, C_6D_6): 7.27-6.89 (m, 16H, aryl), 6.67 (t, $J = 8.3$ Hz, 1H, C_6H_5), 6.37 (d, $J = 8.5$ Hz, 1H, C_6H_5), 5.58 (d, $J = 2.0$ Hz, 1H, H2), 5.16 (d, $J = 2.1$ Hz, 1H, H2'), 4.88 (d, $J = 2.4$ Hz, 1H, H2''), 4.74 (d, $J = 2.0$ Hz, 1H, H2'''), 3.09 (s, 3H, OCH_3), 2.84 (s, 3H, OCH_3), 2.83 (obscured signal, 1H, $\text{CH}_2(\text{C}_6\text{H}_5)$), 2.34 (t, $J = 10.9$ Hz, 1H, $\alpha\text{-CH}_2$), 2.00 (dd, $J = 15.9, 10.9$ Hz, 1H, $\text{CH}_2(\text{C}_6\text{H}_5)$), 1.66 (d, $J = 12.5$ Hz, 1H, $\alpha\text{-CH}$), 0.88 (m, 1H $\beta\text{-CH}$), 0.47 (t, $J = 12.1$ Hz, 1H, $\alpha\text{-CH}_2$).

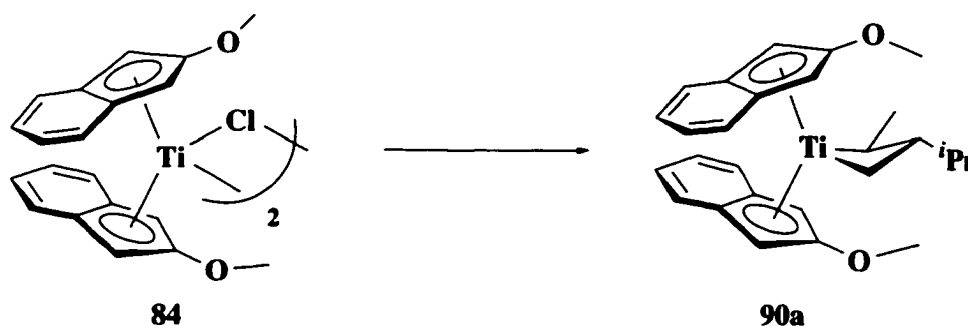
Titanacyclobutane 90a from Crotyl Complex 87:



3-Isopropyl-2-methyl-bis(2-methoxyindenyl)titanacyclobutane 90a. In the drybox, a vial containing a THF solution (5 mL) of bis(2-methoxyindenyl)titanium crotyl **87** (139.8 mg, 0.354 mmol) and SmI_2 (3.55 mL, 0.1 M in THF) was cooled to $-35\text{ }^\circ\text{C}$ and treated with 2-iodopropane (35.3 μL , 0.354 mmol) via syringe. The reaction mixture was left at $-35\text{ }^\circ\text{C}$ for 10 minutes and then allowed to warm to room temperature. On warming the colour of the reaction quickly turned from blue to burgundy and with bright yellow SmI_2X precipitate formation. The solvent was removed under reduced pressure, the burgundy residue was triturated with pentane and filtered through a short plug of Celite. The solution was concentrated and cooled to $-35\text{ }^\circ\text{C}$ yielding purple agglomerated needles of titanacyclobutane complex **90a** in 72% yield (111.3 mg). Thermal instability precluded full characterization of this product. $^1\text{H NMR}$ (360.1 MHz, C_6D_6): δ 7.27 (m, 4H, H4/H5), 6.94 (m, 4H, H4/H5), 5.38 (d, $J = 2.0\text{ Hz}$, 1H, H2), 5.17 (d, $J = 2.3\text{ Hz}$, 1H, H2'), 4.58 (d, $J = 2.1\text{ Hz}$, 1H, H2''), 4.47 (d, $J = 2.4\text{ Hz}$, 1H, H2'''), 2.94 (s, 3H, OCH_3), 2.93 (s, 3H, OCH_3), 2.68 (t, $J = 8.8\text{ Hz}$, 1H, $\alpha\text{-CH}_2$), 1.88 (m, 1H, $\alpha\text{-CH}(\text{CH}_3)$), 1.80 (d, $J = 6.5\text{ Hz}$, 3H, $\text{CH}(\text{CH}_3)_2$), 1.53 (apparent octet, $J = 6.7\text{ Hz}$, 1H, $\text{CH}(\text{CH}_3)_2$), 1.16 (d, $J = 6.5\text{ Hz}$, 3H, $\text{CH}(\text{CH}_3)_2$), 1.14 (obscured signal, 1H, $\alpha\text{-CH}_2$), 1.09 (d, $J = 6.6\text{ Hz}$, 3H, $\text{CH}(\text{CH}_3)_2$), -0.33 (dq, $J = 6.7\text{ Hz}$, 9.0 Hz, 1H, $\beta\text{-CH}$). GCOSY (300 MHz, C_6D_6) select data only: δ 2.68 ($\alpha\text{-CH}_2$) \leftrightarrow δ 1.14 ($\alpha\text{-CH}_2$) \leftrightarrow δ -0.33 ($\beta\text{-CH}$); δ -0.33 ($\beta\text{-CH}$) \leftrightarrow δ 1.88 ($\alpha\text{-CH}(\text{CH}_3)$) \leftrightarrow δ 1.80 ($\text{CH}(\text{CH}_3)_2$); δ -0.33 ($\beta\text{-CH}$) \leftrightarrow δ 1.53 ($\text{CH}(\text{CH}_3)_2$) \leftrightarrow δ

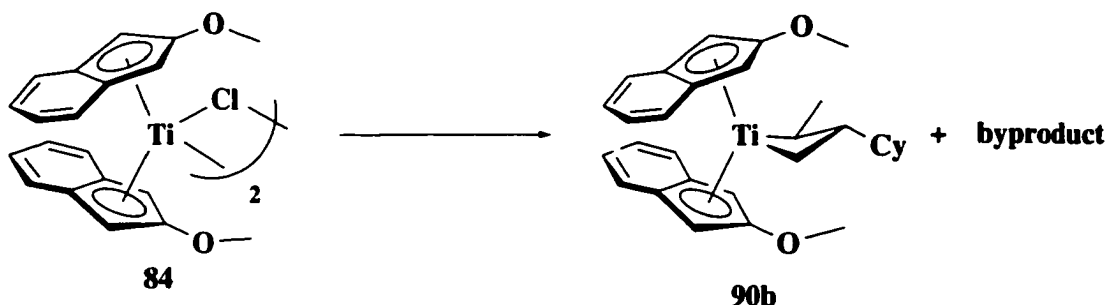
1.16 (CH(CH₃)₂), δ 1.09 (CH(CH₃)₂). ¹³C NMR (100.6 MHz, C₆D₆): δ 157.5, 156.3, 125.6, 125.4, 124.7, 123.3, 123.2, 122.9, 122.8, 118.5, 117.5, 117.2, 117.0, 96.3, 91.8, 90.5, 87.1, 86.8, 85.3, 56.6, 56.2, 34.5, 29.3, 28.6, 24.1, 22.1.

Titanacyclobutane 90a from Bis(2-methoxyindenyl)titanium Chloride 84:



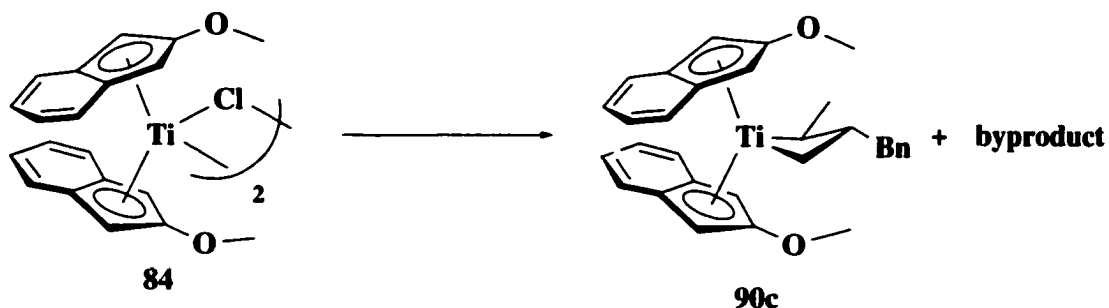
3-Isopropyl-2-methyl-bis(2-methoxyindenyl)titanacyclobutane 90a. In the drybox, a vial containing a THF solution (2 mL) of bis(2-methoxyindenyl)titanium chloride **84** (43.3 mg, 0.116 mmol) was cooled to $-35\text{ }^{\circ}\text{C}$. One equivalent of crotylmagnesium chloride (80 μL , 1.5 M in THF) was added to the solution, which was then left at $-35\text{ }^{\circ}\text{C}$ for 1 h, stirred at room temperature for 0.5 h, and re-cooled to $-35\text{ }^{\circ}\text{C}$. SmI_2 (1.25 mL, 0.1 M in THF) was added to the reaction followed 1 h later by 2-iodopropane (11.9 μL , 0.119 mmol). The resultant reaction mixture was then allowed to warm to room temperature and within 15 minutes the colour of the solution turned from blue/brown to burgundy with bright yellow SmI_2X precipitate formation. The solution was decanted and evaporated to dryness. The residue was triturated with pentane, filtered through Celite and evaporated to dryness yielding 98% (49.6 mg) of titanacyclobutane complex **90a** which was found to be spectroscopically identical to that previously prepared from crotyl complex **87**.

Titanacyclobutane **90b** from Bis(2-methoxyindenyl)titanium Chloride **84**:



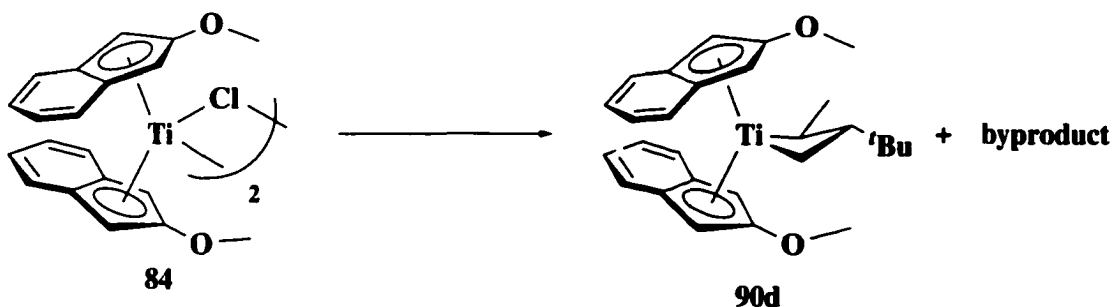
3-Cyclohexyl-2-methyl-bis(2-methoxyindenyl)titanacyclobutane **90b.** In the drybox, to a vial containing a THF solution (2 mL) of bis(2-methoxyindenyl)titanium chloride (42.0 mg, 0.112 mmol) cooled to $-35\text{ }^{\circ}\text{C}$, was added one equivalent of crotylmagnesium chloride (75 μL , 1.5 M in THF). The reaction mixture was left at $-35\text{ }^{\circ}\text{C}$ for 1 h, stirred at room temperature for 0.5 h, re-cooled to $-35\text{ }^{\circ}\text{C}$, and treated with SmI_2 (1.15 mL, 0.1 M in THF). After 1 h, one equivalent of iodocyclohexane (14.5 μL) was added to the reaction mixture which was then left to warm to room temperature. After stirring 2 h, the colour of the solution turned from blue/brown to burgundy with bright yellow SmI_2X precipitate formation. The solution was decanted and evaporated to dryness *in vacuo*. The product was extracted into pentane, filtered and the pentane evaporated under reduced pressure. A ^1H NMR spectrum of the crude indicated formation of the titanacyclobutane **90b** as well as small amounts of a byproduct (^1H NMR data given pp. 77). Further purification or characterization was not attempted. ^1H NMR (360.1 MHz, C_6D_6): δ 7.28 (m, 4H, H4/H5), 6.89 (m, 4H, H4/H5), 5.37 (d, $J = 1.9$ Hz, 1H, H2), 5.19 (d, $J = 1.9$ Hz, 1H, H2'), 4.59 (d, $J = 1.7$ Hz, 1H, H2''), 4.49 (d, $J = 1.7$ Hz, 1H, H2'''), 2.96 (s, 3H, OCH_3), 2.95 (s, 3H, OCH_3), 2.71 (t, $J = 8.8$ Hz, 1H, $\alpha\text{-CH}_2$), 2.03 (d, $J = 12.1$ Hz, 1H, H_{cy}), 1.96 (m, 1H, H_{cy}), 1.84 (m, 1H, $\text{CH}(\text{CH}_3)$), 1.80 (d, $J = 6.6$ Hz, 3H, $\text{CH}(\text{CH}_3)$), 1.72 (m, 2H, H_{cy}), 1.64 (m, 2H, H_{cy}), 1.52 (m, 2H, H_{cy}), 1.30 (m, 4H, $\alpha\text{-CH}_2$, H_{cy}), -0.33 (m, 1H, $\beta\text{-CH}$).

Titanacyclobutane 90c from Bis(2-methoxyindenyl)titanium Chloride 84:



3-Benzyl-2-methyl-bis(2-methoxyindenyl)titanacyclobutane 90c. In the drybox, a vial containing a THF solution (4 mL) of bis(2-methoxyindenyl)titanium chloride (45.0 mg, 0.120 mmol) cooled to $-35\text{ }^{\circ}\text{C}$ was treated with one equivalent of crotylmagnesium chloride (80.0 μL , 1.5 M in THF). After leaving the reaction mixture at $-35\text{ }^{\circ}\text{C}$ for 1 h, it was then stirred at room temperature for 0.5 h and re-cooled to $-35\text{ }^{\circ}\text{C}$. SmI_2 (1.20 mL, 0.1 M in THF) was added to the reaction mixture followed 1 h later by one equivalent of benzyl chloride (13.8 μL). The reaction was left at $-35\text{ }^{\circ}\text{C}$ for an additional 0.5 h and then allowed to warm to room temperature. Upon warming, the colour of the solution turned from blue/brown to grey to red. The reaction mixture was decanted from the yellow SmI_2X precipitate, evaporated under reduced pressure to dryness, triturated with pentane and filtered. The pentane extracts were evaporated under reduced pressure to afford a red oil. ^1H NMR spectroscopy of the crude suggests formation of titanacyclobutane **90c** in addition to an uncharacterized byproduct. Further purification was not attempted. ^1H NMR (360.1 MHz, C_6D_6 , the complexity of the spectrum does not allow for full assignment): δ 5.33 (d, $J = 2.3$ Hz, 1H, H2), 4.88 (d, $J = 2.2$ Hz, 1H, H2'), 4.68 (d, $J = 2.0$ Hz, 1H, H2''), 4.53 (d, $J = 2.1$ Hz, 1H, H2'''), 2.89 (s, 3H, OCH_3), 2.86 (s, 3H, OCH_3), 2.59 (t, $J = 8.4$ Hz, 1H, $\alpha\text{-CH}_2$), 2.24 (dd, $J = 10.5, 8.0$ Hz, 1H, $\text{CH}_2(\text{C}_6\text{H}_5)$), 1.72 (m, 1H, $\text{CH}(\text{CH}_3)$), 1.69 (d, $J = 6.8$ Hz, 3H, $\text{CH}(\text{CH}_3)$), 1.05 (t, $J = 8.3$ Hz, 1H, $\alpha\text{-CH}_2$), 0.75 (m, 1H, $\beta\text{-CH}$).

Titanacyclobutane 90d from Bis(2-methoxyindenyl)titanium Chloride 84:



3-*tert*-Butyl-2-methyl-bis(2-methoxyindenyl)titanacyclobutane 90d. In the drybox, a vial containing a THF solution (2 mL) of bis(2-methoxyindenyl)titanium chloride **84** (47.0 mg, 0.126 mmol) cooled to $-35\text{ }^{\circ}\text{C}$ was treated with one equivalent of crotylmagnesium chloride (84.0 μL , 1.5 M in THF). The reaction mixture was left at $-35\text{ }^{\circ}\text{C}$ for 1 h, stirred at room temperature for 0.5 h, re-cooled to $-35\text{ }^{\circ}\text{C}$ and treated with SmI_2 (1.30 mL, 0.1 M in THF); 1h later *tert*-butyl chloride (13.4 μL , 0.126 mmol) was added. The reaction mixture was left at $-35\text{ }^{\circ}\text{C}$ overnight. The following morning, the colour of the solution had turned from blue/brown to grey. The reaction mixture was left to stir at room temperature for an additional 1 h and, thereafter, decanted from the yellow SmI_2X precipitate. The purple solution was evaporated under reduced pressure to dryness, the products were extracted into pentane, filtered and concentrated under reduced pressure to purple oil. A ^1H NMR spectrum of the crude indicated formation of titanacyclobutane **90d**, 3,4-dimethylpentene and an additional byproduct. Further purification was not attempted. ^1H NMR (300.1 MHz, C_6D_6): δ 7.28 (m, 4H, H4/H5), 6.89 (m, 4H, H4/H5), 5.66 (s, 1H, H2), 5.50 (s, 1H, H2'), 4.51 (s, 1H, H2''), 4.46 (s, 1H, H2'''), 2.94 (s, 3H, OCH_3), 2.93 (s, 3H, OCH_3), 2.60 (t, $J = 8.7\text{ Hz}$, 1H, $\alpha\text{-CH}_2$), 1.82 (m, 1H, $\text{CH}(\text{CH}_3)$), 1.78 (d, $J = 8.0\text{ Hz}$, 3H, $\text{CH}(\text{CH}_3)$), 1.11 (t, $J = 8.6\text{ Hz}$, 1H, $\alpha\text{-CH}_2$), 0.83 (s, 9H, $\text{C}(\text{CH}_3)_3$), 0.021 (q, $J = 8.6\text{ Hz}$, 1H, $\beta\text{-CH}$).

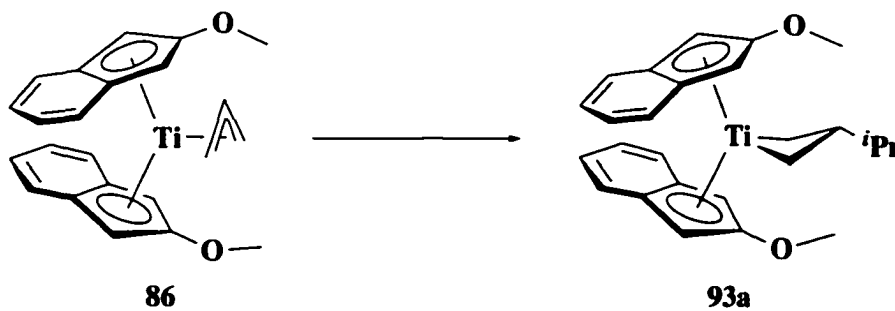
Synthesis of the uncharacterized byproduct:

Method 1. In the drybox, a vial containing a THF solution (4 mL) of bis(2-methoxyindenyl)titanium chloride **84** (44.0 mg, 0.118 mmol) cooled to $-35\text{ }^{\circ}\text{C}$ was treated with one equivalent of crotylmagnesium chloride (82.0 μL , 1.5 M in THF) and then left at $-35\text{ }^{\circ}\text{C}$ for 1 h followed by 30 minutes at room temperature. Following the addition of SmI_2 (1.20 mL, 0.1 M in THF) the reaction mixture was re-cooled to $-35\text{ }^{\circ}\text{C}$, treated with crotyl bromide (11.0 μL , 0.118 mmol) and left at $-35\text{ }^{\circ}\text{C}$ for 48 h. During this time the colour of the solution was not seen to change from the brown/blue colour originally observed, however a bright yellow precipitate of SmI_2X formed. The solution was decanted and evaporated to dryness under reduced pressure. The brown residue was triturated with a benzene/hexane mixture (1 : 4), filtered through Celite, and the solvent removed *in vacuo*. Further purification was not attempted. ^1H NMR (360.1 MHz, C_6D_6 , the identity of this compound remains unknown; the signal with the smallest integration is assigned 1H): δ 7.01 (m, 1H), 6.83 (m 2H), 6.14 (m, 2H), 5.98 (m, 2H), 5.67 (m, 1H), 3.25 (dt, $J = 6.9\text{ Hz}, 3.7\text{ Hz}$, 1H), 3.22 (s, 3H), 2.02 (m, 1H), 1.73 (m, 1H), 1.50 (d, $J = 8.3\text{ Hz}$, 1H), 1.25 (m, 1H), 1.21 (d, $J = 5.8\text{ Hz}$, 3H), 0.30 (m, 1H), -0.16 (m, 2H), -0.65 (d, $J = 12.8\text{ Hz}$, 1H).

Method 2. In the drybox, a vial containing a THF solution (2 mL) of bis(2-methoxyindenyl)titanium chloride (24.5 mg, 0.0655 mmol) was cooled to $-35\text{ }^{\circ}\text{C}$. Following the addition of one equivalent of crotylmagnesium chloride (45.0 μL , 1.5 M in THF), the reaction was left at $-35\text{ }^{\circ}\text{C}$ for 1 h, treated with half of an equivalent of PbCl_2 (9.1 mg, 0.0328 mmol) and left at $-35\text{ }^{\circ}\text{C}$ for an additional 30 minutes. The reaction was allowed to warm to room temperature. After stirring 1 h, the reaction mixture was filtered through Celite to removed elemental lead and evaporated to dryness under reduced pressure. The residue was triturated with benzene/hexane mixture (1 : 4), filtered through Celite and dried *in vacuo*. ^1H NMR spectroscopy indicated that the

product formed was identical to the product formed in Method 1 as well as the byproduct observed in the syntheses of crotyl-derived titanacyclobutane complexes.

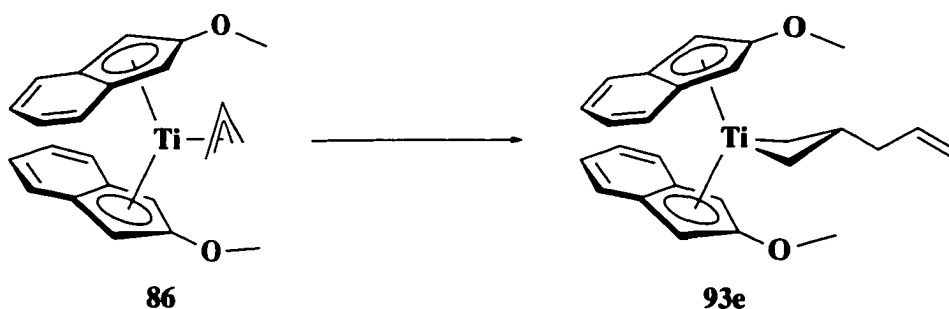
Titanacyclobutane 93a from Allyl Complex 86:



3-Isopropyl-bis(2-methoxyindenyl)titanacyclobutane 93a. In the drybox, a vial containing a THF solution (5 mL) of bis(2-methoxyindenyl)titanium allyl **86** (92.4 mg, 0.243 mmol) was cooled to $-35\text{ }^{\circ}\text{C}$ and treated with SmI_2 (2.70 mL, 0.1 M in THF). The reaction mixture was re-cooled to $-35\text{ }^{\circ}\text{C}$, treated with 2-iodopropane (24.3 μL , 0.243 mmol), left at $-35\text{ }^{\circ}\text{C}$ for 0.5 h, and then allowed to warm to room temperature. On warming, the colour of the solution quickly turned red with formation of SmI_2X precipitate. The THF was removed under reduced pressure and the resultant red residue was extracted into pentane and filtered. Recrystallization from a cold ($-35\text{ }^{\circ}\text{C}$) concentrated pentane solution afforded dark red agglomerated needles (50.6 mg, 49%). ^1H NMR (300 MHz, C_6D_6): δ 7.24 (2nd order m, 2H, H4/H5), 7.17 (2nd order m, 2H, H4/H5), 6.86 (2nd order m, 4H, H4/H5), 4.79 (s, 2H, H2), 4.77 (s, 2H, H2'), 2.89 (s, 3H, OCH_3), 2.88 (s, 3H, OCH_3), 2.22 (dd, $J = 10.4, 8.7$ Hz, 2H $\alpha\text{-CH}_2$), 1.91 (t, $J = 8.5$ Hz, 2H, $\alpha\text{-CH}_2$), 1.23 (d, $J = 6.3$ Hz, 6H, $\text{CH}(\text{CH}_3)_2$), 1.07 (dseptets, $J = 6.4, 2.4$ Hz, 1H, $\text{CH}(\text{CH}_3)_2$), 0.02 (apparent sextet, $J = 8.6$ Hz, 1H, $\beta\text{-CH}$). GCOSY (300 Mz, C_6D_6) select data only: δ 2.22 ($\alpha\text{-CH}_2$) \leftrightarrow δ 1.91 ($\alpha\text{-CH}_2$) \leftrightarrow δ 0.02 ($\beta\text{-CH}$), δ 1.23 ($\text{CH}(\text{CH}_3)_2$) \leftrightarrow δ 1.07 ($\text{CH}(\text{CH}_3)_2$), δ 1.07 ($\text{CH}(\text{CH}_3)_2$) \leftrightarrow δ 0.02 ($\beta\text{-CH}$). ^{13}C NMR (75 MHz, C_6D_6): δ

157.6 (C1), 155.5 (C1'), 125.7 (C4/C5), 125.5 (C4/C5), 123.0 (C4/C5), 122.8 (C4/C5), 117.3 (C3), 116.7 (C3'), 89.3 (C2), 88.5 (C2'), 87.5 (α -CH₂), 56.4 (OCH₃), 56.2 (OCH₃), 37.0 ($\underline{\text{C}}\text{H}(\text{CH}_3)_2$), 24.3 ($\underline{\text{C}}\text{H}(\text{CH}_3)_2$), 21.3 (β -CH). HMQC (300 MHz, C₆D₆) select data only: δ 89.3 (C2) \leftrightarrow δ 4.79 (H2); δ 88.5 (C2') \leftrightarrow δ 4.77 (H2'); δ 87.5 (α -CH₂) \leftrightarrow δ 2.22 (α -CH₂) \leftrightarrow δ 1.91 (α -CH₂); δ 56.4 (OCH₃) \leftrightarrow δ 2.89 (OCH₃); δ 56.2 (OCH₃) \leftrightarrow δ 2.88 (OCH₃); δ 37.0 ($\underline{\text{C}}\text{H}(\text{CH}_3)_2$) \leftrightarrow δ 1.07 ($\underline{\text{C}}\text{H}(\text{CH}_3)_2$); δ 24.3 ($\underline{\text{C}}\text{H}(\text{CH}_3)_2$) \leftrightarrow δ 1.23 ($\underline{\text{C}}\text{H}(\text{CH}_3)_2$); δ 21.3 (β -CH) \leftrightarrow δ 0.02 (β -CH). HRMS calcd. for C₂₆H₃₀O₂Ti, not found; C₂₃H₂₃O₂Ti (titanocene allyl) *m/z* 379.11774, found 379.11848 (0.24%); C₂₀H₁₈O₂Ti (titanocene template) *m/z* 338.07861, found 338.07975 (13%).

Titanacyclobutane 93e from Allyl Complex 86:



3-Allyl-bis(2-methoxyindenyl)titanacyclobutane 93e. In the drybox, a vial containing a THF solution (2 mL) of bis(2-methoxyindenyl)titanium allyl **86** (37.2 mg, 0.0980 mmol) and SmI₂ (1.10 mL, 0.1 M in THF) was cooled to -35 °C. The reaction mixture was treated with allyl bromide (10.0 μ L, 0.108 mmol) and left at -35 °C for 0.5 h, followed by 10 minutes at room temperature. On warming, the colour of the solution quickly turned red with formation of SmI₂X precipitate. The THF was removed under reduced pressure, the resulting red residue was extracted into pentane, filtered, and evaporated to dryness. A ¹H NMR of the resultant red oil suggests the formation of titanacyclobutane **93e**, however decomposition of complex **93e** occurs prior to crystallization from a concentrated cooled (-35 °C) pentane solution. ¹H NMR (300

MHz, C₆D₆): δ 7.23 (2nd order m, 4H, H4/H5), 6.85 (2nd order m, 4H, H4/H5), 6.14 (ddt, $J = 16.2, 9.4, 6.0$ Hz, 1H, CH₂CH=CH₂), 5.15 (overlapping signals, 2H, CH₂CH=CH₂), 4.75 (s, 2H, H2), 4.65 (s, 2H, H2'), 2.88 (s, 3H, OCH₃), 2.87 (s, 3H, OCH₃), 2.41 (dd, $J = 10.9, 8.7$ Hz, 2H, α -CH₂), 2.22 (m, 1H, CH₂CH=CH₂), 1.91 (t, $J = 8.0$ Hz, 2H, α -CH₂), 0.45 (m, 1H, β -CH).

F. References

1. (a) Kirmse, W.; Loosen, K. *Chem. Ber.* **1981**, *114*, 400. (b) Kirmse, W.; Loosen, K.; Sluma, H. -D. *J. Am. Chem. Soc.* **1981**, *103*, 5935. (c) Mironov, V. A.; Luk'yanov, V. T.; Bernadskii, A. A. *J. Org. Chem. USSR* **1984**, 61. (d) Olson, D. R.; Platz, M. S. *J. Phys. Org. Chem.* **1996**, *9*, 759.
2. (a) Keefe, J. R.; Kresge, A. J.; Yin, Y. *J. Am. Chem. Soc.* **1988**, *110*, 8202. (b) Eliasson, B.; Edlund, U. *J. Chem. Soc., Perkin. Trans.* **1981**, *2*, 403.
3. (a) Foster, P.; Rausch, M. D.; Chien, J. C. W. *J. Organomet. Chem.* **1997**, *527*, 71. (b) Lieno, R.; Luttikhedde, H.; Wilén, C. -E.; Sillanpää, R.; Näsman, J. H. *Organometallics*, **1996**, *15*, 2450.
4. Manzer, L. E. *Inorg. Synth.* **1982**, *21*, section 31.
5. The molar ratio of **84** to **84**•LiCl(THF)₂ could not be determined precisely; the yield of the reaction is estimated assuming conversion to the complex **84** alone. The yield of the reaction is actually lower.
6. Monomeric complexes: (a) Pattisina, J. W.; Heeres, H. J.; van Bolhuis, F.; Meetsma, A.; Teuben, J. H. *Organometallics* **1987**, *6*, 1004. (b) Castellani, M. P.; Geib, S. J.; Rheingold, A. L.; Trogler, W. C. *Organometallics* **1987**, *6*, 2524. (c) Urazowski, I. F.; Ponomaryov, V. I.; Ellert, O. G.; Nifant'ev, I. E.; Lemenovskii, D. A. *J. Organomet. Chem.* **1988**, *356*, 181. (d) Troyanov, S. I.; Rybakov, V. B.; Thewalt, U.; Varga, V.; Mach, K. *J. Organomet. Chem.* **1993**, *447*, 221. Dimeric complexes: (e)

- Jungst, R.; Sekutowski, D.; Davis, J.; Luly, M.; Stucky, G. *Inorganic Chem.* **1977**, *16*, 1645. (f) Martin, J.; Fauconet, M.; Moïse, C. *J. Organomet. Chem.* **1989**, *371*, 87.
7. Carter, C. A. G.; McDonald, R.; Stryker, J. M. *Organometallics* **1999**, *18*, 820.
 8. Martin, H. A.; Jellinek, F. *J. Organomet. Chem.* **1967**, *8*, 115.
 9. Martin, H. A.; Jellinek, F. *J. Organomet. Chem.* **1968**, *12*, 149.
 10. (a) Martin, H. A.; Lemaire, P. J.; Jellinek, F. *J. Organomet. Chem.* **1968**, *14*, 149. (b) Yasuda, H.; Kajihara, Y.; Mashima, K.; Nagasuna, K.; Nakamura, A. *Chem. Lett.* **1981**, 671. Mashima, K.; Yasuda, H.; Asami, K.; Nakamura, A. *Chem. Lett.* **1983**, 219. (c) Blenkins, J.; de Liefde Meijer, H. J.; Teuben, J. H. *J. Organomet. Chem.* **1981**, *218*, 383. (d) McDade, C.; Bercaw, J. E. *J. Organomet. Chem.* **1985**, *279*, 281. (e) Highcock, W. J.; Mills, R. M.; Spencer, J. L.; Woodward, P. *J. Chem. Soc., Dalton Trans.* **1986**, 829, and references therein. (f) Larson, E. J.; van Dort, P. C.; Lakanen, J. R.; O'Neill, D. W.; Pederson, L. M.; McCandless, J. J.; Silver, M. E.; Russo, S. O.; Huffman, J. D. *Organometallics* **1988**, *7*, 1183. Vance, P. J.; Prins, T. J.; Hauger, B. E.; Silver, M. E.; Wemple, M. E.; Pederson, L. M.; Kort, D. A.; Kannisto, M. R.; Geerligs, S. J.; Kelly, R. S.; McCandless, J. J.; Huffman, J. D.; Peters, D. G. *Organometallics* **1991**, *10*, 917. (g) Tjaden, E. B.; Stryker, J. M. *J. Am. Chem. Soc.* **1993**, *115*, 2083.
 11. Girard, P.; Namy, J. L.; Kagan, H. B. *J. Am. Chem. Soc.* **1980**, *102*, 2693.
 12. Casty, G. L.; Stryker, J. M. *J. Am. Chem. Soc.* **1995**, *117*, 7814.
 13. Ogoshi, S.; Stryker, J. M. *J. Am. Chem. Soc.* **1998**, *120*, 3514.
 14. Tjaden, E. B. Ph. D. Thesis, Indiana University, 1993.
 15. (a) Howard, T. R.; Lee, J. B.; Grubbs, R. H. *J. Am. Chem. Soc.* **1980**, *102*, 6876. (b) Lee, J. B.; Ott, K. C. Grubbs, R. H. *J. Am. Chem. Soc.* **1982**, *104*, 7491. (c) Ikariya, T.; Ho, S. C. H.; Grubbs, R. H. *Organometallics* **1985**, *4*, 199.
 16. Casty, G. L. Ph. D Thesis, Indiana University, 1994.
 17. Carter, C. A. G. Ph. D Thesis, University of Alberta, 1994.

18. (a) Lee, J. B.; Gajda, G. J.; Schaefer, W. P.; Howard, T. R.; Ikariya, T.; Straus, D. A.; Grubbs, R. H. *J. Am. Chem. Soc.* **1981**, *103*, 7358. (b) Gilliom, L. R.; Grubbs, R. H. *Organometallics* **1986**, *5*, 721. (c) Straus, D. A.; Grubbs, R. H. *J. Mol. Catal.* **1985**, *28*, 9. (d) Stille, J. R.; Santarsiero, B. D.; Grubbs, R. H. *J. Org. Chem.* **1990**, *55*, 843.
19. (a) Seetz, J. W. F. L.; Schat, G.; Akkerman, O. S.; Bickelhaupt, F. *Angew. Chem. Int. Ed. Engl.* **1983**, *22*, 248. (b) Seetz, J. W. F. L.; Van de Heisteeg, B. J.; Schat, G.; Akkerman, O. S.; Bickelhaupt, F. *J. Mol. Catal.* **1985**, *28*, 71.
20. Polse, J. L.; Kaplan, A. W.; Anderson, R. A.; Bergman, R. G. *J. Am. Chem. Soc.* **1998**, *120*, 6316. (b) Polse, J. L.; Anderson, R. A.; Bergman, R. G. *J. Am. Chem. Soc.* **1996**, *118*, 8737.
21. This assignment was based on a similar ¹H NMR spectrum reported for bis(indenyl)titanium dicarbonyl; in addition, both complexes have the same colour: Rausch, M. D.; Moriarty, K. J.; Atwood, J. L.; Hunter, W. E.; Samuel, E. J. *Organomet. Chem.* **1987**, *327*, 39.
22. Messerle, L. in *Experimental Organometallic Chemistry*, Wayda, A. L., Darensburg, M. Y., ed.; The American Chemistry Society: Washington, 1987, Chapter 7.
23. SHELXS-86: Sheldrick, G. M. *Acta Crystallogr.* **1990**, *A46*, 467–473; DIRDIF-96: Beurskens, P. T.; Beurskens, G.; Bosman, W. P.; de Gelder, R.; Garcia Granda, S.; Gould, R. O.; Israel, R.; Smits, J. M. M. (1996). The DIRDIF-96 program system. Crystallography Laboratory, University of Nijmegen, The Netherlands.
24. Sheldrick, G. M. *SHELXL-93*. Program for crystal structure determination. University of Göttingen, Germany, 1993.
25. Baker, K. V.; Brown, J. M.; Hughes, N.; Skarnulis, A. J.; Sexton, A. *J. Org. Chem.* **1991**, *56*, 698.
26. Ready, T. E.; Chein, J. C. W.; Rausch, M. D. *J. Organometallic Chem.* **1999**, *583*, 11.

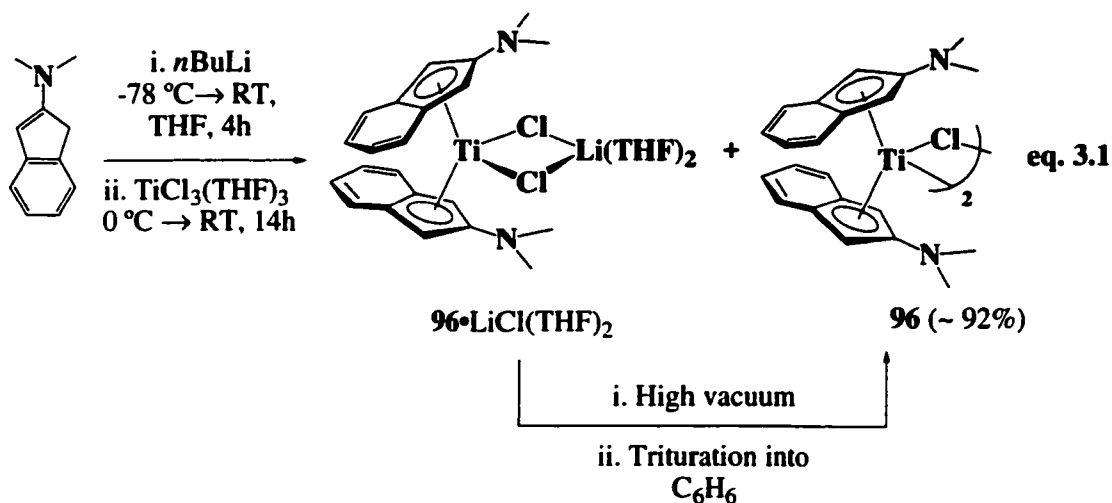
27. (a) Keefe, *J. Am. Chem. Soc.* **1988**, *110*, 8202. (b) Eliasson, B.; Edlund, U. *J. Chem. Soc., Perkin. Trans.* **1981**, *2*, 403.
28. Manzer, L. E. in *Inorg. Synth.* **1982**, *21*, section 31.

Chapter 3. Central Carbon Radical Alkylation of Bis(2-*N,N*-dimethylaminoindenyl)titanium(III) η^3 -Allyl Complexes

All evidence indicates that templates that are strongly electron-donating and sterically unimposing promote regioselective central carbon alkylation at substituted allyl ligands. Although alkylation of substituted allyl complexes **60** and **61**, with ansa-bridged ancillary ligands (p. 25), provides the highest yields of 2,3-disubstituted titanacyclobutane complexes, it is the bis(2-piperidinoindenyl)titanium(III) template **52**, that was best suited for further functionalization of resultant titanacyclobutane complexes to give *trans*-2,3-disubstituted cyclobutanones.^{1,2} The use of the piperidinoindenyl template, as previously discussed, appears to be limited to alkylations using unstabilized alkyl radicals and suffers from rapid β -hydride elimination from titanacycles bearing an α -methyl substituent.^{1,3} Unfavourable steric interactions generated by the relatively large piperidino substituent on the indenyl rings were postulated to be at least partly responsible for the relative facility of this β -hydride elimination.

A. Synthesis of Bis(2-*N,N*-dimethylaminoindenyl)titanium(III) η^3 -Allyl Complexes

To combat these limitations, the development of the less sterically demanding but similarly electron-rich bis(2-*N,N*-dimethylaminoindenyl)titanium(III) template, **96**, was initiated. The synthesis of this template was accomplished by lithiation of 2-*N,N*-dimethylaminoindene⁴ using *n*-butyllithium in THF and *in situ* slow addition of this solution to a suspension of $\text{TiCl}_3 \cdot \text{THF}$ at room temperature (eq. 3.1). The addition of isolated 2-*N,N*-dimethylaminoindenyllithium as an amorphous solid to a suspension of $\text{TiCl}_3 \cdot 3\text{THF}$ failed to give complex **96**, as did the use of 2-*N,N*-dimethylamino-1-trimethylsilylindene⁵ or 1-tributylstannyl-2-*N,N*-dimethylaminoindene⁶ as milder ligand transfer reagents. Initial crystallization of complex **96** from THF layered with hexane gave a mixture of green crystals and an amorphous terra cotta red solid. Slow



recrystallization of this mixture from THF afforded a low yield of green single crystals suitable for X-ray crystallography. The complex was revealed to incorporate an equivalent of lithium chloride, as well as two THF ligands completing the lithium ion coordination sphere (Figure 3.1). The green crystals of complex $96 \cdot \text{LiCl}(\text{THF})_2$, upon extensive drying under high vacuum, returned to a terra cotta red amorphous powder. This red powder was taken up into benzene, filtered and recrystallized from THF layered with hexane to analytical purity. Whereas elemental analysis is consistent with formation of bis(2-*N,N*-dimethylaminoindenyl)titanium chloride **96**, the solid state structure of this complex is likely dimeric, as the considerable steric hindrance needed in the ancillary ligands to prevent dimerization is absent (*vide supra*).⁷ As the molar ratio of complex **96** to complex $96 \cdot \text{LiCl}(\text{THF})_2$ could not be determined precisely, the yield of the reaction is estimated based on conversion to complex **96** alone (92%), as it is the major product isolated in this procedure. The actual yield of the reaction is somewhat lower. Further support for the identity of complex **96** is garnered by PbCl_2 oxidative chlorination to give the dichloride complex **97** (eq. 3.2), which has been fully characterized.

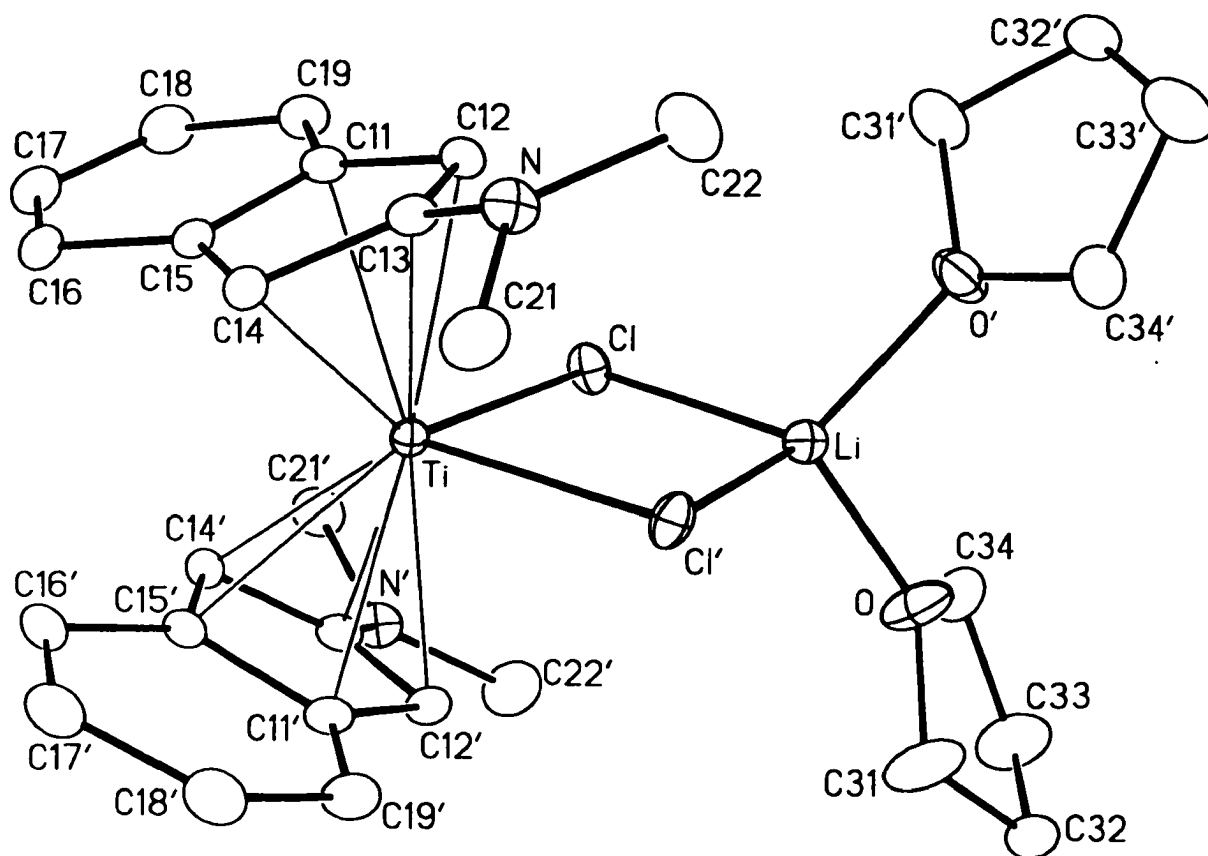
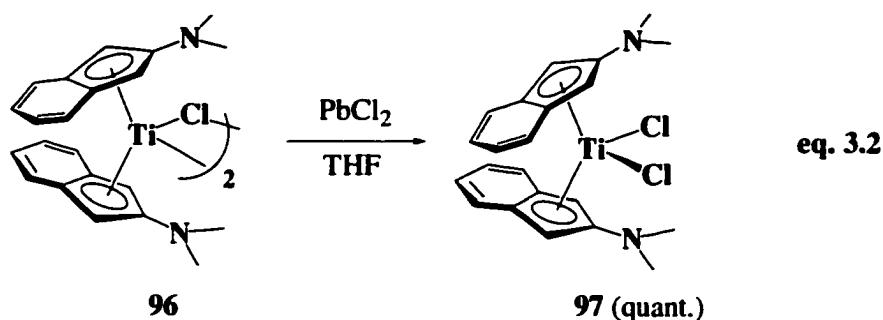


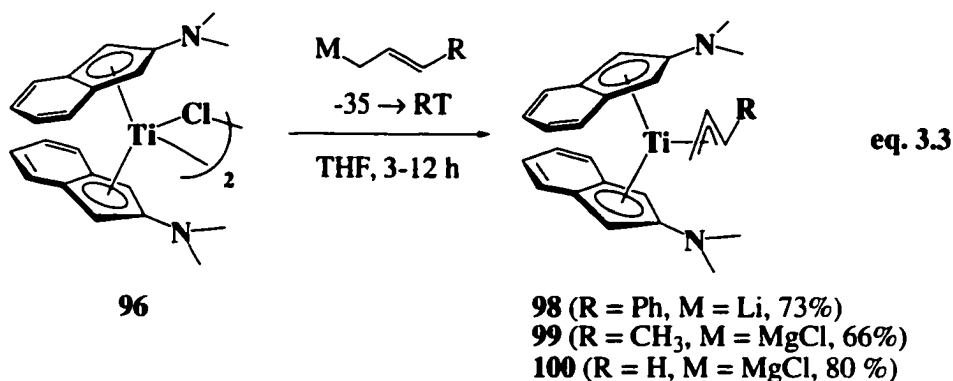
Figure 3.1 The molecular structure of bis(2-*N,N*-dimethylaminoindenyl)titanium chloride-lithium chloride·2THF, **96**·LiCl(THF)₂. Selected interatomic distances are listed in Table 3.4. Crystallographic details are given in Appendix I.



The synthesis of bis(2-*N,N*-dimethylaminoindenyl)titanium chloride **96** thus leads initially to bis(2-*N,N*-dimethylaminoindenyl)titanium chloride-lithium chloride•2THF, which on drying loses THF and lithium chloride to give complex **96**. In the synthesis of bis(2-methoxyindenyl)titanium chloride **84** (eq. 2.2, pg. 45), it is thus likely that the complex also initially exists as a lithium chloride adduct, as the bulk material isolated in equation 2.2 was never extensively dried under high vacuum and purification was attempted only by recrystallization. Though elemental analysis was reproducible, values obtained were inconsistent with the formation of analytically pure salt-free **84** which accounts for the speculation that the product mixture analyzed was actually obtained as a mixture of **84** and **84**•LiCl(THF)₂.

The cinnamyl, crotyl and allyl complexes **98**, **99** and **100** were obtained upon treatment of complex **96** with cinnamyllithium, crotylmagnesium chloride and allylmagnesium chloride, respectively, at -35 °C in THF (eq. 3.3). The cinnamyl complex **98** was isolated as a deep green crystalline material in 73% yield. This complex is mildly unstable and over the course of several months at room temperature decomposes to an intractable brown solid. The green colour of complex **98** is again attributed to the extended conjugation afforded by the phenyl substituent on the allyl ligand; the unsubstituted allyl complex **100** is orange. Structural characterization of complex **98** was accomplished by X-ray diffraction of a single crystal obtained from a

dilute solution of the complex in THF layered with hexane and cooled to -35°C . In addition, infrared spectroscopy, elemental analysis and high resolution mass spectrometry were used.

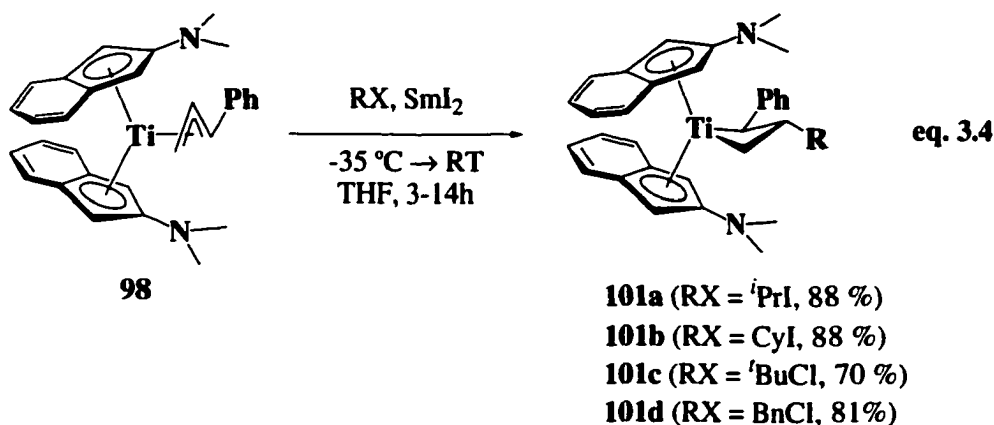


Crotyl complex **99** was isolated as a very dark red oil in 66% yield. Interestingly, the use of crotylmagnesium bromide in place of the chloride leads to a significantly lower yield. Characterization of this very air sensitive material was difficult. Elemental analysis of this paramagnetic complex was not within tolerable allowances, a problem also observed for other oxophilic early metal complexes,⁸ and high resolution mass spectrometry failed to provide a parent ion peak. As this complex coordinates an allylic anion, an infrared absorption band between 1480 and 1540 cm^{-1} of moderate to strong intensity is expected for the allylic asymmetric C=C stretch.^{9,10} However, in the IR spectrum of **99**, three bands were observed in this region (1548 (vs), 1529 (s), 1486 (m)). The presence of these three bands makes it difficult to assign the coordination between the crotyl substituent and titanium. After repeated recrystallization from dilute solutions of diethyl ether carefully layered with hexane, single crystals suitable for X-ray crystallographic analysis were obtained, which unambiguously identified the *syn*- η^3 -coordination of the crotyl ligand to the titanium template in the solid state. A more detailed analysis of the crystal structures of complexes **98** and **99** is given in Section C of this chapter.

Unsubstituted allyl complex **100**, obtained in good yield, was characterized by IR spectroscopy. In contrast to crotyl complex **99**, only one $C=C_{\text{asym}}$ stretch was observed (1546 cm^{-1}). The positioning of this band occurs near the highest energy $C=C_{\text{asym}}$ stretch observed for crotyl complex **99**. This result is surprising as it indicates that the presence of a methyl group has little effect on this asymmetric stretch.^{9,10} Nonetheless, elemental analysis is consistent with simple allyl coordination to the 2-*N,N*-dimethylaminoindenyl template.

B. Radical Addition to Crotyl and Cinnamyl Complexes

Despite the apparently subtle change in structure and electron donating capability on proceeding from the 2-piperidinoindenyl to the 2-*N,N*-dimethylaminoindenyl system, the latter is compatible with an extended range of radical alkylations and dramatically increases the thermal stability of α -methyl substituted titanacyclobutane complexes. The complex 3-isopropyl-2-phenyl-bis(2-*N,N*-dimethylaminoindenyl)titanacyclobutane, **101a**, can be synthesized from the Ti(III) cinnamyl complex **98** upon addition of one equivalent of both isopropyl iodide and samarium diiodide at low temperature (eq. **3.4**). That the central carbon alkylation step proceeds below room temperature again suggests that the electron-rich Ti(III) complex **98** reacts directly with isopropyl iodide, leading to the formation of an allyltitanium(IV) iodo intermediate and the isopropyl radical, the latter of which alkylates the remaining Ti(III) allyl complex (see Scheme **2.1**, pg. 48). The allyl Ti(IV) halide intermediate is then reduced by SmI_2 to regenerate the allyltitanium(III) complex. It is also possible that an adventitious titanium complex provides the catalyst required for the reaction at low temperature. Thermally stable and deep red in colour, single crystals of complex **101a** were isolated by recrystallization from cold ($-35\text{ }^\circ\text{C}$) THF layered with hexane in 88% yield.



Spectroscopic analysis reveals that complex **101a** is fluxional at room temperature: warming the complex in solution (70 °C) results in the sharpening of the two broad indenyl singlets observed at δ 4.27 and 4.05 into mutually coupled doublets with a coupling constant of 2.1 Hz, suggesting hindered rotation for one of the dimethylaminoindenyl rings. Together with the two additional indenyl resonances observed at δ 5.44 (d, $J = 2.3$ Hz) and 5.42 (d, $J = 2.3$ Hz) and the inequivalent dimethylamino groups at δ 2.43 and 2.38, the top to bottom, as well as side to side, dissymmetry expected in this 2,3-disubstituted titanacyclobutane complex is evident. Once this fast exchange limit is reached, the featureless titanacyclobutane α -CH₂ signal also sharpens into a triplet at δ 0.56 with a coupling constant of 9.6 Hz. The other signals for the four-membered titanacycle ring are the upfield resonance for the β -hydrogen atom observed as a multiplet at δ 1.10 and downfield resonances for the additional α -methylene hydrogen atom at δ 2.61 (t, $J = 9.0$ Hz) and α -methine hydrogen atom at δ 3.28 (d, $J = 10.7$ Hz). The chemical shift difference between the two α -methylene protons and the pronounced downfield shift for the β -methine hydrogen (more typically observed upfield of 0.5 ppm) mirrors both the 2-methoxyindenyl (*vide supra*) and 2-piperidinoindenyl¹ analogues and supports structural similarity among these three complexes. The isopropyl substituent is characterized by two doublets at δ 1.16 ($J = 6.5$ Hz) and δ 1.06 ($J = 6.5$) for the diastereotopic methyl groups and the isopropyl methine

proton at δ 1.57 that appears as a coincidental octet ($J = 7.0$ Hz). Overlapping signals with indenyl resonances precludes full assignment of the phenyl substituent. These assignments were identified by, and are fully consistent with, the GCOSY spectrum taken of complex **101a**, and have been tabulated into Table 3.1. A ^1H NMR spectrum acquired at -60 °C identified the presence of three rotational isomers in a ratio of 2 : 2 : 1; the complexity of this spectrum discouraged any attempt at complete assignment. Characteristic ^{13}C NMR resonances for the titanacyclobutane ring at room temperature, determined by HMQC experiments, occur at δ 87.6 and 80.0 for the α -methine and α -methylene carbons, respectively, and a typical high field signal at δ 26.5 for the β -carbon. Based on the spectroscopic similarity to the piperidinoindenyl titanacyclobutane complex **55a**¹ and 2-methoxyindenyl titanacyclobutane complex **89a** (see Table 2.1, pg. 48), the titanacyclobutane substituents were assigned the expected *trans* stereochemistry; this was also verified crystallographically (*vide infra*).

Cinnamyl complex **98** also traps cyclohexyl radicals to give the expected 3-cyclohexyl-2-phenyl titanacyclobutane **101b** (eq. 3.4) in high yield under reaction conditions identical to those given above to **101a**. Characterization of this complex was accomplished in a manner similar to complex **101a**. Pertinent ^1H NMR spectroscopic data for complex **101b**, given in Table 3.1, indicates the structural similarity to the isopropyl complex **101a**. The GCOSY spectrum of complex **101b** confirms that the α -methylene and α -methine resonances in the ^1H NMR occur at δ 2.69 (t, $J = 8.8$ Hz), 0.61 (br m) and 3.33 (d, $J = 10.7$ Hz), respectively. All of these signals are coupled to the β -methine signal observed upfield at δ 1.11. HMQC correlations were consistent with the α -methylene and α -methine carbon signals in the ^{13}C NMR at δ 80.9 and 87.2, respectively. The typical upfield signal for the β -carbon occurs at δ 25.5. Cyclohexyl-substituted titanacyclobutane complex **101b** was crystallized out of a concentrated THF solution layered with hexane cooled to -35 °C, giving dark brown rhomboid crystals in

88% yield. ^1H NMR spectroscopy indicates that the isolated crystals contain a nonstoichiometric amount of entrained THF, fully consistent with the elemental analysis of this complex.

Table 3.1 Room Temperature ^1H NMR Resonances of Titanacyclobutane Complexes **101a-d**

	101a , R = 'Pr δ (m, J, I)*	101b , R = Cy δ (m, J, I)*	101c , R = 'Bu δ (m, J, I)*	101d , R = BnCl δ (m, J, I)*
Ti-CH ₂	2.65 (t, 9.0, 1H) 0.61 (br s, 1H)	2.69 (t, 8.8, 1H) 0.61 (br s, 1H)	2.65 (t, 9.5, 1H) 1.38 (br s, 1H)	2.57 (t, 9.4, 1H) 0.22 (t, 9.1, 1H)
Ti-CH(Ph)	3.32 (d, 10.7, 1H)	3.33 (d, 10.7, 1H)	3.58 (d, 11.3, 1H)	3.04 (d, 2H)
-CH	1.04 (m, 1H)	1.11 (obscured, 1H)	0.18 (br s, 1H)	1.51 (dqintets, 8.5, 4.3 1H)
CH(Indeny l)	5.41 (d, 1.7, 1H) 5.31 (d, 2.3, 1H) 4.27 (br s, 1H) 4.05 (br s, 1H)	5.42 (s, 1H) 5.34 (d, 2.2, 1H) 4.27 (s, 1H) 4.02 (s, 1H)	5.79 (d, 2.3, 1H) 5.66 (s, 1H) 4.05 (br s, 1H) 3.89 (br s, 1H)	5.31 (d, 2.2, 1H) 4.88 (d, 2.2, 1H) 4.44 (s, 1H) 4.25 (s, 1H)
NMe ₂	2.36 (s, 6H) 2.23 (s, 6H)	2.36 (s, 6H) 2.26 (s, 6H)	2.42 (br s, 6H) 2.28 (br s, 6H)	2.36 (s, 6H) 2.13 (s, 6H)
R	1.50 (m, 1H) 1.15 (d, 6.6, 3H) 1.05 (d, 6.7, 3H)	2.17 (m, 1H) 1.83 (t, 12.9, 2H) 1.68 (d, 5.3, 2H) 1.34-1.15 (m, 6H)	1.03 (s, 9H)	3.04 (overlapping doublets, 2H) 2.38 (obscured, 1H)

* δ = chemical shift, m = multiplicity, J = JHH in Hz, I = integral

Bulky *tert*-butyl radicals can also be trapped by cinnamyl complex **98** to give 3-*tert*-butyl-2-phenyl titanacyclobutane complex **101c** in moderate yield (eq. **3.4**). As in the two previous cases, the reaction proceeds at low temperatures, suggesting that it is the titanium complex that reacts with the alkyl halide to generate the radical despite the bulk of *tert*-butyl chloride. The fluxionality of complex **101c** manifests itself in the broad nature of the room temperature ^1H NMR spectrum. In addition to several indeterminate aryl resonances, the only sharp signals present are a doublet at δ 3.58 ($J = 11.3$ Hz, α -

methine proton) and a triplet at δ 2.65 ($J = 9.5$ Hz, deshielded α -methylene proton), indicating that the fluxionality does not directly involve the titanacyclobutane ring. Cooling the sample to -60 °C provides a static spectrum of the complex where two non-interconverting conformers of complex **101c** exist in a 5 : 1 ratio. In the limiting spectrum, the titanacyclobutane core of the major isomer gives rise to a typical doublet at δ 3.48 ($J = 11.1$ Hz) for the α -methine proton, triplets at δ 2.73 ($J = 9.4$ Hz) and 0.71 ($J = 9.8$ Hz) for the α -methylene signals, and a quartet (expected dt) at δ 1.58 ($J = 10.0$ Hz) for the β -methine hydrogen atom. These assignments were verified by 2-dimensional ^1H NMR spectroscopy. The *tert*-butyl substituent is observed as singlet at δ 1.15. Although not fully characterized, the most significant signal for the minor isomer is a triplet located at δ -1.44 ($J = 10.0$ Hz), which is likely to arise from an α -methylene proton. If this is indeed the case, the orientation of the indenyl ligands in the two conformers is likely as illustrated in Figure 3.2. In the major conformer (Structure A) the titanacyclobutane core experiences less shielding from the indenyl rings, whereas in the minor isomer (Structure B), the bottom indenyl ring shields one of the α -methylene signals. The ^{13}C NMR spectrum of these static structures was also collected. Based on correlations obtained from the HMQC experiment, the titanacyclobutane signals for the major isomer are observed at δ 77.1 for the α -methine carbon, δ 72.0 for the α -methylene carbon, and a slightly more upfield signal for the β -methine carbon at δ 14.6 caused by anisotropic shielding from one of the indenyl rings. The high temperature limiting spectrum for complex **101c** could not be obtained due to thermal decomposition (presumably cycloreversion) that occurs at the temperature needed to obtain this spectrum (>70 °C). ^1H NMR spectroscopy reveals that the crystals obtained by concentrating the complex in THF, layering with hexane and cooling to -35 °C contain a stoichiometric amount of entrained THF; this is consistent with the elemental analysis of complex **101c**.

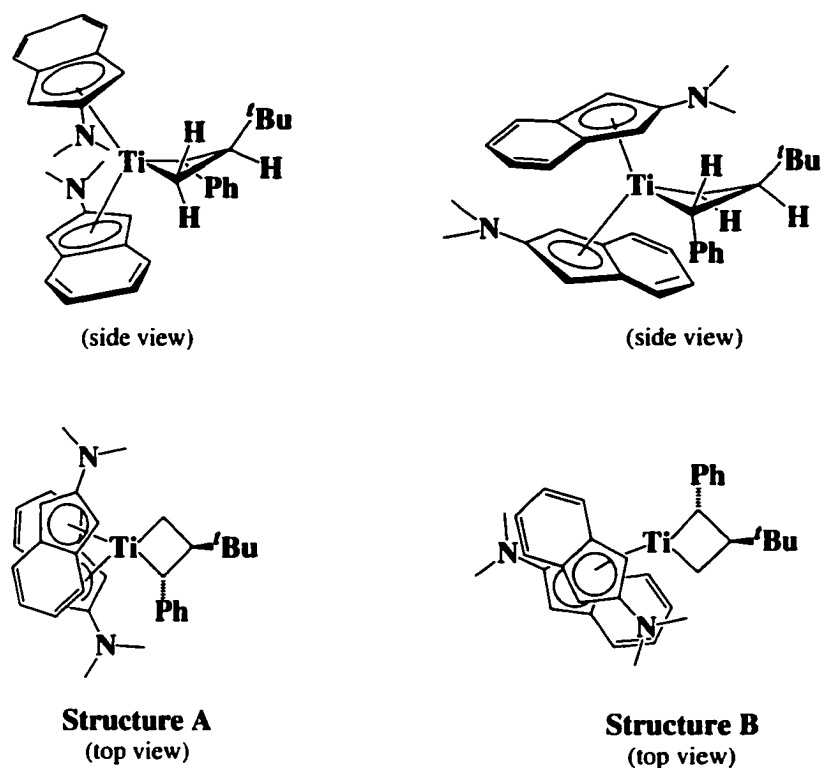


Figure 3.2 Proposed Structures for Non-interconverting Conformers of 101c at -60 °C

Not only does the addition of benzyl radical to cinnamyl complex **98** result in the formation of thermally *stable* 2-phenyl-3-benzyl titanacyclobutane complex **101d**, it does so efficiently (eq. 3.4). The spectral and analytical data obtained for complex **101d** are fully consistent with the assigned structure (Table 3.1).

Surprisingly, the addition of allyl radical to cinnamyl complex **98** does not result in the formation of a titanacyclobutane complex. Although the colour change over the course of the reaction (green → brown) is consistent with all previously examined radical reactions of this template, the ^1H NMR spectrum of the crude reaction mixture does not indicate the formation of the desired titanacyclobutane complex. Observed instead are very broad signals characteristic of paramagnetic titanium material. The addition of the

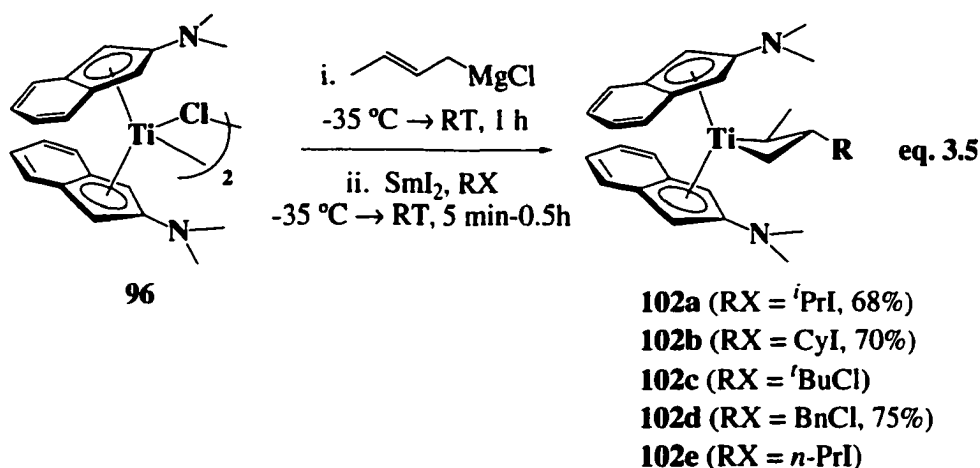
n-propyl radical to cinnamyl complex **98** does appear to result in titanacyclobutane formation; however, the resonances in the crude ¹H NMR spectrum also indicate the formation of a substantial amount of an unknown byproduct. All attempts to separate the two complexes by selectively crystallizing one product out of the reaction mixture resulted in complete decomposition to a paramagnetic amorphous red material, which could not be characterized.

From a synthetic standpoint, a one pot procedure for the synthesis of titanacyclobutane complexes is highly desirable. For this reason, the one pot procedure developed for the 2-methoxyindenyl template **84** was extended to the 2-*N,N*-dimethylaminoindenyl template. To obtain cinnamyl-derived titanacyclobutane complexes **101a-d**, the chloride complex **96** was alkylated *in situ* with cinnamyl lithium and then treated directly with the respective alkyl halide and samarium diiodide at low temperature. The reaction mixture was allowed to warm to room temperature and the reaction worked up in a manner identical to the two-step synthesis described above. The yields for this one pot procedure are comparable to, if not better than, the overall yields obtained when cinnamyl complex **98** is isolated (Table 3.2).

Table 3.2 Yields of One Pot Procedure for Titanacyclobutane Complexes **101a-d**

Complex	R-X	Yield (one pot, %)	Yield (two-step 96 → 98 → 101 , %)
101a	^t PrI	74	64
101b	CyI	60	64
101c	^t BuCl	49	51
101d	BnCl	53	59

Because isolation of crotyltitanium(III) complex **99** in crystalline form was so difficult, the one pot alkylation procedure was used to obtain crotyl-derived titanacyclobutane complexes, avoiding the isolation of this troublesome intermediate. Thus, chloride complex **96** was alkylated with crotyl Grignard, followed directly by addition of one equivalent each of isopropyl iodide and samarium diiodide to afford analytically pure titanacyclobutane complex **102a** as dark purple microcrystals in an overall 68% yield (eq. 3.5). In contrast to the thermally unstable titanacyclobutane complexes derived from bis(2-piperidinoindenyl)titanium(η^3 -crotyl) **54**, the dimethylaminoindenyl complex **102a** is substantially more stable; notable decomposition is observed only after several hours in solution at room temperature.



Identification of this complex was again accomplished by spectroscopic and analytical analysis and is fully consistent with a 2,3-disubstituted titanacyclobutane structure. Worthy of comment, however, is the upfield shift of the β -methine signal in the ^1H NMR spectrum at δ -0.015 (dq, $J = 9.9, 6.5$ Hz) relative to the cinnamyl-derived titanacyclobutane complexes. This significantly more shielded environment for the β -methine proton indicates that the orientation of the ancillary ligands in the solution structure of complex **102a** is likely similar to Structure B, illustrated in Figure 3.2.

Comparative ^1H NMR data for all crotyl-derived titanacyclobutane complexes are provided in Table 3.3.

Table 3.3 Room Temperature ^1H NMR Resonances of Titanacyclobutane Complexes **102a-e**

	102a , R = 'Pr δ (m, J, I)*	102b , R = Cy δ (m, J, I)*	102c , R = 'Bu δ (m, J, I)*	102d , R = BnCl δ (m, J, I)*	102e , R = Pri δ (m, J, I)*
Ti-CH ₂	2.46 (t, 9.1, 1H) 0.79 (t, 9.7, 1H)	2.49 (t, 8.9, 1H) 0.78 (t, 9.7, 1H)	1.28 (t, 9.6, 1H) 0.88 (t, 8.7, 1H)	2.47 (t, 9.0, 1H) 0.75 (t, 9.9, 1H)	2.45 (t, 8.7, 1H) 1.06 (t, 9.6, 1H)
Ti-CH(CH ₃)	2.22 (dq, 6.9, 9.9, 1H)	2.24 (dq, 9.2, 4.7, 1H)	2.32 (obscured, 1H)	1.86 (obscured, 1H)	1.27 (obscured, 1H)
Ti-CH(CH ₃)	1.83 (d, 6.9, 3H)	1.85 (d, 6.6, 3H)	1.28 (d, 6.9, 3H)	1.81 (d, 6.1, 3H)	1.29 (d, 6.3, 3H)
β -CH	-0.015 (dq, 9.9, 6.5, 1H)	-0.001 (dq, 8.9, 4.0, 1H)	0.41 (dt, 9.5, 8.2, 1H)	0.40 (dq, 8.1, 4.1, 1H)	-0.062 (m, 1H)
CH _(indenyl)	5.34 (d, 2.2, 1H) 5.10 (d, 2.3, 1H) 4.15 (d, 2.2, 1H) 4.07 (d, 2.2, 1H)	5.33 (d, 1.8, 1H) 5.11 (d, 2.0, 1H) 4.15 (d, 1.9, 1H) 4.05 (d, 2.1, 1H)	5.65 (d, 2.1, 1H) 5.52 (d, 2.1, 1H) 4.08 (s, 2H)	5.22 (d, 2.3, 1H) 4.82 (d, 2.3, 1H) 4.22 (d, 2.2, 1H) 4.06 (d, 2.2, 2H)	5.12 (d, 1.8, 1H) 4.84 (d, 1.8, 1H) 4.22 (d, 1.2, 1H) 4.11 (d, 1.5, 1H)
NMe ₂	2.31 (s, 6H) 2.29 (s, 6H)	2.31 (s, 6H) 2.30 (s, 6H)	2.33 (s, 6H) 2.31 (s, 6H)	2.29 (s, 6H) 2.15 (s, 6H)	2.33 (s, 6H) 2.29 (s, 6H)
R	1.71 (octet, 6.7, 1H) 1.24 (d, 6.7, 3H) 1.18 (d, 6.6, 3H)	2.07 (d, 13.2, 1H) 1.89 (obscured, 2H) 1.77 (d, 9.1, 2H) 1.39-1.11 (m, 6H)	1.11 (s, 9H)	3.11 (dd, 12.7, 3.9, 1H) 2.30 (obscured, 1H)	1.90 (m, 2H) 1.55 (m, 2H) 1.11 (t, 7.2, 1H)

δ = chemical shift, m = multiplicity, J = J_{HH} in Hz, I = integral

Making use of this one pot methodology, 3-cyclohexyl-2-methyl-titanacyclobutane **102b** was obtained in 70% yield by alkylating chloride complex **96** with crotyl Grignard, followed by addition of an equivalent of both iodocyclohexane and samarium diiodide (eq. 3.5). Spectroscopic analysis of complex **102b** is fully consistent with the assigned structure (Table 3.3). In solution, this thermally unstable titanacyclobutane complex decomposes via β -hydride elimination at a faster rate than the

isopropyl analogue **102a**. Although cooling a concentrated pentane solution containing complex **102b** gives cubic crystals, the elemental analysis of these crystals was not within tolerances, perhaps as a result of thermal instability in the solid state.

The bulky *tert*-butyl radical can also be trapped under the aforementioned reaction conditions, giving 3-*tert*-butyl-2-methyl titanacyclobutane complex **102c**, albeit in lower yield (eq. 3.5). Complete characterization of this complex was precluded by rapid decomposition in solution at room temperature and thus characterization rests on ¹H NMR spectroscopy alone. Nonetheless, the ¹H NMR spectrum clearly reveals the expected resonances for a 3-alkyl-2-methyl titanacyclobutane complex. The titanacyclobutane ring is represented by triplets at δ 1.28 ($J = 9.6$ Hz) and 0.88 ($J = 8.7$ Hz) for the α -methylene protons. Although the α -methine proton at δ 2.32 is obscured by dimethylamino resonances, the β -methine proton resonates as a typical doublet of triplets at δ 0.41 ($J = 9.5, 8.2$ Hz). The α -methyl substituent appears as a doublet at δ 1.28 ($J = 6.9$ Hz) and the β -*tert*-butyl group appears as a singlet at δ 1.11. Interestingly, the α -methylene protons of complex **102c** do not show significantly different chemical shifts, nor is the β -methine signal shifted significantly upfield. This suggests strongly that neither of the arene rings of the dimethylaminoindenyl ligands are located above the titanacyclobutane core, as is suspected for complexes **102a** and **102b**. Instead we propose that the dimethylamino groups are likely to flank the titanacyclobutane, similar to Structure A, Figure 3.2.

A more thermally stable 3-benzyl-2-methyl titanacyclobutane complex **102d** is obtained from chloride complex **96** upon alkylation with crotyl Grignard and subsequent treatment with benzyl chloride and samarium diiodide (eq. 3.5). The spectral data are fully consistent with the assigned structure (Table 3.3). Analytically pure red/purple prisms of complex **102d** were obtained by cooling a concentrated pentane solution of the

complex. Unfortunately, successful alkylation could not be obtained using allyl bromide as a radical source, paralleling the result obtained for alkylation of the cinnamyl complex **98** with allyl radical (*vide supra*).

This one pot methodology also allows for the synthesis of 2-methyl-3-propyl titanacyclobutane **102e** (eq. 3.5). The ¹H NMR spectrum of the crude reaction mixture clearly defines the resonances of the four-membered titanacycle: triplets at 2.45 (*J* = 8.7 Hz) and 1.06 (*J* = 9.6 Hz) for the α -methylene hydrogen atoms, multiplets at δ 1.27 and -0.062 for the α -methine and β -methine protons. Further purification of this complex was not possible, again due to the relatively rapid decomposition in solution.

Conclusions. The bis(2-*N,N*-dimethylaminoindenyl)titanium(III) template affords improved results for regioselective central carbon alkylation of substituted allyl complexes relative to the previously reported bis(2-piperidinoindenyl)titanium(III) template.^{1,3} Central carbon alkylation proceeds in acceptable yields upon reaction with both stabilized and unstabilized radicals under mild reaction conditions.

Titanacyclobutane complexes can also be prepared *in situ* using allylic Grignard or lithium reagents and samarium-mediated alkylation of the intermediate allyl complexes without isolation. Titanacyclobutane complexes derived from cinnamyl complex **98** are reasonably robust, but generally decompose at temperatures above 70 °C. The crotyl-derived titanacyclobutane complexes, which possess β -hydrogen atoms on the titanacyclobutane α -substituent, undergo decomposition by β -hydride elimination, but are thermally less sensitive than the complexes derived from the 2-piperidinoindenyl template. Larger substituents (e.g., *tert*-butyl) in the 3-position of the titanacyclobutane ring appear to promote β -hydride elimination, whereas complexes with smaller substituents (e.g. *iso*-propyl), are reasonably stable and allow for further functionalization (Chapter 5).

C. Crystallographic Investigation of Substituted Allyltitanium(III) and Titanacyclobutane Complexes

1. Introduction

Relative to cyclopentadienyl as an ancillary ligand, indenyl is thought to possess lower electron-donor strength due to the aromatic character of the indenyl arene ring.¹¹ The difference in pK_a for indene and cyclopentadiene, however implies that this may not be the case (indene has a pK_a value of 21 whereas cyclopentadiene has a pK_a value of 16).¹² The successful alkylation of the aminoindenyl complexes suggests that the nitrogen lone pair interacts with the indenyl ligand to promote electron richness at the metal and central carbon alkylation. To gain insight into the effectiveness of dialkylaminoindenyl templates in promoting the alkylation of substituted allyl ligands and to probe the differences between the piperidino- and dimethylamino-substituted indenyl ligands, a comparative crystallographic investigation of both substituted allyl complexes of titanium(III) and derived titanacyclobutane complexes for each of the two ligand systems was undertaken.

2. Crystallographic Analysis of Titanium(III) Complexes $96 \cdot LiCl(THF)_2$, **98 and **99****

The solid state molecular structure of cinnamyl complex **98** together with the atomic labeling scheme is shown in Figure 3.3. The crotyl complex **99** crystallizes as two equally abundant conformational isomers **99** and **99'**;¹³ the molecular structure of each conformer, as well as the atomic labeling schemes, are shown in Figures 3.4a and 3.4b. The two conformers of the crotyl complex do not exist as crystallographically-independent molecules, but in fact occur at the same site; the 2-*N,N*-dimethylaminoindenyl ligand containing the atoms N1, C10 through C19, C30 and C34 (all of which are refined at full occupancy) is common to both conformers **99** and **99'**. Two sets of positions, in equal abundance (50% structural occupancy), are found for the titanium atom, the crotyl group, and the second 2-*N,N*-dimethylaminoindenyl ligand. An

ORTEP diagram of the superimposed disordered conformer structures is given in Appendix I (Figure C.2). Selected bond lengths and angles are presented in Table 3.4 for complex **96**•LiCl(THF)₂, Table 3.5 for complex **98** and Table 3.6 for complexes **99** and **99'**.

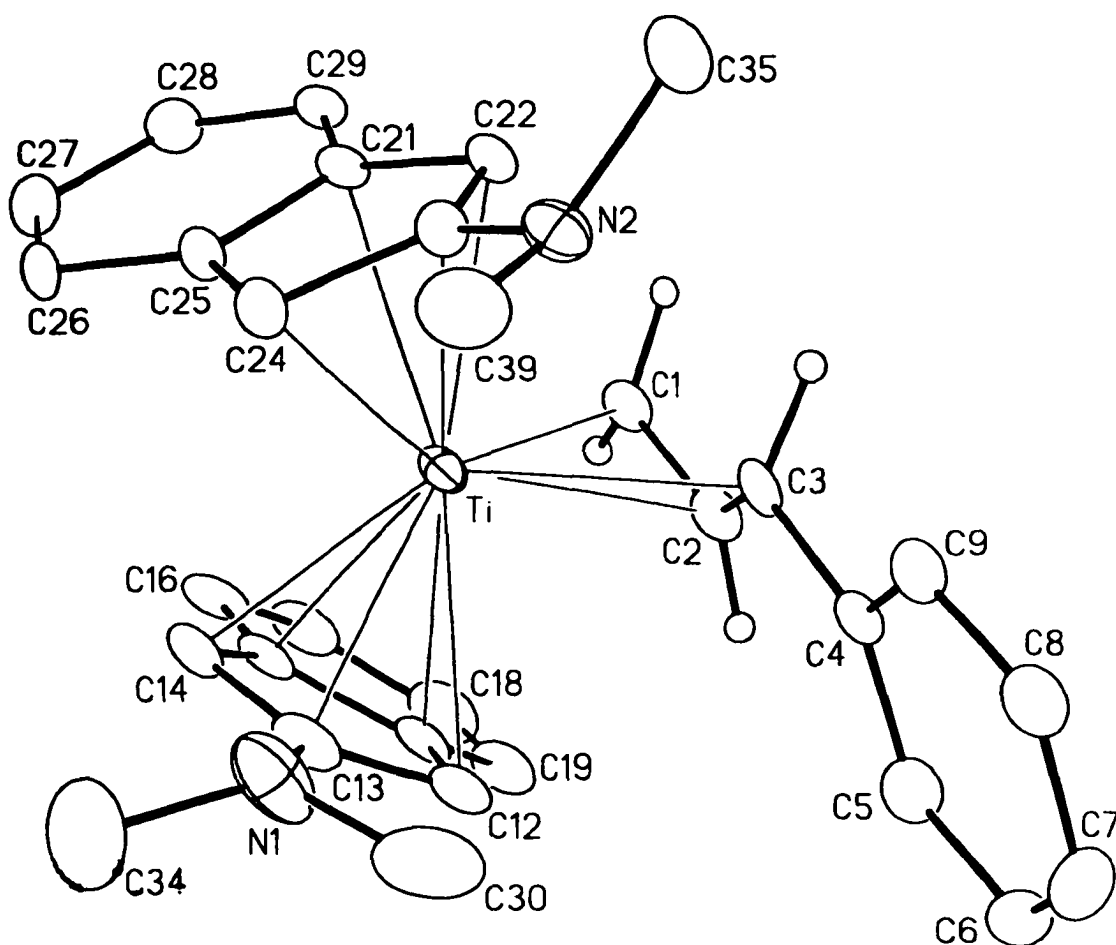


Figure 3.3 The molecular structure of bis(2-*N,N*-dimethylaminoindenyl)titanium(cinnamyl), **98**. Selected interatomic distances are listed in Table 3.5. Crystallographic details are given in Appendix I.

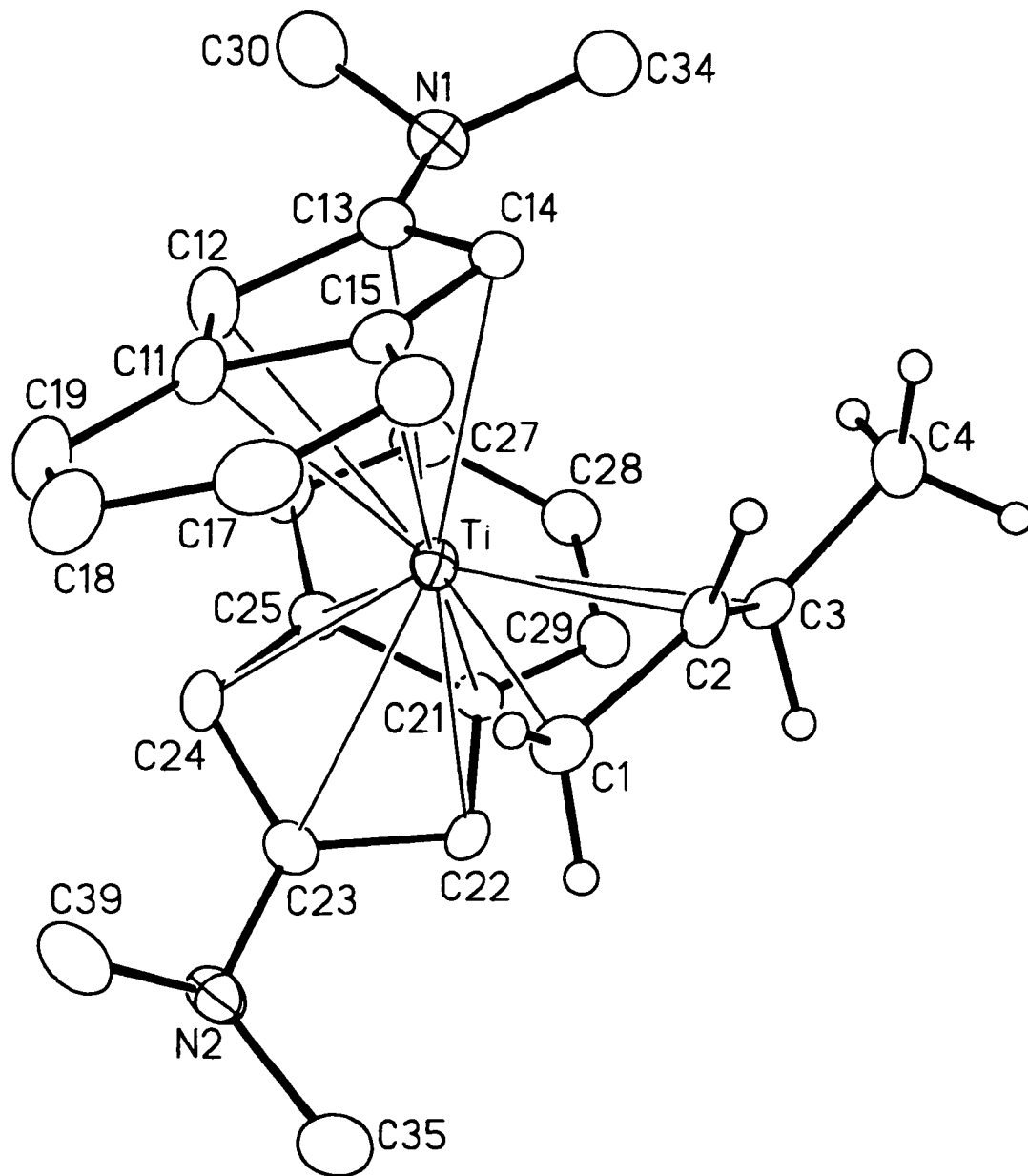


Figure 3.4a The molecular structure of bis(2-*N,N*-dimethylaminoindenyl)titanium(crotyl), **99**. Selected interatomic distances are listed in Table 3.6. Crystallographic details are given in Appendix I.

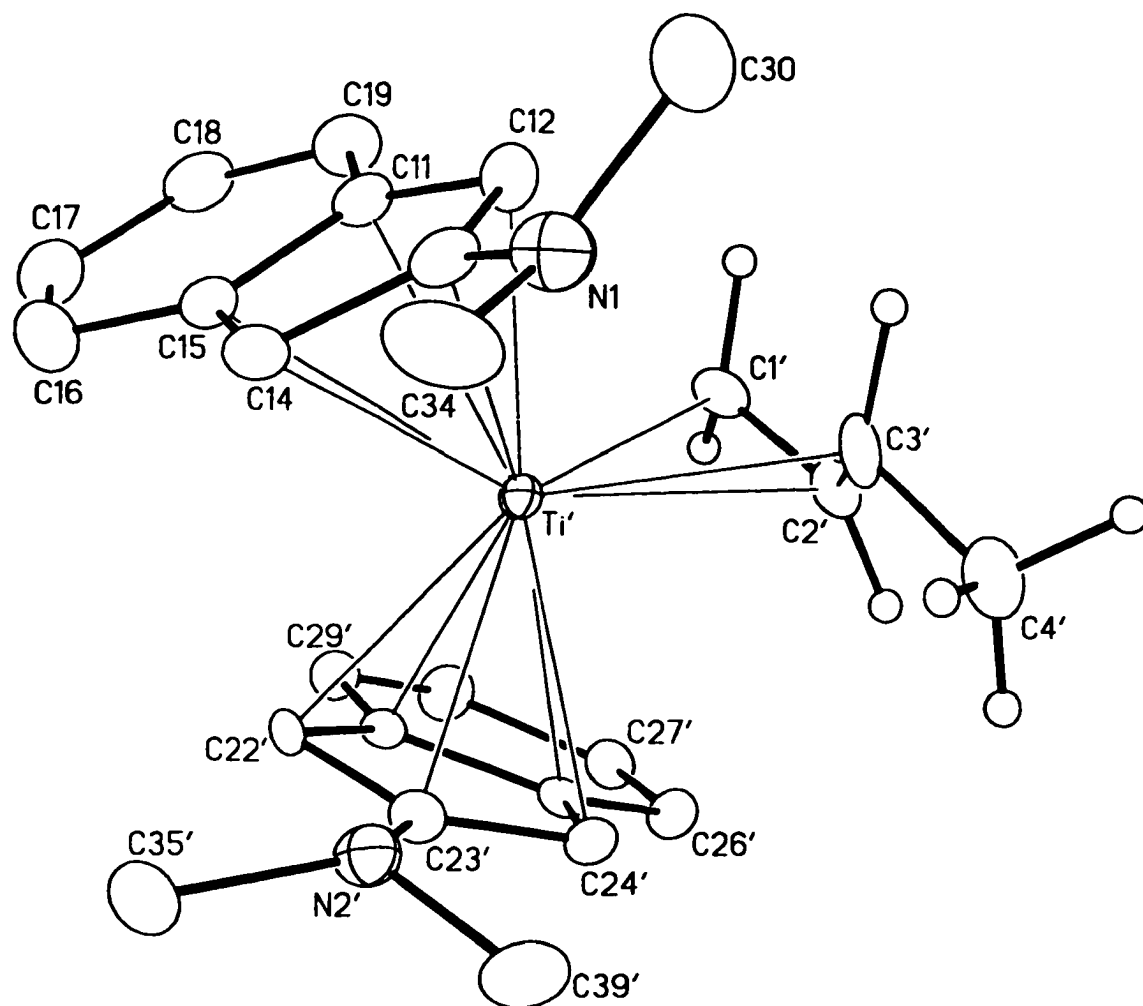


Figure 3.4b The molecular structure of bis(2-*N,N*-dimethylaminoindenyl)titanium(crotyl), **99'**. Selected interatomic distances are listed in Table 3.6. Crystallographic details are given in Appendix I.

Table 3.4 Selected Bond Lengths and Angles for **96**•LiCl₂(THF)₂

Bond Lengths (Å)			
Ti-Cl	2.5184(6)	N1-C13	1.372(3)
Li-Cl	2.284(4)	N1-C21	1.456(3)
Li-O	1.923(4)	N1-C22	1.448(3)
Ti-C11	2.4114(19)	Ti-Cp(cent) ^a	2.108
Ti-C12	2.3855(19)	Ti-Cp(plane) ^b	2.1067(9)
Ti-C13	2.517(2)		
Ti-C14	2.400(2)		
Ti-C15	2.443(2)		
Angles (°)			
Cl-Ti-Cl'	84.97(3)	C13-N1-C21	119.18(19)
Cl-Li-Cl'	96.3(2)	C13-N1-C22	119.2(2)
Cp(cent)-M-Cp(cent) ^a	134.5	C22-N1-C21	117.0(2)
Cp(plane)-M-Cp(plane) ^b	45.89(6)		

^aCentroid of the indenyl ligand, ^bCalculated normal to plane of indenyl ligand

The solid state structure of complex **96**•LiCl(THF)₂ (Figure 3.1, pg. 86) possesses a crystallographic twofold rotational axis passing through the titanium and lithium atoms. The planar TiCl₂Li-core possesses Ti-Cl distances that are elongated with respect to the statistical range determined for Ti(IV)-Cl bond lengths (2.442-2.476 Å)¹⁴ and shortened with respect to reported Ti(III)-Cl bond lengths (2.527-2.555 Å).¹⁴ This unusual TiCl₂-Li core has only twice been crystallographically characterized in the chemistry of titanium(III) halides: Gambarotta reports that addition of two equivalents of dicyclohexylamidolithium or bis[(trimethylsilyl)benzamidoinato]lithium-TMEDA complex to a THF suspension of TiCl₃(THF)₃ containing excess TMEDA results in the formation of lithium chloride adducts **103** and **104**, respectively (Scheme 3.1).^{15,16}

The cinnamyl and crotyl substituents in the crystal structures of complexes **98** and **99** adopt the anticipated η³-coordination, *syn* substituent stereochemistry, partially

Table 3.5 Selected Bond Lengths and Angles for 98

Bond Lengths (Å)			
Ti-C1	2.336(6)	N1-C13	1.399(9)
Ti-C2	2.364(6)	N1-C30	1.423(10)
Ti-C3	2.475(6)	N1-C34	1.371(9)
Ti-C11	2.488(6)	N2-C23	1.382(8)
Ti-C12	2.447(7)	N2-C35	1.464(7)
Ti-C13	2.434(7)	N2-C39	1.454(8)
Ti-C14	2.344(6)	C1-C2	1.420(9)
Ti-C15	2.428(6)	C2-C3	1.416(8)
Ti-C21	2.486(6)	C3-C4	1.451(9)
Ti-C22	2.437(6)	Ti-Cp(cent) ^a	2.108, 2.131
Ti-C24	2.370(6)	Ti-Cp(plane) ^b	2.105(3), 2.130(3)
Ti-C25	2.466(6)		

Angles (°)			
C1-Ti-C3	63.4(2)	C13-N1-C30	117.1(8)
C1-C2-C3	126.3(6)	C13-N1-C34	117.3(7)
C2-C3-C4	125.1(6)	C30-N1-C34	116.9(7)
Cp(cent)-M-Cp(cent) ^a	133.9	C23-N2-C35	115.9(6)
Cp(plane)-M-Cp(plane) ^b	50.6(3)	C23-N2-C39	116.7(6)
		C35-N2-C39	113.6(5)

^aCentroid of the indenyl ligand, ^bCalculated normal to plane of indenyl ligand

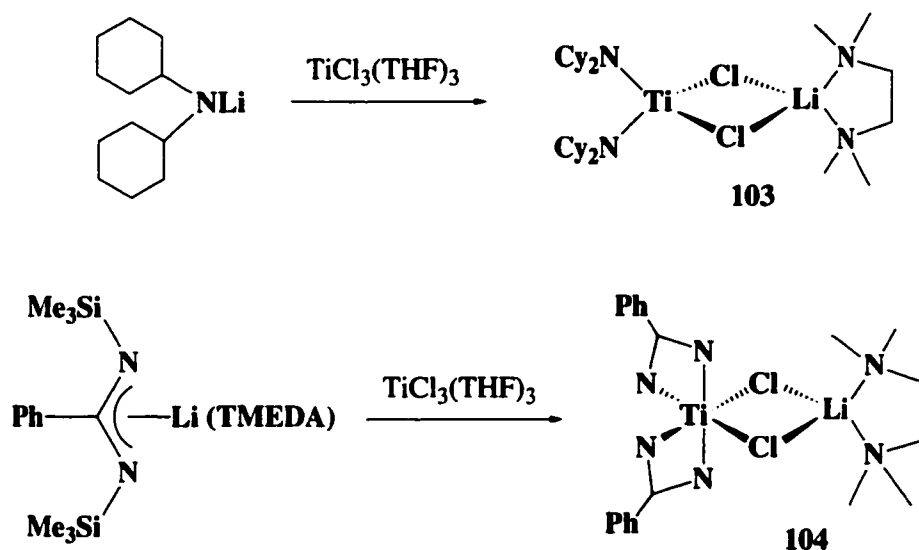
Scheme 3.1

Table 3.6 Selected Bond Lengths and Angles for 99 and 99'

Bond Lengths (Å)			
Ti-C1	2.292(5)	Ti'-C1'	2.272(11)
Ti-C2	2.350(6)	Ti'-C2'	2.335(10)
Ti-C3	2.484(10)	Ti'-C3'	2.447(12)
Ti-C11	2.473(4)	Ti'-C11	2.432(4)
Ti-C12	2.537(4)	Ti'-C12	2.243(4)
Ti-C13	2.588(4)	Ti'-C13	2.362(4)
Ti-C14	2.401(4)	Ti'-C14	2.461(4)
Ti-C15	2.394(4)	Ti'-C15	2.566(4)
Ti-C21	2.453(5)	Ti'-C21'	2.411(4)
Ti-C22	2.425(8)	Ti'-C22'	2.323(4)
Ti-C23	2.506(6)	Ti'-C23'	2.454(9)
Ti-C24	2.403(13)	Ti'-C24'	2.457(5)
Ti-C25	2.432(11)	Ti'-C25'	2.496(7)
N1-C13	1.396(3)	N2'-C23'	1.408(13)
N1-C30	1.431(3)	N2'-C35'	1.453(8)
N1-C34	1.440(3)	N2'-C39'	1.430(11)
N2-C23	1.407(6)	C1'-C2'	1.402(15)
N2-C35	1.440(14)	C2'-C3'	1.45(3)
N2-C39	1.435(7)	C3'-C4'	1.46(3)
C1-C2	1.394(8)	Ti-Cp(cent) ^a	2.167, 2.124 (Ti), 2.094, 2.107 (Ti')
C2-C3	1.354(11)	Ti-Cp(plane) ^b	2.1569(12), 2.133(5) (Ti) 2.073(3), 2.102(4) (Ti')
C3-C4	1.519(15)		
Bond Angles (°)			
C1-Ti-C3	61.3(3)	C1'-Ti'-C3'	64.8(6)
C1-C2-C3	125.1(6)	C1'-C2'-C3'	125.0(11)
C2-C3-C4	123.9(7)	C2'-C3'-C4'	120.1(16)
C13-N1-C30	118.5(2)		
C13-N1-C34	116.4(2)		
C30-N1-C34	115.1(2)		
C23-N2-C35	117.3(7)	C23'-N2'-C35'	118.2(7)
C23-N2-C39	117.2(5)	C23'-N2'-C39'	116.4(7)
C35-N2-C39	114.7(7)	C35'-N2'-C39'	116.2(8)
Cp(cent)-M-Cp(cent) ^a			133.2 (Ti), 131.2 (Ti')
Cp(plane)-M-Cp(plane) ^b			42.9(3) (Ti), 45.27(15) (Ti')

^aCentroid of the indenyl ligand, ^bCalculated normal to plane of indenyl ligand

pyramidalized allyl terminal carbons and unsymmetrical coordination of the allyl carbon atoms to the metal.^{1,17} The tilt angle that the allyl ligand plane makes with the Ti(III) template in complexes **98**, **99** and **99'** falls within the range reported for other Ti(III) allyl complexes (Table 3.7).¹⁷ In complex **98**, the shortened C3-C4 bond and the coplanarity of the phenyl and allyl π -systems suggest the presence of substantial conjugative stabilization within the cinnamyl ligand.

Table 3.7 Comparison of Bond Lengths (Å) and Angles (°) for (allyl)Ti(III) Complexes

Complex	Tilt Angle	Ti-C(1)	Ti-C(2)	Ti-C(3)	C(1)-C(2)	C(2)-C(3)	C(3)-C(4)
53 [‡]	111.8(6)	2.318(6)	2.351(6)	2.448(6)	1.387(8)	1.381(8)	1.480(8)
98	113.2(5)	2.336(6)	2.364(6)	2.475(6)	1.420(9)	1.416(8)	1.451(9)
99	110.0(6)	2.292(5)	2.350(6)	2.484(10)	1.394(8)	1.354(11)	1.519(15)
99'	113.8(9)	2.272(11)	2.335(10)	2.447(12)	1.402(15)	1.45(3)	1.46(3)

[‡] For comparison, the data for 1-phenylallyl-bis(2-piperidinoindenyl)titanium(III) is also given here.

The relative spatial orientation of the 2-*N,N*-dimethylaminoindenyl ligands can be represented by the indenyl rotational angle parameter.¹⁸ A measured indenyl rotation angle of 0° defines perfectly eclipsed indenyl rings; a 180° rotational angle is indicative of staggered indenyl rings. In cinnamyl complex **98**, the two *N,N*-dimethylamino substituents are roughly *syn* to each other with a measured indenyl rotational angle of 41.9°. Despite the steric differences, the orientation of the ancillary ligands in 2-*N,N*-dimethylaminoindenyl complex **98** is nearly identical to that determined for the 2-piperidinoindenyl cinnamyl complex **53** (Figure 3.5) in which an indenyl rotation angle of 36.9° was measured.¹

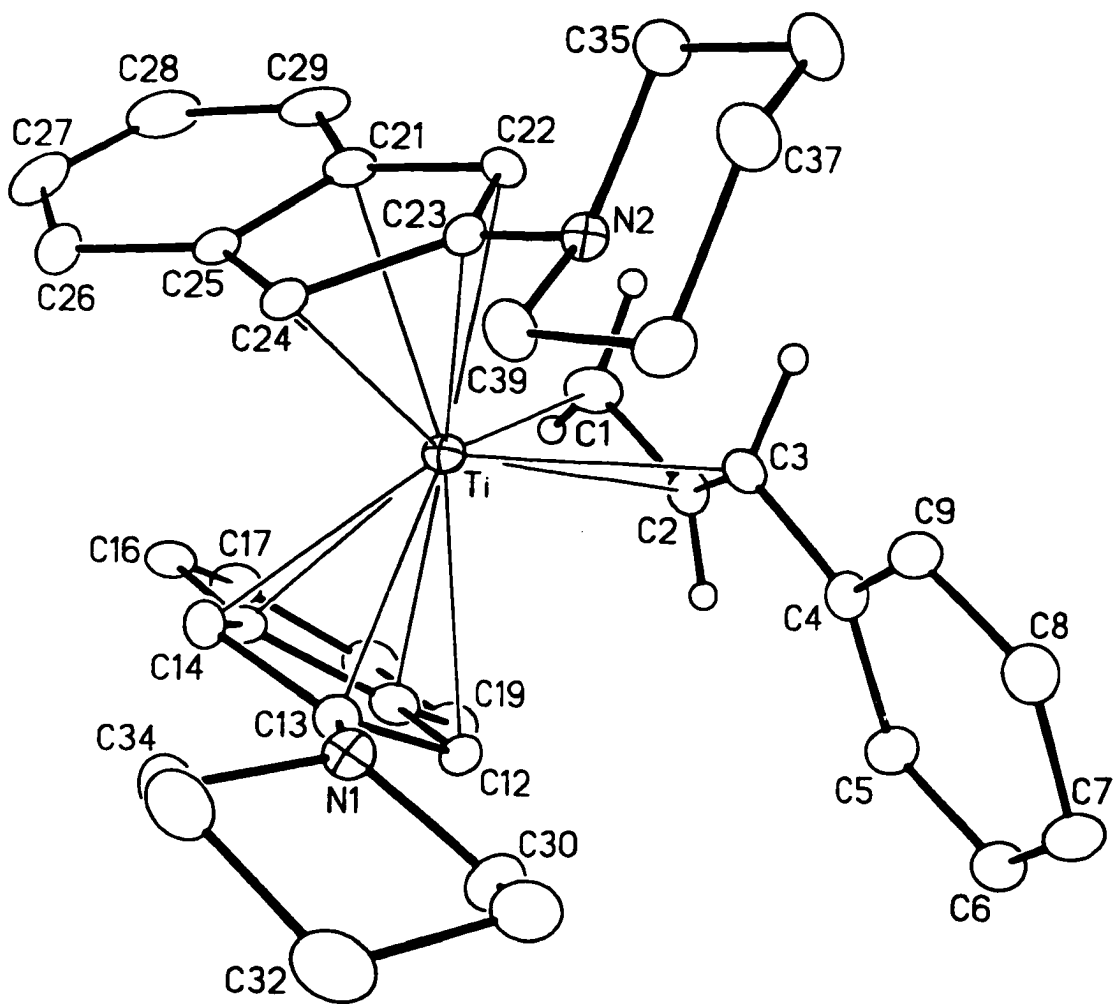
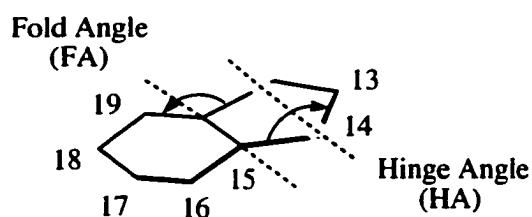


Figure 3.5 The molecular structure of bis(2-piperidinoindenyl)titanium(cinnamyl), **53**.¹

For the crotyl complex, the most significant difference between the two conformers **99** and **99'** is in the relative orientations of the ancillary ligands. In the ORTEP diagram of conformer **99**, the indenyl ligands are oriented *anti*; an indenyl rotational angle of 177.8 ° was obtained. In conformer **99'**, the ancillary ligands approach a *syn* orientation with a corresponding indenyl rotational angle of 41.6°, almost identical to that observed in the cinnamyl complex **98**. The ancillary ligands in complex **96**•LiCl(THF)₂, the structure with the least sterically encumbering substituents in the wedge, are positioned with an indenyl rotational angle of 129.6°, where the dimethylamino groups flank each side of the TiCl₂Li core.

Figure 3.6. Schematic diagram illustrating the folding axes of the indenyl ligand



Many indenyl complexes are prone to ring slippage away from the symmetrical η^5 -coordination mode to η^3 -coordination.^{18,19,20} This allows the indenyl π -system to rehybridize, increasing the residual aromatic character of the indenyl arene ring. Three parameters have been devised to quantify these distortions:²¹ (1) the slip parameter Δ_{M-C} , (2) hinge angle HA, and (3) fold angle FA.¹⁹ The slip parameter Δ_{M-C} is a measure of the hapticity of indenyl coordination to the metal (η^5 - to η^3 -coordination) and is defined as the difference in the average bond lengths of the metal to the ring-junction carbons, e.g., C(11) and C(15) and the metal to the adjacent carbon atoms of the five-membered ring, e.g., C(12), C(13) and C(14) (Figure 3.6). The hinge angle (HA) measures distortion in the planarity of the cyclopentadienyl ring and is defined as the angle between the planes [C(12), C(13), C(14)] and [C(12), C(11), C(15), C(14)]. The fold angle (FA) is the angle

between the two rings in the indenyl system and is defined by the difference in the planes of the five-membered ring, [C(12), C(11), C(15), C(14)], and the six-membered ring, [C(19), C(11), C(15), C(16)], (Figure 3.6). Values for these parameters range from values less than 0.030 Å (Δ_{M-C}), 2.5° (HA), and 4.4° (FA) for ‘true’ η^5 -complexes^{18a} to values greater than 0.8 Å (Δ_{M-C}), and 28° (FA) for ‘true’ η^3 -complexes,²² with intermediate values of 0.11-0.43 Å (Δ_{M-C}), 7-14° (HA), and 6-13° (FA) observed for ‘distorted’ complexes,²⁰ in which some degree of bonding occurs from the metal to the ring junction carbon atoms. These data have been calculated for complexes **96**•LiCl₂(THF)₂, **98**, **99**, and **99'** and can be found in Table 3.8 (along with data for the corresponding titanium(IV) complexes, 2-*N,N*-dimethylaminoindenyl titanacyclobutane **101a** and 2-piperidinoindenyl titanacyclobutane **55a**). In addition to these parameters, a symmetrically coordinated η^5 -indenyl ring will have significant bond alternation in the carbon-carbon bond lengths of the non-coordinated arene ring, reflecting a partially localized cyclohexatriene structure.²⁰ Slipped η^3 -coordinated complexes¹⁹ will possess nearly equal internal carbon-carbon bond lengths in the arene ring, as observed in fully delocalized benzene itself. The arene ring carbon-carbon bond lengths in the indenyl ligands in complexes **98**, **99** and **99'** are tabulated in Table 3.9.

The geometry and rotational orientation of the amino substituents on the indenyl rings were also determined. For the greatest donation of electron density from the ancillary ligands to the metal, the lone pair on the nitrogen atom ideally aligns parallel to the π -system of the cyclopentadienyl ring and the hybridization of the nitrogen atom approaches sp². The degree of pyramidalization can be calculated by summing the bond angles surrounding nitrogen and subtracting this value from the sum of bond angles around a perfectly sp² hybridized nitrogen center. The resulting value is then divided by the difference between the sum of bond angles for an sp² center and an sp³ center (eq. 3.6). The alignment is measured as the twist angle, defined as the angle between the axis

Table 3.8 Structural Data For Indenyl Coordination

Complex	Δ_{M-C} (Å) ^a	Fold Angle (°) ^b	Hinge Angle(°) ^c
96 •LiCl ₂ (THF) ₂	-0.0070	5.80(10)	11.5(1)
52 ^d	0.0450	2.8(5)	6.3(8)
	0.0490	6.7(4)	8.5(8)
98	0.0497	3.6(3)	5.9(4)
	0.0625	5.1(3)	8.9(6)
99	-0.0751	3.4(2)	7.3(2)
	-0.0022	4.0(4)	9.4(6)
99'	0.1437	3.4(2)	7.3(2)
	0.0422	3.0(2)	7.2(4)
55a	0.0653	4.0 (2)	5.8(4)
	0.0313	5.4(2)	11.3(3)
101a	0.0178	5.6(2)	12.6(4)
	0.0235	4.0(2)	10.5(4)

^a Δ_{M-C} -the difference in bond lengths of the metal to C(11) and C(15) and the metal to C(12), C(13) and C(14)

^bHA- angle between planes [C(12), C(13), C(14)] and [C(11), C(12), C(14), C(15)]

^cFA- angle between planes [C(11), C(12), C(13), C(14), C(15)] and [C(11), C(15), C(16), C(17), C(18), C(19)]

^dFor comparison, the data for cinnamyl bis(2-piperidinoindenyl)titanium(III) is also given here.

3.6). The alignment is measured as the twist angle, defined as the angle between the axis of the lone electron pair on nitrogen and the π -electron system of the indenyl ring, that is the [C12-C13-C14] plane. Together with the degree of pyramidalization and twist angle, the indenyl carbon-nitrogen bond lengths indicate the extent of electron donation from the amino group into the indenyl ring. These values have been determined for complexes **96**•LiCl₂(THF)₂, **98** and **99/99'** and are collected in Table 3.10. The 2-*N,N*-dimethylamino groups in cinnamyl and crotyl complexes **98** and **99/99'** are significantly pyramidal, deviate markedly from coplanarity with the indenyl ring, and possess C_{Ind-N} bond lengths only minimally contracted from normal C-N single bonds. The structural

Table 3.9 Indenyl Carbon-Carbon Bond Lengths (Å)

Comp-lex	C(11)-C(12)	C(12)-C(13)	C(13)-C(14)	C(14)-C(15)	C(11)-C(15)	C(15)-C(16)	C(16)-C(17)	C(17)-C(18)	C(18)-C(19)	C(19)-C(11)
96-LiCl-(THF) ₂	1.435(3)	1.420(3)	1.421(3)	1.431(3)	1.431(3)	1.420(3)	1.372(4)	1.402(4)	1.373(3)	1.415(3)
98	1.438(9)	1.413(10)	1.404(9)	1.406(9)	1.431(9)	1.423(9)	1.362(10)	1.406(11)	1.314(10)	1.414(9)
	1.430(8)	1.397(8)	1.430(8)	1.437(8)	1.428(8)	1.419(8)	1.366(9)	1.405(9)	1.361(8)	1.399(8)
99	1.419(3)	1.416(3)	1.406(3)	1.415(3)	1.426(3)	1.423(4)	1.352(4)	1.404(4)	1.347(4)	1.413(3)
	1.442(9)	1.405(8)	1.405(13)	1.425(15)	1.440(11)	1.37(2)	1.45(3)	1.410(19)	1.356(6)	1.419(5)
99'	1.438(10)	1.429(10)	1.380(9)	1.423(8)	1.433(7)	1.417(8)	1.378(12)	1.445(14)	1.367(6)	1.397(4)
53	1.439(8)	1.401(8)	1.427(8)	1.435(8)	1.418(8)	1.429(8)	1.374(8)	1.397(9)	1.343(9)	1.424(8)
	1.433(8)	1.418(8)	1.417(8)	1.423(8)	1.432(8)	1.401(8)	1.378(9)	1.383(10)	1.361(10)	1.419(8)
55a	1.417(3)	1.422(3)	1.418(3)	1.428(3)	1.428(3)	1.416(3)	1.365(4)	1.413(4)	1.364(4)	1.419(3)
	1.425(3)	1.424(3)	1.409(3)	1.431(3)	1.427(4)	1.416(3)	1.370(4)	1.401(5)	1.365(4)	1.414(4)
101a	1.436(4)	1.414(4)	1.423(4)	1.427(4)	1.422(4)	1.433(4)	1.360(4)	1.415(4)	1.371(4)	1.418(4)
	1.425(4)	1.416(4)	1.427(4)	1.430(4)	1.432(4)	1.426(4)	1.364(4)	1.409(4)	1.365(4)	1.412(4)

and orientational parameters of the ancillary ligands in piperidinoindenyl and dimethylaminoindenyl complexes **53** and **98** are remarkably similar to each other.

$$\% \text{ pyramidalization} = [360 - \sum \text{carbon-nitrogen bonds}] / [360 - 328.5] \cdot 100 \quad (\text{eq. 3.6})$$

Table 3.10 Structural Data for Amino Group

Complex	Pyramidalization (%)	C _{Ind} -N (Å)	Twist Angle(°)
96 •LiCl ₂ (THF) ₂	15	1.372(3)	11.8
98	28	1.399(9)	21.4
	43	1.382(8)	16.9
99	32	1.396(3)	17.1
	34	1.407(6)	-158.8
99'	32	1.396(3)	7.0
	30	1.408(13)	4.8
53	51	1.416(7)	7.1
	74	1.409(7)	28.3
55a	43	1.397(3)	6.4
	54	1.399(3)	8.6
101a	3	1.366(4)	-171.4
	22	1.375(4)	5.8

The above detailed analysis of the crystal structures for the two 17-electron Ti(III) dimethylaminoindenyl complexes **98** and **99/99'**, with respect to piperidinoindenyl complex **53**, allows for a direct comparison of the two ancillary ligand systems in an attempt to identify potential structural origins for the noted differences in reactivity. In the case of cinnamyl complexes **98** and **53**, striking similarities in the general appearance are evident. Upon close inspection, however, many subtle differences are noted. In the coordination of the cinnamyl ligand, the phenyl-substituted Ti-C(3) bond is longer in dimethylaminoindenyl complex **98** as compared to piperidinoindenyl complex **53**, while

the C(3)-C(4) bond is longer in complex **53** than in complex **98** (Table 3.7). One interpretation of this data is that in piperidinoindenyl complex **53** the substituted allyl ligand is distorted toward η^1, η^2 -(σ, π)-coordination. The bond to the benzylic carbon thus has greater σ -character, leaving the bond between C(1) and C(2) with greater π -character. This is consistent with the shorter C1-C2 bond observed in this complex. As a result, the phenyl group is expected to be less conjugated to the allyl framework; this is reflected directly in the longer C(3)-C(4) bond observed. While it is counterintuitive that the more sterically crowded complex **53** should display the shorter benzylic carbon-titanium bond, the more symmetrical π -allyl structure defined for the dimethylaminoindenyl complex **98** correlates with the improved reactivity toward organic radicals. It is, however, possible that (intermolecular) crystal packing forces in the extended lattices alone account for the observed differences in cinnamyl ligand coordination, so that these structural differences may be irrelevant to the solution behaviour.

The difference in nitrogen parameters between piperidinoindenyl complex **53** and dimethylaminoindenyl complex **98** are suggestive of varying electron richness at the metal center, although the effects of crystal packing forces on these parameters again cannot be disregarded. While the differences in twist angle are ambiguous, the amino substituents in complex **53** show greater pyramidalization and longer $C_{\text{ind}}\text{-N}$ bond lengths than observed in complex **98**, implying that the slightly more electron-rich piperidinoindenyl ligands in complex **53** provide *less* electron density to the metal than do the dimethylaminoindenyl ligands in complex **98** (Table 3.10).

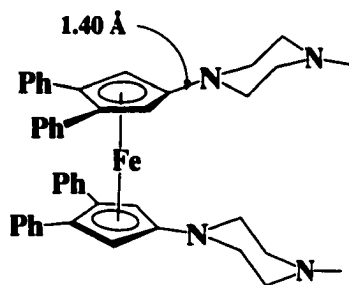
Although the slip parameters, hinge angles and fold angles do not indicate significant ring slip in the ancillary ligands of complexes **98** and **53**, a close examination of bond alternation for the internal carbon-carbon bond lengths of the benzene ring

(Table 3.9) indicates greater retention of the arene aromaticity in piperidinoindenyl complex **53**. The 2-*N,N*-dimethylaminoindenyl ancillary ligands in complex **98** show a pattern more consistent with an η^5 -cyclopentadienyl bonding, as evidenced by the significant bond length alternation in the carbon-carbon bond lengths of the arene rings. While this also suggests that greater electron density is delivered to the metal in dimethylaminoindenyl complex **98**, the extent to which these differences affect the reactivity of the two titanocene templates remains unclear.

Amine substituents on coordinated cyclopentadienyl rings are known to provide variable amounts of electron density to the metal center, depending on the electronic state of the metal. Carbon-nitrogen bond lengths in η^5 -aminocyclopentadienyl complexes are longer in electron-rich organometallic systems such as ferrocene complex **105** (ca. 1.41 Å),^{23c,e} and shorter when coordinated to electron deficient organometallic fragments such as cymantrene complex **106** (ca. 1.36 Å) (Scheme 3.2).^{23d} This clearly indicates that in all of the Ti(III) complexes the amine functionality is capable of providing far greater donation of electron density to the ligand system than is required by the metal and the system at least partially 'deconjugates' the nitrogen center.

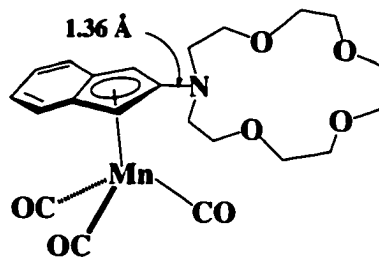
Examination of the structural parameters of crotyl complexes **99** and **99'** must be taken with due consideration to the observed positional disorder in the structure. Cautiously interpreted, it does appear that among the structurally characterized Ti(III) allyl complexes,^{1,16} crotyl complexes **99** and **99'** display the shortest Ti-C1 and Ti-C2 bonds reported, reflective of relatively strong $d \rightarrow \pi^*$ back donation from the d^1 -metal center. The longer Ti-C3 bond arises from steric and electronic effects introduced by the terminal methyl substituent. Coordination of the crotyl ligand differs remarkably between the conformers **99** and **99'**. Analogous to complex **53**, in conformer **99** the allyl ligand appears distorted toward η^1, η^2 -(σ, π)-coordination, whereas in conformer **99'** the

Scheme 3.2



105

Amino-coordination to an electron rich organometallic fragment.



106

Amino-coordination to an electron deficient organometallic fragment.

allyl coordination is more symmetrical. These two modes of crotyl coordination may be the origin of the three bands observed in the IR spectrum representative of $C=C_{\text{asym}}$. Regardless, these differences illustrate that there is considerable coordinative freedom in these complexes and underscore the importance of crystal packing forces on structural detail.

More interesting are the differing modes of coordination of the ancillary ligands in conformers **99** and **99'** and their deviation from true η^5 -coordination (Table 3.8). Although the Δ_{M-C} value of 0.1437 Å is not complemented by a significant hinge angle, the data clearly illustrate the longer titanium-ring junction carbons relative to the remaining titanium-carbon bonds in the five-membered ring, indicating distortion toward η^3 -coordination of one of the indenyl rings in conformer **99'**. In conformer **99**, the reverse is observed. The longest titanium-carbon bond in both five-membered rings is the bond to the carbon bearing the dimethylamino substituent; much stronger coordination occurs between titanium and the ring junction carbons, as reflected in the hinge angles measured. In complex **99'**, the pyramidalization and $C_{\text{ind}}\text{-N}$ bond lengths observed are consistent with those observed in complexes **98**, **99**, and **53**; however, the

alignment of the nitrogen lone pair and the indenyl π -system is nearly perfect. This boost in electron density, attributable to the loss of electron density arising from the 'slipped' coordination of one indenyl ring, may result in the stronger coordination of the crotyl ligand in **99'** relative to conformer **99**.

3. Crystallographic Analysis of Titanium (IV) Complexes **55a** and **101a**

Both 3-isopropyl-2-phenyl-bis(2-*N,N*-dimethylaminoindenyl)titanacyclobutane **101a** and 3-isopropyl-2-phenyl-bis(2-piperidinoindenyl)titanacyclobutane **55a**¹ are synthesized from the Ti(III) cinammyl precursors **98** (*vide supra*) and **53**, respectively. Single crystals of the previously reported¹ complex **55a** were obtained by recrystallization from diethyl ether layered with pentane. ORTEP diagrams of complexes **101a** and **55a**, together with the atomic labeling schemes, are shown in Figures 3.7 and 3.8, respectively. Selected intramolecular bond lengths and angles are presented in Tables 3.11 and 3.12. Homonuclear decoupling experiments, difference NOE measurements and ¹H-¹³C heteronuclear correlated spectroscopy were used to determine the solution structure of complex **55a**, which supported a tentative assignment of the substituent stereochemistry as *trans*.¹ The single-crystal X-ray diffraction analyses confirms the spectroscopic characterization of both complexes **101a** and **55a**.

Crystallographic analysis of titanacyclobutane complexes **101a** and **55a** reveal core structures very similar to previously reported 2,3-disubstituted titanacyclobutane complexes.²⁴ In complexes **101a** and **55a**, the Ti-C(1) and Ti-C(3) bond distances, respectively, are essentially equidistant and fall close to the statistical range determined for Ti-C_{sp3} bonds (2.14 - 2.21 Å).¹⁴ The unsubstituted Ti-C(1) bond in both complexes is consistently shorter than Ti-C(3), presumably due to absence of a substituent and the inherently weaker bonding expected to a benzylic position. The carbon-carbon bond lengths in the titanacyclobutane rings are roughly equal and comparable to previously

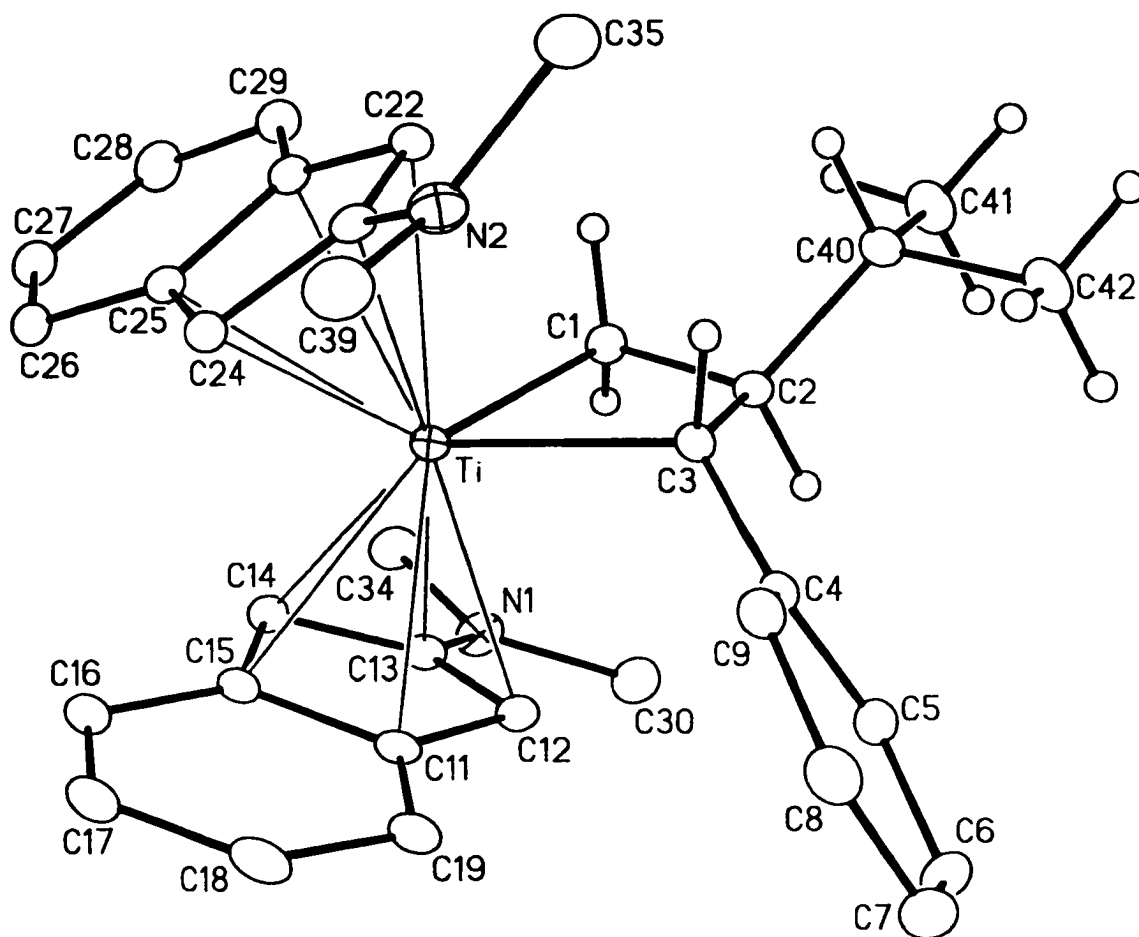


Figure 3.7 The molecular structure of 3-isopropyl-2-phenyl-bis(2-*N,N*-dimethylaminoindenyl)titanacyclobutane, **101a**. Selected interatomic distances are listed in Table 3.11. Crystallographic details are given in Appendix I.

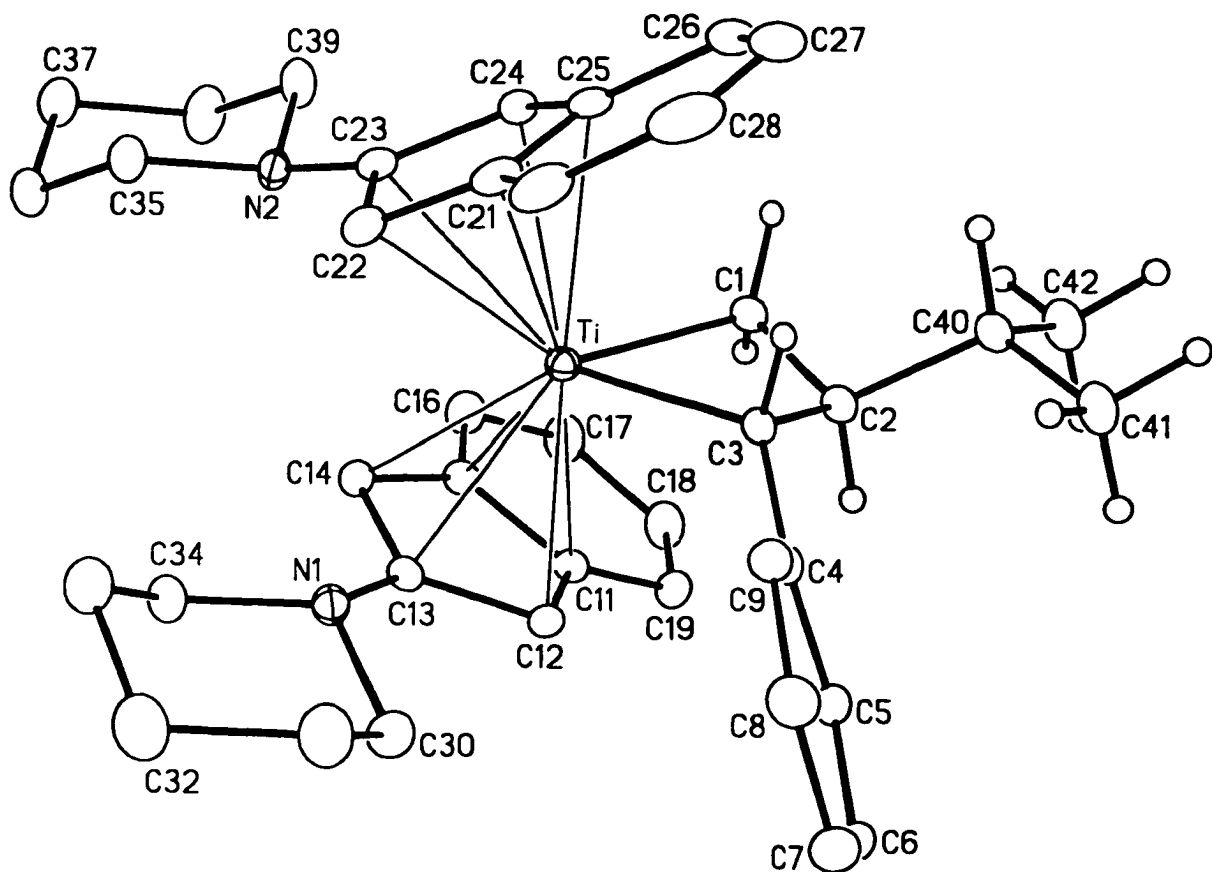


Figure 3.8 The molecular structure of 3-isopropyl-2-phenyl-bis(2-piperidinoindenyl)titanacyclobutane, **55a**. Selected interatomic distances are listed in Table 3.12. Crystallographic details are given in Appendix I.

Table 3.11 Selected Bond Lengths (Å) and Angles (°) for Complex 101a

Bond Lengths (Å)			
Ti-C1	2.128(3)	N1-C13	1.366(4)
Ti-C3	2.202(2)	N1-C30	1.450(4)
Ti-C11	2.439(3)	N1-C34	1.448(4)
Ti-C12	2.401(3)	N2-C23	1.375(4)
Ti-C13	2.516(3)	N2-C35	1.452(4)
Ti-C14	2.381(3)	N2-C39	1.442(4)
Ti-C15	2.462(3)	C1-C2	1.559(4)
Ti-C21	2.463(3)	C2-C3	1.557(4)
Ti-C22	2.423(3)	Ti-Cp(cent) ^a	2.104, 2.117
Ti-C23	2.504(3)	Ti-Cp(plane) ^b	2.099(3), 2.116(3)
Ti-C24	2.387(3)		
Ti-C25	2.460(3)		
Angles (°)			
C1-Ti-C3	71.84(10)	C13-N1-C30	120.0(2)
C1-C2-C3	109.3(2)	C13-N1-C34	120.0(2)
Cp(cent)-M-Cp(cent) ^a	133.1	C30-N1-C34	119.0(2)
Cp(plane)-M-	49.8(3)	C23-N2-C35	116.9(2)
Cp(plane) ^b		C23-N2-C39	118.6(2)
		C35-N2-C39	117.6(3)

^aCentroid of the indenyl ligand, ^bCalculated normal to plane of indenyl ligand

characterized titanacyclobutane complexes.²⁴ The metallacycle rings are puckered, with dihedral angles of 156.5° and 157.0° for the C(1)-Ti-C(3) and C(1)-C(2)-C(3) planes of complexes **101a** and **55a**, respectively. Such puckering is anticipated for α,β -disubstituted titanacyclobutane complexes.^{24b-d} The ancillary ligands in complexes **101a** and **55a** are positioned with indenyl rotational angles of 124.0° and 106.9°, respectively. In titanacyclobutane **55a**, the arene ring of one 2-piperidinoindenyl ligand flanks each side of the metallacycle fragment; however, in complex **101a** the dimethylamino groups flank each side of the titanacyclobutane core, presumably a consequence of the lower

steric demand of the dimethylamino substituents.

Table 3.12 Selected Bond Lengths (Å) and Angles (°) for Complex 55a

Bond Lengths (Å)			
Ti-C1	2.121(2)	N1-C13	1.397(3)
Ti-C3	2.190(2)	N1-C30	1.453(3)
Ti-C11	2.497(2)	N1-C34	1.466(3)
Ti-C12	2.418(3)	N2-C23	1.399(3)
Ti-C13	2.420(2)	N2-C35	1.463(3)
Ti-C14	2.367(2)	N2-C39	1.465(3)
Ti-C15	2.437(2)	C1-C2	1.553(3)
Ti-C21	2.479(3)	C2-C3	1.552(3)
Ti-C22	2.393(3)	Ti-Cp(cent) ^a	2.105, 2.158
Ti-C23	2.529(3)	Ti-Cp(plane) ^b	2.1029(12), 2.1569(12)
Ti-C24	2.460(3)		
Ti-C25	2.505(3)		
Bond Angles (°)			
C1-Ti-C3	71.33(9)	C13-N1-C30	117.1(2)
C1-C2-C3	108.09(19)	C13-N1-C34	116.5(2)
Cp(cent)-M-Cp(cent) ^a	131.3	C30-N1-C34	112.9(2)
Cp(plane)-M-	52.03(11)	C23-N2-C35	114.4(2)
Cp(plane) ^b		C23-N2-C39	116.07(19)
		C35-N2-C39	112.4(2)

^aCentroid of the indenyl ligand, ^bCalculated normal to plane of indenyl ligand

The change in oxidation state to titanium(IV) upon alkylation is clearly reflected in the accompanying changes in nitrogen pyramidalization, C_{Ind}-N bond length, and tilt angle of the amino substituents, as compared to the Ti(III) precursors. The amine functionality on each indenyl ring is significantly less pyramidal (Table 3.10), the C_{Ind}-N bond length is shorter, and the tilt angle is smaller, all indicative of stronger donation of electron density into the indenyl ligands of these higher oxidation state products. The slip parameters, hinge and fold angles, and carbon-carbon bond lengths for each of the indenyl rings (Tables 3.8 and 3.9) suggest mildly distorted η⁵-coordination. This

presumably arises from the longer titanium-carbon bonds to the nitrogen-substituted positions (Ti-C(13) and Ti-C(23)) relative to the remaining titanium-carbon bonds to the five-membered ring. Interestingly, the pyramidalization (14.6%), $C_{\text{ind}}\text{-N}$ bond length and tilt angle (11.8 °) of the dimethylamino substituents observed in titanium chloride complex **96**•LiCl₂(THF)₂ are located at intermediate values, between those observed for Ti(III) complexes **98** and **99** and Ti(IV) complex **101a**.

The torsional angle between H-C(2)-C(3)-H in piperidinoindenyl complex **55a** is calculated to be 155.6°, corresponding to a coupling constant of approximately 10 Hz based on the Karplus relation.²⁵ This prediction is in good agreement with the 11.6 Hz coupling observed in the ¹H NMR spectrum, indicating that the solution structure of the titanacyclobutane core is reasonably modeled by the solid state structure. For dimethylaminoindenyl titanacyclobutane complex **102a**, the torsional angle between H-C(2)-C(3)-H is 147.3°, again in good agreement with the 10.7 Hz coupling observed in the ¹H NMR spectrum. The principal difference in the solid state structures of the complexes **102a** and **55a** lies in the relative orientation of the ancillary ligands. The increased steric demand of the larger piperidine substituents in complex **55a** presumably forces the indenyl rings to rotate, placing the two substituents behind the titanocene wedge. In contrast, the dimethylamino substituents in complex **102a**, project somewhat forward over the titanacyclobutane ring. It is not obvious, however, that such a conformational change would necessarily be observed in the corresponding crotyl-derived titanacyclobutane complexes and how, if observed, such a change might engender the differences in the observed rates of β-hydride elimination.

The change in oxidation state at the metal that accompanies central carbon alkylation reaction is accented by rehybridization of the nitrogen atoms and rotation of the amine functionality with respect to the indenyl plane. The greater ability of the

nitrogen-substituted ancillary ligand system to facilitate the oxidation state increase at the metal in the transition state for central carbon alkylation may, at least in part, account for the successful alkylation of substituted allyl complexes.

Although the piperidinoindenyl ligands in complex **55a** indeed report the change in oxidation state relative to complex **53**, the nitrogen pyramidalization is greater and $C_{\text{ind}}\text{-N}$ bond lengths are longer than what is observed in either 1,1'-bis(*N,N*-dimethylamino)titanocene dichloride^{23a} or any of the previously reported bis(dialkylaminoindenyl)zirconocene dichlorides.^{23d,f,g,i} Only the *ansa*-bridged bis(dialkylaminoindenyl)zirconium(IV) systems exhibit nitrogen pyramidalizations and $C_{\text{ind}}\text{-N}$ bond lengths that approach the values present in complex **55a**, although these features are attributed to specific steric interactions with the ligand bridges.^{23g,h} In contrast, the crystal structure of dimethylaminoindenyl complex **101a** reveals that the amine functionality is essentially sp^2 -hybridized. The observed $C_{\text{ind}}\text{-N}$ bond lengths indicate strong double bond character (*cf.*, imine $C=N$: 1.38 Å) and fall within the range observed for other dialkylamino-substituted indenyl complexes of Ti(IV) and Zr(IV).²³ The twist angle is similarly decreased, confirming the strong donation of electron density into the indenyl rings. The pronounced differences in the structural parameters of the aminoindenyl ligands for such closely analogous complexes can not be readily rationalized by simple steric and electronic considerations.

Conclusions. The ORTEP diagrams of Ti(III) and Ti(IV) complexes **96**•LiCl₂(THF)₂, **98**, **99**, **101a**, **53** and **55a** reveal interesting structural features presumably attributable to the variable electron demands of titanium centers in the different ligand and oxidation state environments. The crystal structures clearly indicate that the ancillary ligands are capable of providing greater electron density than is required by the metal, facilitating the oxidation state change that occurs during central carbon radical alkylation. Based on this

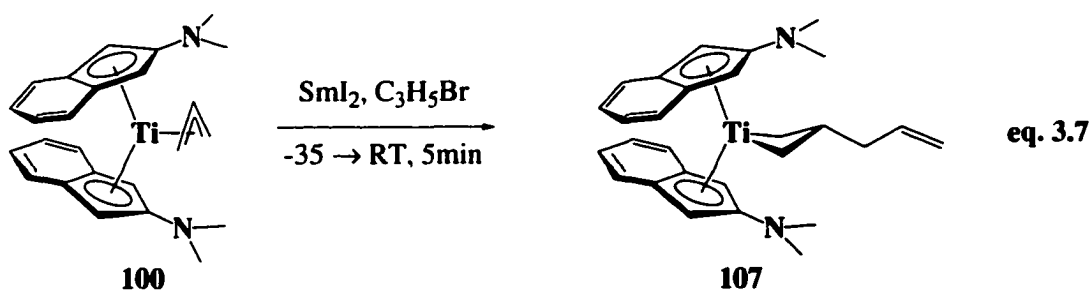
'oversupply' of electron richness, our investigation next turned to the development of less electron-rich indenyl templates, to determine the minimum electron density required to promote regioselective central carbon alkylation of substituted allyl systems (Chapter 4).

D. β -Carbon Cleavage: A New Decomposition Pathway for Titanacyclobutane Complexes

Although the bis(2-*N,N*-dimethylaminoindenyl)titanium(III) template affords improved results for regioselective central carbon radical alkylation of substituted allyl complexes relative to the previously reported bis(2-piperidinoindenyl)titanium(III) template, the effectiveness with stabilized radicals remains limited. Central carbon alkylation proceeds in acceptable yields upon reaction of cinnamyl complex **98** and crotyl complex **99** with benzyl radical; the addition of allyl radical to either complex does not afford a titanacyclobutane product. Titanacyclobutane complexes derived from cinnamyl complex **98** are robust and are generally stable at temperatures up to about 70 °C. Crotyl-derived titanacyclobutane complexes, which possess β -hydrogen atoms on the titanacyclobutane α -substituent, are subject to β -hydride elimination. Thus, while the inability to observe a crotyl-derived titanacyclobutane upon addition of allyl radical might be rationalized by proposing decomposition by β -hydride elimination, this explanation can not be extended to a titanacyclobutane complex derived from the addition of allyl radical to cinnamyl complex **98**.

The reactivity of the unsubstituted allyl complex **100** was thus investigated. The addition of one equivalent each of allyl bromide and samarium diiodide at low temperature to allyl complex **100** resulted in a colour change suggestive of titanacyclobutane formation (blue to bright red). On workup, however, the red solution quickly lost colour and gave way to a light brown paramagnetic material. Believing that the desired titanacyclobutane complex had indeed been formed, another attempt was

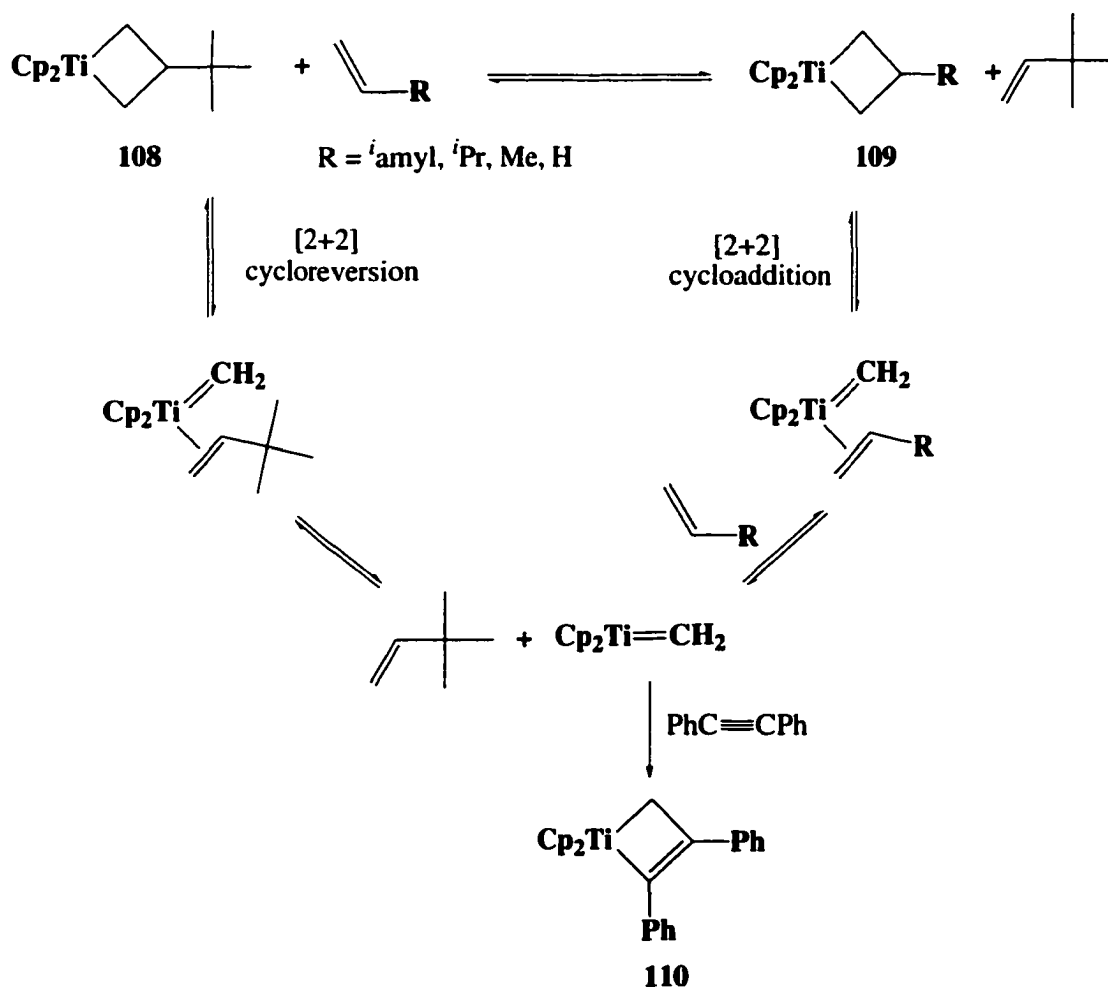
made to isolate the kinetic product of the reaction. Five minutes after the addition of allyl bromide and samarium diiodide, the reaction mixture was added to a large excess of cold pentane. The resultant red suspension was filtered and concentrated under vacuum. A ^1H NMR spectrum of the crude product shows signals characteristic of 3-allyl titanacyclobutane complex **107** (eq. 3.7). As anticipated, the titanacyclobutane core is identified by triplets at δ 2.03 ($J = 10.0$ Hz) and 1.78 ($J = 8.4$ Hz) for the four α -methylene protons; the β -methine proton is obscured by pentane resonances. The allyl substituent is characterized by a multiplet at δ 6.23 for the vinyl methine signal, overlapping signals at δ 5.15 for the terminal methylene signals and a multiplet at 2.59 ppm for the internal methylene signal. Further characterization of complex **107** was not possible as the titanacycle decomposed quickly in solution to a paramagnetic material. The similarity of this spectrum to previously characterized 3-allyl-bis(pentamethylcyclopentadienyl)titanacyclobutane²⁶ however, lends additional support to the structural assignment.



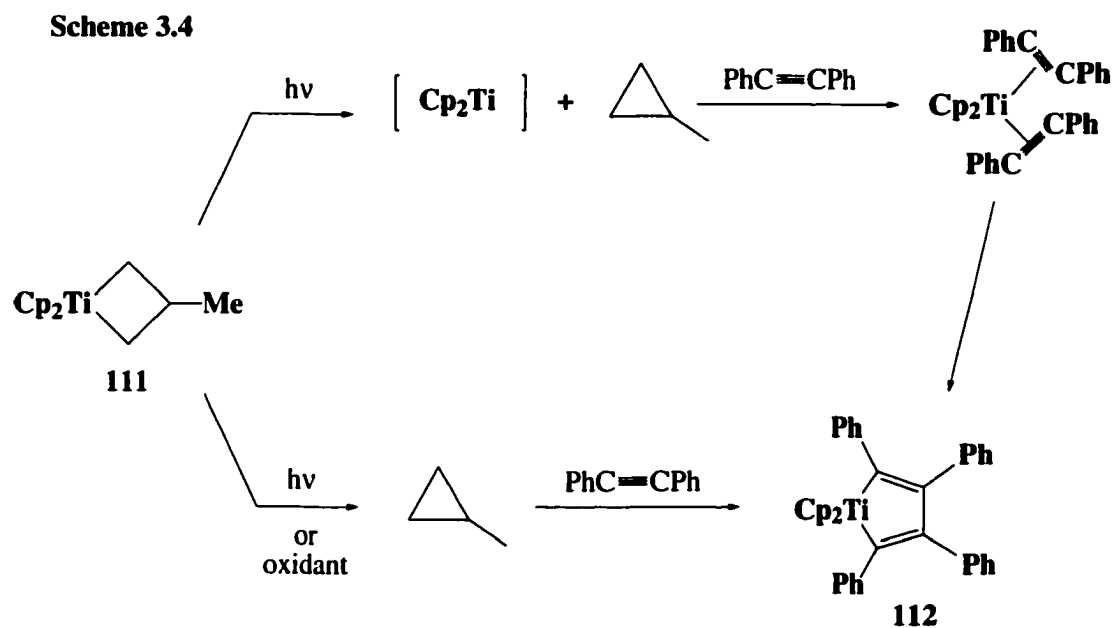
There are two established decomposition pathways for titanacyclobutane complexes that do not bear a hydrogen atom on an α -substituent.²⁷⁻²⁹ The most common pathway is [2+2] cycloreversion; the second is oxidatively induced reductive elimination. Transition metal catalyzed olefin metathesis has been extensively investigated; it has been revealed that the reaction proceeds through metal alkylidene and metallacyclobutane as intermediates.²⁷ In this reaction, [2+2] cycloreversion and [2+2] cycloaddition are the

key steps to the formation of these intermediates, respectively (Scheme 3.3). The existence of these intermediates was clearly established by the treatment of titanacyclobutane complex **108** with various olefins and observation of the corresponding metallacyclobutanes **109**. The suspected titanium alkylidene intermediate was trapped by diphenylacetylene to give the corresponding stable titanacyclobutene **110**.²⁷ The rate of cleavage of the titanacyclobutane to the titanocene methylidene olefin complex was found to decrease in the presence of electron-donating substituents.²⁸

Scheme 3.3



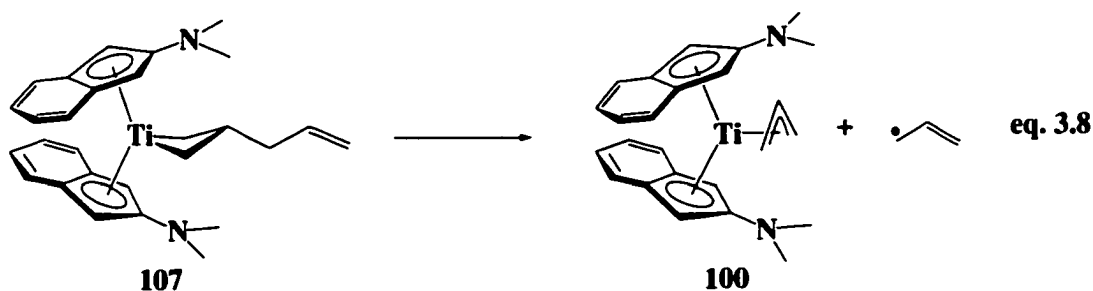
In the oxidative decomposition pathway, the presence of an oxidant or light promotes the conversion of titanacyclobutane complexes to cyclopropanes.²⁹ Irradiating titanacyclobutane complex **111** in the presence of diphenylacetylene induces reductive elimination of the organic fragment from the metal center. Diphenylacetylene coordinates to the metal center and oxidatively couples to give titanacyclopentadiene complex **112** (Scheme 3.4). Similarly, treating titanacyclobutane complex **111** with a one electron oxidant such as tetrakis(trifluoromethyl)cyclopentadienone (TTFC), Ag⁺, 2,3-dichloro-5,6-dicyano-1,4-benzoquinone (DDQ), 7,7,8,8-tetracyanonquinodimethane (TCNQ) or [Cp₂Fe]⁺ results in quantitative production of the cyclopropane.^{29d}



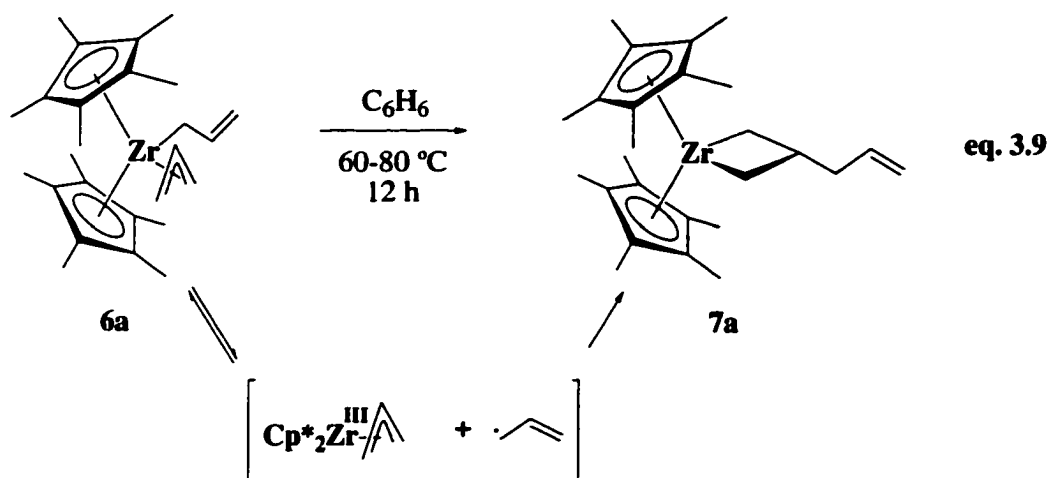
To determine if either of these decomposition pathways is operative in the decomposition of 2-allyltitanacyclobutane complex **107**, one equivalent each of allyl bromide and samarium diiodide at low temperature were added to allyl complex **100**. As the reaction turned red, indicating titanacyclobutane formation, two equivalents of diphenylacetylene were added to the reaction mixture. The reaction was left to stir for

two hours at room temperature. Workup of the reaction mixture afforded quantitative recovery of diphenylacetylene. No diamagnetic titanium product could be detected.

The loss of diamagnetic titanium suggested strongly that titanacyclobutane complex **107** decomposes reductively to paramagnetic Ti(III). The most probable route for this decomposition involves homolytic β -carbon-carbon cleavage of the allyl substituent to regenerate Ti(III) allyl complex **100** and allyl radical (eq. 3.8), although titanium-carbon bond homolysis cannot be discounted. Although β -carbon-carbon cleavage is unprecedented in titanacyclobutane chemistry, such speculation is suggested by the thermal rearrangement of permethylzirconocene benzyl allyl complex **6c** (*vide supra*), and the quantitative conversion of permethylzirconocene bis(allyl) complex **6a** to β -allyl zirconacyclobutane **7a** on warming to ≥ 50 °C (eq. 3.9).^{30,31} Mechanistic investigations suggest that the rearrangement occurs via a free radical pathway involving the hydrocarbyl ligand migrating as a free radical to the β -carbon of the η^3 -allyl moiety. The microscopic reverse, β -carbon-carbon cleavage, suspected in the decomposition of titanacyclobutane **107**, was not detected in the zirconium series.



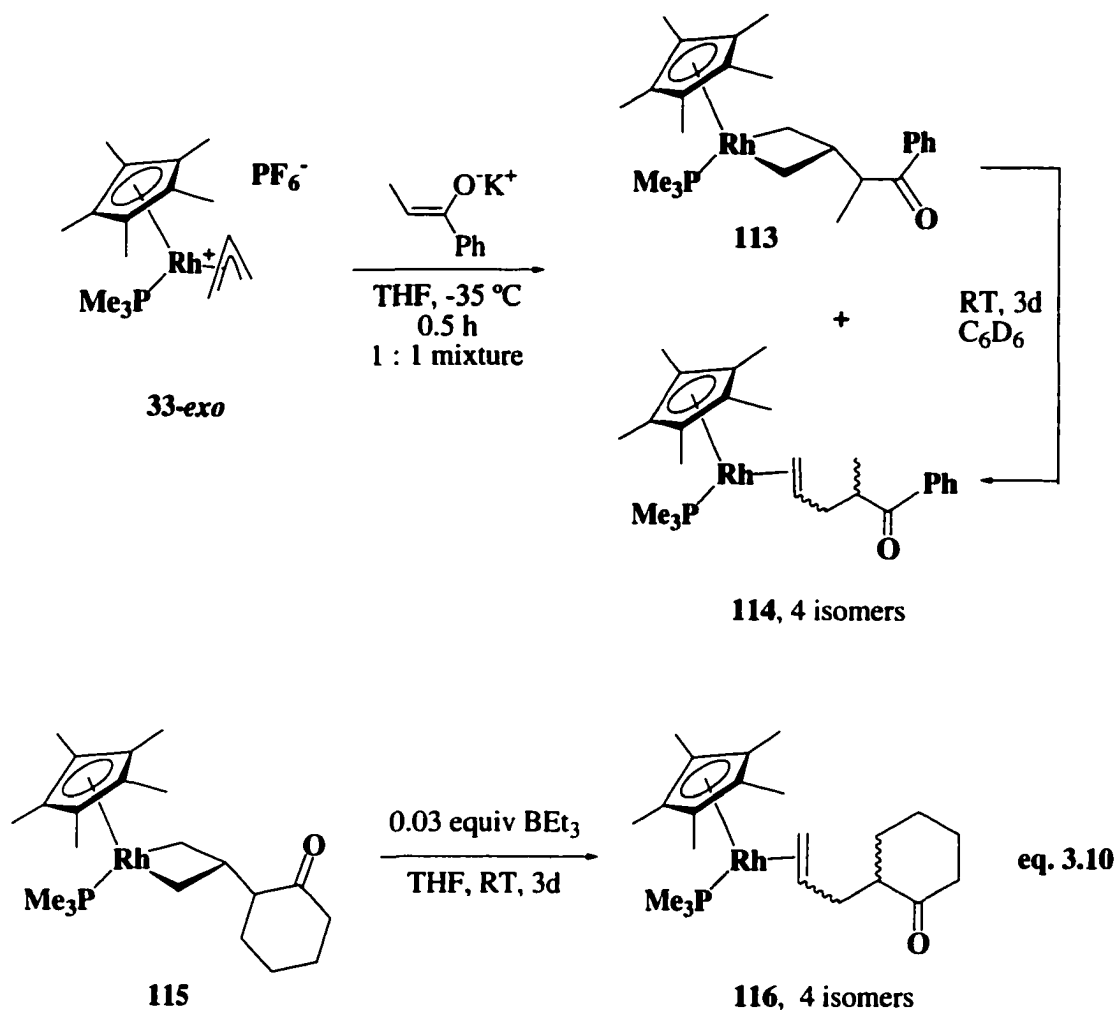
The observation of β -alkyl elimination has been documented in a number of early transition metal complexes;³² several cases have been found to be reversible.³³ β -Alkyl elimination is recognized as a key step in the chain termination of olefin polymerization



catalysis.³⁴ Reversible β -alkyl elimination, as well as alkyl migration, has also been observed in late metal systems.^{35,36} Interestingly and more specifically, β -alkyl migration has been observed in other metallacyclobutane rearrangements, although these systems have not been reported to proceed via radical scission. As previously discussed, both terminal and central carbon alkylation are observed on treatment of $[\text{Cp}^*(\text{PMe}_3)\text{Rh}(\eta^3\text{-allyl})]^+\text{PF}_6^-$ **33** with the enolate of propiophenone. However, metallacyclobutane formation, in this instance, was followed by re-ionization and re-addition to give the thermodynamically preferred terminal carbon olefin adduct **114** (Scheme 3.5), a process that can be catalyzed by added Lewis acids (eq. 3.10).^{26,31,37,38}

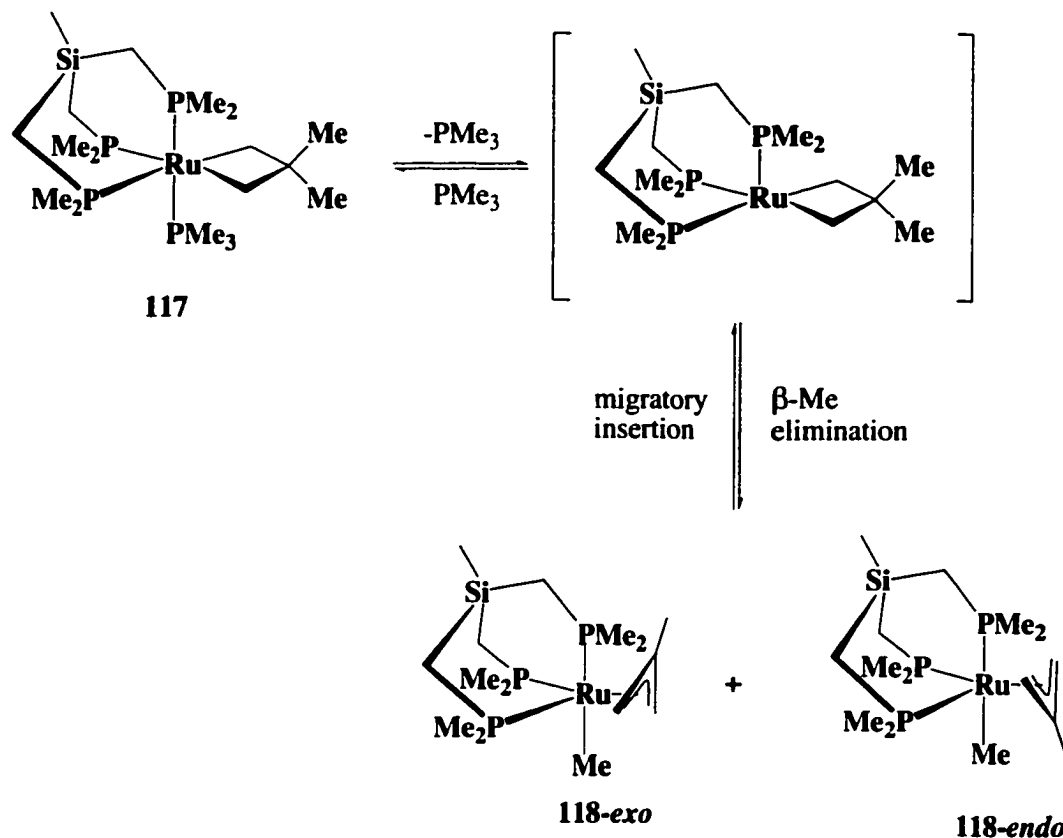
More recently, the Bergman group reported the interconversion of a 3,3-(dimethyl)ruthenacyclobutane and a methyl(2-methallyl)ruthenium complex. Thermolysis of **117** produces complex **118** as a mixture of *endo* and *exo* isomers (Scheme 3.6).³⁹ From the results of kinetic and labelling studies, the interconversion was proposed to take place by reversible β -methyl elimination/insertion.

Scheme 3.5

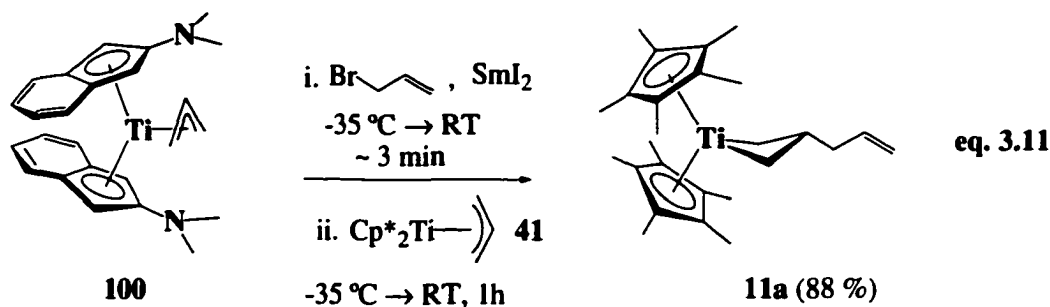


Calculated enthalpies of reaction for a series of β -alkyl elimination reactions at the Cp*₂Zr fragment, based on extensive thermochemical studies by the Marks group, provided the prediction that this process will vary between endothermic (+21 kcal/mol) and weakly exothermic (-6 kcal/mol) depending on the substrate.⁴⁰ In zirconacenes, β -alkyl elimination is predicted to be endothermic for an *n*-propyl group (+6 kcal/mol) and exothermic for a neopentyl group (-2 kcal/mol).

Scheme 3.6



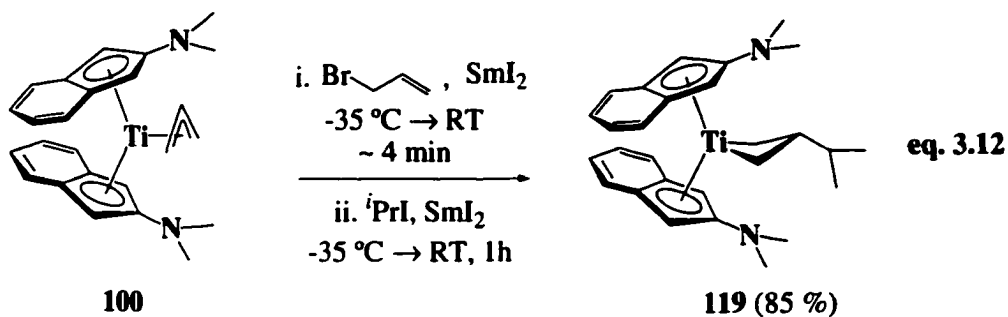
Testing the hypothesis that tentatively identified titanacyclobutane complex **107** decomposes by β -carbon-carbon cleavage requires trapping both decomposition products. Permethyltitanocene allyl complex **41** forms stable titanacyclobutane complexes upon addition of stabilized radicals and thus was expected to be an effective trap for the allyl radical. Thus, equimolar amounts of allyl complex **100** and SmI_2 were dissolved in THF, cooled, and then treated with a cold solution of allyl bromide in THF. The reaction was monitored visually: once the blue colour of unreacted SmI_2 disappeared and was replaced with a bright red colour characteristic of titanacyclobutane complexes (~ 3 min), a molar equivalent of permethyltitanocene allyl complex **41** was added to solution (eq. **3.11**). After one hour, the reaction mixture was evaporated to dryness, and triturated with



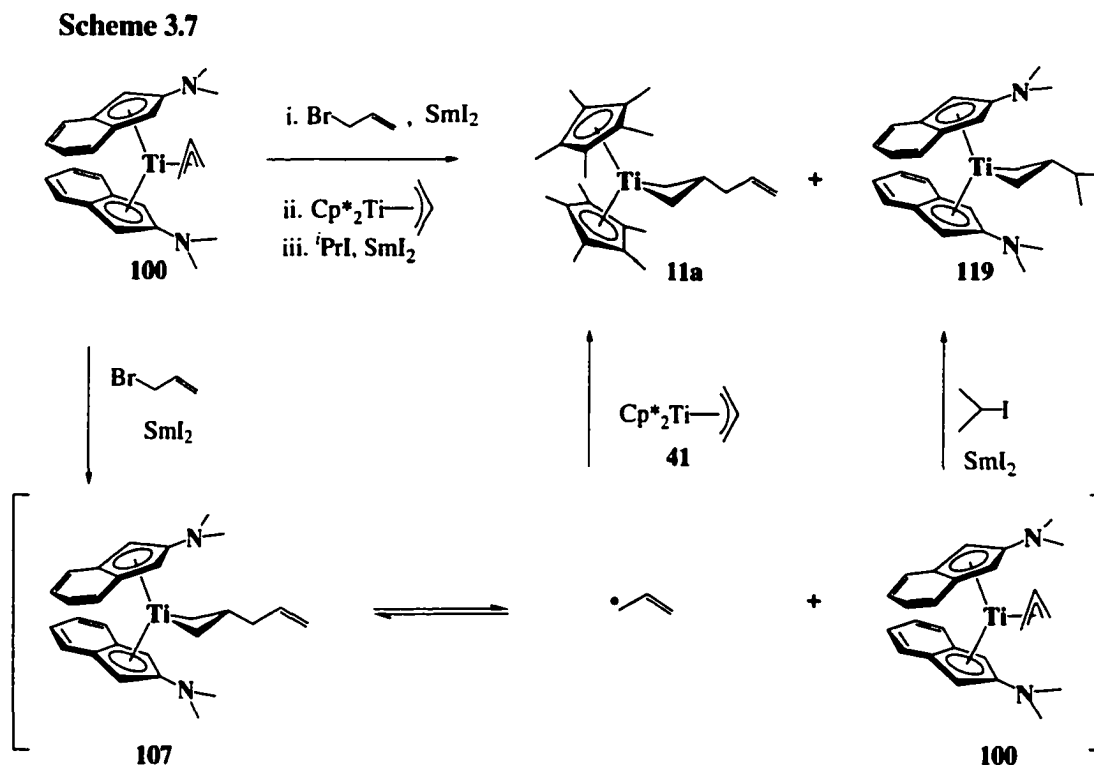
pentane. The resultant red solution was shown to contain 2-allyl bis(permethylcyclopentadienyl)titanacyclobutane complex **11a** as the only diamagnetic product by ¹H NMR spectroscopy. This result is a strong indication that allyl radical is indeed formed in the decomposition of bis(2-*N,N*-dimethylaminoindenyl)titanacyclobutane **107**.

To identify the re-formation of 2-*N,N*-dimethylaminoindenyl titanium allyl complex **100**, the other intermediate expected in the proposed decomposition of titanacyclobutane complex **107**, the subsequent addition of a non-stabilized alkyl radical was investigated. To accomplish this, the reaction described above was repeated, however, the addition of permethyltitanocene allyl complex **41** was replaced by the addition of one equivalent each of SmI₂ and isopropyl iodide. The reaction was left to stir for an additional hour resulting in exclusive isolation of 2-isopropyl-bis(2-*N,N*-dimethylaminoindenyl)titanacyclobutane complex **119**, as determined by ¹H NMR spectroscopy (eq. 3.12) and independent synthesis (Section E). This result provides additional support to the proposed homolytic β-carbon-carbon cleavage of the allyl substituent.

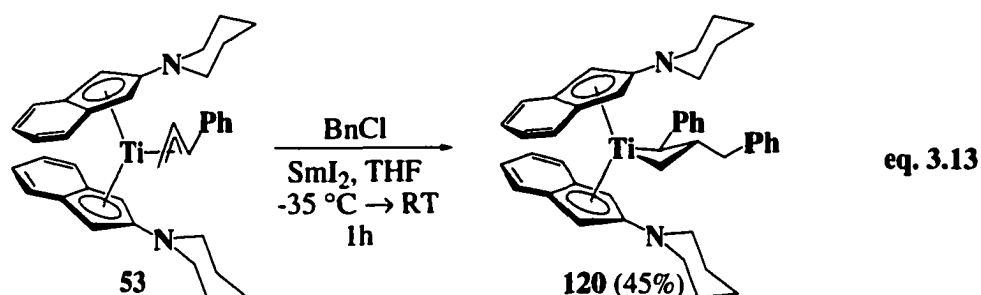
Further substantiation of this decomposition pathway was garnered by trapping both decomposition products in one pot. Thus, a THF solution of bis(2-*N,N*-dimethylaminoindenyl)titanium allyl complex **100** was mixed with cold solutions of SmI₂



and allyl bromide. After the blue colour representative of unreacted SmI₂ had completely disappeared (~ 4 min) one equivalent of permethyltitanocene allyl complex **41** was added to the reaction mixture. This reaction mixture was left to stir until the red colour of the solution re-emerged (~ 3 min). Finally, THF solutions of SmI₂ and isopropyl iodide were added to the reaction mixture. After work-up, ¹H NMR spectroscopy established the formation of 2-allyl bis(permethylcyclopentadienyl)titanacyclobutane complex **11a** and 2-isopropyl bis(2-*N,N*-dimethylaminoindenyl)titanacyclobutane complex **119** in near quantitative material balance (Scheme 3.7).

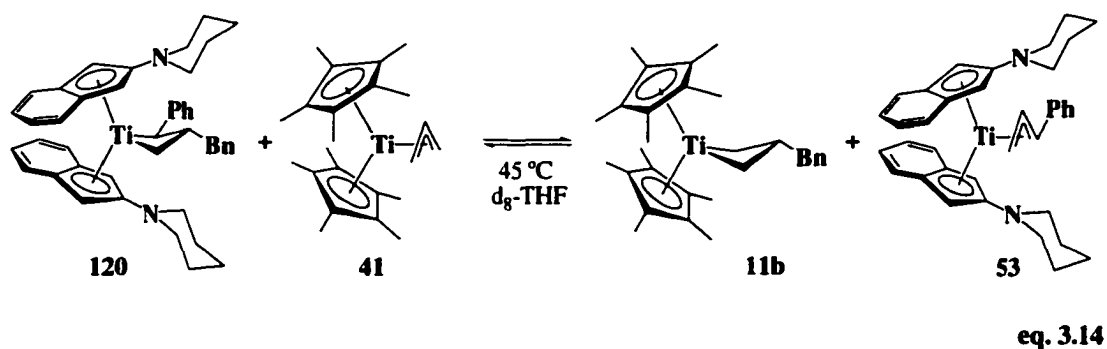


To determine if this unprecedented decomposition pathway is operative in a more general context, a brief reinvestigation of the 2-piperidinoindenyl template was undertaken. Stabilized radicals failed to undergo central carbon alkylation in this series (*vide supra*). Bis(2-piperidinoindenyl)titanium cinnamyl complex **53** was treated with both SmI_2 and benzyl chloride at low temperature. Within one hour of the addition, the colour of the solution had turned red/brown. Immediate ^1H NMR spectroscopy of the crude reaction material clearly indicated the formation of 3-benzyl-2-phenyl-bis(piperidinoindenyl)titanacyclobutane complex **120**, the desired titanacycle (eq. 3.13). However, when left in a THF solution at room temperature overnight, complex **120** decomposed to paramagnetic material. It was even possible to induce precipitation of complex **120** from diethyl ether layered with pentane cooled to $-35\text{ }^\circ\text{C}$, giving bis(2-piperidinoindenyl)titanacyclobutane complex **120** as an impure dark brown powder in 45% yield. NMR spectroscopy (^1H , ^{13}C , COSY and HMQC) was used to confirm the assignment of this product.

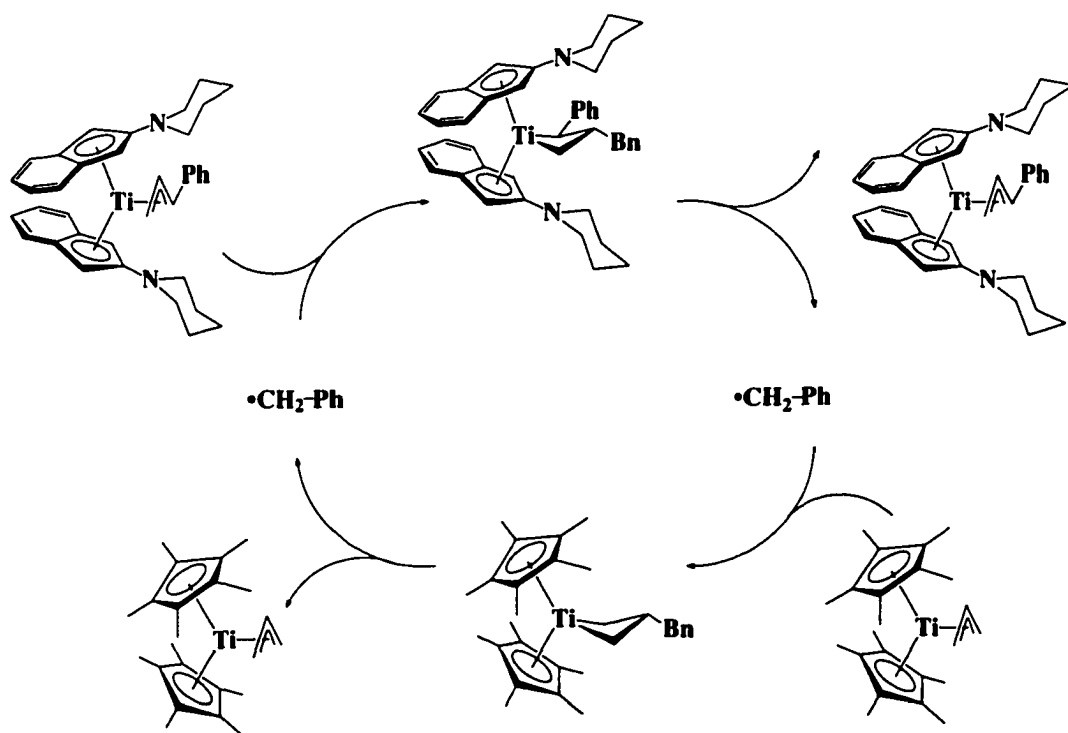


To establish that decomposition of titanacyclobutane complex **120** occurs via β -carbon-carbon bond homolysis, this complex was added to an excess of permethyltitanocene allyl complex **41**, dissolved in THF-d_8 and heated to $45\text{ }^\circ\text{C}$. Within one hour, trace amounts of 2-benzyl-bis(pentamethylcyclopentadienyl)titanacyclobutane complex **11b** were observed spectroscopically and within 12 hours, complex **11b**

constituted over 90% of the material observable by ^1H NMR spectroscopy (eq. 3.14). That the reaction does not go to completion even after three days implies that 3-benzyl bis(pentamethylcyclopentadienyl)titanacyclobutane **11b** may also be capable of β -carbon-carbon homolytic cleavage reversibly, reforming 2-piperidinoindenyl titanacyclobutane complex **120** (Scheme 3.8).



Scheme 3.8



The observed instability of 2-piperidinoindenyl titanacyclobutane complex **120** and of 3-benzyl-2-phenyl-bis(2-methoxyindenyl)titanacyclobutane complex **89c** compared to the remarkable stability of the dimethylaminoindenyl analogue **98d** illustrates the subtle influence exerted by different electron-donating substituents on the ancillary ligands. The steric effects introduced by placing bulky piperidino rings on indene may affect the stability of titanacyclobutane complex **120**, however, this explanation can not be easily extended to understand the instability of 2-methoxyindenyl titanacyclobutane complex **89c**. The stability of these complexes is thus likely dictated by a combination of steric and electronic factors imparted by the ancillary ligand system on the titanacyclobutane core.

The difference in stability of titanacyclobutane complexes derived from benzyl and allyl radicals, presumed to be similar in both stability and reactivity,⁴¹ may be attributed to a subtle substituent effect, akin to the substituent effect reported by Marks in the calculation of enthalpies for a series of β -alkyl eliminations (*vide infra*).⁴⁰ It remains unclear, however, why 3-allyl-bis(pentamethylcyclopentadienyl) titanacyclobutane complex **11a** is significantly more stable than the corresponding aminoindenyl and alkoxyindenyl titanacyclobutane complexes.

In the investigation into the reactivity of $\text{Cp}^*_2\text{Sm}(\text{THF})_2$ with various unsaturated substrates Evans attributes the facile interconversion of samarium oxidation states to the electronic flexibility afforded by the permethylcyclopentadienyl ligands as these ligands are suspected to accept/donate electron density as directed by the metal center.⁴² The difference in reactivity may also be due to the 'indenyl effect'. Basolo first described the 'indenyl effect' upon comparison of the reactivity of $(\eta^5\text{-indenyl})\text{Rh}(\text{CO})_2$ to the corresponding cyclopentadienyl species, with the former found to be far more reactive.⁴³ It is now well known that transition-metal indenyl complexes show enhanced reactivity

towards substitution and related reactions compared to their cyclopentadienyl analogues.¹¹ This rate enhancement has generally been attributed to a facile ring slippage from η^5 - toward η^3 -coordination in an associative transition state. The low barrier to ring slip in indenyl complexes is driven by the aromaticity that is 'regained' by the six-membered ring.

The dialkylaminoindenyl ancillary ligands may be providing titanium with electronic flexibility, promoting the interconversion between the trivalent and tetravalent oxidation states which allows for the electronic conditions required for homolysis of the β -carbon-carbon bond. More specifically, if, in the Ti(IV) oxidation state, ring slip occurs, the loss of electron density at titanium may promote extrusion of the β -alkyl substituent to regain electron density as extrusion reduces titanium to the Ti(III) oxidation state.

In conjunction with the above argument, 16-electron bis(indenyl)titanium, -zirconium, and -hafnium complexes exhibit greater thermal and oxidative stabilities relative to their cyclopentadienyl counterparts.⁴⁴ Group IV indenyl complexes form relatively strong carbon-metal σ -bonds and, expectantly, are less prone to homolytic cleavage of σ -bonded organic groups in comparison to Group IV cyclopentadienyl complexes.⁴⁵ The thermal stability of aminoindenyl titanacyclobutane complexes is reflected in the high temperatures required for [2+2] retrocyclization (>70 °C). Thus, it is perhaps not surprising that for bis(2-*N,N*-dimethylaminoindenyl) titanacyclobutane complexes the weakest bond may in fact be the β -carbon-carbon bond.

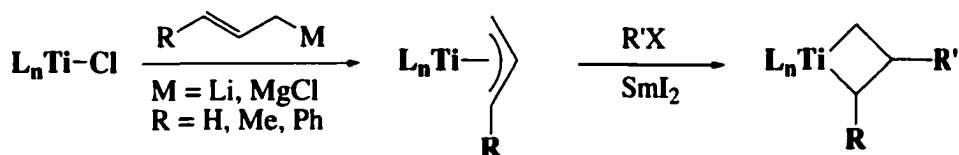
The difficulty in determining the underlying cause of the differences in stability of the benzyl radical-derived products as the difference in stability between 2-allyl titanacyclobutane complex **11a** and **107** illustrates the need for a detailed theoretical

investigation. The indenyl ligand differs from the cyclopentadienyl ligand in the larger number of ligand π -orbitals. The direct result is that bonding and antibonding combinations between the metal and the ancillary ligands determined for the ligation of cyclopentadienyl rings cannot necessarily be extended to indenyl rings. These differences, coupled with the different steric and electronic environment for each of the ancillary ligand systems, can likely only be addressed by computational methods.

E. One Pot All-Samarium Mediated Synthesis of Titanacyclobutane Complexes

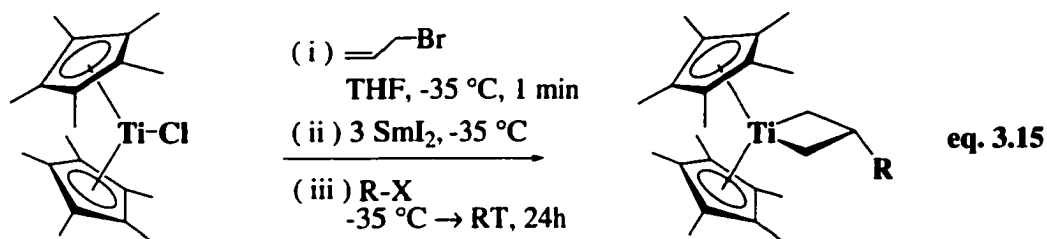
The preparation of titanacyclobutane complexes by radical alkylation requires two organometallic reactions, which can be conducted separately or in one pot. In the first reaction the titanocene chloride complex is treated with an allylic Grignard or lithium reagent to afford an allyl complex. In the second reaction, free radical alkylation generates the titanacyclobutane complex (Scheme 3.9). Particularly because of limitations experienced using the pentamethylcyclopentadienyl template,²⁶ it was important to develop a synthesis of titanacyclobutane complexes that avoids the use of allylmetal reagents. This was first accomplished by Chen, who developed samarium-mediated methodology to generate 2-alkyl bis(pentamethylcyclopentadienyl)titanacyclobutanes from the titanocene chloride, allyl bromide and an alkyl halide.^{2,46}

Scheme 3.9



Synthesis of titanacyclobutane complexes using the ‘Chen procedure’ requires the initial addition of one equivalent of allyl bromide in THF to Cp^*_2TiCl at low temperature

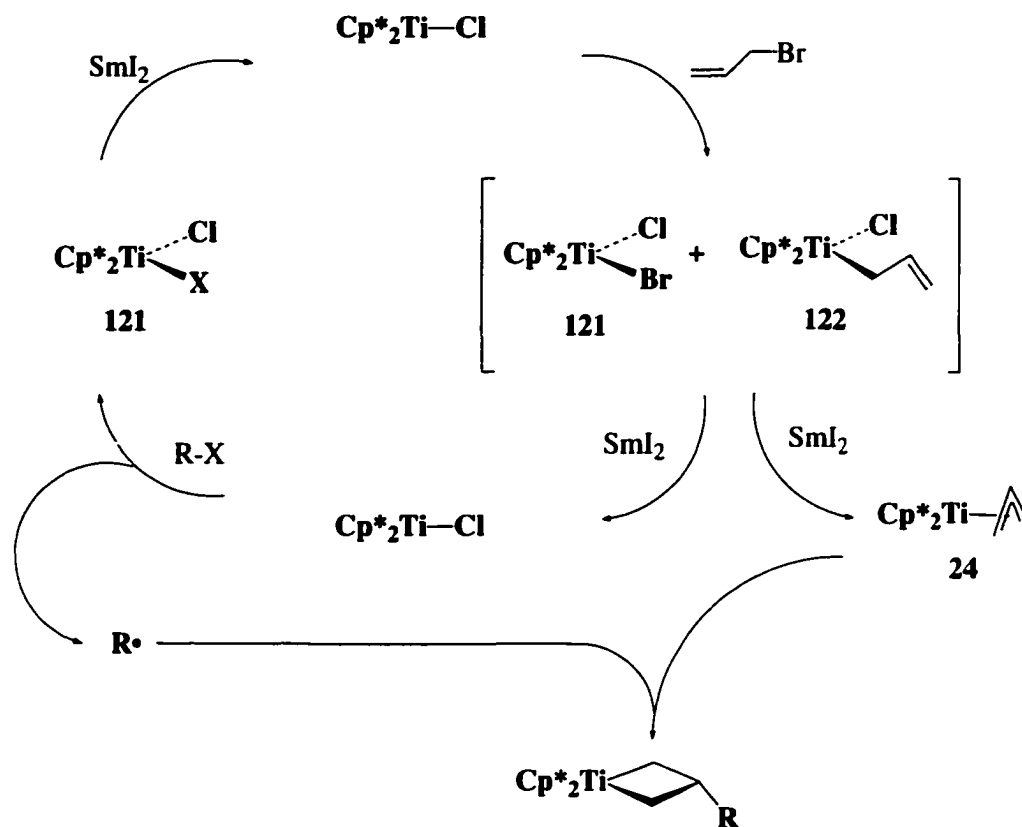
(-35 °C). The resultant reaction mixture is stirred for no more than one minute and subsequently treated with three equivalents of cold SmI₂, followed immediately by the addition of one equivalent of the alkyl halide in cold THF. The reaction mixture is allowed to warm to room temperature and maintained there until the blue colour of unreacted SmI₂ has completely disappeared (6-24h) (eq. 3.15). In addition to avoiding the formation of 2-allyl bis(pentamethylcyclopentadienyl)titanacyclobutane **11a**, a byproduct common to the two-step methodology, the yields using this procedure are near quantitative.



The reaction mechanism under these conditions is believed to occur in two stages: (i) generation of the allyl titanium intermediate and (ii) alkyl radical formation and addition. Experimental observations indicate that the initial interaction of allyl bromide with Cp*₂TiCl generates 0.5 equivalents of Ti(IV) dihalide complex **121** and 0.5 equivalents of the allyltitanocene halide **122** (Scheme 3.10). In the presence of samarium diiodide, both of these Ti(IV) complexes are reduced back to Ti(III), the dihalide complex **121** to a monohalide complex²⁶ and the allyl chloride complex to allyltitanium(III) complex **41**, which subsequently undergoes alkylation to generate the titanacyclobutane complexes. As each of these reactions proceeds at or below room temperature, we believe that during the alkylation stage, Cp*₂TiCl or an adventitious Ti(III) catalyst reacts with the alkyl halide to produce the alkyl radical and a Ti(IV) dihalide complex (e.g., complex **121**). The alkyl radical reacts quantitatively with allyltitanocene **41** and the Ti(IV) dihalide complex is reduced by SmI₂ back to

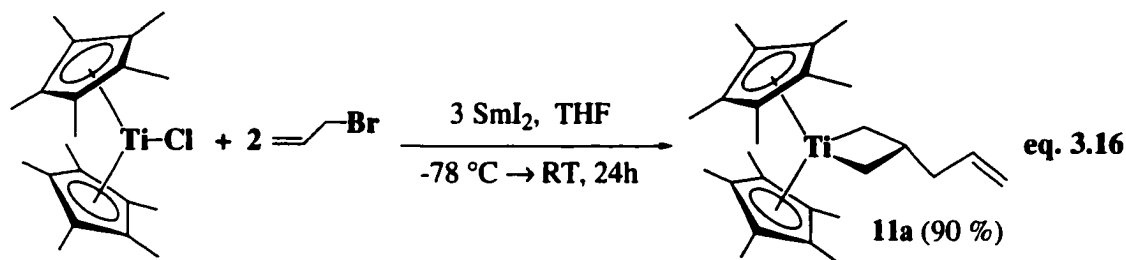
monohalide Ti(III). The regeneration of monohalide Ti(III) in both stages continues until all the allyl bromide has reacted.

Scheme 3.10



Nomura earlier found that although treatment of Cp^*_2TiCl with two equivalents of allyl bromide in the presence of samarium diiodide affords β -allyl titanacyclobutane **11a** in high yield (eq. 3.16), the use of crotyl bromide in this reaction was unsuccessful.⁴⁷ Since the use of substituted allyl for central carbon alkylation is successful using alkoxy- or aminoindenyl titanocene templates, the extension of this procedure to such templates was pursued. A preliminary investigation into the reactivity of unsubstituted allyl complexes revealed that treatment of 2-methoxyindenyl titanocene **84**, 2-piperidinoindenyl titanocene **52** and 2-*N,N*-dimethylaminoindenyl titanocene **96** under these reaction conditions results in the formation of 3-isopropyl titanacyclobutane

complexes **93a**, **123**, and **119**, respectively in moderate to high yields (eq. 3.17 and Table 3.13).



The extension of this reactivity pattern to include substituted allyl substrates was met with only limited success. Treating 2-methoxyindenyl titanocene **84** with crotyl bromide, samarium iodide and isopropyl iodide under reaction conditions identical to those presented above does result in the formation of 2-methyl-3-isopropyl titanacyclobutane **90a**, however the yield of the reaction is significantly lower (eq. 3.17 and Table 3.13). Surprisingly, the use of cinnamyl chloride as the allyl substrate does not generate any of the expected titanacycle. The major product under these reaction conditions is 1,6-diphenylhexa-1,5-diene, presumably from dimerization of cinnamyl radical. Similarly, when 2-*N,N*-dimethylaminoindenyl titanocene **96** is treated with crotyl bromide, samarium diiodide and isopropyl iodide in accordance with the 'Chen procedure', 2-methyl-3-isopropyl titanacyclobutane **102a** is generated, again in lower yield with respect to the unsubstituted allyl case (eq. 3.17 and Table 3.13). Although a trace amount of 3-isopropyl-2-phenyl titanacyclobutane **101a** is formed when 2-*N,N*-dimethylaminoindenyl titanocene **96** is treated with cinnamyl chloride, samarium iodide and isopropyl iodide at low temperature, the major product isolated is again 1,6-diphenylhexa-1,5-diene.

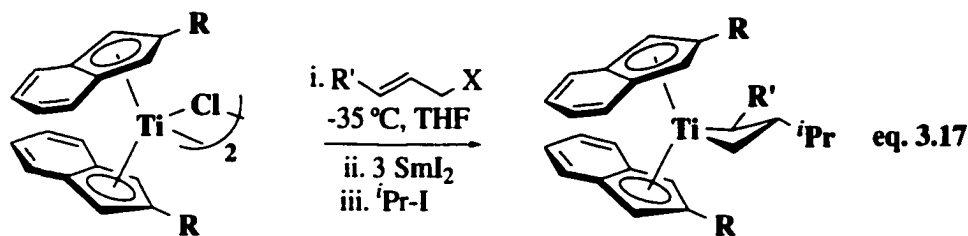


Table 3.13 Titanacyclobutane Formation Using Samarium Mediated Methodology

Starting complex	R	R'	X	Product	Yield ¹
84	OMe	H	Br	93a	93%
84	OMe	CH ₃	Br	90a	49%
84	OMe	Ph	Cl	89a	0%
96	NMe ₂	H	Br	119	95%
96	NMe ₂	CH ₃	Br	102a	53%
96	NMe ₂	Ph	Cl	101a	trace
52	piperidino	H	Br	123	78%
52	piperidino	CH ₃	Br	56a	60%
52	piperidino	Ph	Cl	55a	43% ²

¹Crude isolated yield.

²Isolated yield after recrystallization.

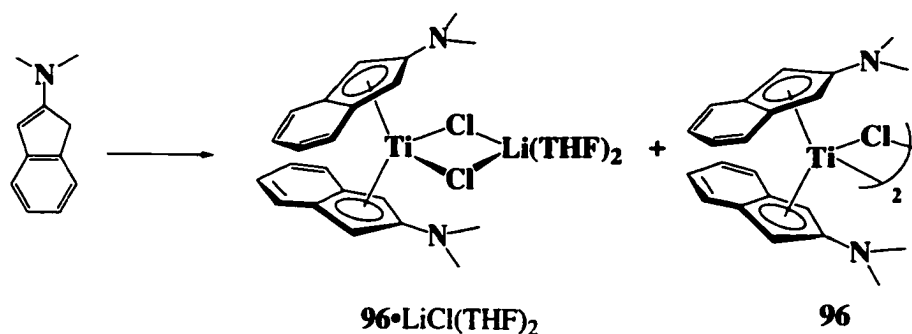
Slightly more encouraging results were obtained using the samarium-mediated reaction conditions for generating titanacyclobutanes from 2-piperidinoindenyl titanocene **52**. Using crotyl bromide and the reaction conditions described by Chen, it was possible to isolate 3-isopropyl-2-methyl titanacyclobutane complex **56a** in a 60% overall yield (eq. 3.17, Table 3.13). In addition, for the first time, a cinnamyl derived product, 3-isopropyl-2-phenyl titanacyclobutane complex **55a** was obtained by treating titanocene **52** with cinnamyl chloride under the 'Chen procedure.' Extraction of the crude product into hexane followed by crystallization resulted in a remarkable 43% isolated yield.

For the synthesis of 2,3-disubstituted titanacyclobutane complexes it is the two step methodology employing the use of allylmetal reagents that affords higher yields, despite numerous attempts to optimize the samarium-mediated reaction conditions. The major byproduct under these reaction conditions appears to result from dimerization of the allyl-derived radical generated. The reaction thus appears to be hampered by the preferential extrusion of cinnamyl or crotyl radical over the SmI_2 -induced reduction of the Ti(IV) allyl halide intermediate (Scheme 3.11). The success of the unsubstituted allyl substrate and increasing failure of crotyl and cinnamyl substrates correlate with the increasing stability of the allylic radical fragment. To improve upon these results a more halophilic one-electron reducing agent is clearly required. It appears counterintuitive that the bulky 2-piperidinoindenyl titanocene template **53** should afford the highest yield of 3-isopropyl-2-phenyl titanacyclobutane complex under the samarium-mediated reaction conditions. Considering the solid state structure of titanacyclobutane **55a**, however, it is clear that the large piperidino groups can locate 'behind' the titanocene wedge. This ancillary ligand orientation may allow for the rapid reduction of the cinnamyl halide Ti(IV) intermediate and subsequent formation of titanacyclobutane **55a**. It may also be that the 2-piperidinoindenyl system has a lower barrier to ring slip of the indenyl ligand from η^5 - to η^3 -coordination. Consequently, the allylic ligand may adopt η^3 -coordination, protecting it from rapid homolytic cleavage.

F. Experimental

General Experimental: See Chapter 2, pg. 59.

Bis(2-*N,N*-dimethylaminoindenyl)titanium Chloride **96 from 2-*N,N*-Dimethylaminoindene:**



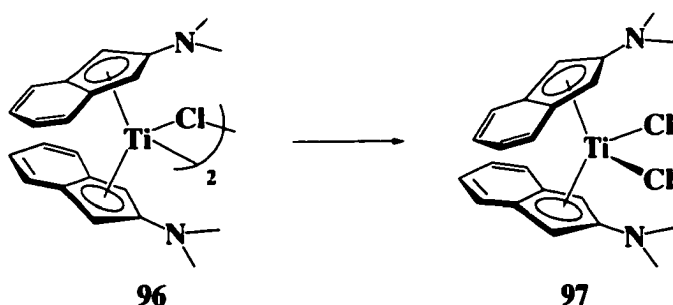
Bis(2-*N,N*-dimethylaminoindenyl)titanium chloride **96.** In a Schlenk flask under an inert atmosphere, 2-*N,N*-dimethylaminoindene⁴ (3.502 g, 22.0 mmol) was dissolved in 30 mL THF and cooled to -40 °C. *n*-Butyllithium (23.1 mmol, 1.6 M) was added dropwise by syringe and the solution was stirred at -40 °C for 3 h before warming to room temperature. In a separate Schlenk flask, $\text{TiCl}_3 \cdot 3\text{THF}$ (4.100 g, 11.0 mmol) was suspended in 40 mL THF. The solution of 2-*N,N*-dimethylaminoindenyllithium was transferred at room temperature via cannula into the titanium solution and left to stir overnight. After 12 h the solvent was removed under reduced pressure from the deep green solution, yielding a red-brown residue. The residue was extracted into benzene and the solution filtered through a sintered glass funnel layered with a short plug of Celite. The benzene was removed under reduced pressure and the residual solid was crystallized from THF/hexane (1 : 2) at -35 °C yielding complex **96** as an amorphous terra-cotta red solid, sprinkled with green crystals (4.05 g, ~92%).⁴⁸ Slow

recrystallization from a dilute solution of THF layered with hexane and cooled to $-35\text{ }^{\circ}\text{C}$ gave green single crystals suitable for analysis by X-ray crystallography, (see Appendix I) establishing the structure as the lithium chloride adduct, bis(2-*N,N*-dimethylaminoindenyl)titanium chloride-lithium chloride \cdot 2THF, **96** \cdot LiCl(THF) $_2$.

Complex **96** \cdot LiCl(THF) $_2$ was then extensively dried, taken up into benzene and filtered to remove all lithium chloride and recrystallized from THF layered with hexane (1 : 4) to give complex **96** as an amorphous terra-cotta red solid. HRMS calcd. for:

$\text{C}_{22}\text{H}_{24}\text{N}_2\text{Ti}^{35}\text{Cl}$ m/z 399.11075, found 399.11036; $\text{C}_{22}\text{H}_{24}\text{N}_2\text{Ti}^{37}\text{Cl}$ m/z 401.10779, found 401.10803. Anal. calcd. for $\text{C}_{22}\text{H}_{24}\text{N}_2\text{TiCl}$: C, 66.10; H, 6.05; N, 7.01; found C, 66.08, H, 6.11, N, 6.53.

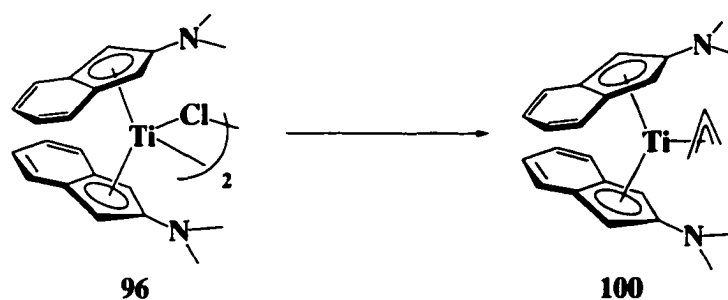
Bis(2-*N,N*-dimethylaminoindenyl)titanium Dichloride 97 from Bis(2-*N,N*-dimethylaminoindenyl)titanium Chloride 96:



Bis(2-*N,N*-dimethylaminoindenyl)titanium dichloride 97. A small sample of complex **96** (50.0 mg, 0.125 mmol) was oxidized using 0.5 equivalent PbCl_2 (17.4 mg) in THF at room temperature overnight. The residual lead was removed via filtration and the remaining solution was concentrated and cooled to $-35\text{ }^{\circ}\text{C}$ to give the corresponding diamagnetic dichloride complex as lustrous black crystals (53 mg, quant.). ^1H NMR (200 MHz, C_6D_6): δ 7.60 (2nd order m, 4H, H4/H5), 6.91 (2nd order m, 4H, H4/H5), 4.57 (br s, 4H, H2), 2.39 (s, 6H, $\text{N}(\text{CH}_3)_2$). ^{13}C NMR (50.3 MHz, C_6D_6): δ 160.4 (C1), 128.3

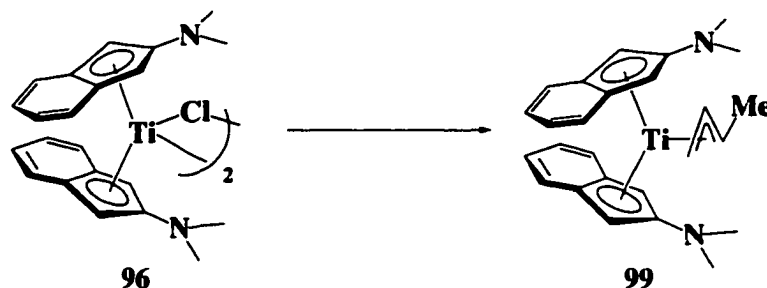
(C3) 125.8 (C4/C5), 123.7 (C4/C5), 92.1 (C2), 39.2 (N(CH₃)₂). HRMS calcd. for C₂₂H₂₄N₂TiCl₂ *m/z* 434.07504, found 434.07553. Anal. calcd. C, 60.46; H, 5.52; N, 6.63; found C, 60.05, H, 5.66, N 6.42.

Bis(2-*N,N*-dimethylaminoindenyl)titanium(η^3 -allyl) 100 from Bis(2-*N,N*-dimethylaminoindenyl)titanium Chloride 96:



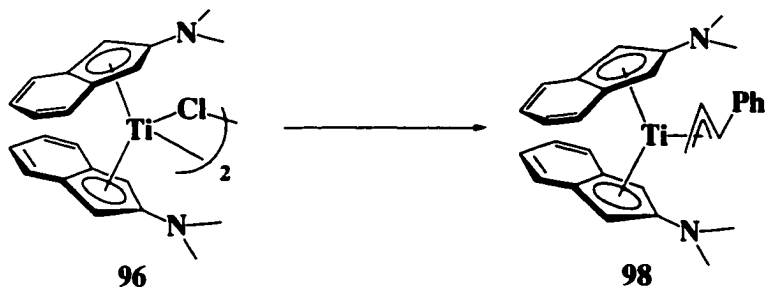
Bis(2-*N,N*-dimethylaminoindenyl)titanium(η^3 -allyl) 100. In the drybox, a vial containing a cooled (-35 °C) THF solution (3 mL) of bis(2-*N,N*-dimethylaminoindenyl)titanium chloride **96**, (27.9 mg, 0.0690 mmol) was mixed with equally cold allylmagnesium chloride (38 μ L, 2.0 M in THF) that had been further diluted in THF (1 mL). The reaction mixture was allowed to warm to room temperature and stir for 2 h. Under reduced pressure the THF was removed, leaving a dark orange residue. The product was extracted into hexane and filtered through a sintered glass funnel layered with a short plug of Celite. The hexane was evaporated under reduced pressure and the resulting solid was crystallized from THF layered with hexane (1 : 10) cooled to -35° C to afford orange prisms (22.5 mg, 80%). IR (cm⁻¹, hexane cast): 2940 (m), 2867 (m), 2794 (m), 1588 (s), 1546 (vs), 1448 (s), 1428 (s), 1360 (s), 1126 (s), 1060 (m), 987 (m), 801 (s), 774 (s), 737 (vs), 624 (m). Anal. calcd. C, 74.07; H, 7.21; N, 6.91; found C, 73.37; H, 7.09; N, 6.69.

Bis(2-*N,N*-dimethylaminoindenyl)titanium(η^3 -crotyl) 99 from Bis(2-*N,N*-dimethylaminoindenyl)titanium Chloride 96:



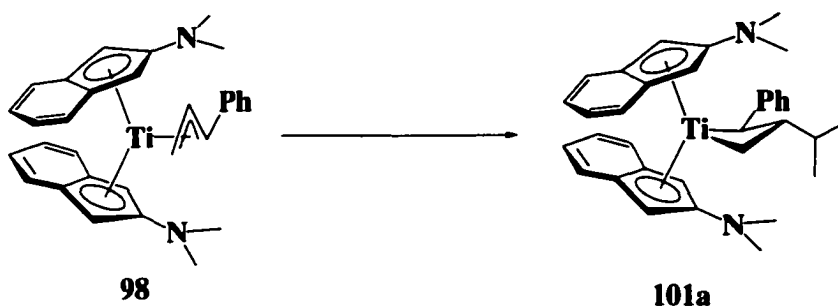
Bis(2-*N,N*-dimethylaminoindenyl)titanium(η^3 -1-methylallyl) 99. In the drybox, a vial containing a THF solution (5 mL) of bis(2-*N,N*-dimethylaminoindenyl)titanium chloride **96**, (57.5 mg, 0.144 mmol) was cooled to -35 °C. Crotylmagnesium chloride (0.100 mL, 1.5 M in THF) was diluted in THF (5 mL) and cooled to -35 °C. The two solutions were mixed together, allowed to warm to room temperature and stir for an additional 3 h. Removal of the THF *in vacuo* gave a dark red viscous oil, which was extracted into benzene and filtered through a sintered glass funnel layered with a short plug of Celite. The benzene was removed under reduced pressure. Purification of the residue from diethyl ether/hexane (1 : 5) gave a very dark red oil (39.8 mg, 66%). IR (cm⁻¹, pentane cast): 2931 (s), 2800 (m), 1588 (vs), 1548 (vs), 1529 (s), 1486 (m), 1449 (m), 1384 (m), 1362 (m), 1261 (w), 1126 (s), 1060 (s), 991(w), 802 (m), 747 (m), 698 (m), 625 (m). Anal. calcd. C, 74.45; H, 7.45; N, 6.68; found (trial 1) C, 71.87; H, 7.45; N, 6.15 (trial 2) C, 71.60; H, 7.39; N, 6.11.⁸ Crystals suitable for X-ray diffraction were obtained by repeated crystallization from dilute solutions of diethyl ether and hexane (see Appendix I).

Bis(2-*N,N*-dimethylaminoindenyl)titanium(η^3 -cinammyl) 98 from Bis(2-*N,N*-dimethylaminoindenyl)titanium Chloride 96:



Bis(2-*N,N*-dimethylaminoindenyl)titanium(η^3 -1-phenylallyl) 98. In the drybox, a vial containing a THF solution (10 mL) of bis(2-*N,N*-dimethylaminoindenyl)titanium chloride 96, (255.5 mg, 0.639 mmol) was cooled to $-35\text{ }^{\circ}\text{C}$. A cooled THF (5 mL) solution ($-35\text{ }^{\circ}\text{C}$) of cinnamyllithium (87.0 mg, 0.703 mmol) was added and the resulting solution was allowed to warm to room temperature and stir overnight. The THF was removed under reduced pressure, leaving a dark green residue. The product was extracted into benzene and filtered through a sintered glass funnel layered with a short plug of Celite. The benzene was removed *in vacuo* and the resulting solid was crystallized from THF layered with hexane (1 : 3) cooled to -35°C , affording dark green diamond-shaped crystals (225 mg, 73%). IR (cm^{-1} , THF cast): 2949 (m), 2866 (m), 2837 (m), 2796 (m), 1592 (s), 1544 (vs), 1528 (vs), 1486 (m), 1449 (m), 1429 (s), 1360 (s), 1251(m), 1125 (m), 1066 (m), 988 (m), 803 (s), 787 (m), 739 (vs), 695 (m). HRMS calcd. for $\text{C}_{31}\text{H}_{33}\text{N}_2\text{Ti}$ m/z 481.2119, found 481.2123. Anal. calcd. C, 77.43; H, 6.91; N, 5.82; found C, 77.21; H, 7.28; N, 5.69. Crystals suitable for X-ray diffraction were obtained from a dilute solution of the complex in THF layered with hexane and cooled to -35°C (see Appendix I).

Titanacyclobutane 101a from Bis(2-*N,N*-dimethylaminoindenyl)titanium Cinnamyl 98:

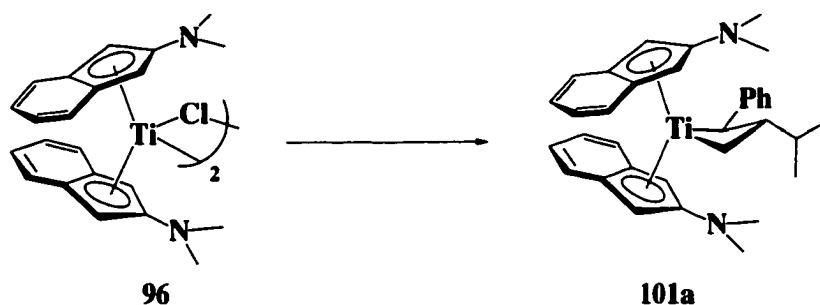


3-Isopropyl-2-phenyl-bis(2-*N,N*-dimethylaminoindenyl)titanacyclobutane 101a. In the drybox, a vial containing a THF solution (5 mL) of bis(2-*N,N*-dimethylaminoindenyl)titanium(η^3 -1-phenylallyl) **98** (103.9 mg, 0.216 mmol), was cooled to -35 °C. A cold solution of SmI₂ (2.25 mL, 0.1 M in THF) was added followed immediately by a cooled solution of 2-iodopropane (22.6 μ L in 1 mL THF). The reaction mixture was allowed to warm to room temperature and stir overnight. Almost immediately upon warming, the blue/green colour of the solution began to dissipate, followed by the emergence of a dark chocolate brown solution. Very little Sm(III) precipitate was observed during the course of the reaction. The solvent was removed *in vacuo*, the brown residue extracted into a 1 : 2 benzene/hexane mixture, and the resultant solution filtered through a sintered glass funnel layered with a short plug of Celite. The solvents were removed *in vacuo* and the resulting residue was crystallized from THF/hexane (1 : 4) at -35 °C to yield the titanacyclobutane complex **101a** as deep red rhomboid crystals suitable for X-ray diffraction (100.1 mg, 88%, see Appendix I for crystal structure determination). ¹H NMR (400 MHz, C₆D₆, RT): δ 7.48 (m, 1H, H4/H5), 7.32 (m, 4H, H4/H5, C₆H₅), 7.00 (t, *J* = 7.3 Hz, 1H, C₆H₅), 6.95 (ddd, *J* = 8.1, 6.9, 1.0, Hz, 1H, C₆H₅), 6.90 (m, 4H, H4/H5), 6.74 (ddd, *J* = 8.1, 6.7, 0.9 Hz, 1H, C₆H₅), 6.12 (d, *J* = 8.0 Hz, 1H, C₆H₅), 5.41 (d, *J* = 1.7 Hz, 1H, H2), 5.31 (d, *J* = 2.3 Hz, 1H,

H2'), 4.27 (br s, 1H, H2''), 4.05 (br s, 1H, H2'''), 3.32 (d, $J = 10.7$ Hz, 1H, α -CH(C₆H₅)), 2.65 (t, $J = 9.0$ Hz, 1H, α -CH₂), 2.36 (s, 6H, N(CH₃)₂), 2.23 (s, 6H, N(CH₃)₂), 1.50 (m, 1H, CH(CH₃)₂), 1.15 (d, $J = 6.6$ Hz, 3H, CH(CH₃)₂), 1.05 (d, $J = 6.7$ Hz, 3H, CH(CH₃)₂), 1.04 (overlapping multiplet with δ 1.05, 1H, β -CH), 0.61 (br m, 1H, α -CH₂). GCOSY (300 MHz, C₆D₆, RT) select data only: δ 3.32 (α -CH(C₆H₅)) \leftrightarrow δ 1.04 (β -CH); δ 2.65 (α -CH₂) \leftrightarrow δ 1.04 (β -CH) \leftrightarrow δ 0.61 (α -CH₂); δ 1.04 (β -CH) \leftrightarrow δ 1.50 (CH(CH₃)₂) \leftrightarrow δ 1.15 (CH(CH₃)₂), δ 1.05 (CH(CH₃)₂). ¹H NMR (400 MHz, C₆D₆, 70 °C): δ 7.50 (m, 1H, H_{aryl}), 7.38 (d, $J = 7.5$ Hz, 2H, H_{aryl}), 7.33 (t, $J = 7.4$ Hz, 2H, H_{aryl}), 7.02 (t, $J = 8.2$ Hz, 4H, H_{aryl}), 6.94 (m, 2H, H_{aryl}), 6.76 (t, $J = 7.5$ Hz, 1H, C₆H₅), 6.19 (d, $J = 8.2$ Hz, 1H, C₆H₅), 5.44 (d, $J = 2.3$ Hz, H2), 5.42 (d, $J = 2.3$ Hz, H2'), 4.44 (d, $J = 2.0$ Hz, H2''), 4.19 (d, $J = 2.2$ Hz, H2'''), 3.28 (d, $J = 10.7$ Hz, 1H, α -CH(C₆H₅)), 2.61 (t, $J = 9.0$ Hz, 1H, α -CH₂), 2.43 (s, 6H, N(CH₃)₂), 2.38 (s, 6H, N(CH₃)₂), 1.57 (apparent octet, 1H, 7.0 Hz, CH(CH₃)₂), 1.16 (d, $J = 6.5$ Hz, 3H, CH(CH₃)₂), 1.10 (overlapping multiplet with δ 1.16 and 1.06, 1H, β -CH), 1.06 (d, $J = 6.5$ Hz, 3H, CH(CH₃)₂), 0.56 (t, $J = 9.6$ Hz, 1H, α -CH₂). ¹H NMR (400 MHz, C₆D₆, -60 °C): three rotational isomers of **101a** are observed in a 2 : 2 : 1 ratio; due to this complexity complete assignment of this spectrum was not attempted. ¹³C NMR (100.6 MHz, C₆D₆, RT): δ 155.4 (C1), 152.0 (C₆H₅), 151.4 (C1'), 127.2 (C_{aryl}), 125.5 (C_{aryl}), 125.1 (C_{aryl}), 125.0 (C_{aryl}), 124.7 (C_{aryl}), 123.3 (C_{aryl}), 123.0 (C_{aryl}), 122.4 (C_{aryl}), 121.7 (C_{aryl}), 121.0 (C_{aryl}), 120.7 (C_{aryl}), 119.3 (C_{aryl}), 91.4 (C2), 90.0 (C2'), 89.9 (C2''), 87.6 (CH(C₆H₅)), 86.0 (C2'''), 80.0 (α -CH₂), 40.5 (N(CH₃)₂), 39.5 (N(CH₃)₂), 36.1 (CH(CH₃)₂), 26.5 (β -CH), 23.5 (CH(CH₃)₂), 21.5 (CH(CH₃)₂), solvent or incidental overlap is likely obscuring missing 3 aryl signals. HMQC (300 MHz, C₆D₆) select data only: δ 91.4 (C2) \leftrightarrow δ 5.31 (H2'); δ 90.0 (C2') \leftrightarrow δ 4.05 (H2'''); δ 89.9 (C2'') \leftrightarrow δ 5.41 (H2); δ 87.6 (CH(C₆H₅)) \leftrightarrow δ 3.32 (α -CH(C₆H₅)); δ 86.0 (C2''') \leftrightarrow δ 4.27 (H2''); δ 80.0 (α -CH₂) \leftrightarrow δ 2.65 (α -CH₂), δ 0.61 (α -CH₂); δ 40.5 (N(CH₃)₂) \leftrightarrow δ 2.36 (N(CH₃)₂); δ 39.5 (N(CH₃)₂) \leftrightarrow δ 2.23 (N(CH₃)₂); δ 36.1 (CH(CH₃)₂) \leftrightarrow δ 1.50 (CH(CH₃)₂); δ 26.5 (β -CH) \leftrightarrow δ 1.04 (β -CH); δ 23.5

(CH(CH₃)₂) ↔ δ 1.15 (CH(CH₃)₂); δ 21.5 (CH(CH₃)₂) ↔ δ 1.05 (CH(CH₃)₂). ¹H NMR spectroscopy indicated that the isolated crystals contained a nonstoichiometric amount of entrained THF; anal. calcd. for a THF adduct of complex (C₃₄H₄₀N₂Ti•C₄H₈O): C, 76.49; H, 8.11; N, 4.69; anal. calcd. for C₃₄H₄₀N₂Ti: C, 77.85; H, 7.69; N, 5.34; found C, 76.92; H, 7.98; N, 5.19.

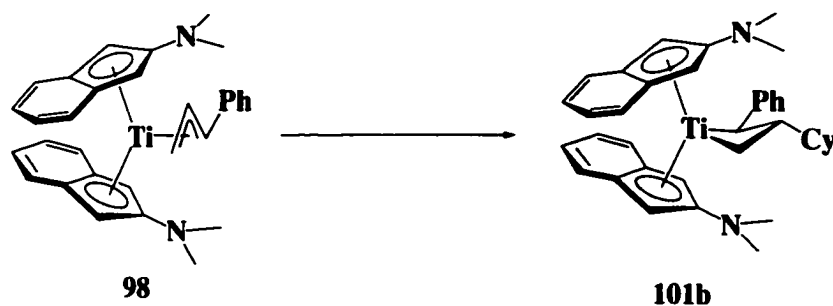
Titanacyclobutane 101a from Bis(2-*N,N*-dimethylaminoindenyl)titanium Chloride 96:



3-Isopropyl-2-phenyl-bis(2-*N,N*-dimethylaminoindenyl)titanacyclobutane 101a. In the drybox, a vial containing a THF solution (10 mL) of bis(2-*N,N*-dimethylaminoindenyl)titanium chloride **96** (202.8 mg, 0.507 mmol) was cooled to -35 °C and treated with a cold solution (-35 °C) of cinnamyllithium (69.2 mg, 0.533 mmol in 5 mL THF). The resultant reaction mixture was allowed to warm to room temperature and stirred for 1 h and then re-cooled to -35 °C. A cold solution (-35 °C) of SmI₂ (5.30 mL, 0.1 M in THF) was added followed immediately by a cooled solution (-35 °C) of isopropyl iodide (53.0 μL in 1 mL THF). The reaction mixture was allowed to warm to room temperature and stir overnight. Quickly the blue/green colour of the solution began to dissipate followed by the emergence of a dark chocolate brown solution. The solvent was removed *in vacuo*, the product was extracted with 1 : 2 benzene/hexane and the extracts filtered through a sintered glass funnel layered with a short plug of Celite. The solvents were removed *in vacuo* and the resulting brown residue was crystallized

from THF/hexane (1:4) yielding the titanacycle complex **101a** as deep red rhomboid crystals (196 mg, 74%). The recovered material was spectroscopically identical to the completely characterized complex given above.

Titanacyclobutane 101b from Bis(2-*N,N*-dimethylaminoindenyl)titanium Cinnamyl 98:



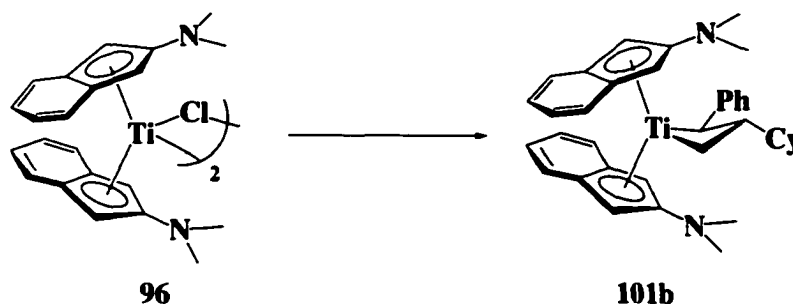
3-Cyclohexyl-2-phenyl-bis(2-*N,N*-dimethylaminoindenyl)titanacyclobutane 101b.

In the drybox, a vial containing a THF solution (5 mL) of bis(2-*N,N*-dimethylaminoindenyl)titanium(η^3 -1-phenylallyl) **98** (60.2 mg, 0.216 mmol) was cooled to -35 °C. A cold solution of SmI₂ (1.30 mL, 0.1 M in THF) was added followed immediately by a cooled solution of iodocyclohexane (22.6 μ L in 1 mL THF). The reaction mixture was allowed to warm to room temperature and stir overnight. It required 8 hours for the blue/green colour of the solution to turn earth brown; only a trace amount of Sm(III) precipitate was observed. The solvent was removed *in vacuo*, the brown residue was triturated with a 1 : 2 benzene/hexane mixture, and the resultant solution filtered through a short plug of Celite. The solvents were removed *in vacuo* and the resulting residue was crystallized from THF/hexane (1 : 10) at -35 °C to yield the titanacyclobutane complex **101b** as dark brown rhomboid crystals (60.8 mg, 88%). ¹H NMR (400 MHz, C₆D₆): δ 7.48 (m, 1H, H4/H5), 7.29 (m, 4H, H4/H5, C₆H₅), 7.15 (obscured signal, 2H, H4/H5), 6.99 (t, *J* = 7.2 Hz, 1H, H4/H5), 6.96 (t, *J* = 7.6, 1.0 Hz, 1H, C₆H₅), 6.90 (t, *J* = 3.1 Hz, 1H, H4/H5), 6.88 (t, *J* = 3.0 Hz, 1H, H4/H5), 6.75 (t, *J* =

7.5 Hz, 1H, C₆H₅), 6.12 (d, *J* = 8.4 Hz, 1H, C₆H₅), 5.42 (s, 1H, H₂), 5.34 (d, *J* = 2.2 Hz, 1H, H₂'), 4.27 (s, 1H, H₂''), 4.02 (s, 1H, H₂'''), 3.33 (d, *J* = 10.7 Hz, 1H, α-CH(C₆H₅)), 2.69 (t, *J* = 8.8 Hz, 1H, α-CH₂), 2.36 (s, 6H, N(CH₃)₂), 2.26 (s, 6H, N(CH₃)₂), 2.17 (m, 1H, H_{cy}), 1.83 (t, *J* = 12.9 Hz, 2H, H_{cy}), 1.68 (d, *J* = 5.3 Hz, 2H, H_{cy}), 1.34-1.15 (m, 6H, H_{cy}) 1.11 (partially obscured signal, 1H, β-CH), 0.61 (br m, 1H, α-CH₂). GCOSY (300 Mz, C₆D₆, RT) select data only: δ 3.33 (α-CH(C₆H₅)) ↔ δ 1.11 (β-CH), δ 2.69 (α-CH₂) ↔ δ 1.11 (β-CH) ↔ δ 0.61(α-CH₂). ¹³C NMR (100.6 MHz, C₆D₆): δ 155.6 (C1), 153.0 (C_{aryl}), 151.4 (C1'), 127.3(C_{aryl}), 125.5 (C_{aryl}), 125.1 (C_{aryl}), 125.0 (C_{aryl}), 124.8 (C_{aryl}), 123.2 (C_{aryl}), 122.9 (C_{aryl}), 122.4 (C_{aryl}), 122.2 (C_{aryl}), 121.7 (C_{aryl}), 121.0 (C_{aryl}), 120.9 (C_{aryl}), 119.5 (C_{aryl}), 91.7 (C2), 90.2 (C2',C2''), 87.2 (CH(C₆H₅)), 86.2 (C2'''), 80.9 (α-CH₂), 47.0 (C_{cy}), 40.7 (N(CH₃)₂), 39.6 (N(CH₃)₂), 34.5 (C_{cy}), 32.8 (C_{cy}), 27.9 (C_{cy}), 27.7 (C_{cy}), 27.6 (C_{cy}), 25.5 (β-CH), solvent or overlap is likely obscuring missing 2 aryl signals. HMQC (300 Mz, C₆D₆) select data only: δ 91.7 (C2) ↔ δ 5.34 (H₂'); δ 90.2 (C2',C2'') ↔ δ 5.42 (H₂), δ 4.02 (H₂'''); δ 87.2 (α-CH(C₆H₅)) ↔ δ 3.33 (α-CH(C₆H₅)); δ 86.2 (C2''') ↔ δ 4.27 (H₂''), δ 80.9 (α-CH₂) ↔ δ 2.69 (α-CH₂), δ 0.64 (α-CH₂); 47.0 (C_{cy}) ↔ δ 1.34-1.15 (H_{cy}); δ 40.7 (N(CH₃)₂) ↔ δ 2.36 (N(CH₃)₂); δ 39.6 (N(CH₃)₂) ↔ δ 2.26 (N(CH₃)₂); 34.5 (C_{cy}) ↔ δ 1.34-1.15 (H_{cy}), δ 1.83 (H_{cy}); 32.8 (C_{cy}) ↔ δ 2.17 (H_{cy}); 27.9 (C_{cy}) ↔ δ 1.83 (H_{cy}), δ 1.68 (H_{cy}); 27.7 (C_{cy}) ↔ δ 1.34-1.15 (H_{cy}); 27.6 (C_{cy}) ↔ δ 1.34-1.15 (H_{cy}); 25.5 (β-CH) ↔ δ 1.11 (β-CH). ¹H NMR spectroscopy indicated that the isolated crystals contained a nonstoichiometric amount of entrained THF; anal. calcd. for a THF adduct of complex (C₃₇H₄₄N₂Ti•C₄H₈O): C, 77.33; H, 8.23; N, 4.40; anal. calcd. for C₃₇H₄₄N₂Ti: C, 78.70; H, 7.85; N, 4.96; found C, 77.83; H, 7.87; N, 4.64.

Titanacyclobutane **101b** from Bis(2-*N,N*-dimethylaminoindenyl)titanium Chloride

96:

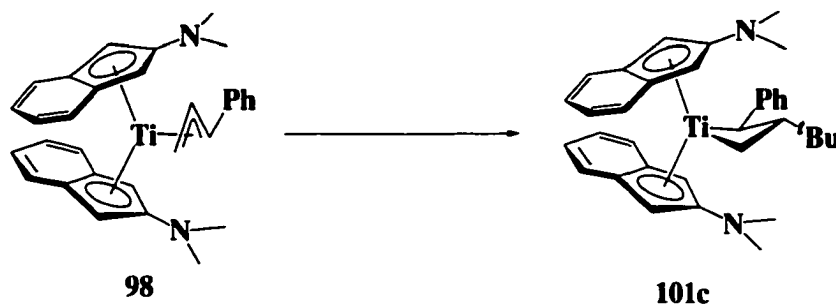


3-Cyclohexyl-2-phenyl-bis(2-*N,N*-dimethylaminoindenyl)titanacyclobutane **101b**.

In the drybox, to a vial containing a THF solution (5 mL) of bis(2-*N,N*-dimethylaminoindenyl)titanium chloride **96** (35.8 mg, 0.0895 mmol) cooled to -35 °C, was added a cooled solution of cinnamyl lithium (11.8 mg, 0.0904 mmol in 1 mL THF). The solution was allowed to warm to room temperature and stir an additional 1 h, after which an equivalent of SmI₂ (0.90 mL, 0.1 M in THF) was added. The reaction mixture was re-cooled to -35 °C, treated with a cold solution (-35 °C) of iodocyclohexane (22.6 μL in 1 mL THF) and allowed to warm to room temperature and stir overnight. The solvent was removed *in vacuo* and the product was extracted into a 1 : 2 benzene/hexane mixture and filtered through a short plug of Celite. The solvents were removed *in vacuo* and the resulting residue was crystallized from THF/hexane (1 : 10) at -35 °C to yield the titanacycle complex **101b** as dark brown rhomboid crystals (30.9 mg, 60%). The recovered material was spectroscopically identical to the completely characterized complex given above.

Titanacyclobutane 101c from Bis(2-*N,N*-dimethylaminoindenyl)titanium Cinnamyl

98:

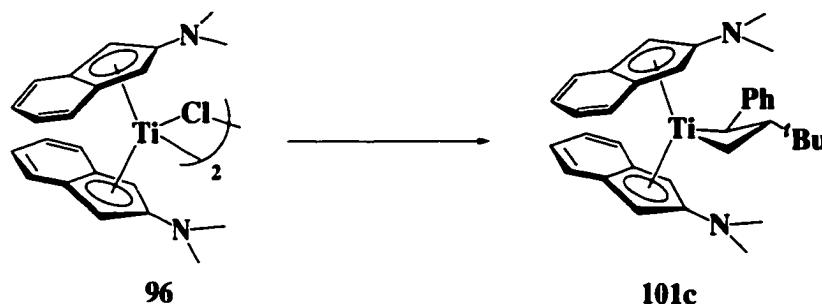


3-*tert*-Butyl-2-phenyl-bis(2-*N,N*-dimethylaminoindenyl)titanacyclobutane 101c. In the drybox, a vial containing a THF solution (5 mL) of bis(2-*N,N*-dimethylaminoindenyl)titanium(η^3 -1-phenylallyl) **98** (21.2 mg, 0.0440 mmol) was cooled to -35 °C and treated successively with cold (-35 °C) solutions of SmI₂ (0.45 mL, 0.1 M in THF) and *tert*-butyl chloride (5.0 μ L in 1 mL THF). The reaction mixture was allowed to warm to room temperature and stir overnight. The reaction stirred for several hours before the blue/green colour of the solution began to dissipate, followed by the emergence of a dark chocolate brown solution. Very little Sm(III) precipitate was observed during the course of the reaction. The solvent was removed *in vacuo*, the brown residue extracted into a 1 : 4 benzene/hexane mixture, and the resultant solution filtered through a short plug of Celite. The solvents were removed *in vacuo* and the brown residue was crystallized from THF/hexane (1 : 6) at -35 °C to yield the titanacyclobutane complex **101c** as brown rhomboid crystals (16.6 mg, 70%). ¹H NMR (400 MHz, CD₃C₆D₅): δ 7.50 (m, 1H, H_{aryl}), 7.39 (m, 2H, H_{aryl}), 7.27 (m, 2H, H_{aryl}), 6.90 (m, 2H, H_{aryl}), 6.83 (m, 3H, H_{aryl}), 6.63 (m, 1H, H_{aryl}), 6.52 (br d, $J = 7.2$ Hz, 1H, H_{ary}), 5.79 (d, $J = 2.3$ Hz, 1H, H₂), 5.77 (br d, $J = 8.0$ Hz, 1H, H_{ary}), 5.66 (s, 1H, H_{2'}), 4.05 (br s, 1H, H_{2''}), 3.89 (br s, 1H, H_{2'''}), 3.58 (d, $J = 11.3$ Hz, 1H, α -CH(C₆H₅)), 2.65 (t, $J = 9.5$ Hz, 1H, α -CH₂), 2.42 (br s, 6H, N(CH₃)₂), 2.28 (br s, 6H, N(CH₃)₂), 1.38 (br s, 1H, α -CH₂), 1.03 (s, 9H, C(CH₃)₃), 0.18 (br s, 1H, β -CH). Due to the broad nature of the room

temperature spectrum, an additional spectrum was recorded at $-60\text{ }^{\circ}\text{C}$; only the major conformer is characterized (major isomer : minor isomer = 5 : 1). ^1H NMR (400 MHz, $\text{CD}_3\text{C}_6\text{D}_5$, $-60\text{ }^{\circ}\text{C}$): δ 7.61 (d, $J = 8.2\text{ Hz}$, 1H, H_{aryl}), 7.55 (t, $J = 7.5\text{ Hz}$, 1H, H_{aryl}), 7.48 (d, $J = 7.3\text{ Hz}$, 1H, H_{aryl}), 7.36 (t, $J = 7.7\text{ Hz}$, 1H, H_{aryl}), 7.25 (d, $J = 8.1\text{ Hz}$, 1H, H_{aryl}), 7.18 (partially obscured signal, 1H, H_{aryl}), 6.94 (t, $J = 7.0\text{ Hz}$, 1H, H_{aryl}), 6.80 (m, 4H, H_{aryl}), 6.57 (d, $J = 7.7\text{ Hz}$, 1H, H_{aryl}), 5.90 (s, 1H, H2), 5.80 (s, 1H, H2'), 5.67 (d, $J = 8.1\text{ Hz}$, 1H, H_{aryl}), 3.71 (s, 1H, H2''), 3.48 (d, $J = 11.1\text{ Hz}$, 1H, $\alpha\text{-CH}(\text{C}_6\text{H}_5)$), 3.36 (s, 1H, H2'''), 2.73 (t, $J = 9.4\text{ Hz}$, 1H, $\alpha\text{-CH}_2$), 2.70 (s, 3H, $\text{N}(\text{CH}_3)_2$), 2.54 (s, 3H, $\text{N}(\text{CH}_3)_2$), 2.01 (s, 3H, $\text{N}(\text{CH}_3)_2$), 1.86 (s, 3H, $\text{N}(\text{CH}_3)_2$), 1.58 (q, $J = 10.0\text{ Hz}$, 1H, $\beta\text{-CH}$), 1.15 (s, 9H, $\text{C}(\text{CH}_3)_3$), 0.71 (t, $J = 9.8\text{ Hz}$, $\alpha\text{-CH}_2$). GCOSY (500 Mz, $\text{CD}_3\text{C}_6\text{D}_5$, $-50\text{ }^{\circ}\text{C}$) select data only: δ 3.48 ($\text{CH}(\text{C}_6\text{H}_5)$) \leftrightarrow δ 1.58 ($\beta\text{-CH}$); δ 2.73 ($\alpha\text{-CH}_2$) \leftrightarrow δ 1.58 ($\beta\text{-CH}$) \leftrightarrow δ 0.71 ($\alpha\text{-CH}_2$). ^{13}C NMR (100.6 MHz, $\text{CD}_3\text{C}_6\text{D}_5$, $-60\text{ }^{\circ}\text{C}$): δ 154.7, 153.8, 150.8, 137.6, 137.3, 137.0, 129.1, 128.2, 127.2, 126.6, 125.9, 125.6, 124.6, 122.7, 122.6, 122.4, 121.8, 121.3, 120.9, 120.6, 120.3, 119.6, 91.9 (C2), 91.7 (C2'), 88.5 (C2''), 87.3 (C2'''), 77.1 ($\alpha\text{-CH}(\text{C}_6\text{H}_5)$), 72.0 ($\alpha\text{-CH}_2$), 41.4 ($\text{N}(\text{CH}_3)_2$), 39.4 ($\text{N}(\text{CH}_3)_2$), 39.3 ($\text{N}(\text{CH}_3)_2$), 38.2 ($\text{N}(\text{CH}_3)_2$), 37.2 ($\text{C}(\text{CH}_3)_3$), 29.3 ($\text{C}(\text{CH}_3)_3$), 14.6 ($\beta\text{-CH}$). HMQC (500 Mz, $\text{CD}_3\text{C}_6\text{D}_5$, $-50\text{ }^{\circ}\text{C}$) select data only: δ 91.9 (C2) \leftrightarrow δ 5.90 (H2); δ 91.7 (C2') \leftrightarrow δ 5.80 (H2'); δ 88.5 (C2'') \leftrightarrow δ 3.71 (H2''); δ 87.3 (C2''') \leftrightarrow δ 3.36 (H2'''); δ 77.1 ($\alpha\text{-CH}(\text{C}_6\text{H}_5)$) \leftrightarrow δ 3.48 ($\alpha\text{-CH}(\text{C}_6\text{H}_5)$); δ 72.0 ($\alpha\text{-CH}_2$) \leftrightarrow δ 2.73 ($\alpha\text{-CH}_2$), δ 0.71 ($\alpha\text{-CH}_2$); δ 41.4 ($\text{N}(\text{CH}_3)_2$) \leftrightarrow δ 2.54 ($\text{N}(\text{CH}_3)_2$); δ 39.4 ($\text{N}(\text{CH}_3)_2$) \leftrightarrow δ 2.70 ($\text{N}(\text{CH}_3)_2$); δ 39.3 ($\text{N}(\text{CH}_3)_2$) \leftrightarrow δ 2.01 ($\text{N}(\text{CH}_3)_2$); δ 38.2 ($\text{N}(\text{CH}_3)_2$) \leftrightarrow δ 1.86 ($\text{N}(\text{CH}_3)_2$); δ 29.3 ($\text{C}(\text{CH}_3)_3$) \leftrightarrow δ 1.15 ($\text{C}(\text{CH}_3)_3$); δ 14.6 ($\beta\text{-CH}$) \leftrightarrow δ 1.58 ($\beta\text{-CH}$). Anal. calcd. for THF adduct $\text{C}_{32}\text{H}_{42}\text{N}_2\text{Ti}\cdot\text{C}_4\text{H}_8\text{O}$: C, 76.69; H, 8.25; N, 4.59; found C, 76.24; H, 7.94; N, 5.08.

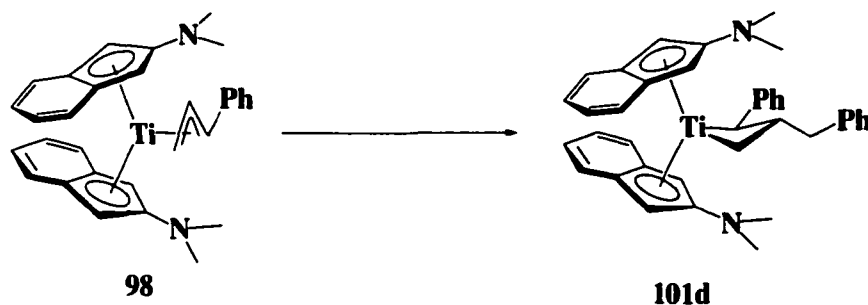
Titanacyclobutane 101c from Bis(2-*N,N*-dimethylaminoindenyl)titanium Chloride

96:



3-*tert*-Butyl-2-phenyl-bis(2-*N,N*-dimethylaminoindenyl)titanacyclobutane 101c. In the drybox, to a vial containing bis(2-*N,N*-dimethylaminoindenyl)titanium chloride **96** (31.3 mg, 0.0785 mmol), dissolved in 3 mL THF and cooled to -35 °C, was added a cold solution (-35 °C) of cinnamyllithium (10.2 mg, 0.0825 mmol in 2 mL THF). The reaction was left to warm to room temperature and stir for 1 h. The resultant green solution was treated with one equivalent of SmI_2 (0.82 mL, 0.1 M in THF) and re-cooled to -35 °C. After the addition of a cooled solution (-35 °C) of *tert*-butyl chloride (9.0 μL in 2 mL THF) the reaction mixture was left to warm to room temperature and stir for an additional 3 h. The solvent was evaporated under reduced pressure, the remaining brown residue was triturated with 1 : 4 benzene/hexane and filtered through a short plug of Celite. The solvents were removed *in vacuo* and the titanacyclobutane complex **101c** was crystallized from THF/hexane (1 : 6) cooled to -35 °C to yield brown rhomboid crystals (21.3 mg, 49%). The recovered material was spectroscopically identical to the completely characterized complex given above.

Titanacyclobutane 101d from Bis(2-*N,N*-dimethylaminoindenyl)titanium Cinnamyl 98:

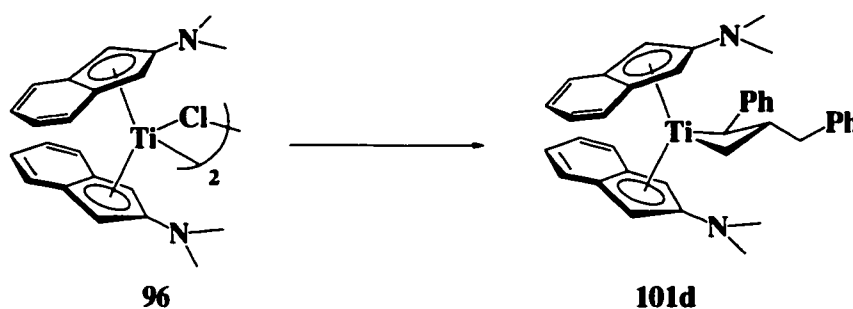


3-Benzyl-2-phenyl-bis(2-*N,N*-dimethylaminoindenyl)titanacyclobutane 101d. In the drybox, a vial containing a THF solution (5 mL) of bis(2-*N,N*-dimethylaminoindenyl)titanium(η^3 -1-phenylallyl) (59.1 mg, 0.122 mmol) **98** was treated with an equivalent of SmI₂ (1.25 mL, 0.1 M in THF), cooled to -35 °C, and treated with a cold solution of benzyl chloride (14.0 μ L in 1 mL THF). The reaction mixture was allowed to warm to room temperature and stir an additional 3 h. Almost immediately upon warming, the blue/green colour of the solution began to dissipate, followed by the emergence of a red/brown solution. Very little samarium(III) precipitate was observed during the course of the reaction. The solvent was removed *in vacuo*, the product extracted into a 1 : 2 benzene/hexane mixture and filtered through a short plug of Celite. The solvents were removed *in vacuo* and the brown residue was crystallized from THF/hexane (1 : 6) at -35 °C to yield the titanacycle complex **101d** as deep red rhomboid crystals (57.1 mg, 81%). ¹H NMR (400.1 MHz, C₆D₆): δ = 7.44-7.38 (m, 3H, H_{aryl}), 7.30-7.20 (m, 6H, H_{aryl}), 7.10 (m, 2H, H_{aryl}), 7.04 (t, 7.2 Hz, 2H, H_{aryl}), 6.93-6.87 (m, 3H H_{aryl}), 6.70 (ddd, *J* = 7.9, 6.7, 0.70 Hz, 1H, α -CH(C₆H₅)), 6.27 (d, *J* = 8.3 Hz, 1H, α -CH(C₆H₅)), 5.31 (d, *J* = 2.2 Hz, 1H, H2), 4.88 (d, *J* = 2.2 Hz, 1H, H2'), 4.44 (s, 1H, H2''), 4.25(s, 1H, H2'''), 3.04 (two overlapping doublets, 2H, CH(C₆H₅), CH₂(C₆H₅)), 2.57 (t, *J* = 9.4 Hz, 1H, α -CH₂), 2.38 (obscured signal, 1H, CH₂(C₆H₅)), 2.36 (s, 6H, N(CH₃)₂), 2.13 (s, 6H, N(CH₃)₂), 1.51 (apparent dq, *J* = 8.5, 4.3 Hz, 1H, β -CH), 0.22 (t, *J* =

9.1 Hz, 1H, α -CH₂). GCOSY (300 Mz, C₆D₆) select data only: δ 3.04 (CH₂(C₆H₅)) \leftrightarrow δ 2.38 (CH₂(C₆H₅)) \leftrightarrow δ 1.51 (β -CH); δ 2.57 (α -CH₂) \leftrightarrow δ 1.51 (β -CH) \leftrightarrow δ 0.22 (α -CH₂). ¹³C NMR (100.6 MHz, C₆D₆): δ = 154.2 (C1), 152.0 (C_{aryl}), 151.4 (C1), 151.1 (C_{aryl}), 142.5(C_{aryl}), 130.2 (C_{aryl}), 125.7 (C_{aryl}), 125.1 (C_{aryl}), 124.7 (C_{aryl}), 124.6 (C_{aryl}), 123.5 (C_{aryl}), 123.3 (C_{aryl}), 122.5 (C_{aryl}), 122.1 (C_{aryl}), 121.6 (C_{aryl}), 121.4 (C_{aryl}), 121.0 (C_{aryl}), 119.1 (C_{aryl}), 91.0 (C2), 90.6 (C2'), 89.4 (C2''), 87.4 (α -CH(C₆H₅)), 85.7 (C2'''), 79.8 (α -CH₂), 41.8 (CH₂(C₆H₅)), 41.0 (N(CH₃)₂), 39.7 (N(CH₃)₂), 22.2 (β -CH). HMQC (300 MHz, C₆D₆) select data only: δ 91.0 (C2) \leftrightarrow δ 4.88 (H2'); δ 90.6 (C2') \leftrightarrow δ 4.25 (H2'''); δ 89.4 (C2'') \leftrightarrow δ 5.31 (H2); δ 87.4 (α -CH(C₆H₅)) \leftrightarrow δ 3.04 (CH(C₆H₅)); δ 85.7 (C2''') \leftrightarrow δ 4.44 (H2''); δ 79.8 (α -CH₂) \leftrightarrow δ 2.57 (α -CH₂), δ 0.22 (α -CH₂); δ 41.8 (CH₂(C₆H₅)) \leftrightarrow δ 3.04 (CH₂(C₆H₅)), δ 2.38 (CH₂(C₆H₅)); δ 41.0 (N(CH₃)₂) \leftrightarrow δ 2.36 (N(CH₃)₂); δ 39.7 (N(CH₃)₂) \leftrightarrow δ 2.13 (N(CH₃)₂); δ 22.2 (β -CH) \leftrightarrow δ 1.51 (β -CH). Anal. calcd. for a THF adduct of complex (C₃₈H₄₀N₂Ti•C₄H₈O): C, 78.24; H, 7.50; N, 4.34; found C, 78.55; H, 7.35; N, 4.77.

Titanacyclobutane 101d from Bis(2-*N,N*-dimethylaminoindenyl)titanium Chloride

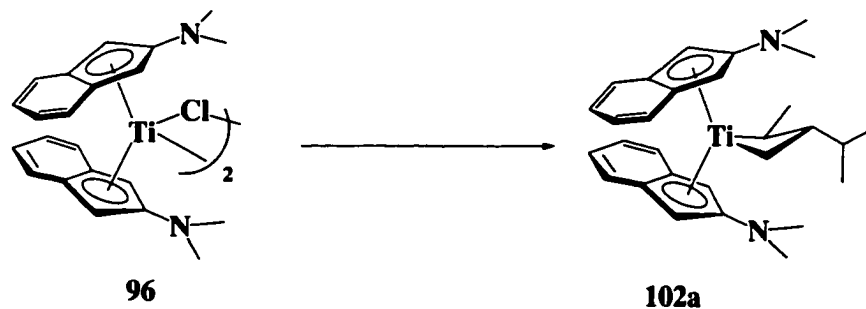
96:



3-Benzyl-2-phenyl-bis(2-*N,N*-dimethylaminoindenyl)titanacyclobutane 101d. In the drybox, to bis(2-*N,N*-dimethylaminoindenyl)titanium chloride **96** (42.3 mg, 0.106 mmol), dissolved in 5 mL THF and cooled to -35 °C, was added a cold solution (-35 °C) of cinnamyllithium (14.5 mg, 0.116 mmol in 2 mL THF). The reaction was left to warm to

room temperature and stirred for 1 h. The resultant green solution was re-cooled to -35 °C and treated with both cold solutions (-35 °C) of SmI₂ (1.10 mL, 0.1 M in THF) and benzyl chloride (12.8 μL in 3 mL THF). The reaction was then left to stir at room temperature for 3 h. Within minutes, the blue/green colour of the solution began to dissipate followed by the emergence of a red/brown solution with no observable Sm(III) precipitate. The solvent was removed *in vacuo*, the brown residue was extracted into 1 : 2 benzene/hexane and filtered through a short plug of Celite. The solvents were removed under reduced pressure and the titanacyclobutane complex was crystallized from Et₂O/hexane (1 : 4) yielding deep red rhomboid crystals (32.2 mg, 53%) of titanacyclobutane complex **101d**, spectroscopically homogeneous and identical to the material prepared above.

Titanacyclobutane 102a from Bis(2-*N,N*-dimethylaminoindenyl)titanium Chloride **96:**

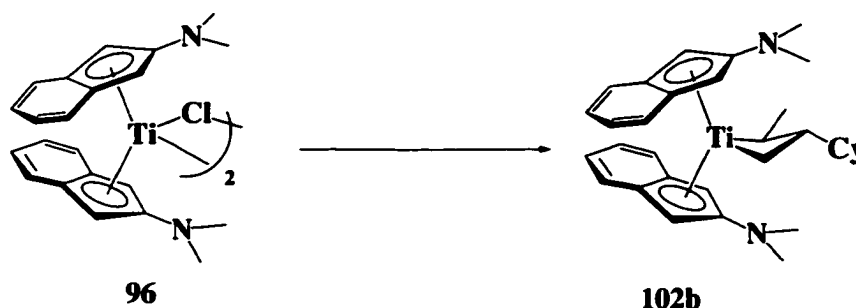


3-Isopropyl-2-methyl-bis(2-*N,N*-dimethylaminoindenyl)titanacyclobutane 102a. In the drybox, a vial containing a THF solution (5 mL) of bis(2-*N,N*-dimethylaminoindenyl)titanium chloride (75.9 mg, 0.190 mmol) **96** was cooled to -35 °C and treated with cooled (-35 °C) crotylmagnesium chloride (128 μL, 1.5 M in THF) that had been further diluted in THF (5 mL). The reaction was left to warm to room temperature, stir for an additional hour and re-cooled to -35 °C. A cold solution of SmI₂ (1.90 mL, 0.1 M in THF) was added to the reaction mixture, followed immediately by a

cold solution of 2-iodopropane (19.2 μL in 2 mL THF). The reaction was warmed to room temperature and stirred for 30 minutes. Almost immediately, the blue colour of the SmI_2 began to dissipate, followed by the emergence of a purple red solution and a bright yellow precipitate of samarium(III). The solution was decanted from the precipitate and the solvent removed *in vacuo*, extracted with pentane, and filtered through a sintered glass funnel layered with a short plug of Celite. The pentane solution was concentrated to approximately half its original volume and cooled to $-35\text{ }^\circ\text{C}$ to yield dark purple microcrystals (56.3 mg, 68%). ^1H NMR (400 MHz, C_6D_6): δ 7.48 (2nd order m, 4H, H4/H5), 7.06 (dt, $J = 8.1, 0.8$ Hz, 1H, H4/H5), 6.97 (2nd order m, 3H, H4/5), 5.34 (d, $J = 2.2$ Hz, 1H, H2), 5.10 (d, $J = 2.3$ Hz, 1H, H2'), 4.15 (d, $J = 2.2$ Hz, 1H, H2''), 4.07 (d, $J = 2.2$ Hz, 1H, H2'''), 2.46 (t, $J = 9.1$ Hz, 1H, $\alpha\text{-CH}_2$), 2.31 (s, 6H, $\text{N}(\text{CH}_3)_2$), 2.29 (s, 6H, $\text{N}(\text{CH}_3)_2$), 2.22 (dq, $J = 6.9, 9.9$ Hz, 1H, $\alpha\text{-CH}(\text{CH}_3)$), 1.83 (d, $J = 6.9$ Hz, 3H, $\alpha\text{-CH}(\text{CH}_3)$), 1.71 (apparent octet, $J = 6.7$ Hz, 1H, $\text{CH}(\text{CH}_3)_2$), 1.24 (d, $J = 6.7$ Hz, 3H, $\text{CH}(\text{CH}_3)_2$), 1.18 (d, $J = 6.6$ Hz, 3H, $\text{CH}(\text{CH}_3)_2$), 0.79 (t, $J = 9.7$ Hz, 1H, $\alpha\text{-CH}_2$), -0.015 (dq, $J = 9.9, 6.5$ Hz, 1H, $\beta\text{-CH}$). GCOSY (300 Mz, C_6D_6) select data only: δ 2.46 ($\alpha\text{-CH}_2$) \leftrightarrow δ 0.79 ($\alpha\text{-CH}_2$) \leftrightarrow δ -0.015 ($\beta\text{-CH}$); δ 1.83 ($\alpha\text{-CH}(\text{CH}_3)$) \leftrightarrow δ 2.22 ($\alpha\text{-CH}(\text{CH}_3)$) \leftrightarrow δ -0.015 ($\beta\text{-CH}$); δ -0.015 ($\beta\text{-CH}$) \leftrightarrow δ 1.71 ($\text{CH}(\text{CH}_3)_2$) \leftrightarrow δ 1.24 ($\text{CH}(\text{CH}_3)_2$), δ 1.18 ($\text{CH}(\text{CH}_3)_2$). ^{13}C NMR (100 MHz, C_6D_6): δ 163.9 (C1), 150.6 (C1'), 126.0 (C3/C4/C5), 125.4 (C3/C4/C5), 124.6 (C3/C4/C5), 123.9 (C3/C4/C5), 122.4 (C3/C4/C5), 122.1 (C3/C4/C5), 121.9 (C3/C4/C5), 121.7 (C3/C4/C5), 121.3 (C3/C4/C5), 120.5 (C3/C4/C5), 119.5 (C3/C4/C5), 119.4 (C3/C4/C5), 91.7 (C2), 87.9 (C2'), 86.9 (C2''), 85.5 (C2'''), 83.4 ($\alpha\text{-CH}(\text{CH}_3)$), 77.8 ($\alpha\text{-CH}_2$), 40.1 ($\text{N}(\text{CH}_3)_2$), 39.6 ($\text{N}(\text{CH}_3)_2$), 34.6 ($\text{CH}(\text{CH}_3)_2$), 31.5 ($\beta\text{-CH}$), 27.4 ($\text{CH}(\text{CH}_3)$), 23.8 ($\text{CH}(\text{CH}_3)_2$), 21.2 ($\text{CH}(\text{CH}_3)_2$). HMQC (300 MHz, C_6D_6) select data only: δ 91.7 (C2) \leftrightarrow δ 5.10 (H2'); δ 87.9 (C2') \leftrightarrow δ 5.34 (H2); δ 86.9 (C2'') \leftrightarrow δ 4.07 (H2'''); δ 85.5 (C2''') \leftrightarrow δ 4.15 (H2''); δ 83.4 ($\alpha\text{-CH}(\text{CH}_3)$) \leftrightarrow δ 2.22 ($\alpha\text{-CH}(\text{CH}_3)$); δ 77.8 ($\alpha\text{-CH}_2$) \leftrightarrow δ 2.46 ($\alpha\text{-CH}_2$), δ 0.79 ($\alpha\text{-CH}_2$); δ 40.1 ($\text{N}(\text{CH}_3)_2$) \leftrightarrow δ 2.31 ($\text{N}(\text{CH}_3)_2$); δ 39.6 ($\text{N}(\text{CH}_3)_2$) \leftrightarrow δ 2.29 ($\text{N}(\text{CH}_3)_2$); δ 34.6 ($\text{CH}(\text{CH}_3)_2$) \leftrightarrow δ 1.71

(CH(CH₃)₂); δ 31.5 (β-CH) ↔ δ -0.015 (β-CH); δ 27.4 (CH(CH₃)) ↔ δ 1.83 (α-CH(CH₃)); δ 23.8 (CH(CH₃)₂) ↔ δ 1.24 (CH(CH₃)₂); δ 21.2 (CH(CH₃)₂) ↔ δ 1.18 (CH(CH₃)₂). Anal. calcd. C, 75.31; H, 8.28; N, 6.06; found C, 75.02; H, 8.33; N, 5.84.

Titanacyclobutane 102b from Bis(2-*N,N*-dimethylaminoindenyl)titanium Chloride 96:

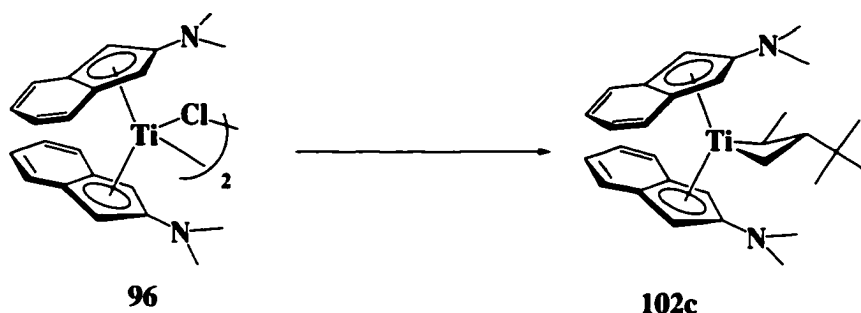


3-Cyclohexyl-2-methyl-bis(2-*N,N*-dimethylaminoindenyl)titanacyclobutane 102b. In the drybox a vial containing a THF solution (3 mL) of bis(2-*N,N*-dimethylaminoindenyl)titanium chloride **96** (31.2 mg, 0.0780 mmol) was cooled to -35 °C and treated with a cold (-35 °C) solution of crotylmagnesium chloride (52.9 μL, 1.5 M in THF), further diluted in 3 mL THF. After being left to stir at room temperature for 1 h, the reaction mixture was returned to the freezer to cool -35 °C and, thereafter, cold solutions (-35 °C) of SmI₂ (0.80 mL, 0.1 M in THF) followed by iodocyclohexane (10.3 μL in 2 mL THF) were added to the reaction mixture which was then left to stir at room temperature. Within five minutes the colour of the solution turned from dark blue/green to red-purple followed by the emergence of a bright yellow Sm(III) precipitate. The solution was then decanted from the precipitate and the solvent removed *in vacuo*. The purple residue was triturated with pentane, filtered through a short plug of Celite concentrated to approximately 3 mL and cooled to -35 °C to afford cubic red/purple crystals of titanacyclobutane complex **102b** (27.6 mg, 70%). ¹H NMR (360 MHz, C₆D₆): δ = 7.48 (m, 2H, H4/H5), 7.38 (d, *J* = 8.0 Hz, 2H, H4/H5), 7.02 (t, *J* = 7.2 Hz, 1H,

H4/H5), 6.92 (m, 3H, H4/H5), 5.33 (d, $J = 1.8$ Hz, 1H, H2), 5.11 (d, $J = 2.0$ Hz, 1H, H2'),
 4.15 (d, $J = 1.9$ Hz, 1H, H2''), 4.05 (d, $J = 2.1$ Hz, 1H, H2'''), 2.49 (t, $J = 8.9$ Hz, 1H, α -
 CH₂), 2.31 (s, 6H, N(CH₃)₂), 2.30 (s, 6H, N(CH₃)₂), 2.24 (partially obscured dq, $J = 9.2$,
 4.7 Hz, 1H, α -CH(CH₃)), 2.07 (d, $J = 13.2$ Hz, 1H, H_{cy}), 1.89 (obscured signal, 2H, H_{cy}),
 1.85 (d, $J = 6.6$ Hz, 3H, α -CH(CH₃)), 1.77 (d, $J = 9.1$ Hz, 2H, H_{cy}), 1.39-1.11 (m, 6H,
 H_{cy}), 0.78 (t, $J = 9.7$ Hz, α -CH₂), -0.001 (dq, $J = 8.9, 4.0$ Hz, 1H, β -CH). GCOSY (300
 Mz, C₆D₆) select data only: δ 2.49 (α -CH₂) \leftrightarrow δ 0.78 (α -CH₂) \leftrightarrow δ -0.001 (β -CH);
 δ -0.001 (β -CH) \leftrightarrow δ 2.24 (α -CH(CH₃)) \leftrightarrow δ 1.77 (α -CH(CH₃)). ¹³C(APT) NMR (100
 MHz, C₆D₆): δ 151.4 (C1), 150.8 (C1'), 126.8 (C4/C5), 126.0 (C4/C5), 125.4 (C4/C5),
 124.6 (C4/C5), 124.0 (C4/C5), 122.2 (C4/C5), 121.8 (C3), 121.6 (C4/C5), 121.3 (C4/C5),
 120.4 (C3'), 119.5 (C3''), 119.4 (C3'''), 91.8 (C2), 87.9 (C2'), 86.3 (C2''), 85.4 (C2'''), 83.0
 (α -CH(CH₃)), 77.9 (α -CH₂), 45.6 (C_{cy}), 40.2 (N(CH₃)₂), 39.6 (N(CH₃)₂), 34.7 (C_{cy}), 32.1
 (C_{cy}), 30.4 (β -CH), 27.9 (C_{cy}), 27.7 (C_{cy}), 27.6 (CH(CH₃)). HMQC (300 MHz, C₆D₆)
 select data only: δ 91.8 (C2) \leftrightarrow δ 5.11 (H2'); δ 87.9 (C2') \leftrightarrow δ 5.33 (H2); δ 86.3
 (C2'') \leftrightarrow δ 4.05 (H2'''); δ 85.4 (C2''') \leftrightarrow δ 4.15 (H2''); δ 83.0 (α -CH(CH₃)) \leftrightarrow δ 2.24 (α -
 CH(CH₃)); δ 77.9 (α -CH₂) \leftrightarrow δ 2.49 (α -CH₂), 0.78 (α -CH₂); δ 45.6 (C_{cy}) \leftrightarrow δ 1.39-1.11
 (H_{cy}); δ 40.2 (N(CH₃)₂) \leftrightarrow δ 2.31 (N(CH₃)₂); δ 39.6 (N(CH₃)₂) \leftrightarrow δ 2.30 (N(CH₃)₂);
 δ 34.7 (C_{cy}) \leftrightarrow δ 1.89 (H_{cy}), 1.39-1.11 (H_{cy}); δ 32.1 (C_{cy}) \leftrightarrow δ 2.07 (H_{cy}), 1.39-1.11 (H_{cy});
 δ 30.4 (β -CH) \leftrightarrow δ -0.001 (β -CH); δ 27.9 (C_{cy}) \leftrightarrow δ 1.39-1.11 (H_{cy}); δ 27.7 (C_{cy}) \leftrightarrow
 δ 1.89 (H_{cy}), 1.77 (H_{cy}); δ 27.6 (CH(CH₃)) \leftrightarrow δ 1.85 (α -CH(CH₃)). Anal. calcd. C, 76.48;
 H, 8.42; N, 5.57; found C, 75.04; H, 8.50; N, 5.14.

Titanacyclobutane 102c from Bis(2-*N,N*-dimethylaminoindenyl)titanium Chloride

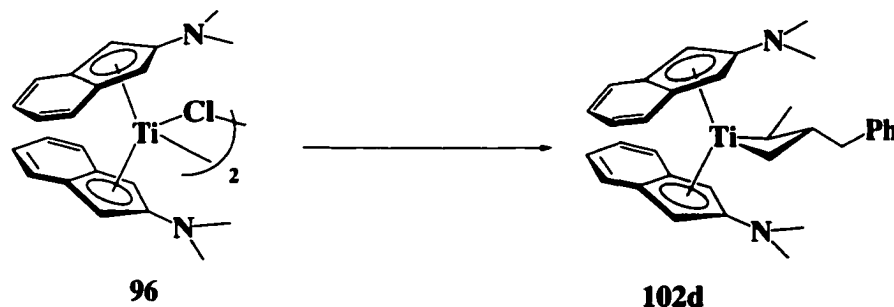
96:



3-*tert*-Butyl-2-methyl-bis(2-*N,N*-dimethylaminoindenyl)titanacyclobutane 102c. In the drybox, a vial containing a THF solution (3 mL) of bis(2-*N,N*-dimethylaminoindenyl)titanium chloride **96** (50.4 mg, 0.0780 mmol), cooled to -35 °C was treated with a cooled (-35 °C) solution of crotylmagnesium chloride (81.2 μL, 1.63 M in THF) further diluted in 3 mL THF. After being left to stir at room temperature for 1 h, the reaction mixture was re-cooled to -35 °C and, thereafter, a cold solutions (-35 °C) of SmI₂ (1.30 mL, 0.1 M in THF) followed by *tert*-butyl chloride (14.4 μL) were added to the reaction mixture which was then left to stir at room temperature. Within five minutes the colour of the solution turned from dark blue/green to red-purple followed by the emergence of a bright yellow Sm(III) precipitate. The solution was then decanted from the precipitate and the solvent removed *in vacuo*. The purple residue was triturated with pentane, vacuum filtered through a short plug of Celite and evaporated to dryness under reduced vacuum to give a deep red oil (30.0 mg, 50%). Further purification of titanacyclobutane **102c** was precluded by rapid decomposition. ¹H NMR (300 MHz, C₆D₆): δ = 7.49 (m, 1H, H4/H5), 7.35 (t, *J* = 7.5 Hz, 3H, H4/H5), 6.99 (t, *J* = 8.1 Hz, 1H, H4/H5), 6.87 (m, 3H, H4/H5), 5.65 (d, *J* = 2.1 Hz, 1H, H2), 5.52 (d, *J* = 2.1 Hz, 1H, H2'), 4.08 (s, 2H, H2''/H2'''), 2.33 (s, 6H, N(CH₃)₂), 2.32 (obscured signal, 1H, CH(CH₃)₃), 2.31 (s, 6H, N(CH₃)₂), 1.28 (d, *J* = 6.9 Hz, 3H, CH(CH₃)₃), 1.11 (s, 9H, C(CH₃)₃), 1.28 (t, *J* = 9.6 Hz, 1H, α-CH₂), 0.88 (t, *J* = 8.7 Hz, 1H, α-CH₂), 0.41 (dt, *J* = 9.5, 8.2 Hz, 1H, β-CH).

GCOSY (300 Mz, C₆D₆) select data only: δ 1.28 (α -CH₂) \leftrightarrow δ 0.88 (α -CH₂) \leftrightarrow δ -0.41 (β -CH); δ 0.41 (β -CH) \leftrightarrow δ 2.32 ($\underline{\text{C}}\text{H}(\text{CH}_3)$) \leftrightarrow δ 1.28 ($\text{C}\text{H}(\text{CH}_3)$).

Titanacyclobutane 102d from Bis(2-*N,N*-dimethylaminoindenyl)titanium Chloride 96:

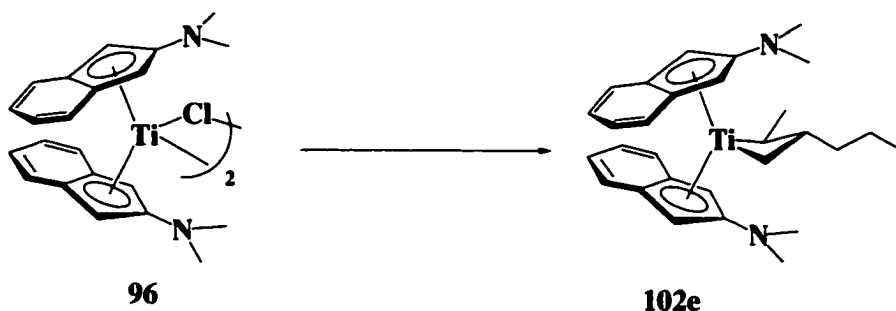


3-Benzyl-2-methyl-bis(2-*N,N*-dimethylaminoindenyl)titanacyclobutane 102d. In the drybox, to a vial containing a THF solution (3 mL) of bis(2-*N,N*-dimethylaminoindenyl)titanium chloride **96** (31.4 mg, 0.0786 mmol), cooled to -35 °C, was added cold (-35 °C) crotylmagnesium chloride (52.9 μL , 1.5 M in THF), diluted further in 3 mL THF. After being left to stir at room temperature for 1 h, the reaction mixture was returned to the freezer to cool -35 °C and, thereafter, cold solutions (-35 °C) of SmI₂ (0.80 mL, 0.1 M in THF) and benzyl chloride (9.1 μL in 2 mL THF) were added in succession to the reaction mixture. The colour of the reaction turned dark brown immediately on addition of benzyl chloride and within 0.5 h turned red-purple followed by the emergence of a bright yellow Sm(III) precipitate. The solution was then decanted from the precipitate and the solvent removed *in vacuo*. The product was extracted into pentane and filtered through a sintered glass funnel layered with a short plug of Celite. The solution was concentrated to approximately 5 mL and cooled to -35 °C to afford red/purple prisms of titanacyclobutane complex **102d** (29.1 mg, 75%). ¹H NMR (400.1 MHz, C₆D₆): δ = 7.45 (t, J = 6.4, 2H, H_{aryl}), 7.35 (four line multiplet, 4H, H_{aryl}), 7.26 (t, J = 7.4 Hz, 2H, H_{aryl}), 7.13 (m, 1H, H_{aryl}), 7.00 – 6.84 (m, 4H, H_{aryl}), 5.22 (d, J = 2.3 Hz, 1H,

H2), 4.82 (d, $J = 2.3$ Hz, 1H, H2'), 4.22 (d, $J = 2.2$ Hz, 1H, H2''), 4.06 (d, $J = 2.2$ Hz, H2'''), 3.11 (dd, $J = 12.7, 3.9$ Hz, 1H, $\text{CH}_2(\text{C}_6\text{H}_5)$), 2.47 (t, $J = 9.0$ Hz 1H, $\alpha\text{-CH}_2$), 2.30 (obscured dd, 1H, $\text{CH}_2(\text{C}_6\text{H}_5)$), 2.29 (s, 6H, $\text{N}(\text{CH}_3)_2$), 2.15 (s, 6H, $\text{N}(\text{CH}_3)_2$), 1.86 (partially obscured m, 1 H, $\alpha\text{-CH}(\text{CH}_3)$), 1.81(d, $J = 6.1$ Hz, 3H, $\alpha\text{-CH}(\text{CH}_3)$), 0.75 (t, $J = 9.9$ Hz, 1H, $\alpha\text{-CH}_2$), 0.40 (apparent dqintet, $J = 8.1, 4.1$ Hz, 1H, $\beta\text{-CH}$). GCOSY (300 Mz, C_6D_6) select data only: δ 3.11 ($\text{CH}_2(\text{C}_6\text{H}_5)$) \leftrightarrow δ 1.86 ($\text{CH}_2(\text{C}_6\text{H}_5)$) \leftrightarrow δ 0.40 ($\beta\text{-CH}$); δ 2.47 ($\alpha\text{-CH}_2$) \leftrightarrow δ 0.75 ($\alpha\text{-CH}_2$) \leftrightarrow δ 0.40 ($\beta\text{-CH}$); δ 0.40 ($\beta\text{-CH}$) \leftrightarrow δ 1.86 ($\alpha\text{-CH}(\text{CH}_3)$) \leftrightarrow δ 1.81 ($\alpha\text{-CH}(\text{CH}_3)$). ^{13}C NMR (100.6 MHz, C_6D_6): $\delta = 151.4$ (C1), 151.0 (C1'), 143.6 (C_6H_5), 125.8 (C_{aryl}), 125.7 (C_{aryl}), 125.2 (C_{aryl}), 124.7 (C_{aryl}), 124.0 (C_{aryl}), 122.4 (C_{aryl}), 122.2(C_{aryl}), 121.9 (C_{aryl}), 121.8 (C_{aryl}), 121.6 (C_{aryl}), 120.3 (C_{aryl}), 119.6 (C_{aryl}), 119.3 (C_{aryl}), 91.5 (C2), 87.8 (C2'), 87.6 ($\alpha\text{-CH}(\text{CH}_3)$), 86.5 (C2''), 85.4 (C2'''), 79.6 ($\alpha\text{-CH}_2$), 43.4 ($\text{CH}_2(\text{C}_6\text{H}_5)$), 40.4 ($\text{N}(\text{CH}_3)_2$), 39.5 ($\text{N}(\text{CH}_3)_2$), 27.0 ($\beta\text{-CH}$), 26.4 ($\alpha\text{-CH}(\text{CH}_3)$), one aryl signal missing, most likely obscured by solvent peak. HMQC (300 MHz, C_6D_6) select data only: δ 91.5 (C2) \leftrightarrow δ 4.82 (H2'); δ 87.8 (C2') \leftrightarrow δ 5.22 (H2); δ 87.6 ($\alpha\text{-CH}(\text{CH}_3)$) \leftrightarrow δ 1.86 ($\alpha\text{-CH}(\text{CH}_3)$); δ 86.5 (C2'') \leftrightarrow δ 4.06 (H2'''); δ 85.4 (C2''') \leftrightarrow δ 4.22 (H2''); δ 79.6 ($\alpha\text{-CH}_2$) \leftrightarrow δ 2.47 ($\alpha\text{-CH}_2$), δ 0.75 ($\alpha\text{-CH}_2$); δ 43.4 ($\text{CH}_2(\text{C}_6\text{H}_5)$) \leftrightarrow δ 3.11 ($\text{CH}_2(\text{C}_6\text{H}_5)$), δ 2.30 ($\text{CH}_2(\text{C}_6\text{H}_5)$); δ 40.4 ($\text{N}(\text{CH}_3)_2$) \leftrightarrow δ 2.29 ($\text{N}(\text{CH}_3)_2$); δ 39.5 ($\text{N}(\text{CH}_3)_2$) \leftrightarrow δ 2.15 ($\text{N}(\text{CH}_3)_2$); δ 27.0 ($\beta\text{-CH}$) \leftrightarrow δ 0.40 ($\beta\text{-CH}$); δ 26.4 ($\alpha\text{-CH}(\text{CH}_3)$) \leftrightarrow δ 1.81 ($\alpha\text{-CH}(\text{CH}_3)$). Anal. calcd. C, 77.63; H, 7.50; N, 5.49; found C, 77.86; H, 7.70; N, 5.44.

Titanacyclobutane 102e from Bis(2-*N,N*-dimethylaminoindenyl)titanium Chloride

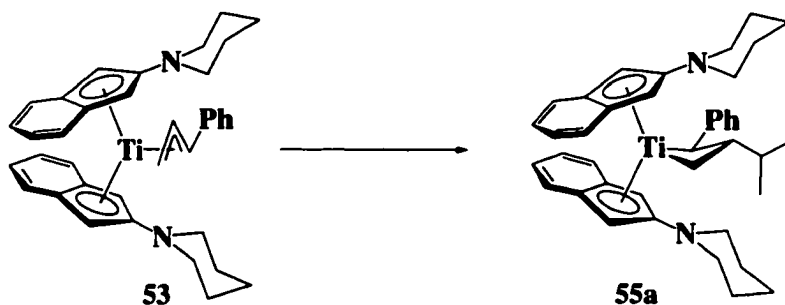
96:



3-Propyl-2-methyl-bis(2-*N,N*-dimethylaminoindenyl)titanacyclobutane 102e. In the drybox a vial containing a THF solution (3 mL) of bis(2-*N,N*-dimethylaminoindenyl)titanium chloride **96** (40.0 mg, 0.100 mmol) was cooled to -35 °C and treated with crotylmagnesium chloride (61.3 μL, 1.63 M in THF). After being left to stir at room temperature for 1 h, one equivalent of SmI₂ (1.00 mL, 0.1 M in THF) was added to the reaction mixture which was then returned to the freezer to cool -35 °C. Following the addition of a cold solution (-35 °C) of iodopropane (9.8 μL in 1 mL THF), the reaction mixture was left to stir at room temperature. Within five minutes the colour of the solution turned from dark blue/green to red-purple followed by the emergence of a bright yellow Sm(III) precipitate. The solution was then decanted from the precipitate and the solvent removed *in vacuo*. The product was extracted into pentane, filtered through a short plug of Celite and evaporated to dryness to give a red oil (crude 24.7 mg, 53%). Due to rapid decomposition in solution further purification of titanacyclobutane complex **102e** was unsuccessful. ¹H NMR (300 MHz, C₆D₆): δ = 7.45 (m, 2H, H4/H5), 7.38 (m, 2H, H4/H5), 6.94 (m, 2H, H4/H5), 5.12 (d, *J* = 1.8 Hz, 1H, H2), 4.84 (d, *J* = 1.8 Hz, 1H, H2'), 4.22 (d, *J* = 1.2 Hz, 1H, H2''), 4.11 (d, *J* = 1.5 Hz, 1H, H2'''), 2.45 (t, *J* = 8.7 Hz, 1H, α-CH₂), 2.33 (s, 6H, N(CH₃)₂), 2.29 (s, 6H, N(CH₃)₂), 1.90 (m, 2H, CH₂CH₂CH₃), 1.55 (m, 2H, CH₂CH₂CH₃), 1.29 (d, 6.3 Hz, 3H, CH(CH₃)), 1.27 (obscured m, 1H, CH(CH₃)), 1.11 (t, *J* = 7.2 Hz, 1H, CH₂CH₂CH₃), 1.06 (t, *J* = 9.6 Hz, 1H, α-CH₂),

-0.062 (m, 1H, β -CH). GCOSY (300 Mz, C_6D_6) select data only: δ 2.45 (α -CH₂) \leftrightarrow δ 1.06 (α -CH₂) \leftrightarrow δ -0.062 (β -CH); δ -0.062 (β -CH) \leftrightarrow δ 1.90 ($CH_2CH_2CH_3$) \leftrightarrow δ 1.55 ($CH_2CH_2CH_3$); δ 1.55 ($CH_2CH_2CH_3$) \leftrightarrow δ 1.11 ($CH_2CH_2CH_3$).

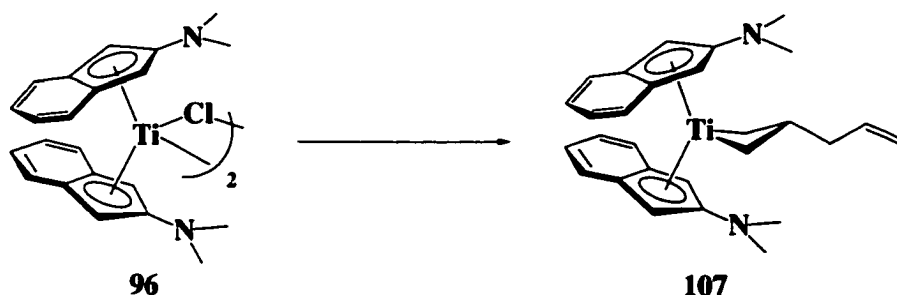
Titanacyclobutane 55a from Bis(2-piperidinoindenyl)titanium Cinnamyl 53:



3-Isopropyl-2-phenyl-bis(2-piperidinoindenyl)titanacyclobutane 55a. This procedure, modified from the previous report¹ was used to obtain crystals suitable for X-ray crystallography. In the drybox, a vial containing a THF solution (3 mL) of bis(2-piperidinoindenyl)titanium (η^3 -1-phenylallyl) (48.9 mg, 0.0870 mmol) **53**, was cooled to -35 °C. A solution of SmI_2 (0.91 mL, 0.1 M in THF at -35 °C) was added, followed immediately by a solution of isopropyl iodide (9.1 μ L in 2 mL THF at -35 °C). The solution was allowed to warm to room temperature and stir for 5 hours. The solvent was removed *in vacuo* and the product was extracted into 1 : 2 benzene/hexane and filtered through a sintered glass funnel layered with a short plug of Celite. The solvents were removed and the resulting solid was crystallized by layering pentane on a solution of the complex in diethyl ether (1 : 4) and cooling to -35 °C, yielding the known titanacyclobutane complex **55a** as diffractable deep red platelets (40.2 mg, 78%, see Appendix I for crystallographic details).

Titanacyclobutane **107** from Bis(2-*N,N*-dimethylaminoindenyl)titanium Chloride **96**

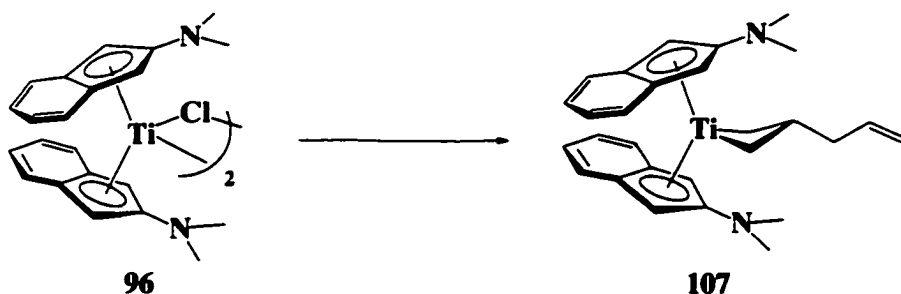
(Procedure A):



3-Allyl-bis(2-*N,N*-dimethylaminoindenyl)titanacyclobutane **107.** In the drybox, a vial containing a cold (-35 °C) THF solution (1 mL) of bis(2-*N,N*-dimethylaminoindenyl)titanium chloride **96** (42.2 mg, 0.106 mmol) was treated with 2 equivalents of a cold (-35 °C) THF solution of allyl bromide (18.7 μ L, in 0.5 mL THF). The reaction mixture was left to stir for one minute and treated with 3 equivalents of cold (-35 °C) SmI₂ (2.1 mL, 0.1 M in THF). The reaction was left to stir at room temperature until the blue solution turned bright red with notable formation of SmI₂X precipitate (2-3 minutes). At this point, the solution was decanted, mixed with 10 mL of cold (-35 °C) pentane, vacuum filtered through a plug of Celite and evaporated to dryness. A ¹H NMR spectrum taken of the crude indicated the formation of titanacyclobutane complex **107**. A yield could not be calculated nor was full characterization possible due to the rapid thermal decomposition. ¹H NMR (360.1 MHz, C₆D₆): δ 7.39 (m, 2H, H4/H5), 7.30 (m, 2H, H4/H5), 6.92 (m, 4H, H4/H5), 6.23 (m, 1H, 1H, CH₂CH=CH₂), 5.15 (overlapping signals, 2H, CH₂CH=CH₂), 4.55 (s, 2H, H2), 4.45 (s, 2H, H2'), 2.59 (m, 1H, CH₂CH=CH₂), 2.30 (s, 6H, N(CH₃)₂), 2.25 (s, 6H, N(CH₃)₂), 2.03 (t, *J* = 10.0 Hz, 2H, α -CH₂), 1.78 (t, *J* = 8.4 Hz, 2H, α -CH₂), β -CH – obscured by residual pentane.

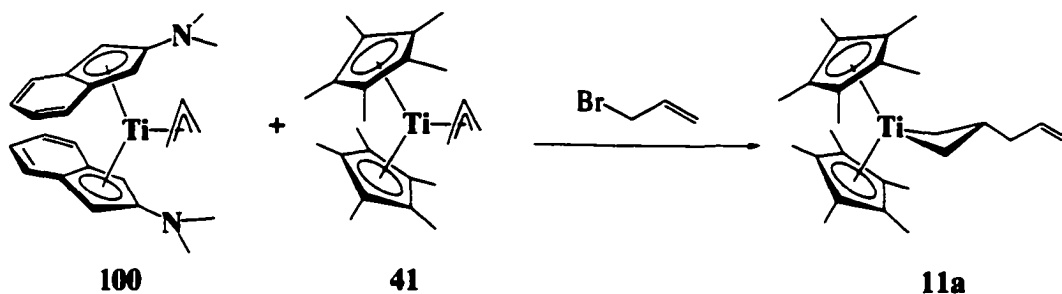
Titanacyclobutane 107 from Bis(2-*N,N*-dimethylaminoindenyl)titanium Chloride 96

(Procedure B):



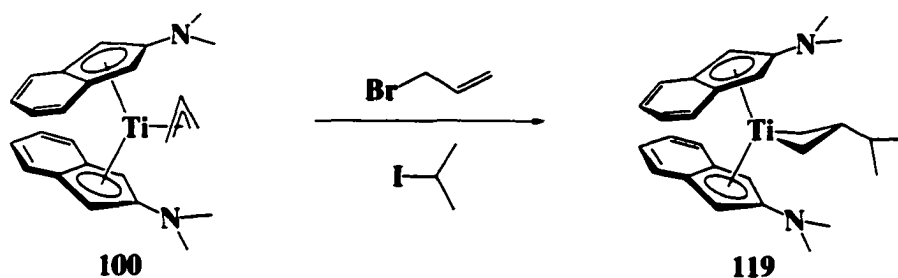
2-Allyl-bis(2-*N,N*-dimethylaminoindenyl)titanacyclobutane 107. In the drybox, a vial containing a cold ($-35\text{ }^{\circ}\text{C}$) THF solution (1 mL) of bis(2-*N,N*-dimethylaminoindenyl)titanium chloride (29.3 mg, 0.0733 mmol) was treated with one equivalent of allylmagnesium chloride (73.3 μL , 1.0 M in THF). The solution was allowed to warm to room temperature, stirred for an additional hour and treated with an equivalent of SmI_2 (0.73 mL, 0.1 M in THF). The reaction mixture was re-cooled to $-35\text{ }^{\circ}\text{C}$ and treated with an equivalent of allyl bromide (6.3 μL). On warming the reaction to room temperature, the blue colour of the solution was quickly (approximately 5 minutes) replaced by a brilliant red solution and a bright yellow SmI_2X precipitate. The solution was decanted, mixed with 10 mL of cold ($-35\text{ }^{\circ}\text{C}$) pentane, vacuum filtered through a plug of Celite and evaporated to dryness. The ^1H NMR spectrum taken was spectroscopically homogeneous and identical to the material prepared above.

Thermal Decomposition of Titanacyclobutane 107:



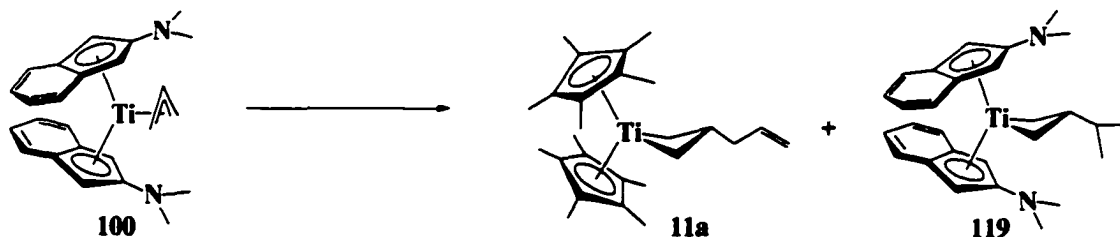
Trapping of allyl radical. In the drybox, to a vial containing a cooled (-35 °C) THF solution of bis(2-*N,N*-dimethylaminoindenyl)titanium allyl complex **100** (21.8 mg, 0.0538 mmol) and SmI₂ (0.54 mL, 0.1 M in THF) was added an equally cold solution of allyl bromide (4.6 μL in 1 mL THF). After approximately 3 minutes the colour of the solution had turned from dark blue to bright red. At this point, a cold (-35 °C) THF solution containing bis(pentamethylcyclopentadienyl)titanium allyl complex **41** (19.3 mg, 0.0538 mmol) was added to the reaction. The colour of the reaction darkened, and within minutes regained its original brightness. The reaction was left to stir at room temperature for 1 h, evaporated to dryness under reduced pressure and triturated with pentane. The pentane extracts were filtered through Celite and evaporated to dryness to yield 19.0 mg of a dark red oil (88%) identified by ¹H NMR as 2-allyl bis(pentamethylcyclopentadienyl)titanacyclobutane complex **11a**, spectroscopically homogeneous and identical to material previously characterized.²⁶

Thermal Decomposition of Titanacyclobutane 107:



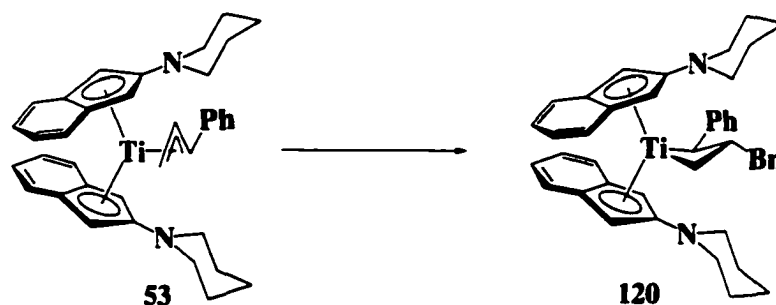
Trapping of allyl complex 100. In the drybox, to a vial containing a cooled (-35 °C) THF solution of bis(2-*N,N*-dimethylaminoindenyl)titanium allyl complex **100** (20.0 mg, 0.0493 mmol) and SmI₂ (0.50 mL, 0.1 M in THF) was added an equally cold solution of allyl bromide (4.3 μL in 1 mL THF). After approximately 3 minutes the colour of the solution turned from dark blue to bright red. At this point, an additional equivalent of SmI₂ (0.50 mL), cooled to -35 °C, was added to the reaction followed by an equivalent of 2-iodopropane (5.0 μL in 1 mL THF at -35 °C). The colour of the reaction darkened, and within 5 minutes had regained its original brightness. The reaction was left to stir at room temperature for 1 h, evaporated to dryness under reduced pressure and triturated with pentane. The pentane extracts were filtered through Celite and evaporated to dryness to yield 18.9 mg of a dark red oil (85%) identified by ¹H NMR as 2-isopropyl bis(2-*N,N*-dimethylaminoindenyl)titanacyclobutane complex **119**, spectroscopically homogeneous and identical to the material prepared on pg. 177.

Thermal Decomposition of Titanacyclobutane 107:



Trapping of both allyl radical and allyl complex 100. In the drybox, a vial containing a cooled ($-35\text{ }^{\circ}\text{C}$) THF solution of bis(2-*N,N*-dimethylaminoindenyl)titanium allyl complex **100** (20.0 mg, 0.0493 mmol) and SmI_2 (0.50 mL, 0.1 M in THF) was treated with an equally cold solution of allyl bromide (3.9 μL in 1 mL THF). After approximately 4 minutes the colour of the solution had turned from dark blue to bright red. At this point, a THF solution containing bis(pentamethylcyclopentadienyl)titanium allyl complex **41** (17.7 mg, 0.0493 mmol), cooled to $-35\text{ }^{\circ}\text{C}$, was added to the reaction. The colour of the reaction darkened and within 3 minutes regained its original brightness. After stirring an additional minute, an additional equivalent of SmI_2 (0.50 mL) cooled to $-35\text{ }^{\circ}\text{C}$ was added followed by an equivalent of 2-iodopropane (4.9 μL in 1 mL THF at $-35\text{ }^{\circ}\text{C}$). The colour of the reaction darkened significantly, but within 1 h fully regained its original brightness and formed a yellow SmI_2X precipitate. The reaction was evaporated to dryness under reduced pressure and triturated with pentane. The pentane extracts were filtered through Celite and evaporated to dryness to yield 40.8 mg of a dark red oil identified by ^1H NMR as an approximate 1 : 1 ratio of 2-isopropyl bis(2-*N,N*-dimethylaminoindenyl)titanacyclobutane complex **119** and 2-allyl bis(pentamethylcyclopentadienyl)titanacyclobutane complex **41**, spectroscopically homogeneous and identical to the materials previously characterized. Based on a material balance for the reaction, 97% of the expected total mass is recovered.

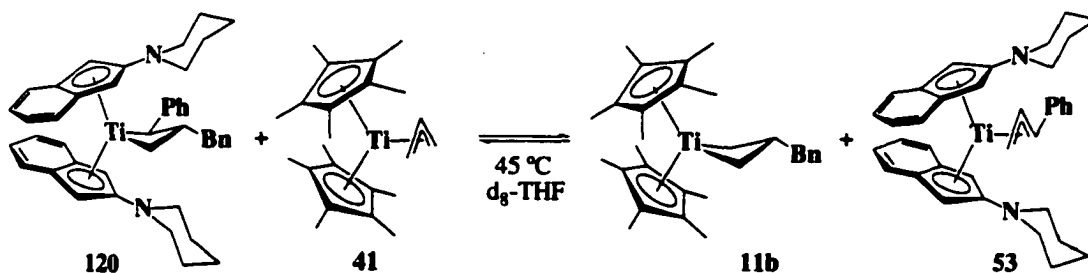
Titanacyclobutane 120 from Bis(2-piperidinoindenyl)titanium Cinnamyl 53:



3-Benzyl-2-phenyl bis(2-piperidinoindenyl)titanacyclobutane 120. In the drybox, a vial containing a THF solution (3 mL) of bis(2-piperidinoindenyl)titanium (η^3 -1-phenylallyl) **53** (48.0 mg, 0.0855 mmol) was cooled to $-35\text{ }^\circ\text{C}$. A cold ($-35\text{ }^\circ\text{C}$) solution of SmI_2 (0.85 mL, 0.1 M in THF at $-35\text{ }^\circ\text{C}$) was added, followed immediately by a cold ($-35\text{ }^\circ\text{C}$) solution of benzyl chloride (9.8 μL in 1 mL THF at $-35\text{ }^\circ\text{C}$). The reaction mixture was allowed to warm to room temperature and stir for 2 h. The solvent was removed *in vacuo* and the product was extracted into hexane and filtered through a sintered glass funnel layered with a short plug of Celite. The solvents were removed and the resulting solid was purified by layering pentane on a solution of the complex in diethyl ether (1 : 4) and cooling to $-35\text{ }^\circ\text{C}$, yielding titanacyclobutane complex **120** as a dark brown powder (24.3 mg, 44%). $^1\text{H NMR}$ (400.1 MHz, C_6D_6): δ 7.35-7.09 (m, 10H, H_{aryl}), 7.01-9.93 (m, 6H, H_{aryl}), 6.70 (t, $J = 7.7\text{ Hz}$, 1H, C_6H_5), 6.60 (d, $J = 8.2\text{ Hz}$, 1H, C_6H_5), 5.20 (s, 1H, H2), 5.12 (s, 1H, H2'), 4.95 (s, 1H, H2''), 4.92 (s, 1H, H2'''), 2.95 (dd, $J = 2.2, 12.7\text{ Hz}$, 1H, $\text{CH}_2(\text{C}_6\text{H}_5)$), 2.83-2.68 (m, 4H, $\text{CH}_2(\text{piperidino})$), 2.50 (t, $J = 9.3\text{ Hz}$, 1H, $\alpha\text{-CH}_2$), 2.42 (m, 2H, $\text{CH}_2(\text{piperidino})$), 2.16 (dd, $J = 8.7, 12.5\text{ Hz}$, 1H, $\text{CH}_2(\text{C}_6\text{H}_5)$), 1.78 (d, $J = 11.4\text{ Hz}$, 1H, $\alpha\text{-CH}(\text{C}_6\text{H}_5)$), 1.36 (m, 4H, $\text{CH}_2(\text{piperidino})$), 1.23 (m, 10H, $\text{CH}_2(\text{piperidino})$), 1.22 (obscured signal, $\beta\text{-CH}$), -0.22 (t, $J = 9.2\text{ Hz}$, 1H, $\alpha\text{-CH}_2$). GCOSY (300 Mz, C_6D_6) select data only: δ 2.95 ($\text{CH}_2(\text{C}_6\text{H}_5)$) \leftrightarrow δ 2.16 ($\text{CH}_2(\text{C}_6\text{H}_5)$); δ -0.22 ($\alpha\text{-CH}_2$) \leftrightarrow δ 2.50 ($\alpha\text{-CH}_2$) \leftrightarrow δ 1.22 ($\beta\text{-CH}$); δ 1.78 ($\alpha\text{-CH}(\text{C}_6\text{H}_5)$) \leftrightarrow δ 1.22 ($\beta\text{-CH}$). $^{13}\text{C NMR}$ (100.6 MHz, C_6D_6): δ

154.6 (C₆H₅), 151.3 (C1), 149.0 (C1'), 142.7 (C₆H₅), 129.9 (C_{aryl}), 128.3 (C_{aryl}), 125.3 (C_{aryl}), 125.1 (C_{aryl}), 124.3 (C_{aryl}), 124.1 (C_{aryl}), 123.7 (C_{aryl}), 123.3 (C_{aryl}), 123.2 (C_{aryl}), 122.7 (C_{aryl}), 122.5 (C_{aryl}), 121.9 (C_{aryl}), 121.1 (C_{aryl}), 117.9 (C_{aryl}), 93.5 (C2), 90.9 (α-CH(C₆H₅)), 90.6 (C2'), 89.1 (C2''), 86.0 (C2'''), 81.6 (α-CH₂), 50.8 (CH₂(piperidino)), 49.4 (CH₂(piperidino)), 39.5 (CH₂(C₆H₅)), 31.7 (CH₂(piperidino)), 25.5 (CH₂(piperidino)), 24.8 (CH₂(piperidino)), 24.2 (CH₂(piperidino)), 24.1 (CH₂(piperidino)), 22.8 (CH₂(piperidino)), 22.6 (β-CH). HMQC (300 MHz, C₆D₆) select data only: δ 93.5 (C2) ↔ δ 4.95 (H2''); δ 90.9 (α-CH(C₆H₅)) ↔ δ 1.78 (α-CH(C₆H₅)); δ 90.6 (C2') ↔ δ 5.20 (H2); δ 89.1 (C2'') ↔ δ 4.92 (H2''); δ 86.0 (C2''') ↔ δ 5.12 (H2'); δ 81.6 (α-CH₂) ↔ δ 2.50 (α-CH₂), δ -0.22 (α-CH₂); δ 39.5 (CH₂(C₆H₅)) ↔ δ 2.95 (CH₂(C₆H₅)), δ 2.16 (CH₂(C₆H₅)); δ 22.6 (β-CH) ↔ δ 1.22 (β-CH).

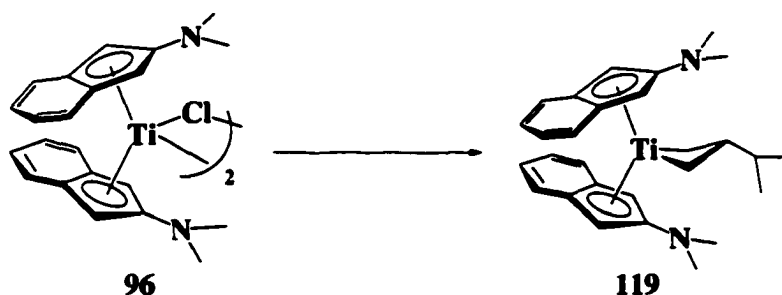
Thermal Decomposition of 3-Benzyl-2-phenyl-bis(2-piperidinoindenyl)titanacyclobutane 120:



Trapping the benzyl radical. In the drybox, 3-benzyl-2-phenyl bis(2-piperidinoindenyl)titanacyclobutane **120** (16.0 mg, 0.0245 mmol) and bis(pentamethylcyclopentadienyl)titanium allyl complex **41** (18.0 mg, 0.0500 mmol) were dissolved in ~ 1 mL d₈-THF and transferred into a NMR tube. The cap of the NMR tube was wrapped with parafilm and removed from the drybox. The tube was heated in an oil bath at 45 °C for one hour. ¹H NMR indicated trace amounts of 3-benzyl bis(pentamethylcyclopentadienyl)titanacyclobutane complex **11b** in addition to 3-benzyl-

2-phenyl bis(2-piperidinoindenyl)titanacyclobutane **120**. Continued thermolysis at 45°C resulted in >90 % conversion of to 3-benzyl-2-phenyl bis(2-piperidinoindenyl)titanacyclobutane **120** to 3-benzyl bis(pentamethylcyclopentadienyl)titanacyclobutane complex **11b** in 12 h. The reaction was heated for a total of 3 days, at which point the only remaining species in solution was 3-benzyl bis(pentamethylcyclopentadienyl)titanacyclobutane complex **11b**. Confirmation of 3-benzyl bis(pentamethylcyclopentadienyl)titanacyclobutane complex **11b** identity was performed by spiking the NMR tube with independently synthesized material.²⁶

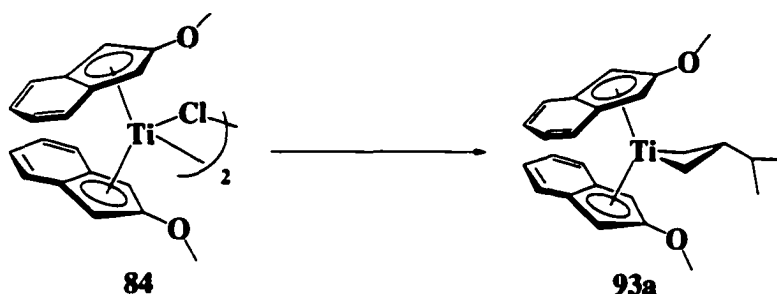
Titanacyclobutane 119 from Bis(2-*N,N*-dimethylaminoindenyl)titanium Chloride 96 (all SmI₂ procedure):



3-Isopropyl-bis(2-*N,N*-dimethylaminoindenyl)titanacyclobutane 119. In the drybox, a cold (-35 °C) THF solution (1 mL) of bis(2-*N,N*-dimethylaminoindenyl)titanium chloride **96** (27.5 mg, 0.0688 mmol) was treated with a cold (-35 °C) THF solution of allyl bromide (6.0 μL, in 0.5 mL THF). The reaction mixture was left to stir for one minute and, thereafter, 3 equivalents of cooled SmI₂ (2.1 mL, 0.1 M in THF) were added to solution followed immediately by a cooled solution of 2-iodopropane (7.0 μL, in 0.5 mL THF). The reaction was allowed to warm slowly to room temperature. On the addition of SmI₂, the colour of the solution turned dark blue/brown; on warming to room temperature, the colour turned bright red with the formation of SmI₂X precipitate. After

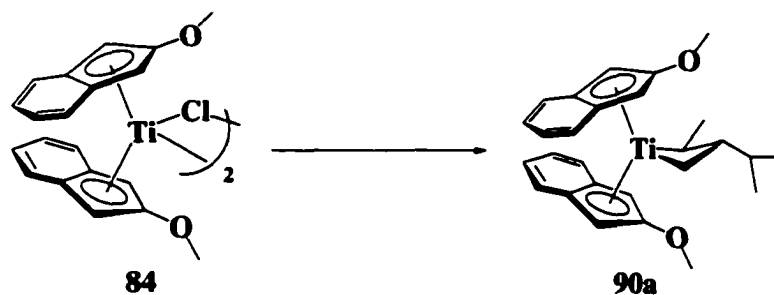
1 h, the solution was decanted from the precipitate and evaporated under reduced pressure to dryness. The red residue was triturated with pentane, filtered through a plug of Celite and evaporated to dryness under reduced pressure, giving complex **119** in a crude yield of 95 %. The red oil was re-dissolved in pentane, concentrated to approximately 1 mL and cooled to $-35\text{ }^{\circ}\text{C}$ to afford dark red agglomerates of titanacyclobutane **119** (26.0 mg, 84 %). $^1\text{H NMR}$ (400 MHz, C_6D_6): δ 7.37 (dd, $J = 6.3, 3.1$ Hz, 2H, H3/H4), 7.34 (dd, $J = 6.3, 3.1$ Hz, 2H, H4/H5), 6.92 (dd, $J = 6.3, 3.1$ Hz, 4H, H4/H5), 4.57 (s, 2H, H2), 4.55 (s, 2H, H2'), 2.30 (s, 6H, $\text{N}(\text{CH}_3)_2$), 2.28 (s, 6H, $\text{N}(\text{CH}_3)_2$), 1.78 (dd, $J = 10.0, 8.8$ Hz, 2H, $\alpha\text{-CH}_2$), 1.69 (t, $J = 8.4$ Hz, 2H, $\alpha\text{-CH}_2$), 1.27 (d, $J = 6.4$ Hz, 6H, $\text{CH}(\text{CH}_3)_2$), 1.09 (dseptet, $J = 2.9, 6.6$ Hz, 1H, $\text{CH}(\text{CH}_3)_2$), 0.20 (m, 1H, $\beta\text{-CH}$). GCOSY (300 Mz, C_6D_6) select data only: δ 1.78 ($\alpha\text{-CH}_2$) \leftrightarrow δ 1.69 ($\alpha\text{-CH}_2$) \leftrightarrow δ 0.20 ($\beta\text{-CH}$); δ 1.27 ($\text{CH}(\text{CH}_3)_2$) \leftrightarrow δ 1.09 ($\text{CH}(\text{CH}_3)_2$); δ 1.09 ($\text{CH}(\text{CH}_3)_2$) \leftrightarrow δ 0.20 ($\beta\text{-CH}$). $^{13}\text{C NMR}$ (100.6 MHz, C_6D_6): δ 151.3 (C1), 149.2 (C1'), 125.2 (C4/C5), 124.9 (C4/C5), 121.9 (C4/C5), 121.6 (C4/C5), 120.1 (C3), 119.5 (C3'), 88.3 (C2), 87.6 (C2'), 77.3 ($\alpha\text{-CH}_2$), 40.0 ($\text{N}(\text{CH}_3)_2$), 39.8 ($\text{N}(\text{CH}_3)_2$), 37.9 ($\text{CH}(\text{CH}_3)_2$), 23.9 ($\text{CH}(\text{CH}_3)_2$), 23.7 ($\beta\text{-CH}$). HMQC (300 MHz, C_6D_6) select data only: δ 88.3 (C2) \leftrightarrow δ 4.57 (H2); δ 87.6 (C2') \leftrightarrow δ 4.59 (H2'); δ 77.3 ($\alpha\text{-CH}_2$) \leftrightarrow δ 1.78 ($\alpha\text{-CH}_2$), δ 1.69 ($\alpha\text{-CH}_2$); δ 40.0 ($\text{N}(\text{CH}_3)_2$) \leftrightarrow δ 2.30 ($\text{N}(\text{CH}_3)_2$); δ 39.8 ($\text{N}(\text{CH}_3)_2$) \leftrightarrow δ 2.28 ($\text{N}(\text{CH}_3)_2$); δ 37.9 ($\text{CH}(\text{CH}_3)_2$) \leftrightarrow δ 1.09 ($\text{CH}(\text{CH}_3)_2$); δ 23.9 ($\text{CH}(\text{CH}_3)_2$) \leftrightarrow δ 1.27 ($\text{CH}(\text{CH}_3)_2$); δ 23.7 ($\beta\text{-CH}$) \leftrightarrow δ 0.20 ($\beta\text{-CH}$). Anal. calcd. C, 74.98; H, 8.09; N, 6.25; found C, 75.26; H, 8.21; N, 6.10.

Titanacyclobutane 93a from Bis(2-methoxyindenyl)titanium Chloride 84 (all SmI₂ procedure):



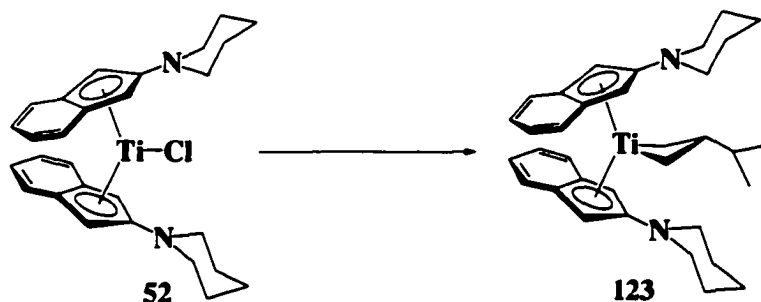
3-Isopropyl-bis(2-methoxyindenyl)titanacyclobutane 93a. In the drybox, a vial containing a THF solution (3 mL) of bis(2-methoxyindenyl)titanium chloride **84** (27.1 mg, 0.0725 mmol) was cooled to $-35\text{ }^{\circ}\text{C}$. Allyl bromide (6.4 μL , in 1 mL THF) was placed into a separate vial and cooled to $-35\text{ }^{\circ}\text{C}$ and then added to the monochloride complex **84**. The reaction was left to stir for approximately 1 minute after which three equivalents of cooled ($-35\text{ }^{\circ}\text{C}$) samarium iodide (2.2 mL, 0.1 M in THF) followed immediately by an equivalent of equally cooled 2-iodopropane (7.3 μL in 1 mL THF) were added to the reaction. The resultant reaction mixture was allowed to warm to room temperature and stir overnight. Evaporation of the solvent followed by trituration of the crude reaction mixture with pentane and filtration through Celite afforded titanacyclobutane complex **93a** in 93% yield (28.1 mg), spectroscopically homogeneous and identical to that previously prepared (pg. 78).

Titanacyclobutane 90a from Bis(2-methoxyindenyl)titanium Chloride 84 (all SmI₂ procedure):



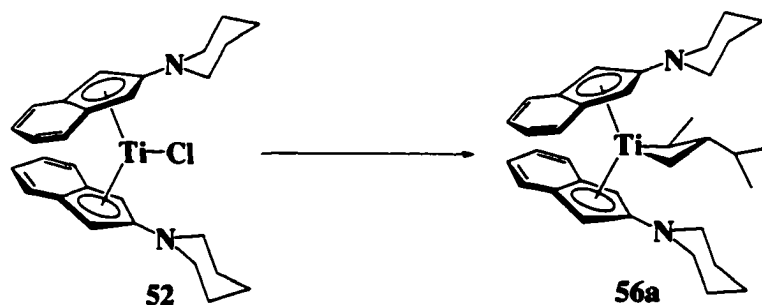
3-Isopropyl-2-methyl-bis(2-methoxyindenyl)titanacyclobutane 90a. As described above, crotyl bromide (7 μ L in 1 mL THF) was added to a cooled (-35 $^{\circ}$ C) THF solution (3 mL) of bis(2-methoxyindenyl)titanium chloride **84** (28.0 mg, 0.0750 mmol) followed by the addition of three equivalents of cooled (-35 $^{\circ}$ C) samarium iodide (2.3 mL, 0.1 M in THF) and an equivalent of equally cooled 2-iodopropane (7.5 μ L in 1 mL THF). The resultant reaction mixture was allowed to warm to room temperature and stir an additional hour. Evaporation of the solvent followed by trituration of the crude reaction mixture with pentane and filtration through Celite afforded titanacyclobutane complex **90a** in 49 % yield (16.0 mg), spectroscopically homogeneous and identical to that previously prepared (pg. 72).

Titanacyclobutane 123 from Titanocene Chloride 52 (all SmI₂ procedure):



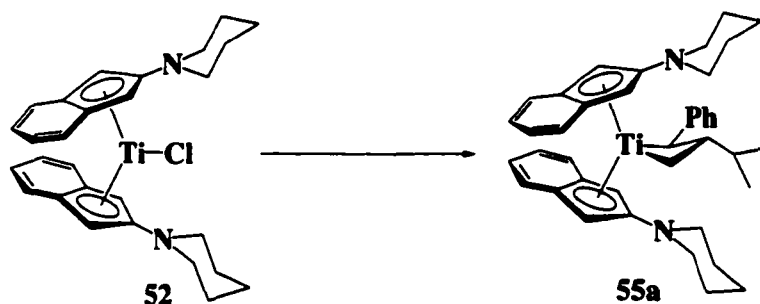
3-Isopropyl-bis(2-piperidinoindenyl)titanacyclobutane 123. As described above, a vial containing a THF solution (3 mL) of bis(2-piperidinoindenyl)titanium chloride **52** (38.1 mg, 0.0794 mmol) was cooled to $-35\text{ }^{\circ}\text{C}$ and treated with allyl bromide (7.0 μL , in 1 mL THF), three equivalents of cooled ($-35\text{ }^{\circ}\text{C}$) samarium iodide (2.4 mL, 0.1 M in THF) and an equivalent of equally cooled 2-iodopropane (8.0 μL in 1 mL THF). The resultant reaction mixture was allowed to warm to room temperature and stir overnight. Evaporation of the solvent followed by trituration of the crude reaction mixture with pentane and filtration through Celite afforded titanacyclobutane complex **123** in 71% yield (29.6 mg), spectroscopically homogeneous and identical to that previously reported.³

Titanacyclobutane 56a from Bis(2-piperidinoindenyl)titanium Chloride 52 (all SmI₂ procedure):



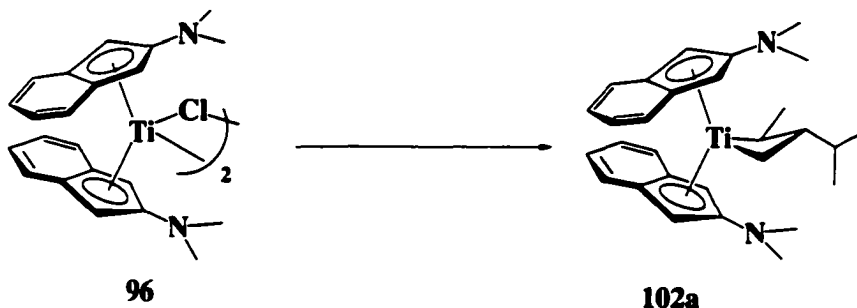
3-Isopropyl-2-methyl-bis(2-piperidinoindenyl)titanacyclobutane 56a. As described above, a vial containing a THF solution (3 mL) of bis(2-piperidinoindenyl)titanium chloride **52** (23.7 mg, 0.0494 mmol) was cooled to $-35\text{ }^{\circ}\text{C}$ and treated with crotyl bromide (4.6 μL , in 1 mL THF), three equivalents of cooled ($-35\text{ }^{\circ}\text{C}$) samarium iodide (1.5 mL, 0.1 M in THF) and an equivalent of equally cooled 2-iodopropane (5.0 μL in 1 mL THF). The resultant reaction mixture was allowed to warm to room temperature and stir an additional hour. Evaporation of the solvent followed by trituration of the crude reaction mixture with pentane and filtration through Celite afforded titanacyclobutane complex **56a** in 60% yield (15.7 mg), spectroscopically homogeneous and identical to that previously reported.³

Titanacyclobutane 55a from Bis(2-piperidinoindenyl)titanium Chloride 52 (all SmI₂ procedure):



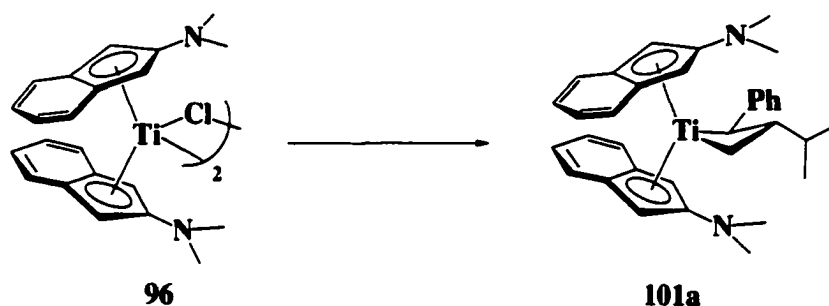
3-Isopropyl-2-phenyl-bis(2-piperidinoindenyl)titanacyclobutane 55a. As described above, a vial containing a THF solution (3 mL) of bis(2-piperidinoindenyl)titanium chloride 52 (35.2 mg, 0.0733 mmol) was cooled to $-35\text{ }^{\circ}\text{C}$ and treated with cinnamyl chloride (10.7 μL , in 1 mL THF), three equivalents of cooled ($-35\text{ }^{\circ}\text{C}$) samarium iodide (2.2 mL, 0.1 M in THF) and an equivalent of equally cooled 2-iodopropane (7.7 μL in 1 mL THF). The resultant reaction mixture was allowed to warm to room temperature and left overnight. Evaporation of the solvent was followed by trituration of the crude reaction mixture with benzene/hexane (1 : 5) and filtration through Celite. Recrystallization from THF layered with hexane (1 : 5) afforded titanacyclobutane complex 55a in 43% yield (19.0 mg), spectroscopically homogeneous and identical to that previously reported.¹

Titanacyclobutane 102a from Bis(2-*N,N*-dimethylaminoindenyl)titanium Chloride 96 (all SmI₂ procedure):



3-Isopropyl-2-methyl-bis(2-*N,N*-dimethylaminoindenyl)titanacyclobutane 102a. As described above, a cold (-35 °C) THF solution (2 mL) of bis(2-*N,N*-dimethylaminoindenyl)titanium chloride **96** (31.4 mg, 0.0786 mmol) was treated with a cold (-35 °C) THF solution of crotyl bromide (7.4 μL, in 0.5 mL THF) followed by 3 equivalents of cooled (-35 °C) SmI₂ (2.4 mL, 0.1 M in THF) and an equally cooled solution of 2-iodopropane (7.9 μL, in 0.5 mL THF). The solution was left to warm to room temperature and stir for 1 h. The solution was decanted from the Sm(III) precipitate and evaporated to dryness. The purple/red residue was triturated with pentane, filtered through Celite to afford titanacyclobutane complex **102a** in 53% yield (19.4 mg), spectroscopically homogeneous and identical to that previously prepared (pg. 161).

Titanacyclobutane 101a from Bis(2-*N,N*-dimethylaminoindenyl)titanium Chloride 96 (all SmI_2 procedure):



3-Isopropyl-2-phenyl-bis(2-*N,N*-dimethylaminoindenyl)titanacyclobutane 101a. As described above, a cold ($-35\text{ }^\circ\text{C}$) THF solution (2 mL) of bis(2-*N,N*-dimethylaminoindenyl)titanium chloride **96** (27.9 mg, 0.0698 mmol) was treated with a cold ($-35\text{ }^\circ\text{C}$) THF solution of cinnamyl chloride (9.8 μL , in 0.5 mL THF) followed by 3 equivalents of cooled ($-35\text{ }^\circ\text{C}$) SmI_2 (2.1 mL, 0.1 M in THF) and an equally cooled solution of 2-iodopropane (7.0 μL , in 0.5 mL THF). The solution was left to warm to room temperature and stir overnight. Evaporation of the solvent followed by trituration of the crude reaction mixture with benzene/hexane (1 : 5) and filtration through Celite afforded trace amounts of titanacyclobutane complex **101a** as observed by ^1H NMR spectroscopy of the crude reaction mixture.

G. References

1. Carter, C. A. G.; McDonald, R.; Stryker, J. M. *Organometallics* **1999**, *18*, 820
2. Carter, C. A. G.; Greidanus, G; Chen, J.-X.; Stryker, J. M., manuscript submitted.
3. Carter, C. A. G. Ph. D. Dissertation, University of Alberta, 1998.
4. Edlund, U. *Acta. Chem. Scand.* **1973**, *27*, 4027.
5. The synthesis of 2-(*N,N*-dimethylamino)-1-(trimethylsilyl)indene was based on a method reported by Clark: Cardoso, A. M.; Clark, R. J.; Moorhouse, S. J. *J. Chem.*

- Soc., Dalton Trans.* **1980**, 1156. Coordination of silylated cyclopentadienyl ligands to titanium: Winter, C. H.; Zhou, X.-X.; Dobbs, D. A.; Heeg, M. J. *Organometallics* **1991**, *10*, 210.
6. The synthesis of 1-tributylstannyl-2-*N,N*-dimethylaminoindene is based on the method described by Schlosser. Desponds, O.; Schlosser, M. *J. Organomet. Chem.* **1991**, *409*, 93. Coordination of cyclopentadienyl tin derivatives to titanium: (a) Abel, E. W. Moorhouse, S. *J. Chem. Soc., Dalton Trans.* **1973**, 1706. (b) Jutzi, P.; Kuhn, M. *J. Organomet. Chem.* **1979**, *173*, 221. (c) O' Hare, D.; Murphy, V.; Diamond, G. M.; Arnold, P.; Mountford, P. *Organometallics* **1994**, *13*, 4689. (d) Hart, S. L.; Duncalf, D. J.; Hastings, J. J.; McCamley, A.; Taylor, P.C. *J. Chem. Soc., Dalton Trans.* **1996**, 2843.
 7. Monomeric complexes: (a) Pattisina, J. W.; Heeres, H. J.; van Bolhuis, F.; Meetsma, A.; Teuben, J. H. *Organometallics* **1987**, *6*, 1004. (b) Castellani, M. P.; Geib, S. J.; Rheingold, A. L.; Trogler, W. C.; *Organometallics* **1987**, *6*, 2524. (c) Urazowski, I. F.; Ponomaryov, V. I.; Ellert, O. G.; Nifant'ev, I. E.; Lemenovskii, D. A. *J. Organomet. Chem.* **1988**, *356*, 181. (d) Troyanov, S. I.; Rybakov, V. B.; Thewalt, U.; Varga, V.; Mach, K. *J. Organomet. Chem.* **1993**, *447*, 221. Dimeric complexes: (e) Jungst, R.; Sekutowski, D.; Davis, J.; Luly, M.; Stucky, G. *Inorganic Chem.* **1977**, *16*, 1645. (f) Martin, J.; Fauconet, M.; Moïse, C. *J. Organomet. Chem.* **1989**, *371*, 87.
 8. For a comment on this problem, common to certain classes of early transition metal complexes, see supporting information in Carney, M. J.; Walsh, P. J.; Bergman, R. G. *J. Am. Chem. Soc.* **1990**, *112*, 6426.
 9. Martin, H. A.; Jellinek, F. *J. Organomet. Chem.* **1967**, *8*, 115.
 10. Martin, H. A.; Jellinek, F. *J. Organomet. Chem.* **1968**, *12*, 149.
 11. Review: O'Connor, J. M.; Casey, C. P. *Chem. Rev.* **1987**, *87*, 307. (a) Kakkar, A. K.; Taylor, N. J.; Marder, T. B. *Organometallics* **1989**, *8*, 1765. (b) Taraki, N. N.; Huggins, J. M.; Lebioda, L. *Inorg. Chem.* **1988**, *27*, 424. (c) Marder, T. B.; Williams,

I.D. *J. Chem. Soc.; Chem. Commun.* **1987**, 1478. (d) Rest, A. J.; Witwell, L.; Graham, W. A.; Hoyano, J. K.; McMaster, A. D. *J. Chem. Soc.; Chem. Commun.* **1984**, 624. (e) Rerek, M. E.; Basolo, F. *Organometallics* **1984**, *3*, 740. (f) Caddy, P.; Green, M.; O'Brien, E.; Smart, L. E.; Woodward, P. *J. Chem. Soc. Dalton Trans.* **1980**, 962. (g) Marder, T. B.; Roe, D. C.; Milstein, S. *Organometallics* **1988**, *7*, 1451. (h) Borrini, A.; Diversi, P.; Ingrosso, G.; Lucherini, A.; Serra, G. *J. Mol. Catal.* **1985**, *30*, 181. Bonneman, H. *Angew. Chem., Int. Ed. Engl.* **1985**, *24*, 248. (i) Ceccon, A.; Gambaro, A.; Saverio, S.; Valle, G.; Venzo, A. *J. Chem. Soc., Chem. Commun.* **1989**, 51. (j) Habib, A.; Tanke, R. S.; Holtz, E. M.; Crabtree, R. H. *Organometallics* **1989**, *8*, 1225. (k) Merola, J. S.; Kacmarcik, R. T. *Organometallics* **1989**, *8*, 778. (l) Bonifaci, C.; Ceccon, A.; Santi, S.; Mealli, C.; Zoeller, R. *Inorg. Chim. Acta* **1995**, *240*, 541. (m) Huang, Y.; Neto, C. C.; Pevear, K. A.; Holl, M. M. B.; Swiegart, D. A.; Chung, Y. K. *Inorg. Chim. Acta* **1994**, *226*, 53. (n) Pevear, K. A.; Holl, M. M. B.; Carpenter, G. B.; Rieger, A. L.; Rieger, P. H.; Swiegart, D. A. *Organometallics* **1995**, *14*, 512. (o) Okuda, J.; König, P.; Rushkin, I. L.; Kang, H.-C.; Massa, W. *J. Organomet. Chem.* **1995**, *501*, 37. (p) Sato, T.; Nishio, M.; Ishii, Y.; Yamazaki, H.; Hidai, M. *J. Organomet. Chem.* **1998**, *569*, 99. (q) Szajek, L. P.; Lawson, J.; Shapley, J. R. *Organometallics* **1991**, *10*, 357. (r) Rufanov, K.; Avtomonov, E.; Kazennova, N.; Kotov, V.; Khvorost, A.; Lemenovskii, D.; Lorberth, J. *J. Organomet. Chem.* **1997**, *536*, 361. (s) Frankcom, T. M.; Green, J. C.; Nagy, A.; Kakkar, A.; Marder, T. B. *Organometallics* **1993**, *12*, 3688. Calhorda, M. J.; Gamelas, C. A.; Romão, C. C.; Veiros, L. F. *Eur. J. Inorg. Chem.* **2000**, 331. (t) Veiros, L. F. *Organometallics* **2000**, *19*, 3127. (u) Bitterwolf, T. E.; Lukmanova, D.; Gallagher, S.; Rheingold, A. L.; Guzei, I. A.; Liable-Sands, L. *J. Organomet. Chem.* **2000**, *605*, 168. (v) Bassetti, M.; Casellato, P.; Gamasa, M. P.; Gimeno, J. González-Bernardo, C.; Martín-Vaca, B. *Organometallics* **1997**, *16*, 5470.

12. Roberts, J. D.; Caserio, M. P. *Basic Principles of Organic Chemistry*, 2nd ed. Menlow Park, CA: W. A. Benjamin, 1977.
13. The unit cells of $(C_5H_5)_2Ti(1,3\text{-dimethylallyl})$ and $(C_5H_5)_2Ti(2\text{-methylallyl})$ both contain two independent molecules in a crystallographic asymmetric unit.
14. Orpen, A. G.; Brammer, L.; Allen, F. H.; Kennard, O.; Watson, D. G.; Taylor, R. J. *Chem. Soc., Dalton Trans.* **1989**, S1.
15. Scoles, L.; Minhas, R.; Duchateau, R.; Jubb, J.; Gambarotta, S. *Organometallics* **1994**, *13*, 4978.
16. Dick, D. G.; Duchateau, R.; Edema, J. J. H.; Gambarotta, S. *Inorg. Chem.* **1993**, *32*, 1959.
17. Helmholdt, R. B.; Jellinek, F.; Martin, H. A.; Vos, A. *Recl. Trav. Chim. Pays-Bas* **1967**, *86*, 1263. (b) Chen, J.; Kai, Y.; Nasai, N.; Yasuda, H.; Yamamoto, H.; Nakamura, A. *J. Organomet. Chem.* **1991**, *407*, 191.
18. (a) Westcott, S. A.; Kakkar, A. K.; Stringer, G.; Taylor, N. J.; Marder, T. B. *J. Organomet. Chem.* **1990**, *394*, 777. (b) O'Hare, D.; Green, J. C.; Marder, T.; Collins, S.; Stringer, G.; Kakkar, A. T.; Kaltsoyannis, N.; Kuhn, A.; Lewis, R.; Mehnert, C.; Scott, P.; Kurmoo, M.; Pugh, S. *Organometallics* **1992**, *11*, 48. (c) O'Hare, D.; Murphy, V. J.; Kaltsoyannis, N. *J. Chem. Soc., Dalton Trans.* **1993**, 383. (d) O'Hare, D.; Murphy, V.; Diamond, G. M.; Arnold, P.; Mountford, P. *Organometallics*, **1994**, *13*, 4689.
19. η^3 -Indenyl coordination: (a) O'Connor, J. M.; Casey, C. P. *Chem. Rev.* **1987**, *87*, 307, and references therein. (b) Merola, J. S.; Kacmarcik, R. T.; Van Engen, D. *J. Am. Chem. Soc.* **1986**, *108*, 329. (c) Kowalewski, R. M.; Rheingold, A. L.; Trogler, W. C.; Basolo, F. *J. Am. Chem. Soc.* **1986**, *108*, 2460. (d) Forschner, T. C.; Cutler, A. R.; Kullnig, R. K. *Organometallics* **1987**, *6*, 889. (e) Poli, R.; Mattamana, S. P.; Falvello, L. R. *Gazz. Chim. Ital.* **1992**, *112*, 315. (f) Ascenso, J. R.; de Azevedo, C. G.; Gonçalves, I. S.; Herdtweck, E.; Moreno, D. S.; Romão, C. C.; Zühlke, J.

- Organometallics* **1994**, *13*, 429. (g) Le Husebo, T.; Jensen, C. M. *Organometallics*, **1995**, *14*, 1087. (h) Ascenso, J. R.; de Azevedo, C. G.; Gonçalves, I. S.; Herdtweck, E.; Moreno, D. S.; Pessanha, M.; Romão, C. C. *Organometallics* **1995**, *14*, 3901. (i) Kakkar, A. K.; Stringer, G.; Taylor, N. J.; Marder, T. B. *Can. J. Chem.* **1995**, *73*, 981. (j) Calhorda, M. J.; Gamelas, I.S.; Gonçalves, I. S.; Herdtweck, E.; Romão, C. C.; Veiros, L. F. *Organometallics*, **1998**, *17*, 2597.
20. Intermediate η^3 - to η^5 -indenyl coordination: see references 17(a), 20(a), 20(i) and the following: (a) Marder, T. B.; Calabrese, J. C.; Roe, D. C.; Tulip, T. H. *Organometallics*, **1987**, *6*, 2012. (b) Carl, R. T.; Hughes, R. P.; Rheingold, A. L.; Marder, T. B.; Taylor, N. J. *Organometallics*, **1988**, *7*, 1613. (c) Kakkar, A. K.; Taylor, N. J.; Calabrese, J. C.; Nugent, W. A.; Roe, D. C.; Connaway, E. A.; Marder, T. B. *J. Chem. Soc., Chem. Commun.* **1989**, 990. (d) Kakkar, A. K.; Jones, S. F.; Taylor, N. J.; Collins, S.; Marder, T. B. *J. Chem. Soc., Chem. Commun.* **1989**, 1454. (e) Kakkar, A. K.; Taylor, N. J.; Marder, T. B.; Shen, J. K.; Hallinan, N.; Basolo, F. *Inorg. Chim. Acta.* **1992**, *198-200*, 219. (f) Morandini, F.; Pilloni, G.; Consiglio, G.; Sironi, A.; Moret, M.; *Organometallics* **1993**, *12*, 3495. (g) Frankcom, T.M.; Green, J. C.; Nagy, A.; Marder, T. B. *Organometallics* **1993**, *12*, 3688. (h) Rau, D.; Behrens, U.; *J. Organomet. Chem.* **1993**, *461*, 151. (i) Zhou, Z.; Jablonski, C.; Bridson, J. J. *Organomet. Chem.* **1993**, *461*, 215. (j) Westcott, A. S.; Stringer, G.; Anderson, S.; Taylor, N. J.; Marder, T. B. *Inorg. Chem.* **1994**, *33*, 4589. (k) Kakkar, A. K.; Stringer, G.; Taylor, N. J.; Marder, T. B. *Can. J. Chem.* **1995**, *73*, 981. (l) Comstock, M. C.; Shapley, R. J.; *Organometallics* **1997**, *16*, 4816. (m) Bassetti, M.; Casellato, P.; Gamasa, M. P.; Gimeno, J.; González-Bernardo, C.; Martin-Vaca, B. *Organometallics* **1997**, *16*, 5470. (n) Stradiotto, M.; Hughes, D. W.; Bain, A. D.; Brook, M. A.; McGlinchey, M. J. *Organometallics* **1997**, *16*, 5563. (o) Huber, T. A.; Bayrakdarian, M.; Dion, S.; Dubuc, I.; Bélanger-Gariépy, F. Zargarian, D. *Organometallics* **1997**, *16*, 5811. (p) Cecchetto, P.; Ceccon, A.; Gambaro, A.; Santi,

- S.; Ganis, P.; Gobetto, R.; Valle, G.; Venzo, A.; *Organometallics* **1998**, *17*, 752, and refs therein. (q) Westcott, S. A.; Taylor, N. J.; Marder, T. B. *Can. J. Chem.* **1999**, *77*, 199. (r) Gamelas, C. A.; Herdtweck, E.; Lopes, J. P.; Romao, C. C.; *Organometallics* **1999**, *18*, 506. (s) Calhorda, M. J. Gamalas, C. A.; Romao, C. C.; Veiros, L. F. *Eur. J. Inorg. Chem.* **2000**, *2*, 331.
21. Other workers have selected different, but related, parameters to quantify indenyl ligand distortions: see, Faller, J. W.; Crabtree, R. H.; Habib, A. *Organometallics* **1985**, *5*, 929.
22. In several specific examples the authors do not report HA values.^{21ac}
23. (a) Stahl, K. P.; Boche, G.; Massa, W. *J. Organomet. Chem.* **1984**, *277*, 113. (b) Bernheim, M.; Boche, G. *Angew. Chem. Int. Ed. Engl.* **1990**, *19*, 1010. (c) Plenio, H.; Burth, D. *Angew. Chem. Int. Ed. Engl.* **1995**, *34*, 800. (d) Plenio, H.; Burth, D. *Organometallics*, **1996**, *15*, 1151. (e) Plenio, H.; Burth, D. *Organometallics*, **1996**, *15*, 4054. (f) Plenio, H.; Burth, D. *J. Organomet. Chem.* **1996**, *519*, 269. (g) Barsties, E.; Schaible, S.; Prosenc, M. -H.; Rief, U.; Röhl W.; Weyand, O.; Dorer, B.; Brintzinger, H.-H. *J. Organomet. Chem.* **1996**, *520*, 63. (h) Luttkhedde, H. J. G.; Leino, R.; Ahlgrén, M. J.; Pakkanen, T. A.; Näsman, J. H. *J. Organomet. Chem.* **1998**, *557*, 227. (i) Knüppel, S.; Fauré, J.-L.; Erker, G.; Kehr, G.; Nissenen, M.; Fröhlich, R. *Organometallics* **2000**, *19*, 1262.
24. (a) Lee, J. B.; Gajda, G. J.; Schaefer, W. P.; Howard, T. R.; Ikariya, T.; Straus, D. A.; Grubbs, R. H. *J. Am. Chem. Soc.* **1981**, *103*, 7358. (b) Stille, R. J.; Santarsiero, B. D.; Grubbs, R. H. *J. Org. Chem.* **1990**, *55*, 843. (c) Polse, J. L.; Anderson, R. A.; Bergman, R. G. *J. Am. Chem. Soc.* **1996**, *118*, 8737. (d) Polse, J. L.; Kaplan, A. W.; Anderson, R. A.; Bergman, R. G. *J. Am. Chem. Soc.* **1998**, *120*, 6316.
25. Silverstein, R. M.; Webster, F. X. *Spectroscopic Identification of Organic Compounds*, 6th ed., New York: John Wiley & Sons, Inc., 1998.

26. (a) Casty, G. L. Ph. D. Thesis, Indiana University, 1994. (b) Tjaden, E. B.; Casty, G. L.; Stryker, J. M. *J. Am. Chem. Soc.* **1993**, *115*, 9814.
27. (a) Howard, T. R.; Lee, J. B.; Grubbs, R. H. *J. Am. Chem. Soc.* **1980**, *102*, 6876. (b) Lee, J. B.; Ott, K. C. Grubbs, R. H. *J. Am. Chem. Soc.* **1982**, *104*, 7491. (c) Ikariya, T.; Ho, S. C. H.; Grubbs, R. H. *Organometallics* **1985**, *4*, 199.
28. Finch, W. C.; Anslyn, E. V.; Grubbs, R. H. *J. Am. Chem. Soc.* **1988**, *110*, 2406.
29. Ho, S. C. H.; Straus, D. A.; Grubbs, R. H. *J. Am. Chem. Soc.* **1984**, *106*, 1533. (b) Tumas, W.; Wheeler, D. R.; Grubbs, R. H. *J. Am. Chem. Soc.* **1987**, *109*, 6182. (c) Burk, M. J. Staley, D. L.; Tumas, W. *J. Chem. Soc. Chem. Commun.* **1990**, 809. (d) Burk, M. J.; Tumas, W.; Wheeler, D. R. *J. Am. Chem. Soc.* **1990**, *112*, 6133.
30. Tjaden, E. B.; Stryker, J. M. *J. Am. Chem. Soc.* **1993**, *115*, 2085.
31. Tjaden, E. B. Ph. D Thesis, Indiana University, 1993.
32. Corker, J.; Lefebvre, F.; Lécuyer, C.; Dufaud, V.; Quignard, F.; Choplin, A.; Evans, J.; Basset, J. -M. *Science* **1996**, *271*, 966. (b) Watson, P. L.; Parshall, G. W. *Acc. Chem. Res.* **1985**, *18*, 51. (c) Watson, P.L.; Roe, D. C. *J. Am. Chem. Soc.* **1982**, *104*, 6471. (d) Bunel, D.; Berger, B. J.; Bercaw, J. E. *J. Am. Chem. Soc.* **1988**, *110*, 976. (e) Bercaw, J. E. *Pure Appl. Chem.* **1990**, *62*, 1151. (f) Hajela, S.; Bercaw, J. E. *Organometallics*, **1994**, *11*, 362. (g) Eshuis, J. J. W.; Tan, Y. Y.; Teuben J. H.; Renkema, J. *J. Mol. Catal.* **1990**, *62*, 277. (h) Eshuis, J. J. W.; Tan, Y. Y.; Meetsma, A.; Teuben, J. H.; Renkema, J.; Evens, G. G.; *Organometallics* **1992**, *11*, 362. (i) Ketsi, M. R.; Waymouth, R. M. *J. Am. Chem. Soc.* **1992**, *114*, 3565. (j) Resconi, L.; Piemontesi, F.; Francisocono, G.; Abis, L.; Fiorani, T. *J. Am. Chem. Soc.* **1992**, *114*, 1025. (k) Yang, X.; Jia, L.; Marks, T. J. *J. Am. Chem. Soc.* **1993**, *115*, 3392. (l) Horton, A. D. *Organometallics* **1996**, *15*, 2675. (m) Etienne, M.; Mathieu, R.; Donnadieu, B. *J. Am. Chem. Soc.* **1997**, *119*, 3218.

33. See references 33(m) and the following: (a) Etienne, M.; Mathieu, R.; Donnadiu, B. *J. Am. Chem. Soc.* **1997**, *119*, 3218. (b) Corradi, M. M.; Pindado, G. J.; Sarsfield, M. J.; Thorton-Pett, M.; Bochmann, M. *Organometallics* **2000**, *19*, 1150.
34. See references 33 (g-l) and the following: (a) Eshuis, J. J. W.; Tan, Y. Y.; Teuben J. H.; Renkema, J. *J. Mol. Catal.* **1990**, *62*, 277. (b) Eshuis, J. J. W.; Tan, Y. Y.; Meetsma, A.; Teuben, J. H.; Renkema, J.; Evens, G. G.; *Organometallics* **1992**, *11*, 362. (c) Resconi, L.; Piemontesi, F.; Francisocono, G.; Abis, L.; Fiorani, T. *J. Am. Chem. Soc.* **1992**, *114*, 1025. Kesti, M. R.; Waymouth, R. M. *J. Am. Chem. Soc.* **1992**, *114*, 3565. Yang, X.; Jia, L.; Marks, T. J. *J. Am. Chem. Soc.* **1993**, *115*, 3392. Horton, A. D. *Organometallics* **1996**, *15*, 2675. (a) Mise, T.; Kageyama, A.; Miya, S.; Yamazaki, H. *Chem. Lett.* **1991**, 1525. (b) Resconi, L.; Camurati, I.; Sudmeijer, O. *Top. Catal.* **1999**, *7*, 145.
35. Dimauro, P. T.; Wolczanski, P. T. *Polyhedron* **1995**, *14*, 149.
36. Benfield, F. W. S.; Green M. L. H. *J. Chem. Soc., Dalton Trans.* **1974**, 1324. (b) Eilbracht, P. *Chem. Ber.* **1976**, *109*, 1429. (c) Eilbracht, P.; Dahler, P. *Chem. Ber.* **1980**, *113*, 542. (d) Eilbracht, P.; Dahler, P. Mayser, U.; Henkes, E. *Chem. Ber.* **1980**, *113*, 1033. (e) Eilbracht, P.; Mayser, U. Tiedtke, G. *Chem. Ber.* **1980**, *113*, 1420. (f) Eilbracht, P.; Mayser, U. *Chem. Ber.* **1980**, *113*, 2211. (g) Crabtree, R. H.; Dion, R. P. *J. Chem. Soc., Chem. Commun.* **1984**, 1260.
37. Schwiebert, K. E.; Stryker, J. M. *Organometallics* **1993**, *12*, 600. (b) Tjaden, E. B.; Casty, G. L.; Stryker, J. M. *J. Am. Chem. Soc.* **1993**, *115*, 9814. (c) Tjaden, E. B.; Stryker, J. M. *Organometallics* **1992**, *11*, 16. (d) Tjaden, E. B.; Schwiebert, K. E.; Stryker, J. M. *J. Am. Chem. Soc.* **1992**, *114*, 1100.
38. Schwiebert, K. E. Ph. D. Thesis, Indiana University, 1993.
39. (a) McNeill, K, Anderson, R. A.; Bergman, R. G. *J. Am. Chem. Soc.* **1995**, *117*, 3625. (b) McNeill, K, Anderson, R. A.; Bergman, R. G. *J. Am. Chem. Soc.* **1997**, *119*, 11244.

40. Schock, L. E.; Marks, T. J. *J. Am. Chem. Soc.* **1988**, *110*, 7701.
41. Ege, S. N. *Organic Chemistry*, 4th ed., New York: Houghton Mifflin Company, 1999.
42. Evans, W. J.; Keyer, R. A.; Rabe, G. W.; Drummond, D. K.; Ziller, J. W. *Organometallics* **1993**, *12*, 4664.
43. Samuel, E.; Rausch, M. D. *J. Am. Chem. Soc.* **1973**, *95*, 6263.
44. Brintzinger, H.; Bercaw, J. *J. Am. Chem. Soc.* **1970**, *92*, 6182.
45. Rerek, M. E.; Basolo, F. Ji, L. N. *Chem. Commun.* **1983**, 1208.
46. Chen, J. -X. Ph. D. Thesis, University of Alberta, 1999.
47. Nomura, N. Unpublished results.
48. The molar ratio of complex **96** to complex **96**•LiCl(THF)₃ could not be determined precisely; the yield of the reaction is estimated assuming conversion to complex **96** alone, as it is the major material isolated in this procedure. The actual yield is lower.

Chapter 4. Development of Less Electron Rich Indenyl Templates for Central Carbon Alkylation of Titanium(III) Allyl Complexes

A. Introduction

The structural study of aminoindenyl Ti(III) and Ti(IV) complexes indicates that the available electron density provided by the ancillary ligands is greater than what is required to form stable products. What remains unclear is how essential this overabundance of electron density is to facilitate the oxidation state change that occurs during central carbon radical alkylation. Based on this, our investigation turned to the development of simpler, less electron-rich indenyl templates to determine the minimum electron density required to promote regioselective central carbon alkylation of substituted allyl systems.

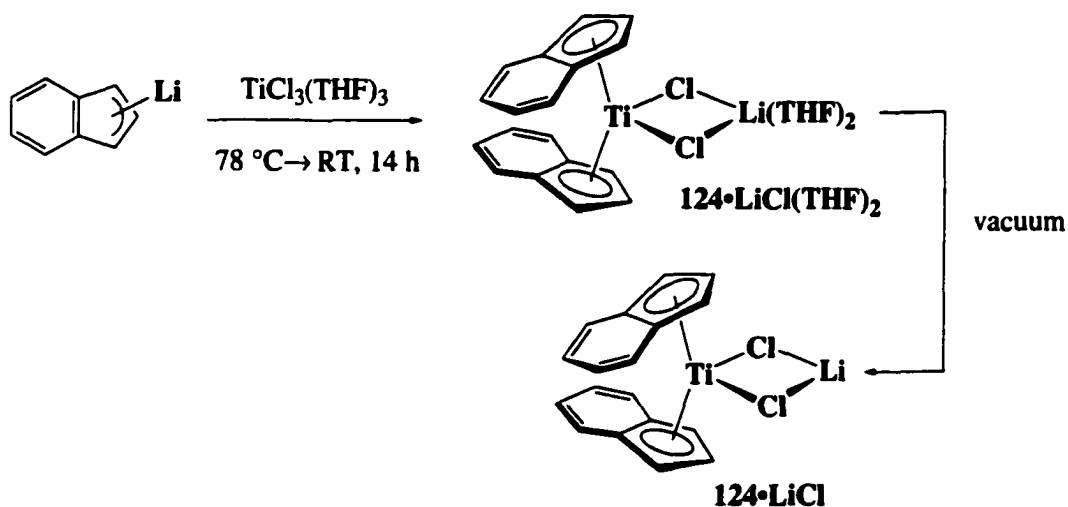
B. Bis(indenyl)titanium(III) as a Template for Central Carbon Alkylation

1. Preparation of Bis(indenyl)titanium(III) η^3 -Allyl Complexes

The unsubstituted indenyl ligand represents the least electron-rich ancillary ligand in this investigation. The synthesis of the requisite titanocene(III) chloride complex was accomplished by transferring a solution of indenyllithium¹ via cannula into a suspension of $\text{TiCl}_3(\text{THF})_3$ in THF at low temperature and allowing the reaction to warm slowly and stir overnight. The deep green solution yielded a red-brown residue which, following crystallization from cooled THF layered with hexane (1 : 2), gave not the expected bis(indenyl)titanocene(III) chloride complex **124**, but the lithium chloride adduct, **124**• $\text{LiCl}(\text{THF})_2$ in 78% yield as green prisms (Scheme 4.1). Under vacuum, these green prisms turn into an amorphous bright red solid and, under the conditions described above, can be recrystallized to again yield green prisms. While high resolution mass spectrometry of the red solid indicates the formation of bis(indenyl)titanocene(III) chloride, elemental analysis is consistent with the presence of lithium chloride in the

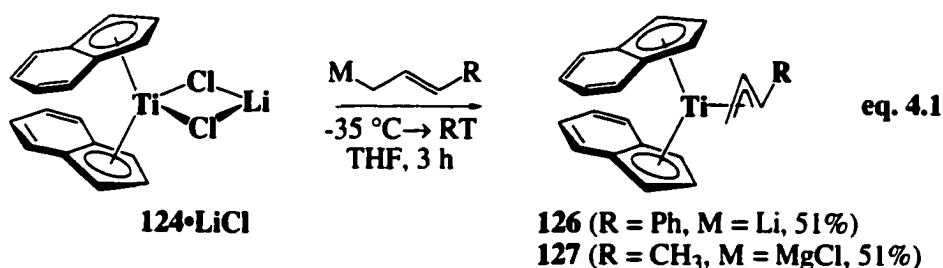
titanocene coordination sphere; the exact structure of complex **124**•LiCl remains unknown. Prolonged exposure to high vacuum, followed by repurification was unsuccessful at removing the coordinated lithium chloride from the complex (*cf.*, bis(2-*N,N*-dimethylaminoindenyl)titanocene **96**•LiCl(THF)₂). Oxidation of complex **124**•LiCl with PbCl₂, expected to yield bis(indenyl)titanocene dichloride **125**, was unsuccessful, although oxidative chlorination using carbon tetrachloride afforded dichloride complex **125**. Rausch previously noted the instability and low solubility² of dichloride complex **125** which together prevented full characterization of this complex. It remains unclear why lead chloride oxidation, which successfully oxidizes numerous titanocene(III) chloride complexes to the corresponding dichloride,³ is unsuccessful here.

Scheme 4.1



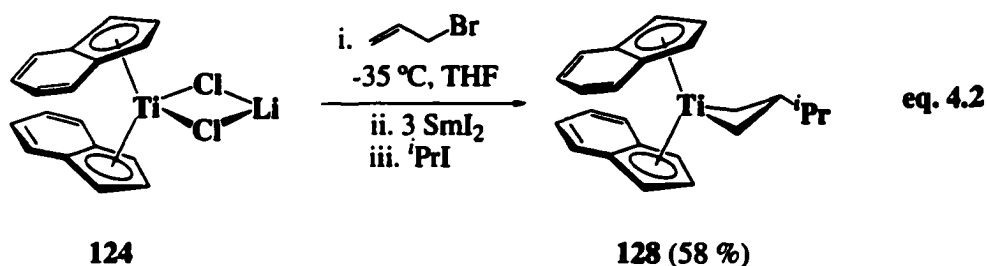
Cinnamyl (η^3 -1-phenylallyl) complex **126** and crotyl (η^3 -1-methylallyl) complex **127** were obtained by treating bis(indenyl)titanium chloride•LiCl **124** with cinnamyl lithium and crotyl Grignard, respectively, in THF at -35 °C (eq. 4.1). The cinnamyl complex **126** was isolated as a green crystalline material in 51% yield and characterized by infrared spectroscopy and elemental analysis. Crotyl complex **127** was isolated as impure medium brown agglomerates in 51% yield and was characterized by IR spectroscopy

only. The infrared spectrum of crotyl complex **127** displays a band at 1532 cm^{-1} for the allylic asymmetric C=C stretch^{4,5} suggesting *syn*- η^3 -crotyl coordination to titanium.

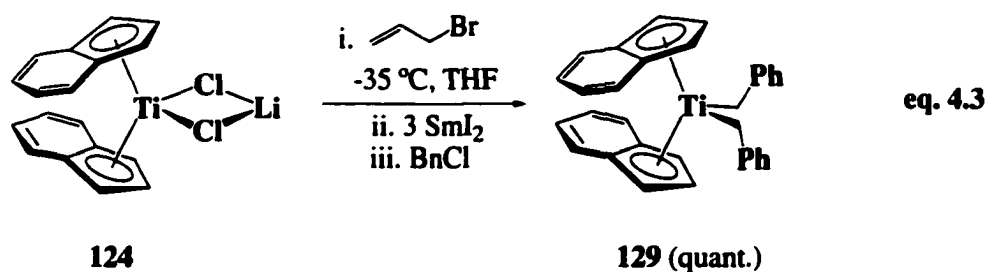


2. Radical Additions to Substituted and Unsubstituted Allyl Complexes of Bis(indenyl)titanium(III)

To evaluate central carbon alkylation of the unsubstituted allyl complex, the *in situ* ‘Chen procedure’ was employed. Bis(indenyl)titanium chloride complex **124**•LiCl, when treated with allyl bromide in THF at low temperature ($-35\text{ }^{\circ}\text{C}$), followed by SmI_2 and 2-iodopropane, results in the formation of titanacyclobutane complex **128** in 58% isolated yield (eq. 4.2). The ^1H NMR spectrum of complex **128** clearly indicates a β -substituted bis(indenyl)titanacyclobutane; characteristic signals at δ 1.81 (t, $J = 9.3\text{ Hz}$) and 0.25 (t, $J = 8.5\text{ Hz}$) are observed for the α -methylene protons and the β -methine signal appears at δ -0.41 as a coincidental sextet. The top to bottom dissymmetry in complex **128** is indicated by the two sets of distinct signals observed for the five-membered ring of the indenyl ligands. These assignments were confirmed by ^1H - ^1H correlated spectroscopy and HMQC correlations.



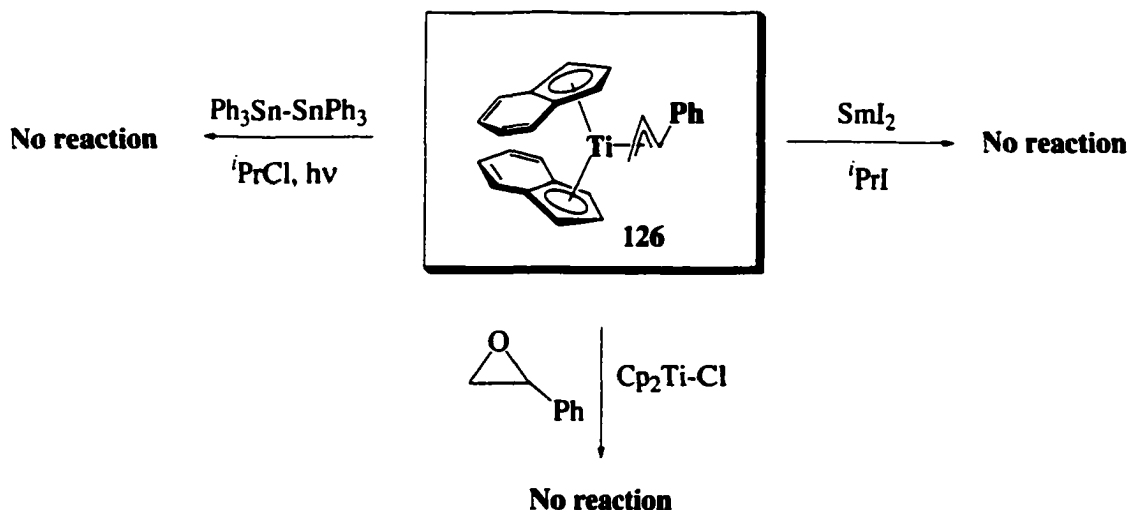
The use of stabilized radicals however, met with only limited success. While colour changes representative of titanacyclobutane formation were observed, the addition of allyl radical led to product decomposition before ^1H NMR spectroscopy could be performed. The use of benzyl chloride gave a dramatically different result: instead of isolating the expected 2-benzyl-bis(indenyl)titanacyclobutane, bis(benzyl)bis(indenyl)titanium(IV) **129** was formed quantitatively (eq. 4.3), as determined by spectroscopic analysis. The origin of this product will be discussed below.



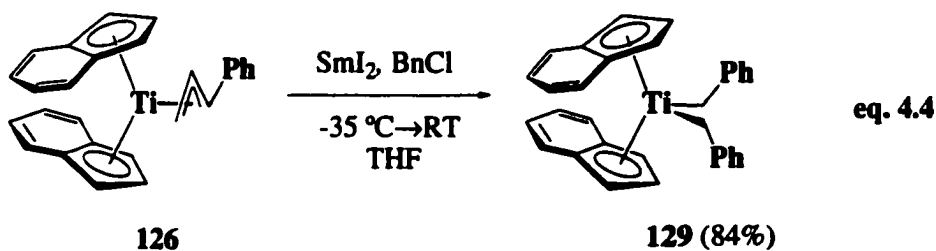
As the primary focus of this study was to probe central carbon radical alkylation of substituted allyl complexes, cinnamyl complex **126** was mixed with SmI_2 , cooled to -35 $^\circ\text{C}$ and treated with 2-iodopropane. Under these conditions, however, central carbon alkylation does not occur, nor is titanacyclobutane formation observed under warmer reaction conditions (> 50 $^\circ\text{C}$) (Scheme 4.2). Other radical generating methodologies were also investigated in an attempt to force cinnamyl complex **126** to undergo central carbon alkylation. Photolytic initiation by hexaphenylditin⁶ to generate isopropyl radicals in the presence of cinnamyl complex **126** does not result in the expected titanacyclobutane formation. Similarly β -oxyalkyl radicals, generated by titanium (III)-mediated opening of epoxides,⁷ do not add to cinnamyl complex **126**.

The addition of a simple stabilized radical to cinnamyl complex **126** was investigated. The addition of benzyl chloride and SmI_2 , however, again provided only bis(benzyl)

Scheme 4.2

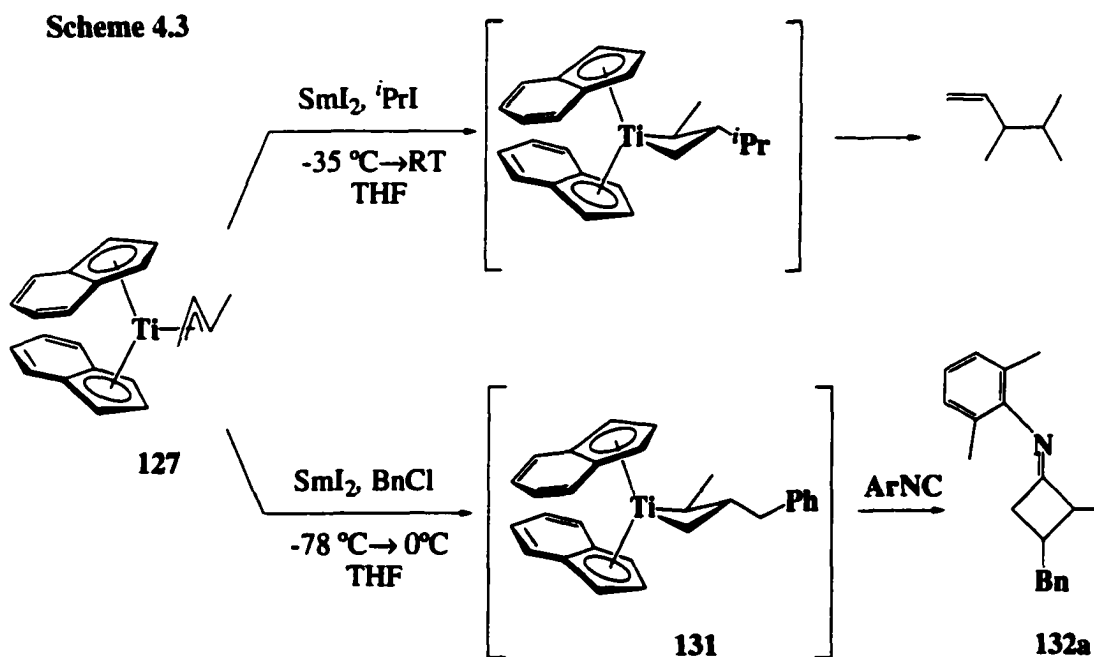


complex **129** (eq. 4.4). Worthy of comment are the colour changes that accompany this reaction. As the reaction mixture warms to room temperature, the blue/green colour of the solution dissipates and is replaced by a medium brown colour accompanied by yellow Sm(III) precipitate. If the reaction is left to stir for an additional hour, the solution returns to green. This colour change is consistent with β -carbon-carbon cleavage (as it requires regeneration of the green cinnamyl complex **126**), however rapid ${}^1\text{H}$ NMR spectroscopy failed to conclusively establish the intermediate formation of the anticipated 3-benzyl-2-phenyl-titanacyclobutane complex **130**.



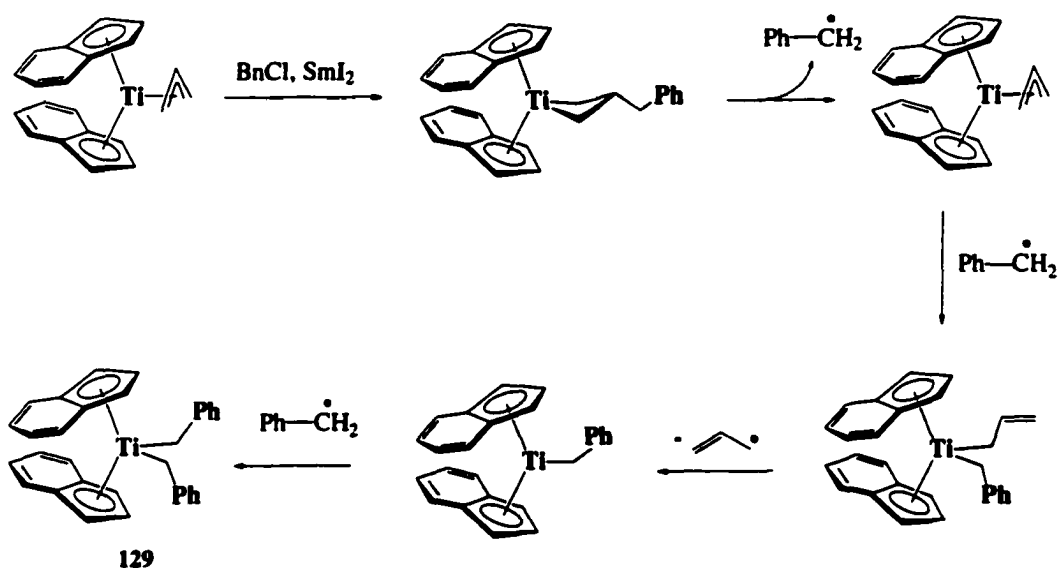
For comparison, the reactivity of crotyl complex **127** was also investigated. Treating crotyl complex **127** with one equivalent of both SmI_2 and isopropyl iodide at low temperature resulted in a colour change of the reaction mixture from blue/brown to red,

and the formation of samarium(III) precipitate prior to the reaction warming to room temperature. Despite the visual observations characteristic of titanacyclobutane formation, it was impossible to isolate the expected titanacyclobutane complex, due to rapid β -hydride elimination from the α -methyl substituent following titanacyclobutane formation. Verification for this mode of decomposition was obtained by identification of 3,4-dimethyl-1-pentene in the crude reaction mixture using GCIR spectroscopy (Scheme 4.3). The treatment of crotyl complex **127** with benzyl radical resulted in formation of a marginally more stable 3-benzyl-2-methyl titanacyclobutane complex **131**. Although titanacyclobutane complex **131** also could not be isolated, its identity was inferred by detecting at least some cyclobutanimine **132a** by HRMS. This was accomplished by performing the alkylation at low temperature and treating the crude product immediately with excess 2,6-dimethylphenyl isonitrile (Scheme 4.3). (The insertion process will be described in detail in Chapter 5.) Without the addition of isonitrile, these reaction conditions result in formation of only trace amounts of (< 10 %) the bis(benzyl) complex **129**.



Taken together, the data provide circumstantial evidence for the addition of benzyl radicals to substituted allyl complexes **126** and **127** to afford titanacyclobutane complexes **130** and **131**, respectively. The formation of stable 3-isopropyl bis(indenyl)titanacyclobutane complex **128** and the inability to observe the 3-allyl analogue of complex **128**, coupled with the formation of bis(benzyl)bis(indenyl)titanium **129**, indicate that the indenyl titanacyclobutane complexes, formed upon addition of stabilized radicals, are prone to β -carbon-carbon bond cleavage. Re-addition of the ejected benzyl radical to the metal center can ultimately result in the formation of the bis(benzyl) titanocene **129** (Scheme 4.4). The complimentary observation of bis(benzyl) titanocene **129** upon addition of benzyl radical to cinnamyl complex **127** supports this postulate, as do the organic compounds detected in the crude reaction mixtures formed on radical addition to crotyl complex **126**. Decomposition of these crotyl-derived titanacyclobutane complexes primarily occurs via β -hydride elimination, as only trace amounts of the bis(benzyl) titanocene **129** are observed.

Scheme 4.4

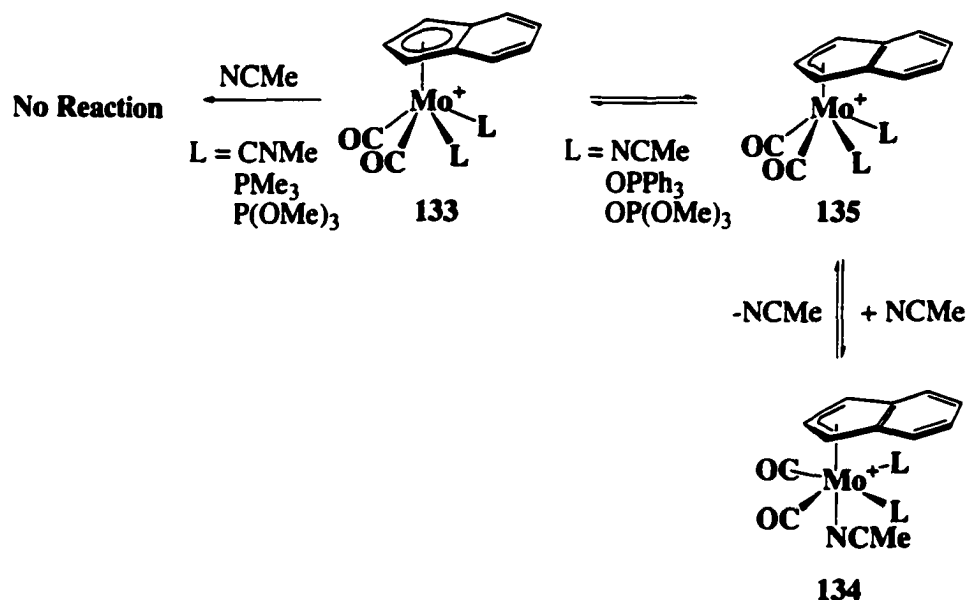


These findings have some interesting implications. The assumption of a minimum electron density requirement from the ancillary ligands for central carbon alkylation appears not to be entirely accurate. That $\text{Cp}_2\text{Ti}(\text{C}_3\text{H}_5)$ does not undergo central carbon alkylation, except in the case of *tert*-butyl radical,⁸ implies that it may be the ‘indenyl effect’ that allows for the alkylation using the indenyl template, as titanium coordinated to two cyclopentadienyl rings is certainly more electron rich. The activation barrier for radical alkylation may somehow be lowered by the facile ring slippage in the indenyl complex. As these radical reactions are conducted in a donor solvent, it may be that coordination of THF to the metal center induces ring slip to η^3 -indenyl coordination. The combination of THF coordination and η^3 -coordination of an indenyl ligand may increase the preference for η^3 -coordination of the allyl ligand and enhance delocalization of the odd-electron density onto the central carbon, facilitating alkylation, although exactly how this might facilitate alkylation remains unknown.

While it may appear counterintuitive that ring slip should induce central carbon alkylation, a study performed by Romão and Verios may provide some precedent for this claim.⁹ The authors found that acetonitrile reversibly adds to the cationic complex $[(\eta^5\text{-indenyl})\text{Mo}(\text{L})_2(\text{CO})_2]^+$ **133** only in the cases where L is a weaker ligand (L = NCMe, OPPh₃, OP(OMe)₃) to form the η^3 -indenyl complex $[(\eta^3\text{-indenyl})\text{Mo}(\text{NCMe})(\text{L})_2(\text{CO})_2]^+$ **134** (Scheme 4.6) as determined by ¹H NMR spectroscopy. When L is a strong ligand, *i.e.* CNMe, PMe₃, P(OMe)₃, no η^3 -indenyl complex is observed nor does there appear to be a reaction with the complex. To explain these results, DFT calculations were performed that indicated that the addition of weaker, more labile π -donors such as NCMe and oxygen ligands assist in the ring slippage adduct formation by electron donation into the metal orbitals that enhance metal-carbonyl backbonding. It is believed that there is a rapid $\eta^5 \rightleftharpoons \eta^3$ pre-equilibrium that gives rise to the electronically unsaturated species $[(\eta^3\text{-indenyl})\text{Mo}(\text{L})_2(\text{CO})_2]^+$ **135**, a complex that is ‘en route’ to the substitution product.

This complex is intercepted by weak ligands, eventually forming a stable entity (complex **134**). The addition of strong ligands does not provide this stabilizing effect, instead, the complexes are very energetic and give rapid substitutions (complex **133** possessing two coordinated acetonitrile ligands will exchange these ligands with PMe_3 at room temperature without the detection of an η^3 -intermediate). Reversible acetonitrile addition was not observed for the η^5 -cyclopentadienyl analogue of complex **133**.

Scheme 4.5



To test this hypothesis for bis(indenyl)titanium templates requires the detection of η^3 -indenyl complexes. The paramagnetism of titanium(III) complexes precludes identification by ^1H NMR spectroscopy; crystallographic analysis of an allyl titanium(III) complex with a slipped indenyl ring may be possible only in the presence of a non-labile donor ligand. The coordination of various donors to allyl bis(indenyl)titanocene(III) complexes may be observable by IR, or UV-vis spectroscopy and potentially could indicate ring-slippage of the indenyl ligand, or changes in allyl coordination. Secondly, an 'indenyl effect' would be strongly implied if a mixed indenyl-cyclopentadienyl

titanocene(III) allyl complex is observed to undergo central carbon alkylation, particularly with substituted allyl complexes. Such investigations have yet to be undertaken.

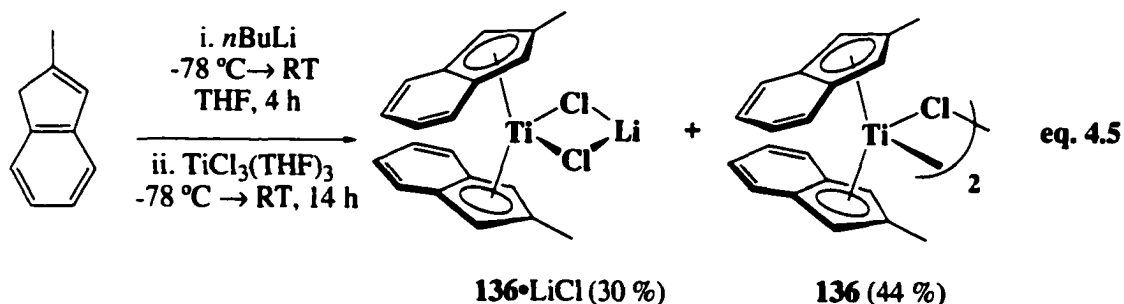
The observed difference in reactivity between cyclopentadienyl and indenyl systems may also be attributed to a simple steric effect. The larger, more sterically congesting indenyl rings direct radical attack to the allyl ligand for radicals with a larger steric profile (e.g., isopropyl radical); otherwise, attack occurs at the metal center. In the sterically, more open cyclopentadienyl system it has been postulated that smaller radicals add to the accessible metal center, whereas only the very large *tert*-butyl radical adds selectively to the allyl group.⁸

C. Bis(2-methylindenyl)titanium(III) as a Template for Central Carbon Alkylation

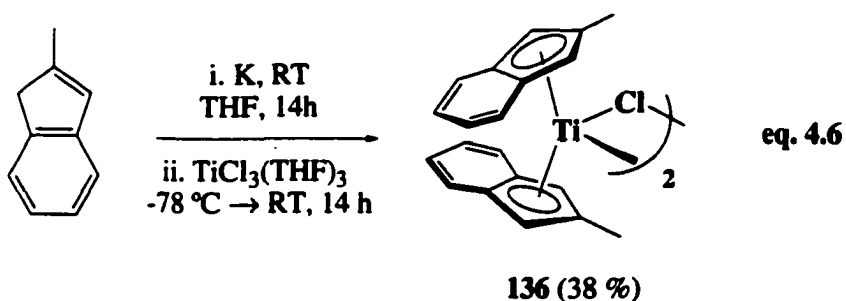
1. Preparation of Bis(2-methylindenyl)titanium(III) η^3 -Allyl Complexes

The effect that electron-donating substituents on the indenyl rings have on central carbon alkylation was investigated by preparing the slightly more electron-rich 2-methylindenyl analogue of complex **124**. The synthesis of bis(2-methylindenyl)titanocene(III) chloride **136** was readily accomplished by treating 2-methylindene¹ with *n*-butyllithium in THF followed by slow addition of this solution to a suspension of TiCl₃•THF at low temperature (eq. 4.5). The crude red residue was initially triturated with benzene and the extracted material was precipitated from THF/hexane (1 : 1) at -35 °C to yield the chloride complex **136** as an amorphous burgundy red solid in 44% yield.¹⁰ The remaining crude product was extracted into THF to give a forest green solution. Concentrating this solution, followed by careful layering with an equal amount of hexane and cooling to -35 °C, gave pale green prisms, which on drying turn to an amorphous bright red powder. Elemental analysis of the red powder is consistent with the lithium chloride adduct of the 2-methylindenyl titanocene **136**•LiCl,

obtained in 30% yield. Oxidation of complexes **136** and **136**•LiCl with PbCl₂ to yield the corresponding titanocene dichloride complex was not successful.

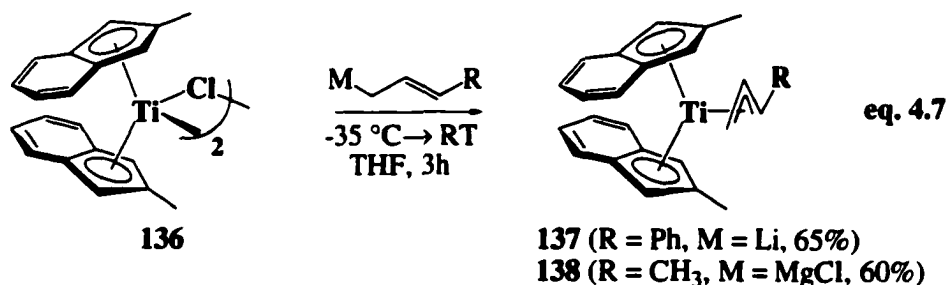


Further support for the incorporation of an equivalent of lithium chloride into the coordination sphere of the titanocene(III) chloride complex **136**•LiCl was garnered from synthesis of complex **136** from 2-methylindenylpotassium. The burgundy-red solution obtained from this reaction provided a purple residue that dissolved almost completely in benzene. Precipitation from THF/hexane (1 : 1) cooled to -35 °C afforded analytically pure titanocene(III) complex **136** as an amorphous burgundy red solid in 38% yield (eq. 4.6). The larger size of the potassium cation (1.33 Å vs. 0.60 Å for Li⁺) and its greater ionic character apparently prevent it from remaining within the coordination sphere of the titanium complex.



The synthesis of bis(2-methylindenyl)titanium cinnamyl **137** and bis(2-methylindenyl)titanium crotyl **138** was accomplished by treating bis(2-methylindenyl)titanium chloride complex **136** with equivalents of cinnamyllithium and

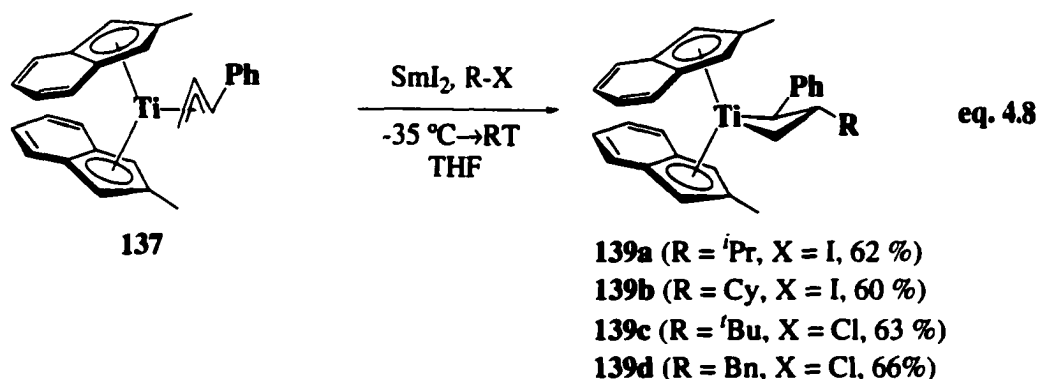
crotyl Grignard, respectively, at low temperature (-35 °C) in THF (eq. 4.7). The cinnamyl complex **137** was isolated as analytically pure crystalline green diamonds in 65% yield. The crotyl complex **138** was isolated as an analytically pure amorphous lime green solid in 60% yield. The allylic asymmetric C=C stretch for the allylic anion in crotyl complex **138** is observed in the infrared spectrum at 1540 cm⁻¹, suggesting a typical *syn*-η³-crotyl coordination to titanium.



2. Radical Additions to Cinnamyl and Crotyl Bis(2-methylindenyl)titanium(III) Complexes

The presence of a single methyl substituent on the indenyl ring has a profound effect on the ability of the cinnamyl complex to trap organic radicals. When a mixture of cinnamyl complex **137** and samarium iodide in THF is treated with isopropyl iodide, 3-isopropyl-2-phenyl titanacyclobutane complex **139a** is obtained in 62% yield as analytically pure dark brown rhomboid crystals following purification (eq. 4.8). ¹H NMR spectroscopy of complex **139a** shows strong similarities to the spectra of previously characterized 2-methoxyindenyl, 2-*N,N*-dimethylaminoindenyl and 2-piperidinoindenyl analogues of this complex. The titanacyclobutane core is represented by signals at δ 3.07 (d, *J* = 11.1 Hz) for the α-methine proton, triplets at δ 1.93 (*J* = 9.6 Hz) and 0.086 (*J* = 9.3) for the α-methylene protons and a doublet of quartets at δ 0.44 (*J* = 9.9, 6.6 Hz) for the β-methine proton. ¹H NMR spectroscopy also indicates that at room temperature

complex **139a** is rigid or rapidly undergoing ligand rotations; the broad signals of interconverting conformers, as was recorded in the ^1H NMR spectrum of 2-*N,N*-dimethylaminoindenyl complex **101a** and 2-piperidinoindenyl complex **55a**, are not observed.¹¹ Presumably the sharpness of the ^1H NMR spectrum is due to the less sterically encumbering ancillary ligands.



Under similar reaction conditions, cinnamyl complex **137** also traps cyclohexyl, benzyl and *tert*-butyl radicals, yielding 3-alkyl-2-phenyl titanacyclobutane complexes **139b-d** in moderate yields (eq. 4.8). Selected ^1H NMR spectroscopic data for these complexes are presented in Table 4.1. Titanacyclobutane complexes **139a-d** can also be obtained in comparable if not better yields using a one-pot procedure. Thus, 2-methylindenyltitanocene chloride **136** is alkylated with cinnamyllithium and subsequently treated *in situ* with an equivalent of SmI_2 and the respective alkyl halide at low temperature. Table 4.2 provides the yields obtained under these reaction conditions, as well as the overall yield provided by the two-step synthesis.

Single crystals of 3-*tert*-butyl-2-phenyl titanacyclobutane **139c** were obtained from a concentrated THF solution of the complex layered with hexane. An ORTEP diagram of complex **139c** is shown in Figure 4.1. A molecule of hexane, the

crystallization solvent, was also incorporated into the lattice. Selected intramolecular bond lengths and angles are presented in Table 4.3.

Table 4.1 Room Temperature ^1H NMR Resonances of Titanacyclobutane Complexes **139a-d**

	139a , R = ^iPr δ (m, J, I)*	139b , R = Cy δ (m, J, I)*	139c , R = ^tBu δ (m, J, I)*	139d , R = BnCl δ (m, J, I)*
Ti-CH ₂	1.93 (t, 9.6, 1H) 0.086 (t, 9.3, 1H)	2.00 (t, 9.3, 1H) 0.12 (t, 9.6, 1H)	2.10 (t, 9.6, 1H) -0.094 (t, 9.6, 1H)	1.86 (t, 9.6, 1H) -0.036 (t, 9.4, 1H)
Ti-CH(Ph)	3.07 (d, 11.1, 1H)	3.07 (d, 11.4, 1H)	3.94 (d, 11.7, 1H)	2.53 (d, 11.4, 1H)
β -CH	0.44 (dq, 9.9, 6.6, 1H)	0.44 (dq, 10.2, 6.0, 1H)	0.65 (q, 9.9, 1H)	0.90 (m, 1H)
CH _(Indenyl)	5.68 (d, 0.9, 1H) 5.67 (d, 0.9, 1H) 5.54 (d, 2.1, 1H) 5.34 (d, 1.8, 1H)	5.68 (d, 2.1, 1H) 5.67 (d, 2.1, 1H) 5.40 (d, 1.8, 1H) 5.34 (d, 1.8, 1H)	5.88 (s, 1H) 5.77 (s, 1H) 5.75 (s, 1H) 5.38 (s, 1H)	5.67 (s, 1H) 5.47 (s, 1H) 5.32 (s, 1H) 5.30 (s, 1H)
Me _(Indenyl)	1.79 (s, 3H) 1.22 (s, 3H)	1.80 (s, 3H) 1.32 (s, 3H)	1.72 (s, 3H) 0.97 (s, 3H)	1.79 (s, 3H) 1.30 (s, 3H)
R	1.44 (octet, 6.6, 1H) 0.94 (d, 6.6, 3H) 0.91(d, 6.6, 3H.)	1.85-1.74 (m, 3H) 1.67-1.59 (m, 3H) 1.21-0.98 (m, 5H)	0.94 (s, 9H)	2.93 (dd, 12.8, 2.9, 1H) 2.04 (dd, 12.7, 8.5, 1H)

δ = chemical shift, m = multiplicity, J = J_{HH} in Hz, I = integral.

Table 4.2 Yields of One Pot Procedure for Titanacyclobutane Complexes **139a-d**

Complex	R-X	Yield (one pot, %)	Yield (two-step 136 \rightarrow 137 \rightarrow 139, %)
139a	^iPrI	47	40
139b	CyI	26	39
139c	$^t\text{BuCl}$	33	41
139d	BnCl	35	43

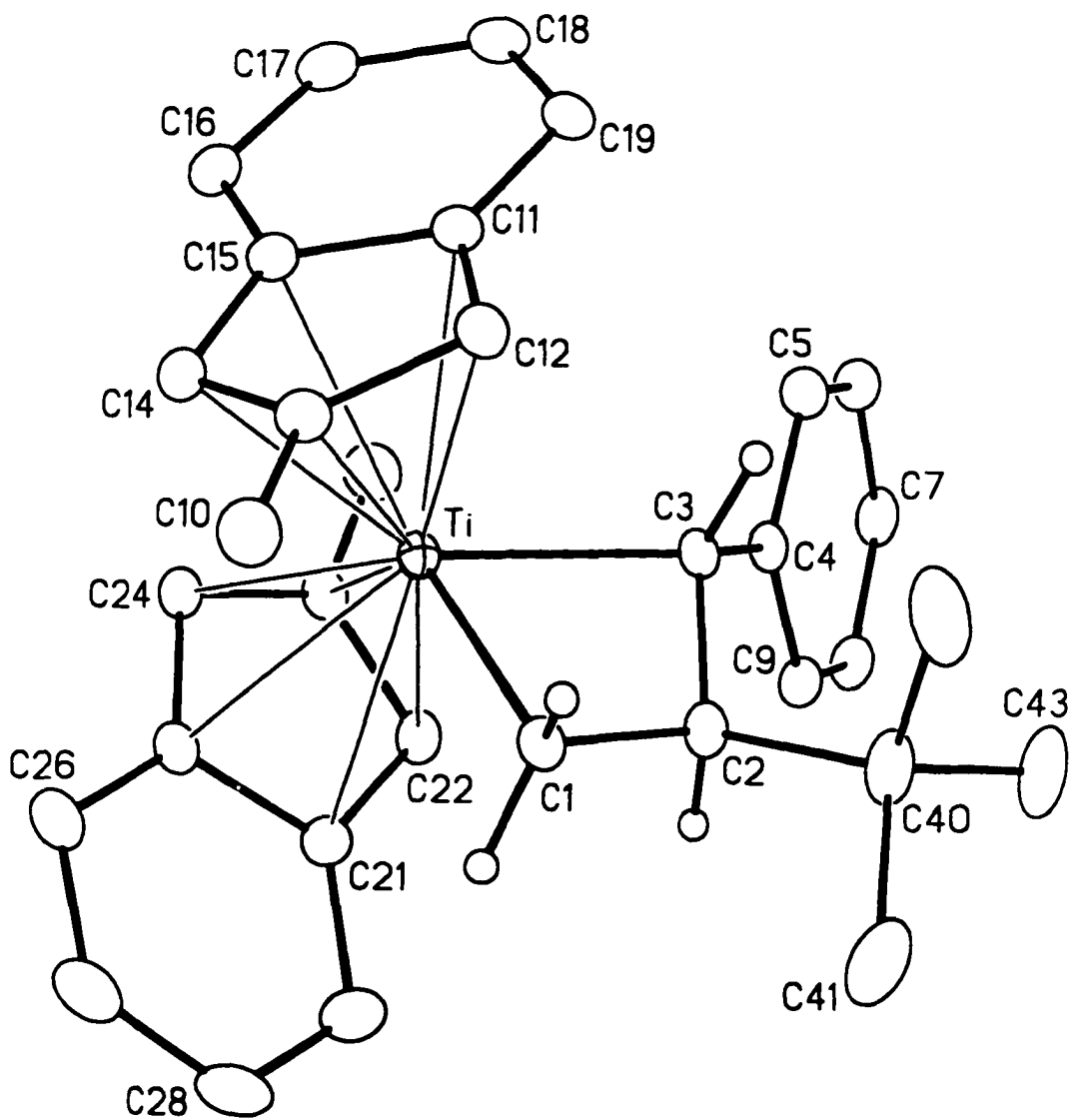


Figure 4.1 The molecular structure of 3-*tert*-butyl-2-phenyl-bis(2-methylindenyl)titanacyclobutane, **139c**. Selected interatomic distances are listed in Table 4.3. Crystallographic details are provided in Appendix I.

Table 4.3 Selected Bond Lengths (Å) and Angles (°) for Complex 139c

Bond Lengths (Å)			
Ti-C1	2.103(2)	C10-C13	1.494(4)
Ti-C3	2.208(3)	C20-C23	1.505(4)
Ti-C11	2.498(2)	C2-C40	1.581(4)
Ti-C12	2.418(2)	C3-C4	1.487(3)
Ti-C13	2.435(2)	C1-C2	1.551(3)
Ti-C14	2.410(3)	C2-C3	1.558(3)
Ti-C15	2.494(3)	Ti-Cp(cent) ^a	2.134, 2.124
Ti-C21	2.546(2)	Ti-Cp(plane) ^b	2.1321(12), 2.1147(12)
Ti-C22	2.464(2)		
Ti-C23	2.411(2)		
Ti-C24	2.354(2)		
Ti-C25	2.436(2)		
Bond Angles (°)			
C1-Ti-C3	72.01(9)	Cp(cent)-M-Cp(cent) ^a	132.2
C1-C2-C3	109.4(2)	Cp(plane)-M- Cp(plane) ^b	51.78(9)

^aCentroid of the indenyl ligand, ^bCalculated normal to plane of indenyl ligand

Remarkably, there are very few differences in the structure of this titanacyclobutane complex with respect to either the 2-piperidinoindenyl and 2-*N,N*-dimethylaminoindenyl titanacyclobutane complexes previously described or to any of the previously reported 2,3-disubstituted titanacyclobutane complexes.¹² With respect to the titanacyclobutane core, the Ti-C(1) and Ti-C(3) bond distances in complex 139c are essentially equidistant and fall close to the statistical range determined for Ti-C_{sp}³ bonds (2.14 - 2.21 Å),¹³ where the unsubstituted Ti-C(1) bond is again shorter than Ti-C(3), presumably due to absence of a phenyl substituent. The carbon-carbon bond lengths in the titanacyclobutane rings are roughly equal in length. The metallacycle ring, as expected, is puckered, with dihedral angles of 153.9° for the C(1)-Ti-C(3) and C(1)-C(2)-C(3) planes. The torsional angle between H-C(2)-C(3)-H in complex 139c is calculated to be 158.4°, corresponding to a coupling constant of approximately 11 Hz based on the

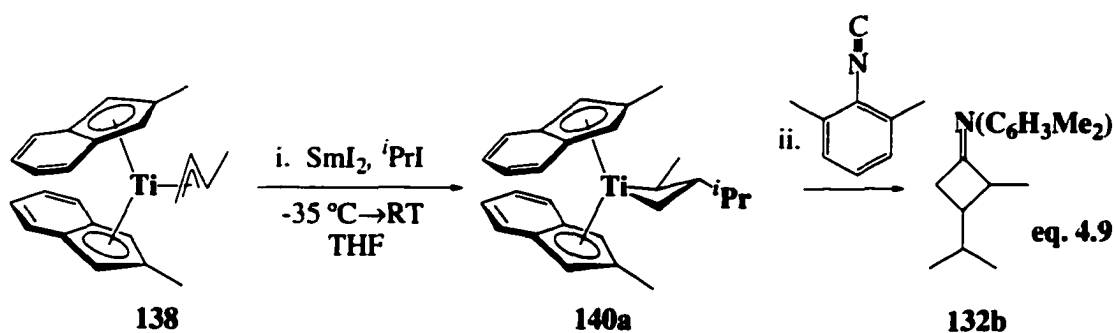
Karplus relation.¹⁴ This prediction is in good agreement with the 11.7 Hz coupling observed in the ¹H NMR spectrum, indicating that the solution structure of the core (but not necessarily the ligands) is reasonably modeled by the solid state structure.

The ancillary ligands in complex **139c** are nearly perfectly staggered, positioned with an indenyl rotational angle of 178°. The coordination parameters of the indenyl rings are given in Table 4.4 and indicate only mildly distorted η⁵-indenyl coordination, caused by the slightly longer ring junction titanium-carbon bonds relative to the remaining titanium-carbon bonds in the five-membered ring. Although 2-methylindenyl zirconocene dichloride is known, no crystal structure has been reported.¹⁵

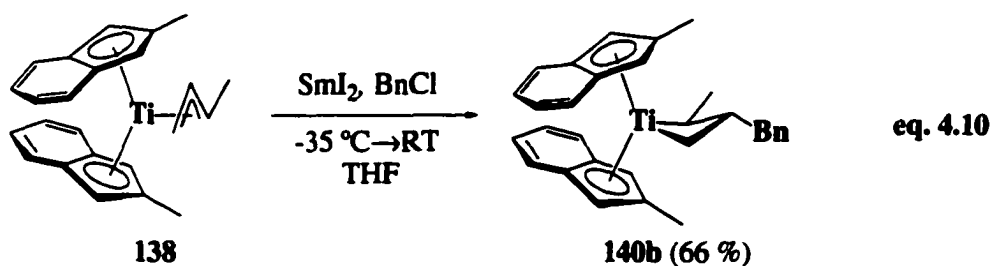
Table 4.4 Structural Data For Indenyl Coordination

Complex	Δ _{M-C} (Å)	Fold Angle (°)	Hinge Angle(°)
139c	0.0700	4.62(19)	4.9(4)
	0.0813	3.93(9)	3.58(16)

The ability of crotyl complex **138** to trap organic radicals was also investigated. Treating a mixture of crotyl complex **138** and an equivalent of SmI₂ with isopropyl iodide at low temperature affords 2-methyl-3-isopropyl titanacyclobutane complex **140a**. As observed for the indenyl analogue (*vide supra*), this complex decomposes rapidly via β-hydride elimination prior to characterization by ¹H NMR spectroscopy. To verify its formation, the reaction was repeated and following the disappearance of SmI₂, the reaction mixture was transferred onto cooled pentane, filtered, and treated with excess 2,6-dimethylphenylisocyanide. Under these conditions, the organic from the titanacyclobutane core was retrieved from complex **140a** as cyclobutanamine **132b** in undetermined yield (eq. 4.9).



Exposure of crotyl complex **138** to benzyl radical results in the formation of titanacyclobutane complex **140b**, a complex which is significantly more stable than complex **140a** (eq. 4.10). Complex **140b** is isolated as deep red rhomboid crystals in 66% yield by triturating the crude reaction mixture with pentane, concentrating, and cooling ($-35\text{ }^{\circ}\text{C}$) the resultant extracts. In the ^1H NMR spectrum of complex **140b**, the titanacyclobutane core is represented by triplets at δ 1.88 ($J = 9.7\text{ Hz}$.) and 0.01 ($J = 10.4\text{ Hz}$) for the inequivalent α -methylene signals, the α -methine proton is obscured at δ 1.87, and a multiplet is observed at δ -0.17 for the β -methine signal. The improvement in stability of complex **140b** relative to **140a** is believed to be due to the smaller steric profile of the benzyl substituent, which does not force the α -methyl substituent as close to the metal center.



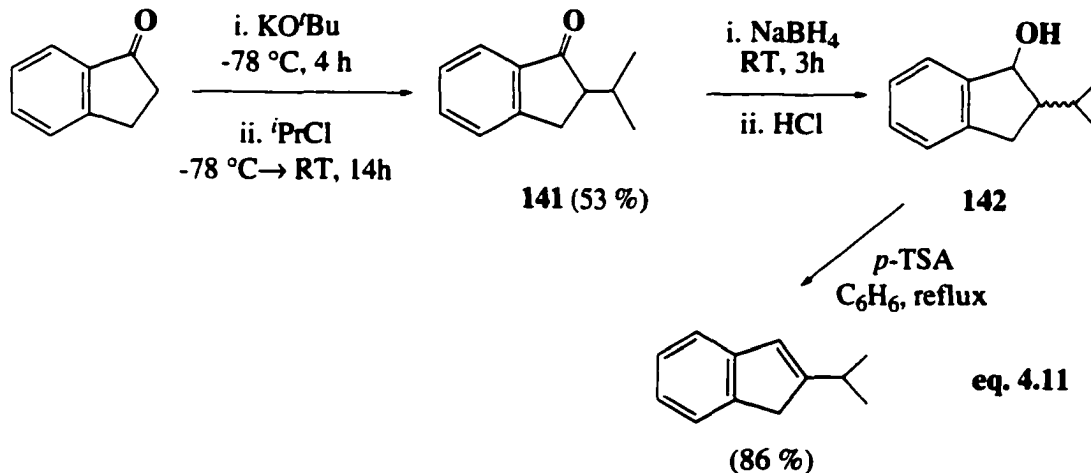
The effect of placing a methyl group at the 2-position of the indenyl ligands significantly enhances the reactivity of the cinnamyl and crotyl complexes. The ligand methyl groups not only improve the stability of crotyl-derived titanacyclobutane complexes, but provides sufficient electron-richness to promote general central carbon

alkylation of cinnamyl complex **137** and makes 3-benzyl-2-phenyl titanacyclobutane **139d** unreactive toward β -carbon-carbon bond homolysis. All of the central carbon alkylation reactions occur at or below room temperature with relatively short reaction times, again indicating that the mechanism of organic radical formation likely does not involve samarium directly.

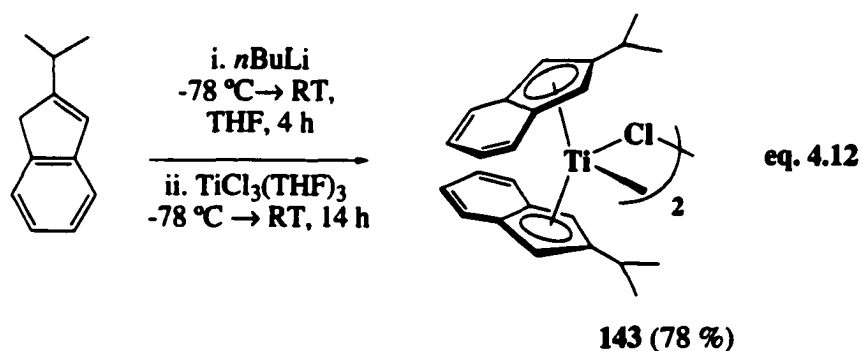
D. Bis(2-isopropylindenyl)titanium(III) as a Template for Central Carbon Alkylation

1. Preparation of Bis(2-isopropylindenyl)titanium(III) η^3 -Allyl Complexes

To provide further insight into the performance of the 2-*N,N*-dimethylaminoindenyl ligand system, an investigation into the relatively electron poor, but virtually isostructural, 2-isopropylindenyl system was undertaken. The synthesis of 2-isopropylindene proved to be unexpectedly challenging. That 2-indanone is readily converted to its enolate under mildly basic conditions¹⁶ prevents 2-indanone from undergoing addition with Grignard reagents. Typically, this problem can be overcome by alkylating under less basic reaction conditions using organocerium or organolanthanum reagents.¹⁷ Such a procedure ultimately led to the synthesis of bis(2-isopropylindenyl)zirconium dichloride,¹⁵ but the ligand synthesis was found to be unreliable and generally low yielding, particularly on a larger scale. For these reasons, a more reproducible synthesis amenable to scale-up was developed. This was accomplished by deprotonating 1-indanone with potassium *tert*-butoxide and alkylating the resultant enolate using 2-chloropropane. Following purification by column chromatography, 2-isopropyl-1-indanone **141** was isolated in 54% yield as a pale yellow oil (eq. **4.11**). Indanone **141** was reduced to a mixture of *cis* and *trans*-2-isopropylindanol **142** and dehydrated to afford 2-isopropylindene in 86% yield for the two steps.

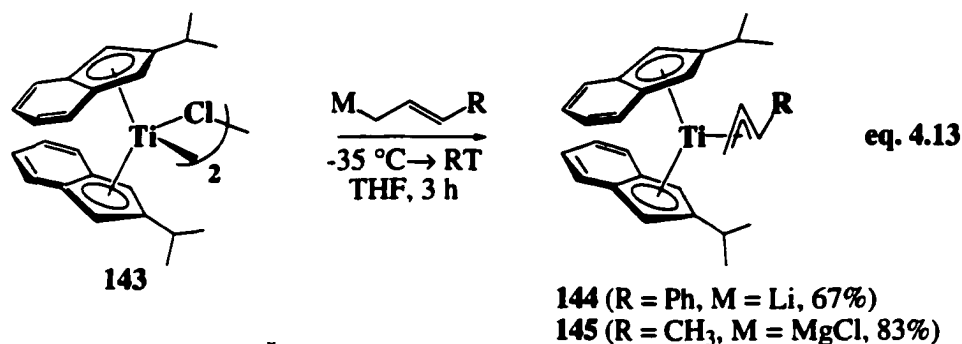


The synthesis of bis(2-isopropylindenyl)titanium(III) chloride complex **143** was accomplished in the usual manner (eq. 4.12). The deep green crude product was extensively dried under high vacuum to yield a red-brown residue which precipitates from cold THF layered with hexane (1 : 2), to afford analytically pure bis(2-isopropylindenyl)titanium(III) chloride complex **143** as a burgundy red powder in 78% yield. Under such rigorous drying conditions the lithium chloride adduct was not detected.



As expected, cinnamyl and crotyl titanocene (III) complexes **144** and **145** were obtained on treating titanocene(III) chloride complex **143** with cinnamyllithium and

crotyl Grignard, respectively, at low temperature (eq. 4.13). Cinnamyl complex **144** can be isolated in 67% yield as bright green diamond shaped crystals. Despite numerous recrystallizations, twinned crystals were repeatedly obtained, precluding characterization of the complex by X-ray crystallography. Single diffractable crystals were obtained for crotyl complex **145** in 83% yield from concentrated THF layered with hexane at $-35\text{ }^{\circ}\text{C}$. The resultant ORTEP diagram, together with an atomic labeling scheme, can be seen in Figure 4.2. Selected intramolecular bond lengths and angles are presented in Table 4.5. Two spacial orientations are observed for the isopropyl substituent on one of the indenyl ligands, 2/3 occupancy for one orientation (C40A-C42A) and 1/3 of the other (C40B-C42B).



The crotyl substituent in the crystal structure of complex **145** adopts the anticipated η^3 -coordination, *syn* substituent stereochemistry, partially pyramidalized allyl terminal carbons, and unsymmetrical coordination of the allyl fragment.^{11,18} Infrared spectroscopy reveals the allylic asymmetric C=C stretch in crotyl complex **145** at 1538 cm^{-1} , in accordance with the observed *syn*- η^3 -crotyl coordination to titanium. The tilt angle that the allyl ligand plane makes with the Ti(III) template falls within the range reported for other Ti(III) allyl complexes (Table 4.6).¹⁸ Compared to the aminoindenyl Ti(III) complexes **53**, **98**, **99** and **99'**, complex **145** possesses surprisingly short Ti-C1 and

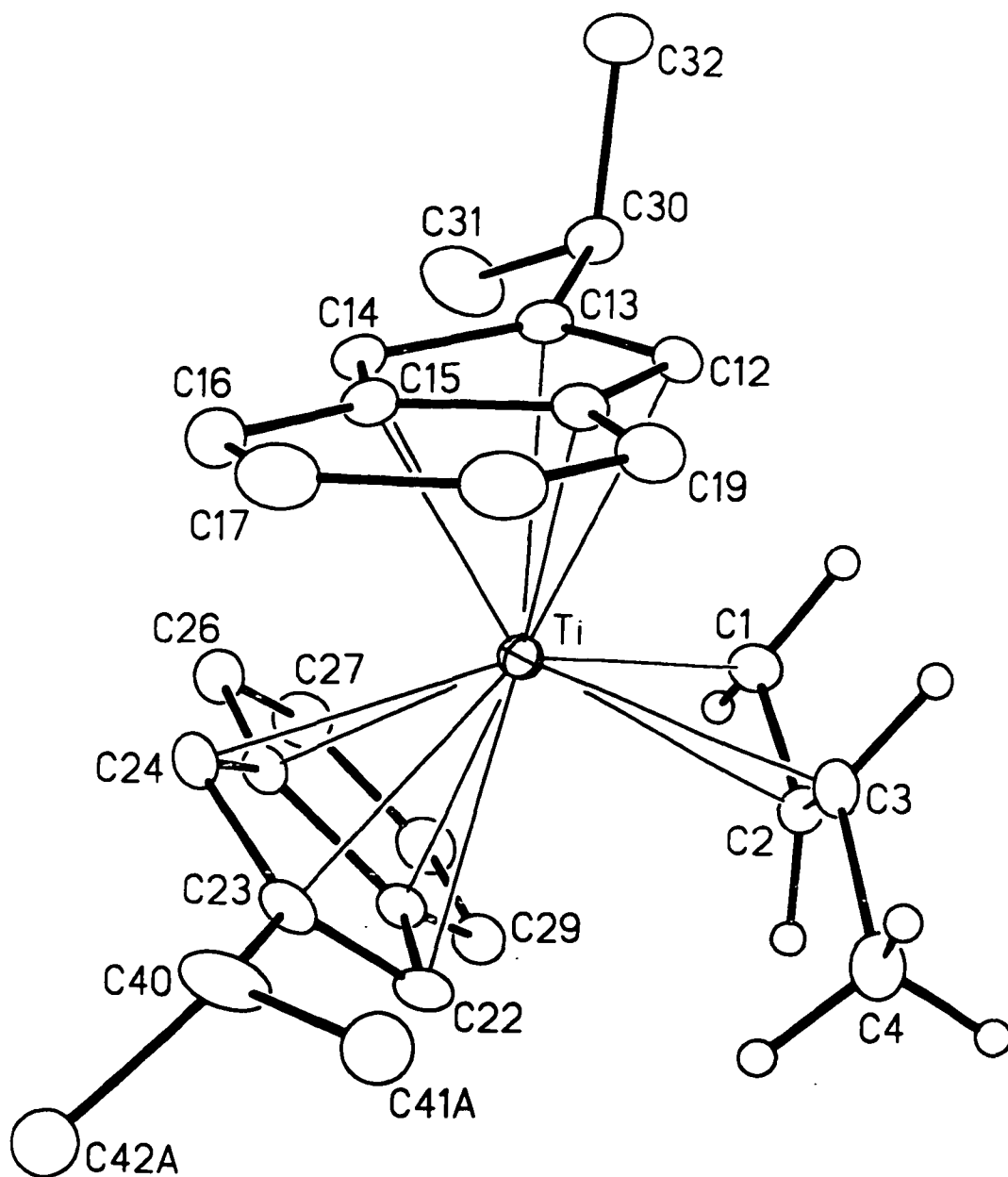


Figure 4.2 The molecular structure of bis(2-isopropylindenyl)titanium(η^3 -crotyl), **145**. Selected interatomic distances are listed in Table 4.5. Crystallographic details are given in Appendix I.

Table 4.5 Selected Bond Lengths (Å) and Angles (°) for Complex 145

Bond Lengths (Å)			
Ti-C1	2.312(3)	C13-C30	1.517(3)
Ti-C2	2.379(3)	C30-C31	1.516(4)
Ti-C3	2.490(3)	C30-C32	1.522(4)
Ti-C11	2.459(3)	C23-C40A	1.553(6)
Ti-C12	2.398(3)	C23-C40B	1.503(12)
Ti-C13	2.426(3)	C40A-C41A	1.513(7)
Ti-C14	2.389(3)	C40A-C42A	1.524(7)
Ti-C15	2.465(3)	C40B-C41B	1.521(14)
Ti-C21	2.496(3)	C40B-C42B	1.528(13)
Ti-C22	2.448(3)	C3-C4	1.514(4)
Ti-C23	2.433(3)	C1-C2	1.410(4)
Ti-C24	2.367(3)	C2-C3	1.379(4)
Ti-C25	2.442(2)	Ti-Cp(cent) ^a	2.105, 2.117
		Ti-Cp(plane) ^b	2.1321(12), 2.1173(11)
Bond Angles (°)			
C1-Ti-C3	61.73(9)	Cp(cent)-M-Cp(cent) ^a	132.2
C1-C2-C3	124.5(3)	Cp(plane)-M-	48.13(12)
C2-C3-C4	121.7(3)	Cp(plane) ^b	

Ti-C2 bonds, reflective of relatively strong $d \rightarrow \pi^*$ back donation from the d^1 -metal center.

Table 4.6 Bond Lengths (Å) and Angles (°) for Crotyl Ti(III) Complex 145

Complex	Tilt Angle	Ti-C(1)	Ti-C(2)	Ti-C(3)	C(1)-C(2)	C(2)-C(3)	C(3)-C(4)
145	111.6	2.312(3)	2.379(3)	2.490(3)	1.410(4)	1.379(4)	1.514(4)

More interesting is the indenyl ligand coordination in this complex. The indenyl rings are *anti* to each other with an indenyl rotation angle of 173°. The calculated values for $\Delta_{M,C}$, FA and HA (Table 4.7) classify the indenyl bonding as essentially η^5 -

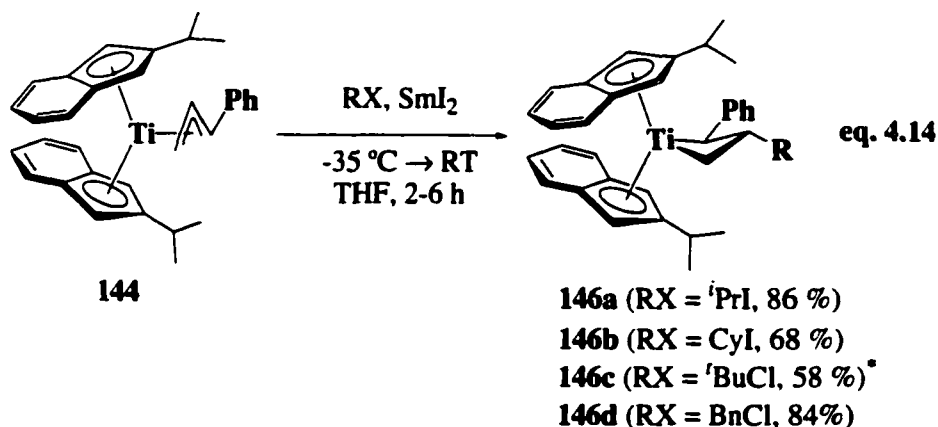
coordinate. In fact, the hinge angles, fold angles and values for Δ_{M-C} indicate less deviation from true η^5 -coordination in this Ti(III) allyl complex than in any of the aminoindenyl Ti(III) complexes. It appears that the indenyl rings are also more symmetrically bound to titanium than in 2-methylindenyl titanacyclobutane complex **139c**, in which the titanium is in the +4 oxidation state.

Table 4.7 Structural Data For Indenyl Coordination

Complex	Δ_{M-C} (Å) ^a	Fold Angle (°) ^b	Hinge Angle (°) ^c
145c	0.0577	4.23(11)	5.14(15)
	0.0530	2.57(19)	4.1(4)

2. Radical Additions to Cinnamyl and Crotyl Bis(2-isopropylindenyl)titanium(III) Complexes

The treatment of cinnamyl complex **144** with organic radicals results in near quantitative crude yields of the central carbon alkylation products. As the highly soluble complexes are not easily crystallized, these yields are not reflected in the isolated yields. Isopropyl titanacyclobutane complex **146a**, for example, is isolated in 86% yield as brown rhomboid crystals, although the crude yield of the reaction is quantitative (eq. **4.14**). Spectroscopic analysis indicates the complex is slowly fluxional at room temperature (Table 4.8). Significant broadening of indenyl as well as the titanacyclobutane core resonances are observed; presumably the bulky *iso*-propyl group hinders rotation of the α -phenyl substituent which in turn affects the ability of the sterically encumbering isopropylindenyl ligands to fully rotate. On warming to 70 °C, both the upfield α -methylene proton and β -methine proton sharpen into a triplet at δ 0.042 ($J = 9.3$ Hz) and an apparent doublet of quartets at δ 0.45 ($J = 9.9, 7.1$ Hz), respectively. The low temperature limiting spectrum was not acquired.



*This result was obtained using 10 mol % [(2-isopropylindenyl)₂TiCl]₂, **143**

Table 4.8 Room Temperature ¹H NMR Resonances of Titanacyclobutane Complexes **146a-d**

	146a , R = ⁱ Pr δ (m, J, I)*	146b , R = Cy δ (m, J, I)*	146c , R = ^t Bu [†] δ (m, J, I)*	146d , R = BnCl δ (m, J, I)*
Ti-CH ₂	2.71 (t, 9.1, 1H.) 0.054 (br s, 1H)	2.75 (t, 9.1, 1H) 0.43 (br m, 1H)	2.62 (m, 2H) -0.83 (t, 10.2, 1H)	2.64 (t, 9.4, 1H) -0.014 (t, 9.0, 1H)
Ti-CH(Ph)	2.68 (m, 2H)	2.38 (br m, 1H)	4.03 (d, 11.4, 1H)	2.13 (m, 3H)
β-CH	0.41 (br s, β-CH)	0.075 (br m, 1H)	0.33 (q, 10.8, 1H)	1.00 (obscured signal, 1H)
CH _(Indenyl)	5.91 (br s, 1H) 5.64 (br s with a shoulder, 2H) 5.52 (br s, 1H)	5.92 (s, 1H) 5.64 (s, 1H) 5.58 (s, 1H) 5.51 (s, 1H)	6.11 (s, 1H) 5.98 (s, 1H) 5.84 (s, 1H) 5.34 (s, 1H)	5.73 (s, 1H) 5.63 (s, 2H) 5.17 (s, 1H)
CH(CH ₃) ₂ (^{is} indenyl)	2.68 (m, 2H) 1.05 (d, 7.0, 3H) 0.97 (d, 6.6, 3H) 2.19 (m, 1H) 1.03 (d, 7.7, 3H) 0.52 (d, 6.8, 3H)	2.71 (septet, 6.8, 1H) 1.06 (d, 5.1, 3H) 0.97 (d, 6.6, 1H) 2.23 (septet, 6.6, 1H) 1.04 (d, 5.1, 3H) 0.54 (d, 6.7, 1H)	2.62 (m, 2H) 1.02 (obscured signal, 6H) 1.73 (br m, 1H) 0.99 (d, 6.4, 3H) 0.24 (d, 5.9, 3H)	2.65 (septet, 6.9, 1H) 1.02 (d, 6.8, 3H) 0.94 (d, 6.7, 3H) 2.13 (m, 3H) 0.99 (d, 6.9, 3H) 0.50 (d, 6.7, 3H)
R	1.38 (dseptet, 13.4, 6.8, 1H) 0.97 (d, 6.6, 3H) 0.89 (d, 6.7, 3H)	1.93 (d, 10.1, 1H) 1.77 (d, 11.5, 1H) 1.59 (d, 8.5, 3H) 1.22 - 0.94 (m, 6H)	0.96 (s, 9H)	2.85 (dd, 12.7, 3.3, 1H) 2.13 (m, 3H)

* δ = chemical shift, m = multiplicity, J = J_{HH} in Hz, I = integral. [†] Spectrum recorded at -30 °C.

In a similar manner, 3-cyclohexyl-2-phenyl titanacyclobutane **146b** can be obtained from iodocyclohexane, albeit in lower isolated yield (68%) (eq. 4.14). *Tert*-butyl radical is relatively inert, requiring a very lengthy reaction time for addition to cinnamyl complex **144**. The low reaction temperatures and short reaction times required for central carbon alkylation of the previous templates implicate the direct interaction of the titanium with the alkyl halide. Given the sterically encumbering ancillary ligands and cinnamyl ligand blocking access to the metal center, we propose that access to the metal is severely diminished for the large *tert*-butyl chloride. To test this hypothesis, the reaction was repeated in the presence of a catalytic amount of the less hindered titanocene(III) chloride complex **143**. Under these conditions, the reaction proceeds to completion at a significantly higher rate and complex **146c** was isolated as brown rhomboid crystals in 58% yield (eq. 4.14). Due to the broadness of the room temperature spectrum, the low temperature limiting spectrum was acquired at $-30\text{ }^{\circ}\text{C}$. Two isomers were observed in a 7 : 2 ratio; only the major isomer was analyzed. At this temperature, ^1H NMR spectroscopy reveals typical titanacyclobutane core resonances. The high temperature limiting spectrum of this complex could not be obtained due to the thermal instability of this complex at $70\text{ }^{\circ}\text{C}$.

Central carbon alkylation of cinnamyl complex **144** with the benzyl radical occurs efficiently without the addition of a catalyst. The expected titanacyclobutane complex **146d** was obtained as deep red rhomboid crystals in 84% yield (eq. 4.14). ^1H NMR spectroscopy reveals that the complex is freely fluxional at room temperature; the benzyl substituent does not interfere with the α -phenyl substituent rotation in the complex. The *n*-propyl radical also adds to the central carbon of cinnamyl complex **144**; however, as for the 2-*N,N*-dimethylaminoindenyl template, the reaction produces unknown byproducts that inhibit the isolation and characterization of the desired titanacyclobutane. As observed using the other templates, the one pot procedure allows

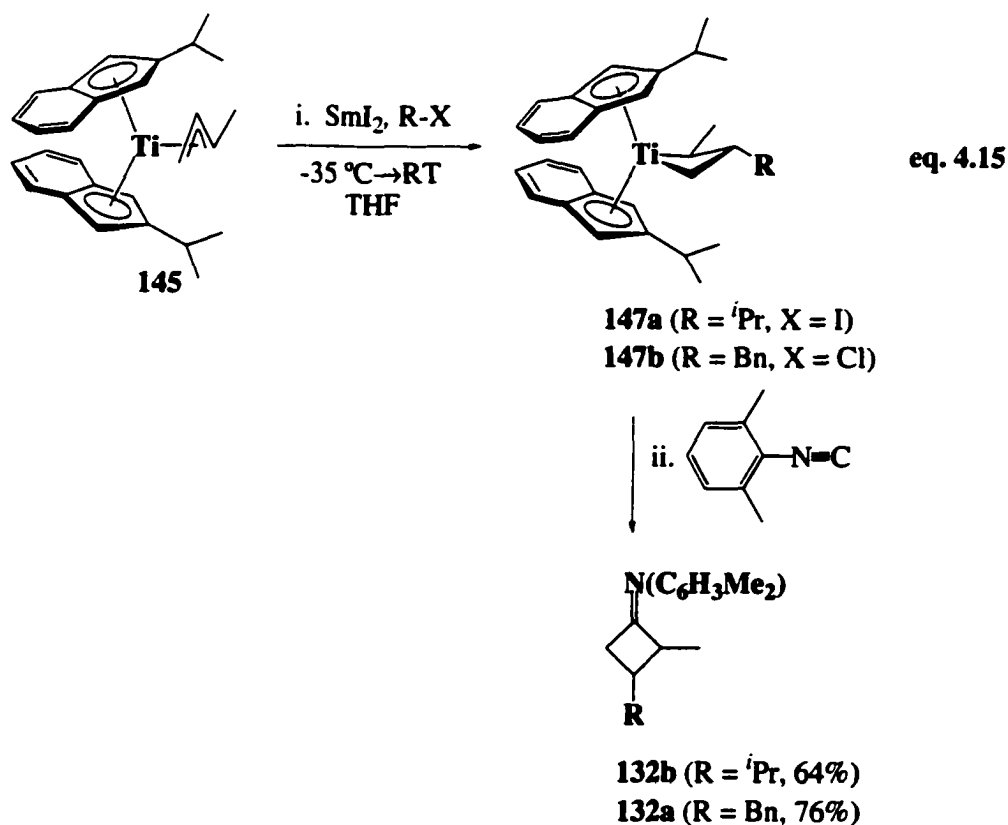
titanacyclobutane. As observed using the other templates, the one pot procedure allows for the single-step synthesis of these complexes in comparable or better overall yields (Table 4.9).

Table 4.9 Yields of One Pot Procedure for Titanacyclobutane Complexes 146a-d

Complex	R-X	Yield (one pot, %)	Yield (two-step 143 → 144 → 146, %)
146a	PrI	60	58
146b	CyI	56	46
146c	^t BuCl	57	39
146d	BnCl	57	56

The addition of organic radicals to crotyl complex **145** was met, as expected, with more limited success. Central carbon alkylation provides titanacyclobutanes complexes that are exceptionally prone to β -hydride elimination. For this reason, it was not possible to directly characterize any of the derived titanacyclobutane complexes. However, *in situ* 2,6-dimethylphenylisonitrile insertion proceeds cleanly, permitting the isolation of cyclobutanimes **132a** and **132b** in 76% and 64% isolated yields, respectively (eq. 4.15).

Conclusion. These results demonstrate the addition of stabilized and unstabilized radicals to crotyl and cinnamyl complexes **145** and **144**, respectively. For the cinnamyl complex, central carbon alkylation proceeds in yields that are high enough for synthetic application. However, it appears that an excessively bulky ancillary ligand system does not stabilize crotyl derived titanacyclobutane complexes sufficiently for isolation. Although the derivatization of the titanacyclobutane complexes was possible using isonitrile insertion, it is not clear how general such *in situ* reactions may be.



E. Conclusions

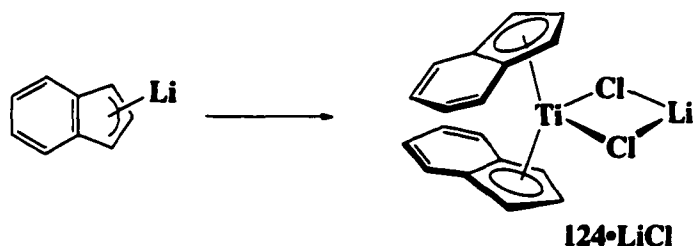
A reasonable level of electron density provided to the metal center by the indenyl ancillary ligands is necessary to observe central carbon alkylation in good yields. Surprising however, is the relatively minimal level of electron density necessary to promote clean conversion of substituted allyl complexes. The reactivity of even the unsubstituted indenyl system is suggestive of central carbon alkylation, however, for practical applications, the isopropylindenyl system allows for the synthesis of robust 2-phenyl substituted titanacyclobutane complexes in good to excellent yields. The extension to 2-methyl substituted titanacyclobutanes remains problematic, but another template with similar electron density but different steric profile may indeed generate

stable α -methyl titanacyclobutane complexes. Such systems are currently under investigation.

F. Experimental

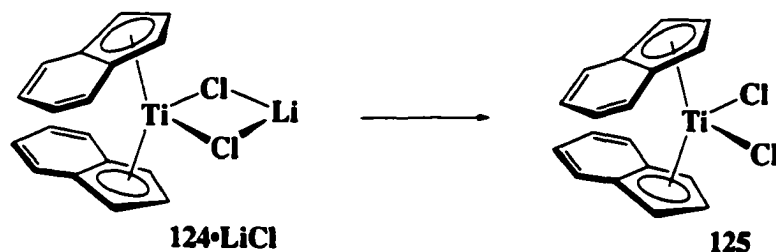
General Experimental: See Chapter 2, pg. 59.

Bis(indenyl)titanium Chloride•Lithium Chloride, 124•LiCl from Indenyllithium:



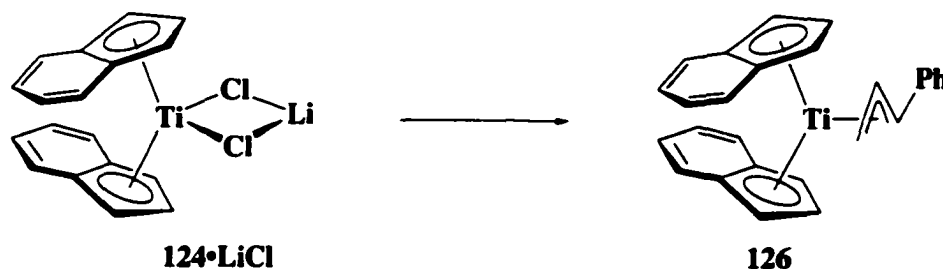
Bis(indenyl)titanium chloride•lithium chloride 124•LiCl. In a Schlenk flask under an inert atmosphere, indenyllithium¹ (1.06 g, 8.51 mmol) was dissolved in 30 mL THF and cooled to -78 °C. In a separate Schlenk flask, TiCl₃•3THF (1.50 g, 4.05 mmol) was suspended in 25 mL THF and, after cooling to -78 °C, the solution of indenyllithium was transferred via cannula onto the titanium solution and left to slowly warm to room temperature and stir overnight. After 12 hours, the solvent was removed under reduced pressure from the deep green solution, yielding a red-brown residue. The residue was extracted into benzene/THF (1 : 1) and the solution filtered through a sintered glass funnel layered with a short plug of Celite. The solvents were removed under reduced pressure and the residual solid was recrystallized from THF/hexane (1 : 2) at -35 °C yielding complex **124•LiCl** as green prisms which, under vacuum, turned into an amorphous bright red solid (1.13 g, 78%). HRMS calcd. for: C₁₈H₁₄Ti³⁵Cl *m/z* 313.02634, found 313.02766; C₂₂H₂₆Ti³⁷Cl *m/z* 315.02341, found 315.02415. Anal. calcd. for C₁₈H₁₄TiCl•LiCl: C, 60.72; H, 3.96; found C, 60.96, H, 4.06.

Bis(indenyl)titanium Dichloride 125 from Bis(indenyl)titanium Chloride•Lithium Chloride 124•LiCl:



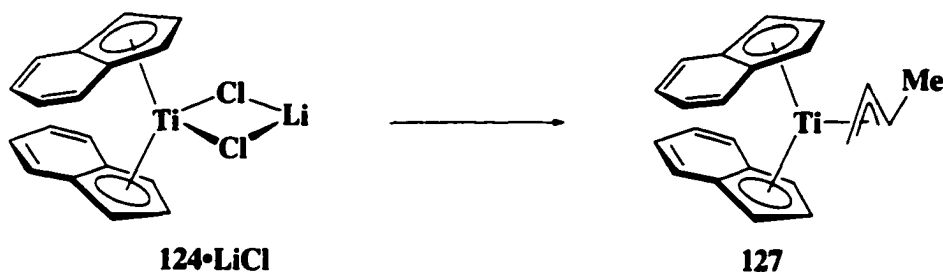
Bis(indenyl)titanium dichloride 125. In the drybox, a NMR tube containing a deuterated benzene solution of bis(indenyl)titanium chloride•LiCl, **124•LiCl** (40.0 mg, 0.112 mmol) was capped with a rubber septum, removed from the drybox and treated with carbon tetrachloride (11.4 μ L, 0.118 mmol) via syringe. As bis(indenyl)titanium chloride•LiCl slowly dissolved into solution, precipitation of dark brown dichloride complex **125** was observed on the sides of the NMR tube. Due to the insolubility and thermal instability of dichloride complex **125** characterization was performed by ^1H NMR spectroscopy alone.² ^1H NMR (360.1 MHz, C_6D_6): δ 7.31 (2nd order m, 2H, H4/5), 6.94 (2nd order m, 2H, H4/5), 5.93 (t, J = 3.2 Hz, 1H, H2), 5.82 (d, J = 3.2 Hz, 2H, H1).

Bis(indenyl)titanium Cinammyl 126 from Bis(indenyl)titanium Chloride 124•LiCl:



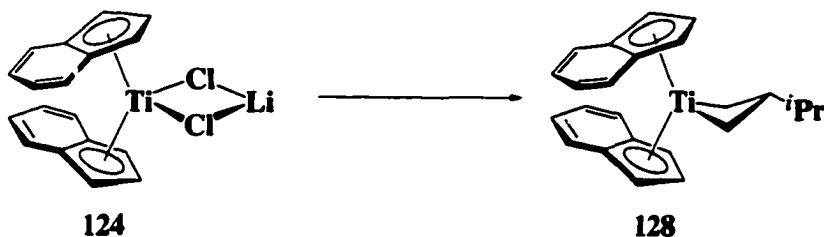
Bis(indenyl)titanium(η^3 -1-phenylallyl) 126. In the drybox, a vial containing a THF solution (3 mL) of bis(indenyl)titanium chloride•LiCl, **124•LiCl** (67.4 mg, 0.189 mmol) was cooled to $-35\text{ }^\circ\text{C}$ and treated with a cooled ($-35\text{ }^\circ\text{C}$) THF solution (1 mL) of cinnamyl lithium (28.0 mg, 0.226 mmol). Within 30 seconds the colour of the solution turned from forest green to brown to emerald green. After an additional 3 h at room temperature, the THF was removed under reduced pressure, leaving a dark green residue. The product was extracted into benzene and filtered through a sintered glass funnel layered with a short plug of Celite. The benzene was removed *in vacuo* and the resulting solid was crystallized from THF layered with hexane (1 : 2) cooled to $-35\text{ }^\circ\text{C}$, affording bright green diamond-shaped crystals (40.1 mg, 51%) of cinnamyl complex **126**. IR (cm^{-1} , hexane cast): 3032 (w), 2980 (m), 1594 (m), 1530 (s), 1484 (w), 1448 (m), 1430 (w), 1339 (s), 1320 (m), 1258 (m), 1214 (m), 1178 (w), 1148 (w), 1098 (w), 1038 (m), 997 (w), 894 (w), 867 (w), 835 (w), 815 (s), 791 (s), 779 (vs), 753 (vs), 694 (s). Anal. calcd. C, 82.02; H, 5.86; found C, 81.29; H, 6.03.

Bis(indenyl)titanium Crotyl 127 from Bis(indenyl)titanium Chloride 124•LiCl:



Bis(indenyl)titanium(η^3 -1-methylallyl) 127. In the drybox, a vial containing a THF solution (3 mL) of bis(indenyl)titanium chloride•LiCl, **124•LiCl** (134.6 mg, 0.378 mmol) cooled to $-35\text{ }^\circ\text{C}$ was treated with a cooled ($-35\text{ }^\circ\text{C}$) solution (1 mL) of crotyl Grignard (250 μL , 1.63 M further diluted in 1 mL THF). The colour of the solution turned slowly from red to medium brown in ~ 3 minutes. After an additional 2 h at room temperature, the THF was removed under reduced pressure, leaving a dark brown residue. The product was extracted into benzene and filtered through a sintered glass funnel layered with a short plug of Celite. The benzene was removed *in vacuo* and the resulting solid was crystallized from THF layered with hexane (1 : 4) cooled to -35°C , affording brown agglomerated crystals (64.3 mg, 51%) of crotyl complex **127**. IR (cm^{-1} , diethyl ether cast): 3043 (m), 3005 (m), 2918 (m), 2874 (m), 2847 (m), 2743 (s), 1912 (w), 1782 (w), 1686 (w), 1607 (w), 1532 (m), 1480 (w), 1449, 1436 (m), 1341 (vs), 1374 (m), 1257 (m), 1214 (s), 1152 (w), 1120 (m), 1046 (s), 1027 (m), 1009 (m), 997 (m), 970 (w), 869 (s), 795 (vs), 741 (vs), 668 (s). Elemental analysis was not within tolerances.²¹

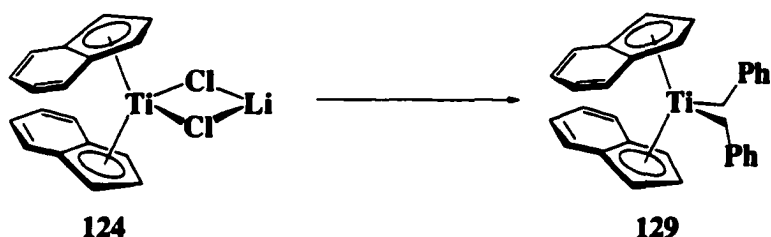
Titanacyclobutane Complex 128 from Bis(indenyl)titanium Chloride 124•LiCl:



3-Isopropyl-bis(2-indenyl)titanacyclobutane 128. In the drybox, a vial containing a THF solution (3 mL) of bis(indenyl)titanium chloride•LiCl, **124**•LiCl (39.2 mg, 0.110 mmol) was cooled to -35 °C and treated with a cold (-35 °C) THF solution (1 mL) of allyl bromide (10.3 μL, 0.119 mmol). After stirring the resultant reaction 1 minute, cold (-35 °C) SmI₂ (3.6 mL, 0.1 M in THF) was added to the vial followed immediately by a cold solution of 2-iodopropane (11.9 μL, in 1 mL THF). After allowing the reaction to warm to room temperature and stir an additional 3 h, the supernatant was removed from the samarium (III) precipitate and the solvent removed under reduced pressure, leaving a mixed red and green residue. The product was extracted into pentane and filtered through a short plug of Celite, concentrated to approximately 2 mL and cooled to -35 °C, affording red cube shaped crystals (23.2 mg, 58%) of titanacyclobutane complex **128**. ¹H NMR (400.1 MHz, C₆D₆): δ 7.09 (m, 4H, H4/H5), 6.88 (2nd order m, 2H, H4/H5), 6.86 (2nd order m, 2H, H4/H5), 5.80 (d, *J* = 3.0 Hz, 2H, H2), 5.64 (t, *J* = 2.9 Hz, 1H, H1), 5.55 (d, *J* = 3.0 Hz, 2H, H2'), 4.87 (t, *J* = 3.0 Hz, 1H, H1'), 1.81 (t, *J* = 9.3 Hz, 2H α-CH₂), 1.02 (d, *J* = 6.5 Hz, 6H, CH(CH₃)₂), 0.65 (m, 1H, CH(CH₃)₂), 0.25 (t, *J* = 8.5 Hz, 2H, α-CH₂), -0.41 (apparent sextet, *J* = 9.2 Hz, 1H, β-CH). GCOSY (300 Mz, C₆D₆) select data only: δ 1.81 (α-CH₂) ↔ δ 0.25 (α-CH₂) ↔ δ -0.41 (β-CH); δ 1.02 (CH(CH₃)₂) ↔ δ 0.65 (CH(CH₃)₂), δ 0.65 (CH(CH₃)₂) ↔ δ -0.41 (β-CH). ¹³C NMR (100.6 MHz, C₆D₆): δ 125.3 (C4/C5), 125.0 (C4/C5), 124.9 (C4/C5), 124.5 (C4/C5), 121.8 (C3), 116.4 (C1), 114.2 (C1'), 102.7 (C2), 101.4 (C2'), 79.4 (α-CH₂), 33.9

($\underline{\text{CH}}(\text{CH}_3)_2$), 23.6 ($\text{CH}(\underline{\text{C}}\text{H}_3)_2$), 22.9 ($\beta\text{-CH}$), missing C3' signal likely obscured by solvent. HMQC (300 MHz, C_6D_6): select data only δ 116.4 (C1) \leftrightarrow δ 5.64 (H1); δ 114.2 (C1') \leftrightarrow δ 4.87 (H1'); δ 102.7 (C2) \leftrightarrow δ 5.80 (H2); δ 101.4 (C2') \leftrightarrow δ 5.55 (H2'); δ 79.4 ($\alpha\text{-CH}_2$) \leftrightarrow δ 1.81 ($\alpha\text{-CH}_2$), δ 0.25 ($\alpha\text{-CH}_2$); δ 33.9 ($\underline{\text{CH}}(\text{CH}_3)_2$) \leftrightarrow δ 0.65 ($\text{CH}(\underline{\text{C}}\text{H}_3)_2$); δ 23.6 ($\text{CH}(\underline{\text{C}}\text{H}_3)_2$) \leftrightarrow δ 1.02 ($\text{CH}(\underline{\text{C}}\text{H}_3)_2$); δ 22.9 ($\beta\text{-CH}$) \leftrightarrow δ -0.41 ($\beta\text{-CH}$). Elemental analysis was not within tolerable allowances.²¹

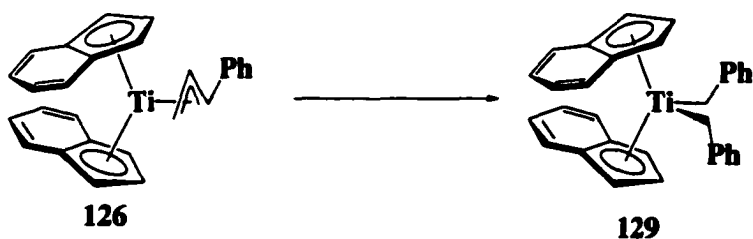
Bis(benzyl)bis(indenyl)titanocene 129 from Bis(indenyl)titanium Chloride 124•LiCl:



Bis(benzyl)bis(indenyl)titanocene 129. In the drybox, to a vial containing a THF solution (3 mL) of bis(indenyl)titanium chloride•LiCl, **124**•LiCl (32.8 mg, 0.0921 mmol) cooled to -35 °C was added a cold (-35 °C) THF solution (1 mL) of allyl bromide (8.4 μL , 0.119 mmol). After stirring the resultant reaction 1 minute, cold (-35 °C) SmI_2 (2.8 mL, 0.1 M in THF) was added to the vial followed immediately by an equally cold solution of benzyl chloride (11.3 μL , in 1 mL THF). After allowing the reaction to warm to room temperature and stir an additional hour, the supernatant was removed from the samarium (III) precipitate and the solvent removed under reduced pressure, leaving a red brown residue. The product was extracted into pentane, and filtered through a short plug of Celite, and evaporated to dryness, affording quantitatively bis(benzyl)bis(indenyl)titanocene (crude: 24.3 mg). This material was not further purified. ^1H NMR (400.1 MHz, C_6D_6): δ 7.20 (t, $J = 7.6$ Hz, 4H, $\text{CH}_2\text{C}_6\text{H}_5$), 7.07 (2nd order m, 4H, H4/H5), 6.93 (t, $J = 7.3$ Hz, 2H, $\text{CH}_2\text{C}_6\text{H}_5$), 6.90 (2nd order m, 4H, H4/H5), 6.83 (d, $J = 7.1$ Hz, 4H, $\text{CH}_2\text{C}_6\text{H}_5$), 5.67 (d, $J = 3.3$ Hz, 4H, H1), 5.59 (t, $J = 3.3$ Hz, 2H,

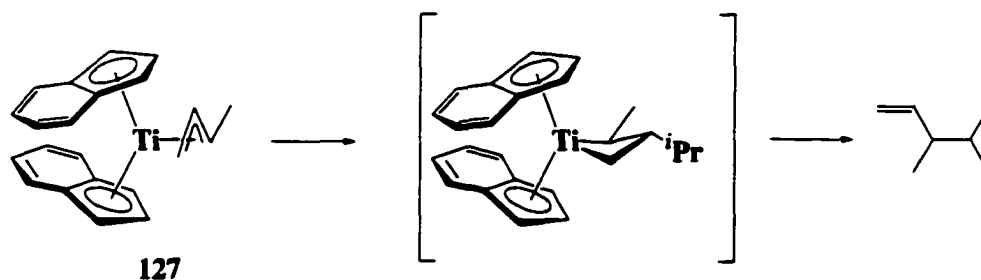
H2), 1.01 (s, 4H, $\text{CH}_2\text{C}_6\text{H}_5$). GCOSY (300 Mz, C_6D_6) select data only: 7.20 ($\text{CH}_2\text{C}_6\text{H}_5$) \leftrightarrow δ 6.93 ($\text{CH}_2\text{C}_6\text{H}_5$) \leftrightarrow δ 6.83 ($\text{CH}_2\text{C}_6\text{H}_5$). ^{13}C NMR (100.6 MHz, C_6D_6): δ 153.9 ($\text{CH}_2\text{C}_6\text{H}_5$), 128.1 (C_{aryl}), 126.3 (C_{aryl}), 126.2 (C_{aryl}), 125.3 (C_{aryl}), 122.0 (C_{aryl}), 121.1 (C1), 108.8 (C2), 79.5 ($\text{CH}_2\text{C}_6\text{H}_5$). HMQC (300 MHz, C_6D_6): select data only δ 121.1 (C1) \leftrightarrow δ 5.67 (H1); δ 108.8 (C2) \leftrightarrow δ 5.59 (H2); δ 79.5 ($\text{CH}_2\text{C}_6\text{H}_5$) \leftrightarrow δ 1.01 ($\text{CH}_2\text{C}_6\text{H}_5$).

Bis(benzyl)bis(indenyl)titanocene 129 from Bis(indenyl)titanium Cinnamyl 126:



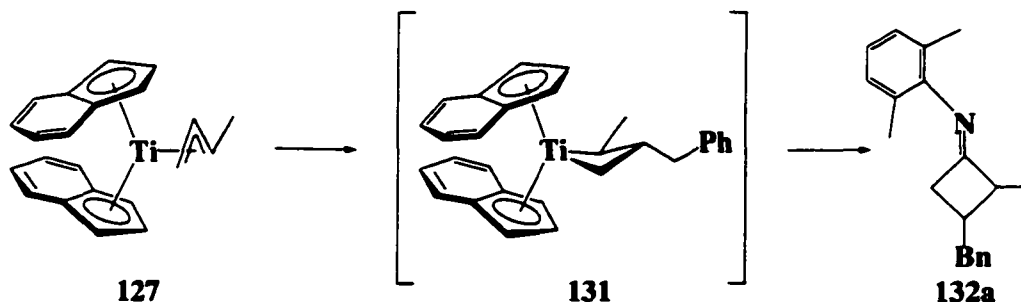
Bis(benzyl)bis(indenyl)titanocene 129. In the drybox, a vial containing a THF solution (3 mL) of bis(indenyl)titanium cinnamyl **126** (23.6 mg, 0.0597 mmol) and SmI_2 (0.63 mL, 0.1 M in THF) cooled to $-35\text{ }^\circ\text{C}$ was treated with a cold ($-35\text{ }^\circ\text{C}$) THF solution (1 mL) of benzyl chloride (7.2 μL , in 1 mL THF). After allowing the reaction to warm to room temperature and stir an additional hour, the supernatant was removed from the samarium (III) precipitate and the solvent removed under reduced pressure, leaving a mixture of red and green residue. The product was extracted into pentane, filtered through a short plug of Celite, and evaporated to dryness to yield bis(benzyl)bis(indenyl)titanocene (crude: 12.1 mg, 84%). The material obtained was spectroscopically homogeneous and identical to that prepared above.

**Thermal Decomposition of 2-Methyl-3-isopropyl-bis(indenyl)titanacyclobutane:
Detection of 3,4-Dimethyl-1-pentene.**



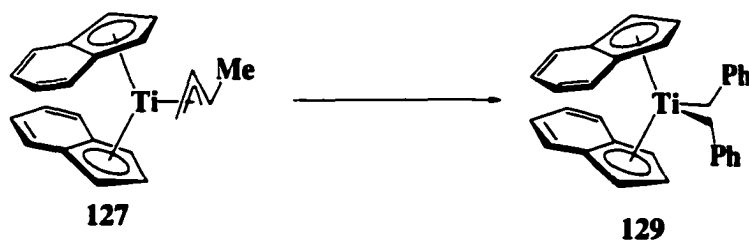
2-Methyl-3-isopropyl-bis(indenyl)titanacyclobutane. In the drybox, a vial containing a THF solution (2 mL) of bis(indenyl)titanium crotyl **127** (14.3 mg, 0.0432 mmol) and SmI_2 (0.45 mL, 0.1 M in THF) cooled to $-35\text{ }^\circ\text{C}$ was treated with a cold ($-35\text{ }^\circ\text{C}$) THF solution (1 mL) of isopropyl iodide (4.5 μL , 0.0432 mmol). After allowing the reaction to warm to room temperature and stir an additional hour, the supernatant was removed from the samarium (III) precipitate and submitted for GCIR spectroscopy. Analysis of the supernatant confirmed the presence of 3,4-dimethyl-1-pentene, indirectly indicating some formation of 2-methyl-3-isopropyl-bis(indenyl)titanacyclobutane.

Derivatization of 2-Methyl-3-benzyl-bis(indenyl)titanacyclobutane 131 with 2,6-Dimethylphenylisonitrile: Detection of N-[*Trans*-(3-benzyl-2-methyl)-1-cyclobutylidene]-N-[2,6-dimethylphenyl]amine 132a.



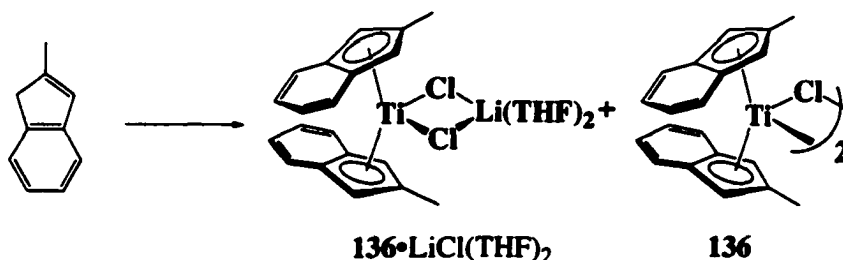
2-Methyl-3-Benzyl-bis(indenyl)titanacyclobutane 131. In the drybox, a vial containing a THF solution (2 mL) of bis(indenyl)titanium crotyl 127 (21.7 mg, 0.0655 mmol) and SmI_2 (0.69 mL, 0.1 M in THF) cooled to $-35\text{ }^\circ\text{C}$ was treated with a cold ($-35\text{ }^\circ\text{C}$) THF solution (1 mL) of benzyl chloride (4.5 μL , 0.0432mmol). After allowing the reaction to stir at room temperature for 5 minutes, the reaction mixture was poured onto 10 mL of cold ($-35\text{ }^\circ\text{C}$) pentane, filtered, and treated with a cold solution of 2,6-dimethylphenylisonitrile (25.7 mg, 0.196 mmol in 5 mL THF). After stirring for one hour at room temperature for 3 h, the solvents were removed under reduced pressure and the residue submitted for HRMS. HRMS calcd. for $\text{C}_{20}\text{H}_{23}\text{N}$ m/z 277.18304, found 277.18274.

Bis(benzyl)bis(indenyl)titanium 129 from Bis(indenyl)titanium Crotyl 127:



Bis(benzyl)bis(indenyl)titanium 129. As described above, a THF solution of crotyl complex **127** (10.0 mg, 0.0302) and SmI_2 (0.30 mL, 0.1 M in THF) were treated with benzyl chloride (3.5 μL , 0.0300mmol). After allowing the reaction to warm to room temperature and stir an additional hour, the supernatant was removed from the samarium(III) precipitate and the solvent removed under reduced pressure, leaving a red brown residue. The product was extracted into pentane, filtered through a short plug of Celite, and evaporated to dryness to yield bis(benzyl)bis(indenyl)titanocene (crude: < 2.0 mg, ~10%). The material obtained was spectroscopically homogeneous and identical to material previously prepared (pg. 227).

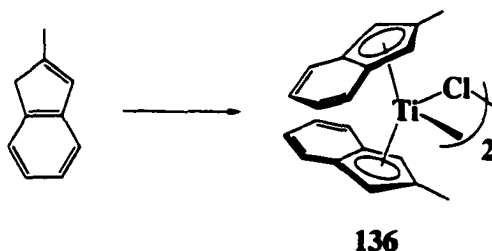
Bis(2-methylindenyl)titanium chloride 136 and 136•LiCl from 2-methylindenyllithium:



Bis(2-methylindenyl)titanium chloride 136 and 136•LiCl. In a 100 mL Schlenk flask, under an inert atmosphere, 2-methylindene¹ (2.00 g, 15.4 mmol) was dissolved in 25 mL THF and cooled to -78 °C. *n*-Butyllithium (15.4 mmol, 2.5 M in hexanes) was added

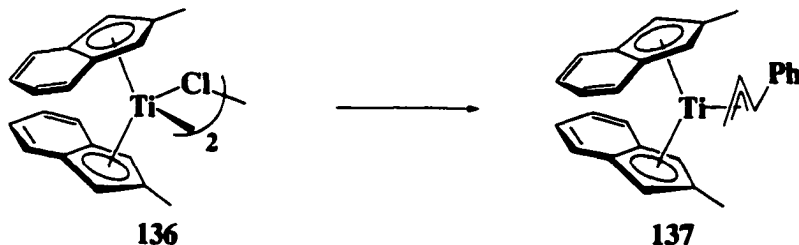
dropwise by syringe and the solution was stirred at $-78\text{ }^{\circ}\text{C}$ for 3 hours, warmed to room temperature to stir for an additional 2 hours and re-cooled to $-78\text{ }^{\circ}\text{C}$. In a separate 250 mL Schlenk flask, $\text{TiCl}_3 \cdot 3\text{THF}$ (2.71 g, 7.31 mmol) was suspended in 50 mL THF and cooled to $-78\text{ }^{\circ}\text{C}$. The solution of 2-methylindenyl lithium was transferred at $-78\text{ }^{\circ}\text{C}$ via cannula onto the titanium solution and left to warm slowly to room temperature overnight. The solvent was removed under reduced pressure from the brown solution to leave a red residue. The Schlenk flask was placed under vacuum and returned to the drybox, where some of the residue was extracted into benzene (4 x 30 mL). These extracts were filtered through a sintered glass funnel layered with a short plug of Celite and evaporated to dryness under reduced pressure. The residual solid was precipitated from THF/hexane (1 : 1) at $-35\text{ }^{\circ}\text{C}$, yielding the chloride complex **136** as an amorphous burgundy red solid, (1.10 g, 44%).¹⁰ The remaining red residue was extracted into THF. The forest green solution was filtered through a short plug of Celite, concentrated, and layered carefully with an equal amount of hexane. Cooling the solution to $-35\text{ }^{\circ}\text{C}$ afforded pale green prisms, which upon drying turned to an amorphous red powder corresponding to bis(2-methylindenyl)titanium chloride•lithium chloride **136**•LiCl (0.83 g, 30 %).¹⁹ **Bis(2-methylindenyl)titanium chloride 136**: HRMS calcd. for: $\text{C}_{20}\text{H}_{18}\text{Ti}^{35}\text{Cl}$ m/z 341.05765, found 341.05792 (100%); $\text{C}_{20}\text{H}_{18}\text{Ti}^{37}\text{Cl}$ m/z 343.05469, found 343.05553; anal. calcd. for $\text{C}_{20}\text{H}_{18}\text{TiCl}$: C, 70.37; H, 5.32; found C, 70.86, H, 5.52. **Bis(2-methylindenyl)titanium chloride•lithium chloride 136**•LiCl. Anal. calcd. for $\text{C}_{20}\text{H}_{18}\text{TiCl}\cdot\text{LiCl}$: C, 62.54; H, 4.72; found C, 62.78, H, 4.63.

Bis(2-methylindenyl)titanium Chloride from 2-Methylindenylpotassium:



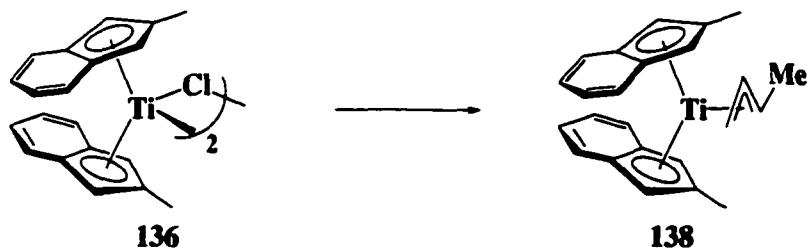
Bis(2-methylindenyl)titanium chloride 136. In the drybox, to a 50 mL Schlenk flask containing 2-methylindene¹ (400 mg, 3.07 mmol) dissolved in 25 mL THF, was added potassium metal (120.1 mg, 3.07 mmol). The stopcock of the Schlenk flask was left in the open position to relieve H₂ evolution. The reaction was stirred overnight and the following morning 38 mg (0.97 mmol) of potassium metal was retrieved from the reaction flask. The flask was removed from the drybox and cooled to -78 °C. In a separate 100 mL Schlenk flask, TiCl₃•3THF (540 mg, 1.46 mmol) was suspended in 25 mL THF and cooled to -78 °C. The solution of 2-methylindenylpotassium was slowly transferred via cannula onto the titanium solution and left to slowly warm to room temperature stirring a total of 14 h. The solvent was removed under reduced pressure from the burgundy red solution to leave a purple residue. The Schlenk flask was returned to the drybox where the entire residue was extracted into benzene (4 x 25 mL) and filtered through a sintered glass funnel layered with a short plug of Celite. The benzene was removed under reduced pressure and the solid was precipitated from THF/hexane (1 : 1) at -35 °C yielding the chloride complex **136** as an amorphous burgundy red solid, (0.1354 g, 38%)²⁰ identical by elemental analysis to the material prepared previously.

Bis(2-methylindenyl)titanium Cinnamyl 137 from Bis(2-methylindenyl)titanium Chloride 136:



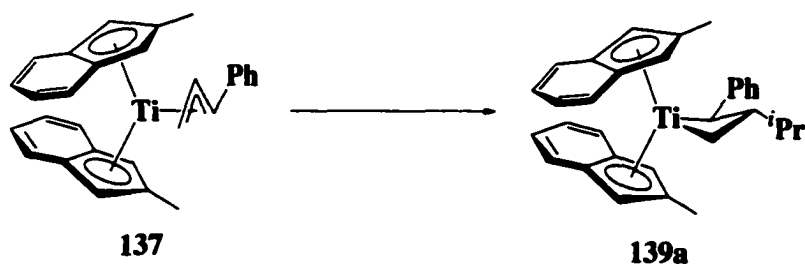
Bis(2-methylindenyl)titanium(η^3 -1-phenylallyl) 137. In the drybox, to a vial containing a THF solution (5 mL) of bis(2-methylindenyl)titanium chloride **136** (96.0 mg, 0.281 mmol) cooled to $-35\text{ }^\circ\text{C}$, was added a cold ($-35\text{ }^\circ\text{C}$) THF solution (3 mL) of cinnamyl lithium (37.0 mg, 0.295 mmol). Instantaneously, the colour of the solution turned from red/brown to emerald green. After an additional 1 h at room temperature, the THF was removed under reduced pressure leaving a dark green residue. The product was extracted into benzene and filtered through a short plug of Celite. The benzene was removed *in vacuo* and the resulting solid was crystallized from THF layered with hexane (1 : 3) cooled to $-35\text{ }^\circ\text{C}$, to afford bright green diamond-shaped crystals of complex **137** (76.9 mg, 65%). IR (cm^{-1} , THF cast): 3039 (w), 2916 (w), 1593 (w), 1526 (m), 1485 (w), 1447 (m), 1380 (m), 1354 (m), 1329 (w), 1282, (w), 1245 (m), 1212 (m), 1174 (w), 1152 (w), 1117 (w), 1071 (m), 1030 (m), 995 (m), 964 (m), 847 (m), 850 (s), 799 (s), 742 (vs), 693 (s), 642 (m). It is suspected that one THF molecule is entrained in the crystals isolated: anal. calcd. for $\text{C}_{29}\text{H}_{27}\text{Ti}$: C, 82.26; H, 6.43; anal. calcd. for $\text{C}_{29}\text{H}_{27}\text{Ti}\cdot\text{C}_4\text{H}_8\text{O}$: C, 79.99; H, 7.12; found (trial 1): C, 80.39; H, 6.55; (trial 2): C, 80.44; H, 6.64.

Bis(2-methylindenyl)titanium Crotyl 138 from Bis(2-methylindenyl)titanium Chloride 136:



Bis(2-methylindenyl)titanium(η^3 -1-methylallyl) 138. In the drybox, a vial containing a THF solution (5 mL) of bis(2-methylindenyl)titanium chloride **136**, (106.9 mg, 0.312 mmol), cooled to $-35\text{ }^{\circ}\text{C}$, was treated with a cold solution of crotylmagnesium chloride (0.200 mL, 1.63 M in THF further diluted in 3 mL THF). The reaction was left to warm to room temperature and stir for an additional 3 hours. The colour of the solution turned from red/brown to army green over the course of 5 minutes. Removal of the THF *in vacuo* gave a dark green residue, which was extracted into hexane and filtered through a sintered glass funnel layered with a short plug of Celite. The hexane was removed under reduced pressure and further purification from THF/hexane (1 : 3), cooled to $-35\text{ }^{\circ}\text{C}$, powdered a out lime green solid (67.5 mg, 60%) corresponding to crotyl complex **138**. IR (cm^{-1} , hexane cast): 3039 (w), 2916 (w), 2845 (w), 1651 (w), 1540 (w), 1437 (w), 1355 (w), 1329 (w), 1291 (w), 1212 (w), 1104 (m), 1076 (m), 1025 (m), 962 (w), 888 (w), 847 (s), 823 (s), 740 (vs), 642 (w). Anal. calcd. C, 79.77; H, 6.97; found C, 79.61; H, 7.10.

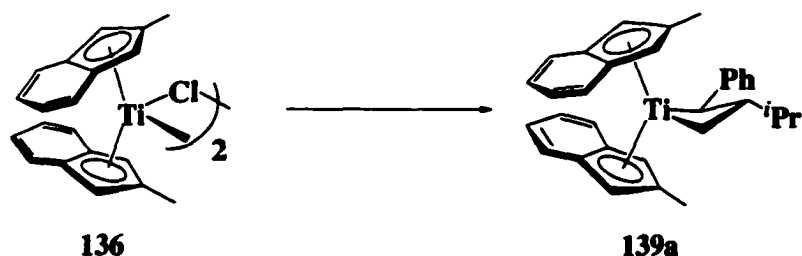
Titanacyclobutane 139a from Bis(2-methylindenyl)titanium Cinnamyl 137:



3-Isopropyl-2-phenyl-bis(2-methylindenyl)titanacyclobutane 139a. In the drybox, a vial containing a THF solution (2 mL) of bis(2-methylindenyl)titanium cinnamyl **137** (23.8 mg, 0.0562 mmol) and SmI_2 (0.60 mL, 0.1 M in THF) was cooled to $-35\text{ }^\circ\text{C}$. Following the addition of a cold ($-35\text{ }^\circ\text{C}$) solution of isopropyl iodide (5.9 μL in 1 mL THF), the reaction mixture was allowed to warm to room temperature and stir an additional 2 h. After 0.5 h, the blue/green colour of the solution dissipated into a dark chocolate brown solution. The solvent was removed *in vacuo*, the brown residue extracted into hexane, and the resultant solution filtered through a short plug of Celite. The hexane solution was concentrated to approximately 2 mL and cooled to $-35\text{ }^\circ\text{C}$ to yield titanacyclobutane complex **139a** as dark brown agglomerated rhomboids (16.2 mg, 62%). ^1H NMR (400 MHz, C_6D_6): δ 7.28 – 7.17 (m, 5H, H_{aryl}), 7.02 (ddd, $J = 8.4, 6.3, 1.2$ Hz, 2H, H_{aryl}), 6.94 (m, 2H, H_{aryl}), 6.89 (m, 2H, H_{aryl}), 6.72 (m, 2H, H_{aryl}), 5.68 (d, $J = 0.9$ Hz, 1H, H2), 5.67 (d, $J = 0.9$ Hz, 1H, H2'), 5.54 (d, $J = 2.1$ Hz, 1H, H2''), 5.34 (d, $J = 1.8$ Hz, 1H, H2'''), 3.07 (d, $J = 11.1$ Hz, 1H, α -CH), 1.93 (t, $J = 9.6$ Hz, 1H, α - CH_2), 1.79 (s, 3H, CH_3), 1.44 (coincidental octet, $J = 6.6$ Hz, 1H, $\text{CH}(\text{CH}_3)_2$), 1.22 (s, 3H, CH_3), 0.94 (d, $J = 6.6$ Hz, 3H, $\text{CH}(\text{CH}_3)_2$), 0.91 (d, $J = 6.6$ Hz, 3H, $\text{CH}(\text{CH}_3)_2$), 0.44 (dq, $J = 9.9, 6.6$ Hz, 1H, β -CH), 0.086 (t, $J = 9.3$ Hz, 1H, α - CH_2). GCOSY (300 Mz, C_6D_6) select data only: δ 3.07 (α -CH) \leftrightarrow δ 0.44 (β -CH); δ 1.93 (α - CH_2) \leftrightarrow δ 0.44 (β -CH) \leftrightarrow δ 0.086 (α - CH_2), δ 0.44 (β -CH) \leftrightarrow δ 1.44 ($\text{CH}(\text{CH}_3)_2$) \leftrightarrow δ 0.94 ($\text{CH}(\text{CH}_3)_2$), δ 0.91 ($\text{CH}(\text{CH}_3)_2$). ^{13}C

NMR (100.6 MHz, C₆D₆): δ 155.1 (C_{aryl}), 128.7 (C_{aryl}), 128.3 (C_{aryl}), 128.0 (C_{aryl}), 127.5 (C_{aryl}), 127.1 (C_{aryl}), 126.9 (C_{aryl}), 126.6 (C_{aryl}), 125.6 (C_{aryl}), 124.9 (C_{aryl}), 124.8 (C_{aryl}), 124.6 (C_{aryl}), 124.5 (C_{aryl}), 124.2 (C_{aryl}), 124.1 (C_{aryl}), 124.0 (C_{aryl}), 123.4 (C_{aryl}), 121.4 (C_{aryl}), 119.4 (C_{aryl}), 113.9 (C2), 105.2 (C2'), 102.0 (C2''), 100.6 (C2'''), 92.3 (α -CH), 89.2 (α -CH₂), 33.3 (CH(CH₃)₂), 23.7 (CH(CH₃)₂), 23.0 (β -CH), 20.9 (CH(CH₃)₂), 16.8 (CH₃), 14.1 (CH₃). HMQC (300 Mz, C₆D₆) select data only: δ 113.9 (C2) \leftrightarrow δ 5.68 (H2'/H2); δ 105.2 (C2') \leftrightarrow δ 5.68 (H2/H2'); δ 102.0 (C2'') \leftrightarrow δ 5.54 (H2''); δ 100.6 (C2''') \leftrightarrow δ 5.34 (H2'''); δ 92.3 (α -CH) \leftrightarrow δ 3.07 (α -CH); δ 89.2 (α -CH₂) \leftrightarrow δ 1.93 (α -CH₂), δ 0.086 (α -CH₂); δ 33.3 (CH(CH₃)₂) \leftrightarrow δ 1.44 (CH(CH₃)₂); δ 23.7 (CH(CH₃)₂) \leftrightarrow δ 0.94 (CH(CH₃)₂); δ 23.0 (β -CH) \leftrightarrow δ 0.44 (β -CH); δ 20.9(CH(CH₃)₂) \leftrightarrow δ 0.91(d, *J* CH(CH₃)₂); δ 16.8 (CH₃) \leftrightarrow δ 1.79 (CH₃); δ 14.1 (CH₃) \leftrightarrow δ 1.22 (CH₃). ¹H NMR spectroscopy indicates that the crystals entrain approximately one THF molecule: anal. calcd. for C₃₂H₃₄Ti•C₄H₈O: C, 79.96; H, 7.86; found: C, 79.46; H, 7.29.

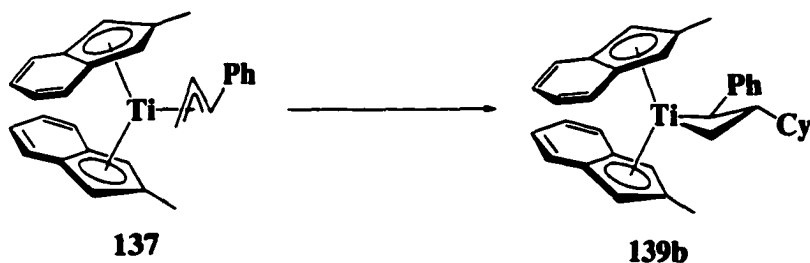
Titanacyclobutane 139a from Bis(2-methylindenyl)titanium Chloride 136:



3-Isopropyl-2-phenyl-bis(2-methylindenyl)titanacyclobutane 139a. In the drybox, a vial containing a THF solution (5 mL) of bis(2-methylindenyl)titanium chloride 136 (40.8 mg, 0.119 mmol) was cooled to -35 °C. Cinnamyl lithium (15.6 mg, 0.125 mmol) was dissolved in 2 mL THF and cooled to -35 °C. The two solutions were mixed together, allowed to warm to room temperature and stirred for 1 h. After Sml₂ (1.25 mL,

0.1 M in THF) was added via syringe into solution, the resulting green/blue solution was re-cooled to $-35\text{ }^{\circ}\text{C}$ and treated with cold ($-35\text{ }^{\circ}\text{C}$) isopropyl iodide (11.9 μL in 1 mL THF, 0.119 mmol). The reaction mixture was left to warm to room temperature and stir for an additional 3 h. Within 1 h the blue/green colour of the solution had completely dissipated with the emergence of a dark chocolate brown solution. The solvent was removed *in vacuo*, the brown residue was extracted with a hexane/benzene mixture (3 : 1) and the solution filtered through a short plug of Celite. The solvents were removed under reduced pressure and the crude recrystallized from THF/hexane (1:6) cooled to $-35\text{ }^{\circ}\text{C}$ affording 26.2 mg (47%) of titanacyclobutane complex **139a** as brown agglomerates, spectroscopically homogeneous and identical to the material prepared above.

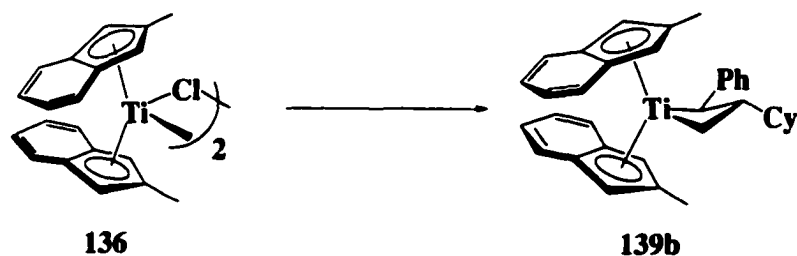
Titanacyclobutane 139b from Bis(2-methylindenyl) Cinnamyl 137:



3-Cyclohexyl-2-phenyl-bis(2-methylindenyl)titanacyclobutane 139b. In the drybox, a vial containing a THF solution (2 mL) of bis(2-methylindenyl)titanium cinnamyl **137** (23.5 mg, 0.0555 mmol), mixed with an equivalent of SmI_2 (0.60 mL, 0.1 M in THF), was cooled to $-35\text{ }^{\circ}\text{C}$. Following the addition of a cold solution of cyclohexyl iodide (7.5 μL in 1 mL THF) the reaction mixture was left to warm to room temperature and stir overnight. The solvent was removed under reduced pressure, the product was extracted into hexane, filtered through a short plug of Celite, and concentrated *in vacuo*. The concentrated solution, when cooled to $-35\text{ }^{\circ}\text{C}$, afforded a dark brown powder (16.8 mg)

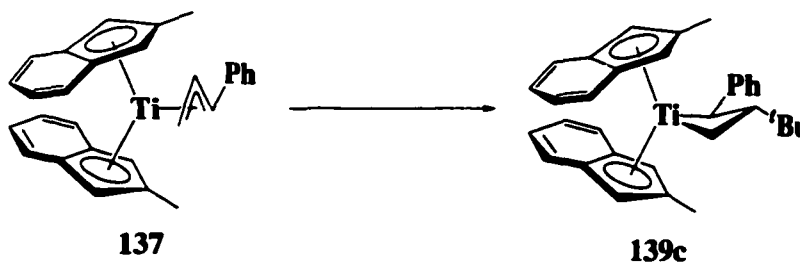
corresponding to titanacyclobutane complex **139b** (60 % yield). ^1H NMR (400 MHz, C_6D_6): δ 7.28 (dt, $J = 8.0$ Hz, 0.6 Hz, 1H, C_6H_5), 7.22 (t, $J = 9.0$ Hz, 2H, H_{aryl}), 7.21 (d, $J = 7.2$ Hz, 2H, H_{aryl}), 7.05 (ddd, $J = 8.4, 6.0, 1.5$ Hz, 1H, C_6H_5), 6.99 (d, $J = 7.8$ Hz, 2H, aryl), 6.88 (m, 3H, H_{aryl}), 6.73 (m, 2H, H_{aryl}), 5.68 (d, $J = 2.1$ Hz, 1H, H2), 5.67 (d, $J = 2.1$ Hz, 1H, H2'), 5.40 (d, $J = 1.8$ Hz, 1H, H2''), 5.34 (d, $J = 1.8$ Hz, 1H, H2'''), 3.07 (d, $J = 11.4$ Hz, 1H, α -CH), 2.00 (t, $J = 9.3$ Hz, 1H, α -CH₂), 1.85-1.74 (m, 3H, H_{cy}), 1.80 (s, 3H, CH₃), 1.67-1.59 (m, 3H, H_{cy}), 1.32 (s, 3H, CH₃), 1.21-0.98 (m, 5H, H_{cy}), 0.44 (dq, $J = 10.2, 6.0$ Hz, 1H, β -CH), 0.12 (t, $J = 9.6$ Hz, 1H, α -CH₂). GCOSY (300 Mz, C_6D_6) select data only: δ 3.07 (α -CH) \leftrightarrow δ 0.44 (β -CH); δ 2.00 (α -CH₂) \leftrightarrow δ 0.44 (β -CH) \leftrightarrow δ 0.12 (α -CH₂). ^{13}C NMR (125.3 MHz, C_6D_6): δ 155.5 (C_6H_5), 128.9 (C_{aryl}), 128.5 (C_{aryl}), 128.3 (C_{aryl}), 128.1 (C_{aryl}), 127.9 (C_{aryl}), 127.7 (C_{aryl}), 126.8 (C_{aryl}), 125.9 (C_{aryl}), 125.1₍₂₎ (C_{aryl}), 125.1₍₀₎ (C_{aryl}), 124.9 (C_{aryl}), 124.8 (C_{aryl}), 124.7 (C_{aryl}), 124.5 (C_{aryl}), 124.2₍₇₎ (C_{aryl}), 124.2₍₆₎ (C_{aryl}), 123.9 (C_{aryl}), 123.6 (C_{aryl}), 121.6 (C_{aryl}), 119.6 (C_{aryl}), 114.3 (C2), 105.5 (C2'), 102.2 (C2''), 100.9 (C2'''), 92.2 ($\underline{\text{C}}\text{H}(\text{C}_6\text{H}_5)$), 90.6 (α -CH₂), 44.3 (C_{cy}), 34.9 (C_{cy}), 32.4 (C_{cy}), 27.9 (C_{cy}), 27.6 (C_{cy}), 27.5 (C_{cy}), 22.3 (β -CH), 17.0 (CH₃), 14.3 (CH₃). HMQC (300 Mz, C_6D_6) select data only: δ 114.3 (C2) \leftrightarrow δ 5.68 (H2); δ 105.5 (C2') \leftrightarrow δ 5.67 (H2'); δ 102.2 (C2'') \leftrightarrow δ 5.40 (H2''); δ 100.9 (C2''') \leftrightarrow δ 5.34 (H2'''); δ 92.2 (α -CH) \leftrightarrow δ 3.07 (α -CH); δ 90.6 (α -CH₂) \leftrightarrow δ 2.00 (α -CH₂), δ 0.12 (α -CH₂); δ 44.3 (C_{cy}) \leftrightarrow δ 1.21-0.98 (H_{cy}); δ 34.9 (C_{cy}) \leftrightarrow δ 1.21-0.98 (H_{cy}), δ 1.67-1.59 (H_{cy}); δ 32.4 (C_{cy}) \leftrightarrow δ 1.85-1.74 (H_{cy}), δ 1.21-0.98 (H_{cy}); δ 27.9 (C_{cy}) \leftrightarrow δ 1.21-0.98 (H_{cy}); δ 27.6 (C_{cy}) \leftrightarrow δ 1.85-1.74 (H_{cy}); δ 27.5 (C_{cy}) \leftrightarrow δ 1.67-1.59 (H_{cy}); δ 22.3 (β -CH) \leftrightarrow δ 0.44 (β -CH); δ 17.0 (CH₃) \leftrightarrow δ 1.80 (CH₃); δ 14.3 (CH₃) \leftrightarrow δ 1.32 (CH₃). Elemental analysis of complex **139b** was not within tolerances.²¹

Titanacyclobutane 139b from Bis(2-methylindenyl)titanium Chloride 136:



3-Cyclohexyl-2-phenyl-bis(2-methylindenyl)titanacyclobutane 139b. In the drybox, a vial containing a THF solution (5 mL) of bis(2-methylindenyl)titanium chloride **136** (33.4 mg, 0.0977 mmol) was cooled to $-35\text{ }^{\circ}\text{C}$. An equally cold solution of cinnamyllithium (12.7 mg, 0.103 mmol in 1 mL THF) was added and the solution was allowed to warm to room temperature and stir for 1 additional hour. The reaction mixture was treated with SmI_2 (1.05 mL, 0.1 M in THF), cooled to $-35\text{ }^{\circ}\text{C}$, and treated with a cold ($-35\text{ }^{\circ}\text{C}$) solution of cyclohexyl iodide (13.3 μL in 1 mL THF). The reaction mixture was allowed to warm to room temperature and stir overnight. The solvent was removed *in vacuo*, the product extracted into a hexane/benzene mixture (5 : 1), and the extracts filtered through a short plug of Celite. The solvents were removed and the crude product recrystallized from THF layered with hexane (1 : 6) cooled to $-35\text{ }^{\circ}\text{C}$ affording titanacycle complex **139b** as a dark brown powder (13.0 mg, 26%), spectroscopically homogeneous and identical to the material prepared above.

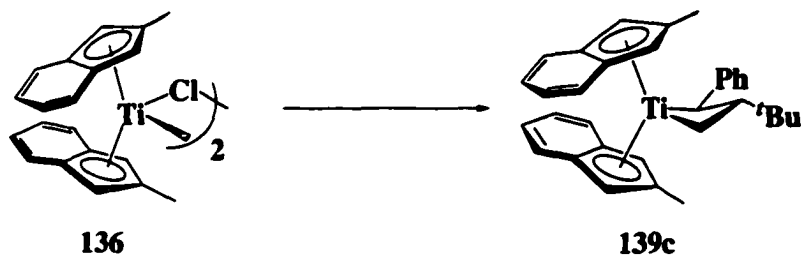
Titanacyclobutane 139c from Bis(2-methylindenyl)titanium Cinnamyl 137:



3-tert-Butyl-2-phenyl-bis(2-methylindenyl)titanacyclobutane 139c. In the drybox, a vial containing a THF solution (3 mL) of bis(2-methylindenyl)titanium cinnamyl (23.9 mg, 0.0564 mmol) and an equivalent of SmI_2 (0.60 mL, 0.1 M in THF) was cooled to -35°C . Following the addition of a cold (-35°C) solution of *tert*-butyl chloride (6.4 μL in 1 mL THF), the reaction mixture was allowed to warm to room temperature and stir overnight. The reaction stirred for six hours before the blue/green colour of the solution turned dark chocolate brown. The solvent was removed *in vacuo*, the product extracted into hexane, and filtered through a short plug of Celite. The hexane extracts were concentrated to approximately 2 mL and cooled to -35°C to afford single crystals of complex (17.2 mg, 63%, see Appendix I for crystallographic details). ^1H NMR (300 MHz, C_6D_6): δ 7.36 (dd, $J = 8.4, 0.7$ Hz, 2H, H_{aryl}), 7.05 (dd, $J = 4.8, 2.8$ Hz, 1H, H_{aryl}), 7.02 (dd, $J = 4.9, 2.8$ Hz, 1H, H_{aryl}), 6.93 – 6.80 (m, 3H, H_{aryl}), 6.70 (m, 2H, H_{aryl}), 5.88 (s, 1H, H2), 5.77 (s, 1H, H2'), 5.75 (s, 1H, H2''), 5.38 (s, 1H, H2'''), 3.94 (d, $J = 11.7$ Hz, 1H, $\alpha\text{-CH}(\text{C}_6\text{H}_5)$), 2.10 (t, $J = 9.6$ Hz, 1H, $\alpha\text{-CH}_2$), 1.72 (s, 3H, CH_3), 0.97 (s, 3H, CH_3), 0.94 (s, 9H, $\text{C}(\text{CH}_3)_3$), 0.65 (q, $J = 9.9$ Hz, 1H, $\beta\text{-CH}$), -0.094 (t, $J = 9.6$ Hz, 1H, $\alpha\text{-CH}_2$). GCOSY (300 Mz, C_6D_6) select data only: δ 3.94 ($\alpha\text{-CH}(\text{C}_6\text{H}_5)$) \leftrightarrow δ 0.65 ($\beta\text{-CH}$); δ 2.10 ($\alpha\text{-CH}_2$) \leftrightarrow δ 0.65 ($\beta\text{-CH}$) \leftrightarrow δ -0.094 ($\alpha\text{-CH}_2$). ^{13}C NMR (125.3 MHz, C_6D_6): δ = 155.3 (C_6H_5), 129.1 (C_{aryl}), 128.5 (C_{aryl}), 128.3 (C_{aryl}), 127.6 (C_{aryl}), 127.4 (C_{aryl}), 127.1 (C_{aryl}), 126.1 (C_{aryl}), 125.1 (C_{aryl}), 125.0 (C_{aryl}), 124.8 (C_{aryl}), 124.5 (C_{aryl}).

124.4 (C_{aryl}), 124.0 (C_{aryl}), 123.8 (C_{aryl}), 123.6 (C_{aryl}), 121.2 (C_{aryl}), 119.9 (C_{aryl}), 115.1 (C2), 105.2 (C2'), 104.1 (C2''), 100.7 (C2'''), 90.5 (α-CH₂), 85.6 (α-CH(C₆H₅)), 37.2 (C(CH₃)₃), 29.6 (C(CH₃)₃), 27.5 (β-CH), 16.8 (CH₃), 13.8 (CH₃). HMQC (300 Mz, C₆D₆) select data only: δ 115.1 (C2) ↔ δ 5.88 (H2); δ 105.2 (C2') ↔ δ 5.77 (H2'); δ 104.1 (C2'') ↔ δ 5.75 (H2''); δ 100.7 (C2''') ↔ δ 5.38 (H2'''); δ 90.5 (α-CH₂) ↔ δ 2.10 (α-CH₂), δ -0.094 (α-CH₂); δ 85.6 (α-CH(C₆H₅)) ↔ δ 3.94 (α-CH(C₆H₅)); δ 29.6 (C(CH₃)₃) ↔ δ 0.94 (C(CH₃)₃); δ 27.5 (β-CH) ↔ δ 0.65 (β-CH); δ 16.8 (CH₃) ↔ δ 1.72 (CH₃); δ 13.8 (CH₃) ↔ δ 0.97 (CH₃). Anal. calcd. for C₃₃H₃₆Ti: C, 82.48; H, 7.55; found: C, 82.00; H, 7.43.

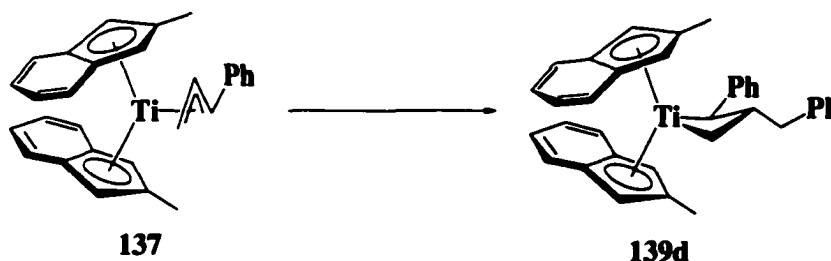
Titanacyclobutane 139c from Bis(2-methylindenyl)titanium Chloride 136:



3-tert-Butyl-2-phenyl-bis(2-methylindenyl)titanacyclobutane 139c. In the drybox, to a vial containing bis(2-methylindenyl)titanium chloride (37.2 mg, 0.109 mmol), dissolved in 3 mL THF and cooled to -35 °C, was added a cold solution (-35 °C) of cinnamylolithium (14.2 mg, 0.114 mmol in 2 mL THF). The reaction was left to warm to room temperature and stirred for 1 h. The resultant green solution was treated with an equivalent of SmI₂ (1.15 mL, 0.1 M in THF) and cooled to -35 °C. A cooled solution (-35 °C) of *tert*-butyl chloride (12.4 μL in 1 mL THF) was added to the reaction mixture, which was then left to warm to room temperature and stir overnight. The solvent was evaporated under reduced pressure and the remaining brown residue was triturated with a hexane/benzene mixture (5 : 1) and filtered through a short plug of Celite. The solvents

were removed *in vacuo* and the brown crude product was recrystallized from THF layered with pentane (1 : 6) cooled to $-35\text{ }^{\circ}\text{C}$ to afford titanacyclobutane complex **139c** as brown needles (18.2 mg) in 35% yield, spectroscopically homogeneous and identical to the material prepared above.

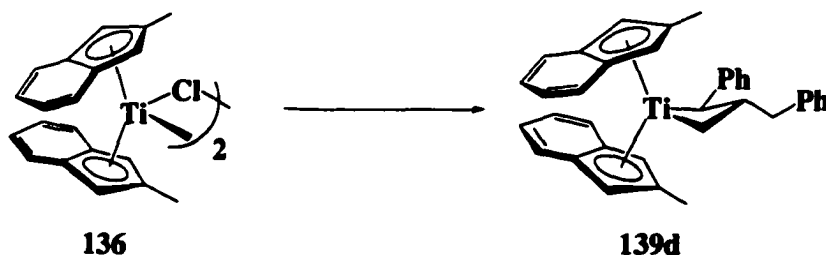
Titanacyclobutane 139d from Bis(2-methylindenyl)titanium Cinnamyl 137:



3-Benzyl-2-phenyl-bis(2-methylindenyl)titanacyclobutane 139d. In the drybox, a vial containing a THF solution (3 mL) of bis(2-methylindenyl)titanium cinnamyl **137** (22.8 mg, 0.0538 mmol) was treated with an equivalent of SmI_2 (0.60 mL, 0.1 M in THF) and cooled to $-35\text{ }^{\circ}\text{C}$. Following the addition of cold solution of benzyl chloride (6.5 μL in 1 mL THF), the reaction mixture was allowed to warm to room temperature and stir an additional 1.5 hours. Almost immediately upon warming, the blue/green colour of the solution began to dissipate, followed by the emergence of a red brown solution. The solvent was removed *in vacuo*, the residue extracted into hexane, and filtered through a short plug of Celite. The extracts were concentrated to approximately 3 mL and cooled to $-35\text{ }^{\circ}\text{C}$ to yield titanacyclobutane complex **139d** as deep red rhomboid crystals (18.2 mg, 66%). $^1\text{H NMR}$ (400.1 MHz, C_6D_6): $\delta = 7.31$ (t, $J = 7.6$ Hz, 2H, H_{aryl}), 7.20 (m, 5H, H_{aryl}), 7.10 (m, 5H, H_{aryl}), 6.99 (t, $J = 7.2$ Hz, 1H, H_{aryl}), 6.88 (m, 3H, H_{aryl}), 6.72 (d, $J = 8.4$ Hz, 1H, H_{aryl}), 6.60 (t, $J = 6.9$ Hz, 1H, H_{aryl}), 5.67 (s, 1H, H2), 5.47 (s, 1H, H2'), 5.32 (s, 1H, H2''), 5.30 (s, 1H, H2'''), 2.93 (dd, $J = 12.8, 2.9$ Hz, 1H, $\text{CH}_2(\text{C}_6\text{H}_5)$), 2.53 (d, $J = 11.4$ Hz, 1H, $\alpha\text{-CH}$), 2.04 (dd, $J = 12.7, 8.5$ Hz, 1H, $\text{CH}_2(\text{C}_6\text{H}_5)$), 1.86 (t, $J = 9.6$ Hz, 1H,

α -CH₂), 1.79 (s, 3H, CH₃), 1.30 (s, 3H, CH₃), 0.90 (m, 1H, β -CH), -0.036 (t, J = 9.4 Hz, 1H, α -CH₂). GCOSY (300 Mz, C₆D₆) select data only: δ 2.93 (CH₂(C₆H₅)) \leftrightarrow δ 2.04 (CH₂(C₆H₅)) \leftrightarrow δ 0.90 (β -CH); δ 2.53 (α -CH) \leftrightarrow δ 0.90 (β -CH); δ 1.86 (α -CH₂) \leftrightarrow δ 0.90 (β -CH) \leftrightarrow δ -0.036 (α -CH₂). ¹³C NMR (100.6 MHz, C₆D₆): δ = 154.0 (C_{aryl}), 142.2 (C_{aryl}), 130.0 (C_{aryl}), 129.0 (C_{aryl}), 128.6 (C_{aryl}), 127.4 (C_{aryl}), 126.4 (C_{aryl}), 125.9 (C_{aryl}), 125.8 (C_{aryl}), 125.3 (C_{aryl}), 125.2 (C_{aryl}), 124.9 (C_{aryl}), 124.8 (C_{aryl}), 124.7 (C_{aryl}), 124.6 (C_{aryl}), 124.4 (C_{aryl}), 124.2 (C_{aryl}), 124.1 (C_{aryl}), 122.1 (C_{aryl}), 119.6 (C_{aryl}), 113.0 (C2), 105.0 (C2'), 101.5 (C2''), 101.3 (C2'''), 92.9 (α -CH(C₆H₅)), 88.0 (α -CH₂), 39.2 (CH₂(C₆H₅)), 19.1 (β -CH), 17.0 (CH₃), 14.5 (CH₃). HMQC (300 MHz, C₆D₆) select data only: δ 113.0 (C2) \leftrightarrow δ 5.67 (H2); δ 105.0 (C2') \leftrightarrow δ 5.47 (H2'); δ 101.5 (C2'') \leftrightarrow δ 5.32 (H2''/H2'''); δ 101.3 (C2''') \leftrightarrow δ 5.32 (H2''/H2'''); δ 92.9(α -CH(C₆H₅)) \leftrightarrow δ 2.53 (α -CH); δ 88.0 (α -CH₂) \leftrightarrow δ 1.86 (α -CH₂), δ -0.036 (α -CH₂); δ 39.2 (CH₂(C₆H₅)) \leftrightarrow δ 2.93 (CH₂(C₆H₅)), δ 2.04 (CH₂(C₆H₅)); δ 19.1 (β -CH) \leftrightarrow δ 0.90 (β -CH); δ 17.0 (CH₃) \leftrightarrow δ 1.79 (CH₃); δ 14.5 (CH₃) \leftrightarrow δ 1.30 (CH₃). Anal. calcd. for (C₄₀H₄₂Ti): C, 84.19; H, 7.41; found C, 84.00; H, 7.23.

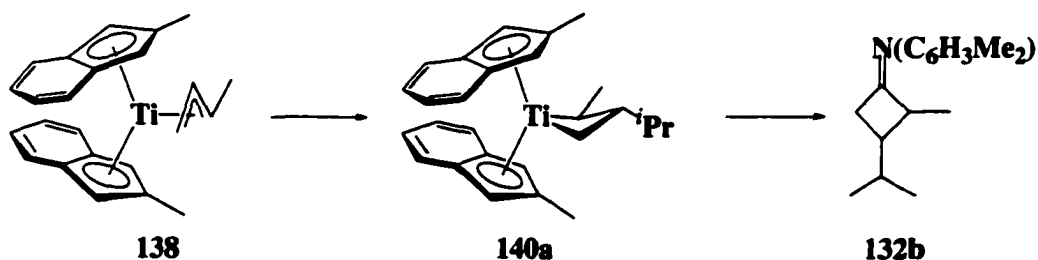
Titanacyclobutane 139d from Bis(2-methylindenyl)titanium Chloride 136:



3-Benzyl-2-phenyl-bis(2-methylindenyl)titanacyclobutane 139d: In the drybox, to bis(2-methylindenyl)titanium chloride 136 (36.8 mg, 0.107 mmol), dissolved in 3 mL THF and cooled to -35 °C, was added a cold solution (-35 °C) of cinnamyl lithium (14.0 mg, 0.113 mmol in 1 mL THF). The reaction was left to warm to room temperature and

stirred for 1 h. The resultant green solution was treated with an equivalent of SmI_2 (1.15 mL, 0.1 M in THF) and cooled to $-35\text{ }^\circ\text{C}$. After adding a cold solution ($-35\text{ }^\circ\text{C}$) of benzyl chloride (13.0 μL in 1 mL THF), the reaction was left to stir at room temperature for 3 h. Within 0.5 h the blue/green colour of the solution began to dissipate followed by the emergence of a red-brown solution. The solvent was removed under reduced pressure, the brown residue triturated with hexane, and the hexane extracts filtered through a short plug of Celite. The hexane extracts were concentrated to approximately 3 mL and cooled to $-35\text{ }^\circ\text{C}$ to crystallize titanacyclobutane complex **139b** as deep red rhomboid crystals (17.9 mg) in 33 % yield, spectroscopically homogeneous and identical to the material prepared above.

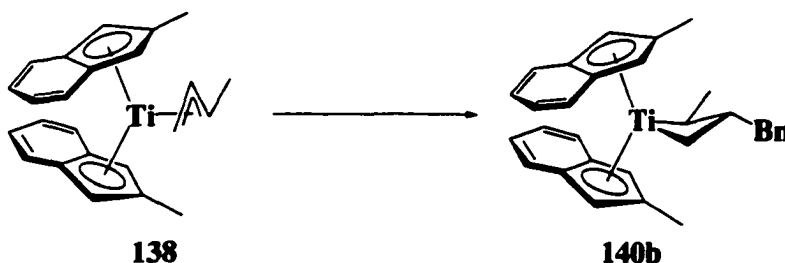
Derivatization of 3-Isopropyl-2-methyl Bis(2-methylindenyl)titanacyclobutane 140a with 2,6-Dimethylphenylisonitrile: Detection of N-[*trans*-(3-Isopropyl-2-methyl)-1-cyclobutylidene]-N-[2,6-dimethylphenyl]amine 132b.



3-Isopropyl-2-methyl-bis(2-methylindenyl)titanacyclobutane 140a. In the drybox, a vial containing a THF solution (2 mL) of bis(2-methylindenyl)titanium crotyl **138** (23.7 mg, 0.0655 mmol) and SmI_2 (0.69 mL, 0.1 M in THF) cooled to $-35\text{ }^\circ\text{C}$ was treated with a cold ($-35\text{ }^\circ\text{C}$) THF solution (1 mL) of isopropyl iodide (6.9 μL , 0.0690 mmol). After allowing the reaction to stir at room temperature for 5 minutes, the reaction mixture was poured onto 10 mL of cold ($-35\text{ }^\circ\text{C}$) pentane, filtered, and treated with a cold solution of 2,6-dimethylphenylisonitrile (25.7 mg, 0.196 mmol in 5 mL THF). After stirring for one

hour at room temperature, the solvents were removed under reduced pressure and ^1H NMR spectroscopy performed on the crude residue. Signals diagnostic of cyclobutanimine **132b** were clearly evident, however, due to difficulty in purification, no yield could be determined.

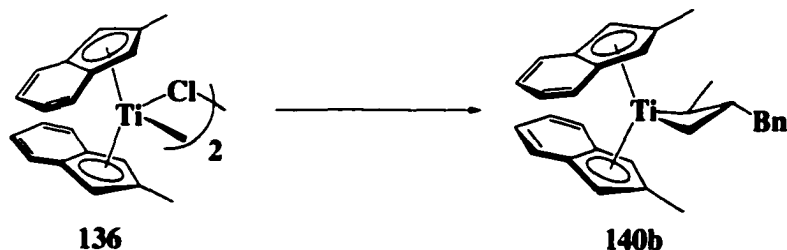
Titanacyclobutane 140b from Bis(2-methylindenyl)titanium Crotyl 138:



3-Benzyl-2-methyl-bis(2-methylindenyl)titanacyclobutane 140b. In the drybox, a vial containing a THF solution (2 mL) of bis(2-methylindenyl)titanium crotyl **138** (36.2 mg, 0.100 mmol) and one equivalent of SmI_2 (1.05 mL, 0.1 M in THF), was cooled to $-35\text{ }^\circ\text{C}$. A cooled ($-35\text{ }^\circ\text{C}$) solution of benzyl chloride (12.0 μL in 1 mL THF) was added to the reaction mixture which was subsequently left to warm to room temperature and stir 0.5 h. The colour of the solution quickly turned from blue/green to grey to red. The solvent was removed *in vacuo*, the red residue extracted into pentane, and the resultant solution filtered through a short plug of Celite. The pentane solution was concentrated to approximately 2 mL and cooled to $-35\text{ }^\circ\text{C}$ to yield titanacycle complex **140b** as thermally unstable dark red agglomerated prisms (21.9 mg, 48%). ^1H NMR (400 MHz, C_6D_6): 7.20 (m, 5H, H_{aryl}), 7.11 (m, 1H, H_{aryl}), 7.02 (m, 1H, H_{aryl}), 6.83 (m, 4H, H_{aryl}), 6.60 (dd, $J = 8.2, 6.8$ Hz, 2H, H_{aryl}), 5.88 (d, $J = 1.4$ Hz, 1H, H2), 5.43 (d, $J = 1.5$ Hz, 1H, H2'), 5.31 (d, $J = 1.5$ Hz, 1H, H2''), 5.16 (d, $J = 1.5$ Hz, 1H, H2'''), 2.96 (dd, $J = 12.6, 4.0$ Hz, 1H, $\text{CH}_2(\text{C}_6\text{H}_5)$), 2.21 (dd, $J = 12.7, 8.7$ Hz, 1H, $\text{CH}_2(\text{C}_6\text{H}_5)$), 1.88 (t, $J = 9.7$ Hz, 1H, $\alpha\text{-CH}_2$),

1.87 (obscured signal, 1H, α -CH(CH₃)), 1.78 (s, 3H, CH₃), 1.65 (d, J = 6.9 Hz, 1H, α -CH(CH₃)), 1.63 (s, 3H, CH₃), 0.015 (t, J = 10.4 Hz, 1H, α -CH₂), -0.17 (m, 1H, β -CH). GCOSY (300 Mz, C₆D₆) select data only: δ 2.96 (CH₂(C₆H₅)) \leftrightarrow δ 2.21 (CH₂(C₆H₅)) \leftrightarrow δ -0.17 (β -CH); δ 1.88 (α -CH₂) \leftrightarrow δ 0.015 (α -CH₂) \leftrightarrow δ -0.17 (β -CH); δ 1.87 (α -CH(CH₃)) \leftrightarrow δ 1.65 (α -CH(CH₃)), δ -0.17 (β -CH). ¹³C NMR (100.6 MHz, C₆D₆): δ 142.4 (C_{aryl}), 129.9 (C_{aryl}), 128.4 (C_{aryl}), 126.0 (C_{aryl}), 125.7 (C_{aryl}), 124.6 (C_{aryl}), 124.2 (C_{aryl}), 123.8 (C_{aryl}), 123.5 (C_{aryl}), 123.3 (C_{aryl}), 123.2 (C_{aryl}), 123.0 (C_{aryl}), 122.8 (C_{aryl}), 119.5 (C_{aryl}), 107.4 (C2), 104.4 (C2'), 103.7 (C2''), 100.3 (C2'''), 92.4 (α -CH(CH₃)), 87.1 (α -CH₂), 40.8 (α -CH₂(C₆H₅)), 26.4 (α -CH(CH₃)), 25.0 (β -CH), 16.5 (CH₃), 14.9 (CH₃). HMQC (300 Mz, C₆D₆): select data only δ 107.4 (C2) \leftrightarrow δ 5.88 (H2); δ 104.4 (C2') \leftrightarrow δ 5.31 (H2''); δ 103.7 (C2'') \leftrightarrow δ 5.16 (H2'''); δ 100.3 (C2''') \leftrightarrow δ 5.43 (H2'); δ 92.4 (α -CH(CH₃)) \leftrightarrow δ 1.87 (α -CH(CH₃)); δ 87.1 (α -CH₂) \leftrightarrow δ 1.88 (α -CH₂), δ 0.015 (α -CH₂); δ 40.8 (α -CH₂(C₆H₅)) \leftrightarrow δ 2.96 (CH₂(C₆H₅)), δ 2.21 (CH₂(C₆H₅)); δ 26.4 (α -CH(CH₃)) \leftrightarrow δ 1.65 (α -CH(CH₃)); δ 25.0 (β -CH) \leftrightarrow δ -0.17 (β -CH); δ 16.5 (CH₃) \leftrightarrow δ 1.78 (CH₃); δ 14.9 (CH₃) \leftrightarrow δ 1.63 (CH₃). HRMS calcd. for C₃₁H₃₂Ti m/z 452.79381; not found, calculated for C₂₀H₁₈TiC₄H₇ (bis(2-methylindenyl)titanium crotyl): m/z 361.12359, found 361.14338; for C₂₀H₁₈Ti (bis(2-methylindenyl)titanium): 306.08881; found, 306.08915 (100%). Anal. calc. for C₃₁H₃₂Ti: C, 82.29; H, 7.13; found (trial 1): C, 80.72; H, 7.45; trial 2: C, 80.97; H, 7.43.²¹

Titanacyclobutane 140b from Bis(2-methylindenyl)titanium Chloride 136:



3-Benzyl-2-methyl-bis(2-methylindenyl)titanacyclobutane 140b. In the drybox, a vial containing a THF solution (2 mL) of bis(2-methylindenyl)titanium chloride **136** (37.2 mg, 0.109 mmol), cooled to $-35\text{ }^{\circ}\text{C}$, was treated with an equivalent of crotylmagnesium chloride (70.1 μL , 1.63 M in THF). The reaction mixture was left to warm to room temperature and stir one additional hour. After the addition of one equivalent of SmI_2 (1.15 mL, 0.1 M in THF), the reaction was re-cooled to $-35\text{ }^{\circ}\text{C}$ and treated with a cold ($-35\text{ }^{\circ}\text{C}$) solution of benzyl chloride (13.2 μL in 1 mL THF). The reaction mixture was allowed to warm to room temperature and stir 0.5 hours. Under reduced pressure, the solvent was removed from the reaction mixture and the residue triturated with pentane and filtered through a plug of Celite. Concentrating and cooling ($-35\text{ }^{\circ}\text{C}$) the pentane extracts afforded deep purple mounds (15.0 mg, 30 %) of titanacyclobutane complex **140b**, spectroscopically homogeneous and identical to the material prepared above.

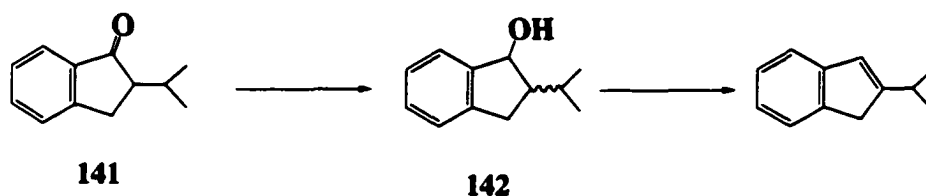
2-Isopropyl-1-indanone 141 from 1-Indanone:



2-Isopropyl-1-indanone 141. In a 200 mL Schlenk flask under an inert atmosphere, 1-indanone (4.88 g, 37.0 mmol) was dissolved in 100 mL dry THF and cooled to $-78\text{ }^{\circ}\text{C}$.

In a separate 500 mL Schlenk flask, potassium *t*-butoxide (4.60 g, 41.0 mmol) was suspended in 100 mL dry THF and cooled to $-78\text{ }^{\circ}\text{C}$. Over the course of 1 hour, the indanone was added to the potassium *t*-butoxide solution via cannula. After stirring 4 h at $-78\text{ }^{\circ}\text{C}$, 2-iodopropane (5.0 mL, 50 mmol) was added and the reaction mixture left to warm slowly to room temperature and stir overnight. The following morning, the deep blue solution was quenched with 100 mL H_2O . The product was extracted with diethyl ether (3 x 100 mL), washed with brine, and dried over magnesium sulfate. Purification by column chromatography (10 % ethyl acetate/hexane) afforded **141** as a pale yellow oil (3.50 g, 54%). ^1H NMR (400.1 MHz, CDCl_3): δ 7.73 (d, $J = 7.7$ Hz, 1H, H4), 7.56 (dt, $J = 7.5$ Hz, 1.2 Hz, 1H, H5), 7.46 (dt, $J = 7.7$ Hz, 0.92 Hz, 1H, H4'), 7.34 (dt, $J = 7.7$ Hz, 0.70 Hz, 1H, H5'), 3.14 (dd, $J = 18.5$ Hz, 8.1 Hz, 1H, CH_2), 2.92 (dd, $J = 17.4$ Hz, 4.0 Hz, 1H, CH_2), (dt, $J = 8.1$ Hz, 4.2 Hz, 1H, H1), 2.41 (dseptets, $J = 4.4$ Hz, 6.9 Hz, 1H, $\text{CH}(\text{CH}_3)_2$), 1.04 (d, $J = 6.9$ Hz, 3H, $\text{CH}(\text{CH}_3)_2$), 0.78 (d, $J = 6.8$ Hz, 3H, $\text{CH}(\text{CH}_3)_2$). ^{13}C NMR (100.6 MHz, CDCl_3): δ 208.8, 154.1, 137.6, 134.5, 127.2, 126.4, 123.6, 53.1, 29.0, 28.3, 20.8, 17.3. IR (cm^{-1} , CHCl_3 cast): 1709 (C=O); HRMS calcd. for: $\text{C}_{12}\text{H}_{14}\text{O}$ m/z 174.10458, found 174.10458.

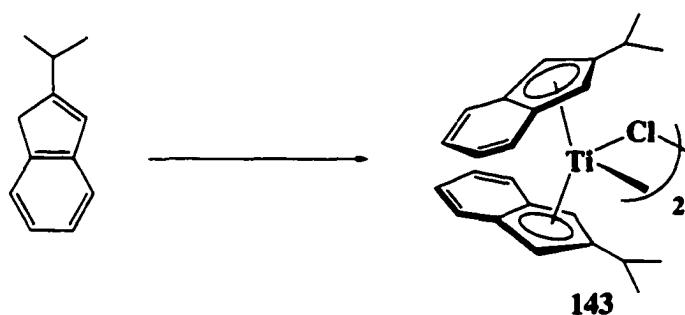
2-Isopropylindene from 2-Isopropyl-1-indanone **141**:



2-Isopropylindene. In a 50 mL round bottomed flask, 2-isopropyl-1-indanone (0.76 g, 4.36 mmol) was dissolved in 25 mL methanol. Sodium borohydride (1.45 g, 43.6 mmol) was added slowly to the flask. The reaction mixture was left to stir for 3 h and then quenched with 10% HCl. The organic product, 2-isopropylindanol **142**, was extracted

into ether, washed with brine and dried with magnesium sulfate. Compound **142** was further purified by column chromatography (10 % ethyl acetate/hexanes), dissolved in 50 mL benzene, treated with a catalytic amount of *p*-toluenesulfonic acid (1 mg) and heated to reflux for 3 h. The solvent was removed under reduced pressure and the crude residue purified by column chromatography (hexane) to afford 2-isopropylindene as a colourless oil (0.69 g, 86%) spectroscopically homogeneous and identical to the material reported.¹⁵

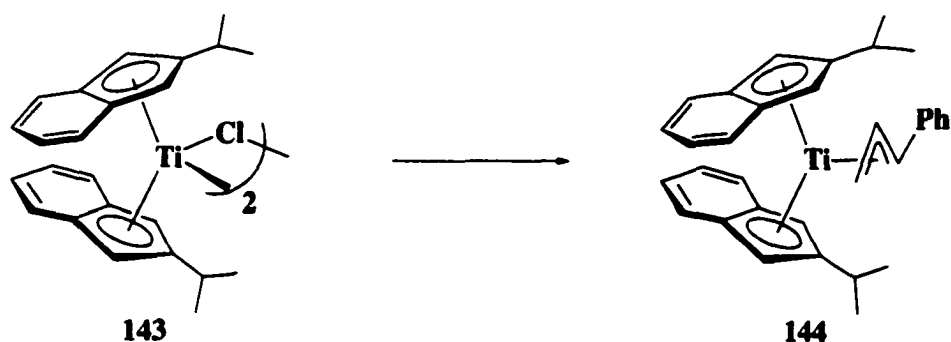
Bis(2-isopropylindenyl)titanium Chloride 143 from 2-Isopropylindene:



Bis(2-isopropylindenyl)titanium chloride 143. In a Schlenk flask, under an inert atmosphere, 2-isopropylindene (2.30 g, 14.5 mmol) was dissolved in 30 mL THF and cooled to $-78\text{ }^{\circ}\text{C}$. *n*-Butyllithium (15.3 mmol, 2.5 M) was added dropwise by syringe and the reaction was stirred at $-78\text{ }^{\circ}\text{C}$ for 3 h, warmed to room temperature to stir for an additional 2 h, and re-cooled to $-78\text{ }^{\circ}\text{C}$. In a separate Schlenk flask, $\text{TiCl}_3 \cdot 3\text{THF}$ (2.55 g, 6.88 mmol) was suspended in 40 mL THF and cooled to $-78\text{ }^{\circ}\text{C}$. The solution of 2-isopropylindenyllithium was transferred at $-78\text{ }^{\circ}\text{C}$ via cannula onto the titanium solution and left to warm slowly to room temperature. After 12 h, the solvent was removed under reduced pressure from the deep green solution and dried extensively (3 days at 0.5 mm Hg), yielding a red-brown residue. The product was extracted into benzene and filtered through a sintered glass funnel layered with a short plug of Celite. The benzene was

removed under reduced pressure and the residual solid was precipitated from THF/hexane (1 : 2) at -35 °C yielding complex **143** as an amorphous burgundy red solid (2.14 g, 78%). HRMS calcd. for: $C_{22}H_{26}Ti^{35}Cl$ m/z 397.12024, found 397.11973 (100%); $C_{22}H_{26}Ti^{37}Cl$ m/z 399.11731, found 399.11792. Anal. calcd. for $C_{22}H_{26}TiCl$: C, 72.46; H, 6.59; found C, 72.16, H, 6.74.

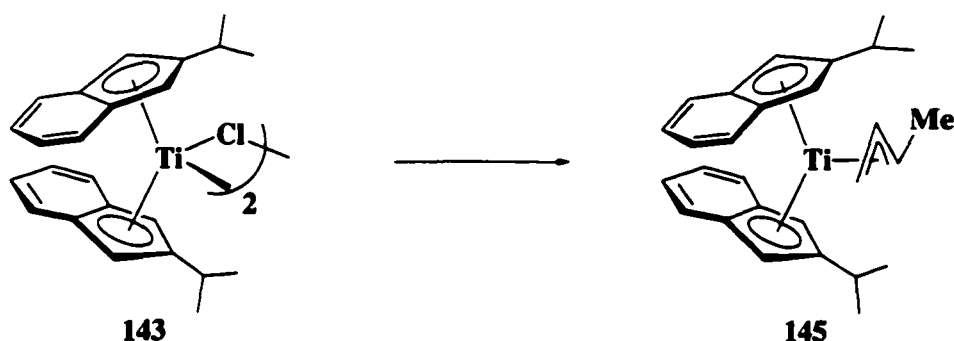
Bis(2-isopropylindenyl)titanium Cinnamyl **144 from Bis(2-isopropylindenyl)titanium Chloride **143**:**



Bis(2-isopropylindenyl)titanium(η^3 -1-phenylallyl) **144.** In the drybox, to a vial containing a THF solution (10 mL) of bis(2-isopropylindenyl)titanium chloride **143** (304 mg, 0.764 mmol) cooled to -35 °C was added a cold (-35 °C) THF solution (5 mL) of cinnamyllithium (104 mg, 0.840 mmol). Instantaneously, the colour of the solution turned from red/brown to emerald green. After stirring an additional 3 h at room temperature, the THF was removed under reduced pressure, leaving a dark green residue. The product was extracted into benzene and filtered through a sintered glass funnel layered with a short plug of Celite. The benzene was removed in *vacuo* and the resulting solid was crystallized from THF layered with hexane (1 : 2) cooled to -35° C, affording bright green diamond-shaped crystals of cinnamyl complex **144** (244 mg, 67%). IR

(cm^{-1} , THF cast): 2958 (m), 2924 (w), 2867 (w), 2837 (m), 1592 (w), 1535 (w), 1457 (w), 1358 (w), 1332 (w), 1302 (w), 1277 (w), 1254 (w), 1204 (w), 1170 (w), 1102 (m), 1070 (m), 897 (w), 847 (m), 832 (m), 800 (s), 743 (s), 718 (m), 695 (m), 668 (m). LRMS calcd. for $\text{C}_{33}\text{H}_{35}\text{Ti}$ m/z 479.2, found 479.2 (100%). Anal. calcd.: C, 82.66; H, 7.36; found C, 81.87; H, 7.46.²¹

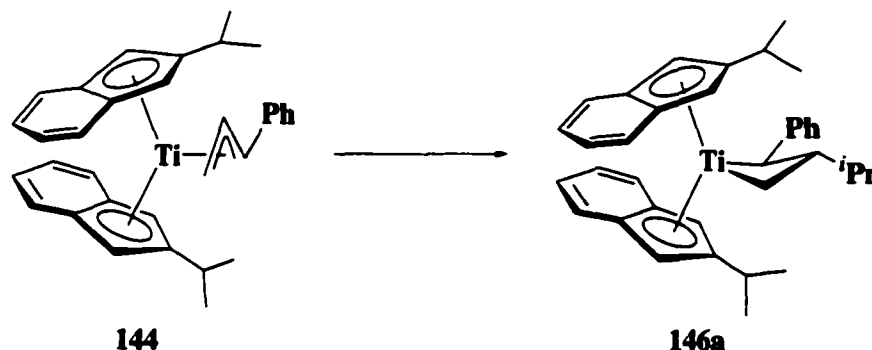
Bis(2-isopropylindenyl)titanium Crotyl 145 from Bis(2-isopropylindenyl)titanium Chloride 143:



Bis(2-isopropylindenyl)titanium(η^3 -1-methylallyl) 145. In the drybox, a vial containing a THF solution (5 mL) of bis(2-isopropylindenyl)titanium chloride **143**, (304 mg, 0.764 mmol) was cooled to $-35\text{ }^\circ\text{C}$ and treated with cold ($-35\text{ }^\circ\text{C}$) crotylmagnesium chloride (0.516 mL, 1.63 M in THF) further diluted in THF (3 mL). The resultant solution was left to warm to room temperature and stir for an additional 3 h. The colour of the solution turned from red/brown to army green over the course of 5 minutes. Removal of the THF in *vacuo* gave a dark green residue that was triturated with hexane and filtered through a sintered glass funnel layered with a short plug of Celite. The hexane was removed under reduced pressure and the residue was recrystallized from THF/hexane (1 : 3) cooled to $-35\text{ }^\circ\text{C}$ to afford dark green prisms of crotyl complex **145** suitable for X-ray crystallography (267 mg, 83%, crystallographic detail is given in Appendix I). IR (cm^{-1} , hexane cast): 3036 (w), 2958 (s), 2925 (m), 2868 (m), 1695 (w),

1685(w), 1652 (w), 1644 (w), 1606 (w), 1538 (w), 1456 (m), 1381 (m), 1359 (m), 1335 (w), 1260 (m), 1205 (m), 1170 (m), 1108 (m), 1078 (m), 1023 (m), 950 (w), 837 (m), 818 (s), 743 (s), 665 (w). Anal. calcd.: C, 80.56; H, 7.97; found C, 80.18; H, 8.25.

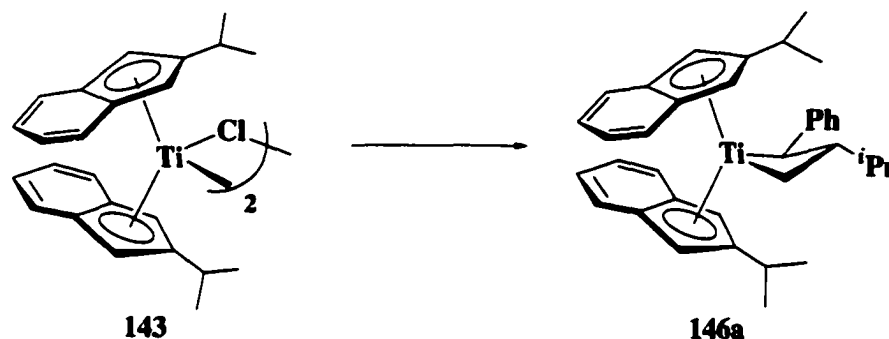
Titanacyclobutane 146a from Bis(2-isopropylindenyl)titanium Cinnamyl 144:



3-Isopropyl-2-phenyl-bis(2-isopropylindenyl)titanacyclobutane 146a. In the drybox, a vial containing a THF solution (2 mL) of bis(2-isopropylindenyl)titanium cinnamyl **144** (32.7 mg, 0.0682 mmol) and one equivalent of SmI₂ (0.72 mL, 0.1 M in THF) was cooled to -35 °C. Following the addition of a cold (-35 °C) solution of isopropyl iodide (7.3 μL in 1 mL THF) the reaction mixture was allowed to warm to room temperature and stir an additional 6 h. After approximately 4 h, the blue/green colour of the solution dissipated into a dark chocolate brown solution with the formation of trace amounts of Sm(III) precipitate. The solvent was removed *in vacuo*, the residue extracted with hexane, and the resultant solution filtered through a short plug of Celite. The hexane solution was concentrated to approximately 3 mL and cooled to -35 °C to yield the titanacyclobutane complex **146a** as dark brown rhomboid crystals (30.7 mg, 86%). ¹H NMR (400 MHz, C₆D₆, RT): δ 7.32 (t, J = 7.9 Hz, 2H, H_{aryl}), 7.23 (m, 3H, H_{aryl}), 7.03 – 6.87 (m, 6H, H_{aryl}), 6.73 (t, J = 8.0 Hz, 1H, C₆H₅), 6.56 (br d, J = 7.3 Hz, 1H, C₆H₅), 5.91 (br s, 1H, H2), 5.64 (br s with a shoulder, 2H, H2', H2''), 5.52 (br s, 1H, H2'''), 2.71 (t, J = 9.1 Hz, 1H, α-

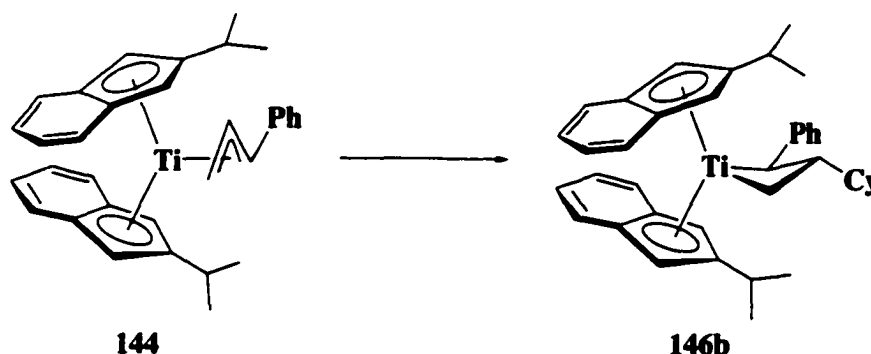
CH_2), 2.68 (m, 2H, $\alpha\text{-CH}$, $\text{CH}(\text{CH}_3)_2$), 2.19 (m, 1H, $\text{CH}(\text{CH}_3)_2$), 1.38 (dseptet, $J = 13.4$, 6.8 Hz, 1H, $\text{CH}(\text{CH}_3)_2$), 1.05 (d, $J = 7.0$ Hz, 3H, $\text{CH}(\text{CH}_3)_2$), 1.03 (d, $J = 7.7$ Hz, 3H, $\text{CH}(\text{CH}_3)_2$), 0.97 (d, $J = 6.6$ Hz, 3H, $\text{CH}(\text{CH}_3)_2$), 0.89 (d, $J = 6.7$ Hz, 3H, $\text{CH}(\text{CH}_3)_2$), 0.52 (d, $J = 6.8$ Hz, 3H, $\text{CH}(\text{CH}_3)_2$), 0.41 (br s, 1H, $\beta\text{-CH}$), 0.054 (br s, 1H, $\alpha\text{-CH}_2$). GCOSY (300 MHz, C_6D_6) select data only: δ 2.71 ($\alpha\text{-CH}_2$) \leftrightarrow δ 0.41 ($\beta\text{-CH}$) \leftrightarrow δ 0.054 ($\alpha\text{-CH}_2$); 2.68 ($\alpha\text{-CH}$) \leftrightarrow δ 0.41 ($\beta\text{-CH}$); δ 2.68 ($\text{CH}(\text{CH}_3)_2$) \leftrightarrow δ 1.05 ($\text{CH}(\text{CH}_3)_2$), 0.97 ($\text{CH}(\text{CH}_3)_2$); δ 2.19 ($\text{CH}(\text{CH}_3)_2$) \leftrightarrow δ 1.03 ($\text{CH}(\text{CH}_3)_2$), 0.52 ($\text{CH}(\text{CH}_3)_2$); δ 0.41 ($\beta\text{-CH}$) \leftrightarrow δ 1.38 ($\text{CH}(\text{CH}_3)_2$) \leftrightarrow δ 0.98 ($\text{CH}(\text{CH}_3)_2$), 0.89 ($\text{CH}(\text{CH}_3)_2$). ^1H NMR (400 MHz, C_6D_6 , 70 °C): δ 7.34 (d, $J = 8.2$ Hz, 2H, H_{aryl}), 7.21 (m, 2H, H_{aryl}), 7.00 (t, $J = 7.8$ Hz, 1H, H_{aryl}), 6.94 (m, 2H, H_{aryl}), 6.91 (m, 2H, H_{aryl}), 6.70 (t, $J = 7.8$ Hz, 1H, C_6H_5), 6.55 (d, $J = 8.4$ Hz, 1H, C_6H_5), 5.94 (s, 1H, H2), 5.68 (s, 1H, H2'), 5.62 (s, 2H, H2'', H2'''), 2.71 (m, 2H, $\text{CH}(\text{CH}_3)_2$, $\alpha\text{-CH}_2$), 2.63 (d, $J = 11.2$ Hz, 1H, $\alpha\text{-CH}(\text{C}_6\text{H}_5)$), 2.23 (septet, $J = 6.8$ Hz, 1H, $\text{CH}(\text{CH}_3)_2$), 1.43 (dseptet, $J = 13.4$, 6.8 Hz, 1H, $\text{CH}(\text{CH}_3)_2$), 1.07 (d, $J = 6.8$ Hz, 3H, $\text{CH}(\text{CH}_3)_2$), 1.04 (d, $J = 6.9$ Hz, 3H, $\text{CH}(\text{CH}_3)_2$), 1.00 (d, $J = 6.8$ Hz, 3H, $\text{CH}(\text{CH}_3)_2$), 0.93 (d, $J = 6.6$ Hz, 3H, $\text{CH}(\text{CH}_3)_2$), 0.86 (d, $J = 6.7$ Hz, 3H, $\text{CH}(\text{CH}_3)_2$), 0.52 (d, $J = 6.7$ Hz, 3H, $\text{CH}(\text{CH}_3)_2$), 0.45 (partially obscured dq, $J = 9.9$, 7.1 Hz, 1H, $\beta\text{-CH}$), 0.042 (t, $J = 9.3$ Hz, 1H, $\alpha\text{-CH}_2$). ^{13}C NMR (400 MHz, C_6D_6 , RT): δ 155.5, 141.2, 128.6, 127.4, 127.1, 126.9, 125.6, 125.5, 125.2, 124.6, 124.4, 124.3, 124.0, 121.7, 104.0, 94.5, 30.1, 29.8, 28.9, 25.8, 25.1, 24.6, 23.9, 22.4, 21.6, 20.9. ^{13}C NMR (400 MHz, C_6D_6 , 70 °C): δ 155.5, 141.4, 139.9, 126.9, 125.6, 125.4, 125.2, 125.1, 124.7, 124.3, 124.0, 121.9, 120.8, 109.2, 104.1, 101.5, 100.1, 94.6, 86.7, 34.2, 29.8, 29.0, 25.6, 25.0, 24.8, 23.7, 22.5, 22.2, 21.4, 21.1. Anal. calcd. C, 82.73; H, 8.10; found C, 82.44, 8.40.

Titanacyclobutane 146a from Bis(2-isopropylindenyl)titanium Chloride 143:



3-Isopropyl-2-phenyl-bis(2-isopropylindenyl)titanacyclobutane 146a. In the drybox, a vial containing a THF solution (5 mL) of bis(2-isopropylindenyl)titanium chloride 143 (38.9 mg, 0.0978 mmol) was cooled to $-35\text{ }^{\circ}\text{C}$. Cinnamyl lithium (12.7 mg, 0.103 mmol) was dissolved in 2 mL THF and cooled to $-35\text{ }^{\circ}\text{C}$. The two solutions were mixed together, left to warm to room temperature and stirred for 1 h. One equivalent of SmI_2 (1.00 mL, 0.1 M in THF) was added via syringe into solution and the resultant green/blue solution was re-cooled to $-35\text{ }^{\circ}\text{C}$. A cold ($-35\text{ }^{\circ}\text{C}$) solution of 2-iodopropane (10.0 μL in 1 mL THF) was added to the reaction mixture that was then left to warm to room temperature and stirred for an additional 2 h. Within 1 h the blue/green colour of the solution had completely dissipated to leave a dark chocolate brown solution. The solvent was removed *in vacuo*, the brown residue was triturated with hexane, and the solution filtered through a short plug of Celite. The solution was concentrated to approximately 3 mL and cooled to $-35\text{ }^{\circ}\text{C}$ to afford titanacyclobutane complex 146a as brown rhomboid crystals (30.7 mg, 60%). The isolated material was found to be spectroscopically homogeneous and identical to the material prepared above.

Titanacyclobutane 146b from Bis(2-isopropylindenyl)titanium Cinnamyl 144:

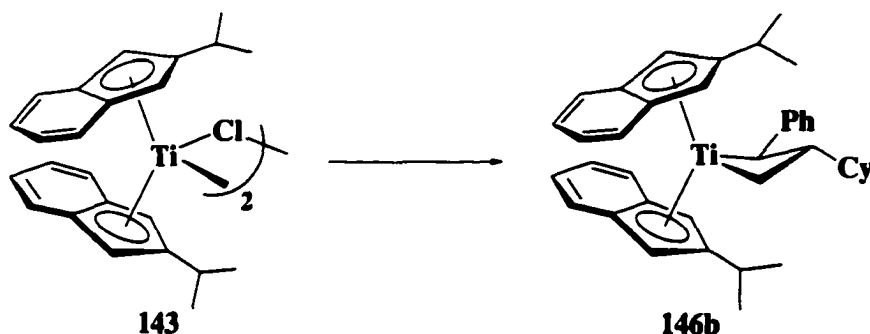


3-Cyclohexyl-2-phenyl-bis(2-isopropylindenyl)titanacyclobutane 146b. In the drybox, a vial containing a THF solution (3 mL) of bis(isopropylindenyl)titanium cinnamyl **144** (36.0 mg, 0.751 mmol) mixed with an equivalent of SmI_2 (0.79 mL, 0.1 M in THF), was cooled to $-35\text{ }^\circ\text{C}$. Following the addition of a cold ($-35\text{ }^\circ\text{C}$) solution of cyclohexyl iodide (10.2 μL in 1 mL THF) the reaction mixture was left to warm to room temperature and stir an additional 6 h, during which trace amounts of Sm(III) precipitate were formed. The solvent was removed *in vacuo*, the product was extracted into hexane, filtered through a short plug of Celite, and concentrated *in vacuo*. The concentrated solution, when cooled to $-35\text{ }^\circ\text{C}$, afforded dark brown rhomboid crystals (28.8 mg) of complex **146b** in 68 % yield. $^1\text{H NMR}$ (400 MHz, C_6D_6): δ 7.34 (t, $J = 8.0$ Hz, 2H, H4/H5, C_6H_5), 7.23 (m, 3H, H4/H5), 7.06 – 6.87 (m, 6H, H4/H5, C_6H_5), 6.74 (t, $J = 8.0$ Hz, 1H, C_6H_5), 6.55 (d, $J = 6.6$ Hz, 1H, C_6H_5), 5.92 (s, 1H, H2), 5.64 (s, 1H, H2'), 5.58 (s, 1H, H2''), 5.51 (s, 1H, H2'''), 2.75 (t, $J = 9.1$ Hz, 1H, $\alpha\text{-CH}_2$), 2.71 (septet, $J = 6.8$ Hz, 1H, $\text{CH}(\text{CH}_3)_2$), 2.38 (br m, 1H, $\alpha\text{-CH}(\text{C}_6\text{H}_5)$), 2.23 (septet, $J = 6.6$ Hz, 1H, $\text{CH}(\text{CH}_3)_2$), 1.93 (d, $J = 10.1$ Hz, 1H, H_{cy}), 1.77 (d, $J = 11.5$ Hz, 1H, H_{cy}), 1.59 (d, $J = 8.5$ Hz, 3H, H_{cy}), 1.22 - 0.94 (m, 6H, H_{cy}), 1.06 (d, $J = 5.1$ Hz, 3H, $\text{CH}(\text{CH}_3)_2$), 1.04 (d, $J = 5.1$ Hz, 3H, $\text{CH}(\text{CH}_3)_2$), 0.97 (d, $J = 6.6$ Hz, 3H, $\text{CH}(\text{CH}_3)_2$), 0.54 (d, $J = 6.7$ Hz, 3H, $\text{CH}(\text{CH}_3)_2$), 0.43

(br m, 1H, α -CH₂), 0.075 (br m, 1H, β -CH). GCOSY (300 Mz, C₆D₆) select data only: δ 2.75 (α -CH₂) \leftrightarrow δ 0.43 (α -CH₂) \leftrightarrow δ 0.075 (β -CH); δ 2.71 (CH(CH₃)₂) \leftrightarrow δ 1.06 (CH(CH₃)₂), δ 0.97 (CH(CH₃)₂); δ 2.38 (α -CH(C₆H₅)) \leftrightarrow δ 0.075 (β -CH); δ 2.23 (CH(CH₃)₂) \leftrightarrow δ 1.04 (CH(CH₃)₂), δ 0.54 (CH(CH₃)₂). ¹³C NMR (100.6 MHz, C₆D₆): δ 155.5 (C_{aryl}), 141.1 (C1), 139.5 (C1'), 125.5(C_{aryl}), 125.4 (C_{aryl}), 125.0 (C_{aryl}), 124.9 (C_{aryl}), 124.7 (C_{aryl}), 124.5 (C_{aryl}), 124.3 (C_{aryl}), 124.2 (C_{aryl}), 123.8 (C_{aryl}), 123.6 (C_{aryl}), 123.4 (C_{aryl}), 121.7 (C_{aryl}), 120.3 (C_{aryl}), 114.8 (C_{aryl}), 108.8 (C2), 103.8 (C2'), 101.1 (C2''), 99.3 (C2'''), 93.9 (CH(C₆H₅)), 87.1 (α -CH₂), 44.7 (C_{cy}), 34.7 (C_{cy}), 32.9 (C_{cy}), 29.8 (CH(CH₃)₂), 29.0 (CH(CH₃)₂), 27.8 (CH(CH₃)₂), 27.6 (C_{cy}), 27.4 (C_{cy}), 25.9 (C_{cy}), 25.3 (CH(CH₃)₂), 23.6 (β -CH), 22.4 (CH(CH₃)₂), 21.0 (CH(CH₃)₂). HMQC (300 Mz, C₆D₆) select data only: δ 108.8 (C2) \leftrightarrow δ 5.64 (H2'); δ 103.8 (C2') \leftrightarrow δ 5.92 (H2); δ 101.1 (C2'') \leftrightarrow δ 5.58 (H2''); δ 99.3 (C2''') \leftrightarrow δ 5.51 (H2'''); δ 93.9 (CH(C₆H₅)) \leftrightarrow δ 2.38 (α -CH(C₆H₅)); δ 87.1 (α -CH₂) \leftrightarrow δ 2.75 (α -CH₂), δ 0.43 (α -CH₂); δ 44.7 (C_{cy}) \leftrightarrow δ 1.22 - 0.94 (H_{cy}); δ 34.7 (C_{cy}) \leftrightarrow δ 1.59 (H_{cy}), δ 1.22 - 0.94 (H_{cy}); δ 32.9 (C_{cy}) \leftrightarrow δ 1.93 (H_{cy}), 1.22 - 0.94 (H_{cy}); δ 29.8 (CH(CH₃)₂) \leftrightarrow δ 2.71 (CH(CH₃)₂); δ 29.0 (CH(CH₃)₂) \leftrightarrow δ 2.23 (CH(CH₃)₂); δ 27.8 (CH(CH₃)₂) \leftrightarrow δ 1.06 (CH(CH₃)₂); δ 27.6 (C_{cy}) \leftrightarrow δ 1.77 (H_{cy}), δ 1.59 (H_{cy}); δ 27.4 (C_{cy}) \leftrightarrow δ 1.22 - 0.94 (H_{cy}); δ 25.9 (C_{cy}) \leftrightarrow δ 1.59 (H_{cy}), δ 1.22 - 0.94 (H_{cy}); δ 25.3 (CH(CH₃)₂) \leftrightarrow δ 1.04 (CH(CH₃)₂); δ 23.6 (β -CH) \leftrightarrow δ 0.075 (β -CH); δ 22.4 (CH(CH₃)₂) \leftrightarrow δ 0.97 (CH(CH₃)₂); δ 21.0 (CH(CH₃)₂) \leftrightarrow δ 0.54 (CH(CH₃)₂).

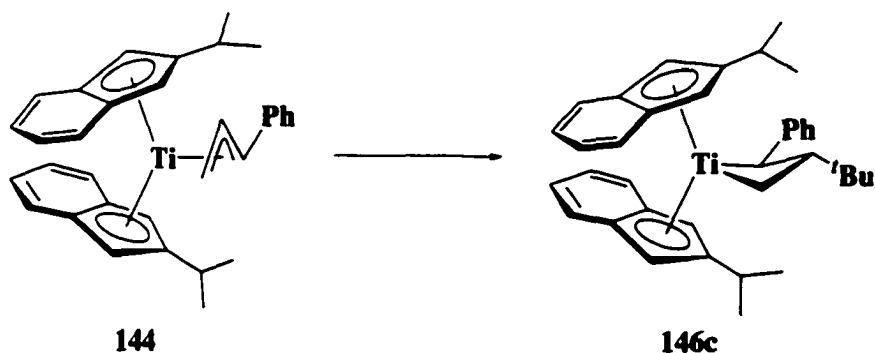
Anal. calcd.: C, 83.25; H, 8.24; found C, 82.96; H, 8.34.

Titanacyclobutane 146b from Bis(2-isopropylindenyl)titanium Chloride 143:



3-Cyclohexyl-2-phenyl-bis(2-isopropylindenyl)titanacyclobutane 146b. In the drybox, a vial containing a THF solution (5 mL) of bis(2-isopropylindenyl)titanium chloride **143** (40.8 mg, 0.102 mmol) was cooled to $-35\text{ }^{\circ}\text{C}$, treated with a cold ($-35\text{ }^{\circ}\text{C}$) solution of cinnamyl lithium (13.4 mg, 0.108 mmol in 1 mL THF), left to warm to room temperature and stirred an additional 1 h. After the addition of an equivalent of SmI_2 (1.10 mL, 0.1 M in THF), the reaction was cooled to $-35\text{ }^{\circ}\text{C}$ and treated with a cold ($-35\text{ }^{\circ}\text{C}$) solution of iodocyclohexane (13.9 μL in 1 mL THF). The reaction mixture was allowed to warm to room temperature and stir an additional 2 h. The solvent was removed *in vacuo*, the product extracted into hexane, and filtered through a short plug of Celite. The hexane extracts were concentrated to approximately 3 mL and cooled to $-35\text{ }^{\circ}\text{C}$ to afford titanacyclobutane complex **146b** as dark brown rhomboid crystals (32.2 mg, 56%), spectroscopically homogeneous and identical to the material prepared above.

Titanacyclobutane 146c from Bis(2-isopropylindenyl)titanium Cinnamyl 144:

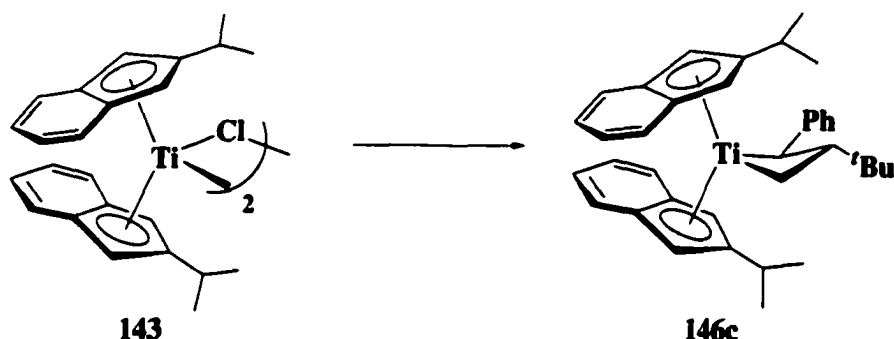


3-*tert*-Butyl-2-phenyl-bis(2-isopropylindenyl)titanacyclobutane 146c. In the drybox, a vial containing a THF solution (5 mL) of bis(2-isopropylindenyl)titanium cinnamyl **144** (23.2 mg, 0.0484 mmol), an equivalent of SmI₂ (0.51 mL, 0.1 M in THF) and a catalytic amount of bis(2-isopropylindenyl)titanium chloride (2.0 mg, 10 mol %) was cooled to -35 °C. Following the addition of a cold (-35 °C) solution of *tert*-butyl chloride (5.5 μL in 1 mL THF) the reaction mixture was allowed to warm to room temperature and stir overnight. The reaction mixture stirred for 6 h before the blue/green colour of the solution turned dark chocolate brown and precipitated trace amounts of samarium(III). The solvent was removed *in vacuo*, the product extracted into hexane, and filtered through a short plug of Celite. The hexane extracts were concentrated to approximately 2 mL and cooled to -35 °C to afford titanacyclobutane complex **146c** as brown rhomboid crystals (15.0 mg, 58%). ¹H NMR (400 MHz, C₆D₆, RT): broad signals only. ¹H NMR (400 MHz, CD₃C₆D₅, -30 °C, major conformational isomer only): δ 7.41 (m, 2H, H_{aryl}), 7.30 (m, 2H, H_{aryl}), 7.22 (d, *J* = 8.0 Hz, 1H, H_{aryl}), 7.18 – 6.85 (multiplets obscured by solvent, H_{aryl}), 6.89 (d, *J* = 7.7 Hz, 1H, H_{aryl}), 6.68 (m, 2H, H_{aryl}), 6.11 (s, 1H, H₂), 5.98 (s, 1H, H₂'), 5.84 (s, 1H, H₂"), 5.34 (s, 1H, H₂'''), 4.03 (d, *J* = 11.4 Hz, 1H, α-CH(C₆H₅)), 2.62 (m, 2H, α-CH₂, CH(CH₃)₂), 1.73 (br m, 1H, CH(CH₃)₂), 1.02 (obscured signal, 6H, CH(CH₃)₂), 0.99 (d, *J* = 6.4 Hz, 3H, CH(CH₃)₂), 0.96 (s, 9H, C(CH₃)₃), 0.33 (q, *J* = 10.8

Hz, 1H, β -CH), 0.24 (d, $J = 5.9$ Hz, 3H, $\text{CH}(\underline{\text{C}}\text{H}_3)_2$), -0.83 (t, $J = 10.2$ Hz, 1H, α - CH_2).

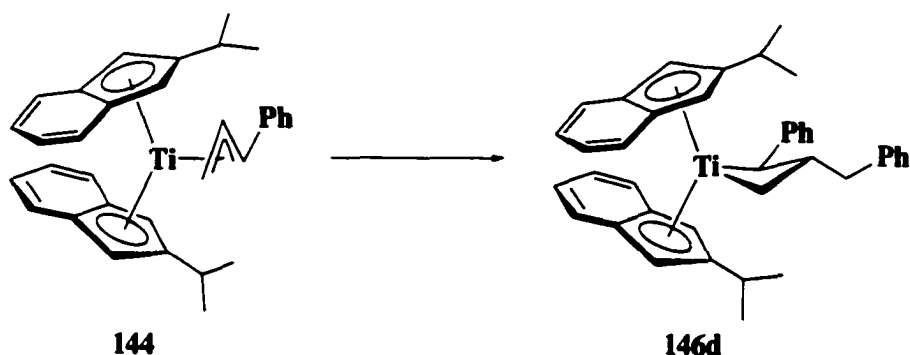
GCOSY (500 Mz, $\text{CD}_3\text{C}_6\text{D}_5$, -30 °C) select data only: δ 4.03 (α - $\text{CH}(\text{C}_6\text{H}_5)$) \leftrightarrow δ 0.33 (β -CH); 2.62 ($\underline{\text{C}}\text{H}(\text{CH}_3)_2$) \leftrightarrow δ 1.02 ($\text{CH}(\underline{\text{C}}\text{H}_3)_2$); δ 2.62 (α - CH_2) \leftrightarrow δ 0.33 (β -CH) \leftrightarrow δ -0.83 (α - CH_2); δ 1.73 ($\text{CH}(\text{CH}_3)_2$) \leftrightarrow δ 0.99 ($\text{CH}(\text{CH}_3)_2$), δ 0.24 ($\text{CH}(\text{CH}_3)_2$). ^{13}C NMR (125.3 MHz, $\text{CD}_3\text{C}_6\text{D}_5$, -30 °C): $\delta = 157.0$ (C_{aryl}), 143.3 (C_{aryl}), 128.3 (C_{aryl}), 127.7 (C_{aryl}), 127.5 (C_{aryl}), 126.5 (C_{aryl}), 125.4 (C_{aryl}), 124.3 (C_{aryl}), 123.5 (C_{aryl}), 122.7 (C_{aryl}), 122.4 (C_{aryl}), 121.6 (C_{aryl}), 121.3 (C_{aryl}), 119.3 (C_{aryl}), 114.1 (C2), 102.9 (C2'), 100.2 (C2''), 97.8 (C2'''), 90.8 (α - CH_2), 87.0 (α - $\underline{\text{C}}\text{H}(\text{C}_6\text{H}_5)$), 36.4 ($\underline{\text{C}}(\text{CH}_3)_3$), 29.9 ($\text{C}(\underline{\text{C}}\text{H}_3)_3$), 29.0 ($\underline{\text{C}}\text{H}(\text{CH}_3)_2$), 28.0 (β -CH), 26.0 ($\underline{\text{C}}\text{H}(\text{CH}_3)_2$), 23.7 ($\text{CH}(\underline{\text{C}}\text{H}_3)_2$), 23.4 ($\text{CH}(\underline{\text{C}}\text{H}_3)_2$), 23.2 ($\text{CH}(\underline{\text{C}}\text{H}_3)_2$), 22.5 ($\text{CH}(\underline{\text{C}}\text{H}_3)_2$). HMQC (500 Mz, $\text{CD}_3\text{C}_6\text{D}_5$, -30 °C) select data only: δ 114.1 (C2) \leftrightarrow δ 6.11 (H2); δ 102.9 (C2') \leftrightarrow δ 5.98 (H2'); δ 100.2 (C2'') \leftrightarrow δ 5.84 (H2''); δ 97.8 (C2''') \leftrightarrow δ 5.34 (H2'''); δ 90.8 (α - CH_2) \leftrightarrow δ 2.62 (α - CH_2), δ -0.83 (α - CH_2); δ 87.0 (α - $\underline{\text{C}}\text{H}(\text{C}_6\text{H}_5)$) \leftrightarrow δ 4.03 (α - $\underline{\text{C}}\text{H}(\text{C}_6\text{H}_5)$); δ 29.9 ($\text{C}(\underline{\text{C}}\text{H}_3)_3$) \leftrightarrow δ 0.96 ($\text{C}(\underline{\text{C}}\text{H}_3)_3$); δ 29.0 ($\underline{\text{C}}\text{H}(\text{CH}_3)_2$) \leftrightarrow δ 2.62, ($\underline{\text{C}}\text{H}(\text{CH}_3)_2$); δ 28.0 (β -CH) \leftrightarrow δ 0.33 (β -CH): δ 26.0 ($\underline{\text{C}}\text{H}(\text{CH}_3)_2$) \leftrightarrow δ 1.73 ($\underline{\text{C}}\text{H}(\text{CH}_3)_2$); δ 23.7 ($\text{CH}(\underline{\text{C}}\text{H}_3)_2$) \leftrightarrow δ 0.99 ($\text{CH}(\underline{\text{C}}\text{H}_3)_2$); δ 23.4 ($\text{CH}(\underline{\text{C}}\text{H}_3)_2$) \leftrightarrow δ 1.02 ($\text{CH}(\underline{\text{C}}\text{H}_3)_2$); δ 23.2 ($\text{CH}(\underline{\text{C}}\text{H}_3)_2$) \leftrightarrow δ 1.02 ($\text{CH}(\underline{\text{C}}\text{H}_3)_2$); δ 22.5 ($\text{CH}(\underline{\text{C}}\text{H}_3)_2$) \leftrightarrow δ 0.24 ($\text{CH}(\underline{\text{C}}\text{H}_3)_2$). Anal. calcd. for $\text{C}_{37}\text{H}_{44}\text{Ti}$: C, 82.81; H, 8.26; found (trial 1): C, 79.74; H, 8.14; (trial 2): C, 79.81; H, 8.18.²¹

Titanacyclobutane 146c from Bis(2-isopropylindenyl)titanium Chloride 143:



3-*tert*-Butyl-2-phenyl-bis(2-isopropylindenyl)titanacyclobutane 146c. In the drybox, to a vial containing bis(2-isopropylindenyl)titanium chloride (39.0 mg, 0.0980 mmol) dissolved in 3 mL THF and cooled to $-35\text{ }^{\circ}\text{C}$, was added a cold solution ($-35\text{ }^{\circ}\text{C}$) of cinnamyl lithium (12.8 mg, 0.103 mmol in 2 mL THF). The reaction mixture was left to warm to room temperature and stirred for 1 h. The resulting green solution was treated with an equivalent of SmI_2 (1.03 mL, 0.1 M in THF) and cooled to $-35\text{ }^{\circ}\text{C}$. A cooled solution ($-35\text{ }^{\circ}\text{C}$) of *tert*-butyl chloride (11.6 μL in 1 mL THF) was added to the reaction mixture which was then left to warm to room temperature and stir for an additional 4 h. The solvent was evaporated under reduced pressure and the remaining brown residue was triturated with hexane and filtered through a short plug of Celite. Concentrating the hexane extracts to approximately 3 mL and cooling to $-35\text{ }^{\circ}\text{C}$ afforded titanacyclobutane complex 146c as brown rhomboid crystals (34.3 mg) in 57% yield, spectroscopically homogeneous and identical to that prepared above.

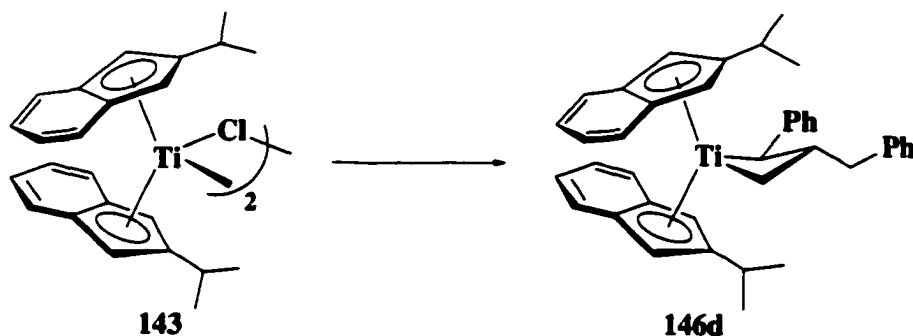
Titanacyclobutane 146d from Bis(2-isopropylindenyl)titanium Cinnamyl 144:



3-Benzyl-2-phenyl-bis(2-isopropylindenyl)titanacyclobutane 146d. In the drybox, a vial containing a THF solution (5 mL) of bis(2-isopropylindenyl)titanium cinnamyl **144** (33.7 mg, 0.0703 mmol) was treated with an equivalent of SmI₂ (0.74 mL, 0.1 M in THF) and cooled to -35 °C. Following the addition of a cold (-35 °C) solution of benzyl chloride (8.5 μL in 1 mL THF), the reaction mixture was left to warm to room temperature and stir an additional 2 h. Almost immediately, the blue/green colour of the solution turned red/brown, depositing trace amounts of Sm(III) precipitate. The solvent was removed *in vacuo*, the brown residue extracted into hexane, and filtered through a short plug of Celite. The extracts were concentrated to approximately 3 mL and cooled to -35 °C to yield titanacycle complex **146d** as deep red rhomboid crystals (37.6 mg, 84%). ¹H NMR (400.1 MHz, C₆D₆): δ = 7.32 (t, *J* = 7.0 Hz, H_{aryl}), 7.26 (d, *J* = 8.4 Hz, 1H, H_{aryl}), 7.20 (m, 5H, H_{aryl}), 7.09 (m, 3H, H_{aryl}), 7.00 (t, *J* = 7.2 Hz, 1H, H_{aryl}), 6.91 (m, 3H H_{aryl}), 6.64 (ddd, *J* = 8.7, 6.6, 0.90 Hz, 1H, CH(C₆H₅)), 6.55 (d, *J* = 8.4 Hz, 1H, CH(C₆H₅)), 5.73 (s, 1H, H₂), 5.63 (s, 2H, H₂', H₂''), 5.17 (s, 1H, H₂''), 2.85 (dd, *J* = 12.7, 3.3 Hz, 1H, CH₂(C₆H₅)), 2.65 (septet, *J* = 6.9 Hz, 1H, CH(CH₃)₂), 2.64 (t, *J* = 9.4 Hz, 1H, α-CH₂), 2.13 (m, 3H, CH₂(C₆H₅), CH(C₆H₅), CH(CH₃)₂), 1.02 (d, *J* = 6.8 Hz, 3H, CH(CH₃)₂), 1.00 (obscured signal, 1H, β-CH), 0.99 (d, *J* = 6.9 Hz, 3H, CH(CH₃)₂), 0.94 (d, *J* = 6.7 Hz, 3H, CH(CH₃)₂), 0.50 (d, *J* = 6.7 Hz, 3H, CH(CH₃)₂), -0.014 (t, *J* = 9.0 Hz,

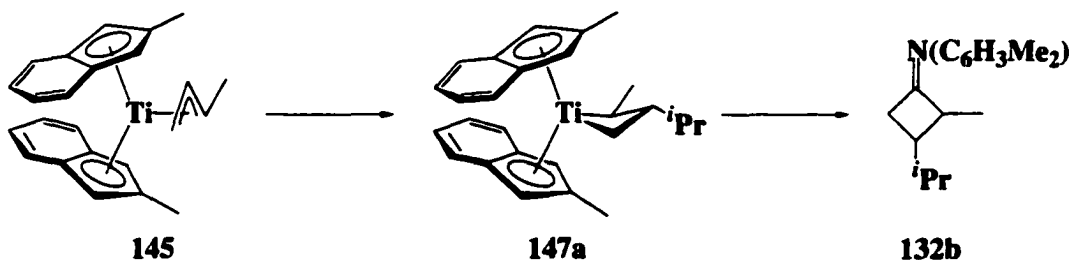
^1H , $\alpha\text{-CH}_2$). GCOSY (300 Mz, C_6D_6) select data only δ 2.85 ($\text{CH}_2(\text{C}_6\text{H}_5)$) \leftrightarrow δ 2.13 ($\text{CH}_2(\text{C}_6\text{H}_5)$) \leftrightarrow δ 1.00 ($\beta\text{-CH}$); δ 2.65 ($\text{CH}(\text{CH}_3)_2$) \leftrightarrow δ 1.02 ($\text{CH}(\text{CH}_3)_2$), δ 0.94 ($\text{CH}(\text{CH}_3)_2$); δ 2.64 ($\alpha\text{-CH}_2$) \leftrightarrow δ 1.00 ($\beta\text{-CH}$) \leftrightarrow δ -0.014 ($\alpha\text{-CH}_2$); δ 2.13 ($\text{CH}(\text{CH}_3)_2$) \leftrightarrow δ 0.99 ($\text{CH}(\text{CH}_3)_2$), δ 0.50 ($\text{CH}(\text{CH}_3)_2$). ^{13}C NMR (100.6 MHz, C_6D_6): δ = 153.9 (C_{aryl}), 142.0 (C1), 141.4 (C1), 130.2 (C_{aryl}), 128.6 (C_{aryl}), 128.3 (C_{aryl}), 128.1 (C_{aryl}), 125.8 (C_{aryl}), 125.5 (C_{aryl}), 125.2 (C_{aryl}), 125.0 (C_{aryl}), 124.6 (C_{aryl}), 124.5 (C_{aryl}), 124.4 (C_{aryl}), 124.3 (C_{aryl}), 124.2 (C_{aryl}), 124.1 (C_{aryl}), 123.9 (C_{aryl}), 122.2 (C_{aryl}), 120.2 (C_{aryl}), 107.6 (C2), 103.4 (C2'), 101.7 (C2''), 99.4 (C2'''), 94.3 ($\alpha\text{-CH}(\text{C}_6\text{H}_5)$), 84.5 ($\alpha\text{-CH}_2$), 39.4 ($\text{CH}_2(\text{C}_6\text{H}_5)$), 29.7 ($\text{CH}(\text{CH}_3)_2$), 28.9 ($\text{CH}(\text{CH}_3)_2$), 25.7 ($\text{CH}(\text{CH}_3)_2$), 25.3 ($\text{CH}(\text{CH}_3)_2$), 22.2 ($\text{CH}(\text{CH}_3)_2$), 21.0 ($\text{CH}(\text{CH}_3)_2$), 20.0 ($\beta\text{-CH}$). HMQC (300 MHz, C_6D_6) select data only: δ 107.6 (C2) \leftrightarrow δ 5.63 (H2', H2''); δ 103.4 (C2') \leftrightarrow δ 5.73 (H2); δ 101.7 (C2'') \leftrightarrow δ 5.63 (H2', H2''); δ 99.4 (C2''') \leftrightarrow δ 5.17 (H2'''); δ 94.3 ($\alpha\text{-CH}(\text{C}_6\text{H}_5)$) \leftrightarrow δ 2.13 ($\text{CH}(\text{C}_6\text{H}_5)$); δ 84.5 ($\alpha\text{-CH}_2$) \leftrightarrow δ 2.64 ($\alpha\text{-CH}_2$), δ -0.014 ($\alpha\text{-CH}_2$); δ 39.4 ($\text{CH}_2(\text{C}_6\text{H}_5)$) \leftrightarrow δ 2.85 ($\text{CH}_2(\text{C}_6\text{H}_5)$), δ 2.13 ($\text{CH}_2(\text{C}_6\text{H}_5)$); δ 29.7 ($\text{CH}(\text{CH}_3)_2$) \leftrightarrow δ 2.65 ($\text{CH}(\text{CH}_3)_2$); δ 28.9 ($\text{CH}(\text{CH}_3)_2$) \leftrightarrow δ 2.13 ($\text{CH}(\text{CH}_3)_2$); δ 25.7 ($\text{CH}(\text{CH}_3)_2$) \leftrightarrow δ 1.02 ($\text{CH}(\text{CH}_3)_2$); δ 25.3 ($\text{CH}(\text{CH}_3)_2$) \leftrightarrow δ 0.99 ($\text{CH}(\text{CH}_3)_2$); δ 22.2 ($\text{CH}(\text{CH}_3)_2$) \leftrightarrow δ 0.94 ($\text{CH}(\text{CH}_3)_2$); δ 21.0 ($\text{CH}(\text{CH}_3)_2$) \leftrightarrow δ 0.50 ($\text{CH}(\text{CH}_3)_2$); δ 20.0 ($\beta\text{-CH}$) \leftrightarrow δ 1.00 ($\beta\text{-CH}$). Anal. calcd.: C, 84.19; H, 7.42; found C, 83.46; H, 7.56.

Titanacyclobutane 146d from Bis(2-isopropylindenyl)titanium Chloride 143:



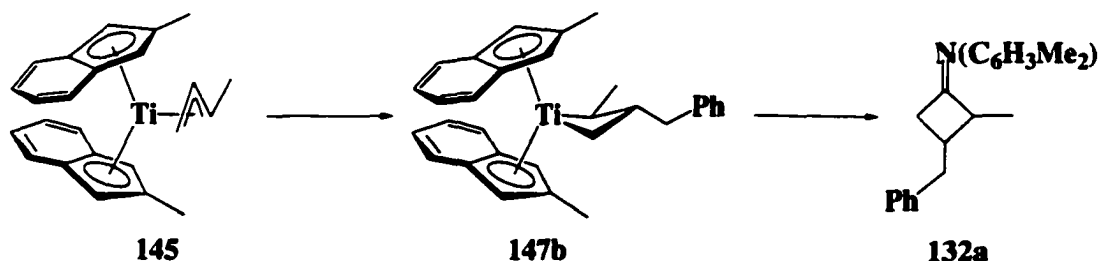
3-Benzyl-2-phenyl-bis(2-isopropylindenyl)titanacyclobutane 146d: In the drybox, to bis(2-isopropylindenyl)titanium chloride (42.0 mg, 0.105 mmol), dissolved in 3 mL THF and cooled to $-35\text{ }^{\circ}\text{C}$, was added a cold solution ($-35\text{ }^{\circ}\text{C}$) of cinnamyl lithium (13.8 mg, 0.110 mmol in 3 mL THF). The reaction was left to warm to room temperature and stirred for 1 h. The resultant green solution was treated with an equivalent of SmI_2 (1.10 mL, 0.1 M in THF) and cooled to $-35\text{ }^{\circ}\text{C}$. A cold ($-35\text{ }^{\circ}\text{C}$) solution of benzyl chloride (12.7 μL in 1 mL THF) was added to the reaction mixture, which was then left to stir at room temperature for 1 h. Within 0.5 h the blue/green colour of the solution began to dissipate followed by the emergence of a red brown solution. The solvent was removed under reduced pressure, the brown residue triturated with hexane, and filtered through a short plug of Celite. The hexane extracts were concentrated to approximately 3 mL and cooled to $-35\text{ }^{\circ}\text{C}$ to afford titanacyclobutane complex **146d** as deep red rhomboid crystals (34.2 mg) in 57% yield.

Derivatization of 3-Isopropyl-2-methyl-bis(2-isopropylindenyl)titanacyclobutane 147a with 2,6-Dimethylphenylisonitrile: Detection of N-[*trans*-(3-Isopropyl-2-methyl)-1-cyclobutylidene]-N-[2,6-dimethylphenyl]amine 132b.



3-Isopropyl-2-methyl-bis(2-isopropylindenyl)titanacyclobutane 147a. In the drybox, a vial containing a THF solution (2 mL) of bis(2-isopropylindenyl)titanium crotyl **145** (20.0 mg, 0.0479 mmol) and SmI_2 (0.50 mL, 0.1 M in THF) cooled to $-35\text{ }^\circ\text{C}$ was treated with a cold ($-35\text{ }^\circ\text{C}$) THF solution (1 mL) of isopropyl iodide (5.0 μL , 0.0690 mmol). After allowing the reaction to stir at room temperature for 5 minutes, the reaction mixture was poured onto 10 mL of cold ($-35\text{ }^\circ\text{C}$) pentane, filtered, and treated with a cold solution of 2,6-dimethylphenylisonitrile (19.3 mg, 0.150 mmol in 5 mL THF). After stirring for 3 h, the solvents were removed under reduced pressure and the crude triturated with pentane, filtered through a plug of Celite, and concentrated. The solution was cooled to $-35\text{ }^\circ\text{C}$ and decanted from the precipitated inorganic material. Concentration of the supernatant afforded cyclobutanimine **132b** as a pale yellow oil in 64 % yield (7.0 mg), spectroscopically homogeneous and identical to the material reported in Chapter 5 (pg. 297).

Derivatization of 3-Benzyl-2-methyl-bis(2-isopropylindenyl)titanacyclobutane 147b with 2,6-Dimethylphenylisonitrile: Detection of N-[*trans*-(3-Benzyl-2-methyl)-1-cyclobutylidene]-N-[2,6-dimethylphenyl]amine 132a.



3-Benzyl-2-methyl-bis(2-isopropylindenyl)titanacyclobutane 147b. As described above, a vial containing a THF solution (2 mL) of bis(2-isopropylindenyl)titanium crotyl **145** (33.0 mg, 0.0791 mmol) was treated with SmI_2 (0.83 mL, 0.1 M in THF) and benzyl chloride (9.5 μL , 0.0830 mmol). After allowing the reaction to stir at room temperature for 5 minutes, the reaction mixture was poured onto 10 mL of cold ($-35\text{ }^\circ\text{C}$) pentane, filtered, and treated with a cold solution of 2,6-dimethylphenylisonitrile (32.7 mg, 0.250 mmol in 5 mL THF). After stirring for 3 h, the reaction was worked-up as described above to afford cyclobutanimine **132a** as a pale yellow oil in 76 % yield (16.0 mg), spectroscopically homogeneous and identical to the material reported in Chapter 5 (pg. 296).

G. References:

1. Ready, T. E.; Chien, J. C. W.; Rausch, M. D. *J. Organomet. Chem.* **1999**, 583, 11.
2. Rausch, M. D.; Moriarty, K. J.; Atwood, J. L.; Hunter, W. E.; Samuel, E. J. *Organomet. Chem.* **1987**, 327, 39.
3. Luinstra, G. A.; Vogelzang, J.; Teuben, J. H. *Organometallics* **1992**, 11, 2273.
4. Martin, H. A.; Jellinek, F. J. *Organomet. Chem.* **1967**, 8, 115.

5. Martin, H. A.; Jellinek, F. *J. Organomet. Chem.* **1968**, *12*, 149.
6. Giese, B. *Radicals in Organic Synthesis: formation of Carbon-Carbon Bonds*. Oxford: Pergamon, 1986.
7. RajanBabu, T. V.; Nugent, W. A. *J. Am. Chem. Soc.* **1994**, *116*, 986 and references therein. (b) RajanBabu, T. V. Nugent, W. A.; Beattie, M. S. *J. Am. Chem. Soc.* **1992**, *114*, 6408. (c) Nugent, W. A.; RajanBabu, T. V. *J. Am. Chem. Soc.* **1989**, *111*, 8561. (d) RajanBabu, T. V.; Nugent, W. A. *J. Am. Chem. Soc.* **1989**, *111*, 4525.
8. (a) Casty, G. L. Ph. D. Thesis, Indiana University, 1994
9. Calhorda, M. J.; Gamelas, C. A.; Gonçalves, I. S.; Herdtweck, E.; Romão, C. C.; Verios, L. *Organometallics* **1998**, *17*, 2597.
10. Yield calculated based on 100% conversion to the dimeric complex.
11. Carter, C. A. G.; McDonald, R.; Stryker, J. M. *Organometallics* **1999**, *18*, 820.
12. (a) Lee, J. B.; Gajda, G. J.; Schaefer, W. P.; Howard, T. R.; Ikariya, T.; Straus, D. A.; Grubbs, R. H. *J. Am. Chem. Soc.* **1981**, *103*, 7358. (b) Stille, R. J.; Santarsiero, B. D.; Grubbs, R. H. *J. Org. Chem.* **1990**, *55*, 843. (c) Polse, J. L.; Anderson, R. A.; Bergman, R. G. *J. Am. Chem. Soc.* **1996**, *118*, 8737. (d) Polse, J. L.; Kaplan, A. W.; Anderson, R. A.; Bergman, R. G. *J. Am. Chem. Soc.* **1998**, *120*, 6316.
13. Orpen, A. G.; Brammer, L.; Allen, F. H.; Kennard, O.; Watson, D. G.; Taylor, R. *J. Chem. Soc., Dalton Trans.* **1989**, S1.
14. Silverstein, R. M.; Webster, F. X. *Spectroscopic Identification of Organic Compounds*, 6th ed., New York: John Wiley & Sons, Inc., 1998.
15. Lee, G. Y.; Kang, M. S.; Kwon, O. C.; Yoon, J. -S.; Lee, Y. -S.; Kim, H. S.; Lee, H.; Lee, I. -M. *J. Organomet. Chem.* **1998**, *558*, 11. (b) Ready, T. E.; Chien, J. C. W.; Rausch, M. D. *J. Organomet. Chem.*, **1996**, *519*, 21.
16. Keeffe, J. R.; Kresge, A. J.; Yin, Y.; *J. Am. Chem. Soc.* **1988**, *110*, 8201.
17. Liu, H. J.; Shia, K. S.; Zhu, B. Y. *Tetrahedron* **1999**, *55*, 3803.

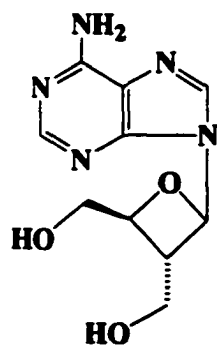
18. Helmholdt, R. B.; Jellinek, F.; Martin, H. A.; Vos, A. *Recl. Trav. Chim. Pays-Bas* **1967**, *86*, 1263. (b) Chen, J.; Kai, Y.; Nasai, N.; Yasuda, H.; Yamamoto, H.; Nakamura, A. *J. Organomet. Chem.* **1991**, *407*, 191.
19. Yield calculated base on 100% conversion to the LiCl-THF free adduct.
20. Yield calculated with potassium as the limiting reagent.
21. For a comment on this problem, common to certain classes of early transition metal complexes, see supporting information in Carney, M. J.; Walsh, P. J.; Bergman, R. G. *J. Am. Chem. Soc.* **1990**, *112*, 6426.

Chapter 5 Functionalization of Titanacyclobutane Complexes: Synthesis of Cyclobutane Derivatives

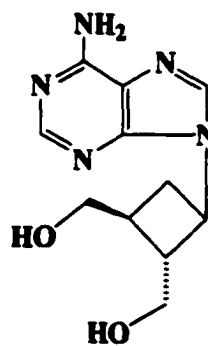
A. Introduction

An investigation into the functionalization of titanacyclobutane complexes using small unsaturated organic compounds was prompted by the importance of the class of synthetic intermediates resulting from the single insertion of carbon monoxide and isonitrile.¹ Specifically, the synthesis of cyclobutanone by the single insertion of carbon monoxide into the titanacyclobutane framework followed by reductive elimination is significant, as cyclobutane derivatives are important precursors to biologically active compounds.² As an illustration, optically active cyclobutanones have proven to be effective templates for nucleoside analogues,³ which hold potential for use as antiviral agents because of their potent activity and greater metabolic stability compared with carbohydrate-derived analogues.⁴ One such example is cyclobut-A **147**, the carbocyclic analogue of oxetanocin A **146**, which demonstrated similarly impressive antiviral activity (Figure 5.1).⁵ The use of appropriately substituted optically active cyclobutanones for the synthesis of cyclobut-A has recently been reported.⁶

Figure 5.1 Structures of Oxetanocin A and Cyclobut-A



Oxetanocin A (146)



Cyclobut-A (147)

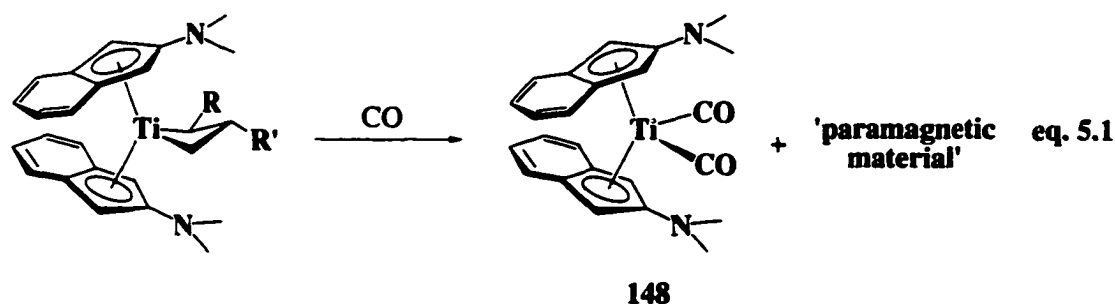
The insertion of isonitriles, the isoelectronic nitrogen-containing analogues of carbon monoxide, into the titanacyclobutane framework, followed by reductive elimination to afford cyclobutanimes has equal potential for applications to organic synthesis. In addition to facile hydrolysis to ketones, alkylation,^{7,8} and reduction,^{8,9} the imines themselves can be used for further synthetic manipulations.^{8,10}

B. Single Insertions of Carbon Monoxide. Synthesis of Cyclobutanones.

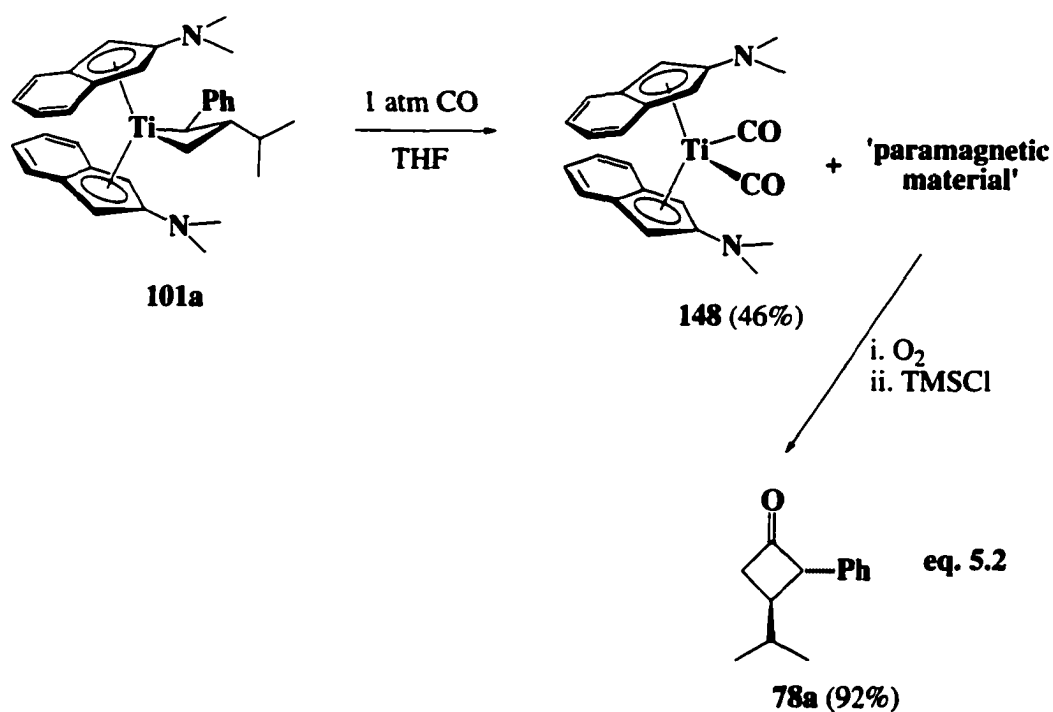
In the Stryker group, general new methodology for the synthesis of substituted cyclobutanones from titanacyclobutane complexes has been recently reported.¹¹ Under appropriate conditions, a single equivalent of carbon monoxide can be incorporated into the titanacyclobutane framework to yield the cyclobutanone exclusively. As described previously, this conversion requires conducting the carbonylation at slightly elevated temperature and low carbon monoxide pressure (*vis-à-vis* double carbonylation). Under these conditions, insertion occurs in very good to excellent yields for complexes derived from the 2-piperidinoindenyl and pentamethylcyclopentadienyl templates to afford substituted cyclobutanones.¹¹ The only exception noted was for the carbonylation of β -allyltitanacyclobutane complex **11a** (see Chapter 1, eq. 1.12). The anomalously low yield obtained in this carbonylation can now be rationalized: β -carbon-carbon bond homolysis occurs competitively with insertion at the temperatures required for single carbonylation.

For the synthesis of 2,3-disubstituted titanacyclobutane complexes, the 2-*N,N*-dimethylaminoindenyl template provides clearly improved reactivity over the 2-piperidinoindenyl template. Thus, we sought reaction conditions leading to single insertion of carbon monoxide for these titanacyclobutane complexes. Adopting the reaction conditions used to carbonylate 2-piperidinoindenyl and permethylcyclopentadienyl titanacyclobutane complexes to 2-*N,N*-dimethylaminoindenyl titanacyclobutane complexes, however, does not liberate cyclobutanone from the titanium

coordination sphere. Obtained instead is a mixture of the dicarbonyl complex **148**, that can be isolated in approximately 50 % yield, and an as yet uncharacterized paramagnetic titanium intermediate that contains all of the organic fragment (eq. 5.1). The organic fragment is released as cyclobutanone from this paramagnetic titanium complex in high yield upon oxidative or hydrolytic workup.

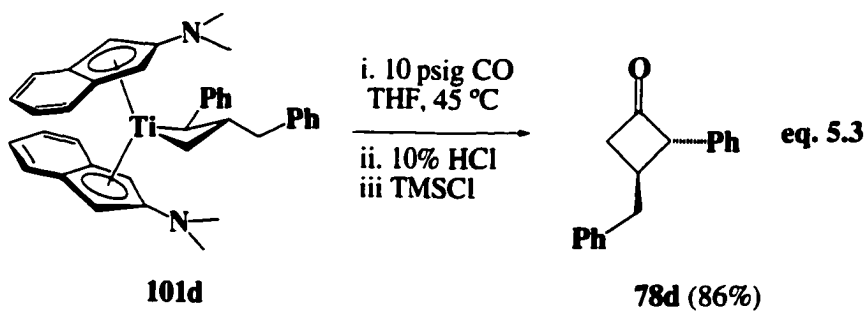


Optimization of reaction conditions for the carbonylation of titanacyclobutane complex **101a** revealed that neither elevated temperature nor high pressure is generally required for efficient carbonylation (eq. 5.2). In fact, simply bleeding carbon monoxide into the reaction vessel to replace the nitrogen atmosphere results in the colour of the solution changing from dark red/brown to forest green in under 5 minutes, a visual indication that the carbonylation is complete. Concentrating and cooling the resultant solution affords dicarbonyl complex **148** as analytically pure green needles in 46% yield. *Trans*-3-isopropyl-2-phenylcyclobutanone **78a** can be retrieved by exposing the supernatant to air. Prior to column chromatography, however, the reaction mixture is treated with an excess of chlorotrimethylsilane to convert the free 2-*N,N*-dimethylaminoindene present in the crude product mixture to the corresponding insoluble ammonium salt, avoiding separation problems in the chromatography of the cyclobutanone. Full characterization of the ammonium byproduct was not pursued. Under these conditions pure *trans*-3-isopropyl-2-phenylcyclobutanone^{11,12} **78a** is isolated in 92% yield.

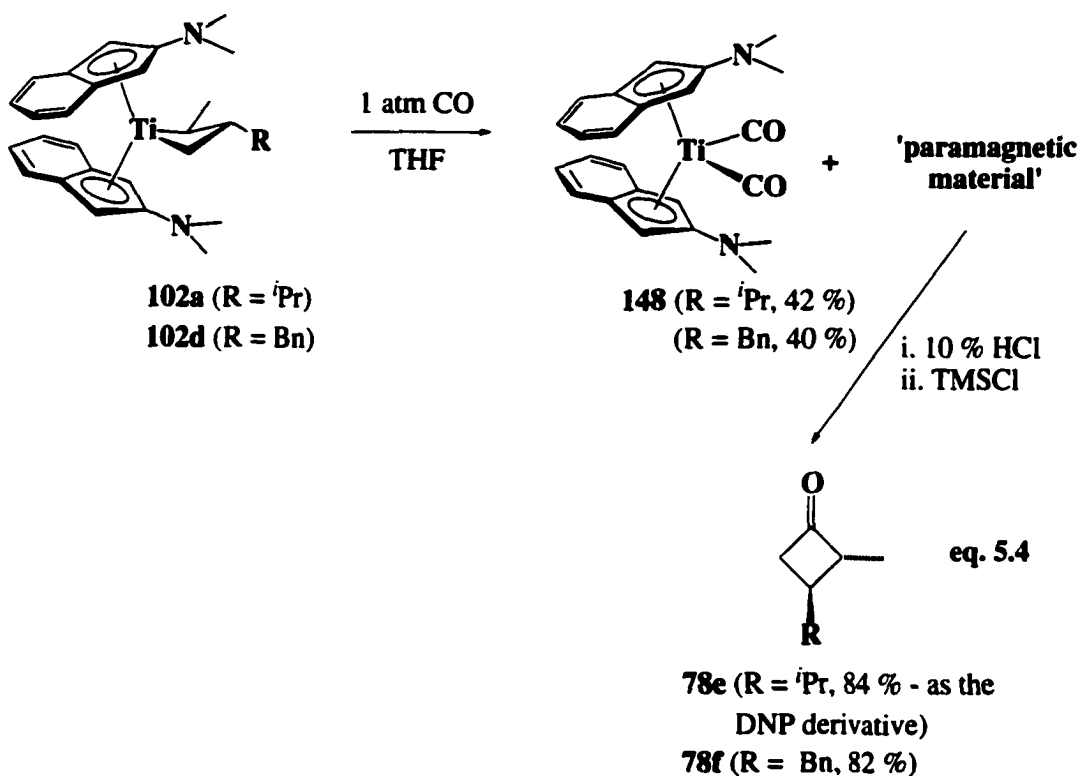


The one atmosphere carbonylation and oxidative workup was ineffective for the carbonylation of 3-benzyl-2-phenyl titanacyclobutane complex **101d**. Instead, it was necessary to perform the carbonylation under higher pressures (10 psig) and warmer temperature (45 °C) (eq. 5.3). These conditions, however do not cleave the organic fragment from the metal and do not lead to the formation of titanium dicarbonyl complex **148**. The organic is retrieved most effectively by using deoxygenated 10% hydrochloric acid; exposure to air severely lowers the yield of the reaction. Following purification, *trans*-3-benzyl-2-phenylcyclobutanone **78d** is obtained in 86% yield.

Due to the greater thermal stability of 2-*N,N*-dimethylaminoindenyl titanacyclobutane complexes bearing a 2-methyl substituent, it is possible to carbonylate both complexes **102a** and **102d** under atmospheric pressure of carbon monoxide (eq. 5.4). Cleavage of the cyclobutanone from the resultant paramagnetic intermediate was most effective under hydrolytic conditions in each case. In this way, 3-benzyl-2-



methylcyclobutanone **78e** was isolated as a colorless oil in 84% yield; 3-isopropyl-2-methylcyclobutanone proved to be volatile and was instead isolated as the 2,4-dinitrophenylhydrazone derivative **78f** in 82% yield.



The synthetic practicality of this reaction process is demonstrated by carrying out the cyclobutanone synthesis in one pot starting with bis(2-*N,N*-dimethylaminoindenyl)titanium chloride **96**. For each of the four examples given above, cyclobutanones **78a** and **78d-f** were isolated in moderate yields avoiding the isolation and manipulation of all air and

moisture sensitive intermediates (eq. 5.5 and Table 5.1). These results are preliminary; however, they clearly demonstrate the synthetic viability of this route to substituted cyclobutanones.

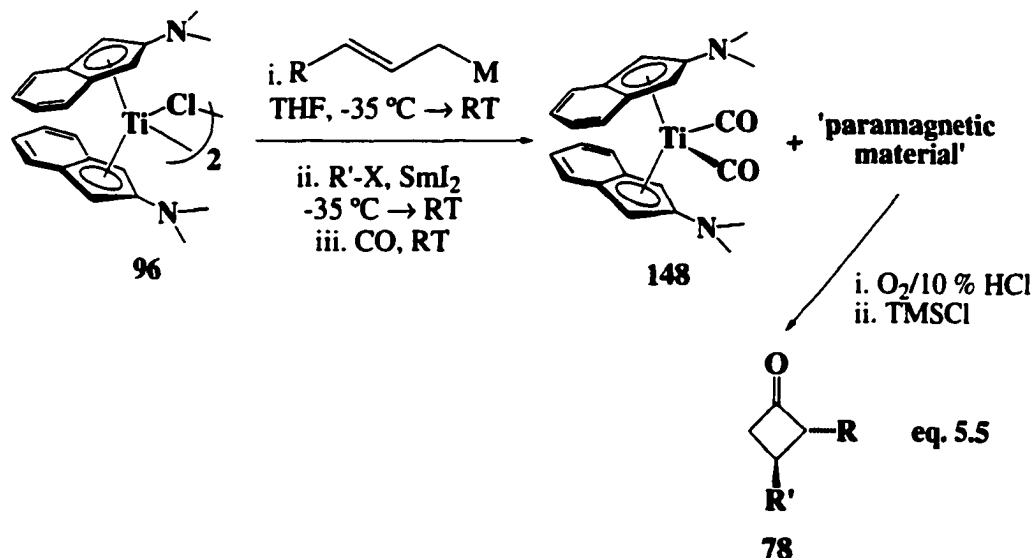


Table 5.1 Titanacyclobutane Formation and Carbonylation to Yield Cyclobutanones

Starting Complex	R	M	R'	X	Complex	Yield	Product	Overall Yield
96	Ph	Li	<i>i</i> Pr	I	148	25 %	78a	48 %
96	Ph	Li	Bn	Cl	148 ¹	26 %	78d	29 % ²
96	CH ₃	MgCl	<i>i</i> Pr	I	148	27 %	78e	33 % ³
96	CH ₃	MgCl	Bn	Cl	148	28 %	78f	44 %

¹Carbonylation at atmospheric pressure

²Carbonylation at 10 psig

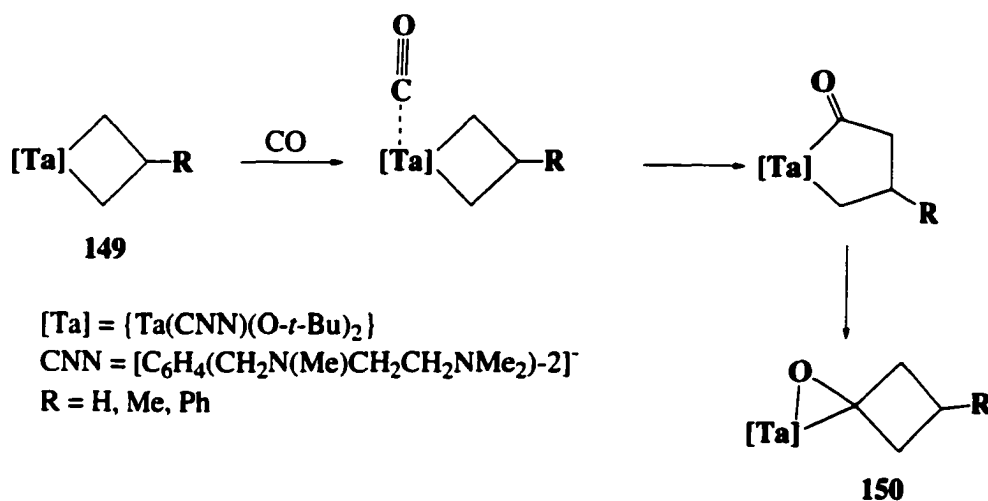
³Isolated as the 2,4-DNP derivative

Characterization of cyclobutanones **78a,d-f** was accomplished by standard analytical techniques and provided spectroscopic data consistent with previously reported 2,3-disubstituted cyclobutanones.¹³ The assigned *trans* stereochemistry is suggested by the

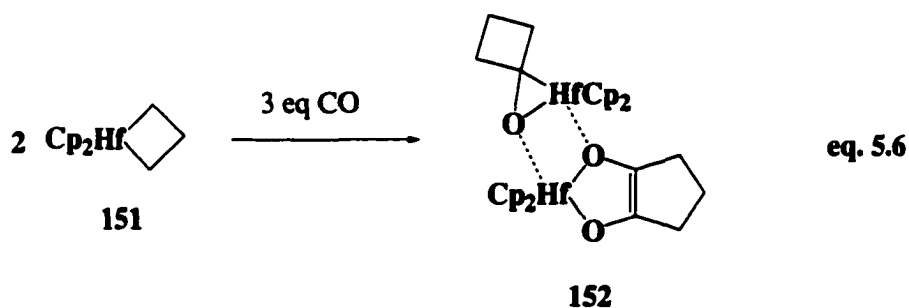
trans-disposition of the substituents in titanacyclobutane complexes **55a** and **101a**, which was confirmed by X-ray crystallography (*vide supra*). In addition, the vicinal coupling constants observed in the ^1H NMR spectra of cyclobutanones **78a,d-f** ($^3J_{\text{cis}} \sim ^3J_{\text{trans}}$) are consistent with the values determined for *trans*-2-butyl-3-methylcyclobutanone.^{13a} The four-bond ^1H - ^1H coupling across the carbonyl group in cyclobutanones **78a,d-f** provided coupling constants $^4J_{\text{cis}}$ and $^4J_{\text{trans}}$ of similar magnitude, commonly observed for disubstituted cyclobutanones.¹³

The formation of a paramagnetic intermediate containing two equivalents of cyclobutanone during the carbonylation of bis(2-*N,N*-dimethylaminoindenyl)-titanacyclobutane complexes was unexpected. Carbon monoxide insertion into metal-carbon bonds to give metal acyl complexes is ubiquitous reactivity in transition metal chemistry;¹⁴ it is generally accepted that formation of the metal acyl involves initial carbon monoxide coordination followed by alkyl migration. In early transition metal chemistry, the formation of an intermediate carbonyl complex is proposed,¹⁵ but as group IV metals in their highest oxidation state are poor π -bases, the intermediate carbon monoxide complexes are unstable¹⁶ and quickly insert to form the observed η^2 -acyl products.¹⁷ This reactivity has been used to convert metallacyclopentane, metallacyclopentene, and related early transition metal complexes into organic five-membered ring compounds via the insertion of one equivalent of carbon monoxide, followed by reductive cyclization.^{18,19,20} Only two isolated instances of single carbonylation in early transition metal metallacyclobutane complexes have been reported. Van Koten described the insertion of carbon monoxide into tantalacyclobutane complexes **149** to afford the η^2 -cyclobutanone adducts **150** (Scheme 5.1). Infrared spectroscopy of complex **150** showed carbon-oxygen stretching at 1181 cm^{-1} suggesting an η^2 -oxatantalacyclopropane fragment, as free cyclobutanone has a $\nu_{\text{C=O}}$ value of 1790 cm^{-1} ; this coordination mode was verified by X-ray crystallography.²¹ A study of the

Scheme 5.1



reaction mechanism implicated initial coordination of carbon monoxide and 1,2-insertion into the tantalum-carbon bond, followed by migratory ring closure. In the second report, Erker unexpectedly observed single carbon monoxide insertion into hafnacyclobutane complex **151**.²² Complex **151** rapidly takes up 1.5 equivalents of carbon monoxide to yield a 1:1 dimetallic adduct consisting of both an η^2 -cyclobutanone moiety and an enediolate complex from double carbonylation (eq. 5.6).



We suspect that the carbonylation of 2-*N,N*-dimethylaminoindenyl titanacyclobutane complexes also proceeds by initial coordination of carbon monoxide, insertion into the titanacyclobutane ring, followed by migratory ring closure to afford the η^2 -cyclobutane adduct. This complex then must undergo unexpected further reaction.

Following carbonylation of titanacyclobutane complex **101a** and removal of the dicarbonyl complex **148** from solution (eq. 5.2), a trace amount of a pale yellow powder can be isolated on further concentration and cooling of the supernatant. IR spectroscopy of this powder revealed a band at 1180 cm^{-1} , consistent with the presence of an η^2 -oxatitanacyclopropane.²³ This alone is not fully diagnostic as the range associated with titanium-alkoxide stretching occurs between $1120\text{-}1170\text{ cm}^{-1}$,²⁴ but it suggests that an η^2 -cyclobutanone fragment may be part of the paramagnetic Ti(III) complex formed in this reaction.

Further investigations into the reaction mechanism have not revealed the identity of this paramagnetic material. Monitoring the reaction by ^1H NMR spectroscopy shows clean conversion to dicarbonyl complex **148** and paramagnetic material with no observable intermediates. That the paramagnetic Ti(III) complex contains all of the organic, in addition to the formation of about 50% yield of a diamagnetic Ti(II) coproduct suggests some kind of disproportionation reaction along the reaction coordinate. Based on these assumptions, a reaction scheme can be proposed involving a disproportionation between the electron rich dicarbonyl complex **148** and an enolate hydride complex **153** (Scheme 5.2). The resultant radical cation complex **154** then abstracts hydride from the radical anion **155** to give Ti(III) enolate complex **156**. Following coordination of free cyclobutanone, the complex undergoes an aldol reaction, resulting in proposed intermediate complex **157**. This mechanistic rationale, however, proved to be incorrect, based on a simple isotopic quenching experiment. The hydrolytic work-up of the paramagnetic material using 10% DCl in D_2O results in no incorporation of deuterium into the cyclobutanone framework. Secondly, carbonylation of complex **101a** in the presence of an equivalent of unsubstituted cyclobutanone does not result in any crossover product. Investigations continue in this area to determine the exact structure of this unknown paramagnetic material.

Extending this reactivity to the indenyl templated titanacyclobutane complexes has met with only limited success. Carbonylation of titanacyclobutane complexes derived from both 2-isopropylindenyl and 2-methylindenyl templates do not afford organic cyclobutanones after various oxidative and hydrolytic work-up conditions. During the carbonylation, however, the observed colour changes are consistent with the formation of titanium dicarbonyl complex. This was verified by ^1H NMR spectroscopy, which also indicated the formation of a paramagnetic complex, which again undoubtedly contains all of the organic product. Unfortunately, conditions to cleave the organic from the paramagnetic intermediate have not yet been determined.

C. Single Insertions of Isonitrile. Synthesis of Cyclobutanimes.

More promising results have been obtained from the insertions of isocyanides into titanacyclobutane complexes (eq. 5.7 and Table 5.2). The treatment of bis(2-*N,N*-dimethylaminoindenyl)titanacyclobutane complexes with three equivalents of 2,6-dimethylphenylisonitrile not only affords *trans*-2,3-disubstituted cyclobutanimes **132** in high yields (as a mixture of geometrical isomers), but the organometallic template is

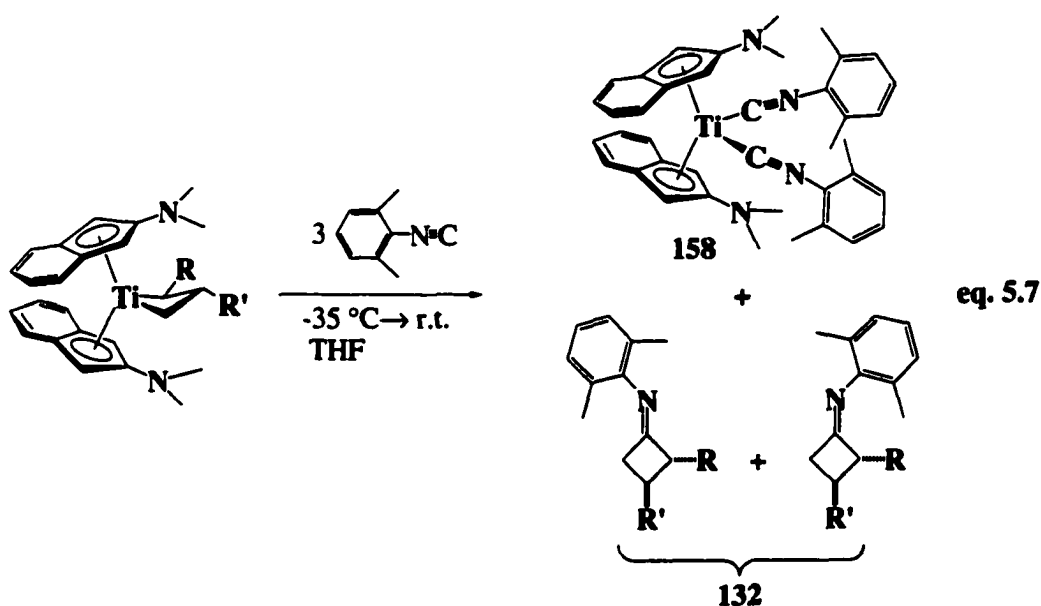


Table 5.2 Isonitrile Insertion to Yield Cyclobutanamines.

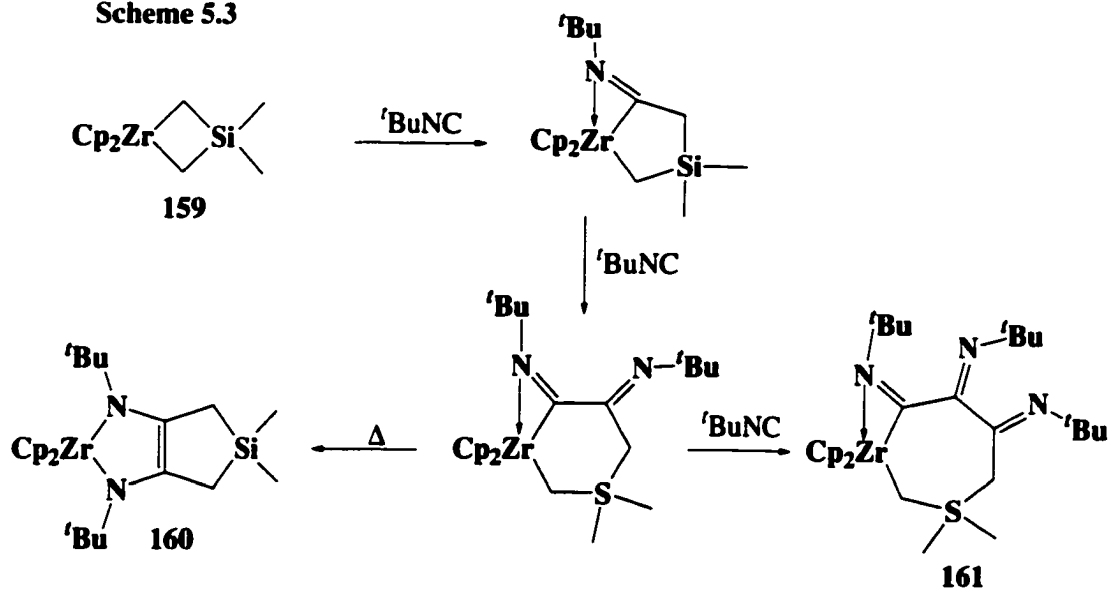
Starting complex	R	R'	Complex	Yield	Product	Yield	Ratio
102a	CH ₃	<i>i</i> Pr	158	84%	132b	90%	>99:<1
102d	CH ₃	Bn	158	quant.	132a	quant.	6:1
101a	Ph	<i>i</i> Pr	158	78%	132c	86 %	10:1
101d	Ph	Bn	158	83 %	132d	quant.	6:1

also recovered as bis(isonitrile)titanium(II) complex **158**, which has been fully characterized. Complex **158** is spectroscopically consistent with other metallocene aryl isocyanide adducts reported in the literature.²⁵

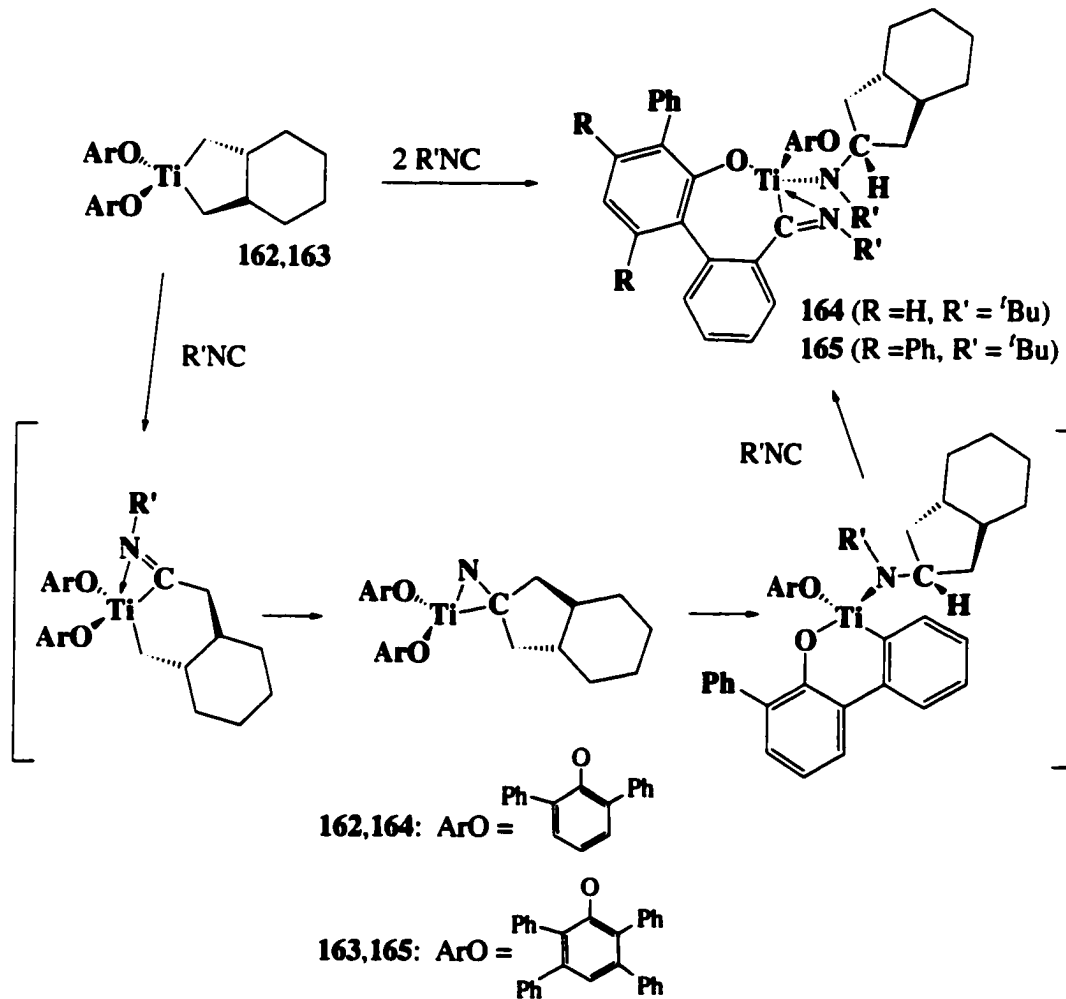
Although much is known about the reactivity between isocyanides and metal-carbon bonds,²⁶ the literature concerning isonitrile insertions in early metal metallacycles is comparatively limited. One extensive study of alkyl isonitrile insertion into 1-sila-3-zirconacyclobutane **159** has been reported by Petersen (Scheme 5.3).²⁷ This mechanistic study focused on the insertion of two equivalents of isonitrile to give enediaminate complex **160**, establishing the consecutive insertion of two isonitrile units into one zirconium carbon bond. The use of three equivalents of isonitrile gave 7-membered ring adduct **161** (Scheme 5.3). Contrasting these studies, the reactions of isonitriles with *trans*-titanabicyclic compounds **162** and **163** demonstrates that migratory ring closure of a mono-iminoacyl complex can be faster than a second isonitrile insertion, resulting in the formation of products **164** and **165**, respectively (Scheme 5.4).²⁸

We propose that the insertion of isonitrile into bis(2-*N,N*-dimethylaminoindenyl)-titanacyclobutane complexes follows a similar pathway. The first insertion is followed

Scheme 5.3

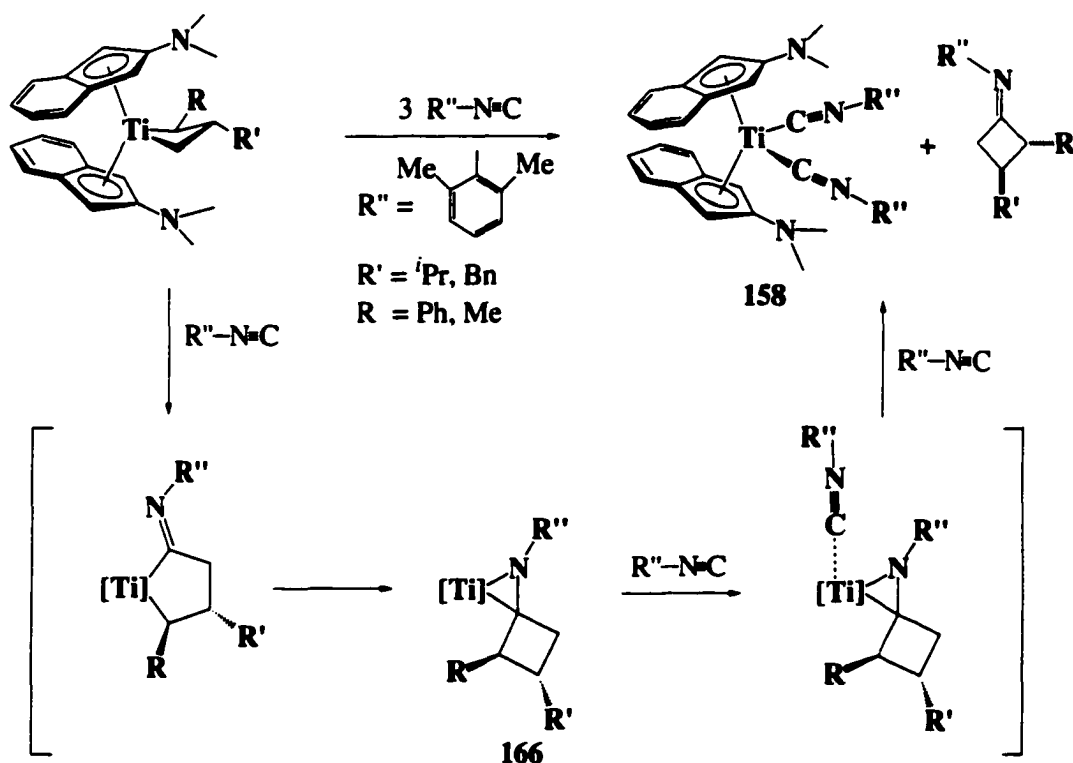


Scheme 5.4



by immediate ring closure to give a η^2 -imine complex **166** (Scheme 5.5). A second equivalent of isonitrile coordinates to the metal center, resulting in loss of coordinated imine and formation of bis(isonitrile) complex **158**. That the isonitrile reaction proceeds cleanly without the formation of an isolable Ti(III) intermediate (*cf.*, carbonylation) can be attributed to the facile reductive decomplexation of the η^2 -iminoacyl group induced by the greater steric bulk of the isonitrile moiety.

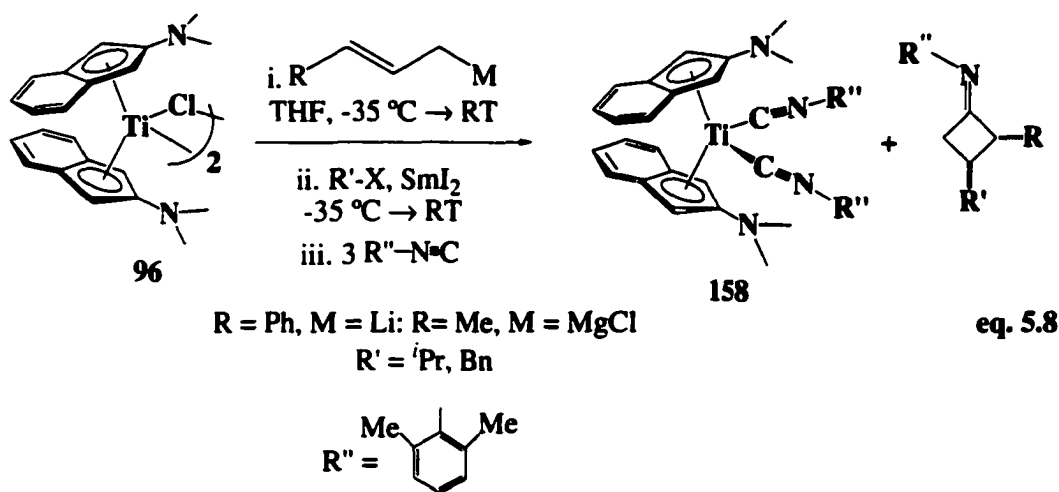
Scheme 5.5



The synthetic practicality of this reaction process is demonstrated by carrying out the cyclobutanamine synthesis starting with either bis(2-methylindenyl)titanium crotyl complex **138** or bis(2-isopropylindenyl)titanium crotyl complex **145**. Isonitrile insertion into the titanacyclobutane framework of 2-methyl and 2-isopropylindenyl titanacyclobutane complexes bearing an α -methyl substituent was observed to occur at a faster rate than β -hydride elimination, and irrefutably established the formation of these

thermally unstable crotyl-derived titanacyclobutane complexes (see Chapter 4, eq. 4.9, eq. 4.15).

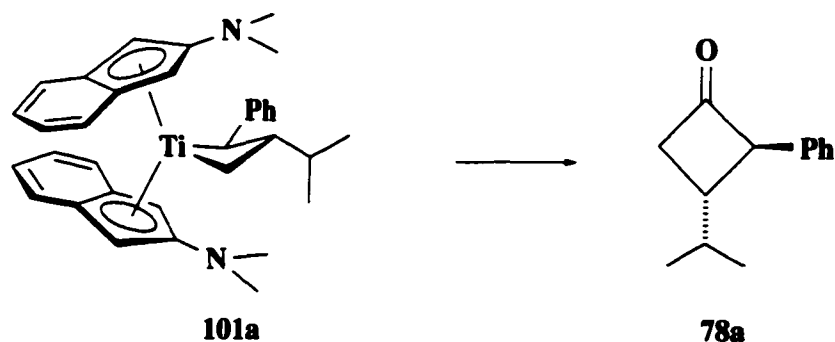
Carrying out the cyclobutanimine synthesis entirely in one pot starting with, for example, bis(2-*N,N*-dimethylaminoindenyl)titanium chloride **96** (eq. 5.8) proved more troublesome. Isonitrile insertion is not impeded, however, the resultant cyclobutanimine compounds are difficult to separate from the byproducts present from titanacyclobutane synthesis, as they are easily hydrolyzed and do not survive purification via column chromatography. Investigations are currently underway to convert the cyclobutanimines directly to cyclobutanones, which can be purified by column chromatography, or to iminium salts, which can be purified through crystallization.



D. Experimental

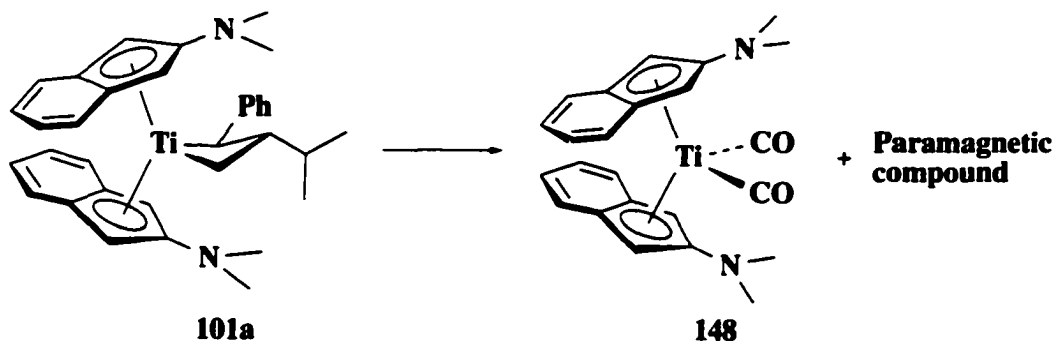
General Experimental: See Chapter 2, pg. 59.

***Trans*-3-isopropyl-2-phenylcyclobutanone 78a from Titanacyclobutane 101a:**



***Trans*-3-isopropyl-2-phenylcyclobutanone 78a.** In the drybox, a glass reaction bomb was charged with titanacyclobutane complex **101a** (20.9 mg, 0.053 mmol) and THF (10 mL). Under a strong purge of nitrogen, the Kontes valve was replaced with a rubber septum. Carbon monoxide was bled into the reaction vessel and vented to replace the nitrogen atmosphere. Within 5 minutes, the dark red/brown solution had turned forest green. The septum was removed and the reaction mixture exposed to air. The green colour of the solution dissipated leaving a colourless solution with a white precipitate. The reaction mixture was treated with trimethylsilyl chloride (1 mL), left to stir for 10 minutes and then filtered.²⁹ After filtration, the solvent was removed *in vacuo* and the residue purified by chromatography on silica gel (5% ethyl acetate in hexane) to give *trans*-3-isopropyl-2-phenylcyclobutanone **78a**^{30,31} (6.4 mg, 92%). The compound was spectroscopically homogeneous and identical to that previously reported.¹²

Isolation of Bis(2-*N,N*-dimethylaminoindenyl)titanium(CO)₂ 148 and the Titanium (III) Intermediate from the Carbonylation of Titanacyclobutane 101a.

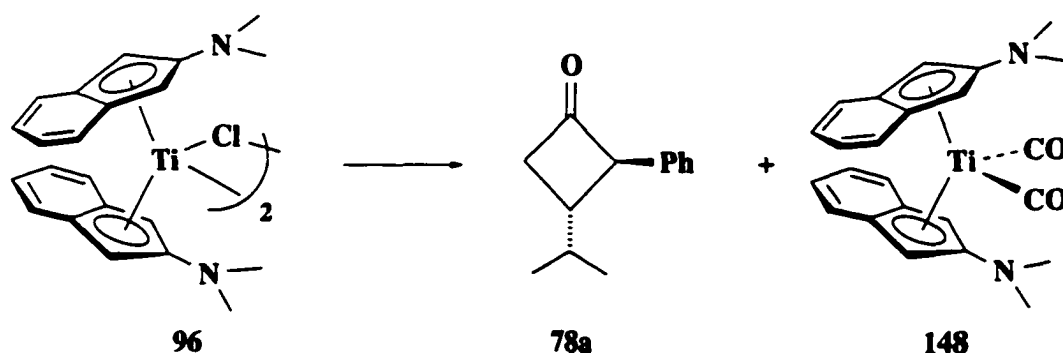


Bis(2-*N,N*-dimethylaminoindenyl)titanium dicarbonyl 148 and uncharacterized Ti(III) intermediate. In the drybox, a glass vessel was charged with titanacyclobutane complex **101a** (35.7 mg, 0.0681 mmol) and THF (10 mL) and carbonylated at atmospheric pressure of CO as described above. After purging the carbon monoxide with nitrogen and sealing the vessel, the reaction mixture was returned to the drybox. The solvent was removed and the green residue triturated with hexanes. The extracts were filtered through Celite, concentrated to approximately 3 mL, and cooled to $-35\text{ }^{\circ}\text{C}$ to afford dark green needles of the bis(2-*N,N*-dimethylaminoindenyl)titanium(CO)₂ **148** (13.2 mg, 46%). The supernatant was further concentrated to half the original volume and re-cooled to $-35\text{ }^{\circ}\text{C}$ to afford trace amounts of a pale yellow powder. Data for dicarbonyl complex **148**: ¹H NMR (300 MHz, C₆D₆): δ 7.38 (2nd order m, 4H, H4/H5), 6.81 (2nd order m, 4H, H4/H5), 3.80 (s, 4H, H2), 2.05 (s, 6H, N(CH₃)₂). ¹³C NMR (75.5 MHz, C₆D₆): δ 223.7 (C≡O), 142.6 (C1), 125.3 (C4/5), 121.2(C4/5), 111.1 (C3), 72.6 (C2), 39.2 (N(CH₃)₂). IR (cm⁻¹, Et₂O cast): 2944 (w), 2869 (w), 2798 (w), 1940 (C≡O, vs), 1855 (C≡O, vs), 1588 (w), 1541 (s), 1525 (s), 1449 (m), 1427 (s), 1383 (m), 1363 (m), 1312 (m), 1234 (w), 1198 (w), 1126 (s), 1063 (m), 998 (w), 984 (m), 793 (s).

773 (s), 748 (s), 638 (m), 622 (m). Anal. calcd. for $C_{24}H_{24}N_2O_2Ti$: C, 68.57; H, 5.75; N, 6.66; found C, 68.10, H, 5.31, N 6.41.

Data for Ti(III) intermediate: IR (cm^{-1} , KBr, cast THF) selected stretches: 1588 (s), 1574 (s), 1462 (s), 1180 (w), 1044 (s), 863 (m), 736 (m), 701 (m), 667 (w).

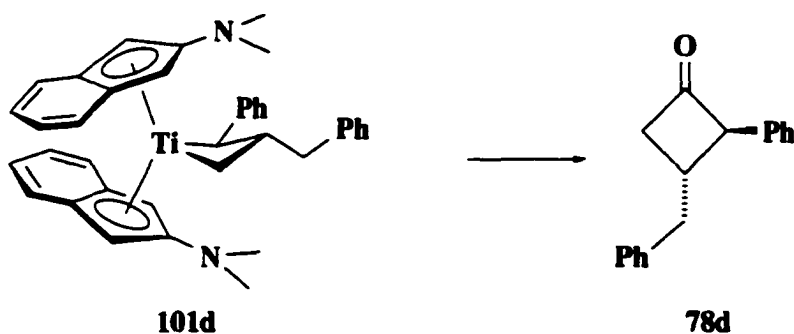
Trans-3-isopropyl-2-phenylcyclobutanone 78a and Dicarbonyl Complex 148 from Bis(2-*N,N*-dimethylaminoindenyl)titanium Chloride 96:



Trans-3-Isopropyl-2-phenylcyclobutanone 78a. In the drybox, a vial containing a THF solution (5 mL) of bis(2-*N,N*-dimethylaminoindenyl)titanium chloride **96** (47.9 mg, 0.120 mmol) was cooled to $-35\text{ }^{\circ}C$. In a separate vial, cinnamyl lithium (15.6 mg, 0.126 mmol) was dissolved in 3 mL THF and cooled to $-35\text{ }^{\circ}C$. The two solutions were mixed together, allowed to warm to room temperature and stirred for 1 h. After the resultant green solution was re-cooled to $-35\text{ }^{\circ}C$, cooled solutions ($-35\text{ }^{\circ}C$) of SmI_2 (0.93 mL, 0.1 M in THF) followed by isopropyl iodide (9.3 μ L in 2 mL THF) were added. The reaction mixture was left to stir for 3 h and transferred to a Schlenk flask fitted with a rubber septum. Carbon monoxide was bled into the reaction vessel and vented to replace the nitrogen atmosphere. Within 5 minutes, the dark red/brown solution had turned forest green. The septum was removed and the reaction exposed to air. The green colour of the solution dissipated leaving a colourless solution with a white precipitate. The reaction

mixture was treated with trimethylsilyl chloride (1 mL), left to stir for 10 minutes and filtered.²⁹ The solvent was removed *in vacuo* and the residue was purified by chromatography on silica gel (5% ethyl acetate in hexane), giving 3-isopropyl-2-phenylcyclobutanone **78a** (10.9 mg, 48%) as a colorless oil, spectroscopically homogeneous and identical to the material previously reported.¹² **Bis(2-*N,N*-dimethylaminoindenyl) Dicarbonyl 148**. As described above, a vial containing a THF solution (5 mL) of bis(2-*N,N*-dimethylaminoindenyl) titanium chloride **96** (58.5 mg, 0.146 mmol) was treated with cinnamyl lithium (19.5 mg, 0.161 mmol), SmI₂ (0.93 mL, 0.1 M in THF) and 2-iodopropane (9.3 μL in 2 mL THF and carbonylated at atmospheric pressure. The solvent was removed *in vacuo* and the Schlenk flask returned to the drybox. The green residue was triturated with hexane and the extracts were filtered through a short plug of Celite. Concentrating the combined extracts to approximately 2 mL and cooling the solution to -35 °C afforded deep green needles of the dicarbonyl complex **148** (15.3 mg, 25%) spectroscopically homogenous and identical to the material prepared above.

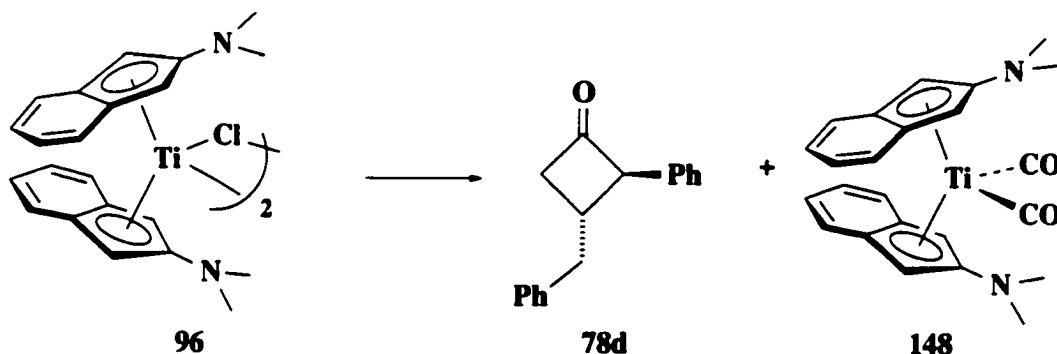
***Trans*-3-benzyl-2-phenylcyclobutanone 78d from Titanacyclobutane 101d:**



***Trans*-3-benzyl-2-phenylcyclobutanone 78d**. In the drybox, a Fischer-Porter bottle charged with 3-benzyl-2-phenyl-1,1-bis(2-*N,N*-dimethylaminoindenyl)titanacyclobutane **101d** (20.5 mg, 0.0358 mmol) and THF (10 mL) was assembled. The bottle was

removed from the drybox and heated to 45 °C in a water bath, pressurized with CO (10 psig), and the reaction mixture stirred for 15 minutes. Within 5 minutes the color of the solution turned from dark brown to light orange. The excess CO was vented, deoxygenated 10% HCl (0.80 μ L, 0.0430 mmol) was added by syringe into the solution, and the reaction mixture stirred for an additional 10 minutes. The reactor was disassembled and the solution transferred to a round-bottom flask. Excess chlorotrimethylsilane²⁹ (1 mL) was added to the reaction mixture and, after 1 h, the reaction was filtered. The solvent was removed under reduced pressure and the residue purified by column chromatography on silica gel (10% ethyl acetate in hexane), giving *trans*-3-benzyl-2-phenylcyclobutanone **101d** (8.4 mg, 86%) as a spectroscopically homogeneous pale yellow oil.^{30,31} Under these vigorous conditions, bis(2-N,N-dimethylaminoindenyl)titanium dicarbonyl **148** was not isolated. ¹H NMR (400 MHz, CDCl₃): δ 7.33-7.27 (m, 4H, phenyl), 7.24-7.22 (m, 4H, phenyl), 7.12 (m, 2H, phenyl), 4.13 (m, 1H, α -CH(C₆H₅)), 3.19 (dd, J = 13.8, 5.7, 1H, α -CH₂), 3.11-3.01 (m, 2H), 2.95-2.84 (m, 2H). ¹³C NMR (50 MHz, CDCl₃) δ 206.2, 139.3, 136.0, 129.0, 128.8, 128.7, 127.2, 127.1, 126.7, 69.1, 49.7, 41.6, 34.0. IR (cm⁻¹, cast): 1777 (C=O). HRMS calcd. for C₁₇H₁₆O m/z 236.12012 found 236.11922.

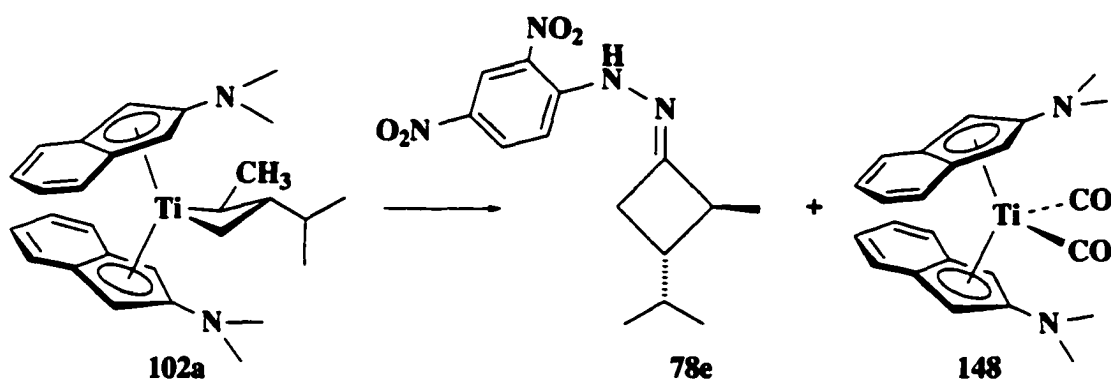
***Trans*-3-benzyl-2-phenylcyclobutanone 78d and Dicarbonyl Complex 148 from Bis(2-*N,N*-dimethylaminoindenyl)titanium Chloride 96:**



***Trans*-3-benzyl-2-phenylcyclobutanone 78d.** In the drybox, to bis(2-*N,N*-dimethylaminoindenyl)titanium chloride **96** (59.8 mg, 0.149 mmol), dissolved in 5 mL THF and cooled to -35 °C, was added a cold solution (-35 °C) of cinnamyllithium (19.5 mg, 0.157 mmol in 3 mL THF). The reaction was left to warm to room temperature and stirred for 1 h. After cooling the resultant green solution to -35 °C, a cooled solution (-35 °C) of SmI₂ (1.60 mL, 0.1 M in THF) was added to the reaction mixture followed immediately by a cooled solution (-35 °C) of benzyl chloride (18.1 μL in 3 mL THF). Within minutes, the blue/green colour of the solution began to dissipate followed by the emergence of a red brown solution. After 1 h, the solution was transferred to a Fischer-Porter bottle. The bottle was taken out of the drybox and heated in a water bath at 50 °C for 15 minutes. The reaction vessel was then pressurized with CO (10 psig) and the reaction mixture was stirred for 15 minutes. Within 5 minutes the colour of the solution turned from dark brown to light orange. The excess CO was vented, deoxygenated 10% HCl (4.5 μL, 0.157 mmol) was added via syringe into the solution, and the reaction was stirred for an additional 10 minutes. The Fischer-Porter bottle was disassembled and the solution transferred to a round-bottomed flask. The reaction was treated with excess trimethylsilyl chloride (1 mL) and was filtered²⁹ after stirring for 1 h. The solvent was removed under reduced pressure and the residue was purified on silica gel using 10%

ethyl acetate in hexane affording cyclobutanone **78d** (10.0 mg, 29%) as a pale yellow oil, spectroscopically homogeneous and identical to the material prepared above. **Dicarbonyl Complex 148**. In the drybox, as described above, vial containing a THF solution (5 mL) of bis(2-*N,N*-dimethylaminoindenyl)titanium chloride **96** (90.8 mg, 0.227 mmol) was treated with cinnamyl lithium (26.9 mg, 0.238 mmol), SmI₂ (2.4 mL, 0.1 M in THF) and benzyl chloride (27.5 μ L in 2 mL THF). Carbon monoxide was bled into the reaction vessel and vented to replace the nitrogen atmosphere. Approximately an hour later, the dark red/brown solution had turned forest green. The solvent was removed *in vacuo* and the Schlenk flask returned to the drybox. The green residue was triturated with hexane and the extracts were filtered through a short plug of Celite. Concentrating the combined extracts to approximately 3 mL and cooling the solution to -35 $^{\circ}$ C afforded deep green needles of the dicarbonyl complex **148** (25.0 mg, 26%).

2,4-Dinitrophenylhydrazone of *Trans*-3-Isopropyl-2-methylcyclobutanone 78e and Dicarbonyl Complex 148 from Titanacyclobutane 102a:

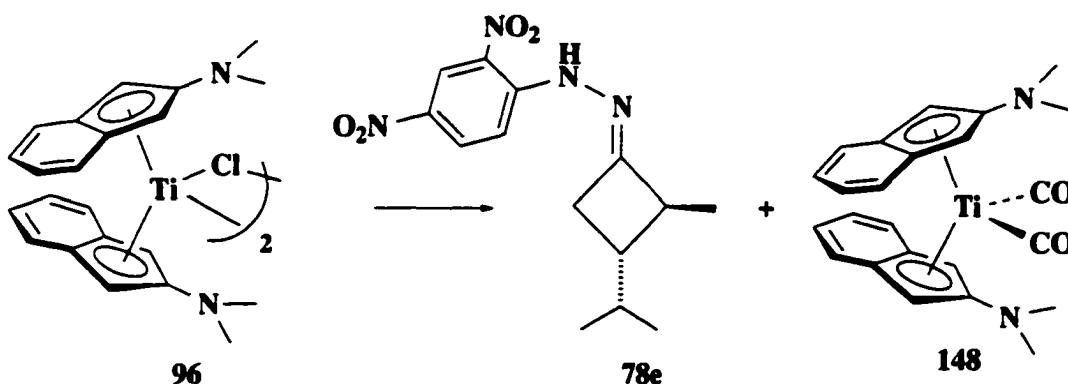


***Trans*-3-isopropyl-2-methylcyclobutanone 78e** (isolated as the non-volatile 2,4-dinitrophenylhydrazone derivative). In the drybox, a glass bomb was charged with 3-benzyl-2-methyl-bis(2-*N,N*-dimethylaminoindenyl)titanacyclobutane **102a** (37.5 mg, 0.0811 mmol) and THF (10 mL) and fitted with a rubber septum. Carbon monoxide was

bled into the reaction vessel and vented to replace the nitrogen atmosphere. Within 10 minutes, the initially purple solution turned forest green. Deoxygenated aqueous 10% HCl (4.0 μ L, 0.216 mmol) was added and the resulting reaction mixture stirred for 20 minutes. Chlorotrimethylsilane²⁹ (1 mL) was added and the stirring was continued for an additional hour. The reaction mixture was filtered into an Erlenmeyer flask containing methanol (10 mL). In a separate vessel, concentrated H₂SO₄ (0.4 mL) was added slowly to a suspension of 2,4-dinitrophenylhydrazine in methanol (0.5 g in 5 mL). The resultant solution was filtered into the crude cyclobutanone solution and the reaction stirred for 1 h. The reaction mixture was diluted with water (20 mL) and extracted with dichloromethane (3 x 20 mL). The combined organic phases were evaporated to dryness under reduced pressure and the residue purified by column chromatography on silica gel (CH₂Cl₂), giving 3-isopropyl-2-methylcyclobutanone-2,4-dinitrophenylhydrazone **78e•DNP** (20.9 mg, 84%) as a red oil. The hydrazone derivative is isolated as a mixture of geometrical isomers; spectroscopic data are provided for the major isomer only. ¹H NMR (400 MHz, CD₂Cl₂): δ 10.71(s, 1H, NH), 9.07 (d, 1H, J = 0.8 Hz, C₆H₃(NO₂)₂), 8.27 (ddd, J = 9.6, 2.6, 0.7 Hz, 1H, C₆H₃(NO₂)₂), 7.89 (d, J = 9.6 Hz, 1H, C₆H₃(NO₂)₂), 3.12-3.00 (m, 2H, CH₂, CHCH₃), 2.55 (dd, J = 16.5, 3.6 Hz, 1H, CH₂), 1.65 (m, 2H, β -CH, CH(CH₃)₂), 1.31 (d, J = 6.9 Hz, 3H, CHCH₃), 0.98 (d, J = 6.2 Hz, 3H, CH(CH₃)₂) 0.93 (d, J = 6.3 Hz, 3H, CH(CH₃)₂). ¹³C NMR (50 MHz, CD₂Cl₂): δ 164.2, 145.4, 137.8, 130.2, 123.9, 121.5, 116.4, 116.2, 47.1, 45.0, 34.7, 34.2, 20.2, 20.0, 17.1. IR (cm⁻¹, cast): 3315 (b), 3107 (wb) 2959 (m), 1618 (s), 1590 (m), 1519 (m), 1424 (m), 1336 (s), 1311 (m), 1135 (m), 1073 (m), 832 (w), 743 (w). MS calcd. for C₁₇H₁₇O₃N₄ m/z 306.13281 found 306.1315. **Dicarbonyl Complex 148**. In the drybox, as described above a glass bomb was charged with titanacyclobutane complex **102a** (31.1 mg, .0672 mmol) and THF (5 mL) and carbonylated. The bomb was returned to the drybox, where the solvent was removed and the green residue triturated with hexane. The extracts were combined, filtered through a plug of Celite, concentrated to approximately 2 mL and

cooled to $-35\text{ }^{\circ}\text{C}$ to afford dark green needles of the dicarbonyl complex **148** (11.8 mg, 42%).

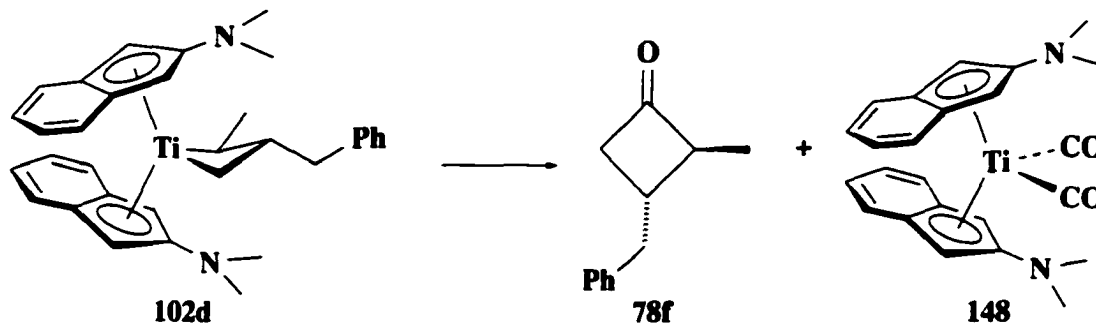
2,4-Dinitrophenylhydrazone of *Trans*-3-isopropyl-2-methylcyclobutanone **78e and Dicarbonyl Complex **148** from Bis(2-*N,N*-dimethylaminoindenyl)titanium Chloride **96**:**



***Trans*-3-isopropyl-2-methylcyclobutanone **78e**.** In the drybox, a vial containing a THF solution (10 mL) of bis(2-*N,N*-dimethylaminoindenyl)titanium chloride **96** (96.3 mg, 0.190 mmol) was cooled to $-35\text{ }^{\circ}\text{C}$ and treated with a cooled ($-35\text{ }^{\circ}\text{C}$) solution of crotylmagnesium chloride (155 μL , 1.63 M in THF further diluted in 5 mL THF). The reaction was left to warm to room temperature and stirred for one additional hour. The solution was re-cooled to $-35\text{ }^{\circ}\text{C}$ and subsequently a cooled solution of SmI_2 (2.50 mL, 0.1 M in THF) was added, followed immediately by a cooled solution ($-35\text{ }^{\circ}\text{C}$) of isopropyl iodide (25.0 μL in 2 mL THF). The solution was left to warm to room temperature and stirred for 30 minutes. Almost immediately, the blue colour of the SmI_2 began to dissipate followed by the emergence of a purple red solution and a bright yellow precipitate of Sm(III). The solution was decanted from the precipitate and transferred to a Schlenk flask fitted with a rubber septum. Carbon monoxide was bled into the reaction vessel and vented to replace the nitrogen atmosphere. Within 10 minutes, the purple

solution turned forest green and was subsequently treated with anaerobic aqueous 10% HCl (4.4 μ L, 0.241 mmol) and left to stir for 20 minutes. The crude reaction mixture was treated with trimethylsilyl chloride²⁹ (1 mL) and stirred an additional hour. The solution was gravity filtered into an Erlenmyer flask containing methanol (10 mL). Meanwhile, concentrated H₂SO₄ (0.4 mL) was slowly added to a methanolic suspension of 2,4-dinitrophenylhydrazine (0.5 g in 5 mL). The resultant solution was gravity filtered into the crude cyclobutanone solution and the reaction was left to stir for one hour. The solution was poured into a separatory funnel containing water (20 mL) and methylene chloride (20 mL). The organic layer was collected and the aqueous layer was washed with methylene chloride (2 x 10 mL). The solvent was removed *in vacuo* and purification of the residue was performed by chromatography on silica gel using CH₂Cl₂ to give the cyclobutanone derivative **78e** (24.5 mg, 33%) as a red oil, spectroscopically homogeneous and identical to the material prepared above. **Dicarbonyl Complex 148**. In the drybox, as described above, a vial containing a THF solution (5 mL) of bis(2-*N,N*-dimethylaminoindenyl)titanium chloride **96** (38.4 mg, 0.190 mmol) was treated with crotylmagnesium chloride (65.0, 1.50 M in THF), SmI₂ (0.97 mL, 0.1 M in THF) and 2-iodopropane (9.7 μ L in 1 mL THF). The resultant purple red solution was separated from the bright yellow precipitate of Sm(III) and evaporated to dryness. The purple residue was triturated with pentane (4 x 5 mL) and filtered through Celite into a Fischer Porter bottle. The bottle was sealed, removed from the drybox, and pressurized and vented with carbon monoxide (3 x 10 psig). Under a CO atmosphere the colour of the solution quickly turned from purple to brown to green. The Fischer Porter bottle was returned to the drybox where the solution was concentrated to three quarters the original volume resulting in the formation of green crystals. These crystals were collected and recrystallized from a concentrated pentane solution cooled to -35 °C to afford green needles of the dicarbonyl complex **148** (10.8 mg, 27%).

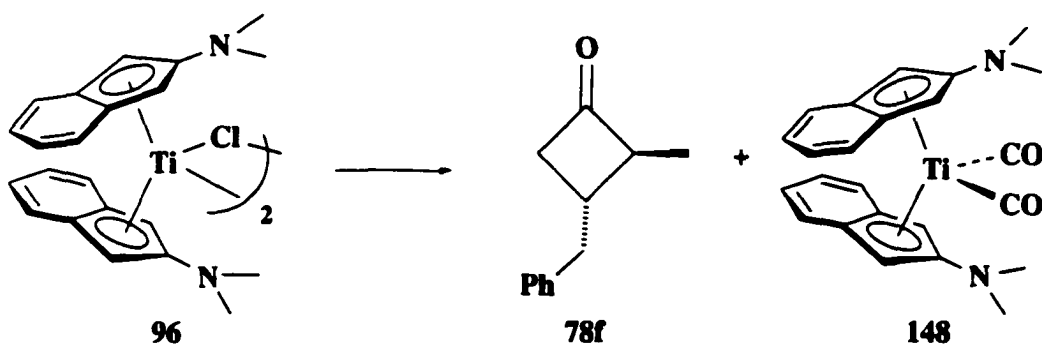
***Trans*-3-benzyl-2-methylcyclobutanone 78f and Dicarbonyl Complex 148 from Titanacyclobutane 102d:**



***Trans*-3-benzyl-2-methylcyclobutanone 78f.** In the drybox, a glass vessel was charged with 3-benzyl-2-methyl-bis(2-*N,N*-dimethylaminoindenyl)titanacyclobutane **102d** (69.7 mg, 0.137 mmol) and THF (10 mL) and fitted with a rubber septum. Carbon monoxide was bled into the reaction vessel and vented to replace the nitrogen atmosphere. The dark red solution turned forest green over 10 minutes, after which the reaction mixture was quenched with deoxygenated aqueous 10% HCl (3.0 μ L, 0.16 mmol) and stirred for 20 minutes. Chlorotrimethylsilane²⁹ (1 mL) was added and reaction stirred for an additional 1 h. The reaction mixture was filtered and the filtrate concentrated under reduced pressure. The residue was purified by silica gel chromatography (5% ethyl acetate in hexane), affording *trans*-3-benzyl-2-methylcyclobutanone **78f**^{30,31} (19.6 mg, 82%) as a colorless oil. ¹H NMR (360 MHz, CD₂Cl₂) δ 7.33-7.29 (m, 2H, C₆H₅), 7.22 (m, 3H, C₆H₅), 3.00-2.91 (m, 4H, α -CH₂, CH₂(C₆H₅), β -CH), 2.75 (ddd, J = 17.5, 8.1, 3.1 Hz, 1H, α -CH₂), 2.21 (apparent sextet, J = 7.6 Hz, 1H, β -CH), 1.00 (d, J = 7.1 Hz, 3H, CH(CH₃)). Due to overlapping signals, the ¹H NMR spectrum was also acquired in deuterated benzene. ¹H NMR (400 MHz, C₆D₆): δ 7.13-7.10 (m, 2H, C₆H₅), 7.05 (m, 1H, C₆H₅), 6.87 (m, 2H, C₆H₅), 2.56 (ddd, J = 16.8, 8.4, 2.5 Hz, 1H, α -CH₂), 2.49 (apparent quintet of t, J = 7.3, 2.5 Hz, 1H, α -CHCH₃), 2.37 (AB part of ABX, *i.e.*, two overlapping AB quartets, J_{AB} = 13.7 Hz, 1H, CH₂C₆H₅), 2.24 (ddd, J = 16.8, 8.0, 2.6 Hz, 1H, α -CH₂), 1.66 (apparent sextet, J =

7.7 Hz, 1H, β -CH), 0.79 (d, $J = 7.2$ Hz, 3H, CHCH₃). ¹H NMR (400 MHz, C₆D₆, homonuclear decoupling experiments): Irr δ 0.79 \leftrightarrow 2.49 (dt, $J = 7.3, 2.5$ Hz); irr δ 1.66 \leftrightarrow 2.56 (dd, $J = 16.8, 2.5$ Hz), 2.49 (dq, $J = 7.3, 3.9$ Hz), 2.38 (AB quartet), 2.24 (dd, $J = 16.8, 2.6$ Hz, 1H); irr δ 2.37 \leftrightarrow 1.66 (q, $J = 7.7$ Hz). ¹³C NMR (100.6 MHz, CD₂Cl₂): δ 210.0, 140.7, 129.0, 128.8, 126.6, 60.1, 50.2, 42.0, 34.8, 13.2. IR (cm⁻¹, cast): 1777 (C=O). HRMS Calcd for C₁₂H₁₄O m/z 174.10446 found 174.10420. **Dicarbonyl Complex 148**. In the drybox, a glass bomb was charged with titanacyclobutane complex **102d** (23.0 mg, 0.0451 mmol) and THF (5 mL) and carbonylated as described above. After replacing the carbon monoxide atmosphere with nitrogen, the bomb was returned to the drybox, where the solvent was removed and the green residue triturated with hexane (3 x 5 mL). The extracts were combined, filtered through a plug of Celite, concentrated to approximately 2 mL and cooled to -35 °C to afford dark green needles of the dicarbonyl complex **148** (7.6 mg, 40%), spectroscopically homogeneous and identical to the material prepared above.

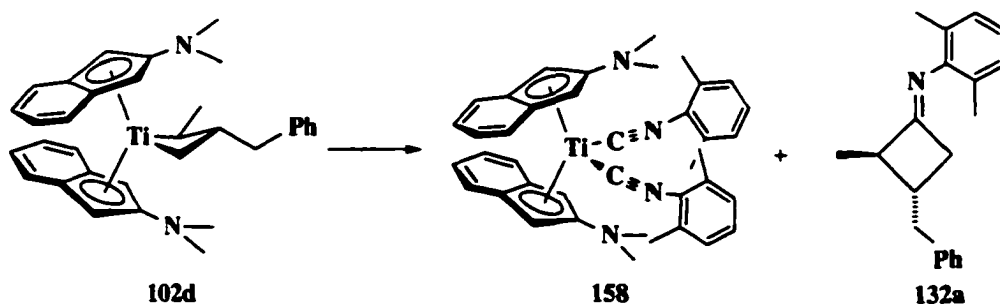
***Trans*-3-benzyl-2-methylcyclobutanone 78f and Dicarbonyl Complex 148 from Bis(2-*N,N*-dimethylaminoindenyl)titanium Chloride 96:**



***Trans*-3-benzyl-2-methylcyclobutanone 78f**. In the drybox, a solution of bis(2-*N,N*-dimethylaminoindenyl)titanium chloride **96** (0.120 g, 0.300 mmol) in THF (10 mL) was

cooled to $-35\text{ }^{\circ}\text{C}$. A solution of crotylmagnesium chloride (0.193 mL, 1.63 M in THF), diluted further with THF (10 mL), cooled to $-35\text{ }^{\circ}\text{C}$, was added and the resulting reaction mixture was warmed to room temperature and stirred for one hour. The resulting red/brown solution was recooled to $-35\text{ }^{\circ}\text{C}$, after which cold solutions ($-35\text{ }^{\circ}\text{C}$) of SmI_2 (3.15 mL, 0.1 M in THF) and benzyl chloride (36 μL in 2 mL THF) were added in succession. The resulting solution turned dark brown immediately and then red-purple within 0.5 h with the emergence of a bright yellow Sm(III) precipitate. The solution was decanted and transferred to a Schlenk flask fitted with a rubber septum. Carbon monoxide was bled into the reaction vessel, venting to replace the nitrogen atmosphere. The dark red/brown solution turned forest green over 10 minutes. The reaction mixture was quenched with deoxygenated 10% HCl (5.5 μL , 0.300 mmol) and, after stirring for 20 minutes, chlorotrimethylsilane²⁹ (1 mL) was added and the stirring continued for 1 h. The reaction mixture was filtered and evaporated to dryness under reduced pressure. The residue was purified by chromatography on silica gel (5% ethyl acetate in hexane), giving 3-benzyl-2-methylcyclobutanone **78f** (23 mg, 44%) as a colorless oil, spectroscopically homogeneous and identical to the material prepared above. **Bis(2-*N,N*-dimethylaminoindenyl)titanium dicarbonyl 148**. In the drybox, to a vial containing a THF solution (10 mL) of bis(2-*N,N*-dimethylaminoindenyl)titanium chloride **96** (75.8 mg, 0.190 mmol) was treated with crotylmagnesium chloride (117 μL , 1.63 M in THF), SmI_2 (2.0 mL, 0.1 M in THF) and benzyl chloride (23.0 μL in 2 mL THF) and carbonylated as described above. The solvent was removed under reduced pressure and the Schlenk flask returned to the drybox. The green residue was triturated with hexane, the extracts collected and filtered through a plug of Celite and concentrated to approximately 3 mL. Cooling the solution ($-35\text{ }^{\circ}\text{C}$) resulted in the formation of deep green needles of dicarbonyl complex **148** (22.0 mg, 28 %).

Trans-3-benzyl-2-methylcyclobutanamine 132a from Titanacyclobutane 102d:



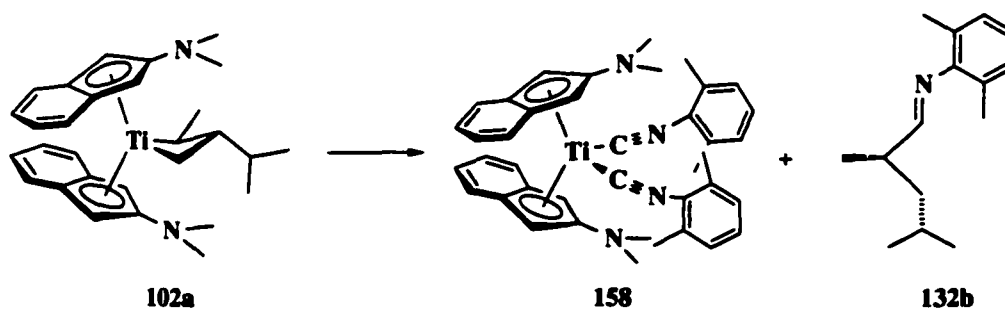
N-[Trans-(3-benzyl-2-methyl)-1-cyclobutylidene]-N-[2,6-dimethylphenyl]amine

132a. In the drybox, a THF solution (2 mL) of titanacyclobutane complex **102d** (14.8 mg, 0.0290 mmol) was cooled to $-35\text{ }^{\circ}\text{C}$ and treated with a cold ($-35\text{ }^{\circ}\text{C}$) THF solution (2 mL) of 2,6-dimethylphenylisocyanide (11.8 mg, 0.0900 mmol). The reaction mixture was left to warm to room temperature and stir for an additional 3 h. Within 5 minutes of mixing, the colour of the solution turned from red to dark purple. The solvent was removed *in vacuo* and the purple residue was extracted with pentane and filtered through Celite. The extracts were concentrated to approximately 3 mL and cooled to $-35\text{ }^{\circ}\text{C}$ to afford dark purple cubes of bis(2-*N,N*-dimethylaminoindenyl)titanium diisocyanide complex **158** (18.2, quant.); the supernatant was removed from the drybox, exposed to air, filtered through Celite to remove any residual organometallic products and evaporated to dryness giving quantitative recovery (7.9 mg) of the cyclobutanamine **132a** as a mixture of two isomers in a 1 : 6 ratio.³² Data for the major isomer: ^1H NMR (400.1 MHz, CDCl_3): δ 7.31 (m, 2H, $\text{CH}_2\text{C}_6\text{H}_5$), 7.12 (m, 3H, $\text{CH}_2\text{C}_6\text{H}_5$), 6.98 (d, $J = 7.5$ Hz, 2H, $\text{C}_6\text{H}_3(\text{CH}_3)_2$), 6.87 (t, $J = 7.0$ Hz, 1H, $\text{C}_6\text{H}_3(\text{CH}_3)_2$), 3.09 (apparent quintet, $J = 7.0, 2.6$ Hz, 1H, $\alpha\text{-CH}(\text{CH}_3)$), 2.93 (dd, $J = 13.8, 6.9$ Hz, 1H, $\text{CH}_2\text{C}_6\text{H}_5$), 2.83 (dd, $J = 13.6, 7.6$ Hz, 1H, $\text{CH}_2\text{C}_6\text{H}_5$), 2.55 (ddd, $J = 16.3, 7.98, 3.05$ Hz, CH_2), 2.26-2.19 (m, 2H, CH_2 , $\beta\text{-CH}$), 2.05 (s, 6H, $\text{C}_6\text{H}_3(\text{CH}_3)_2$), 1.26 (d, $J = 7.0$ Hz, $\alpha\text{-CH}(\text{CH}_3)$). ^{13}C NMR (100.6 MHz, CDCl_3): δ 175.8, 140.1, 128.6, 128.5, 127.5, 126.2, 122.9, 122.7, 119.8,

116.9 51.1, 41.8, 40.2, 37.5, 17.9, 15.7. IR (cm⁻¹, CHCl₃ cast): 3387 (w), 3025 (m), 2963 (s), 2924 (s), 2852 (m), 2781 (m), 1775 (vs), 1715 (s), 1625 (m), 1496 (m), 1476 (s), 1376 (m), 1275 (m), 1138 (m), 1092 (m), 1030 (m), 761 (m), 739 (s), 700 (s). HRMS calcd. for C₂₀H₂₃N *m/z* 277.18304, found 277.18274.

Data for bis(2-*N,N*-dimethylaminoindenyl)bis(2,6-dimethylphenylisonitrile)titanium **158**: ¹H NMR (360.1 MHz, C₆D₆): δ 7.61 (m, 4H, H4/H5), 6.92 (m, 4H, H4/H5), 6.83 (d, *J* = 7.4 Hz, 4H, C₆H₃(CH₃)₂), 6.78 (t, *J* = 6.5 Hz, 2H, C₆H₃(CH₃)₂), 4.35 (s, 4H, H2), 2.36 (s, 12H, N(CH₃)₂), 2.10 (s, 6H, C₆H₃(CH₃)₂). ¹³C NMR (100.6 MHz, C₆D₆): δ 144.6 (C1), 131.0 (C_{aryl}), 128.4 (C_{aryl}), 126.9 (C_{aryl}), 126.2 (C_{aryl}), 120.3 (C_{aryl}), 112.7 (C_{aryl}), 77.2 (C2), 41.0 (N(CH₃)₂), 19.3 C₆H₃(CH₃)₂, not observed: C≡N, one aryl signal. IR (cm⁻¹, pentane cast): 2917 (m), 2799 (w), 2116 (w), 2018 (s), 1988 (m), 1803 (m), 1803 (m), 1586 (vs), 1540 (s), 1463 (s), 1381 (m), 1362 (m), 1311 (m), 1260 (w), 1192 (w), 1127 (m), 1064 (m), 986 (m), 950 (w), 902 (w), 790 (s), 769 (vs), 732 (s), 668 (m), 654 (m). Anal. calcd. for C₃₀H₄₂N₄Ti: C, 76.66; H, 6.75; N, 8.94; found C, 76.18, H, 7.02, N, 8.59.

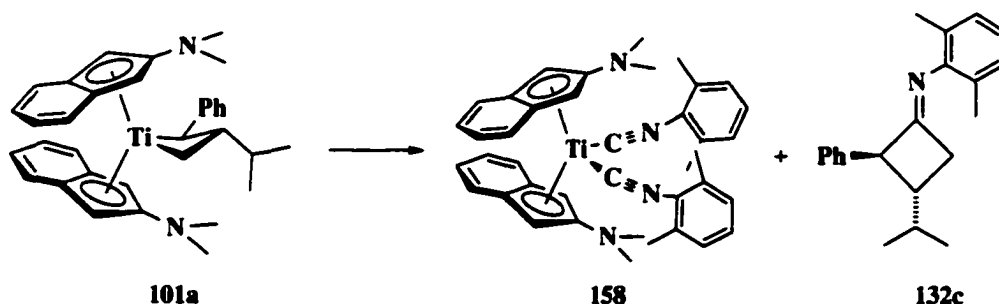
***Trans*-3-Isopropyl-2-methylcyclobutanimine 132b from Titanacyclobutane 102a:**



N-[*Trans*-(3-isopropyl-2-methyl)-1-cyclobutylidene]-N-[2,6-dimethylphenyl]amine 132b. In the drybox, a THF solution (3 mL) of titanacyclobutane complex **102a** (32.0 mg, 0.0689 mmol) was cooled to -35 °C. A cold (-35 °C) THF solution (3 mL) of 2,6-dimethylphenylisonitrile (27.0 mg, 0.206 mmol) was added to the titanacyclobutane

solution and the reaction mixture was allowed to warm to room temperature and stir for an additional 3 h. Within 5 minutes of mixing, the colour of the solution turned dark purple. The solvent was removed *in vacuo* and the purple residue was extracted with pentane and filtered through Celite. The extracts were concentrated to approximately 5 mL and cooled to $-35\text{ }^{\circ}\text{C}$ to afford dark purple cubes of bis(2-*N,N*-dimethylaminoindenyl)titanium diisonitrile complex **158** (36.0, 84%), spectroscopically homogeneous and identical to that prepared above. The supernatant was removed from the drybox, exposed to air, filtered through Celite to remove any residual organometallic products, and evaporated to dryness to give cyclobutanimine **132b** as a spectroscopically homogeneous pale yellow oil (14.1 mg, 90 %).³² ^1H NMR (400.1 MHz, CDCl_3): δ 6.99 (d, $J = 7.4$ Hz, 2H, 2H, $\text{C}_6\text{H}_3(\text{CH}_3)_2$), 6.88 (t, $J = 7.1$ Hz, 1H, $\text{C}_6\text{H}_3(\text{CH}_3)_2$), 3.03 (apparent dqintet, $J = 7.0, 2.6$ Hz, 1H, $\alpha\text{-CH}(\text{CH}_3)$), 2.52 (ddd, $J = 16.6, 7.7, 0.6$ Hz, $\alpha\text{-CH}_2$), 2.12 (ddd, $J = 16.7, 7.8, 0.6$ Hz, 1H, $\alpha\text{-CH}_2$), 2.07 (s, 6H, $\text{C}_6\text{H}_3(\text{CH}_3)_2$), 1.64 - 1.54 (m, 2H, $\text{CH}(\text{CH}_3)_2$, $\beta\text{-CH}$), 1.39 (d, $J = 7.0$ Hz, $\alpha\text{-CH}(\text{CH}_3)$), 0.98 (d, $J = 6.4$ Hz, 3H, $\text{CH}(\text{CH}_3)_2$), 0.85 (d, $J = 6.6$ Hz, 3H, $\text{CH}(\text{CH}_3)_2$). ^{13}C NMR (100.6 MHz, CDCl_3): δ 176.3, 147.8, 127.8, 126.6, 123.0, 50.0, 44.0, 39.1, 34.8, 20.4, 20.2, 18.0, 16.7. IR (cm^{-1} , CHCl_3 , cast): 3018 (m), 2957 (vs), 2924 (vs), 2868 (s), 2116 (w), 1753 (m), 1714 (vs), 1592 (s), 1577 (m), 1467 (s), 1375 (m), 1256 (w), 1208 (w), 1125 (m), 1092 (m), 1031 (w), 984 (w), 917 (w), 800 (w), 762 (s), 743 (m), 717 (w). HRMS calcd. for $\text{C}_{16}\text{H}_{23}\text{N}$ m/z 229.18304, found 229.18314.

Trans-3-isopropyl-2-phenylcyclobutanamine 132c from Titanacyclobutane 101a:

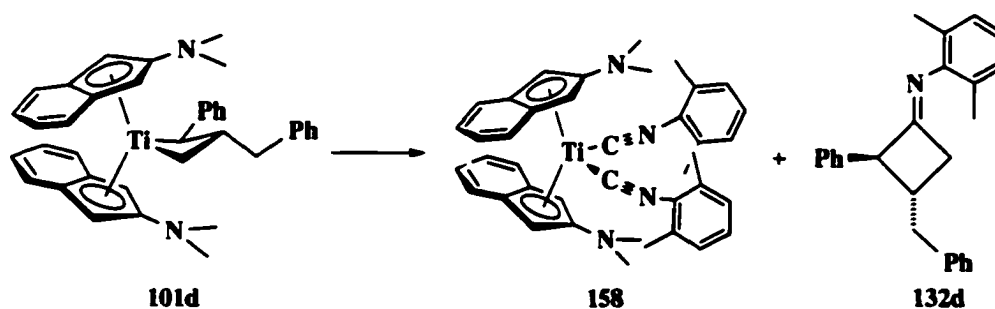


N-[(3-isopropyl-2-phenyl)-1-cyclobutylidene]-N-[2,6-dimethylphenyl]amine 132c.

In the drybox, a THF solution (2 mL) of titanacyclobutane complex **101a** (19.1 mg, 0.0364 mmol) was cooled to $-35\text{ }^{\circ}\text{C}$. A cold ($-35\text{ }^{\circ}\text{C}$) THF solution (2 mL) of 2,6-dimethylphenylisonitrile (14.3 mg, 0.109 mmol) was added and the reaction mixture was left to warm to room temperature and stir for an additional 3 h. Within 5 minutes of mixing, the colour of the solution turned from brown to dark purple. The solvent was removed *in vacuo* and the purple residue was extracted with pentane and filtered through Celite. The extracts were concentrated to approximately 5 mL and cooled to $-35\text{ }^{\circ}\text{C}$ to afford dark purple cubes of bis(2-N,N-dimethylaminoindenyl)titanium diisonitrile complex **158** (16.5, 72%), spectroscopically homogeneous and identical to the material prepared above. The supernatant was removed from the drybox, exposed to air, filtered through Celite to remove residual organometallic products, and evaporated to dryness to give cyclobutanamine **132c** as a spectroscopically homogeneous pale yellow oil (9.1 mg, 86 %, mixture of two isomers in a 1 : 10 ratio).³² Data is provided for the major isomer. ^1H NMR (400.1 MHz, CDCl_3): δ 7.31 (m, 3H, C_6H_5), 7.21 (m, 2H, C_6H_5), 6.94 (d, $J = 7.4$ Hz, 2H, 2H, $\text{C}_6\text{H}_3(\text{CH}_3)_2$), 6.65 (t, $J = 7.4$ Hz, 1H, $\text{C}_6\text{H}_3(\text{CH}_3)_2$), 4.09 (dt, $J = 8.0, 2.5$ Hz, 1H, $\alpha\text{-CH}(\text{C}_6\text{H}_5)$), 3.08 (ddd, $J = 17.4, 8.7, 2.4$ Hz, $\alpha\text{-CH}_2$), 2.85 (ddd, $J = 17.4, 8.1, 2.5$ Hz, 1H, $\alpha\text{-CH}_2$), 2.43 (s, 6H, $\text{C}_6\text{H}_3(\text{CH}_3)_2$), 2.35 (apparent quintet, $J = 8.3$ Hz, 1H, $\beta\text{-CH}$), 1.86 (dseptets, $J = 9.1, 6.6$ Hz, 1H, $\text{CH}(\text{CH}_3)_2$), 1.04 (d, $J = 6.6$ Hz, 3H, $\text{CH}(\text{CH}_3)_2$), 1.00 (d, $J = 6.6$ Hz, 3H, $\text{CH}(\text{CH}_3)_2$). ^{13}C NMR (100.6 MHz, CDCl_3): δ 162.2, 136.5,

128.7, 128.3, 128.1, 127.9, 127.8, 127.6, 127.1, 69.1, 48.6, 39.7, 35.1, 21.0, 20.7, 17.7.
 IR (cm⁻¹, CHCl₃ cast): 3382 (w), 3028 (m), 2958 (s), 2925 (s), 2879 (m), 1780 (vs), 1679 (s), 1632 (m), 1602 (m), 1497 (s), 1448 (m), 1395 (m), 1262 (m), 1168 (m), 1094 (m), 1033 (m), 952 (m), 801 (w), 770 (m), 740 (m), 698 (s), 549 (w). HRMS calcd. for C₂₁H₂₅N *m/z* 291.19870, found 291.19836.

***Trans*-3-benzyl-2-phenylcyclobutanimine 132d from Titanacyclobutane 101d:**



***N*-[*Trans*-(3-benzyl-2-phenyl)-1-cyclobutylidene]-*N*-[2,6-dimethylphenyl]amine 132.**

In the drybox, to THF solution (3 mL) of titanacyclobutane complex **101d** (20 mg, 0.0347 mmol) cooled to -35 °C, was added a cooled THF solution (3 mL) of 2,6-dimethylphenylisonitrile (13.6 mg, 0.104 mol). Within five minutes of mixing the brown solution turned deep purple in colour. The reaction mixture was left to stir an additional 3 h, the solvent removed *in vacuo*, and the products extracted into pentane (4 x 5 mL). The extracts were concentrated to approximately 3 mL and cooled to -35 °C to afford deep purple lustrous crystals of the diisonitrile complex **158** (18.1 mg, 83%), spectroscopically homogeneous and identical to the material prepared above. The supernatant was collected, removed from the drybox, and exposed to air. Filtration through glass wool removed residual organometallic decomposition products and concentration resulted in the isolation of the cyclobutanimine **132d** (12.0 mg, quantitative).³² ¹H NMR (400.1 MHz, CDCl₃): δ 7.37 (m, 5H, H_{aryl}), 7.26 (m, 1H, H_{aryl}),

7.17 (m, 4H, H_{aryl}), 6.99 (d, $J = 7.4$ Hz, 2H, 2H, C₆H₃(CH₃)₂), 6.88 (t, $J = 7.1$ Hz, 1H, C₆H₃(CH₃)₂), 4.23 (dd, $J = 7.4, 2.6$ Hz, 1H, α -CH(C₆H₅)), 3.15 (dd, $J = 13.7, 6.4$ Hz, CH₂(C₆H₅)), 2.91 (dd, $J = 13.5, 8.8$ Hz, CH₂(C₆H₅)), 2.75 (m, 1H, β -CH), 2.64 (ddd, $J = 16.6, 8.6, 2.6$ Hz, 1H, α -CH₂), 2.36 (dd, $J = 16.8, 7.5$ Hz, 1H, α -CH₂), 2.09 (s, 6H, C₆H₃(CH₃)₂). ¹³C NMR (100.6 MHz, CDCl₃): δ 173.1, 147.6, 139.6, 128.9, 128.7, 128.6, 127.9, 127.7, 127.0, 126.5, 123.3, 60.7, 46.5, 41.8, 40.8, 40.2, 38.3, 18.4. IR (cm⁻¹, CHCl₃ cast): 3262 (m), 3061 (m), 3026 (m), 2921 (m), 1775 (w), 1709 (s), 1679 (vs), 1596 (s), 1496 (s), 1473 (s), 1376 (m), 1236 (s), 1091 (m), 1030 (m), 1002 (m), 954 (m), 845 (w), 754 (vs), 700 (vs), 666 (m), 508 (m). HRMS calcd. for C₂₅H₂₅N m/z 339.19870, found 339.19852.

E. References

1. Reviews: (a) Bellus, D.; Ernst, B. *Angew. Chem. Int. Ed.* **1988**, *27*, 797. (b) Lee-Ruff, E. in *Advances in Strain in Organic Chemistry*, Vol. 1; Halton, B.; Ed.; JAI Press: Greenwich, CT, 1991. (c) Nemoto, H.; Fukumoto, K. *Synlett* **1997**, 863. Recent and leading references: (d) Murakami, M.; Tsuruta, T.; Ito, Y. *Angew. Chem. Int. Ed.* **2000**, *39*, 2484. (e) Brown, B.; Hegedus, L. S. *J. Org. Chem.* **2000**, *65*, 1865. Hegedus, L. S.; Raslow, P. B. *Synthesis* **2000**, 953. Riches, A. G.; Wernersbach, L. A.; Hegedus, L. S. *J. Org. Chem.* **1998**, *63*, 4691. (f) Brown, R. C. D.; Keily, J.; Karim, R. *Tetrahedron Lett.* **2000**, *41*, 3247. (g) Miyata, J.; Nemoto, H.; Ihara, M. *J. Org. Chem.* **2000**, *65*, 504. (h) Johnston, D.; McCuster, C. F.; Muir, K.; Proctor, D. J. *J. Chem. Soc., Perkin Trans. 1* **2000**, 681. (i) Jiang, W.; Fuertes, M. J.; Wulff, W. D. *Tetrahedron* **2000**, *56*, 2183. (j) Weber, J.; Haslinger, U.; Brinker, U. *J. Org. Chem.* **1999**, *64*, 6085. (k) Vinson, N. A.; Day, C. S.; Welker, M. E.; Guzei, I.; Rheingold, A. L. *Organometallics* **1999**, *18*, 1824.

2. (a) Norbeck, D. W.; Kern, E.; Hayashi, S.; Rosenbrook, W.; Sham, H.; Herrin, T.; Plattner, J. J.; Ericksen, J.; Clement, J.; Swanson, R.; Shipkowitz, N.; Hardy, D.; Marsh, K.; Arnett, G.; Shannon, W.; Broder, S.; Mitsuya, H. *J. Med. Chem.* **1990**, *33*, 1281. Brown, B.; Hegedus, L. S. *J. Org. Chem.* **1998**, *63*, 8012. Frieden, M.; Giraud, M.; Rees, C. B.; Song, Q. L. *J. Chem. Soc., Perkin Trans. 1* **1998**, 2827. (b) Prasit, P.; Rideneau, D. *Ann. Reports, Med. Chem.* **1997**, *32*, 211. Friesen, R. W.; Dube, D.; Fortin, R.; Frenette, R.; Prescott, S.; Cromlish, W.; Greig, G. M.; Kargman, S.; Wong, E.; Chan, C. C.; Gordon, R.; Xu, L. J.; Rideneau, D. *Bioorg. Med. Chem. Lett.* **1996**, *6*, 2677. (c) Delincee, H.; Pool-Zobel, B. L. *Radiat. Phys. Chem.* **1998**, *52*, 39.
3. Reed, A. D.; Hegedus, L. S. *J. Org. Chem.* **1998**, *63*, 2313.
4. Reviews: (a) Agrofoglio, L.; Sudhas, E.; Farese, A.; Condom, R.; Challand, S. R.; Earl, R. A.; Guedj, R. *Tetrahedron* **1994**, *50*, 10611. (b) Borthwick, A. D.; Biggadike, K. *Tetrahedron* **1992**, *48*, 571. (c) Huryn, D. M.; Okabe, M. *Chem. Rev.* **1992**, *92*, 1745.
5. Norbeck, D. W.; Kern, E.; Hayashi, S.; Rosenbrook, W.; Sham, H.; Herrin, T.; Plattner, J. J.; Erickson, J.; Clement, J.; Swanson, R.; Shipkowitz, N.; Hardy, D.; Marsh, K.; Arnett, G.; Shannon, W.; Broder, S.; Mitsuya, H. *J. Med. Chem.* **1990**, *33*, 1281.
6. (a) Brown, B.; Hegedus, L. S. *J. Org. Chem.* **1998**, *63*, 8012. (b) Frieden, M.; Giraud, M.; Reese, C. B.; Song, Q. *J. Chem. Soc., Perkin Trans. 1* **1998**, 2827.
7. Enders, D.; Rienhold, U. *Tetrahedron: Asymmetry* **1997**, *8*, 3789.
8. Reviews: (a) Adams, J. P. *J. Chem. Soc., Perkin Trans. 1* **2000**, 125. (b) Adams, J. P.; Robertson, G. *Contem. Org. Synth.* **1997**, *4*, 183. (c) Adams, J. P. *Contem. Org. Synth.* **1997**, *4*, 517.
9. Hashiguchi, S.; Uematsu, N.; Noyori, R. *J. Synth. Org. Chem. Jpn.* **1997**, *55*, 99.
10. Kirsme, W. *Eur. J. Org. Chem.* **1998**, *2*. (b) Schroth, W.; Jahn, U. *J. Prakt. Chem./Chem. Ztg.* **1998**, *340*, 287.

11. Carter, C. A. G.; Greidanus, G; Chen, J.-X.; Stryker, J. M., submitted.
12. Carter, C. A. G. Ph. D. Dissertation, University of Alberta, 1998.
13. (a) Chevtchouk, T.; Ollivier, J.; Salaün, *Tetrahedron: Asymmetry* **1997**, *8*, 1011.
See also: (b) Sato, M.; Ohuchi, H.; Abe, Y.; Kaneko, C. *Tetrahedron: Asymmetry* **1992**, *3*, 313. (c) Salaün, J.; Karkour, B.; Ollivier, J. *Tetrahedron* **1989**, *45*, 3151. (d) Salaün, J.; Karkour, B. *Tetrahedron Lett.* **1988**, *29*, 1537. (e) Salaün, J.; Karkour, B. *Tetrahedron Lett.* **1987**, *28*, 4669. (f) Rey, M.; Roberts, S. M.; Dreiding, A. S.; Roussel, A.; Vanlierde, H.; Toppet, S.; Ghosez, L. *Helv. Chim. Acta* **1982**, *65*, 703.
14. Crabtree, R. H. *The Organometallic Chemistry of the Transition Metals* 2nd ed. 1994, John Wiley & Sons, Inc. New York.
15. (a) Erker, G. *Acc. Chem. Res.* **1984**, *17*, 103. (b) Lauher, J. W.; Hoffmann, R. *J. Am. Chem. Soc.* **1976**, *98*, 1729. (c) Tatsumi, K.; Nakamura, A.; Hofmann, P.; Stauffert, P.; Hoffmann, R. *J. Am. Chem. Soc.* **1985**, *107*, 4440 and references therein.
16. Marko, L. et al. *J. Organometal. Chem.* **1980**, *199*, C31.
17. Erker, G. et al. *Angew. Chem., Int. Ed.* **1978**, *17*, 605.
18. Cyclopentanones: (a) McDermott, J. X.; Wilson, M. E.; Whitesides, G. M. *J. Am. Chem. Soc.* **1976**, *98*, 6529. (b) Grubbs, R. H.; Miyashita, A.; Liu, M.; Burk, R. *J. Am. Chem. Soc.* **1978**, *100*, 2418. (c) Manriques, J. M.; McAllister, D. R.; Sanner, R. D.; Bercaw, J. E. *J. Am. Chem. Soc.* **1978**, *100*, 2716. (d) Erker, G. *Acc. Chem. Res.* **1984**, *17*, 103.
19. Cyclopentenones, recent and leading references: (a) Ti: Hicks, F. A.; Buchwald, S. L. *J. Am. Chem. Soc.* **1999**, *121*, 7026. (b) Sturla, S. J.; Buchwald, S. L. *J. Org.* **1999**, *64*, 5547. (c) Hicks, F. A.; Kablaoui, N. M.; Buchwald, S. L. *J. Am. Chem. Soc.* **1999**, *121*, 5881. (d) Chohen, S. A.; Bercaw, J. E. *Organometallics* **1985**, *4*, 1006. Bristow, G. S.; Lappert, M. F.; Martin, T. R.; Atwood, J. L.; Hunter, W. F. *J. Chem. Soc., Dalton Trans.* **1984**, 399. (e) Zr: Negishi, E.-I.; Holmes, S. J.; Tour, J. M.; Miller, J. A.; Cederbaum, F. E.; Swanon, D. R.; Takahashi, T. *J. Am. Chem. Soc.* **1989**, *111*,

3336. (f) Negishi, E.–I. in *Comprehensive Organic Synthesis*; Trost, B. M.; Fleming, I.; Eds.; Pergamon: Oxford, 1991; Vol. F, 1163. (g) Buchwald, S. L.; Lum, R. T.; Fisher, R. A.; Davis, W. M. *J. Am. Chem. Soc.* **1989**, *111*, 9113. (h) Probert, G. D.; Whitbey, R. J.; Coote, S. J. *Tetrahedron Lett.* **1995**, *36*, 4113. (i) Erker, G.; Engel, K.; Kruger, C.; Chiang, A.–P. *Chem. Ber.* **1982**, *115*, 3311.
20. γ -Lactones, leading references: (a) Kablaoui, N.; Hicks, F. A.; Buchwald, S. L. *J. Am. Chem. Soc.* **1997**, *119*, 4424. (b) Crowe, W. E.; Vu, A. T. *J. Am. Chem. Soc.* **1996**, *118*, 5508. (c) Mashima, K.; Haraguchi, H.; Ohyoshi, A.; Sakai, N.; Takaya, H. *Organometallics* **1991**, *10*, 2731.
21. Rietveld, M. H. P.; Hagen H.; van de Water, L.; Grove, D. M.; Kooijman, H.; Veldman, N.; Spek, A. L.; van Koten, G. *Organometallics*, **1997**, *16*, 168.
22. Erker, G.; Czisch, P.; Schlunde, R.; Angermund, K.; Kruger, C. *Angew. Chem. Int. Ed.* **1986**, *25*, 364.
23. This is based on the similarity in $\nu_{C=O}$ observed in η^2 -oxytantalacyclopropane complex **151**.
24. Coutts, R. S. P. Wailes, P. C.; Martin, R. L. *J. Organometal. Chem.* **1973**, *50*, 145.
25. (a) Gambarotta, S.; Floriani, C.; Chiesi-Villa, A.; Guastini, C. *Inorg. Chem.* **1984**, *23*, 1739. (b) Dorer, B.; Prosenc, M. –H.; Rief, U.; Brinzinger, H. –H.; *Collect. Czech. Chem. Commun.* **1997**, *62*, 265. (c) Carrondo, M. A. A. F. de C. T.; Morais, J.; Romão, C. C.; Romão, M. J.; Veiros, L. F. *Polyhedron* **1993**, *12*, 765. (d) Strauch, H. C.; Wibbeling, B.; Frohlich, R.; Erker, G. *Organometallics* **1999**, *18*, 3802.
26. Recent and leading references on isonitrile insertion into transition metal-carbon bonds: (a) Braunstein, P.; Knorr, M.; Reinhard, G.; Schubert, U.; Stahrfeldt, T. *Chem. Eur. J.* **2000**, *6*, 4265. (b) Calhorda, M. J.; Lopez, P. E. M.; Berends, E. J. *New J. Chem.* **2000** *24*, 289. (c) Adams, H.; Cubbon, R. J.; Sarsfield, M. J.; Winter, M. J. *Chem. Commun.* **1999**, 491. (d) Amor, F.; Butt, A.; du Plooy, K. E.; Spaniol, T. P.; Okuda, J. *Organometallics* **1998**, *17*, 5836. (e) Utz, T. L.; Leach, P. A.; Geib, S. J.;

- Cooper, N. J. *Organometallics* **1997**, *16*, 4109. (f) Putzer, M. A.; Neumuller, B.; Dehnicke, K. Z. *Anorg. Allg. Chem.* **1998**, *641*, 57. (f) Braunstein, P.; Knorr, M.; Stern, C. *Coord. Chem. Rev.* **1998**, *180 part 2*, 903.
27. (a) Valero, C.; Grehl, M.; Wingbermuehle, D.; Kloppenburg, L.; Carpenetti, D.; Erker, G.; Petersen, J. L. *Organometallics* **1994**, *13*, 415. (b) Berg, F. J.; Petersen, J. L. *Organometallics* **1991**, *10*, 1599. (c) Petersen, J. L.; Egan, J. W., Jr. *Organometallics* **1987**, *6*, 2007.
28. Thorn, M. G.; Fanwick, P. E.; Rothwell, I. P. *Organometallics* **1999**, *18*, 4442.
29. The presence of free 2-*N,N*-dimethylaminoindene in the crude product mixtures obtained from carbonylation interferes with product purification, co-eluting with the cyclobutanone during column chromatography. The addition of excess chlorotrimethylsilane to the crude reaction mixture removes the 2-*N,N*-dimethylaminoindene by precipitation, presumably by forming the corresponding insoluble ammonium salt. Characterization of this byproduct was not pursued.
30. The *trans* stereochemistry in the 2,3-disubstituted cyclobutanones is suggested by the *trans*-disposition of the substituents in titanacyclobutane complexes **101a** and **55a**, which has been confirmed by X-ray crystallography. The assignment of *trans*-stereochemistry for the substituents in complexes **78a, d-f** is supported by the vicinal coupling constants observed in the ¹H NMR spectra (³*J*_{cis} ~ ³*J*_{trans}) consistent with the values determined for *trans*-2-butyl-3-methylcyclobutanone.¹³
31. Four-bond ¹H-¹H coupling across the carbonyl group of substituted cyclobutanones is commonly observed, with coupling constants, ⁴*J*_{cis} and ⁴*J*_{trans}, of similar magnitude,^{13a-c} as observed for **78a, d-f**.
32. Hydrolysis of imine precluded purification via column chromatography. Minor impurities (> 5%) were present in isolated material.

Chapter 6. Conclusions

Regioselective addition of both stabilized and unstabilized radicals to the central carbon of substituted allyl titanocene complexes has been demonstrated. Although the 'ideal' template for this reactivity pattern has not been found, we have developed one pot procedures allowing titanium(III) chloride complexes to be converted to titanacyclobutanes without the isolation of sensitive allyl titanocene intermediates. For the synthesis of 2,3-disubstituted titanacyclobutane complexes it is the two step methodology employing the use of allylmetal reagents that affords higher yields, despite numerous attempts to optimize the samarium(II)-mediated reaction conditions.

The continued investigation into electron-rich templates indicated that central carbon alkylation of substituted allyl complexes affords titanacyclobutanes in good to high yields under mild reaction conditions, consistent with our previously held hypothesis. A crystallographic study of aminoindenyl Ti(III) and Ti(IV) complexes however, clearly indicated that these ancillary ligands are capable of providing greater electron density than is required by the metal. Our investigations then turned to the development of less electron-rich indenyl templates. Surprising is the relatively minimal level of electron density required by the metal center from the indenyl ancillary ligands for clean conversion of substituted allyl complexes to titanacyclobutanes on addition of organic radicals. Further development of simpler indenyl systems is currently under investigation in the Stryker group to address the relationship between electron richness and central carbon alkylation.

In this investigation, we also uncovered a new decomposition pathway for titanacyclobutane complexes. Various Ti(III) η^3 -allyl complexes undergo reversible regioselective central carbon alkylation, particularly complexes treated with stabilized

organic free radicals. The stability of these titanacyclobutane complexes, however, is subtle and is likely dictated a combination of steric and electronic factors imparted by the ancillary ligand system on the titanacyclobutane core. For these reasons we envision a theoretical investigation into this novel decomposition pathway.

This investigation has also demonstrated that functionalization of titanacyclobutanes with carbon monoxide and isonitriles affords cyclobutanones and cyclobutanimes, respectively, in high yield under mild reaction conditions. We were able to demonstrate the synthetic practicality of this reaction process by carrying out the cyclobutanone synthesis in one pot starting with bis(2-*N,N*-dimethylaminoindenyl)titanium chloride **96**. An investigation into the optimization of this reaction continues in the Stryker group and the development of one pot cyclobutanime synthesis starting from allylmetal reagents is currently underway. Quite unexpected was the paramagnetic Ti(III) intermediate formed on carbonylation of the titanacyclobutane complexes that contained all of the organic fragment. Investigations continue into both the identity of this carbonylation-derived intermediate, and methodology to cleave the organic from the carbonylation intermediates derived from the simpler indenyl templates.

Appendix I – Selected Data from X-ray Crystallographic Structure Determinations

Table of Contents

	page
Part A. Crystallographic details for complex 96 •LiCl(THF) ₂ , report # <i>jms0027</i>	310
Part B. Crystallographic details for complex 98 , report # <i>jms9904</i>	316
Part C. Crystallographic details for complex 99 and 99' , report # <i>jms9909</i>	323
Part D. Crystallographic details for complex 101a , report # <i>jms9901</i>	335
Part E. Crystallographic details for complex 55a , report # <i>jms9908</i>	342
Part F. Crystallographic details for complex 139c , report # <i>jms0043</i>	350
Part G. Crystallographic details for complex 145 , report # <i>jms0037</i>	358

Additional information (including structure factors, etc.) can be obtained directly from Dr. R. McDonald at the University of Alberta Molecular Structure Center, Department of Chemistry, University of Alberta, Edmonton, Alberta, T6G 2G2, Canada. Request report #'s

**Part A. Crystallographic Details for Bis(2-*N,N*-dimethylaminoindenyl)titanium Chloride
•LiCl(THF)₂, Complex **96**.**

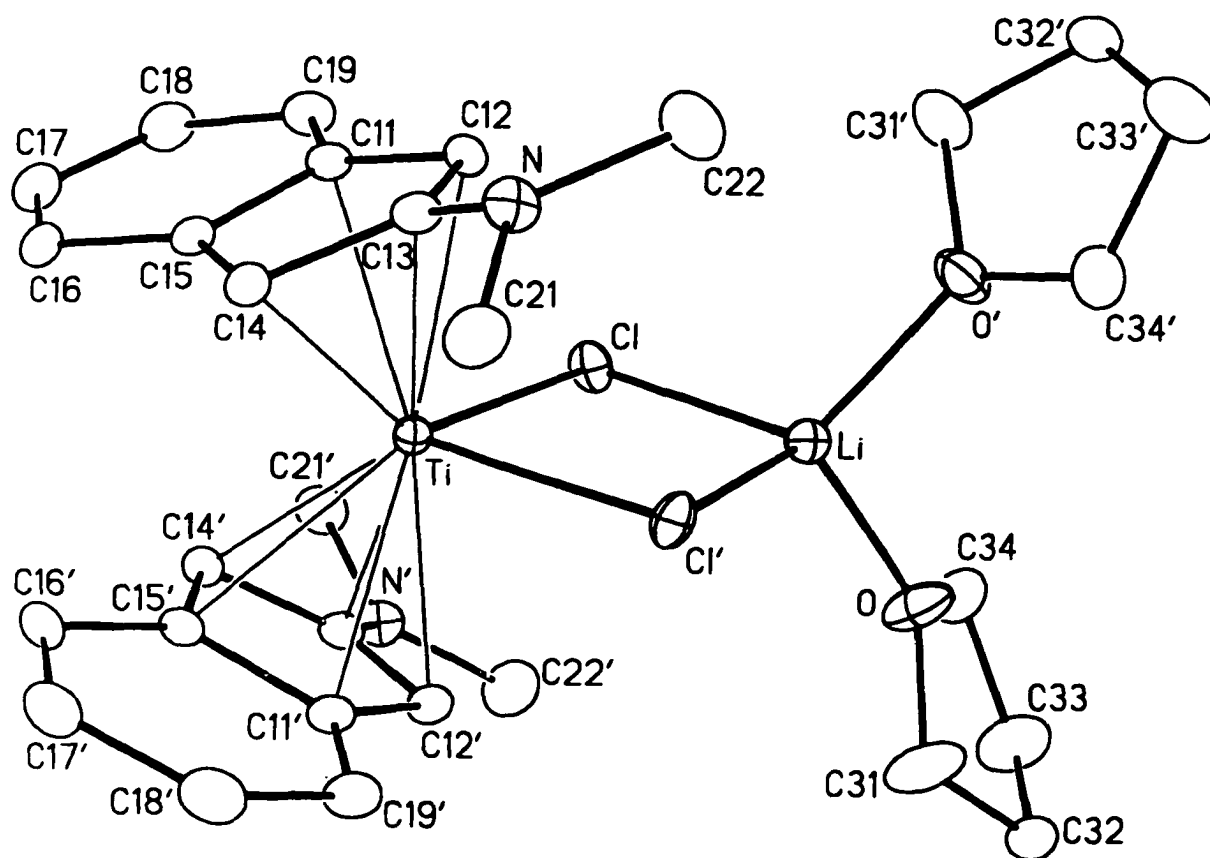


Figure A.1 Perspective view of the [(2-*N,N*-dimethylaminoindenyl)₂Ti(μ-Cl)₂Li(OC₄H₈)₂] complex **96** showing the atom labelling scheme. Non-hydrogen atoms are represented by Gaussian ellipsoids at the 20% probability level. Hydrogen atoms are not shown. Primed atoms are related to unprimed ones via the crystallographic twofold rotational axis (0, *y*, 1/4) passing through the Ti and Li atoms.

Table A.1 Crystallographic Experimental Details

<i>A. Crystal Data</i>	
formula	C ₃₀ H ₄₀ Cl ₂ LiN ₂ O ₂ Ti
formula weight	586.38
crystal dimensions (mm)	0.37 × 0.14 × 0.14
crystal system	monoclinic
space group	<i>C2/c</i> (No. 15)
unit cell parameters ^a	
<i>a</i> (Å)	16.0060 (15)
<i>b</i> (Å)	11.6875 (12)
<i>c</i> (Å)	17.1235 (15)
β (deg)	109.2334 (19)
<i>V</i> (Å ³)	3024.5 (5)
<i>Z</i>	4
ρ _{calcd} (g cm ⁻³)	1.288
μ (mm ⁻¹)	0.488
<i>B. Data Collection and Refinement Conditions</i>	
diffractometer	Bruker P4/RA/SMART 1000 CCD ^b
radiation (λ [Å])	graphite-monochromated Mo Kα (0.71073)
temperature (°C)	-80
scan type	φ rotations (0.3°) / ω scans (0.3°) (30 s exposures)
data collection 2θ limit (deg)	52.74
total data collected	7268 (-20 ≤ <i>h</i> ≤ 17, -14 ≤ <i>k</i> ≤ 14, -8 ≤ <i>l</i> ≤ 21)
independent reflections	3094
number of observed reflections (<i>NO</i>)	2495 [<i>F</i> _o ² ≥ 2σ(<i>F</i> _o ²)]
structure solution method	direct methods (<i>SHELXS-86</i> ^c)
refinement method	full-matrix least-squares on <i>F</i> ²
(<i>SHELXL-93</i> ^d)	
absorption correction method	<i>SADABS</i>
range of transmission factors	0.9348–0.8400
data/restraints/parameters	3094 [<i>F</i> _o ² ≥ -3σ(<i>F</i> _o ²)] / 0 / 175
goodness-of-fit (<i>S</i>) ^e	1.039 [<i>F</i> _o ² ≥ -3σ(<i>F</i> _o ²)]
final <i>R</i> indices ^f	
<i>R</i> ₁ [<i>F</i> _o ² ≥ 2σ(<i>F</i> _o ²)]	0.0411
<i>wR</i> ₂ [<i>F</i> _o ² ≥ -3σ(<i>F</i> _o ²)]	0.1104
largest difference peak and hole	0.391 and -0.317 e Å ⁻³

^aObtained from least-squares refinement of 3984 centered reflections.

^bPrograms for diffractometer operation, data collection, data reduction and absorption correction were those supplied by Bruker. (continued)

Table A.1 Crystallographic Experimental Details (continued)

^cSheldrick, G. M. *Acta Crystallogr.* **1990**, A46, 467–473.

^dSheldrick, G. M. *SHELXL-93*. Program for crystal structure determination. University of Göttingen, Germany, 1993. Refinement on F_o^2 for all reflections (all of these having $F_o^2 \geq -3\sigma(F_o^2)$). Weighted R -factors wR_2 and all goodnesses of fit S are based on F_o^2 ; conventional R -factors R_1 are based on F_o , with F_o set to zero for negative F_o^2 . The observed criterion of $F_o^2 > 2\sigma(F_o^2)$ is used only for calculating R_1 , and is not relevant to the choice of reflections for refinement. R -factors based on F_o^2 are statistically about twice as large as those based on F_o , and R -factors based on ALL data will be even larger.

^e $S = [\sum w(F_o^2 - F_c^2)^2 / (n - p)]^{1/2}$ (n = number of data; p = number of parameters varied; $w = [\sigma^2(F_o^2) + (0.0562P)^2 + 1.6051P]^{-1}$ where $P = [\text{Max}(F_o^2, 0) + 2F_c^2]/3$).

^f $R_1 = \sum ||F_o| - |F_c|| / \sum |F_o|$; $wR_2 = [\sum w(F_o^2 - F_c^2)^2 / \sum w(F_o^4)]^{1/2}$.

Table A.2 Atomic Coordinates and Equivalent Isotropic Displacement Parameters

Atom	<i>x</i>	<i>y</i>	<i>z</i>	<i>U</i> _{eq} , Å ²
Ti	0.0000	-0.13221(4)	0.2500	0.02204(15)*
Cl	0.11135(3)	0.02670(5)	0.26989(3)	0.03582(17)*
O	0.01251(14)	0.25774(19)	0.34202(13)	0.0673(6)*
N	-0.17021(12)	-0.11252(17)	0.05677(11)	0.0368(4)*
C11	0.06185(14)	-0.19098(19)	0.14558(12)	0.0299(5)*
C12	-0.00534(14)	-0.10688(19)	0.11020(12)	0.0299(5)*
C13	-0.08891(14)	-0.15788(18)	0.09955(12)	0.0299(5)*
C14	-0.07363(14)	-0.26439(18)	0.14196(12)	0.0288(5)*
C15	0.01868(15)	-0.28989(18)	0.16357(12)	0.0296(5)*
C16	0.06949(17)	-0.3900(2)	0.19348(13)	0.0380(5)*
C17	0.15881(18)	-0.3882(2)	0.20664(15)	0.0457(6)*
C18	0.20158(17)	-0.2894(2)	0.19286(15)	0.0463(6)*
C19	0.15468(16)	-0.1913(2)	0.16323(14)	0.0397(6)*
C21	-0.24735(16)	-0.1491(2)	0.07744(16)	0.0453(6)*
C22	-0.17489(19)	-0.0015(3)	0.01804(17)	0.0543(7)*
C31	-0.0389(3)	0.2527(3)	0.3962(2)	0.0846(13)*
C32	-0.0159(2)	0.3543(2)	0.44877(15)	0.0482(6)*
C33	0.0785(2)	0.3767(3)	0.4556(2)	0.0761(10)*
C34	0.0893(2)	0.3243(3)	0.37952(19)	0.0576(7)*
Li	0.0000	0.1571(5)	0.2500	0.0409(13)*

Anisotropically-refined atoms are marked with an asterisk (*). The form of the anisotropic displacement parameter is: $\exp[-2\pi^2(h^2a^2U_{11} + k^2b^2U_{22} + l^2c^2U_{33} + 2klb^*c^*U_{23} + 2hla^*c^*U_{13} + 2hka^*b^*U_{12})]$.

Table A.3 Selected Interatomic Distances (Å)

Atom1	Atom2	Distance	Atom1	Atom2	Distance
Ti	Cl	2.5184(6)	C11	C12	1.435(3)
Ti	C11	2.4114(19)	C11	C15	1.431(3)
Ti	C12	2.3855(19)	C11	C19	1.415(3)
Ti	C13	2.517(2)	C12	C13	1.420(3)
Ti	C14	2.400(2)	C13	C14	1.421(3)
Ti	C15	2.443(2)	C14	C15	1.431(3)
Cl	Li	2.284(4)	C15	C16	1.420(3)
O	C31	1.429(3)	C16	C17	1.372(4)
O	C34	1.416(3)	C17	C18	1.402(4)
O	Li	1.923(4)	C18	C19	1.373(3)
N	C13	1.372(3)	C31	C32	1.462(4)
N	C21	1.456(3)	C32	C33	1.500(4)
N	C22	1.448(3)	C33	C34	1.499(4)

Primed atoms are related to unprimed ones via the twofold rotational axis (0, y, 1/4).

Table A.4 Selected Interatomic Angles (deg)

Atom1	Atom2	Atom3	Angle	Atom1	Atom2	Atom3	Angle
Cl	Ti	Cl'	84.97(3)	C13	N	C21	119.18(19)
Cl	Ti	C11	82.25(6)	C13	N	C22	119.2(2)
Cl	Ti	C11'	123.71(5)	C21	N	C22	117.0(2)
Cl	Ti	C12	80.44(6)	Ti	C11	C12	71.60(11)
Cl	Ti	C12'	89.02(5)	Ti	C11	C15	74.06(11)
Cl	Ti	C13	111.26(5)	Ti	C11	C19	120.07(15)
Cl	Ti	C13'	79.23(5)	C12	C11	C15	107.23(19)
Cl	Ti	C14	136.45(5)	C12	C11	C19	132.8(2)
Cl	Ti	C14'	102.97(5)	C15	C11	C19	119.9(2)
Cl	Ti	C15	114.57(5)	Ti	C12	C11	73.58(11)
Cl	Ti	C15'	134.17(5)	Ti	C12	C13	78.33(11)
C11	Ti	C11'	146.90(11)	C11	C12	C13	108.05(19)
C11	Ti	C12	34.82(7)	Ti	C13	N	128.12(14)
C11	Ti	C12'	153.08(7)	Ti	C13	C12	68.13(11)
C11	Ti	C13	55.88(7)	Ti	C13	C14	68.73(11)
C11	Ti	C13'	119.54(7)	N	C13	C12	126.4(2)
C11	Ti	C14	57.48(7)	N	C13	C14	125.8(2)
C11	Ti	C14'	99.84(7)	C12	C13	C14	107.80(19)
C11	Ti	C15	34.29(7)	Ti	C14	C13	77.78(12)
C11	Ti	C15'	113.35(7)	Ti	C14	C15	74.45(12)
C12	Ti	C12'	165.74(11)	C13	C14	C15	107.68(18)
C12	Ti	C13	33.54(7)	Ti	C15	C11	71.65(11)
C12	Ti	C13'	149.66(7)	Ti	C15	C14	71.19(11)
C12	Ti	C14	57.33(7)	Ti	C15	C16	124.93(14)
C12	Ti	C14'	134.39(7)	C11	C15	C14	107.86(18)
C12	Ti	C15	57.09(7)	C11	C15	C16	118.9(2)
C12	Ti	C15'	136.93(7)	C14	C15	C16	133.2(2)
C13	Ti	C13'	166.31(10)	C15	C16	C17	119.3(2)
C13	Ti	C14	33.49(7)	C16	C17	C18	121.6(2)
C13	Ti	C14'	132.89(7)	C17	C18	C19	120.8(2)
C13	Ti	C15	55.31(7)	C11	C19	C18	119.3(2)
C13	Ti	C15'	112.92(7)	O	C31	C32	106.5(2)
C14	Ti	C14'	99.88(10)	C31	C32	C33	103.4(2)
C14	Ti	C15	34.37(7)	C32	C33	C34	105.2(2)
C14	Ti	C15'	81.63(7)	O	C34	C33	106.7(2)
C15	Ti	C15'	82.06(10)	Cl	Li	Cl'	96.3(2)
Ti	Cl	Li	89.39(11)	Cl	Li	O	114.86(8)
C31	O	C34	109.1(2)	Cl	Li	O'	113.31(6)
C31	O	Li	125.44(19)	O	Li	O'	104.6(3)
C34	O	Li	123.21(16)				

Primes are related to unprimed ones via the two fold rotational axis (0,y, 1/4).

Table B.1 Crystallographic Experimental Details**A. Crystal Data**

formula	$C_{31}H_{33}N_2Ti$
formula weight	481.49
crystal dimensions (mm)	$0.27 \times 0.21 \times 0.08$
crystal system	orthorhombic
space group	<i>Pbca</i> (No. 61)
unit cell parameters ^a	
<i>a</i> (Å)	9.8686 (15)
<i>b</i> (Å)	18.510 (3)
<i>c</i> (Å)	27.427 (4)
<i>V</i> (Å ³)	5010.1 (13)
<i>Z</i>	8
ρ_{calcd} (g cm ⁻³)	1.277
μ (mm ⁻¹)	0.363

B. Data Collection and Refinement Conditions

diffractometer	Bruker P4/RA/SMART 1000 CCD ^b
radiation (λ [Å])	graphite-monochromated Mo K α (0.71073)
temperature (°C)	-80
scan type	ϕ rotations (0.3°) / ω scans (0.3°) (30 s
exposures)	
data collection 2θ limit (deg)	51.50
total data collected	25624 ($-11 \leq h \leq 12$, $-22 \leq k \leq 21$, $-33 \leq l \leq 30$)
independent reflections	4778
number of observations (<i>NO</i>)	1687 [$F_o^2 \geq 2\sigma(F_o^2)$]
structure solution method	Patterson interpretation (<i>SHELXS-86</i> ^c)
refinement method	full-matrix least-squares on F^2
(<i>SHELXL-93</i> ^d)	
absorption correction method	<i>SADABS</i>
range of transmission factors	0.9703–0.2272
data/restraints/parameters	4778 [$F_o^2 \geq -3\sigma(F_o^2)$] / 0 / 307
goodness-of-fit (<i>S</i>) ^e	0.838 [$F_o^2 \geq -3\sigma(F_o^2)$]
final <i>R</i> indices ^f	
<i>R</i> ₁ [$F_o^2 \geq 2\sigma(F_o^2)$]	0.0771
<i>wR</i> ₂ [$F_o^2 \geq -3\sigma(F_o^2)$]	0.2237
largest difference peak and hole	0.634 and -0.745 e Å ⁻³

^aObtained from least-squares refinement of 3088 centered reflections.

^bPrograms for diffractometer operation, data collection, data reduction and absorption correction were those supplied by Bruker.

^cSheldrick, G. M. *Acta Crystallogr.* **1990**, *A46*, 467–473.

(continued)

Table B.1 Crystallographic Experimental Details (continued)

^dSheldrick, G. M. *SHELXL-93*. Program for crystal structure determination. University of Göttingen, Germany, 1993. Refinement on F_o^2 for all reflections (all of these having $F_o^2 \geq -3\sigma(F_o^2)$). Weighted R -factors wR_2 and all goodnesses of fit S are based on F_o^2 ; conventional R -factors R_1 are based on F_o , with F_o set to zero for negative F_o^2 . The observed criterion of $F_o^2 > 2\sigma(F_o^2)$ is used only for calculating R_1 , and is not relevant to the choice of reflections for refinement. R -factors based on F_o^2 are statistically about twice as large as those based on F_o , and R -factors based on ALL data will be even larger.

$$^eS = [\sum w(F_o^2 - F_c^2)^2 / (n - p)]^{1/2} \quad (n = \text{number of data}; p = \text{number of parameters varied}; w = [\sigma^2(F_o^2) + (0.0972P)^2]^{-1} \text{ where } P = [\text{Max}(F_o^2, 0) + 2F_c^2]/3).$$

$$^fR_1 = \sum ||F_o| - |F_c|| / \sum |F_o|; \quad wR_2 = [\sum w(F_o^2 - F_c^2)^2 / \sum w(F_o^4)]^{1/2}.$$

Table B.2 Atomic Coordinates and Equivalent Isotropic Displacement Parameters

Atom	<i>x</i>	<i>y</i>	<i>z</i>	<i>U</i> _{eq} , Å ²
Ti	0.34506(11)	0.55334(6)	0.37225(4)	0.0348(3)*
N1	0.4005(9)	0.4199(4)	0.2909(2)	0.082(2)*
N2	0.2344(6)	0.4038(3)	0.4361(2)	0.0466(15)*
C1	0.4266(6)	0.6436(3)	0.4241(2)	0.0398(17)*
C2	0.5265(7)	0.5883(4)	0.4234(2)	0.0428(17)*
C3	0.5068(7)	0.5149(3)	0.4362(2)	0.0381(16)*
C4	0.6088(7)	0.4587(4)	0.4325(2)	0.0410(17)*
C5	0.7397(8)	0.4692(4)	0.4132(2)	0.053(2)*
C6	0.8313(8)	0.4136(5)	0.4116(2)	0.058(2)*
C7	0.7979(8)	0.3450(5)	0.4283(3)	0.063(2)*
C8	0.6718(8)	0.3328(4)	0.4480(2)	0.0511(19)*
C9	0.5793(7)	0.3894(4)	0.4499(2)	0.0437(17)*
C11	0.5148(7)	0.6042(4)	0.3146(2)	0.0456(18)*
C12	0.5357(8)	0.5274(4)	0.3179(2)	0.053(2)*
C13	0.4198(8)	0.4940(4)	0.2977(2)	0.0523(19)*
C14	0.3243(7)	0.5480(4)	0.2872(2)	0.0486(18)*
C15	0.3816(7)	0.6164(4)	0.2957(2)	0.0426(18)*
C16	0.3325(8)	0.6884(4)	0.2911(2)	0.055(2)*
C17	0.4179(10)	0.7440(4)	0.3018(3)	0.064(2)*
C18	0.5515(10)	0.7312(5)	0.3174(3)	0.068(2)*
C19	0.5977(8)	0.6652(5)	0.3233(2)	0.061(2)*
C21	0.1214(6)	0.5867(3)	0.4074(2)	0.0342(16)*
C22	0.1848(6)	0.5351(3)	0.4387(2)	0.0359(16)*
C23	0.1912(6)	0.4680(3)	0.4156(2)	0.0378(16)*
C24	0.1498(6)	0.4794(4)	0.3663(2)	0.0423(16)*
C25	0.0968(6)	0.5514(4)	0.3619(2)	0.0381(16)*
C26	0.0272(6)	0.5881(4)	0.3240(2)	0.0444(18)*
C27	-0.0147(7)	0.6575(4)	0.3317(3)	0.054(2)*
C28	0.0110(7)	0.6908(4)	0.3768(3)	0.0503(18)*
C29	0.0787(6)	0.6581(4)	0.4139(2)	0.0428(17)*
C30	0.5015(10)	0.3728(4)	0.3100(3)	0.090(3)*
C34	0.3370(10)	0.3985(5)	0.2489(4)	0.106(3)*
C35	0.1974(7)	0.3923(4)	0.4872(2)	0.059(2)*
C39	0.2217(8)	0.3394(4)	0.4062(3)	0.065(2)*

Anisotropically-refined atoms are marked with an asterisk (*). The form of the anisotropic displacement parameter is: $\exp[-2\pi^2(h^2a^{*2}U_{11} + k^2b^{*2}U_{22} + l^2c^{*2}U_{33} + 2klb^*c^*U_{23} + 2hla^*c^*U_{13} + 2hka^*b^*U_{12})]$.

Table B.3 Selected Interatomic Distances (Å)

Atom1	Atom2	Distance	Atom1	Atom2	Distance
Ti	C1	2.336(6)	C6	C7	1.389(10)
Ti	C2	2.364(6)	C7	C8	1.375(10)
Ti	C3	2.475(6)	C8	C9	1.391(9)
Ti	C11	2.488(6)	C11	C12	1.438(9)
Ti	C12	2.447(7)	C11	C15	1.431(9)
Ti	C13	2.434(7)	C11	C19	1.414(9)
Ti	C14	2.344(6)	C12	C13	1.413(10)
Ti	C15	2.428(6)	C13	C14	1.404(9)
Ti	C21	2.486(6)	C14	C15	1.406(9)
Ti	C22	2.437(6)	C15	C16	1.423(9)
Ti	C24	2.370(6)	C16	C17	1.362(10)
Ti	C25	2.466(6)	C17	C18	1.406(11)
N1	C13	1.399(9)	C18	C19	1.314(10)
N1	C30	1.423(10)	C21	C22	1.430(8)
N1	C34	1.371(9)	C21	C25	1.428(8)
N2	C23	1.382(8)	C21	C29	1.399(8)
N2	C35	1.464(7)	C22	C23	1.397(8)
N2	C39	1.454(8)	C23	C24	1.430(8)
C1	C2	1.420(9)	C24	C25	1.437(8)
C2	C3	1.416(8)	C25	C26	1.419(8)
C3	C4	1.451(9)	C26	C27	1.366(9)
C4	C5	1.410(9)	C27	C28	1.405(9)
C4	C9	1.400(8)	C28	C29	1.361(8)
C5	C6	1.372(9)			

Table B.4 Selected Interatomic Angles (deg)

Atom1	Atom2	Atom3	Angle	Atom1	Atom2	Atom3	Angle
C1	Ti	C2	35.2(2)	C12	Ti	C15	56.9(2)
C1	Ti	C3	63.4(2)	C12	Ti	C21	165.2(2)
C1	Ti	C11	83.3(2)	C12	Ti	C22	158.0(2)
C1	Ti	C12	104.2(3)	C12	Ti	C24	118.0(3)
C1	Ti	C13	136.8(3)	C12	Ti	C25	133.7(2)
C1	Ti	C14	131.7(2)	C13	Ti	C14	34.1(2)
C1	Ti	C15	97.5(2)	C13	Ti	C15	56.4(2)
C1	Ti	C21	83.8(2)	C13	Ti	C21	134.9(2)
C1	Ti	C22	82.4(2)	C13	Ti	C22	139.7(2)
C1	Ti	C24	137.3(2)	C13	Ti	C24	85.9(2)
C1	Ti	C25	115.0(2)	C13	Ti	C25	101.4(2)
C2	Ti	C3	33.9(2)	C14	Ti	C15	34.2(2)
C2	Ti	C11	76.3(2)	C14	Ti	C21	108.6(2)
C2	Ti	C12	80.3(3)	C14	Ti	C22	133.0(2)
C2	Ti	C13	113.1(3)	C14	Ti	C24	80.5(2)
C2	Ti	C14	131.9(2)	C14	Ti	C25	78.4(2)
C2	Ti	C15	105.6(2)	C15	Ti	C21	110.3(2)
C2	Ti	C21	112.0(2)	C15	Ti	C22	144.0(2)
C2	Ti	C22	94.9(2)	C15	Ti	C24	109.8(2)
C2	Ti	C24	144.6(2)	C15	Ti	C25	93.2(2)
C2	Ti	C25	145.5(2)	C21	Ti	C22	33.75(19)
C3	Ti	C11	97.1(2)	C21	Ti	C24	56.5(2)
C3	Ti	C12	83.1(2)	C21	Ti	C25	33.51(18)
C3	Ti	C13	105.6(2)	C22	Ti	C24	56.2(2)
C3	Ti	C14	138.5(2)	C22	Ti	C25	55.9(2)
C3	Ti	C15	130.9(2)	C24	Ti	C25	34.5(2)
C3	Ti	C21	111.7(2)	C13	N1	C30	117.1(8)
C3	Ti	C22	81.3(2)	C13	N1	C34	117.3(7)
C3	Ti	C24	114.1(2)	C30	N1	C34	116.9(7)
C3	Ti	C25	135.9(2)	C23	N2	C35	115.9(6)
C11	Ti	C12	33.9(2)	C23	N2	C39	116.7(6)
C11	Ti	C13	55.5(2)	C35	N2	C39	113.6(5)
C11	Ti	C14	56.1(2)	Ti	C1	C2	73.5(3)
C11	Ti	C15	33.8(2)	Ti	C2	C1	71.3(4)
C11	Ti	C21	138.6(2)	Ti	C2	C3	77.3(4)
C11	Ti	C22	164.7(2)	C1	C2	C3	126.3(6)
C11	Ti	C24	136.2(2)	Ti	C3	C2	68.8(3)
C11	Ti	C25	127.0(2)	Ti	C3	C4	127.2(4)
C12	Ti	C13	33.7(2)	C2	C3	C4	125.1(6)
C12	Ti	C14	56.8(2)	C3	C4	C5	124.2(6)

Table B.4 Selected Interatomic Angles (continued)

Atom1	Atom2	Atom3	Angle	Atom1	Atom2	Atom3	Angle
C3	C4	C9	119.3(6)	C16	C17	C18	121.2(8)
C5	C4	C9	116.4(6)	C17	C18	C19	121.3(8)
C4	C5	C6	120.8(7)	C11	C19	C18	121.4(8)
C5	C6	C7	121.3(7)	Ti	C21	C22	71.2(3)
C6	C7	C8	119.7(7)	Ti	C21	C25	72.5(3)
C7	C8	C9	119.0(7)	Ti	C21	C29	123.5(4)
C4	C9	C8	122.8(7)	C22	C21	C25	107.1(5)
Ti	C11	C12	71.5(4)	C22	C21	C29	133.3(6)
Ti	C11	C15	70.8(4)	C25	C21	C29	119.6(6)
Ti	C11	C19	125.8(4)	Ti	C22	C21	75.0(3)
C12	C11	C15	108.1(6)	Ti	C22	C23	75.8(4)
C12	C11	C19	134.0(8)	C21	C22	C23	109.9(6)
C15	C11	C19	117.7(7)	Ti	C23	N2	123.4(4)
Ti	C12	C11	74.6(4)	Ti	C23	C22	71.3(3)
Ti	C12	C13	72.7(4)	Ti	C23	C24	68.2(3)
C11	C12	C13	106.9(6)	N2	C23	C22	126.4(6)
Ti	C13	N1	120.9(5)	N2	C23	C24	126.9(6)
Ti	C13	C12	73.7(4)	C22	C23	C24	106.6(6)
Ti	C13	C14	69.4(4)	Ti	C24	C23	77.7(4)
N1	C13	C12	126.3(7)	Ti	C24	C25	76.4(3)
N1	C13	C14	125.5(8)	C23	C24	C25	108.6(5)
C12	C13	C14	108.2(6)	Ti	C25	C21	74.0(3)
Ti	C14	C13	76.5(4)	Ti	C25	C24	69.1(3)
Ti	C14	C15	76.2(4)	Ti	C25	C26	123.9(4)
C13	C14	C15	109.7(7)	C21	C25	C24	106.9(5)
Ti	C15	C11	75.4(4)	C21	C25	C26	120.2(6)
Ti	C15	C14	69.6(3)	C24	C25	C26	132.9(6)
Ti	C15	C16	118.5(4)	C25	C26	C27	119.0(6)
C11	C15	C14	106.7(6)	C26	C27	C28	119.5(6)
C11	C15	C16	119.5(7)	C27	C28	C29	123.5(6)
C14	C15	C16	133.7(7)	C21	C29	C28	118.2(6)
C15	C16	C17	118.6(8)				

Part C. Crystallographic Details for Bis(2-*N,N*-dimethylaminoindenyl)titanium(η^3 -1-methylallyl), Complex **99 and **99'**.**

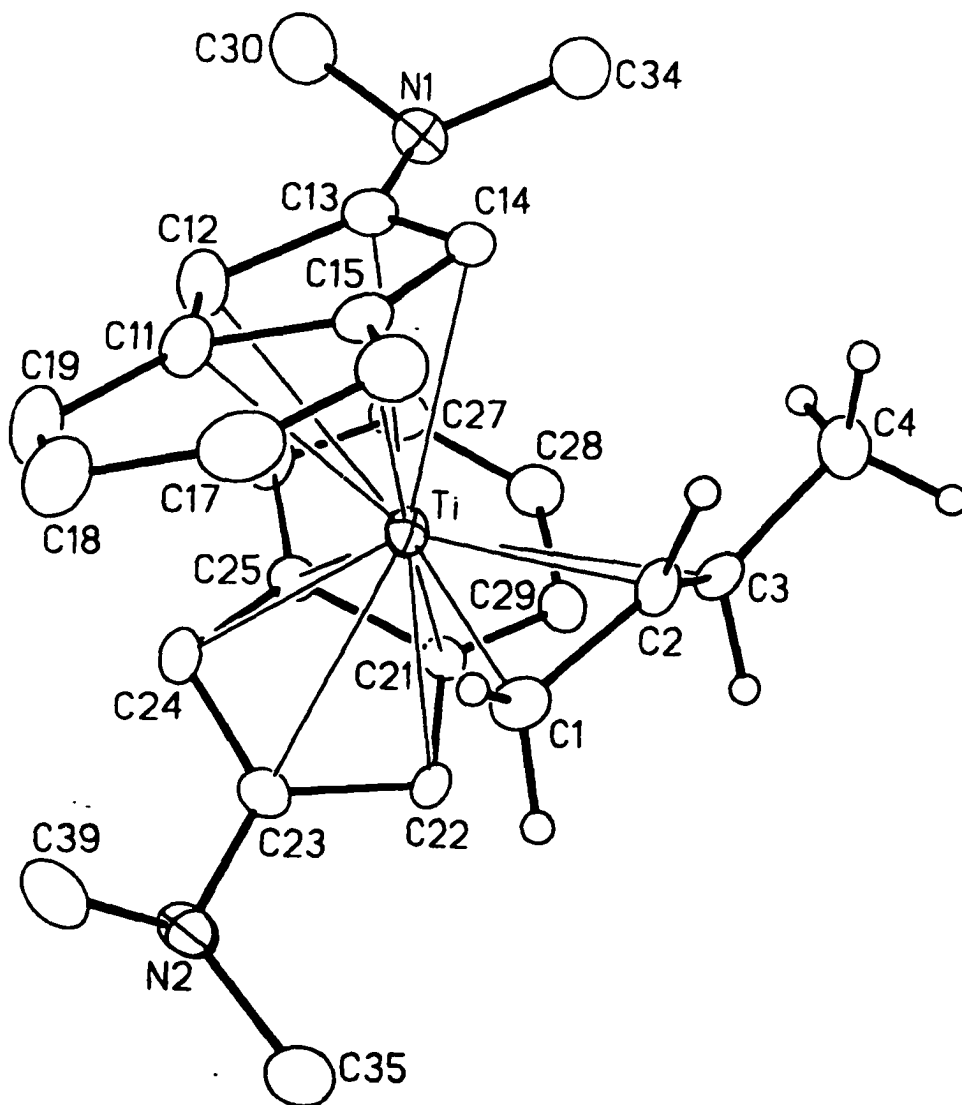


Figure C.1a Perspective view of one of the two equally-abundant independent molecules of $[(\eta^5\text{-2-dimethylaminoindenyl})_2\text{Ti}(\eta^3\text{-crotyl})]$ **99** in the asymmetric unit showing the atom labelling scheme. Non-hydrogen atoms are represented by Gaussian ellipsoids at the 20% probability level. Hydrogen atoms of the crotyl group are shown with arbitrarily small thermal parameters; all other hydrogens are not shown. Note the opposing dispositions of the NMe_2 groups; in this conformation the lone pair on N1 is oriented towards the side of the indenyl plane coordinated to the Ti atom, whereas the lone pair on N2 is directed towards the side of the indenyl plane opposite to the coordinated Ti.

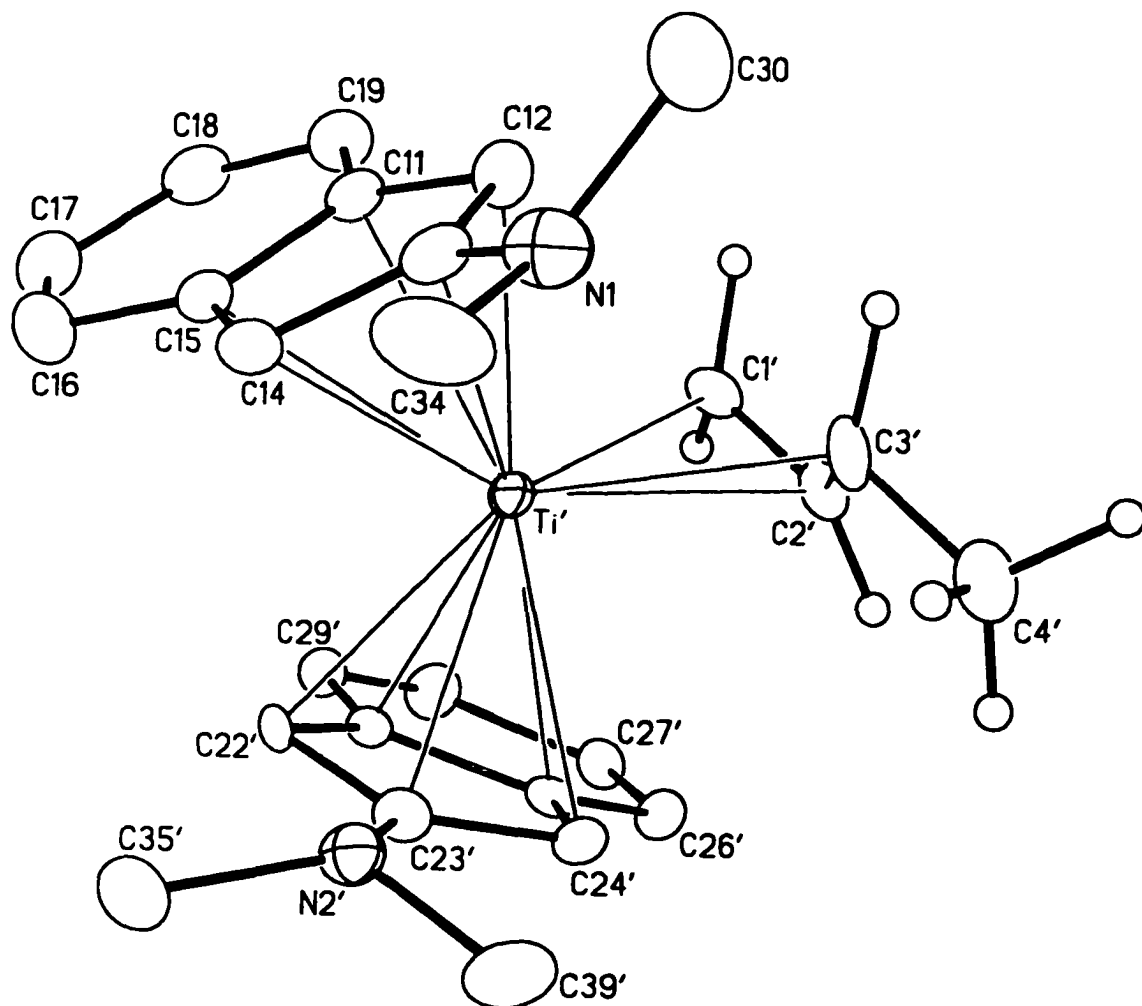


Figure C.1b View of the second $[(\eta^5\text{-2-dimethylaminoindenyl})_2\text{Ti}(\eta^3\text{-crotyl})]$ conformer. In this form the NMe_2 groups are nearly eclipsing, and the nitrogen lone pairs are oriented towards the sides of the indenyl planes coordinated to Ti' .

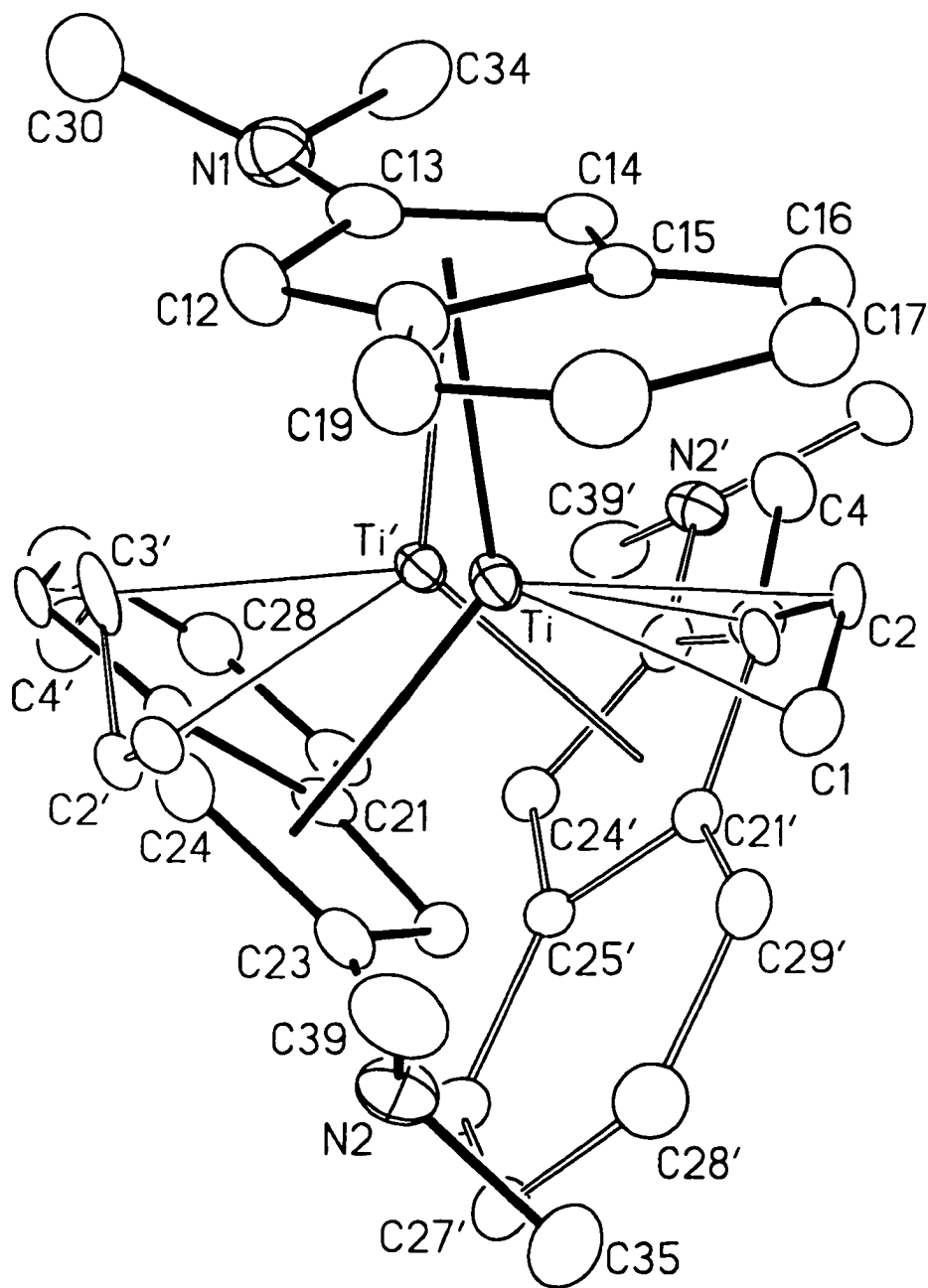


Figure C.2 View of superimposed disordered conformers **99** and **99'**.

Table C.1 Crystallographic Experimental Details**A. Crystal Data**

formula	C ₂₆ H ₃₁ N ₂ Ti
formula weight	419.43
crystal dimensions (mm)	0.45 × 0.27 × 0.09
crystal system	monoclinic
space group	<i>C2/c</i> (No. 15)
unit cell parameters ^a	
<i>a</i> (Å)	28.790 (4)
<i>b</i> (Å)	8.1016 (12)
<i>c</i> (Å)	20.223 (3)
β (deg)	111.707 (3)
<i>V</i> (Å ³)	4382.4 (11)
<i>Z</i>	8
ρ _{calcd} (g cm ⁻³)	1.271
μ (mm ⁻¹)	0.405

B. Data Collection and Refinement Conditions

diffractometer	Bruker PLATFORM/SMART 1000 CCD ^b
radiation (λ [Å])	graphite-monochromated Mo Kα (0.71073)
temperature (°C)	-80
scan type	ω scans (0.3°) (30 s exposures)
data collection 2θ limit (deg)	51.40
total data collected	10604 (-23 ≤ <i>h</i> ≤ 34, -9 ≤ <i>k</i> ≤ 9, -24 ≤ <i>l</i> ≤ 24)
independent reflections	4162
number of observations (<i>NO</i>)	2321 [<i>F</i> _o ² ≥ 2σ(<i>F</i> _o ²)]
structure solution method	direct methods (<i>SHELXS-86</i> ^c)
refinement method	full-matrix least-squares on <i>F</i> ²
(<i>SHELXL-93</i> ^d)	
absorption correction method	<i>SADABS</i>
range of transmission factors	0.9280–0.6987
data/restraints/parameters	4162 [<i>F</i> _o ² ≥ -3σ(<i>F</i> _o ²)] / 0 / 412
goodness-of-fit (<i>S</i>) ^e	0.882 [<i>F</i> _o ² ≥ -3σ(<i>F</i> _o ²)]
final <i>R</i> indices ^f	
<i>R</i> ₁ [<i>F</i> _o ² ≥ 2σ(<i>F</i> _o ²)]	0.0451
<i>wR</i> ₂ [<i>F</i> _o ² ≥ -3σ(<i>F</i> _o ²)]	0.0999
largest difference peak and hole	0.316 and -0.191 e Å ⁻³

^aObtained from least-squares refinement of 2273 centered reflections.

^bPrograms for diffractometer operation, data collection, data reduction and absorption correction were those supplied by Bruker.

(continued)

Table C.1 Crystallographic Experimental Details (continued)

^cSheldrick, G. M. *Acta Crystallogr.* **1990**, *A46*, 467–473.

^dSheldrick, G. M. *SHELXL-93*. Program for crystal structure determination. University of Göttingen, Germany, 1993. Refinement on F_o^2 for all reflections (all of these having $F_o^2 \geq -3\sigma(F_o^2)$). Weighted R -factors wR_2 and all goodnesses of fit S are based on F_o^2 ; conventional R -factors R_1 are based on F_o , with F_o set to zero for negative F_o^2 . The observed criterion of $F_o^2 > 2\sigma(F_o^2)$ is used only for calculating R_1 , and is not relevant to the choice of reflections for refinement. R -factors based on F_o^2 are statistically about twice as large as those based on F_o , and R -factors based on ALL data will be even larger.

$$^e S = [\sum w(F_o^2 - F_c^2)^2 / (n - p)]^{1/2} \quad (n = \text{number of data}; p = \text{number of parameters varied}; w = [\sigma^2(F_o^2) + (0.0433P)^2]^{-1} \text{ where } P = [\text{Max}(F_o^2, 0) + 2F_c^2]/3).$$

$$^f R_1 = \sum ||F_o| - |F_c|| / \sum |F_o|; wR_2 = [\sum w(F_o^2 - F_c^2)^2 / \sum w(F_o^4)]^{1/2}.$$

Table C.2 Atomic Coordinates and Equivalent Isotropic Displacement Parameters

Atom	<i>x</i>	<i>y</i>	<i>z</i>	$U_{\text{eq}}, \text{\AA}^2$
Ti ^a	0.12560(13)	0.1866(4)	0.24161(14)	0.0310(5)*
Ti' ^a	0.12903(12)	0.2184(3)	0.22241(14)	0.0270(5)*
N1	0.14334(9)	0.0377(3)	0.08575(13)	0.0600(6)*
N2 ^a	0.1322(2)	0.5342(5)	0.3521(2)	0.0504(12)*
N2' ^a	0.0284(4)	-0.0306(9)	0.1513(5)	0.0412(19)*
C1 ^a	0.1112(2)	0.1028(7)	0.3406(3)	0.0449(14)*
C2 ^a	0.0860(3)	-0.0109(7)	0.2878(3)	0.0369(16)*
C3 ^a	0.0486(4)	0.0265(10)	0.2255(5)	0.040(2)*
C4 ^a	0.0248(5)	-0.0975(12)	0.1662(6)	0.055(3)*
C1' ^a	0.1644(3)	0.4727(13)	0.2477(7)	0.039(2)*
C2' ^a	0.1225(4)	0.4928(11)	0.1848(7)	0.041(3)*
C3' ^a	0.1130(7)	0.400(2)	0.1196(11)	0.056(4)*
C4' ^a	0.0671(7)	0.4279(19)	0.0579(7)	0.060(3)*
C11	0.21540(9)	0.1255(3)	0.27324(14)	0.0453(7)*
C12	0.19855(10)	0.1692(3)	0.20015(14)	0.0521(7)*
C13	0.16497(10)	0.0463(3)	0.15987(15)	0.0463(7)*
C14	0.15626(10)	-0.0629(3)	0.20815(15)	0.0462(7)*
C15	0.18926(10)	-0.0211(3)	0.27761(15)	0.0446(7)*
C16	0.20037(13)	-0.0959(4)	0.34540(18)	0.0650(9)*
C17	0.23505(12)	-0.0272(4)	0.40380(17)	0.0652(9)*
C18	0.26008(10)	0.1186(4)	0.39926(16)	0.0632(8)*
C19	0.25069(10)	0.1947(4)	0.33581(15)	0.0603(8)*
C21 ^a	0.06202(18)	0.3854(5)	0.1720(3)	0.0354(12)*
C22 ^a	0.0686(3)	0.4029(8)	0.2459(4)	0.0367(17)*
C23 ^a	0.11591(19)	0.4725(5)	0.2821(3)	0.0366(12)*
C24 ^a	0.1428(3)	0.4756(15)	0.2367(7)	0.038(2)*
C25 ^a	0.1090(4)	0.4322(10)	0.1673(6)	0.0340(19)*
C26 ^a	0.1126(6)	0.4379(17)	0.1017(10)	0.038(3)*
C27 ^a	0.0713(7)	0.3846(19)	0.0389(8)	0.051(3)*
C28 ^a	0.0264(2)	0.3365(6)	0.0465(3)	0.0480(14)*
C29 ^a	0.02123(11)	0.3352(4)	0.11044(17)	0.0428(13)*
C21' ^a	0.09404(11)	0.2095(4)	0.31380(17)	0.0269(10)*
C22' ^a	0.08437(11)	0.0583(4)	0.27372(17)	0.0332(18)*
C23' ^a	0.0480(4)	0.0902(9)	0.2044(5)	0.036(2)*
C24' ^a	0.03963(17)	0.2582(5)	0.1982(2)	0.0321(11)*
C25' ^a	0.0649(2)	0.3334(7)	0.2656(4)	0.0285(15)*
C26' ^a	0.06523(18)	0.4962(6)	0.2915(3)	0.0358(12)*
C27' ^a	0.0943(5)	0.5380(16)	0.3605(5)	0.040(2)*
C28' ^a	0.1253(2)	0.4117(7)	0.4064(3)	0.0447(14)*
C29' ^a	0.12468(10)	0.2530(3)	0.38308(13)	0.0406(13)*

Table C.2 Atomic Coordinates and Displacement Parameters (continued)

Atom	x	y	z	$U_{eq}, \text{\AA}^2$
C30	0.17135(10)	0.0973(3)	0.04517(13)	0.0729(9)*
C34	0.11257(12)	-0.1044(4)	0.05638(17)	0.0815(10)*
C35 ^a	0.0974(6)	0.527(2)	0.3880(6)	0.068(4)*
C39 ^a	0.1834(2)	0.5049(7)	0.3968(3)	0.0619(17)*
C35' ^a	0.0257(3)	-0.1998(7)	0.1735(4)	0.053(2)*
C39' ^a	-0.0110(2)	0.0215(7)	0.0875(3)	0.0536(15)*

Anisotropically-refined atoms are marked with an asterisk (*). The form of the anisotropic displacement parameter is: $\exp[-2\pi^2(h^2a^{*2}U_{11} + k^2b^{*2}U_{22} + l^2c^{*2}U_{33} + 2klb^{*c}U_{23} + 2hla^{*c}U_{13} + 2hka^{*b}U_{12})]$. ^aRefined with an occupancy factor of 0.5.

Table C.3 Selected Interatomic Distances (Å)

Atom1	Atom2	Distance	Atom1	Atom2	Distance
Ti	C1	2.292(5)	C2	C3	1.354(11)
Ti	C2	2.350(6)	C3	C4	1.519(15)
Ti	C3	2.484(10)	C1'	C2'	1.402(15)
Ti	C11	2.473(4)	C2'	C3'	1.45(3)
Ti	C12	2.537(4)	C3'	C4'	1.46(3)
Ti	C13	2.588(4)	C11	C12	1.419(3)
Ti	C14	2.401(4)	C11	C15	1.426(3)
Ti	C15	2.394(4)	C11	C19	1.413(3)
Ti	C21	2.453(5)	C12	C13	1.416(3)
Ti	C22	2.425(8)	C13	C14	1.407(3)
Ti	C23	2.506(6)	C14	C15	1.415(3)
Ti	C24	2.403(13)	C15	C16	1.423(4)
Ti	C25	2.432(11)	C16	C17	1.352(4)
Ti'	C1'	2.272(11)	C17	C18	1.404(4)
Ti'	C2'	2.335(10)	C18	C19	1.357(4)
Ti'	C3'	2.447(12)	C21	C22	1.442(9)
Ti'	C11	2.432(4)	C21	C25	1.440(11)
Ti'	C12	2.243(4)	C21	C29	1.419(5)
Ti'	C13	2.362(4)	C22	C23	1.405(8)
Ti'	C14	2.461(4)	C23	C24	1.405(13)
Ti'	C15	2.566(4)	C24	C25	1.425(15)
Ti'	C21'	2.411(4)	C25	C26	1.37(2)
Ti'	C22'	2.323(4)	C26	C27	1.45(3)
Ti'	C23'	2.454(9)	C27	C28	1.410(19)
Ti'	C24'	2.457(5)	C28	C29	1.356(6)
Ti'	C25'	2.496(7)	C21'	C22'	1.4380
N1	C13	1.396(3)	C21'	C25'	1.433(7)
N1	C30	1.431(3)	C21'	C29'	1.397(4)
N1	C34	1.440(3)	C22'	C23'	1.429(10)
N2	C23	1.407(6)	C23'	C24'	1.380(9)
N2	C35	1.440(14)	C24'	C25'	1.423(8)
N2	C39	1.435(7)	C25'	C26'	1.417(8)
N2'	C23'	1.408(13)	C26'	C27'	1.378(12)
N2'	C35'	1.453(8)	C27'	C28'	1.445(14)
N2'	C39'	1.430(11)	C28'	C29'	1.367(6)
C1	C2	1.394(8)			

Table C.4 Selected Interatomic Angles (deg)

Atom1	Atom2	Atom3	Angle	Atom1	Atom2	Atom3	Angle
C1	Ti	C2	34.93(19)	C11	Ti	C24	89.6(2)
C1	Ti	C3	61.3(3)	C11	Ti	C25	105.8(3)
C1	Ti	C11	102.95(19)	C12	Ti	C13	32.07(8)
C1	Ti	C12	135.3(2)	C12	Ti	C14	54.87(11)
C1	Ti	C13	133.72(19)	C12	Ti	C15	55.06(11)
C1	Ti	C14	101.57(17)	C12	Ti	C21	112.34(15)
C1	Ti	C15	83.76(17)	C12	Ti	C22	134.93(18)
C1	Ti	C21	111.0(2)	C12	Ti	C23	111.43(17)
C1	Ti	C22	80.8(2)	C12	Ti	C24	80.3(3)
C1	Ti	C23	84.9(2)	C12	Ti	C25	80.8(3)
C1	Ti	C24	115.6(4)	C13	Ti	C14	32.50(9)
C1	Ti	C25	136.4(3)	C13	Ti	C15	54.45(11)
C2	Ti	C3	32.4(2)	C13	Ti	C21	109.39(16)
C2	Ti	C11	112.1(2)	C13	Ti	C22	143.4(2)
C2	Ti	C12	132.6(2)	C13	Ti	C23	137.97(15)
C2	Ti	C13	110.3(2)	C13	Ti	C24	104.8(3)
C2	Ti	C14	79.73(19)	C13	Ti	C25	89.9(3)
C2	Ti	C15	80.22(18)	C14	Ti	C15	34.33(9)
C2	Ti	C21	107.8(2)	C14	Ti	C21	131.69(18)
C2	Ti	C22	92.5(2)	C14	Ti	C22	160.5(2)
C2	Ti	C23	111.7(2)	C14	Ti	C23	165.25(19)
C2	Ti	C24	144.9(4)	C14	Ti	C24	134.9(3)
C2	Ti	C25	142.1(3)	C14	Ti	C25	121.6(3)
C3	Ti	C11	136.6(2)	C15	Ti	C21	163.84(19)
C3	Ti	C12	137.3(3)	C15	Ti	C22	161.7(2)
C3	Ti	C13	105.5(3)	C15	Ti	C23	135.7(2)
C3	Ti	C14	85.8(2)	C15	Ti	C24	123.4(2)
C3	Ti	C15	102.6(2)	C15	Ti	C25	135.8(3)
C3	Ti	C21	80.0(2)	C21	Ti	C22	34.4(2)
C3	Ti	C22	78.4(3)	C21	Ti	C23	55.35(16)
C3	Ti	C23	108.9(3)	C21	Ti	C24	57.2(2)
C3	Ti	C24	133.7(3)	C21	Ti	C25	34.3(3)
C3	Ti	C25	112.6(3)	C22	Ti	C23	33.0(2)
C11	Ti	C12	32.89(9)	C22	Ti	C24	56.7(3)
C11	Ti	C13	54.14(11)	C22	Ti	C25	56.6(3)
C11	Ti	C14	56.37(11)	C23	Ti	C24	33.2(3)
C11	Ti	C15	34.03(9)	C23	Ti	C25	54.9(3)
C11	Ti	C21	140.05(16)	C24	Ti	C25	34.3(3)
C11	Ti	C22	142.4(2)	C1'	Ti'	C2'	35.4(4)
C11	Ti	C23	109.42(18)	C1'	Ti'	C3'	64.8(6)

Table C.4 Selected Interatomic Angles (continued)

Atom1	Atom2	Atom3	Angle	Atom1	Atom2	Atom3	Angle
C1'	Ti'	C11	83.2(3)	C12	Ti'	C13	35.70(10)
C1'	Ti'	C12	81.2(3)	C12	Ti'	C14	57.70(11)
C1'	Ti'	C13	114.0(3)	C12	Ti'	C15	56.20(11)
C1'	Ti'	C14	136.9(3)	C12	Ti'	C21'	143.63(16)
C1'	Ti'	C15	114.4(3)	C12	Ti'	C22'	132.27(15)
C1'	Ti'	C21'	97.7(4)	C12	Ti'	C23'	139.9(3)
C1'	Ti'	C22'	133.0(4)	C12	Ti'	C24'	158.44(18)
C1'	Ti'	C23'	137.7(3)	C12	Ti'	C25'	165.1(2)
C1'	Ti'	C24'	106.0(3)	C13	Ti'	C14	33.85(9)
C1'	Ti'	C25'	84.9(3)	C13	Ti'	C15	55.08(11)
C2'	Ti'	C3'	35.3(6)	C13	Ti'	C21'	141.51(14)
C2'	Ti'	C11	112.2(3)	C13	Ti'	C22'	109.52(15)
C2'	Ti'	C12	94.2(3)	C13	Ti'	C23'	104.6(3)
C2'	Ti'	C13	112.7(3)	C13	Ti'	C24'	127.23(19)
C2'	Ti'	C14	146.5(3)	C13	Ti'	C25'	159.2(2)
C2'	Ti'	C15	145.2(3)	C14	Ti'	C15	32.62(9)
C2'	Ti'	C21'	105.8(3)	C14	Ti'	C21'	107.68(11)
C2'	Ti'	C22'	133.3(3)	C14	Ti'	C22'	77.79(12)
C2'	Ti'	C23'	113.4(3)	C14	Ti'	C23'	85.2(2)
C2'	Ti'	C24'	81.9(3)	C14	Ti'	C24'	117.00(17)
C2'	Ti'	C25'	77.2(3)	C14	Ti'	C25'	134.06(17)
C3'	Ti'	C11	112.8(5)	C15	Ti'	C21'	92.90(11)
C3'	Ti'	C12	80.7(5)	C15	Ti'	C22'	77.31(11)
C3'	Ti'	C13	83.2(6)	C15	Ti'	C23'	101.3(2)
C3'	Ti'	C14	115.2(6)	C15	Ti'	C24'	132.49(15)
C3'	Ti'	C15	135.1(5)	C15	Ti'	C25'	126.73(16)
C3'	Ti'	C21'	131.9(5)	C21'	Ti'	C22'	35.30(6)
C3'	Ti'	C22'	138.9(5)	C21'	Ti'	C23'	57.1(2)
C3'	Ti'	C23'	105.0(5)	C21'	Ti'	C24'	56.80(14)
C3'	Ti'	C24'	84.1(5)	C21'	Ti'	C25'	33.91(16)
C3'	Ti'	C25'	98.1(6)	C22'	Ti'	C23'	34.7(2)
C11	Ti'	C12	35.05(10)	C22'	Ti'	C24'	56.64(14)
C11	Ti'	C13	57.45(12)	C22'	Ti'	C25'	56.57(16)
C11	Ti'	C14	56.15(11)	C23'	Ti'	C24'	32.6(2)
C11	Ti'	C15	33.02(9)	C23'	Ti'	C25'	54.9(3)
C11	Ti'	C21'	108.57(14)	C24'	Ti'	C25'	33.38(19)
C11	Ti'	C22'	106.67(13)	C13	N1	C30	118.5(2)
C11	Ti'	C23'	134.3(2)	C13	N1	C34	116.4(2)
C11	Ti'	C24'	163.08(14)	C30	N1	C34	115.1(2)
C11	Ti'	C25'	137.7(2)	C23	N2	C35	117.3(7)

Table C.4 Selected Interatomic Angles (continued)

Atom1	Atom2	Atom3	Angle	Atom1	Atom2	Atom3	Angle
C23	N2	C39	117.2(5)	N1	C13	C14	126.2(2)
C35	N2	C39	114.7(7)	C12	C13	C14	107.6(2)
C23'	N2'	C35'	118.2(7)	Ti	C14	C13	81.04(15)
C23'	N2'	C39'	116.4(7)	Ti	C14	C15	72.57(15)
C35'	N2'	C39'	116.2(8)	Ti'	C14	C13	69.21(14)
Ti	C1	C2	74.8(3)	Ti'	C14	C15	77.75(15)
Ti	C2	C1	70.3(3)	C13	C14	C15	108.1(2)
Ti	C2	C3	79.3(4)	Ti	C15	C11	76.00(15)
C1	C2	C3	125.1(6)	Ti	C15	C14	73.10(16)
Ti	C3	C2	68.3(5)	Ti	C15	C16	117.80(19)
Ti	C3	C4	124.6(6)	Ti'	C15	C11	68.33(15)
C2	C3	C4	123.9(7)	Ti'	C15	C14	69.63(15)
Ti'	C1'	C2'	74.8(6)	Ti'	C15	C16	128.04(19)
Ti'	C2'	C1'	69.8(6)	C11	C15	C14	108.3(2)
Ti'	C2'	C3'	76.6(5)	C11	C15	C16	118.6(3)
C1'	C2'	C3'	125.0(11)	C14	C15	C16	133.1(3)
Ti'	C3'	C2'	68.2(7)	C15	C16	C17	119.8(3)
Ti'	C3'	C4'	130.2(11)	C16	C17	C18	121.3(3)
C2'	C3'	C4'	120.1(16)	C17	C18	C19	121.1(3)
Ti	C11	C12	76.04(15)	C11	C19	C18	119.5(3)
Ti	C11	C15	69.97(15)	Ti	C21	C22	71.7(3)
Ti	C11	C19	119.3(2)	Ti	C21	C25	72.0(5)
Ti'	C11	C12	65.19(15)	Ti	C21	C29	121.0(3)
Ti'	C11	C15	78.65(15)	C22	C21	C25	106.0(6)
Ti'	C11	C19	122.7(2)	C22	C21	C29	133.3(5)
C12	C11	C15	106.7(2)	C25	C21	C29	120.6(6)
C12	C11	C19	133.6(3)	Ti	C22	C21	73.9(3)
C15	C11	C19	119.7(3)	Ti	C22	C23	76.7(4)
Ti	C12	C11	71.08(16)	C21	C22	C23	108.1(5)
Ti	C12	C13	75.93(17)	Ti	C23	N2	128.4(3)
Ti'	C12	C11	79.75(17)	Ti	C23	C22	70.3(3)
Ti'	C12	C13	76.73(17)	Ti	C23	C24	69.4(5)
C11	C12	C13	108.7(2)	N2	C23	C22	124.4(5)
Ti	C13	N1	125.52(18)	N2	C23	C24	126.3(6)
Ti	C13	C12	72.00(17)	C22	C23	C24	109.2(6)
Ti	C13	C14	66.46(15)	Ti	C24	C23	77.5(5)
Ti'	C13	N1	119.64(18)	Ti	C24	C25	74.0(6)
Ti'	C13	C12	67.57(16)	C23	C24	C25	107.3(7)
Ti'	C13	C14	76.94(15)	Ti	C25	C21	73.7(5)
N1	C13	C12	126.2(3)	Ti	C25	C24	71.7(6)

Table C.4 Selected Interatomic Angles (continued)

Atom1	Atom2	Atom3	Angle	Atom1	Atom2	Atom3	Angle
Ti	C25	C26	123.9(7)	Ti'	C23'	C22'	67.7(4)
C21	C25	C24	108.5(9)	Ti'	C23'	C24'	73.8(4)
C21	C25	C26	118.9(10)	N2'	C23'	C22'	124.4(6)
C24	C25	C26	132.4(11)	N2'	C23'	C24'	127.5(7)
C25	C26	C27	120.4(13)	C22'	C23'	C24'	107.9(7)
C26	C27	C28	118.4(11)	Ti'	C24'	C23'	73.5(4)
C27	C28	C29	122.3(7)	Ti'	C24'	C25'	74.8(3)
C21	C29	C28	119.2(4)	C23'	C24'	C25'	109.0(5)
Ti'	C21'	C22'	69.02(10)	Ti'	C25'	C21'	69.8(3)
Ti'	C21'	C25'	76.3(3)	Ti'	C25'	C24'	71.8(3)
Ti'	C21'	C29'	118.3(2)	Ti'	C25'	C26'	124.9(4)
C22'	C21'	C25'	105.7(3)	C21'	C25'	C24'	108.3(4)
C22'	C21'	C29'	134.35(16)	C21'	C25'	C26'	118.6(5)
C25'	C21'	C29'	119.9(3)	C24'	C25'	C26'	133.1(5)
Ti'	C22'	C21'	75.68(11)	C25'	C26'	C27'	121.4(7)
Ti'	C22'	C23'	77.7(3)	C26'	C27'	C28'	118.4(9)
C21'	C22'	C23'	108.5(4)	C27'	C28'	C29'	121.2(6)
Ti'	C23'	N2'	119.9(6)	C21'	C29'	C28'	120.4(3)

Part D. Crystallographic Details for 3-Isopropyl-2-phenyl-bis(2-*N,N*-dimethylaminoindenyl)titanacyclobutane, Complex 101a.

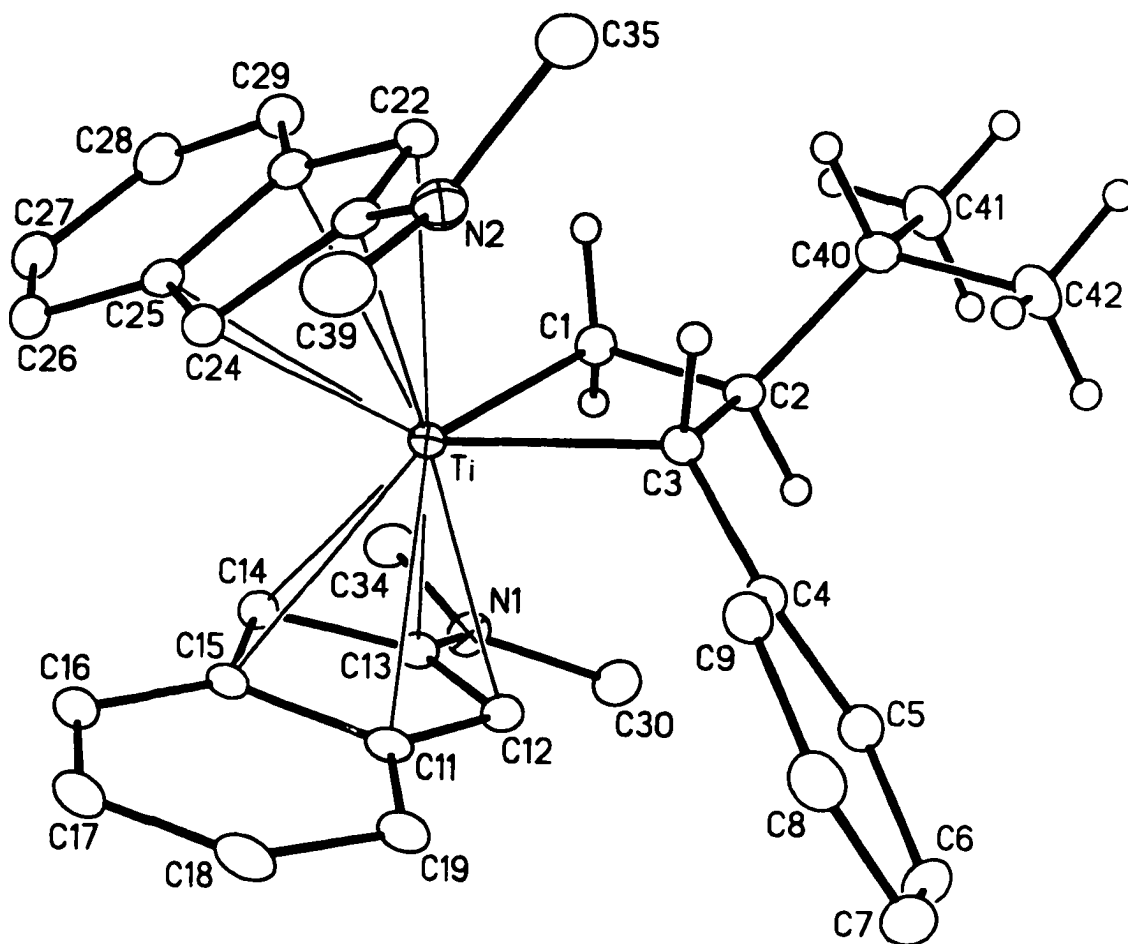


Figure D.1 Perspective view of the $[(\eta^5\text{-2-dimethylaminoindenyl})_2\text{Ti}\{\eta^2\text{-}(\text{C}_6\text{H}_4\text{-CH}(\text{CH}_2\text{CH}_2\text{CH}_3)\text{-CH}_2)\}]$ molecule showing the atom labelling scheme. Non-hydrogen atoms are represented by Gaussian ellipsoids at the 20% probability level. Hydrogen atoms of the titanacyclobutane and isopropyl groups are shown with arbitrarily small thermal parameters; all other hydrogens are not shown.

Table D.1 Crystallographic Experimental Details

A. Crystal Data	
formula	$C_{34}H_{40}N_2Ti$
formula weight	524.58
crystal dimensions (mm)	$0.28 \times 0.26 \times 0.14$
crystal system	triclinic
space group	<i>PI</i> (No. 2)
unit cell parameters ^a	
<i>a</i> (Å)	9.2259 (6)
<i>b</i> (Å)	11.4486 (8)
<i>c</i> (Å)	13.1688 (9)
α (deg)	91.9270 (10)
β (deg)	92.8130 (10)
γ (deg)	93.0000 (10)
<i>V</i> (Å ³)	1386.44 (16)
<i>Z</i>	2
ρ_{calcd} (g cm ⁻³)	1.257
μ (mm ⁻¹)	0.334
B. Data Collection and Refinement Conditions	
diffractometer	Bruker P4/RA/SMART 1000 CCD ^b
radiation (λ [Å])	graphite-monochromated Mo K α (0.71073)
temperature (°C)	-80
scan type	ϕ rotations (0.3°) / ω scans (0.3°) (20 s exposures)
data collection 2θ limit (deg)	51.40
total data collected	7467 ($-11 \leq h \leq 10, -13 \leq k \leq 13, -14 \leq l \leq 16$)
independent reflections	5230
number of observations (<i>NO</i>)	3924 ($F_o^2 \geq 2\sigma(F_o^2)$)
structure solution method	direct methods (<i>SHELXS-86</i> ^c)
refinement method	full-matrix least-squares on F^2
(<i>SHELXL-93</i> ^d)	
absorption correction method	<i>SADABS</i>
range of transmission factors	0.9622–0.6651
data/restraints/parameters	5230 [$F_o^2 \geq -3\sigma(F_o^2)$] / 0 / 334
goodness-of-fit (<i>S</i>) ^e	1.035 [$F_o^2 \geq -3\sigma(F_o^2)$]
final <i>R</i> indices ^f	
$F_o^2 > 2\sigma(F_o^2)$	$R_1 = 0.0545, wR_2 = 0.1453$
all data	$R_1 = 0.0728, wR_2 = 0.1540$
largest difference peak and hole	0.412 and -0.503 e Å ⁻³

^aObtained from least-squares refinement of 5078 centered reflections. (continued)

Table D.1 Crystallographic Experimental Details (continued)

^bPrograms for diffractometer operation, data collection, data reduction and absorption correction were those supplied by Bruker.

^cSheldrick, G. M. *Acta Crystallogr.* **1990**, *A46*, 467–473.

^dSheldrick, G. M. *SHELXL-93*. Program for crystal structure determination. University of Göttingen, Germany, 1993. Refinement on F_o^2 for all reflections (all of these having $F_o^2 \geq -3\sigma(F_o^2)$). Weighted R -factors wR_2 and all goodnesses of fit S are based on F_o^2 ; conventional R -factors R_1 are based on F_o , with F_o set to zero for negative F_o^2 . The observed criterion of $F_o^2 > 2\sigma(F_o^2)$ is used only for calculating R_1 , and is not relevant to the choice of reflections for refinement. R -factors based on F_o^2 are statistically about twice as large as those based on F_o , and R -factors based on ALL data will be even larger.

^e $S = [\sum w(F_o^2 - F_c^2)^2 / (n - p)]^{1/2}$ (n = number of data; p = number of parameters varied; $w = [\sigma^2(F_o^2) + (0.0908P)^2]^{-1}$ where $P = [\text{Max}(F_o^2, 0) + 2F_c^2]/3$).

^f $R_1 = \sum ||F_o| - |F_c|| / \sum |F_o|$; $wR_2 = [\sum w(F_o^2 - F_c^2)^2 / \sum w(F_o^4)]^{1/2}$.

Table D.2 Atomic Coordinates and Equivalent Isotropic Displacement Parameters

Atom	<i>x</i>	<i>y</i>	<i>z</i>	<i>U</i> _{eq} , Å ²
Ti	0.22887(5)	0.33753(4)	-0.25162(4)	0.02183(17)*
N1	0.3179(3)	0.4206(2)	0.00497(18)	0.0330(6)*
N2	0.1251(3)	0.2196(2)	-0.49165(18)	0.0329(6)*
C1	0.0630(3)	0.3083(2)	-0.1472(2)	0.0272(6)*
C2	0.0753(3)	0.1736(2)	-0.1620(2)	0.0250(6)*
C3	0.1704(3)	0.1485(2)	-0.2539(2)	0.0231(6)*
C4	0.2737(3)	0.0539(2)	-0.2521(2)	0.0253(6)*
C5	0.3320(3)	0.0048(2)	-0.1635(2)	0.0305(6)*
C6	0.4382(3)	-0.0761(3)	-0.1668(3)	0.0392(8)*
C7	0.4881(3)	-0.1149(3)	-0.2597(3)	0.0419(8)*
C8	0.4269(3)	-0.0719(3)	-0.3481(3)	0.0379(7)*
C9	0.3219(3)	0.0093(2)	-0.3441(2)	0.0308(6)*
C11	0.4843(3)	0.3008(2)	-0.2168(2)	0.0270(6)*
C12	0.4080(3)	0.2845(2)	-0.1255(2)	0.0257(6)*
C13	0.3706(3)	0.3955(2)	-0.0880(2)	0.0275(6)*
C14	0.3960(3)	0.4770(2)	-0.1653(2)	0.0285(6)*
C15	0.4802(3)	0.4222(2)	-0.2394(2)	0.0287(6)*
C16	0.5582(3)	0.4650(3)	-0.3223(2)	0.0340(7)*
C17	0.6296(3)	0.3890(3)	-0.3809(2)	0.0391(8)*
C18	0.6279(3)	0.2682(3)	-0.3614(2)	0.0375(7)*
C19	0.5579(3)	0.2238(3)	-0.2805(2)	0.0314(7)*
C21	0.0519(3)	0.4680(2)	-0.3266(2)	0.0281(6)*
C22	0.0170(3)	0.3519(2)	-0.3658(2)	0.0254(6)*
C23	0.1266(3)	0.3203(2)	-0.4315(2)	0.0270(6)*
C24	0.2425(3)	0.4080(2)	-0.4196(2)	0.0280(6)*
C25	0.1913(3)	0.5039(2)	-0.3617(2)	0.0280(6)*
C26	0.2480(3)	0.6200(2)	-0.3365(2)	0.0348(7)*
C27	0.1717(3)	0.6930(3)	-0.2779(3)	0.0384(7)*
C28	0.0368(4)	0.6549(3)	-0.2414(3)	0.0404(8)*
C29	-0.0231(3)	0.5452(2)	-0.2647(2)	0.0340(7)*
C30	0.3016(4)	0.3294(3)	0.0780(2)	0.0392(7)*
C34	0.2537(4)	0.5315(3)	0.0241(2)	0.0393(7)*
C35	-0.0156(3)	0.1599(3)	-0.5163(3)	0.0405(8)*
C39	0.2357(4)	0.2088(3)	-0.5646(3)	0.0451(8)*
C40	-0.0763(3)	0.1083(2)	-0.1736(2)	0.0309(7)*
C41	-0.1675(4)	0.1329(3)	-0.0826(3)	0.0447(8)*
C42	-0.0663(4)	-0.0236(3)	-0.1898(3)	0.0438(8)*

Anisotropically-refined atoms are marked with an asterisk (*). The form of the anisotropic displacement parameter is: $\exp[-2\pi^2(h^2a^{*2}U_{11} + k^2b^{*2}U_{22} + l^2c^{*2}U_{33} + 2klb^{*c^{*}}U_{23} + 2hla^{*c^{*}}U_{13} + 2hka^{*b^{*}}U_{12})]$.

Table D.3 Selected Interatomic Distances (Å)

Atom1	Atom2	Distance	Atom1	Atom2	Distance
Ti	C1	2.128(3)	C6	C7	1.394(5)
Ti	C3	2.202(2)	C7	C8	1.385(5)
Ti	C11	2.439(3)	C8	C9	1.379(4)
Ti	C12	2.401(3)	C11	C12	1.436(4)
Ti	C13	2.516(3)	C11	C15	1.433(4)
Ti	C14	2.381(3)	C11	C19	1.418(4)
Ti	C15	2.462(3)	C12	C13	1.414(4)
Ti	C21	2.463(3)	C13	C14	1.423(4)
Ti	C22	2.423(3)	C14	C15	1.427(4)
Ti	C23	2.504(3)	C15	C16	1.422(4)
Ti	C24	2.387(3)	C16	C17	1.360(4)
Ti	C25	2.460(3)	C17	C18	1.415(4)
N1	C13	1.366(4)	C18	C19	1.371(4)
N1	C30	1.450(4)	C21	C22	1.425(4)
N1	C34	1.448(4)	C21	C25	1.432(4)
N2	C23	1.375(4)	C21	C29	1.412(4)
N2	C35	1.452(4)	C22	C23	1.416(4)
N2	C39	1.442(4)	C23	C24	1.427(4)
C1	C2	1.559(4)	C24	C25	1.430(4)
C2	C3	1.557(4)	C25	C26	1.426(4)
C2	C40	1.549(4)	C26	C27	1.364(4)
C3	C4	1.480(4)	C27	C28	1.409(4)
C4	C5	1.407(4)	C28	C29	1.365(4)
C4	C9	1.401(4)	C40	C41	1.526(4)
C5	C6	1.385(4)	C40	C42	1.525(4)

Table D.4 Selected Interatomic Angles (deg)

Atom1	Atom2	Atom3	Angle	Atom1	Atom2	Atom3	Angle
C1	Ti	C3	71.84(10)	C13	Ti	C21	120.72(9)
C1	Ti	C11	124.33(10)	C13	Ti	C22	150.48(9)
C1	Ti	C12	90.01(10)	C13	Ti	C23	165.68(9)
C1	Ti	C13	80.48(10)	C13	Ti	C24	131.86(9)
C1	Ti	C14	104.32(11)	C13	Ti	C25	112.87(9)
C1	Ti	C15	135.25(11)	C14	Ti	C15	34.22(10)
C1	Ti	C21	82.47(10)	C14	Ti	C21	100.58(9)
C1	Ti	C22	80.61(10)	C14	Ti	C22	134.09(9)
C1	Ti	C23	111.03(10)	C14	Ti	C23	132.18(9)
C1	Ti	C24	136.35(10)	C14	Ti	C24	98.72(10)
C1	Ti	C25	114.16(10)	C14	Ti	C25	81.48(9)
C3	Ti	C11	90.77(9)	C15	Ti	C21	113.78(9)
C3	Ti	C12	82.28(9)	C15	Ti	C22	136.14(9)
C3	Ti	C13	109.21(9)	C15	Ti	C23	112.24(9)
C3	Ti	C14	139.48(10)	C15	Ti	C24	80.86(9)
C3	Ti	C15	124.17(10)	C15	Ti	C25	82.40(9)
C3	Ti	C21	118.21(10)	C21	Ti	C22	33.89(9)
C3	Ti	C22	85.97(9)	C21	Ti	C23	55.23(9)
C3	Ti	C23	83.14(9)	C21	Ti	C24	56.92(9)
C3	Ti	C24	111.54(10)	C21	Ti	C25	33.83(9)
C3	Ti	C25	137.91(10)	C22	Ti	C23	33.36(9)
C11	Ti	C12	34.50(9)	C22	Ti	C24	57.06(9)
C11	Ti	C13	55.49(9)	C22	Ti	C25	56.30(9)
C11	Ti	C14	57.21(9)	C23	Ti	C24	33.83(9)
C11	Ti	C15	34.00(9)	C23	Ti	C25	55.29(9)
C11	Ti	C21	146.90(9)	C24	Ti	C25	34.28(9)
C11	Ti	C22	152.31(10)	C13	N1	C30	120.0(2)
C11	Ti	C23	118.96(9)	C13	N1	C34	120.0(2)
C11	Ti	C24	99.32(9)	C30	N1	C34	119.0(2)
C11	Ti	C25	113.55(9)	C23	N2	C35	116.9(2)
C12	Ti	C13	33.33(9)	C23	N2	C39	118.6(2)
C12	Ti	C14	57.22(9)	C35	N2	C39	117.6(3)
C12	Ti	C15	56.67(9)	Ti	C1	C2	90.00(15)
C12	Ti	C21	154.05(10)	C1	C2	C3	109.3(2)
C12	Ti	C22	166.81(9)	C1	C2	C40	111.7(2)
C12	Ti	C23	149.04(9)	C3	C2	C40	112.5(2)
C12	Ti	C24	133.48(9)	Ti	C3	C2	87.40(15)
C12	Ti	C25	136.76(9)	Ti	C3	C4	125.86(18)
C13	Ti	C14	33.65(9)	C2	C3	C4	121.2(2)
C13	Ti	C15	55.09(9)	C3	C4	C5	125.1(3)

Table D.4 Selected Interatomic Angles (continued)

Atom1	Atom2	Atom3	Angle	Atom1	Atom2	Atom3	Angle
C3	C4	C9	119.2(2)	C17	C18	C19	121.1(3)
C5	C4	C9	115.7(3)	C11	C19	C18	118.9(3)
C4	C5	C6	122.0(3)	Ti	C21	C22	71.50(15)
C5	C6	C7	120.5(3)	Ti	C21	C25	72.98(15)
C6	C7	C8	118.3(3)	Ti	C21	C29	121.1(2)
C7	C8	C9	120.8(3)	C22	C21	C25	107.5(2)
C4	C9	C8	122.4(3)	C22	C21	C29	132.5(3)
Ti	C11	C12	71.28(15)	C25	C21	C29	120.0(3)
Ti	C11	C15	73.85(15)	Ti	C22	C21	74.60(16)
Ti	C11	C19	121.23(19)	Ti	C22	C23	76.46(16)
C12	C11	C15	107.2(2)	C21	C22	C23	108.3(2)
C12	C11	C19	132.9(3)	Ti	C23	N2	124.00(18)
C15	C11	C19	120.0(3)	Ti	C23	C22	70.19(16)
Ti	C12	C11	74.22(15)	Ti	C23	C24	68.60(15)
Ti	C12	C13	77.82(16)	N2	C23	C22	126.0(2)
C11	C12	C13	108.1(2)	N2	C23	C24	126.1(3)
Ti	C13	N1	127.97(19)	C22	C23	C24	107.8(2)
Ti	C13	C12	68.85(15)	Ti	C24	C23	77.57(15)
Ti	C13	C14	67.94(15)	Ti	C24	C25	75.67(16)
N1	C13	C12	126.6(2)	C23	C24	C25	107.4(2)
N1	C13	C14	125.8(3)	Ti	C25	C21	73.20(15)
C12	C13	C14	107.6(2)	Ti	C25	C24	70.06(14)
Ti	C14	C13	78.41(16)	Ti	C25	C26	123.38(19)
Ti	C14	C15	76.00(16)	C21	C25	C24	107.8(2)
C13	C14	C15	107.8(2)	C21	C25	C26	118.5(3)
Ti	C15	C11	72.15(15)	C24	C25	C26	133.8(3)
Ti	C15	C14	69.78(15)	C25	C26	C27	120.0(3)
Ti	C15	C16	125.3(2)	C26	C27	C28	120.8(3)
C11	C15	C14	107.6(2)	C27	C28	C29	121.4(3)
C11	C15	C16	119.1(3)	C21	C29	C28	119.3(3)
C14	C15	C16	133.2(3)	C2	C40	C41	111.8(2)
C15	C16	C17	119.4(3)	C2	C40	C42	112.3(2)
C16	C17	C18	121.5(3)	C41	C40	C42	109.6(2)

Part E. Crystallographic Details for 3-Isopropyl-2-phenyl-bis(2-piperidinoindenyl)titanacyclobutane, Complex 55a.

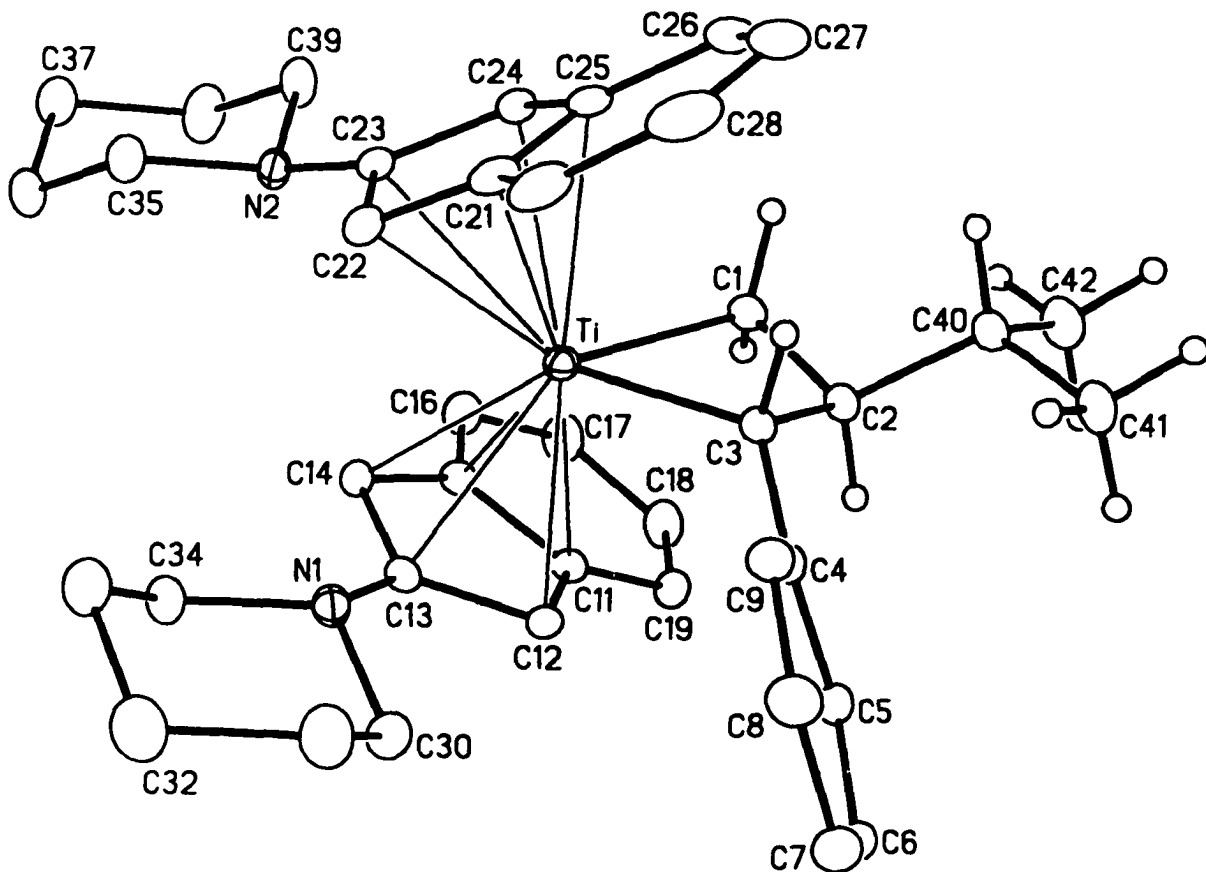


Figure E.1 Perspective view of the $[(\eta^5\text{-2-piperidinoindenyl})_2\text{Ti}(\eta^2\text{-H}_2\text{CCH}^i\text{PrCHPh})]$ molecule **55a** showing the atom labelling scheme. Non-hydrogen atoms are represented by Gaussian ellipsoids at the 20% probability level. Hydrogen atoms of the $\text{H}_2\text{C-CH}^i\text{PrCHPh}$ group are shown with arbitrarily small thermal parameters; all other hydrogens are not shown.

Table E.1 Crystallographic Experimental Details**A. Crystal Data**

formula	C ₄₀ H ₄₈ N ₂ Ti
formula weight	604.70
crystal dimensions (mm)	0.16 _ 0.16 _ 0.06
crystal system	triclinic
space group	<i>PI</i> (No. 2)
unit cell parameters ^a	
<i>a</i> (Å)	11.6351 (8)
<i>b</i> (Å)	12.5204 (8)
<i>c</i> (Å)	11.7615 (8)
α (deg)	83.0481 (13)
β (deg)	88.1276 (12)
γ (deg)	72.7920 (13)
<i>V</i> (Å ³)	1624.63 (19)
<i>Z</i>	2

ρ_{calcd} (g cm⁻³)

1.236

μ (mm⁻¹)

0.294

B. Data Collection and Refinement Conditions

diffractometer	Bruker P4/RA/SMART 1000 CCD ^b
radiation (λ [Å])	graphite-monochromated Mo K α (0.71073)
temperature (°C)	-80
scan type	ϕ rotations (0.3°) / ω scans (0.3°) (30 s exposures)
data collection 2 θ limit (deg)	51.50
total data collected	9065 (-14 ≤ <i>h</i> ≤ 14, -15 ≤ <i>k</i> ≤ 14, -14 ≤ <i>l</i> ≤ 14)
independent reflections	6155
number of observations (<i>NO</i>)	3813 [$F_o^2 \geq 2\sigma(F_o^2)$]
structure solution method	direct methods (<i>SHELXS-86</i> ^c)
refinement method	full-matrix least-squares on F^2
(<i>SHELXL-93</i> ^d)	
absorption correction method	Gaussian integration (face-indexed)
range of transmission factors	0.9778–0.9493
data/restraints/parameters	6155 [$F_o^2 \geq -3\sigma(F_o^2)$] / 0 / 388
goodness-of-fit (<i>S</i>) ^e	0.887 [$F_o^2 \geq -3\sigma(F_o^2)$]
final <i>R</i> indices ^f	
<i>R</i> ₁ [$F_o^2 \geq 2\sigma(F_o^2)$]	0.0482
<i>wR</i> ₂ [$F_o^2 \geq -3\sigma(F_o^2)$]	0.1070
largest difference peak and hole	0.234 and -0.284 e Å ⁻³

^aObtained from least-squares refinement of 4441 centered reflections. (continued)

Table E.1 Crystallographic Experimental Details (continued)

^bPrograms for diffractometer operation, data collection, data reduction and absorption correction were those supplied by Bruker.

^cSheldrick, G. M. *Acta Crystallogr.* **1990**, *A46*, 467–473.

^dSheldrick, G. M. *SHELXL-93*. Program for crystal structure determination. University of Göttingen, Germany, 1993. Refinement on F_o^2 for all reflections (all of these having $F_o^2 \geq -3\sigma(F_o^2)$). Weighted R -factors wR_2 and all goodnesses of fit S are based on F_o^2 ; conventional R -factors R_1 are based on F_o , with F_o set to zero for negative F_o^2 . The observed criterion of $F_o^2 > 2\sigma(F_o^2)$ is used only for calculating R_1 , and is not relevant to the choice of reflections for refinement. R -factors based on F_o^2 are statistically about twice as large as those based on F_o , and R -factors based on ALL data will be even larger.

$$^e S = [\sum w(F_o^2 - F_c^2)^2 / (n - p)]^{1/2} \quad (n = \text{number of data}; p = \text{number of parameters varied}; w = [\sigma^2(F_o^2) + (0.0415P)^2]^{-1} \text{ where } P = [\text{Max}(F_o^2, 0) + 2F_c^2]/3).$$

$$^f R_1 = \sum ||F_o| - |F_c|| / \sum |F_o|; wR_2 = [\sum w(F_o^2 - F_c^2)^2 / \sum w(F_o^4)]^{1/2}.$$

Table E.2 Atomic Coordinates and Equivalent Isotropic Displacement Parameters

Atom	<i>x</i>	<i>y</i>	<i>z</i>	<i>U</i> _{eq} , Å ²
Ti	0.13494(4)	0.23028(3)	-0.20601(4)	0.02464(14)*
N1	0.23793(19)	0.44774(16)	-0.25266(18)	0.0304(5)*
N2	-0.16128(19)	0.41037(16)	-0.21430(18)	0.0307(5)*
C1	0.1438(2)	0.06665(19)	-0.1266(2)	0.0299(6)*
C2	0.2775(2)	0.02486(19)	-0.1636(2)	0.0292(6)*
C3	0.2995(2)	0.11101(18)	-0.2620(2)	0.0260(6)*
C4	0.4220(2)	0.12325(18)	-0.2815(2)	0.0264(6)*
C5	0.5092(2)	0.10509(19)	-0.1964(2)	0.0299(6)*
C6	0.6194(2)	0.1233(2)	-0.2201(2)	0.0362(7)*
C7	0.6497(3)	0.1576(2)	-0.3303(3)	0.0401(7)*
C8	0.5669(3)	0.1720(2)	-0.4165(3)	0.0416(7)*
C9	0.4562(2)	0.1553(2)	-0.3933(2)	0.0340(7)*
C11	0.2105(2)	0.2425(2)	-0.0131(2)	0.0279(6)*
C12	0.2796(2)	0.28348(19)	-0.0996(2)	0.0270(6)*
C13	0.2039(2)	0.38402(19)	-0.1591(2)	0.0266(6)*
C14	0.0849(2)	0.39845(19)	-0.1182(2)	0.0271(6)*
C15	0.0887(2)	0.31194(19)	-0.0260(2)	0.0277(6)*
C16	-0.0012(3)	0.2876(2)	0.0477(2)	0.0363(7)*
C17	0.0312(3)	0.2009(2)	0.1339(2)	0.0442(8)*
C18	0.1526(3)	0.1353(2)	0.1495(2)	0.0429(8)*
C19	0.2413(3)	0.1544(2)	0.0786(2)	0.0337(7)*
C21	0.0680(2)	0.2672(2)	-0.4087(2)	0.0351(7)*
C22	0.0122(2)	0.3625(2)	-0.3500(2)	0.0326(6)*
C23	-0.0763(2)	0.3348(2)	-0.2756(2)	0.0293(6)*
C24	-0.0593(2)	0.2181(2)	-0.2706(2)	0.0314(6)*
C25	0.0241(2)	0.1772(2)	-0.3587(2)	0.0359(7)*
C26	0.0631(3)	0.0721(3)	-0.4030(3)	0.0491(8)*
C27	0.1405(3)	0.0608(3)	-0.4941(3)	0.0596(10)*
C28	0.1842(3)	0.1490(3)	-0.5426(3)	0.0618(10)*
C29	0.1496(3)	0.2510(3)	-0.5012(2)	0.0491(8)*
C30	0.3661(2)	0.4294(2)	-0.2710(2)	0.0394(7)*
C31	0.3906(3)	0.4777(2)	-0.3903(3)	0.0523(9)*
C32	0.3193(3)	0.6011(2)	-0.4164(3)	0.0548(9)*
C33	0.1867(3)	0.6167(2)	-0.3939(3)	0.0473(8)*
C34	0.1681(3)	0.5668(2)	-0.2726(2)	0.0370(7)*
C35	-0.2054(3)	0.5243(2)	-0.2740(3)	0.0417(7)*
C36	-0.2778(3)	0.6060(2)	-0.1962(3)	0.0500(8)*
C37	-0.3810(3)	0.5682(2)	-0.1435(3)	0.0488(8)*
C38	-0.3335(3)	0.4498(2)	-0.0821(3)	0.0561(9)*
C39	-0.2586(3)	0.3698(2)	-0.1612(3)	0.0430(8)*

Table E.2 Atomic Coordinates and Displacement Parameters (continued)

Atom	<i>x</i>	<i>y</i>	<i>z</i>	$U_{eq}, \text{\AA}^2$
C40	0.3094(2)	-0.09648(19)	-0.1991(2)	0.0346(7)*
C41	0.4346(3)	-0.1366(2)	-0.2496(3)	0.0483(8)*
C42	0.2945(3)	-0.1791(2)	-0.0983(3)	0.0508(9)*

Anisotropically-refined atoms are marked with an asterisk (*). The form of the anisotropic displacement parameter is: $\exp[-2\pi^2(h^2a^{*2}U_{11} + k^2b^{*2}U_{22} + l^2c^{*2}U_{33} + 2klb^{*c^*}U_{23} + 2hla^{*c^*}U_{13} + 2hka^{*b^*}U_{12})]$.

Table E.3 Selected Interatomic Distances (Å)

Atom1	Atom2	Distance	Atom1	Atom2	Distance
Ti	C1	2.121(2)	C11	C15	1.428(3)
Ti	C3	2.190(2)	C11	C19	1.419(3)
Ti	C11	2.497(2)	C12	C13	1.422(3)
Ti	C12	2.418(3)	C13	C14	1.418(3)
Ti	C13	2.420(2)	C14	C15	1.428(3)
Ti	C14	2.367(2)	C15	C16	1.416(3)
Ti	C15	2.437(2)	C16	C17	1.365(4)
Ti	C21	2.479(3)	C17	C18	1.413(4)
Ti	C22	2.393(3)	C18	C19	1.364(4)
Ti	C23	2.529(3)	C21	C22	1.425(3)
Ti	C24	2.460(3)	C21	C25	1.427(4)
Ti	C25	2.505(3)	C21	C29	1.414(4)
N1	C13	1.397(3)	C22	C23	1.424(3)
N1	C30	1.453(3)	C23	C24	1.409(3)
N1	C34	1.466(3)	C24	C25	1.431(3)
N2	C23	1.399(3)	C25	C26	1.416(3)
N2	C35	1.463(3)	C26	C27	1.370(4)
N2	C39	1.465(3)	C27	C28	1.401(5)
C1	C2	1.553(3)	C28	C29	1.365(4)
C2	C3	1.552(3)	C30	C31	1.511(4)
C2	C40	1.559(3)	C31	C32	1.521(4)
C3	C4	1.486(3)	C32	C33	1.515(4)
C4	C5	1.399(4)	C33	C34	1.522(4)
C4	C9	1.407(3)	C35	C36	1.503(4)
C5	C6	1.380(3)	C36	C37	1.506(4)
C6	C7	1.384(4)	C37	C38	1.519(4)
C7	C8	1.381(4)	C38	C39	1.511(4)
C8	C9	1.378(4)	C40	C41	1.520(4)
C11	C12	1.417(3)	C40	C42	1.517(3)

Table E.4 Selected Interatomic Angles (deg)

Atom1	Atom2	Atom3	Angle	Atom1	Atom2	Atom3	Angle
C1	Ti	C3	71.33(9)	C13	Ti	C21	109.34(9)
C1	Ti	C11	80.69(9)	C13	Ti	C22	86.73(9)
C1	Ti	C12	103.54(9)	C13	Ti	C23	100.96(8)
C1	Ti	C13	135.58(10)	C13	Ti	C24	133.49(8)
C1	Ti	C14	127.04(9)	C13	Ti	C25	141.31(9)
C1	Ti	C15	92.60(9)	C14	Ti	C15	34.55(8)
C1	Ti	C21	114.21(10)	C14	Ti	C21	111.31(9)
C1	Ti	C22	135.92(10)	C14	Ti	C22	78.29(9)
C1	Ti	C23	110.72(9)	C14	Ti	C23	75.76(8)
C1	Ti	C24	80.82(9)	C14	Ti	C24	104.38(8)
C1	Ti	C25	83.11(10)	C14	Ti	C25	129.16(9)
C3	Ti	C11	96.72(9)	C15	Ti	C21	140.36(9)
C3	Ti	C12	81.29(9)	C15	Ti	C22	106.70(9)
C3	Ti	C13	103.10(9)	C15	Ti	C23	89.49(9)
C3	Ti	C14	136.62(9)	C15	Ti	C24	104.33(9)
C3	Ti	C15	130.33(9)	C15	Ti	C25	137.78(9)
C3	Ti	C21	87.31(9)	C21	Ti	C22	33.96(8)
C3	Ti	C22	117.54(9)	C21	Ti	C23	54.71(9)
C3	Ti	C23	140.15(9)	C21	Ti	C24	55.83(9)
C3	Ti	C24	118.11(9)	C21	Ti	C25	33.28(8)
C3	Ti	C25	87.99(9)	C22	Ti	C23	33.49(8)
C11	Ti	C12	33.47(8)	C22	Ti	C24	56.38(9)
C11	Ti	C13	55.71(8)	C22	Ti	C25	55.88(9)
C11	Ti	C14	56.52(8)	C23	Ti	C24	32.78(8)
C11	Ti	C15	33.61(8)	C23	Ti	C25	54.13(8)
C11	Ti	C21	165.02(9)	C24	Ti	C25	33.47(8)
C11	Ti	C22	134.77(8)	C13	N1	C30	117.1(2)
C11	Ti	C23	123.10(8)	C13	N1	C34	116.5(2)
C11	Ti	C24	132.13(9)	C30	N1	C34	112.9(2)
C11	Ti	C25	160.65(9)	C23	N2	C35	114.4(2)
C12	Ti	C13	34.18(8)	C23	N2	C39	116.07(19)
C12	Ti	C14	57.38(8)	C35	N2	C39	112.4(2)
C12	Ti	C15	56.56(8)	Ti	C1	C2	89.34(14)
C12	Ti	C21	134.42(9)	C1	C2	C3	108.09(19)
C12	Ti	C22	120.25(9)	C1	C2	C40	111.2(2)
C12	Ti	C23	132.57(8)	C3	C2	C40	112.28(19)
C12	Ti	C24	160.20(8)	Ti	C3	C2	86.89(14)
C12	Ti	C25	164.69(9)	Ti	C3	C4	130.06(16)
C13	Ti	C14	34.44(8)	C2	C3	C4	120.1(2)
C13	Ti	C15	56.57(8)	C3	C4	C5	125.1(2)

Table E.4 Selected Interatomic Angles (continued)

Atom1	Atom2	Atom3	Angle	Atom1	Atom2	Atom3	Angle
C3	C4	C9	119.1(2)	C22	C21	C25	107.3(2)
C5	C4	C9	115.7(2)	C22	C21	C29	132.6(3)
C4	C5	C6	121.9(2)	C25	C21	C29	120.1(3)
C5	C6	C7	121.2(3)	Ti	C22	C21	76.30(15)
C6	C7	C8	118.0(3)	Ti	C22	C23	78.48(15)
C7	C8	C9	121.1(3)	C21	C22	C23	107.7(2)
C4	C9	C8	122.0(3)	Ti	C23	N2	124.36(17)
Ti	C11	C12	70.20(14)	Ti	C23	C22	68.03(14)
Ti	C11	C15	70.88(14)	Ti	C23	C24	70.92(15)
Ti	C11	C19	126.28(16)	N2	C23	C22	125.4(2)
C12	C11	C15	107.9(2)	N2	C23	C24	126.5(2)
C12	C11	C19	132.7(2)	C22	C23	C24	108.1(2)
C15	C11	C19	119.4(2)	Ti	C24	C23	76.30(15)
Ti	C12	C11	76.33(14)	Ti	C24	C25	75.01(15)
Ti	C12	C13	72.97(14)	C23	C24	C25	107.5(2)
C11	C12	C13	108.1(2)	Ti	C25	C21	72.33(15)
Ti	C13	N1	115.14(16)	Ti	C25	C24	71.52(15)
Ti	C13	C12	72.85(13)	Ti	C25	C26	123.59(19)
Ti	C13	C14	70.74(13)	C21	C25	C24	108.0(2)
N1	C13	C12	125.5(2)	C21	C25	C26	119.2(3)
N1	C13	C14	125.9(2)	C24	C25	C26	132.7(3)
C12	C13	C14	108.0(2)	C25	C26	C27	118.7(3)
Ti	C14	C13	74.81(13)	C26	C27	C28	122.0(3)
Ti	C14	C15	75.41(13)	C27	C28	C29	120.8(3)
C13	C14	C15	107.9(2)	C21	C29	C28	119.1(3)
Ti	C15	C11	75.51(13)	N1	C30	C31	111.1(2)
Ti	C15	C14	70.03(13)	C30	C31	C32	112.0(2)
Ti	C15	C16	120.70(17)	C31	C32	C33	110.3(2)
C11	C15	C14	107.7(2)	C32	C33	C34	110.3(3)
C11	C15	C16	119.8(2)	N1	C34	C33	110.9(2)
C14	C15	C16	132.5(2)	N2	C35	C36	111.7(2)
C15	C16	C17	119.2(3)	C35	C36	C37	111.3(2)
C16	C17	C18	120.9(3)	C36	C37	C38	109.5(2)
C17	C18	C19	121.7(3)	C37	C38	C39	111.3(2)
C11	C19	C18	118.9(3)	N2	C39	C38	111.8(2)
Ti	C21	C22	69.74(14)	C2	C40	C41	113.6(2)
Ti	C21	C25	74.39(15)	C2	C40	C42	110.5(2)
Ti	C21	C29	122.64(19)	C41	C40	C42	110.2(2)

Part F. Crystallographic Details for 3-*tert*-Butyl-2-phenyl-bis(2-methylindenyl)titanacyclobutane, Complex 139c.

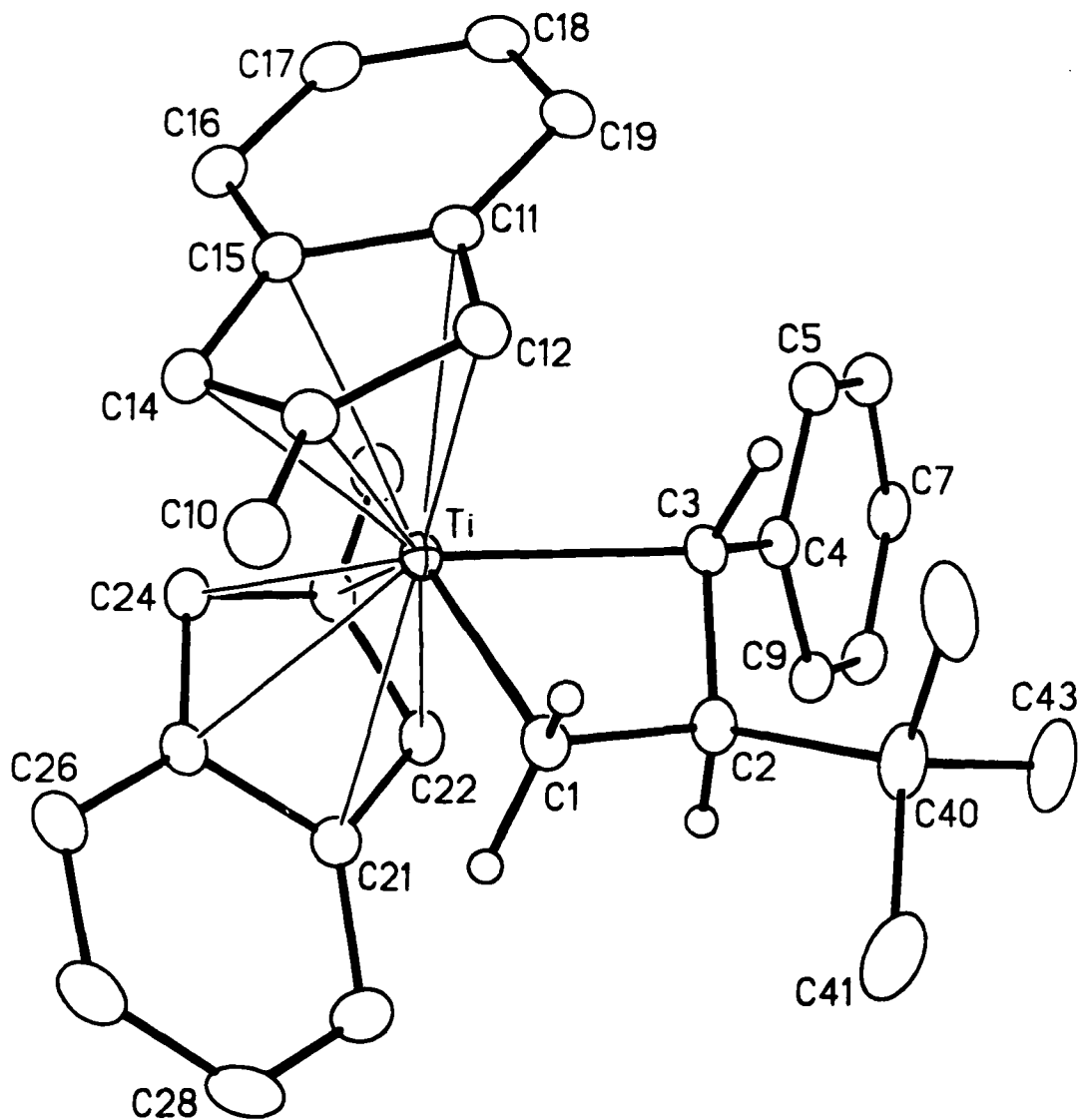


Figure F.1 Perspective view of the $[(\eta^5\text{-2-methylindenyl})_2\text{Ti}\{\kappa^2\text{-H}_2\text{CCH}(\text{'Bu})\text{CHPh}\}]$ molecule showing the atom labelling scheme. Non-hydrogen atoms are represented by Gaussian ellipsoids at the 20% probability level. The hydrogen atoms attached to C1, C2 and C3 are shown with arbitrarily small thermal parameters; all other hydrogens are not shown.

Table F.1 Crystallographic Experimental Details**A. Crystal Data**

formula	C ₃₆ H ₄₃ Ti
formula weight	523.60
crystal dimensions (mm)	0.52 × 0.09 × 0.09
crystal system	monoclinic
space group	<i>P</i> 2 ₁ / <i>c</i> (No. 14)
unit cell parameters ^a	
<i>a</i> (Å)	9.9247 (10)
<i>b</i> (Å)	16.1884 (17)
<i>c</i> (Å)	18.6380 (19)
β (deg)	104.486 (2)
<i>V</i> (Å ³)	2899.3 (5)
<i>Z</i>	4
ρ _{calcd} (g cm ⁻³)	1.200
μ (mm ⁻¹)	0.317

B. Data Collection and Refinement Conditions

diffractometer	Bruker PLATFORM/SMART 1000 CCD ^b
radiation (λ [Å])	graphite-monochromated Mo Kα (0.71073)
temperature (°C)	-80
scan type	ω scans (0.2°) (20 s exposures)
data collection 2θ limit (deg)	53.06
total data collected	17659 (-9 ≤ <i>h</i> ≤ 12, -20 ≤ <i>k</i> ≤ 20, -23 ≤ <i>l</i> ≤ 23)
independent reflections	5951
number of observed reflections (<i>NO</i>)	4037 [<i>F</i> _o ² ≥ 2σ(<i>F</i> _o ²)]
structure solution method	direct methods/fragment search
(<i>DIRDIF-96</i> ^c)	
refinement method	full-matrix least-squares on <i>F</i> ²
(<i>SHELXL-93</i> ^d)	
absorption correction method	<i>SADABS</i>
range of transmission factors	0.9720–0.8523
data/restraints/parameters	5951 [<i>F</i> _o ² ≥ -3σ(<i>F</i> _o ²)] / 0 / 336
goodness-of-fit (<i>S</i>) ^e	1.017 [<i>F</i> _o ² ≥ -3σ(<i>F</i> _o ²)]
final <i>R</i> indices ^f	
<i>R</i> ₁ [<i>F</i> _o ² ≥ 2σ(<i>F</i> _o ²)]	0.0527
<i>wR</i> ₂ [<i>F</i> _o ² ≥ -3σ(<i>F</i> _o ²)]	0.1379
largest difference peak and hole	0.561 and -0.432 e Å ⁻³

^aObtained from least-squares refinement of 4918 centered reflections.

^bPrograms for diffractometer operation, data collection, data reduction and absorption correction were those supplied by Bruker.

(continued)

Table F.1 Crystallographic Experimental Details (continued)

^cBeurskens, P. T.; Beurskens, G.; Bosman, W. P.; de Gelder, R.; Garcia Granda, S.; Gould, R. O.; Israel, R.; Smits, J. M. M. (1996). The *DIRDIF-96* program system. Crystallography Laboratory, University of Nijmegen, The Netherlands.

^dSheldrick, G. M. *SHELXL-93*. Program for crystal structure determination. University of Göttingen, Germany, 1993. Refinement on F_o^2 for all reflections (all of these having $F_o^2 \geq -3\sigma(F_o^2)$). Weighted R -factors wR_2 and all goodnesses of fit S are based on F_o^2 ; conventional R -factors R_1 are based on F_o , with F_o set to zero for negative F_o^2 . The observed criterion of $F_o^2 > 2\sigma(F_o^2)$ is used only for calculating R_1 , and is not relevant to the choice of reflections for refinement. R -factors based on F_o^2 are statistically about twice as large as those based on F_o , and R -factors based on ALL data will be even larger.

$$^e S = [\Sigma w(F_o^2 - F_c^2)^2 / (n - p)]^{1/2} \quad (n = \text{number of data}; p = \text{number of parameters varied}; w = [\sigma^2(F_o^2) + (0.0694P)^2 + 0.4738P]^{-1} \text{ where } P = [\text{Max}(F_o^2, 0) + 2F_c^2] / 3).$$

$$^f R_1 = \Sigma ||F_o| - |F_c|| / \Sigma |F_o|; wR_2 = [\Sigma w(F_o^2 - F_c^2)^2 / \Sigma w(F_o^4)]^{1/2}.$$

Table F.2 Atomic Coordinates and Equivalent Isotropic Displacement Parameters*(a) atoms of [(η^5 -2methylindenyl)₂Ti(κ^2 -H₂CCH(^tBu)CPh)]*

Atom	x	y	z	U_{eq} , Å ²
Ti	0.04690(5)	0.16107(2)	0.29491(2)	0.02546(14)*
C1	-0.0549(3)	0.21107(15)	0.19138(13)	0.0303(6)*
C2	-0.1958(3)	0.19053(15)	0.20909(14)	0.0323(6)*
C3	-0.1733(3)	0.18136(14)	0.29448(14)	0.0287(6)*
C4	-0.2630(3)	0.12513(15)	0.32550(14)	0.0307(6)*
C5	-0.2698(3)	0.13512(17)	0.39939(15)	0.0388(6)*
C6	-0.3465(3)	0.08271(18)	0.43224(16)	0.0420(7)*
C7	-0.4207(3)	0.01808(17)	0.39353(16)	0.0413(7)*
C8	-0.4194(3)	0.00808(16)	0.32010(16)	0.0391(7)*
C9	-0.3435(3)	0.06069(15)	0.28674(15)	0.0334(6)*
C10	0.2240(3)	0.31852(16)	0.23035(16)	0.0415(7)*
C11	0.1026(3)	0.26239(15)	0.39924(14)	0.0337(6)*
C12	0.0843(3)	0.30446(15)	0.33065(15)	0.0354(6)*
C13	0.1933(3)	0.28245(15)	0.29831(14)	0.0334(6)*
C14	0.2735(3)	0.22145(16)	0.34309(14)	0.0340(6)*
C15	0.2219(3)	0.21007(15)	0.40740(14)	0.0341(6)*
C16	0.2708(3)	0.16271(17)	0.47329(15)	0.0409(7)*
C17	0.2018(3)	0.16920(19)	0.52789(15)	0.0469(7)*
C18	0.0847(3)	0.22014(19)	0.51985(16)	0.0477(8)*
C19	0.0334(3)	0.26561(18)	0.45731(15)	0.0430(7)*
C20	0.0411(3)	-0.00323(18)	0.41000(16)	0.0472(8)*
C21	0.0303(3)	0.03581(14)	0.21049(14)	0.0340(6)*
C22	-0.0342(3)	0.01777(14)	0.26851(15)	0.0344(6)*
C23	0.0670(3)	0.01948(14)	0.33632(15)	0.0327(6)*
C24	0.1938(3)	0.04506(14)	0.32233(14)	0.0319(6)*
C25	0.1727(3)	0.05600(14)	0.24422(15)	0.0326(6)*
C26	0.2605(3)	0.08267(16)	0.19919(16)	0.0422(7)*
C27	0.2091(4)	0.08449(18)	0.12448(18)	0.0524(8)*
C28	0.0721(4)	0.05910(18)	0.09107(17)	0.0546(9)*
C29	-0.0178(4)	0.03487(17)	0.13182(16)	0.0485(8)*
C40	-0.3124(3)	0.25409(18)	0.17040(17)	0.0467(7)*
C41	-0.3209(4)	0.2547(2)	0.08704(18)	0.0665(10)*

Table F.2 Atomic Coordinates and Displacement Parameters (continued)

Atom	<i>x</i>	<i>y</i>	<i>z</i>	$U_{\text{eq}}, \text{\AA}^2$
C42	-0.2819(4)	0.34111(18)	0.2011(2)	0.0676(10)*
C43	-0.4523(3)	0.2270(2)	0.1813(2)	0.0663(10)*

(b) solvent n-hexane atoms

Atom	<i>x</i>	<i>y</i>	<i>z</i>	$U_{\text{eq}}, \text{\AA}^2$
C1S	0.5481(8)	0.0238(4)	-0.0114(5)	0.163(3)*
C2S	0.4752(8)	0.0805(4)	-0.0799(3)	0.152(3)*
C3S	0.5795(7)	0.1264(4)	-0.1065(3)	0.126(2)*

Anisotropically-refined atoms are marked with an asterisk (*). The form of the anisotropic displacement parameter is: $\exp[-2\pi^2(h^2a^{*2}U_{11} + k^2b^{*2}U_{22} + l^2c^{*2}U_{33} + 2klb^*c^*U_{23} + 2hla^*c^*U_{13} + 2hka^*b^*U_{12})]$.

Table F.3 Selected Interatomic Distances (Å)*(a) within $[(\eta^5\text{-2-methylindenyl})_2\text{Ti}\{\kappa^2\text{-H}_2\text{CCH}(\text{iBu})\text{CPh}\}]$*

Atom1	Atom2	Distance	Atom1	Atom2	Distance
Ti	C1	2.103(2)	C11	C15	1.432(4)
Ti	C3	2.208(3)	C11	C19	1.421(4)
Ti	C11	2.498(2)	C12	C13	1.409(4)
Ti	C12	2.418(2)	C13	C14	1.405(4)
Ti	C13	2.435(2)	C14	C15	1.429(4)
Ti	C14	2.410(3)	C15	C16	1.426(4)
Ti	C15	2.494(3)	C16	C17	1.365(4)
Ti	C21	2.546(2)	C17	C18	1.402(4)
Ti	C22	2.464(2)	C18	C19	1.365(4)
Ti	C23	2.411(2)	C20	C23	1.505(4)
Ti	C24	2.354(2)	C21	C22	1.418(4)
Ti	C25	2.436(2)	C21	C25	1.433(4)
C1	C2	1.551(3)	C21	C29	1.424(4)
C2	C3	1.558(3)	C22	C23	1.404(4)
C2	C40	1.581(4)	C23	C24	1.410(4)
C3	C4	1.487(3)	C24	C25	1.429(4)
C4	C5	1.405(4)	C25	C26	1.420(4)
C4	C9	1.400(4)	C26	C27	1.358(4)
C5	C6	1.381(4)	C27	C28	1.408(5)
C6	C7	1.375(4)	C28	C29	1.366(5)
C7	C8	1.381(4)	C40	C41	1.535(4)
C8	C9	1.383(4)	C40	C42	1.522(5)
C10	C13	1.494(4)	C40	C43	1.517(4)
C11	C12	1.420(4)			

(b) within the solvent n-hexane molecule

Atom1	Atom2	Distance	Atom1	Atom2	Distance
C1S	C1S'	1.374(11)	C2S	C3S	1.459(8)
C1S	C2S	1.592(9)			

Primed atoms are related to unprimed ones via the crystallographic inversion center ($1/2$, 0, 0).

Table F.4 Selected Interatomic Angles (deg)*(a) within $[(\eta^5\text{-2-methylindenyl})_2\text{Ti}(\kappa^2\text{-H}_2\text{CCH}(\text{tBu})\text{C}_6\text{H}_4)]$*

Atom1	Atom2	Atom3	Angle	Atom1	Atom2	Atom3	Angle
C1	Ti	C3	72.04(9)	C13	Ti	C15	55.67(9)
C1	Ti	C11	115.05(9)	C13	Ti	C21	127.19(9)
C1	Ti	C12	83.61(10)	C13	Ti	C22	158.09(9)
C1	Ti	C13	81.95(9)	C13	Ti	C23	139.26(9)
C1	Ti	C14	112.02(9)	C13	Ti	C24	107.75(9)
C1	Ti	C15	136.26(9)	C13	Ti	C25	102.31(9)
C1	Ti	C21	78.33(9)	C14	Ti	C15	33.82(8)
C1	Ti	C22	96.96(9)	C14	Ti	C21	117.59(9)
C1	Ti	C23	129.93(9)	C14	Ti	C22	133.15(9)
C1	Ti	C24	129.46(9)	C14	Ti	C23	105.75(9)
C1	Ti	C25	95.05(9)	C14	Ti	C24	76.89(9)
C3	Ti	C11	86.06(9)	C14	Ti	C25	84.65(9)
C3	Ti	C12	86.67(9)	C15	Ti	C21	134.15(9)
C3	Ti	C13	117.62(9)	C15	Ti	C22	126.25(9)
C3	Ti	C14	140.49(9)	C15	Ti	C23	92.80(9)
C3	Ti	C15	115.86(9)	C15	Ti	C24	78.93(9)
C3	Ti	C21	101.85(9)	C15	Ti	C25	103.39(9)
C3	Ti	C22	82.28(9)	C21	Ti	C22	32.84(9)
C3	Ti	C23	98.35(9)	C21	Ti	C23	55.12(8)
C3	Ti	C24	132.71(9)	C21	Ti	C24	55.92(9)
C3	Ti	C25	134.85(9)	C21	Ti	C25	33.33(9)
C11	Ti	C12	33.52(9)	C22	Ti	C23	33.46(9)
C11	Ti	C13	55.63(9)	C22	Ti	C24	56.37(9)
C11	Ti	C14	55.91(9)	C22	Ti	C25	55.86(9)
C11	Ti	C15	33.35(8)	C23	Ti	C24	34.39(9)
C11	Ti	C21	166.26(9)	C23	Ti	C25	56.69(9)
C11	Ti	C22	140.46(9)	C24	Ti	C25	34.66(8)
C11	Ti	C23	112.99(9)	Ti	C1	C2	88.51(14)
C11	Ti	C24	110.51(9)	Ti	C2	C1	54.56(12)
C11	Ti	C25	136.50(9)	Ti	C2	C3	58.42(12)
C12	Ti	C13	33.76(9)	Ti	C2	C40	150.00(19)
C12	Ti	C14	56.17(9)	C1	C2	C3	109.4(2)
C12	Ti	C15	55.69(9)	C1	C2	C40	111.1(2)
C12	Ti	C21	156.40(9)	C3	C2	C40	115.4(2)
C12	Ti	C22	168.15(9)	Ti	C3	C2	84.64(14)
C12	Ti	C23	146.08(9)	Ti	C3	C4	126.54(17)
C12	Ti	C24	131.45(10)	C2	C3	C4	120.6(2)
C12	Ti	C25	135.96(9)	C3	C4	C5	119.4(2)
C13	Ti	C14	33.69(9)	C3	C4	C9	125.1(2)

Table F.4 Selected Interatomic Angles (continued)

Atom1	Atom2	Atom3	Angle	Atom1	Atom2	Atom3	Angle
C5	C4	C9	115.5(2)	Ti	C21	C22	70.40(13)
C4	C5	C6	122.1(3)	Ti	C21	C25	69.09(13)
C5	C6	C7	121.1(3)	Ti	C21	C29	126.72(17)
C6	C7	C8	118.2(3)	C22	C21	C25	107.2(2)
C7	C8	C9	121.0(3)	C22	C21	C29	133.1(3)
C4	C9	C8	122.1(3)	C25	C21	C29	119.6(3)
Ti	C11	C12	70.15(14)	Ti	C22	C21	76.76(14)
Ti	C11	C15	73.17(14)	Ti	C22	C23	71.17(14)
Ti	C11	C19	124.20(18)	C21	C22	C23	108.9(2)
C12	C11	C15	107.2(2)	Ti	C23	C20	120.33(17)
C12	C11	C19	133.7(3)	Ti	C23	C22	75.37(14)
C15	C11	C19	119.0(2)	Ti	C23	C24	70.60(13)
Ti	C12	C11	76.33(14)	C20	C23	C22	124.7(3)
Ti	C12	C13	73.80(14)	C20	C23	C24	127.2(3)
C11	C12	C13	109.0(2)	C22	C23	C24	108.1(2)
Ti	C13	C10	122.70(18)	Ti	C24	C23	75.01(14)
Ti	C13	C12	72.44(14)	Ti	C24	C25	75.81(14)
Ti	C13	C14	72.18(14)	C23	C24	C25	108.3(2)
C10	C13	C12	127.2(2)	Ti	C25	C21	77.58(15)
C10	C13	C14	125.0(2)	Ti	C25	C24	69.53(13)
C12	C13	C14	107.8(2)	Ti	C25	C26	117.82(17)
Ti	C14	C13	74.13(15)	C21	C25	C24	107.2(2)
Ti	C14	C15	76.29(15)	C21	C25	C26	119.6(3)
C13	C14	C15	108.7(2)	C24	C25	C26	133.2(3)
Ti	C15	C11	73.49(14)	C25	C26	C27	118.9(3)
Ti	C15	C14	69.89(15)	C26	C27	C28	121.4(3)
Ti	C15	C16	124.65(18)	C27	C28	C29	122.1(3)
C11	C15	C14	107.2(2)	C21	C29	C28	118.1(3)
C11	C15	C16	120.3(2)	C2	C40	C41	108.3(2)
C14	C15	C16	132.5(3)	C2	C40	C42	112.1(3)
C15	C16	C17	118.3(3)	C2	C40	C43	109.9(2)
C16	C17	C18	121.5(3)	C41	C40	C42	109.3(3)
C17	C18	C19	122.0(3)	C41	C40	C43	108.5(3)
C11	C19	C18	118.9(3)	C42	C40	C43	108.7(3)

(b) within the solvent n-hexane molecule

Atom1	Atom2	Atom3	Angle	Atom1	Atom2	Atom3	Angle
C1S'	C1S	C2S	111.1(9)				
C1S	C2S	C3S	110.4(5)				

Primed atoms are related to unprimed ones
via the crystallographic inversion center ($1/2, 0, 0$).

Part G. Crystallographic Details for Bis(2- isopropylindenyl)titanium(η^3 -1-methylallyl), Complex 145.

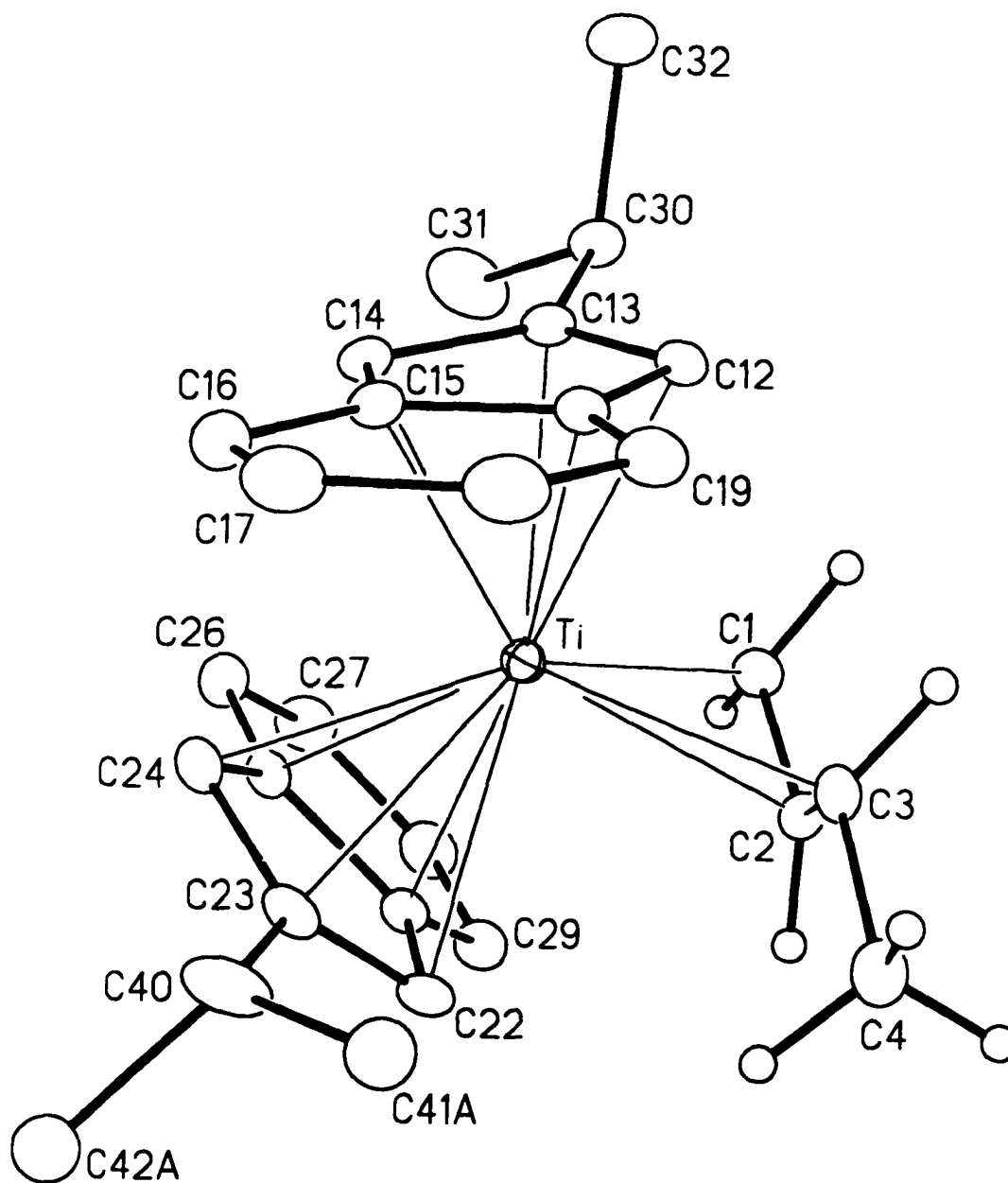


Figure G.1 Perspective view of the $[(\eta^5\text{-2-isopropylindenyl})_2\text{Ti}(\eta^3\text{-crotyl})]$ molecule **145** showing the atom labelling scheme. Non-hydrogen atoms are represented by Gaussian ellipsoids at the 20% probability level. Hydrogen atoms of the crotyl group are shown with arbitrarily small thermal parameters; all other hydrogens are not shown.

Table G.1 Crystallographic Experimental Details

<i>A. Crystal Data</i>	
formula	$C_{28}H_{33}Ti$
formula weight	417.44
crystal dimensions (mm)	$0.34 \times 0.20 \times 0.06$
crystal system	monoclinic
space group	$P2_1/n$ (an alternate setting of $P2_1/c$ [No. 14])
unit cell parameters ^a	
<i>a</i> (Å)	10.2201 (6)
<i>b</i> (Å)	8.2218 (5)
<i>c</i> (Å)	26.6655 (16)
β (deg)	90.5874 (13)
<i>V</i> (Å ³)	2240.5 (2)
<i>Z</i>	4
ρ_{calcd} (g cm ⁻³)	1.238
μ (mm ⁻¹)	0.393
<i>B. Data Collection and Refinement Conditions</i>	
diffractometer	Bruker P4/RA/SMART 1000 CCD ^b
radiation (λ [Å])	graphite-monochromated Mo $K\alpha$ (0.71073)
temperature (°C)	-80
scan type	ϕ rotations (0.3°) / ω scans (0.3°) (30 s exposures)
data collection 2θ limit (deg)	52.74
total data collected	11391 ($-11 \leq h \leq 12$, $-10 \leq k \leq 8$, $-33 \leq l \leq 25$)
independent reflections	4576
number of observed reflections (<i>NO</i>)	3293 [$F_o^2 \geq 2\sigma(F_o^2)$]
structure solution method	direct methods/fragment search (<i>DIRDIF-96</i> ^c)
refinement method	full-matrix least-squares on F^2 (<i>SHELXL-93</i> ^d)
absorption correction method	<i>SADABS</i>
range of transmission factors	0.9768–0.8779
data/restraints/parameters	4576 [$F_o^2 \geq -3\sigma(F_o^2)$] / 0 / 274
goodness-of-fit (<i>S</i>) ^e	1.016 [$F_o^2 \geq -3\sigma(F_o^2)$]
final <i>R</i> indices ^f	
<i>R</i> ₁ [$F_o^2 \geq 2\sigma(F_o^2)$]	0.0510
wR_2 [$F_o^2 \geq -3\sigma(F_o^2)$]	0.1243
largest difference peak and hole	0.447 and -0.382 e Å ⁻³

^aObtained from least-squares refinement of 5737 centered reflections.

^bPrograms for diffractometer operation, data collection, data reduction and absorption correction were those supplied by Bruker.

(continued)

Table G.1 Crystallographic Experimental Details (continued)

^cBeurskens, P. T.; Beurskens, G.; Bosman, W. P.; de Gelder, R.; Garcia Granda, S.; Gould, R. O.; Israel, R.; Smits, J. M. M. (1996). The *DIRDIF-96* program system. Crystallography Laboratory, University of Nijmegen, The Netherlands.

^dSheldrick, G. M. *SHELXL-93*. Program for crystal structure determination. University of Göttingen, Germany, 1993. Refinement on F_o^2 for all reflections (all of these having $F_o^2 \geq -3\sigma(F_o^2)$). Weighted R -factors wR_2 and all goodnesses of fit S are based on F_o^2 ; conventional R -factors R_1 are based on F_o , with F_o set to zero for negative F_o^2 . The observed criterion of $F_o^2 > 2\sigma(F_o^2)$ is used only for calculating R_1 , and is not relevant to the choice of reflections for refinement. R -factors based on F_o^2 are statistically about twice as large as those based on F_o , and R -factors based on ALL data will be even larger.

^e $S = [\sum w(F_o^2 - F_c^2)^2 / (n - p)]^{1/2}$ (n = number of data; p = number of parameters varied; $w = [\sigma^2(F_o^2) + (0.0521P)^2 + 1.1040P]^{-1}$ where $P = [\text{Max}(F_o^2, 0) + 2F_c^2]/3$).

^f $R_1 = \sum ||F_o| - |F_c|| / \sum |F_o|$; $wR_2 = [\sum w(F_o^2 - F_c^2)^2 / \sum w(F_o^4)]^{1/2}$.

Table G.2 Atomic Coordinates and Equivalent Isotropic Displacement Parameters

Atom	<i>x</i>	<i>y</i>	<i>z</i>	<i>U</i> _{eq} , Å ²
Ti	0.15595(4)	0.08561(5)	0.117406(17)	0.02333(14)*
C1	-0.0382(2)	-0.0458(3)	0.09824(11)	0.0320(6)*
C2	0.0596(2)	-0.1404(3)	0.07533(10)	0.0313(6)*
C3	0.1454(2)	-0.0830(3)	0.03992(10)	0.0332(6)*
C4	0.2540(3)	-0.1882(4)	0.01941(12)	0.0457(8)*
C11	0.2035(2)	0.3050(3)	0.05764(10)	0.0294(6)*
C12	0.0654(2)	0.2817(3)	0.06027(10)	0.0296(6)*
C13	0.0222(2)	0.3279(3)	0.10832(10)	0.0304(6)*
C14	0.1339(3)	0.3675(3)	0.13745(11)	0.0317(6)*
C15	0.2461(2)	0.3609(3)	0.10565(10)	0.0302(6)*
C16	0.3797(3)	0.4026(3)	0.11286(12)	0.0401(7)*
C17	0.4628(3)	0.3885(4)	0.07280(14)	0.0483(9)*
C18	0.4204(3)	0.3298(4)	0.02615(13)	0.0465(8)*
C19	0.2941(3)	0.2865(4)	0.01791(11)	0.0388(7)*
C21	0.1640(3)	-0.1238(3)	0.18514(10)	0.0291(6)*
C22	0.2735(3)	-0.1469(3)	0.15334(10)	0.0334(6)*
C23	0.3567(3)	-0.0112(4)	0.15715(10)	0.0331(6)*
C24	0.2951(2)	0.1038(3)	0.18870(10)	0.0318(6)*
C25	0.1774(2)	0.0333(3)	0.20724(9)	0.0283(6)*
C26	0.0828(3)	0.0897(4)	0.24188(10)	0.0373(7)*
C27	-0.0200(3)	-0.0102(4)	0.25342(11)	0.0424(7)*
C28	-0.0326(3)	-0.1652(4)	0.23183(11)	0.0426(8)*
C29	0.0563(3)	-0.2229(4)	0.19839(11)	0.0377(7)*
C30	-0.1207(3)	0.3499(3)	0.12157(11)	0.0356(7)*
C31	-0.1475(3)	0.3346(5)	0.17719(14)	0.0673(11)*
C32	-0.1674(3)	0.5140(4)	0.10195(14)	0.0520(9)*
C40A ^a	0.5013(5)	0.0157(8)	0.1418(2)	0.0330(13)*
C41A ^a	0.5263(4)	-0.0534(7)	0.09016(19)	0.0535(14)*
C42A ^a	0.5905(4)	-0.0635(7)	0.18086(19)	0.0508(13)*
C40B ^b	0.4828(11)	-0.0196(13)	0.1288(4)	0.022(3)
C41B ^b	0.5345(8)	-0.1871(11)	0.1150(3)	0.040(2)
C42B ^b	0.5816(10)	0.0656(12)	0.1632(4)	0.046(2)

Anisotropically-refined atoms are marked with an asterisk (*). The form of the anisotropic displacement parameter is: $\exp[-2\pi^2(h^2a^*U_{11} + k^2b^*U_{22} + l^2c^*U_{33} + 2klb^*c^*U_{23} + 2hla^*c^*U_{13} + 2hka^*b^*U_{12})]$. ^aRefined with an occupancy factor of 2/3.

^bRefined with an occupancy factor of 1/3.

Table G.3 Selected Interatomic Distances (Å)

Atom1	Atom2	Distance	Atom1	Atom2	Distance
Ti	C1	2.312(3)	C15	C16	1.420(4)
Ti	C2	2.379(3)	C16	C17	1.376(4)
Ti	C3	2.490(3)	C17	C18	1.399(5)
Ti	C11	2.459(3)	C18	C19	1.354(4)
Ti	C12	2.398(3)	C21	C22	1.424(4)
Ti	C13	2.426(3)	C21	C25	1.426(4)
Ti	C14	2.389(3)	C21	C29	1.417(4)
Ti	C15	2.465(3)	C22	C23	1.406(4)
Ti	C21	2.496(3)	C23	C24	1.418(4)
Ti	C22	2.448(3)	C23	C40A	1.553(6)
Ti	C23	2.433(3)	C23	C40B	1.503(12)
Ti	C24	2.367(3)	C24	C25	1.427(4)
Ti	C25	2.442(2)	C25	C26	1.422(4)
C1	C2	1.410(4)	C26	C27	1.371(4)
C2	C3	1.379(4)	C27	C28	1.404(5)
C3	C4	1.514(4)	C28	C29	1.364(4)
C11	C12	1.426(4)	C30	C31	1.516(4)
C11	C15	1.424(4)	C30	C32	1.522(4)
C11	C19	1.423(4)	C40A	C41A	1.513(7)
C12	C13	1.411(4)	C40A	C42A	1.524(7)
C13	C14	1.412(4)	C40B	C41B	1.521(14)
C13	C30	1.517(3)	C40B	C42B	1.528(13)
C14	C15	1.433(4)			

Table G.4 Selected Interatomic Angles (deg)

Atom1	Atom2	Atom3	Angle	Atom1	Atom2	Atom3	Angle
C1	Ti	C2	34.96(9)	C11	Ti	C24	110.69(9)
C1	Ti	C3	61.73(9)	C11	Ti	C25	138.49(9)
C1	Ti	C11	111.98(9)	C12	Ti	C13	34.02(9)
C1	Ti	C12	81.31(9)	C12	Ti	C14	56.86(10)
C1	Ti	C13	83.13(9)	C12	Ti	C15	56.22(9)
C1	Ti	C14	114.85(9)	C12	Ti	C21	158.96(9)
C1	Ti	C15	136.21(9)	C12	Ti	C22	163.45(9)
C1	Ti	C21	81.92(10)	C12	Ti	C23	144.59(9)
C1	Ti	C22	97.95(10)	C12	Ti	C24	133.84(10)
C1	Ti	C23	131.40(10)	C12	Ti	C25	140.56(9)
C1	Ti	C24	135.58(10)	C13	Ti	C14	34.10(9)
C1	Ti	C25	101.71(9)	C13	Ti	C15	56.23(9)
C2	Ti	C3	32.80(9)	C13	Ti	C21	130.76(9)
C2	Ti	C11	110.55(10)	C13	Ti	C22	162.53(9)
C2	Ti	C12	94.04(10)	C13	Ti	C23	141.59(10)
C2	Ti	C13	111.36(9)	C13	Ti	C24	111.19(10)
C2	Ti	C14	145.46(9)	C13	Ti	C25	106.71(9)
C2	Ti	C15	144.17(10)	C14	Ti	C15	34.30(9)
C2	Ti	C21	79.21(9)	C14	Ti	C21	120.64(9)
C2	Ti	C22	76.92(10)	C14	Ti	C22	135.79(10)
C2	Ti	C23	107.03(10)	C14	Ti	C23	107.50(10)
C2	Ti	C24	132.10(10)	C14	Ti	C24	79.41(10)
C2	Ti	C25	110.96(10)	C14	Ti	C25	87.66(9)
C3	Ti	C11	82.97(9)	C15	Ti	C21	135.71(9)
C3	Ti	C12	80.44(10)	C15	Ti	C22	125.76(9)
C3	Ti	C13	110.77(9)	C15	Ti	C23	92.37(9)
C3	Ti	C14	136.24(10)	C15	Ti	C24	79.75(9)
C3	Ti	C15	114.76(9)	C15	Ti	C25	104.87(9)
C3	Ti	C21	102.55(9)	C21	Ti	C22	33.46(8)
C3	Ti	C22	84.66(10)	C21	Ti	C23	55.79(9)
C3	Ti	C23	102.04(9)	C21	Ti	C24	56.45(9)
C3	Ti	C24	136.25(9)	C21	Ti	C25	33.54(9)
C3	Ti	C25	135.96(9)	C22	Ti	C23	33.47(9)
C11	Ti	C12	34.13(8)	C22	Ti	C24	56.40(10)
C11	Ti	C13	56.48(8)	C22	Ti	C25	55.91(9)
C11	Ti	C14	56.84(9)	C23	Ti	C24	34.32(9)
C11	Ti	C15	33.63(9)	C23	Ti	C25	56.50(9)
C11	Ti	C21	165.89(9)	C24	Ti	C25	34.49(9)
C11	Ti	C22	136.65(9)	Ti	C1	C2	75.13(15)
C11	Ti	C23	110.56(9)	Ti	C2	C1	69.91(15)

Table G.4 Selected Interatomic Angles (continued)

Atom1	Atom2	Atom3	Angle	Atom1	Atom2	Atom3	Angle
Ti	C2	C3	78.02(16)	C22	C21	C29	133.6(3)
C1	C2	C3	124.5(3)	C25	C21	C29	119.3(2)
Ti	C3	C2	69.18(15)	Ti	C22	C21	75.12(15)
Ti	C3	C4	126.31(18)	Ti	C22	C23	72.67(15)
C2	C3	C4	121.7(3)	C21	C22	C23	109.2(2)
Ti	C11	C12	70.60(14)	Ti	C23	C22	73.86(15)
Ti	C11	C15	73.43(15)	Ti	C23	C24	70.29(14)
Ti	C11	C19	122.59(18)	Ti	C23	C40A	129.7(2)
C12	C11	C15	107.0(2)	Ti	C23	C40B	121.3(5)
C12	C11	C19	132.4(3)	C22	C23	C24	107.5(2)
C15	C11	C19	120.6(2)	C22	C23	C40A	132.1(3)
Ti	C12	C11	75.27(15)	C22	C23	C40B	116.6(4)
Ti	C12	C13	74.10(15)	C24	C23	C40A	119.4(3)
C11	C12	C13	109.1(2)	C24	C23	C40B	135.9(5)
Ti	C13	C12	71.89(15)	Ti	C24	C23	75.39(15)
Ti	C13	C14	71.52(14)	Ti	C24	C25	75.61(15)
Ti	C13	C30	128.11(18)	C23	C24	C25	108.4(2)
C12	C13	C14	107.6(2)	Ti	C25	C21	75.33(14)
C12	C13	C30	123.6(2)	Ti	C25	C24	69.89(14)
C14	C13	C30	128.3(3)	Ti	C25	C26	121.65(18)
Ti	C14	C13	74.39(15)	C21	C25	C24	107.6(2)
Ti	C14	C15	75.74(15)	C21	C25	C26	120.0(2)
C13	C14	C15	108.2(2)	C24	C25	C26	132.3(3)
Ti	C15	C11	72.94(15)	C25	C26	C27	118.6(3)
Ti	C15	C14	69.96(14)	C26	C27	C28	121.2(3)
Ti	C15	C16	124.39(19)	C27	C28	C29	121.7(3)
C11	C15	C14	107.8(2)	C21	C29	C28	119.2(3)
C11	C15	C16	119.0(3)	C13	C30	C31	113.7(3)
C14	C15	C16	133.2(3)	C13	C30	C32	108.9(2)
C15	C16	C17	118.3(3)	C31	C30	C32	110.5(3)
C16	C17	C18	122.1(3)	C23	C40A	C41A	110.9(4)
C17	C18	C19	121.4(3)	C23	C40A	C42A	108.9(4)
C11	C19	C18	118.5(3)	C41A	C40A	C42A	110.8(5)
Ti	C21	C22	71.42(15)	C23	C40B	C41B	117.8(8)
Ti	C21	C25	71.13(14)	C23	C40B	C42B	104.0(8)
Ti	C21	C29	123.83(19)	C41B	C40B	C42B	109.4(9)
C22	C21	C25	107.1(2)				